Mathematical Problems in Engineering

Mathematical Control of Complex Systems

Guest Editors: Zidong Wang, Hamid Reza Karimi, Bo Shen, and Jun Hu

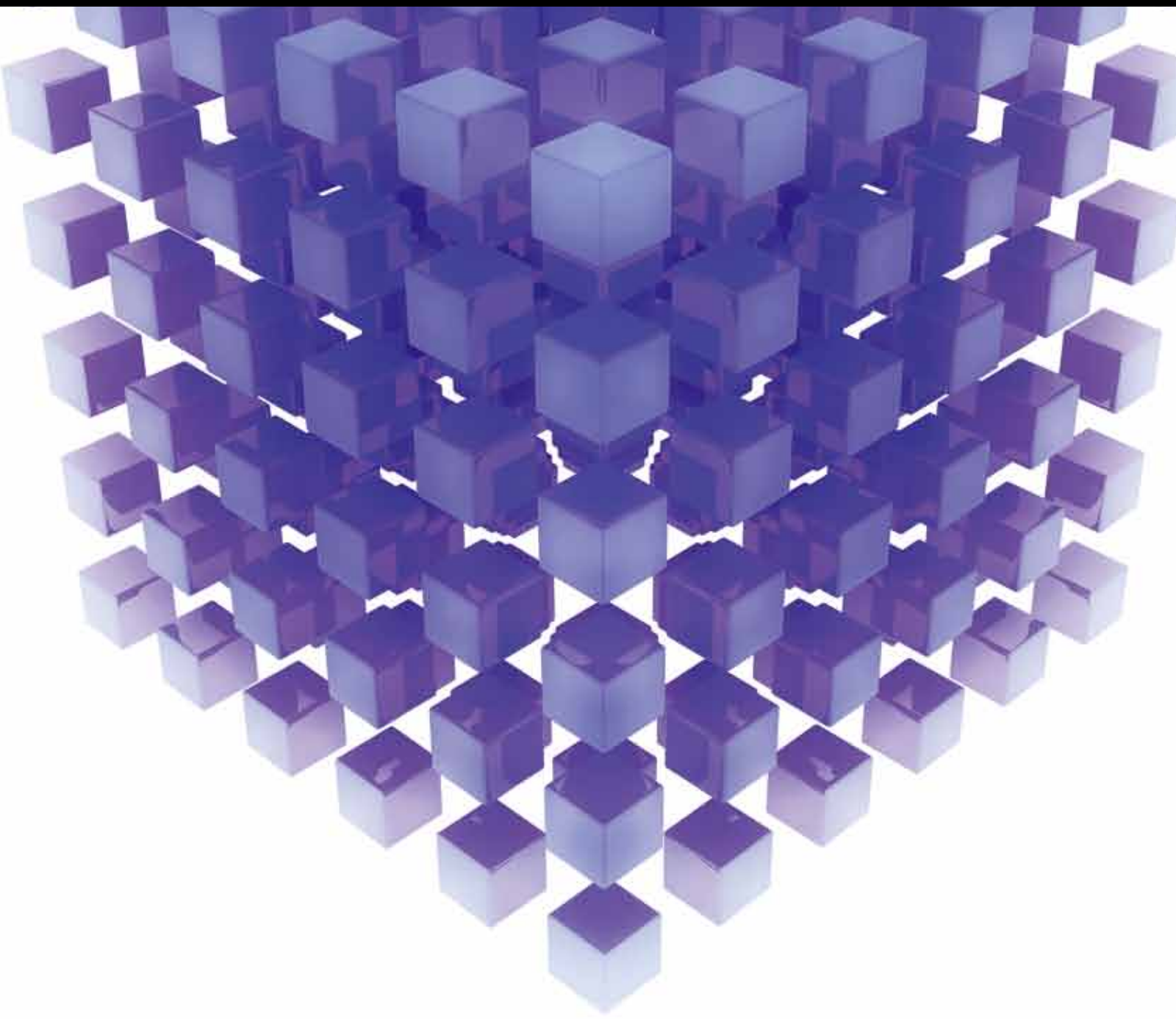

Mathematical Control of Complex Systems

Mathematical Problems in Engineering

Mathematical Control of Complex Systems

Guest Editors: Zidong Wang, Hamid Reza Karimi, Bo Shen, and Jun Hu

Editorial Board

Contents

Hindawi Publishing Corporation
Mathematical Problems in Engineering
Volume 2013, Article ID 407584, 4 pages
http://dx.doi.org/10.1155/2013/407584

Editorial

Mathematical Control of Complex Systems

Zidong Wang,[1,2] Hamid Reza Karimi,[3] Bo Shen,[1] and Jun Hu[4]

[1] *School of Information Science and Technology, Donghua University, Shanghai 200051, China*
[2] *Department of Information Systems and Computing, Brunel University, Uxbridge, Middlesex UB8 3PH, UK*
[3] *Department of Engineering, Faculty of Engineering and Science, University of Agder, N-4898 Grimstad, Norway*
[4] *Research Institute of Intelligent Control and Systems, Harbin Institute of Technology, Harbin, Heilongjiang 150080, China*

Correspondence should be addressed to Zidong Wang; zidong.wang@brunel.ac.uk

Received 17 December 2012; Accepted 17 December 2012

Recent advances in computing and network technologies have contributed much to the successful handling of certain problems in biology, physics, economics, and so forth that until recently were thought too difficult to be analyzed. These complex systems problems tend to share a number of interesting properties from a mathematical viewpoint. A key feature of such systems is that the nonlinear interactions among its components can lead to interesting emergent behavior.

The overall aim of this special issue is to bring together the latest/innovative knowledge and advances in mathematics for handling complex systems, which may depend largely on methods from artificial intelligence, statistics, operational research, and engineering, including nonlinear dynamics, time series analysis, dynamic systems, cellular automata, artificial life, evolutionary computation, game theory, neural networks, multi-agents, and heuristic search methods. The solicited papers in this special issue should provide solutions, or early promises, to modeling, analysis, and control problems of real-world complex systems, such as communication systems, process control, environmental systems, intelligent manufacturing systems, transportation systems, and structural systems. Topics include, but are not limited to: (1) control systems theory (behavioural systems, networked control systems, delay systems, distributed systems, infinite-dimensional systems and positive systems), (2) networked control (channel capacity constraints, control over communication networks, distributed filtering and control, information theory and control, and sensor networks), and (3) stochastic systems (nonlinear filtering, nonparametric methods, particle filtering, partial identification, stochastic control, stochastic realization, and system identification).

We have solicited submissions to this special issue from electrical engineers, control engineers, mathematicians, and computer scientists. After a rigorous peer review process, 29 papers have been selected that provide overviews, solutions, or early promises, to manage, analyze, and interpret dynamical behaviours of complex systems. These papers have covered both the theoretical and practical aspects of complex systems in the broad areas of dynamical systems, mathematics, statistics, operational research, and engineering.

Recently, there have been significant advances on analysis and synthesis of complex systems with randomly occurring incomplete information. In the paper entitled "*A review on analysis and synthesis of nonlinear stochastic systems with randomly occurring incomplete information*" by Z. Wang et al, the focus is to provide a timely review on the recent advances of the analysis and synthesis issues for nonlinear stochastic systems with randomly occurring incomplete information. In the context of systems and control, incomplete information refers to a dynamical system in which knowledge about the system states is limited due to the difficulties in modeling complexity in a quantitative way. The well-known types of incomplete information include parameter uncertainties and norm-bounded nonlinearities. Recently, in response to the development of network technologies, the phenomenon of randomly occurring incomplete information has become more and more prevalent. Most commonly used methods for modeling randomly occurring incomplete information are summarized. Based on the models established, various

filtering, control and fault detection problems with randomly occurring incomplete information are discussed in great detail. Such kind of randomly occurring incomplete information typically appears in a networked environment, which includes randomly occurring uncertainties, randomly occurring nonlinearities, randomly occurring saturation, randomly missing measurements, and randomly occurring quantization. Subsequently, latest results on analysis and synthesis of nonlinear stochastic systems with randomly occurring incomplete information are reviewed. Finally, some concluding remarks are drawn and some possible future research directions are pointed out.

During the past decades, the problems of stability analysis and stabilization synthesis of complex systems have received significant attentions. In the paper entitled "*Almost sure stability and stabilization for hybrid stochastic systems with time-varying delays*" by H. Shu et al., the almost sure stability analysis and stabilization synthesis problems are investigated for hybrid stochastic delay systems. The stability conditions are presented such that the underlying systems are almost sure stable. Following the same idea as in dealing with the stability problem, the linear state feedback controllers are designed such that the special nonlinear or linear closed-loop systems are almost sure stable. The explicit expressions for the desired state feedback controllers are given in terms of the solutions to a set of linear matrix inequalities. Two simulation examples are given to illustrate the effectiveness of the theoretical results. The stability analysis and semistability theorems are given in "*Semistability of nonlinear impulsive systems with delays*" by Y. Gao and X. Mu for delay impulsive systems. A set of Lyapunov-based sufficient conditions is proposed to guarantee the desired stability properties. In the paper entitled "*Stabilization of time-varying system by controllers with internal loop*" by C. Shi and Y. Lu, the concept of stabilization with internal loop is given for infinite-dimensional discrete time-varying systems in the framework of nest algebra. A parameterization of all stabilizing controllers with internal loop is proposed. It is shown that the strong stabilization problem can be completely solved in the closed-loop system with internal loop. Moreover, the problem of controller design is studied in "*L_∞ control with finite-time stability for switched systems under asynchronous switching*" by R. Wang et al. for switched systems under asynchronous switching with exogenous disturbances. It is shown that the switched system is finite-time stabilizable under asynchronous switching satisfying the average dwell-time condition. Furthermore, the problem of L_∞ control for switched systems under asynchronous switching is also investigated. Finally, a numerical example is given to illustrate the effectiveness of the proposed method.

The design of controller has long been the main stream of research topics and much effort has been made for complex systems. In the paper entitled "*MPC schemes guaranteeing ISDS and ISS for nonlinear (time-delay) systems*" by L. Naujok and S. Dashkovskiy, new directions in model predictive control (MPC) are introduced. The input-to-state dynamical stability and MPC are combined for the single and interconnected systems. The MPC schemes are employed to ensure the input-to-state stability of single systems and networks with time delays. Subsequently, the robust finite-time H_∞ control is studied in "*Robust finite-time H_∞ control for impulsive switched nonlinear systems with state delay*" by Z. Xiang et al. for a class of impulsive switched nonlinear systems with time-delay. By employing the piecewise Lyapunov function, sufficient conditions are developed to ensure the finite-time boundedness of the impulsive switched system. In the work entitled "*Robust anti-windup control considering multiple design objectives*" by G. Sun et al., a unified synthesis method of the construction of multi-objective and robust antiwindup controller is proposed for linear systems with actuator saturations, time-varying parametric, and dynamic uncertainties. The analysis and synthesis conditions are developed in terms of the scaled linear matrix inequalities. The impulsive neutral second-order stochastic functional evolution equations are investigated in "*Controllability of second-order semilinear impulsive stochastic neutral functional evolution equations*" by Y. Ding et al. By using the Sadovskii fixed point theorem and the theory of strongly continuous cosine families of operators, the sufficient conditions for the controllability of the system are given. Based on the mean and the standard deviation of lead time demand, in the paper entitled "*Distribution-free continuous review inventory model with controllable lead time and setup cost in the presence of a service level constraint*" by B.-B. Qiu and W.-M MA, the joint decision problem of continuous review inventory is studied.

Networked control systems (NCSs) have attracted much attention owing to their successful applications in a wide range of areas. Accordingly, the design of controller for NCSs has attracted considerable attention. In the paper entitled "*Linear matrix inequalities in multirate control over networks*" by A. Cuenca et al., the networked induced phenomena of bandwidth constraints and time varying delays are considered. Some stability conditions and a state feedback controller design are proposed. Two practical examples are given to illustrate the usefulness of the theoretical results. By utilizing probability-dependent Lyapunov method, the problem of gain-scheduled control is studied in "*Probability-dependent static output feedback control for discrete-time nonlinear stochastic systems with missing measurements*" by G. Wei et al. for a class of discrete time stochastic systems with infinite-distributed delays and missing measurements. A time-varying Lyapunov functional dependent on the missing probability is constructed with hope to improve the performance of the gain-scheduled controller. A static output feedback controller with scheduled gains is designed. In the work entitled "*Observer-based stabilization of stochastic systems with limited communication*" by J. Wu et al., the problem of observer-based stabilization is investigated in stochastic nonlinear systems with limited communication. The phenomena of network-induced delays, data packet dropouts, and measurement quantization are considered. A new stability condition is derived for the stochastic nonlinear system and the design procedure of observer-based controller is given. In the paper entitled "*Finite-time boundedness and stabilization of networked control systems with time delay*" by Y. Sun et al., the finite-time control problem is studied for a class of networked control systems with time delay. Sufficient conditions are given to ensure the finite-time boundedness

and stabilization of the underlying systems. By using the Lyapunov stability theory and discrete Halanay inequality, the exponential synchronization is addressed in "*Exponential synchronization analysis and control for discrete-time uncertain delay complex networks with stochastic effects*" by T. Wang et al.for a class of discrete-time uncertain complex networks with stochastic effects and time delay. Some synchronization criteria and two control methods are obtained.

In the past decades, the issue of parameter estimation has received considerable research interests and has found successful applications in a variety of areas. In the paper entitled "*MIMO LPV state-space identification of open-flow irrigation canal systems*" by A. Grau et al., by identification in a local way using a multimodel approach, a linear parameter-varying (LPV) state-space canal control model is obtained. This LPV identification procedure is based on subspace methods for different operating points of an irrigation canal covering the full operation range. Different subspace algorithms are compared. Subsequently, the parameter estimation problem is studied in "*Asymptotic parameter estimation for a class of linear stochastic systems using Kalman-Bucy filtering*" by H. Shu et al. for a general class of linear stochastic systems. The Kalman-Bucy linear filtering is used to solve the parameter estimation problem. The asymptotic convergence of the estimator is investigated by analyzing Riccati equation and the strong consistent property is studied by comparison theorem. In the work entitled "*Uniform approximate estimation for nonlinear nonhomogenous stochastic system with unknown parameter*" by X. Kan and H. Shu, the error bound in probability between the approximate maximum likelihood estimator (AMLE) and the continuous maximum likelihood estimator (MLE) is investigated for nonlinear nonhomogenous stochastic system with unknown parameter. The rates of convergence of the approximations for Ito and ordinary integral are introduced. Based on these results, the probabilistic rate of convergence of the approximate log likelihood function to the true continuous log-likelihood function is studied for the nonlinear nonhomogenous stochastic system involving unknown parameter. Finally, the error bound in probability between the ALME and the continuous MLE is given. In the paper entitled "*D-Optimal design for parameter estimation in discrete-time nonlinear dynamic systems*" by Y. Liu et al., an optimal input design method is presented for parameter estimation of a discrete nonlinear system. In the paper entitled "*Estimation for stochastic nonlinear systems with randomly distributed time-varying delays and missing measurements*" by H. Shu et al., an estimator is designed such that, for measurements missing and distributed time-varying delays, the estimation error system is mean-square stable.

Over the past decades, the observer/filter problems of complex systems have been investigated extensively since they are very useful in signal processing and engineering applications. In the paper entitled "*Robust H_2/H_∞ filter design for a class of nonlinear stochastic systems with state-dependent noise*" by W. Zhang et al., the problem of robust filter design is studied for a class of nonlinear stochastic systems with state-dependent noise. The state and measurement are corrupted by stochastic uncertain exogenous disturbance and the dynamic system is modeled by Ito-type stochastic differential equations. The robust H_∞ filter can be designed in terms of the solution to the linear matrix inequalities. Moreover, a mixed H_2/H_∞ filtering problem is also solved by minimizing the total estimation error energy when the worst-case disturbance is considered in the design procedure. Subsequently, a cascaded sliding mode observer method is given in "*Fault-reconstruction-based cascaded sliding mode observers for descriptor linear systems*" by J. Yu et al. to reconstruct the actuator faults for a class of descriptor linear systems. Based on a new canonical form, a novel design method is presented to discuss the existence conditions of the sliding mode observer. The proposed method is extended to general descriptor linear systems with actuator faults. In the work entitled "*Data-driven adaptive observer for fault diagnosis*" by S. Yin et al., an approach is given for the data-driven design of fault diagnosis system. The proposed fault diagnosis scheme consists of an adaptive residual generator and a bank of isolation observers, whose parameters are directly identified from the process data without identification of complete process model. To deal with normal variations in the process, the parameters of residual generator are online updated by a standard adaptive technique to achieve reliable fault detection performance. After a fault is successfully detected, the isolation scheme will be activated, in which each isolation observer serves as an indicator corresponding to occurrence of a particular type of fault in the process. The thresholds can be determined analytically or through estimating the probability density function of related variables. A laboratory-scale three-tank system is given to illustrate the usefulness of the proposed method.

The applications of various control schemes have received considerable research interests in the past decades. In the work entitled "*Discrete-time multioverlapping controller design for structural vibration control of tall buildings under seismic excitation*" by F. Palacios-Quinonero et al., a computationally effective strategy to obtain multioverlapping controllers via the inclusion principle is applied to design discrete-time state-feedback multioverlapping LQR controllers for seismic protection of tall buildings. The performance of the proposed multioverlapping controllers has been assessed through numerical simulations. In another paper "*Structural vibration control for a class of connected multistructure mechanical systems*" by F. Palacios-Quinonero et al., the aim is to design the control configurations that combine passive interbuilding dampers with local feedback control systems implemented in the buildings. Moreover, the active-passive control configurations can be properly designed for multibuilding systems requiring different levels of seismic protection. The monocular vision is employed in "*Robot navigation control based on monocular images: an image processing algorithm for obstacle avoidance decisions*" by S. Lauria and W. Benn to control autonomous navigation for a robot in a dynamically changing environment. Subsequently, the optimality condition-based sensitivity analysis of optimal control for hybrid systems with mode invariants and control constraints is addressed in "*Optimality condition-based sensitivity analysis of optimal control for hybrid systems and its application*" by C. Song. The derivatives of the objective functional with respect to control variables are established and

a control vector parameterization method is implemented to obtain the numerical solution to the optimal control problems for hybrid system. In the paper entitled "*Robust H_∞ dynamic output feedback control synthesis with pole placement constraints for offshore wind turbine systems*" by H. R. Karimi and I. Bakka, the problem of robust H_∞ dynamic output feedback control design with pole placement constraints is addressed for a linear parameter-varying model of a floating wind turbine. Finally, a novel multiloop is proposed and the multiobjective cooperative intelligent control system is used in "*Neuroendocrine-based cooperative intelligent control system for multiobjective integrated control of a parallel manipulator*" by K. Hao et al. to improve the performance of position, velocity, and acceleration-integrated control on a complex multichannel plant.

Appendix

Accepted Papers according to Fackled Topics

(1) "A review on analysis and synthesis of nonlinear stochastic systems with randomly occurring incomplete information".

Papers on the Topic of Stability. (2) Almost Sure Stability and *Stabilization for Hybrid Stochastic Systems with Time-Varying Delays*.

(3) Semistability of Nonlinear Impulsive Systems with Delays.

(4) Stabilization of Time-Varying System by Controllers with Internal Loop.

(5) L_∞ Control with Finite-Time Stability for Switched Systems under Asynchronous Switching.

Papers on the Topic of Control for Complex Systems. (6) MPC Schemes Guaranteeing ISDS and ISS for Nonlinear (Time-Delay) Systems.

(7) Robust Finite-Time H_∞ Control for Impulsive Switched Nonlinear Systems with State Delay.

(8) Robust Anti-Windup Control Considering Multiple Design Objectives.

(9) Controllability of Second-Order Semilinear Impulsive Stochastic Neutral Functional Evolution Equations.

(10) Distribution-Free Continuous Review Inventory Model with Controllable Lead Time and Setup Cost in the Presence of a Service Level Constraint.

Papers on the Topic of Control over Networks. (11) Linear Matrix Inequalities in Multirate Control over Networks.

(12) Probability-Dependent Static Output Feedback Control for Discrete-Time Nonlinear Stochastic Systems with Missing Measurements.

(13) Observer-Based Stabilization of Stochastic Systems with Limited Communication.

(14) Finite-Time Boundedness and Stabilization of Networked Control Systems with Time Delay.

(15) Exponential Synchronization Analysis and Control for Discrete-Time Uncertain Delay Complex Networks with Stochastic Effects.

Papers on the Topic of Parameter Estimation. (16) MIMO LPV State-Space Identification of Open-Flow Irrigation Canal Systems.

(17) Asymptotic Parameter Estimation for a Class of Linear Stochastic Systems Using Kalman-Bucy Filtering.

(18) Uniform Approximate Estimation for Nonlinear Nonhomogenous Stochastic System with Unknown Parameter.

(19) D-Optimal Design for Parameter Estimation in Discrete-Time Nonlinear Dynamic Systems.

(20) Estimation for Stochastic Nonlinear Systems with Randomly Distributed Time-Varying Delays and Missing Measurements.

Papers on the Topic of Observer/Filter Design for Complex Systems. (21) Robust H_2/H_∞ Filter Design for a Class of Nonlinear Stochastic Systems with State-Dependent Noise.

(22) Fault-Reconstruction-Based Cascaded Sliding Mode Observers for Descriptor Linear Systems.

(23) Data-Driven Adaptive Observer for Fault Diagnosis.

Papers on the Topic of Applications. (24) Discrete-Time Multioverlapping Controller Design for Structural Vibration Control of Tall Buildings under Seismic Excitation.

(25) Structural Vibration Control for a Class of Connected Multistructure Mechanical Systems.

(26) Robot Navigation Control Based on Monocular Images: An Image Processing Algorithm for Obstacle Avoidance Decisions.

(27) Optimality Condition-Based Sensitivity Analysis of Optimal Control for Hybrid Systems and Its Application.

(28) Robust H_∞ Dynamic Output Feedback Control Synthesis with Pole Placement Constraints for Offshore Wind Turbine Systems.

(29) Neuroendocrine-Based Cooperative Intelligent Control System for Multiobjective Integrated Control of a Parallel Manipulator.

Acknowledgments

This special issue is a timely reflection of the research progress in the area of mathematical control of complex systems. We would like to acknowledge all authors for their efforts in submitting high-quality papers. We are also very grateful to the reviewers for their thorough and on time reviews of the papers.

Zidong Wang
Hamid Reza Karimi
Bo Shen
Jun Hu

Hindawi Publishing Corporation
Mathematical Problems in Engineering
Volume 2012, Article ID 416358, 15 pages
doi:10.1155/2012/416358

Review Article

A Review on Analysis and Synthesis of Nonlinear Stochastic Systems with Randomly Occurring Incomplete Information

Hongli Dong,[1,2] Zidong Wang,[3,4] Xuemin Chen,[5] and Huijun Gao[6]

[1] *College of Electrical and Information Engineering, Northeast Petroleum University, Daqing 163318, China*
[2] *Institute for Automatic Control and Complex Systems, University of Duisburg-Essen 47057, Germany*
[3] *Department of Automation, Tsinghua University, Beijing 100084, China*
[4] *Department of Information Systems and Computing, Brunel University, Uxbridge, Middlesex, UB8 3PH, UK*
[5] *Department of Engineering Technology, Texas Southern University, 3100 Cleburne Street, Houston, TX 77004, USA*
[6] *Research Institute of Intelligent Control and Systems, Harbin Institute of Technology, Harbin 150001, China*

Correspondence should be addressed to Hongli Dong, shiningdhl@gmail.com

Received 11 November 2012; Accepted 21 November 2012

Academic Editor: Bo Shen

In the context of systems and control, incomplete information refers to a dynamical system in which knowledge about the system states is limited due to the difficulties in modeling complexity in a quantitative way. The well-known types of incomplete information include parameter uncertainties and norm-bounded nonlinearities. Recently, in response to the development of network technologies, the phenomenon of randomly occurring incomplete information has become more and more prevalent. Such a phenomenon typically appears in a networked environment. Examples include, but are not limited to, randomly occurring uncertainties, randomly occurring nonlinearities, randomly occurring saturation, randomly missing measurements and randomly occurring quantization. Randomly occurring incomplete information, if not properly handled, would seriously deteriorate the performance of a control system. In this paper, we aim to survey some recent advances on the analysis and synthesis problems for nonlinear stochastic systems with randomly occurring incomplete information. The developments of the filtering, control and fault detection problems are systematically reviewed. Latest results on analysis and synthesis of nonlinear stochastic systems are discussed in great detail. In addition, various distributed filtering technologies over sensor networks are highlighted. Finally, some concluding remarks are given and some possible future research directions are pointed out.

1. Introduction

In the past decade, networked control systems (NCSs) have attracted much attention owing to their successful applications in a wide range of areas for the advantage of decreasing the hardwiring, the installation cost, and implementation difficulties. Nevertheless, the NCS-related challenging problems arise inevitably due to the physical equipment constraints and the complexity and uncertainty of the external environment in the process of modeling or information transmission, which would drastically degrade the system performances. Such network-induced problems include, but are not limited to, missing measurements, communication delays, sensor and actuator saturations, signal quantization, and randomly varying nonlinearities. These phenomena may occur in a probabilistic way that are customarily referred to as the randomly occurring incomplete information. Note that, in the literature concerning systems and control, incomplete information usually refers to a dynamical system in which knowledge about the system states is limited due to the difficulties in modeling complexity in a quantitative way. The well-known types of incomplete information include parameter uncertainties and norm-bounded nonlinearities.

For several decades, nonlinear analysis and stochastic analysis are arguably two of the most active research areas in systems and control. This is simply because (1) nonlinear control problems are of interest to engineers, physicists, and mathematicians because most physical systems are inherently nonlinear in nature and (2) stochastic modelling has come to play an important role in many branches of science and industry as many real world systems and natural processes may be subject to stochastic disturbances. There has been rich literature on the general nonlinear stochastic control problems. A great number of techniques have been developed on filtering, control, and fault detection problems for nonlinear stochastic systems in order to meet the needs of practical engineering. Recently, with the development of networked control systems, the analysis and synthesis problems for nonlinear stochastic systems with randomly occurring incomplete information have become interesting and imperative yet challenging topics that have gained a great deal of research attention.

The focus of this paper is to provide a timely review on the recent advances of the analysis and synthesis issues for nonlinear stochastic systems with randomly occurring incomplete information. Most commonly used methods for modeling randomly occurring incomplete information are summarized. Based on the models established, various filtering, control, and fault detection problems with randomly occurring incomplete information are discussed in great detail. Such kind of randomly occurring incomplete information typically appears in a networked environment, which includes randomly occurring uncertainties, randomly occurring nonlinearities, randomly occurring saturation, randomly missing measurements, and randomly occurring quantization. Subsequently, latest results on analysis and synthesis of nonlinear stochastic systems with randomly occurring incomplete information are reviewed. Finally, some concluding remarks are drawn and some possible future research directions are pointed out.

The rest of this paper is outlined as follows. In Section 2, the phenomenon of randomly occurring incomplete information is addressed and the corresponding models are summarized. In Section 3, the analysis and synthesis problems for nonlinear stochastic systems are reviewed. Section 4 discusses the distributed filtering problems over sensor networks. The latest results on filtering, control, and fault detection problems for nonlinear stochastic systems with randomly occurring incomplete information are reviewed in Section 5. In Section 6, we give some concluding remarks and also point out some future directions.

2. Randomly Occurring Incomplete Information

Accompanied by the rapid development of communication and computer technology, NCSs have become more and more popular for their successful applications in modern complicated industry processes, for example, aircraft and space shuttle, nuclear power stations and high-performance automobiles. However, the insertion of network makes the analysis and synthesis problems much more complex due to the randomly occurring incomplete information that is mainly caused by the limited bandwidth of the digital communication channel. The randomly occurring incomplete information under consideration mainly includes missing measurements, communication delays, sensor and actuator saturations, signal quantization, and randomly varying nonlinearities.

2.1. Missing Measurements

In practical systems within a networked environment, the measurement signals are usually subject to probabilistic information missing (data dropouts or packet losses), which may be caused for a variety of reasons, such as the high manoeuvrability of the tracked target, a fault in the measurement, intermittent sensor failures, network congestion, accidental loss of some collected data, or some of the data may be jammed or coming from a very noisy environment, and so forth. Such a missing measurement phenomenon that typically occurs in networked control systems has attracted considerable attention during the past few years, see [1–11] and the references therein. Various approaches have been presented in the literature to model the packet-dropout phenomenon. For example, in [12, 13], the data packet-dropout phenomenon has been described as a binary switching sequence that is specified by a conditional probability distribution taking on values of 0 and 1. In [14], a discrete-time linear system with Markovian jumping parameters has been employed to construct the random packet-dropout model. In [15], a model that comprises former measurement information of the process output has been introduced to account for the successive packet dropout phenomenon. A model of multiple missing measurements has been proposed in [11, 16] by using a diagonal matrix to describe the different missing probabilities for individual sensors.

2.2. Communication Delays

Owing to the fact that time delays commonly reside in practical systems and constitute a main source for system performance degradation or even instability, the past decade has witnessed a significant progress on analysis and synthesis for systems with various types of delays, and a large amount of literature has appeared on the general topic of time-delay systems. For example, in [17], the stability of NCSs under the network-induced delay has been studied by using a hybrid system technique. The optimal stochastic control method has been proposed in [18] to control the communication delays in NCSs. A networked controller has been designed in the frequency domain using the robust control theory in [19], in which the network delays are considered as an uncertainty. However, most of the relevant literature mentioned above has focused on the *constant time delays*. Delays resulting from network transmissions are inherently *random* and *time varying* [20–22]. This is particularly true when signals are transmitted over the internet and therefore existing control methods for constant time delay cannot be directly utilized [23]. Recently, some researchers have started to model the network-induced time delays in multiform

probabilistic ways and, accordingly, some initial results have been reported. For example, in [24, 25], the random communication delays have been modeled as Markov's chains and the resulting closed-loop systems have been represented as Markovian jump linear systems with two jumping parameters. In [26], two kinds of random delays, which happen in the channels from the controller to the plant and from the sensor to the controller, have been simultaneously considered. The random delays have been modeled in [26] as a linear function of the stochastic variable satisfying Bernoulli random binary distribution. Different from [26], the problem of stability analysis and stabilization control design has been studied in [27] for the Takagi-Sugeno (T-S) fuzzy systems with a probabilistic interval delay, and the Bernoulli distributed sequence has been utilized to describe the probability distribution of the time-varying delay taking values in an interval. It should be mentioned that, among others, the binary representation of the random delays has been fairly popular because of its practicality and simplicity in describing communication delays.

However, most research attention has been centered on the *single* random delay having a *fixed* value if it occurs. This would lead to conservative results or even degradation of the system performance since, at a certain time, the NCSs could give rise to multiple time-varying delays but with different occurrence probabilities. Therefore, a more advanced methodology is needed to handle time varying network-induced time-delays in a closed-loop control system.

2.3. Signal Quantization

As is well-known, quantization always exists in computer-based control systems employing finite-precision arithmetic. Moreover, the performance of NCSs will be inevitably subject to the effect of quantization error owing to the limited network bandwidth caused possibly by strong signal attenuation and perturbation in the operational environment. Hence, the quantization problem of NCSs has long been studied and many important results have been reported in [28–35] and the references therein. For example, in [36], the time-varying quantization strategy has been firstly proposed where the number of quantization levels is fixed and finite while at the same time the quantization resolution can be manipulated over time. In [37], the problem of input-to-state stable with respect to the quantization error for nonlinear continuous-time systems has been studied. In this framework, the effect of quantization is treated as an additional disturbance whose effect is overcome by a Lyapunov redesign of the control law. In [38], a switching control strategy with dwell time has been proposed to use a quantizer for single-input systems. The quantizer employed in this framework is in fact an extension of the static logarithmic quantizer in [39] to continuous case. So far, there have been mainly two different types of quantized communication models adopted in the literature: uniform quantization [28, 33, 34] and logarithmic quantization [30–32, 35]. It has been proved that, as compared to the uniform quantizer, the logarithmic quantization is more preferable since fewer bits need to be communicated. In [40], a sector bound scheme has been proposed to handle the logarithmic quantization effects in feedback control systems, and such an elegant scheme has then been extensively employed later on, see, for example [7, 35, 41, 42], and the references therein. However, we note that the methods that most of the references cited above could not be directly applied to NCSs, because in NCSs the effects of network-included delay and packet dropout should be also considered.

2.4. Sensor and Actuator Saturations

In practical control systems, sensors and actuators cannot provide unlimited amplitude signal due primarily to the physical, safety, or technological constraints. In fact, the actuator/sensor saturation is probably the most common nonlinearity encountered in practical control systems, which can degrade the system performance or even cause instability if such a nonlinearity is ignored in the controller/filter design. Because of their theoretical significance and practical importance, considerable attention has been focused on the filtering and control problems for systems with *actuator saturation* [43–46]. As for *sensor saturation*, the associated results have been relatively few due probably to the technical difficulty [47–49]. Nevertheless, in the scattered literature regarding sensor saturation, it has been implicitly assumed that the occurrence of sensor saturations is deterministic, that is, the sensor always undergoes saturation. Such an assumption, however, does have its limitation especially in a sensor network. The sensor saturations may occur in a probabilistic way and are randomly changeable in terms of their types and/or levels due to the random occurrence of network-induced phenomena such as random sensor failures, sensor aging, or sudden environment changes. To reflect the reality in networked sensors, in [8], a new phenomenon of sensor saturation, namely, randomly occurring sensor saturation (ROSS), has been put forward in order to better reflect the reality in a networked environment. A novel sensor model has then been established to account for both the ROSS and missing measurement in a unified representation by using two sets of the Bernoulli distributed white sequences with known conditional probabilities. It should be mentioned that very few results have dealt with the systems with simultaneous presence of actuator and sensor saturations [50] although such a presence is quite typical in engineering practice.

2.5. Randomly Varying Nonlinearities

It is well known that nonlinearities exist universally in practice and it is quite common to describe them as additive nonlinear disturbances that are caused by environmental circumstances. In a networked system such as the internet-based three-tank system for leakage fault diagnosis, such nonlinear disturbances may occur in a probabilistic way due to the random occurrence of network-induced phenomenon. For example, in a particular moment, the transmission channel for a large amount of packets may encounters severe network-induced congestions due to the bandwidth limitations, and the resulting phenomenon could be reflected by certain randomly occurring nonlinearities where the occurrence probability can be estimated via statistical tests. As discussed in [51, 52], in nowadays prevalent networked control system, the nonlinear disturbances themselves may experience random abrupt changes due to random changes and failures arising from network-induced phenomenon, which give rise to the so-called randomly varying nonlinearities. In other words, the type and intensity of the so-called randomly varying nonlinearities could be changeable in a probabilistic way.

3. The Analysis and Synthesis of Nonlinear Stochastic Systems

For several decades, stochastic systems have received considerable research attention in which stochastic differential equations are the most useful stochastic models with broad applications in aircraft, chemical or process control system, and distributed networks.

Generally speaking, stochastic systems can be categorized into two types, namely, internal stochastic systems and external stochastic systems [53].

As a class of internal stochastic systems with finite operation modes, the Markovian jump systems (MJSs) have gained particular research interests in the past two decades because of their practical applications in a variety of areas such as power systems, control systems of a solar thermal central receiver, networked control systems, manufacturing systems, and financial markets. So far, existing results about MJSs have covered a wide range of research problems including those for stability analysis [54–56], filter design [57–64], and controller design [65, 66]. Nevertheless, compared to the fruitful results for filtering and control problems of MJSs, the corresponding fault detection problem of MJSs has received much less attention [67, 68] due primarily to the difficulty in accommodating the multiple fault detection performances. In the literature concerning the MJSs, most results have been reported by supposing that the transition probabilities (TPs) in the jumping process are completely accessible. However, this is not always true for many practical systems. For example, in networked control systems, it would be extremely difficult to obtain precisely all the TPs via time-consuming yet expensive statistical tests. In other words, some of TPs are very likely to be incomplete (i.e., uncertain or even unknown). So far, some initial efforts have been made to address the incomplete probability issue for MJSs. For example, the problems of uncertain TPs and partially unknown TPs have been addressed in [56, 62] and [63, 69], respectively. Furthermore, the concept of deficient statistics for modes transitions has been put forward in [70] to reflect different levels of the limitations in acquiring accurate TPs. Unfortunately, up to now, the filtering/control/fault detection problem for discrete-time Markovian jump systems with randomly varying nonlinearities has not been fully investigated yet.

For external stochastic systems, stochasticity is always caused by external stochastic noise signal and can be modelled by stochastic differential equations with stochastic processes [53]. Furthermore, recognizing that nonlinearities exist universally in practice and both nonlinearity and stochasticity are commonly encountered in engineering practice, the robust H_∞ filtering, H_∞ control, and fault detection problems for nonlinear stochastic systems have stirred a great deal of research interests. For the fault detection problems, we refer the readers to [46, 71–73] and the references therein. With respect to the H_∞ control and filtering problems, we mention some representative work as follows. The stochastic H_∞ filtering problem for time-delay systems subject to sensor nonlinearities have been dealt with in [74, 75]. The robust stability and controller design problems for networked control systems with uncertain parameters have been studied in [25, 76], respectively. The stability issue has been addressed in [77] for a class of T-S fuzzy dynamical systems with time delays and uncertain parameters. In [78], the robust H_∞ filtering problem for affine nonlinear stochastic systems with state and external disturbance-dependent noise has been studied, where the filter can be designed by solving second-order nonlinear Hamilton-Jacobi inequalities. So far, in comparison with the fruitful literature available for continuous-time systems, the corresponding H_∞ filtering results for discrete-time systems have been relatively few. Also, to the best of our knowledge, the analysis and design problems for *nonlinear discrete-time stochastic systems with randomly occurring incomplete information have not been properly investigated yet, which still remain as challenging research topics*.

4. Distributed Filtering over Sensor Networks

In the past decade, sensor networks have been attracting increasing attention from many researchers in different disciplines owing to the extensive applications of sensor networks

in many areas including surveillance, environment monitoring, information collection, industrial automation, and wireless networks [79–88]. A sensor network typically consists of a large number of sensor nodes and also a few control nodes, all of which are distributed over a spatial region. The distributed filtering or estimation, as an important issue for sensor networks, has been an area of active research for many years. Different from the traditional filtering for a single sensor [58, 61, 89], the information available for the filter algorithm on an individual node of the sensor network is not only from its own measurement but also from its neighboring sensors' measurements according to the given topology. As such, the objective of filtering based on a sensor network can be achieved in a distributed yet collaborative way. It is noticed that one of the main challenges for distributed filtering lies in how to handle the complicated coupling issues between one sensor and its neighboring sensors.

In recent years, the distributed filtering problem for sensor networks has received considerable research interest and a lot of research results have been available in the literature, see, for example, [79, 82, 83, 87, 90–93]. The distributed diffusion filtering strategy has been established in [79, 90] for the design of distributed Kalman filters and smoothers, where the information is diffused across the network through a sequence of Kalman iterations and data-aggregation. A distributed Kalman Filtering (DKF) algorithm has been introduced in [93] through which a crucial part of the solution is used to estimate the average of n signals in a distributed way. Furthermore, three novel distributed Kalman filtering algorithms have been introduced in [92] with the first one being a modification of the previous DKF algorithm [93]. Also, a continuous-time DKF algorithm has been rigorously derived and analyzed in [92], and the corresponding extension to the discrete-time setting has been conducted in [83] which includes the optimality and stability analysis.

It should be pointed out that, so far, most reported distributed filter algorithms for sensor networks have been mainly based on the traditional Kalman filtering theory that requires exact information about the plant model. In the presence of unavoidable parameter drifts and external disturbances, a desired distributed filtering scheme should be made as robust as possible. However, the robust performance of the available distributed filters has not yet been thoroughly studied, and this would inevitably restrict the application potential in practical engineering. Therefore, it is of great significance to introduce the H_∞ performance requirement with the hope to enhance the disturbance rejection attenuation level of designed distributed filters. Note that some initial efforts have been made to address the robustness issue. Very recently, a new distributed H_∞-consensus performance has been proposed in [86] to quantify the consensus degree over a finite horizon and the distributed filtering problem has been addressed for a class of linear time-varying systems in the sensor network, and the filter parameters have been designed recursively by resorting to the difference linear matrix inequalities. In [94], an H_∞-type performance measure of disagreement between adjacent nodes of the network has been included and a robust filtering approach has been proposed to design the distributed filters for uncertain plants. On the other hand, since nonlinearities are ubiquitous in practice, it is necessary to consider the distributed filtering problem for target plants described by nonlinear systems.

Unfortunately, up to now, the distributed nonlinear H_∞ filtering problem for sensor networks has gained very little research attention despite its practical importance.

5. Latest Progress

In [95, 96], the H_∞ filtering and control problems have been investigated for systems with repeated scalar nonlinearities and missing measurements. The nonlinear system is described

by a discrete-time state equation involving a repeated scalar nonlinearity which typically appears in recurrent neural networks. The H_∞ filtering problem has been first considered in [95] for the systems with missing measurements. The missing measurements have been modeled by a stochastic variable satisfying the Bernoulli random binary distribution. The quadratic Lyapunov function has been used to design both full- and reduced-order H_∞ filters such that, for the admissible random measurement missing and repeated scalar nonlinearities, the filtering error system is stochastically stable and preserves a guaranteed H_∞ performance. In addition, in [96], the notion of missing measurements has been extended to the multiple missing measurements, where the missing probability for each sensor is governed by an individual random variable satisfying a certain probabilistic distribution in the interval $[0, 1]$. An observer-based feedback controller has been designed to stochastically stabilize the networked system. Both the stability analysis and controller synthesis problems have been investigated in detail.

In [97], the robust H_∞ filtering problem has been studied for a class of uncertain nonlinear networked systems with both multiple stochastic time-varying communication delays and multiple packet dropouts. The missing measurements have been modeled via a diagonal matrix consisting of a series of mutually independent random variables satisfying certain probabilistic distributions on the interval $[0, 1]$. Such a modeling approach can describe the following packet dropouts situations for the measurement signals: completely missing, completely available, partially missing, and the case when the individual sensor has different missing probability is also included. A new model has been proposed to account for the randomly occurring communication delays. Furthermore, the discrete-time system under consideration has been also subject to parameter uncertainties, state-dependent stochastic disturbances, and sector-bounded nonlinearities. By constructing new Lyapunov functionals, intensive stochastic analysis has been carried out to obtain the desired robust H_∞ filter parameters. Furthermore, in [98], by using similar analysis techniques, some parallel results have been extended to the robust H_∞ fuzzy output feedback control problem for a class of uncertain discrete-time fuzzy systems with both multiple probabilistic delays and multiple missing measurements.

Considering the case that the transfer function method cannot effectively deal with the nonlinear time-varying systems, a recursive matrix inequalities technique has been proposed in [16] in time domain to deal with the robust finite-horizon filtering problem for a class of uncertain nonlinear discrete time-varying stochastic systems with multiple missing measurements and error variance constraints. All the system parameters are time varying and the uncertainty enters into the state matrix. By developing a new filter design algorithm for finite-horizon case, sufficient conditions have been derived for a finite-horizon filter to satisfy the estimation error variance constraints, robustness, and the prescribed H_∞ performance requirement. A simulation example about the target tracking problem has demonstrated the effectiveness and practicality of the developed filter design scheme. This paper has addressed the open finite-horizon filtering problem satisfying multiple performance indices for a class of uncertain nonlinear discrete time-varying stochastic systems with limited communication. Moreover, by using similar analysis techniques, some parallel results have also been derived in [99] for the corresponding robust H_∞ finite-horizon output feedback control problem with both sensor and actuator saturations. The obtained results have practical meaning for the tracking problem of highly maneuvering targets.

In [57, 100], the filtering and fault detection problems have been investigated for discrete-time Markovian jump systems with randomly varying nonlinearities (RVNs) and sensor saturation. The issue of RVNs has been first addressed and the considered transition

probability matrix includes the case with polytopic uncertainties and the case with partially unknown transition probabilities, respectively. The H_∞ filtering problem has been first considered in [57], where the randomly occurring nonlinearities have been modeled by the Bernoulli distributed white sequences with known conditional probabilities. Sufficient conditions have been derived for the filtering augmented system under consideration to satisfy the H_∞ performance constraint. The corresponding robust H_∞ filters have been designed by solving sets of recursive linear matrix inequalities. Based on this, the corresponding fault detection filter design problem has been studied in [100]. Two energy norm indices have been utilized for the fault detection problem in order to account for, respectively, the restraint of disturbance and the sensitivity of faults. A locally optimized fault detection filter has been designed by developing a novel algorithm such that the effect from the exogenous disturbance on the residual is attenuated with respect to a minimized H_∞ norm, and the sensitivity of the residual to the fault is enhanced in terms of a maximized H_∞ norm.

By noticing that the aforementioned scheme cannot be applied to complex dynamic systems with transmission delay or state delay, in [41, 101], the fault detection problems have been dealt with for two classes of discrete-time nonlinear mixed stochastic time delay systems with limited communication. The mixed time delays involve both the multiple time-varying discrete delays and the infinite distributed delays. The fault detection problem has been first addressed in [41] for a class of discrete-time systems with randomly occurring nonlinearities and mixed stochastic time delays as well as measurement quantizations. Sufficient conditions have been established via intensive stochastic analysis for the existence of the desired fault detection filters, and then the explicit expression of the desired filter gains has been derived by means of the feasibility of certain matrix inequalities. Moreover, in [101], the developed scheme has been extended to the robust fault detection problem for a class of uncertain discrete-time T-S fuzzy systems with stochastic mixed time delays and successive packet dropouts. Two practical examples have been provided to show the usefulness and effectiveness of the proposed design methods.

Considering the case that the occurrence of incomplete information in sensor network is more complex and severer, the studies in [102–104] have investigated the distributed filtering problem for several classes of nonlinear stochastic systems over lossy sensor networks. The issues of average H_∞ performance constraints have been brought up in [102], and then the distributed H_∞ filtering problem has been investigated for system with repeated scalar nonlinearities and multiple probabilistic packet losses. Moreover, in [103], the distributed filtering problem has been further extended to the nonlinear time-varying systems with limited communication. The time-varying system (target plant) is subject to randomly vary nonlinearities caused by environmental circumstances. The lossy sensor network suffers from quantization errors and successive packet dropouts that are described in a unified framework. A new distributed finite-horizon filtering technique by means of a set of recursive linear matrix inequalities has been proposed to satisfy the prescribed average filtering performance constraint. In addition, the distributed H_∞ filtering problem has been investigated in [104] for a class of discrete-time Markovian jump nonlinear time-delay systems with deficient statistics of mode transitions. A novel model that describes the deficient statistics of modes transitions has been proposed to account for known, bounded uncertain, and unknown transition probabilities. The system measurements have been collected through a lossy sensor network subject to randomly occurring quantizations errors (ROQEs) and randomly occurring packet dropouts (ROPDs). Two sets of the Bernoulli distributed white sequences have been introduced to govern the phenomena of ROQEs and

ROPDs in the lossy sensor network. The system model (dynamical plant) includes the mode-dependent Lipschitz-like nonlinearities. The distributed filters have been designed to obtain sufficient conditions for ensuring stochastic stability as well as the prescribed average H_∞ performance constraint.

In [105], a new approach has been proposed in virtue of the solvability of certain coupled recursive Riccati difference equations (RDEs) to deal with the distributed H_∞ state estimation problem for a class of discrete time-varying nonlinear systems with both stochastic parameters and stochastic nonlinearities. By employing the completing squares method and the stochastic analysis technique, a necessary and sufficient condition has been established to ensure the dynamics of the estimation error to satisfy the H_∞ performance constraint. Furthermore, the estimator gains have been explicitly characterized by means of the solutions to two coupled backward recursive RDEs. Finally, an illustrative example has been provided that highlights the usefulness of the developed state estimation approach.

6. Conclusions and Future Work

In this paper, we have reviewed some recent advances on the analysis and synthesis problems for nonlinear stochastic systems with randomly occurring incomplete information. Most commonly used randomly occurring incomplete information models have been summarized. Based on this, various filtering, control, and fault detection problems have been discussed. In addition, the various distributed filtering technologies over sensor networks have been given. Latest results on analysis and synthesis problems for nonlinear stochastic systems with randomly occurring incomplete information have been surveyed. Based on the literature review, some related topics for the future research work are listed as follows.

(1) The nonlinearities considered in the existing results have been assumed to satisfy certain constraints for the purpose of simplifying the analysis, thereby bringing a great deal of conservatism. It would be a promising research topic to analyze and synthesize the general nonlinear systems with randomly occurring incomplete information.

(2) Another future research direction is to further investigate multiobjective H_2/H_∞ control and filtering problems for nonlinear systems with randomly occurring incomplete information.

(3) It would be interesting to investigate the problems of fault detection and fault tolerant control for time-varying systems with randomly occurring incomplete information over a finite time horizon.

(4) A trend for future research is to generalize the methods obtained in the existing results to the control, synchronization, and filtering problems for nonlinear stochastic complex networks systems with randomly occurring incomplete information.

(5) A practical engineering application of the existing theories and methodologies would be fault detection for petroleum well systems.

Acknowledgments

This work was supported in part by the National Natural Science Foundation of China under Grants 61273156, 61134009, 61273201, 61021002, and 61004067, the Engineering and Physical

Sciences Research Council (EPSRC) of the UK under Grant GR/S27658/01, the Royal Society of the UK, the National Science Foundation of the USA under Grant No. HRD-1137732, and the Alexander von Humboldt Foundation of Germany.

References

[1] G. Chen, "Simple treatment for suboptimal Kalman filtering in case of measurement data missing," *IEEE Transactions on Aerospace and Electronic Systems*, vol. 26, no. 2, pp. 413–415, 1990.

[2] F. O. Hounkpevi and E. E. Yaz, "Robust minimum variance linear state estimators for multiple sensors with different failure rates," *Automatica*, vol. 43, no. 7, pp. 1274–1280, 2007.

[3] S. Nakamori, R. Caballero-Águila, A. Hermoso-Carazo, J. D. Jiménez-López, and J. Linares-Pérez, "Signal estimation with nonlinear uncertain observations using covariance information," *Journal of Statistical Computation and Simulation*, vol. 79, no. 1-2, pp. 55–66, 2009.

[4] B. Shen, Z. Wang, H. Shu, and G. Wei, "On nonlinear H_∞ filtering for discrete-time stochastic systems with missing measurements," *IEEE Transactions on Automatic Control*, vol. 53, no. 9, pp. 2170–2180, 2008.

[5] B. Shen, Z. Wang, H. Shu, and G. Wei, "H_∞ filtering for uncertain time-varying systems with multiple randomly occurred nonlinearities and successive packet dropouts," *International Journal of Robust and Nonlinear Control*, vol. 21, no. 14, pp. 1693–1709, 2011.

[6] S. Sun, L. Xie, W. Xiao, and Y. C. Soh, "Optimal linear estimation for systems with multiple packet dropouts," *Automatica*, vol. 44, no. 5, pp. 1333–1342, 2008.

[7] Z. Wang, B. Shen, H. Shu, and G. Wei, "Quantized H_∞ control for nonlinear stochastic time-delay systems with missing measurements," *IEEE Transactions on Automatic Control*, vol. 57, no. 6, pp. 1431–1444, 2012.

[8] Z. Wang, B. Shen, and X. Liu, "H_∞ filtering with randomly occurring sensor saturations and missing measurements," *Automatica*, vol. 48, no. 3, pp. 556–562, 2012.

[9] Z. Wang, F. Yang, D. W. C. Ho, and X. Liu, "Robust H_∞ filtering for stochastic time-delay systems with missing measurements," *IEEE Transactions on Signal Processing*, vol. 54, no. 7, pp. 2579–2587, 2006.

[10] Z. Wang, F. Yang, D. W. C. Ho, and X. Liu, "Robust H_∞ control for networked systems with random packet losses," *IEEE Transactions on Systems, Man, and Cybernetics B*, vol. 37, no. 4, pp. 916–924, 2007.

[11] G. Wei, Z. Wang, and H. Shu, "Robust filtering with stochastic nonlinearities and multiple missing measurements," *Automatica*, vol. 45, no. 3, pp. 836–841, 2009.

[12] H. Gao, Y. Zhao, J. Lam, and K. Chen, "H_∞ fuzzy filtering of nonlinear systems with intermittent measurements," *IEEE Transactions on Fuzzy Systems*, vol. 17, no. 2, pp. 291–300, 2009.

[13] Z. Wang, D. W. C. Ho, Y. Liu, and X. Liu, "Robust H_∞ control for a class of nonlinear discrete time-delay stochastic systems with missing measurements," *Automatica*, vol. 45, no. 3, pp. 684–691, 2009.

[14] Z. Shu, J. Lam, and J. Xiong, "Non-fragile exponential stability assignment of discrete-time linear systems with missing data in actuators," *IEEE Transactions on Automatic Control*, vol. 54, no. 3, pp. 625–630, 2009.

[15] M. Sahebsara, T. Chen, and S. L. Shah, "Optimal H_2 filtering with random sensor delay, multiple packet dropout and uncertain observations," *International Journal of Control*, vol. 80, no. 2, pp. 292–301, 2007.

[16] H. Dong, Z. Wang, D. W. C. Ho, and H. Gao, "Variance-constrained H_∞ filtering for a class of nonlinear time-varying systems with multiple missing measurements: the finite-horizon case," *IEEE Transactions on Signal Processing*, vol. 58, no. 5, pp. 2534–2543, 2010.

[17] W. Zhang, M. S. Branicky, and S. M. Phillips, "Stability of networked control systems," *IEEE Control Systems Magazine*, vol. 21, no. 1, pp. 84–99, 2001.

[18] J. Nilsson, *Real-time control systems with delays [Ph.D. dissertation]*, Lund Institute of Technology, Lund, Sweden, 1998.

[19] F. Gokas, *Distributed control of systems over communication networks [Ph.D. dissertation]*, University of Pennsylvania, Philadelphia, Pa, USA, 2000.

[20] H. Gao and X. Li, "H_∞ filtering for discrete-time state-delayed systems with finite frequency specifications," *IEEE Transactions on Automatic Control*, vol. 56, no. 12, pp. 2935–2941, 2011.

[21] H. Gao, T. Chen, and J. Lam, "A new delay system approach to network-based control," *Automatica*, vol. 44, no. 1, pp. 39–52, 2008.

[22] Z. Wang and D. W. C. Ho, "Filtering on nonlinear time-delay stochastic systems," *Automatica*, vol. 39, no. 1, pp. 101–108, 2006.

[23] B. Chen and X. Liu, "Delay-dependent robust H_∞ control for T-S fuzzy systems with time delay," *IEEE Transactions on Fuzzy Systems*, vol. 13, no. 4, pp. 544–556, 2005.

[24] M. Liu, D. W. C. Ho, and Y. Niu, "Stabilization of Markovian jump linear system over networks with random communication delay," *Automatica*, vol. 45, no. 2, pp. 416–421, 2009.

[25] H. Zhang, M. Li, J. Yang, and D. Yang, "Fuzzy model-based robust networked control for a class of nonlinear systems," *IEEE Transactions on Systems, Man, and Cybernetics A*, vol. 39, no. 2, pp. 437–447, 2009.

[26] F. Yang, Z. Wang, Y. S. Hung, and M. Gani, "H_∞ control for networked systems with random communication delays," *IEEE Transactions on Automatic Control*, vol. 51, no. 3, pp. 511–518, 2006.

[27] D. Yue, E. Tian, Y. Zhang, and C. Peng, "Delay-distribution-dependent stability and stabilization of T-S fuzzy systems with probabilistic interval delay," *IEEE Transactions on Systems, Man, and Cybernetics B*, vol. 39, no. 2, pp. 503–516, 2009.

[28] D. V. Dimarogonas and K. H. Johansson, "Quantized agreement under time-varying communication topology," in *American Control Conference (ACC '08)*, pp. 4376–4381, Seattle, Wash, USA, June 2008.

[29] H. Gao and T. Chen, "A new approach to quantized feedback control systems," *Automatica*, vol. 44, no. 2, pp. 534–542, 2008.

[30] Z. Gao and S. X. Ding, "Actuator fault robust estimation and fault-tolerant control for a class of nonlinear descriptor systems," *Automatica*, vol. 43, no. 5, pp. 912–920, 2007.

[31] H. R. Karimi, "Robust H_∞ filter design for uncertain linear systems over network with network-induced delays and output quantization," *Modeling, Identification and Control*, vol. 30, no. 1, pp. 27–37, 2009.

[32] T. Nakamura, "Development of self-learning vision-based mobile robots for acquiring soccer robots behaviors," in *Proceedings of the IEEE International Conference on Robotics and Automation. Part 1 (of 4)*, pp. 2592–2598, Leuven, Belgium, May 1998.

[33] H. Sun, N. Hovakimyan, and T. Basar, "L_1 adaptive controller for quantized systems," in *Proceedings of the American Control Conference*, pp. 582–587, San Francisco, Calif, USA, 2011.

[34] C. Y. Tsai and K. T. Song, "Visual tracking control of a wheeled mobile robot with system model and velocity quantization robustness," *IEEE Transactions on Control Systems Technology*, vol. 17, no. 3, pp. 520–527, 2009.

[35] N. Xiao, L. Xie, and M. Fu, "Stabilization of Markov jump linear systems using quantized state feedback," *Automatica*, vol. 46, no. 10, pp. 1696–1702, 2010.

[36] R. W. Brockett and D. Liberzon, "Quantized feedback stabilization of linear systems," *IEEE Transactions on Automatic Control*, vol. 45, no. 7, pp. 1279–1289, 2000.

[37] D. Liberzon, "On stabilization of linear systems with limited information," *IEEE Transactions on Automatic Control*, vol. 48, no. 2, pp. 304–307, 2003.

[38] H. Ishii and B. A. Francis, "Stabilizing a linear system by switching control with dwell time," *IEEE Transactions on Automatic Control*, vol. 47, no. 12, pp. 1962–1973, 2002.

[39] N. Elia and S. K. Mitter, "Stabilization of linear systems with limited information," *IEEE Transactions on Automatic Control*, vol. 46, no. 9, pp. 1384–1400, 2001.

[40] M. Fu and L. Xie, "The sector bound approach to quantized feedback control," *IEEE Transactions on Automatic Control*, vol. 50, no. 11, pp. 1698–1711, 2005.

[41] H. Dong, Z. Wang, and H. Gao, "On design of quantized fault detection filters with randomly occurring nonlinearities and mixed time-delays," *Signal Processing*, vol. 92, no. 4, pp. 1117–1125, 2012.

[42] M. Fu and C. E. de Souza, "State estimation for linear discrete-time systems using quantized measurements," *Automatica*, vol. 45, no. 12, pp. 2937–2945, 2009.

[43] H. Fang, Z. Lin, and T. Hu, "Analysis of linear systems in the presence of actuator saturation and L_2-disturbances," *Automatica*, vol. 40, no. 7, pp. 1229–1238, 2004.

[44] T. Hu and Z. Lin, *Control Systems With Actuator Saturation: Analysis and Design*, Birkäuser, Boston, Mass, USA, 2001.

[45] L. Lv and Z. Lin, "Analysis and design of singular linear systems under actuator saturation and L_2/L_∞ disturbances," *Systems and Control Letters*, vol. 57, no. 11, pp. 904–912, 2008.

[46] L. Wu and D. W. C. Ho, "Fuzzy filter design for Itô stochastic systems with application to sensor fault detection," *IEEE Transactions on Fuzzy Systems*, vol. 17, no. 1, pp. 233–242, 2009.

[47] Y.-Y. Cao, Z. Lin, and B. M. Chen, "An output feedback H_∞ controller design for linear systems subject to sensor nonlinearities," *IEEE Transactions on Circuits and Systems I*, vol. 50, no. 7, pp. 914–921, 2003.

[48] Y. Xiao, Y.-Y. Cao, and Z. Lin, "Robust filtering for discrete-time systems with saturation and its application to transmultiplexers," *IEEE Transactions on Signal Processing*, vol. 52, no. 5, pp. 1266–1277, 2004.

[49] Z. Zuo, J. Wang, and L. Huang, "Output feedback H_∞ controller design for linear discrete-time systems with sensor nonlinearities," *IEE Proceedings*, vol. 152, no. 1, pp. 19–26, 2005.

[50] G. Garcia, S. Tarbouriech, and J. M. G. da Silva Jr., "Dynamic output controller design for linear systems with actuator and sensor saturation," in *Proceedings of the American Control Conference (ACC '07)*, pp. 5834–5839, July 2007.

[51] J. Liang, Z. Wang, and X. Liu, "Distributed state estimation for discrete-time sensor networks with randomly varying nonlinearities and missing measurements," *IEEE Transactions on Neural Networks*, vol. 22, no. 3, pp. 486–496, 2011.

[52] Z. Wang, Y. Wang, and Y. Liu, "Global synchronization for discrete-time stochastic complex networks with randomly occurred nonlinearities and mixed time delays," *IEEE Transactions on Neural Networks*, vol. 21, no. 1, pp. 11–25, 2010.

[53] M. Liu, *Network-based stability analysis and synthesis for stochastic system with Markovian switching [Ph.D. dissertation]*, City University of Hong Kong, Hong Kong, 2009.

[54] Z. Fei, H. Gao, and P. Shi, "New results on stabilization of Markovian jump systems with time delay," *Automatica*, vol. 45, no. 10, pp. 2300–2306, 2009.

[55] H. Gao, Z. Fei, J. Lam, and B. Du, "Further results on exponential estimates of Markovian jump systems with mode-dependent time-varying delays," *IEEE Transactions on Automatic Control*, vol. 56, no. 1, pp. 223–229, 2011.

[56] J. Xiong, J. Lam, H. Gao, and D. W. C. Ho, "On robust stabilization of Markovian jump systems with uncertain switching probabilities," *Automatica*, vol. 41, no. 5, pp. 897–903, 2005.

[57] H. Dong, Z. Wang, D. W. C. Ho, and H. Gao, "Robust H_∞ filtering for Markovian jump systems with randomly occurring nonlinearities and sensor saturation: the finite-horizon case," *IEEE Transactions on Signal Processing*, vol. 59, no. 7, pp. 3048–3057, 2011.

[58] H. Liu, F. Sun, K. He, and Z. Sun, "Design of reduced-order H_∞ filter for Markovian jumping systems with time delay," *IEEE Transactions on Circuits and Systems II*, vol. 51, no. 11, pp. 1837–1837, 2004.

[59] L. Ma, F. Da, and K.-J. Zhang, "Exponential H_∞ filter design for discrete time-delay stochastic systems with Markovian jump parameters and missing measurements," *IEEE Transactions on Circuits and Systems I*, vol. 58, no. 5, pp. 994–1007, 2011.

[60] M. H. Terra, J. Y. Ishihara, and G. Jesus, "Information filtering and array algorithms for discrete-time Markovian jump linear systems," *IEEE Transactions on Automatic Control*, vol. 54, no. 1, pp. 158–162, 2009.

[61] L. Wu, P. Shi, H. Gao, and C. Wang, "H_∞ filtering for 2D Markovian jump systems," *Automatica*, vol. 44, no. 7, pp. 1849–1858, 2008.

[62] J. Xiong and J. Lam, "Fixed-order robust H_∞ filter design for Markovian jump systems with uncertain switching probabilities," *IEEE Transactions on Signal Processing*, vol. 54, no. 4, pp. 1421–1430, 2006.

[63] L. Zhang, "H_∞ estimation for discrete-time piecewise homogeneous Markov jump linear systems," *Automatica*, vol. 45, no. 11, pp. 2570–2576, 2009.

[64] X. Zhang and Y. Zheng, "Nonlinear H_∞ filtering for interconnected Markovian jump systems," *Journal of Systems Engineering and Electronics*, vol. 17, no. 1, pp. 138–146, 2006.

[65] L. Wu, P. Shi, and H. Gao, "State estimation and sliding-mode control of Markovian jump singular systems," *IEEE Transactions on Automatic Control*, vol. 55, no. 5, pp. 1213–1219, 2010.

[66] J. Zhang, Y. Xia, and E. K. Boukas, "New approach to H_∞ control for Markovian jump singular systems," *IET Control Theory and Applications*, vol. 4, no. 11, pp. 2273–2284, 2010.

[67] X. He, Z. Wang, and D. H. Zhou, "Robust fault detection for networked systems with communication delay and data missing," *Automatica*, vol. 45, no. 11, pp. 2634–2639, 2009.

[68] M. Zhong, H. Ye, P. Shi, and G. Wang, "Fault detection for Markovian jump systems," *Proceedings of the Institution of Electrical Engineers*, vol. 152, no. 4, pp. 397–402, 2005.

[69] L. Zhang, E.-K. Boukas, and J. Lam, "Analysis and synthesis of Markov jump linear systems with time-varying delays and partially known transition probabilities," *IEEE Transactions on Automatic Control*, vol. 53, no. 10, pp. 2458–2464, 2008.

[70] Y. Zhao, L. Zhang, S. Shen, and H. Gao, "Robust stability criterion for discrete-time uncertain markovian jumping neural networks with defective statistics of modes transitions," *IEEE Transactions on Neural Networks*, vol. 22, no. 1, pp. 164–170, 2011.

[71] S. X. Ding, T. Jeinsch, P. M. Frank, and E. L. Ding, "A unified approach to the optimization of fault detection systems," *International Journal of Adaptive Control and Signal Processing*, vol. 14, no. 7, pp. 725–745, 2000.

[72] Y. Zheng, H. Fang, and H. O. Wang, "Takagi-Sugeno fuzzy-model-based fault detection for networked control systems with Markov delays," *IEEE Transactions on Systems, Man, and Cybernetics B*, vol. 36, no. 4, pp. 924–929, 2006.

[73] M. Zhong, S. X. Ding, and E. L. Ding, "Optimal fault detection for linear discrete time-varying systems," *Automatica*, vol. 46, no. 8, pp. 1395–1400, 2010.

[74] Z. Wang, Y. Liu, and X. Liu, "H_∞ filtering for uncertain stochastic time-delay systems with sector-bounded nonlinearities," *Automatica*, vol. 44, no. 5, pp. 1268–1277, 2008.

[75] G. Wei, Z. Wang, H. Shu, and J. Fang, "A delay-dependent approach to H_∞ filtering for stochastic delayed jumping systems with sensor non-linearities," *International Journal of Control*, vol. 80, no. 6, pp. 885–897, 2007.

[76] X. Jiang and Q. L. Han, "On designing fuzzy controllers for a class of nonlinear networked control systems," *IEEE Transactions on Fuzzy Systems*, vol. 16, no. 4, pp. 1050–1058, 2008.

[77] Z. Wang, D. W. C. Ho, and X. Liu, "A note on the robust stability of uncertain stochastic fuzzy systems with time-delays," *IEEE Transactions on Systems, Man, and Cybernetics A*, vol. 34, no. 4, pp. 570–576, 2004.

[78] W. Zhang, B.-S. Chen, and C.-S. Tseng, "Robust H_∞ filtering for nonlinear stochastic systems," *IEEE Transactions on Signal Processing*, vol. 53, no. 2, pp. 589–598, 2005.

[79] F. S. Cattivelli and A. H. Sayed, "Diffusion strategies for distributed Kalman filtering and smoothing," *IEEE Transactions on Automatic Control*, vol. 55, no. 9, pp. 1520–1520, 2010.

[80] L. Chai, B. Hu, and P. Jiang, "Distributed state estimation based on quantized observations in a bandwidth constrained sensor network," in *Proceedings of the 7th World Congress on Intelligent Control and Automation (WCICA '08)*, pp. 2411–2415, June 2008.

[81] M. Farina, G. Ferrari-Trecate, and R. Scattolini, "Distributed moving horizon estimation for sensor networks," in *Proceedings of the 1st IFAC Workshop on Estimation and Control of Networked Systems (NecSys '09)*, pp. 126–131, Venice, Italy, September 2009.

[82] M. Kamgarpour and C. Tomlin, "Convergence properties of a decentralized Kalman filter," in *Proceedings of the 47th IEEE Conference on Decision and Control (CDC '08)*, pp. 3205–3210, Cancun, Mexico, December 2008.

[83] R. Olfati-Saber, "Kalman-consensus filter: optimality, stability, and performance," in *Proceedings of the 48th IEEE Conference on Decision and Control held Jointly with 28th Chinese Control Conference (CDC/CCC '09)*, pp. 7036–7042, New Orleans, La, USA, December 2009.

[84] R. Olfati-Saber, "Flocking for multi-agent dynamic systems: algorithms and theory," *IEEE Transactions on Automatic Control*, vol. 51, no. 3, pp. 401–420, 2006.

[85] B. Shen, Z. Wang, and X. Liu, "A stochastic sampled-data approach to distributed H_∞ filtering in sensor networks," *IEEE Transactions on Circuits and Systems I*, vol. 58, no. 9, pp. 2237–2246, 2011.

[86] B. Shen, Z. Wang, and Y. S. Hung, "Distributed consensus H_∞ filtering in sensor networks with multiple missing measurements: the finite-horizon case," *Automatica*, vol. 46, no. 10, pp. 1682–1688, 2010.

[87] B. Shen, Z. Wang, Y. S. Hung, and G. Chesi, "Distributed H_∞ filtering for polynomial nonlinear stochastic systems in sensor networks," *IEEE Transactions on Industrial Electronics*, vol. 58, no. 5, pp. 1971–1979, 2011.

[88] W. Yu, G. Chen, Z. Wang, and W. Yang, "Distributed consensus filtering in sensor networks," *IEEE Transactions on Systems, Man, and Cybernetics B*, vol. 39, no. 6, pp. 1568–1577, 2009.

[89] H. Zhang, G. Feng, G. Duan, and X. Lu, "H_∞ filtering for multiple-time-delay measurements," *IEEE Transactions on Signal Processing*, vol. 54, no. 5, pp. 1681–1688, 2006.

[90] F. S. Cattivelli and A. H. Sayed, "Diffusion strategies for distributed Kalman filtering: formulation and performance analysis," in *Proceedings of the Cognitive Information Processing*, pp. 36–41, Santorini, Greece, 2008.

[91] R. Carli, A. Chiuso, L. Schenato, and S. Zampieri, "Distributed Kalman filtering based on consensus strategies," *IEEE Journal on Selected Areas in Communications*, vol. 26, no. 4, pp. 622–633, 2008.

[92] R. Olfati-Saber, "Distributed Kalman filtering for sensor networks," in *Proceedings of the 46th IEEE Conference on Decision and Control (CDC '07)*, pp. 5492–5498, New Orleans, La, USA, December 2007.

[93] R. Olfati-Saber and J. S. Shamma, "Consensus filters for sensor networks and distributed sensor fusion," in *Proceedings of the 44th IEEE Conference on Decision and Control, and the European Control Conference (CDC-ECC '05)*, pp. 6698–6703, Seville, Spain, December 2005.

[94] V. A. Ugrinovskii, "Distributed robust filtering with H_∞ consensus of estimates," in *Proceedings of the American Control Conference (ACC '10)*, pp. 1374–1379, July 2010.

[95] H. Dong, Z. Wang, and H. Gao, "H_∞ filtering for systems with repeated scalar nonlinearities under unreliable communication links," *Signal Processing*, vol. 89, no. 8, pp. 1567–1575, 2009.

[96] H. Dong, Z. Wang, and H. Gao, "Observer-based H_∞ control for systems with repeated scalar nonlinearities and multiple packet losses," *International Journal of Robust and Nonlinear Control*, vol. 20, no. 12, pp. 1363–1378, 2010.

[97] H. Dong, Z. Wang, and H. Gao, "Robust H_∞ filtering for a class of nonlinear networked systems with multiple stochastic communication delays and packet dropouts," *IEEE Transactions on Signal Processing*, vol. 58, no. 4, pp. 1957–1966, 2010.

[98] H. Dong, Z. Wang, D. W. C. Ho, and H. Gao, "Robust H_∞ fuzzy output-feedback control with multiple probabilistic delays and multiple missing measurements," *IEEE Transactions on Fuzzy Systems*, vol. 18, no. 4, pp. 712–725, 2010.

[99] Z. Wang, D. W. C. Ho, H. Dong, and H. Gao, "Robust H_∞ finite-horizon control for a class of stochastic nonlinear time-varying systems subject to sensor and actuator saturations," *IEEE Transactions on Automatic Control*, vol. 55, no. 7, pp. 1716–1722, 2010.

[100] H. Dong, Z. Wang, and H. Gao, "Fault detection for Markovian jump systems with sensor saturations and randomly varying nonlinearities," *IEEE Transactions on Circuits and Systems I*, vol. 59, no. 10, pp. 2354–2362, 2012.

[101] H. Dong, Z. Wang, J. Lam, and H. Gao, "Fuzzy-model-based robust fault detection with stochastic mixed time-delays and successive packet dropouts," *IEEE Transactions on Systems, Man, and Cybernetics B*, vol. 42, no. 2, pp. 365–376, 2012.

[102] H. Dong, J. Lam, and H. Gao, "Distributed H_∞ filtering for repeated scalar nonlinear systems with random packet losses in sensor networks," *International Journal of Systems Science*, vol. 42, no. 9, pp. 1507–1519, 2011.

[103] H. Dong, Z. Wang, and H. Gao, "Distributed filtering for a class of time-varying systems over sensor networks with quantization errors and successive packet dropouts," *IEEE Transactions on Signal Processing*, vol. 60, no. 6, pp. 3164–3173, 2012.

[104] H. Dong, Z. Wang, and H. Gao, "Distributed H_∞ filtering for a class of Markovian jump nonlinear time-delay systems over lossy sensor networks ," *IEEE Transactions on Industrial Electronics*. In press.

[105] D. Ding, Z. Wang, H. Dong, and H. Shu, "State estimation with stochastic parameters and nonlinearities through sensor networks: the finite-horizon case," *Automatica*, vol. 48, no. 8, pp. 1575–1585, 2012.

Hindawi Publishing Corporation
Mathematical Problems in Engineering
Volume 2012, Article ID 948936, 16 pages
doi:10.1155/2012/948936

Research Article

MIMO LPV State-Space Identification of Open-Flow Irrigation Canal Systems

Yolanda Bolea,[1] Nicolas Chefdor,[2] and Antoni Grau[1]

[1] *Automatic Control Department, Technical University of Catalonia, 08028 Barcelona, Spain*
[2] *Embedded Systems and Automatic Group, Engineering School of ESEO, 49009 Angers, France*

Correspondence should be addressed to Antoni Grau, antoni.grau@upc.edu

Received 22 June 2012; Accepted 2 October 2012

Academic Editor: Jun Hu

Canal systems are complex nonlinear, distributed parameter systems with changing parameters according to the operating point. In this paper, a linear parameter-varying (LPV) state-space canal control model is obtained by identification in a local way using a multimodel approach. This LPV identification procedure is based on subspace methods for different operating points of an irrigation canal covering the full operation range. Different subspace algorithms have been used and compared. The model that best represents the canal behavior in a precise manner has been chosen, and it has been validated by error functions and analysis correlation of residuals in a laboratory multireach pilot canal providing satisfactory results.

1. Introduction

Water is one of the most used resources by industrial and agricultural sectors, and obviously by population. One fundamental use of water is the irrigation activity, and one the main challenges in this area is to prevent water losses and to permit an efficient use of this scarce and vital resource. These aspects have led to the usage of automatic control systems and the implementation of different advanced control algorithms for the regulation of open-flow irrigation canals. Hence, those control techniques will allow fulfilling the desired performance and the ecological flow in irrigation as well as saving water at the same time. To design an effective controller, a good control model is needed. Therefore, advanced process modeling techniques are required to make an accurate control model.

Modeling and control of nonlinear complex systems is a challenging task. Nonlinear effects can no longer be neglected to meet the specifications imposed on today's complex control systems. Unfortunately, the higher the complexity, the lower our ability to deal with it

and to understand it. Open-flow canals are complex systems, that is, they are large distributed parameter systems that have the following main characteristics: nonlinear behavior and dependence of the parameters with the operating point and coupling among pools [1]. This type of systems can be fully described by Saint-Venant's equations [2]. This representation is the most used model to describe the physical dynamics of a real irrigation canal. However, this complex model is based on a nonlinear hyperbolic partial differential equations system that has analytical solution only in very special cases, requiring the use of numerical methods to solve it properly [3]. This complex representation of the system is suitable for simulation models, but it is not suitable to design controllers that fulfill the control design needs. Then, linearization and simplification of Saint-Venant's equations are currently studied by the irrigation researchers' community of control [4] to develop simpler control models.

Distributed parameter systems with a very large number of states, that is, systems with coupling, have been approximated by decoupled low-order linear time invariant (LTI) models in order to use classical linear control design tools, as a usual practice in control engineering. In fact, control researchers' community has usually used linear control techniques (such as fuzzy control [5], robust control [6], etc.), and even nonlinear control approaches (such as, sliding control [7–9], etc.) for this kind of systems. LTI control models widely used are Hayami model [10], Muskingum model [3], IDZ model [4, 11], or black-box models identified using parameter estimation by classical identification methods [1, 12, 13]. However, these systems are not completely amenable using conventional linear modeling approaches due to the lack of precise, formal knowledge about the system; strongly nonlinear behavior; high degree of uncertainty; time varying characteristics; dynamic parameters changing over the operating point and coupling between pools. Then, simplified control model structures are needed preserving their information. Taking into account these previous properties, a linear parameter varying (LPV) model is required, which consists in a model that regards both the parameter and delay variations with respect to the operating points. In this way, the system information is preserved while it would be lost with a linear control model. These LPV control models permit the design and computation of LPV controllers that rigorously guarantee the system stability and performance [14] for smooth variations of system parameters as well as abrupt ones [15]; this is the case of irrigation canals. The preferred representation scheme for complex plants (multivariable systems involving large system orders) is a state-space model. Then, subspace-based system identification methods are a branch that has been recently developed in system identification attracting much attention thanks to their computational simplicity and effectiveness in identifying dynamic state-space linear multivariable systems. These algorithms are numerically robust and do not involve nonlinear optimization techniques, being fast and accurate.

Due to applications of large dimensions commonly found in industrial processes, subspace identification methods are very promising in this field. In the basis of the aspects explained above, in our case (a multireach canal system) a state-space model representation is suitable instead of a transfer function system description. For this reason, an LPV state-space control model has been developed through LPV identification techniques.

Besides, since system canals are nonlinear, a common engineering approach to deal with this complexity is the divide-and-conquer strategy: decompose the complex problem into several subproblems easier to solve. According to this previous strategy, a method to model complex nonlinear systems has arisen. It is based on partitioning the whole operating range of the nonlinear system into multiple, smaller operating regimes and modeling the system for each and every of these regimes. The task of finding a complete global model for the system is thus replaced by determining linear local models and subsequently combining

these local models into a global description for the system obtaining the LPV model (local LPV identification). This multiple model approach is often referred to as operating regime decomposition [16] or multimodel identification. Interactions between the relevant system phenomena are less complex locally than globally. From the divide-and-conquer point of view, it is desirable to choose the local models such that they are less complex than the global nonlinear model. It is expected that the simpler the local models are, the more models and thus the more operating regimes are needed to describe the global system accurately enough. A trade-off has to be made, because too simple local models lead to an explosion of the number of operating regimes needed. Another manner to identify the nonlinear systems is by the use of specific identification methods in a global way in one-shot through optimization [17] (global LPV identification). Although it is possible to use nonlinear local models (see, e.g., [18]) a common choice is to use local linear models. The main reasons for this choice are a solid theory for linear systems has been developed over the years, linear models are easy to understand, and they are widely used by engineers.

Specifically, the main contribution of the paper is the design of a low-order LPV state-space multivariable control model describing the water flow dynamics in a multireach irrigation canal. The model is estimated over the full operation point range using local LPV identification. Several subspace identification methods are applied and their performances are compared in order to select the subspace algorithm that yields the best control model. This model will be suitable to design LPV controllers that will warranty the stability and the desired performance around all operating points of the system with rigorous formality [14, 15].

The structure of this paper is as follows: in the next section, the main issues related to LPV identification and subspace identification methods used in this study are presented. Section 3 briefly presents the two reach irrigation canal used in this research. Section 4 discusses the important steps (generation and pretreatment of the data set, order estimation, performance quality criteria, and global model obtained by interpolation) in developing a suitable LPV subspace model for the system and compares the performance of the used subspace identification algorithms (N4SID, MOESP, and CVA) carrying out the model validation. Finally, Section 5 provides conclusions.

2. LPV Subspace Identification Methods

Linear time-invariant (LTI) models are not suitable to control systems such as open-flow canals with coupled pools and distributed parameters with nonlinear behaviour that depend on the operating points. However, by an LPV model (with varying parameters depending on the operating points), to preserve the aforementioned information of the system (nonlinearity, coupling, etc.) is also possible, obtaining a more accurate and faithful behaviour with the reality. As it has been emphasized in Section 1, there are two procedures to carry out LPV identification: (i) multimodel identification (local LPV identification) and (ii) one-shot LPV identification (global LPV identification). The former approach consists in a two-step procedure where (1) LTI models at several different equilibrium (operating condition) are identified by classical methods [13, 19]; (2) a global multi-model is obtained by interpolation among the local LTI models, and different interpolation techniques can be used such as membership fuzzy functions [20], polynomial interpolation [21], among others. The latter approach consists in carrying out a one-shot identification in a global way as proposed in [17]. The local approach has the important practical advantage that many engineers are well experienced in LTI identification experiments and that the local LTI models can be

estimated using a wide variety of well-established and widely spread LTI identification algorithms. To properly interpolate these local models, all local LPV identification techniques require that the local models are represented in a consistent state-space form.

The discrete-time subspace identification methods refer to a kind of algorithms which allow identifying a robust and reliable state-space model of MIMO linear systems estimating state sequences directly from the input-output measurements. Based on orthogonal or oblique projected subspaces generated by the rows or columns of Hankel matrices of the input-output data, the process is followed by a singular value decomposition so as to determine the order of the model and the observability matrices. Finally, the state-space model is obtained through the solution of a least squares problem. Subspace-based methods for state-space modeling have their origin in state-space realization, as developed by [22]. The term "subspace identification method" was introduced in the early 90s. The subspace identification can use many different versions of subspace methods such as Canonical Variate Analysis (CVA), Multivariable Output-Error State-Space model identification (MOESP), State-Space System Identification (N4SID), Canonical Correlation Analysis (CCA), and Deterministic and Stochastic Subspace System Identification and Realization (DSR) [10]. These algorithms attract much attention because they present many advantages: their computational simplicity and effectiveness to determinate dynamic linear multivariable systems. Nevertheless, a drawback which can be noticed is that these algorithms require a large amount of data to build accurate models. So the experiments to collect data can be large and time consuming. For this reason in control problems usually an off-line identification is used.

LPV models obtained using subspace identification methods are mathematically described by the following form:

$$\begin{aligned} x_{k+1} &= A(\theta_k)x_k + B(\theta_k)u_k, \\ y_k &= C(\theta_k)x_k + D(\theta_k)u_k, \end{aligned} \tag{2.1}$$

where the vectors $u_k \in R^m$ and $y_k \in R^l$ are the observations at the discrete time k of m inputs and l outputs of the process, respectively. The vector $x_k \in R^n$ represents the state vector of the process at discrete time instant k and contains the numerical values of n states, and θ_k is the parameter vector.

LPV system can be viewed as a nonlinear system that is linearized along a time-varying trajectory determined by the time-varying parameter vector p_k. Hence, the time-varying parameter vector of an LPV system corresponds to the operating point of the nonlinear system. In the LPV framework, it is assumed that this parameter is measurable for control. In many industrial applications, such as process control, the operating point can indeed be determined from measurements, making the LPV approach viable. Control design for LPV systems is an active research area. Within the LPV framework, systematic techniques for designing gain-scheduled controllers can be developed. Such techniques allow tighter performance bounds and can deal with fast variations of the operating point. Furthermore, control design for LPV systems has a close connection with modern robust control techniques based on linear fractional transformations [23]. The important role of LPV systems in control system design motivates the development of identification techniques that can determine such systems from measured data, the LPV identification [23, 24].

Local linear modeling is one of the many possibilities to approximate a nonlinear dynamic system. It is based on partitioning the full operating range of the nonlinear system

into multiple, smaller operating regimes and modeling the system for each of these regimes by a linear model. By making a weighted combination of these linear models, it is expected to describe the complete nonlinear behaviour accurate enough. The local lineal model structure is

$$x_{k+1} = \sum_{i=1}^{s} p_i(\theta_k)(A_i x_k + B_i u_k),$$
$$y_k = \sum_{i=1}^{s} p_i(\theta_k)(C_i x_k + D_i u_k), \tag{2.2}$$

where s is the number of local models and $p_i(\theta_k)$ and the other variables have the same meaning that in (2.1). The weighting vectors p_i are unknown functions of the scheduling vector θ_k. This scheduling vector corresponds to the operating point of the system. This system is closely related to the LPV system in (2.1). The weighting functions can be interpreted as model validity functions: they indicate which model or combination of models is active for a certain operating regime of the system. A weighted combination of local linear models can be used to approximate a smooth nonlinear system up to an arbitrary accuracy by increasing the number of local models. As it is stated, the local linear state-space system is closely related to the LPV system: consider that time-varying parameters are known, while for the local linear model structure the weighting functions have to be determined from input and output data [24].

In this work, the plant is identified by several local LPV subspace identification methods (cited above) to estimate the space-state representation that describes the system dynamics suitably. The LPV identification method used for the experimental modeling of our pilot two-pool canal (presented in the next section) is a two-step procedure where (1) linear state-space models are identified at several different operating points by subspace identification methods over the full range of operation; (2) a global state-space multi-model is obtained at the end interpolating the local state-space models using polynomials [21]. In this paper, the following identification methods have been used: N4SID, the standard method (i.e., N4SID1 from now on) and the robust method (i.e., N4SID2 from now on), CVA algorithm, and MOESP procedure [10]. These methods are used to estimate the model in each operating point. The local identification method forces the local models to fit the system separately and locally. The steps of the identification procedure are explained in Section 4.

3. Description of the Process

An experimental canal prototype is used in this research. This canal consists in two tanks TT and TD with cross section A. The full structure of the canal prototype is presented in Figure 1 (up) and Figure 2. The two tanks are serially connected with pipes, and they are slightly tilted to allow the flow of the water. There is a reservoir at the bottom of the plant to supply water to the tanks. A first pump (with a flow of 3,800 liters/h), named u_1 in Figure 1 (up), permits to collect water from the reservoir to fill the upper tank TT. An ultrasound sensor attached to the metallic structure at the end of the first tank, named y_1, measures the water level. A second pump, named u_2, (with a flow of 1,300 liters/h) allows to drain the upper tank and to fill the lower tank TD.

A second ultrasound sensor positioned also at the end of the tank, named y_2, enables to measure the water level. Finally, a third pump, called u_3, gives the possibility to drain

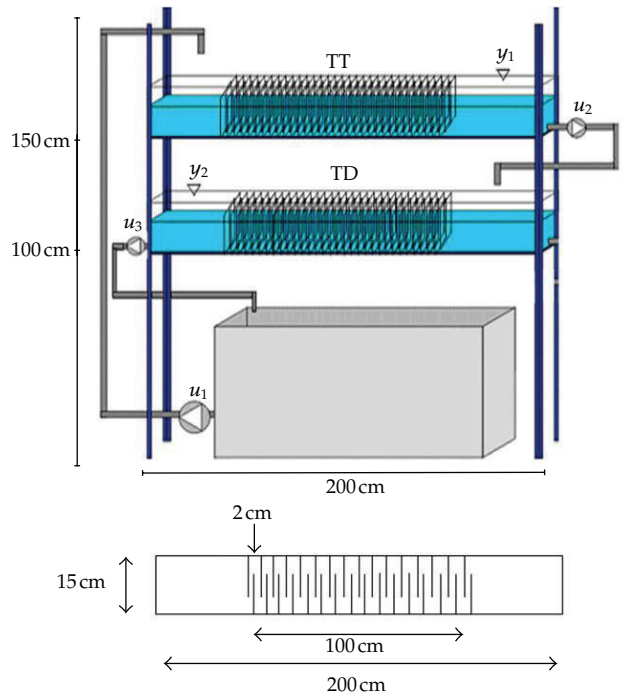

Figure 1: (Up) Full structure of the canal and (down) details of the zenital internal structure of the canal.

away the last tank to the reservoir. The sensors and the pumps are directly connected to an electronic board, which allows to power them and to exchange data between a Matlab program (executed on a PC shown in Figure 2) and the canal. The program uses the Real Time Windows Target (Matlab toolbox) to communicate with the electronic board and the canal. Finally, it is important to emphasize that the prototype canal constitutes a closed system. The water leaves from the bottom reservoir to the tank TT and arrives to the tank TD via the pump u_2. Then, the water returns to the reservoir via the pump u_3. That constitutes a coupled system where the first tank has a big influence on the second one.

There are many methacrylate plates along the two tanks TT and TD shown in Figure 1 (down). These plates are 2 centimeters apart creating a zigzag path in each tank. That provides a delay in the water to reach the other extremity of the tank where the sensor is located. This delay has to be taken into account for the identification. The delay changes depending on the water level in the canal. The more the water in the canal, the smaller the delay. This fact justifies the use of LPV identification to deal with this problem. Each sensor measures the canal level at the end of its path with a precision of 1 mm. The maximum allowed level is 15 cm to avoid the overflow.

4. Identification of an LPV Subspace Model for Two-Reach Pilot Canal

In this section, the different subspace estimation methods in an LPV local way (see Section 2) are applied to the multivariable pilot canal plant. The identification process is carried out following the steps: (1) design of the experiment, collection of input-output data in each operating point (taking into account a suitable selection of the excitation input of the system), and pretreatment of these data; due to the system delays, those delays are estimated and

Figure 2: Laboratory pilot canal.

removed from the identification data; (2) selection of the model order via different criteria, singular value decomposition (SVD), and Akaike information criterion (AIC); (3) estimation of the local space-state models for each operating point by the aforementioned subspace identification methods and their interpolation to obtain a global model by Nearest Neighbour interpolation [10, 25]; (4) validation of the model in all the operation range by error functions (MRSE and MVAF) and correlation analysis of residuals. The identification results of each estimation algorithm (N4SID1, N4SID2, CVA, and MOESP) are compared and studied. When canal models are identified, two problems have to be considered: the problem of large and variable delays and the nonlinearity of the dynamics and its variability with the operating points [26, 27]. These problems are separately treated. The parameters models are estimated using the state-space algorithms in each operating point without the delay effect, previously calibrated by correlation method [13].

4.1. Generation and Pretreatment of the Data Set

It is not an easy task to select either the input or the output variables of a process. In this experiment, two inputs (u_1, u_2) and two outputs (y_1, y_2) are considered. The input u_1 corresponds to the voltage of the first canal pump; u_2 corresponds to the voltage of the second pump; the output y_1 is the downstream level of pool 1, and y_2 the downstream level of the pool 2. Pseudorandom Binary Sequences (PBRS) are widely used in the identification process [13]. These signals are persistent input signals that contain a large number of frequencies representative of the dynamics of the plant. In order to choose the number of operation points (OPs) of the canal plant in a rigorous manner, the optimized OP multipoint technique is used [28]. In this paper, four equidistant operating points have been used. The local model identification will be performed in every operating point because the system is not linear.

In our experiment, a pulse generator creates a train of PBRS as pump input voltage signals which adequately excite the system at different operating points. For the first pump, the PBRS signal, u_1, changes the pump opening at intervals of 800 s and for a period of 10 s. The identification procedure was carried out off-line using 3200 samples of the data set. In Figure 3, the train of PBRS signals of each pump is shown.

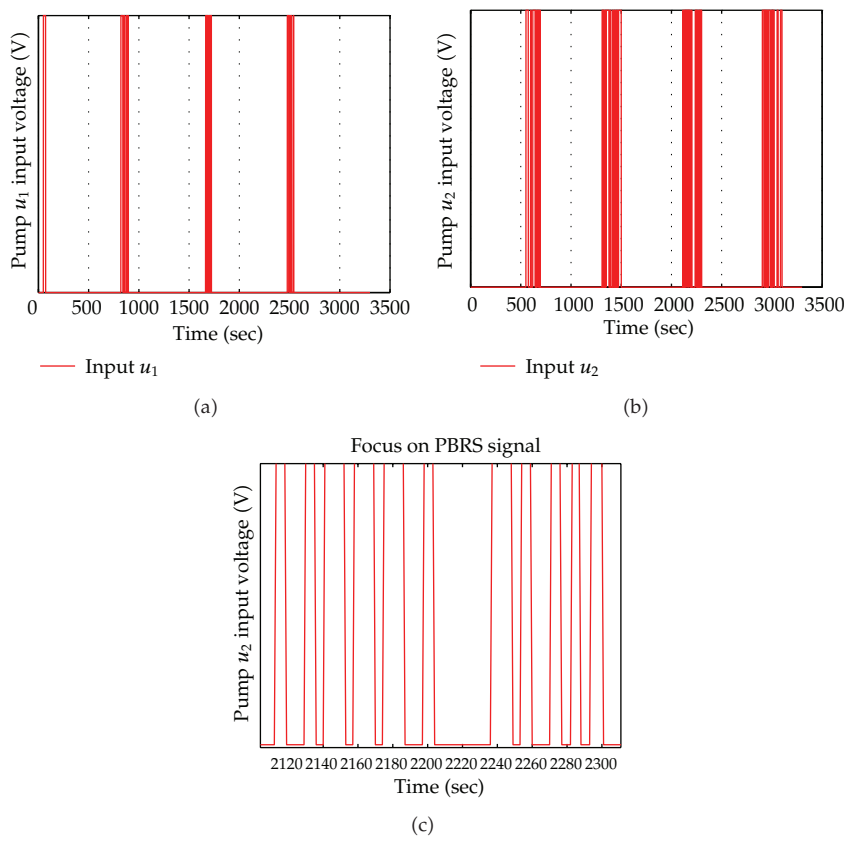

Figure 3: (a) Input signal for pump u_1 and (b) input signal for pump u_2 with (c) focus on the PBRS signal.

4.2. Calibration of the Delay and Order Model Selection

In this subsection, the delay in both pools will be estimated. It is known that open-flow canals present large delays that change with the operating point (in this case, the pump operation, i.e., the upstream level of each canal pool) [26]. In this work, the delay estimation has been derived using correlation method [1, 13]. The delay estimation error is equal or less than 1% in all cases. Next, the identification will be performed having removed the delays.

In subspace-based algorithms, the determination of the model order (n) can be complex. This order can be determined calculating the number of singular values (SVD) different from zero of the orthogonal (or oblique) projections of row spaces of data block-Hankel matrices. However, it is difficult to calculate it when the system data are corrupted by noise. It is also not straightforward to calculate this number, so that the decision is taken by detecting a gap in the spectrum of the singular values. As it can be seen in Figure 4 for N4SID2, the gap is difficult to determinate and hence the application of this strategy becomes really subjective. Therefore, the decision of the model order will be taken with the following criterion.

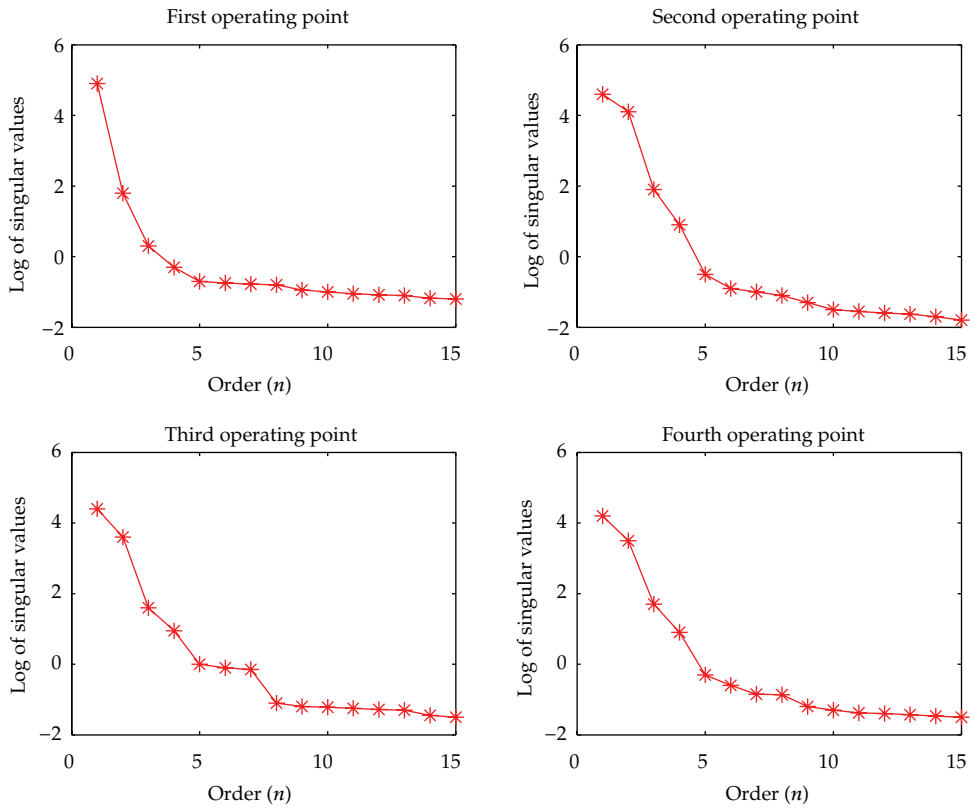

Figure 4: Log of singular values in each operating point.

A reliable technique is Akaike's final prediction error (FPE) criterion and his related Akaike Information Criterion (AIC). AIC procedure allows determining the order n of a system, and it is defined as

$$\mathrm{AIC} = \log\left(V\left(1 + 2\frac{d}{N}\right)\right), \tag{4.1}$$

where V is the loss function (quadratic fit) for the structure, N is the length of the data, and d is the total number of estimated parameters. Using the AIC criterion, the best order model is given by the minimum AIC(n) value. In Figure 4, the results of this criterion using N4SID2 algorithm on each operating point can be seen. A second-order model has been selected by the AIC's criterion for all the above subspace identification methods in the full operation range of the canal. Note that in Figure 5 a substantial difference between first and second order models can be seen, but choosing higher order models is irrelevant for the results using N4SID2. Therefore, a second-order model is enough to achieve a suitable control model.

The above fact demonstrates why engineers widely accept a first-order model with delay (IDZ model) or a second-order model with delay (Hayami model) for an irrigation canal approximation. As it is stated in [11, 29], the chosen model structure depends on the celerity coefficients, diffusion, and length of the canal. In our case, the canal is large enough

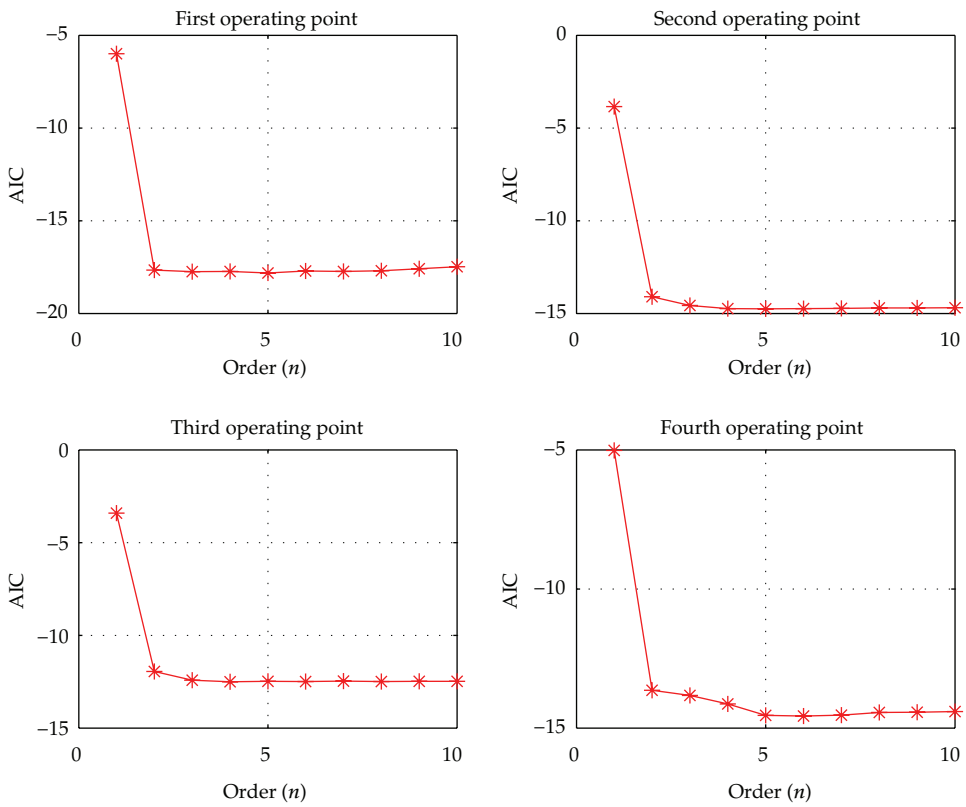

Figure 5: AIC results for N4SID2 in each operating point.

to consider a second-order model, corroborating the model order selection by the chosen statistical method.

4.3. Results and Performance Quality Criteria

After having chosen the best order n, the goal is to determine the best algorithm to obtain the final model. In this study, various subspace algorithms have been tested in the full operation range along the identification process. In order to select the best algorithm for identification, these methodologies have been compared among them to see which one fits best with data. The degree of adaptation of each one has been quantified by means of a cross-validation method, using the following typical performance indicators: MRSE (mean relative square error) and MVAF (mean variance-accounted for).

MRSE:

$$\%\text{MRSE} = \frac{1}{l}\sum_{i=1}^{l}\sqrt{\frac{\sum_{j=1}^{N}\left(y_i(j)-\hat{y}_i(j)\right)^2}{\sum_{j=1}^{N}y_i(j)^2}} \times 100 \quad (\text{in } \%). \tag{4.2}$$

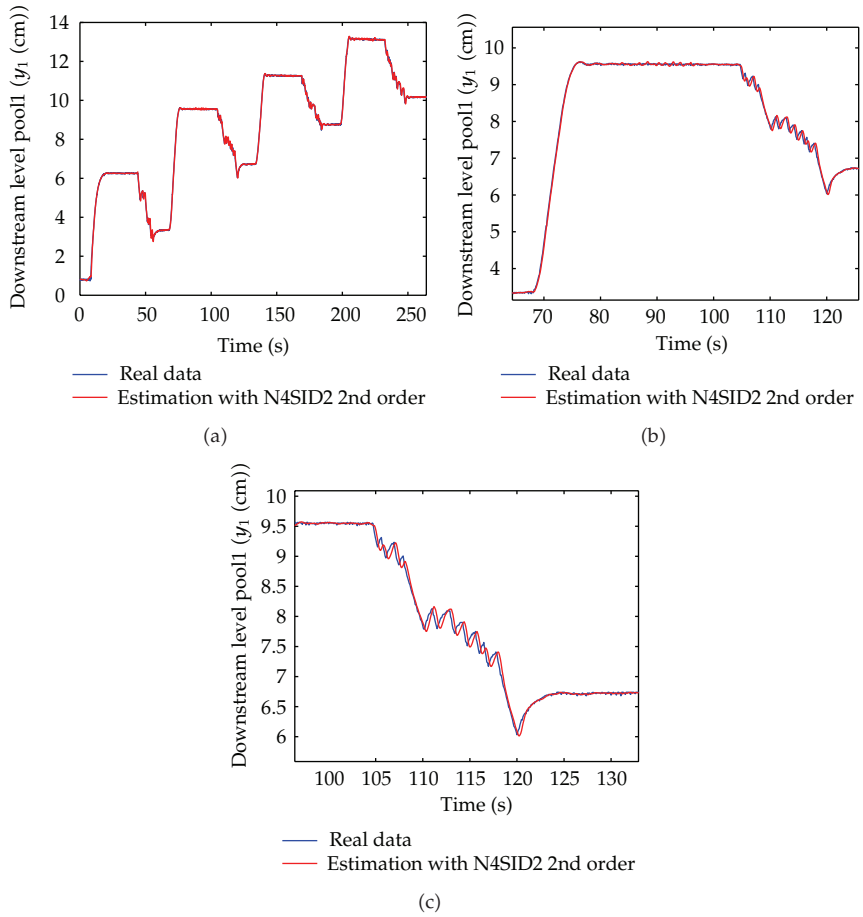

Figure 6: (a) Comparison between measured and estimated downstream level for pool 1, (b) a detail, and (c) a closer detail.

MVAF:

$$\%\text{MVAF} = \frac{1}{l}\sum_{i=1}^{l}\left(1 - \frac{\text{variance}(y_i - \widehat{y}_i)}{\text{variance}(y_i)}\right) \times 100 \quad (\text{in } \%). \tag{4.3}$$

With y_i being the ith real output, $\widehat{y}_i$ the ith simulated output produced by the model, and l is the number of repetitions of the experiment. The MRSE index given by (4.2) is used to measure the mean relative square error between the real process outputs and the outputs predicted by the model. As stated by (4.2), an MRSE index of 0 indicates a perfect model. MVAF in (4.3) is a measure for evaluating the dynamic properties of the produced models. If the ratio of variance $(y_i - \widehat{y}_i)$/variance (y_i) is small, the MVAF is close to 1. This index constitutes a quantitative measure of the model quality.

An experiment around the full the operating point range has been carried out and the best method has been selected. In Table 1, the goodness of the each algorithm (N4SID1, N4SID2, MOESP, and CVA) is shown. We can observe that all the methods provide a suitable prediction to obtain a control model.

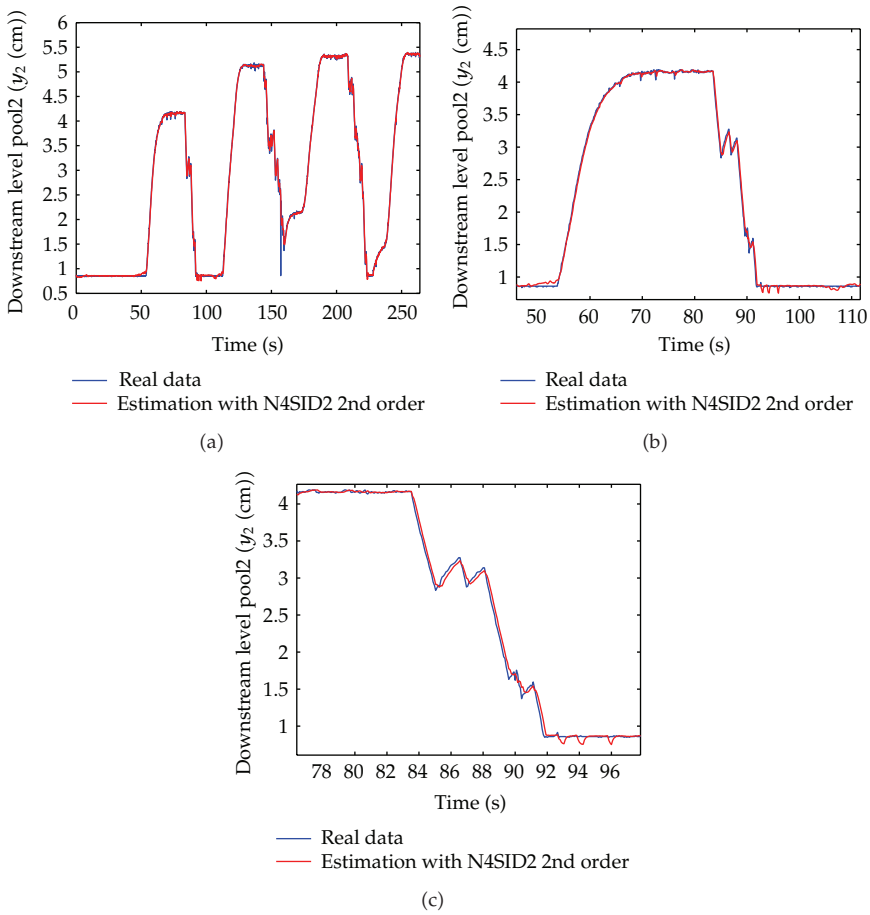

Figure 7: (a) Comparison between measured and estimated downstream level for pool 2, (b) a detail, and (c) a closer detail.

In average, N4SID2 is the most precise method in the full system operating range. However, in the central operating points, MOESP and CVA have a 4% more of precision, and in the highest operating point N4SID1 is 1% more precise. In Figures 6 and 7, the comparison between the measured and predicted downstream level of both pools is shown for a specific set-up around the full system operation range demonstrating the goodness and precision of the selected subspace identification method.

Those results were already expected because MOESP algorithm has the inherent drawback that it estimates the state sequence using a certain past window, possibly leading to biased results. Similar approximations are made in the subspace LTI algorithm N4SID; however, by making the past window larger, and larger this bias will tend to zero.

Apart from this error function used to validate the identified model, a correlation analysis of residuals is required. One of the most basic tests [2] is to compute the correlation between the regressors, the past inputs in this case, and the residuals:

$$\hat{r}^N(\tau) = \frac{1}{N} \sum u(t-\tau)\varepsilon(t). \tag{4.4}$$

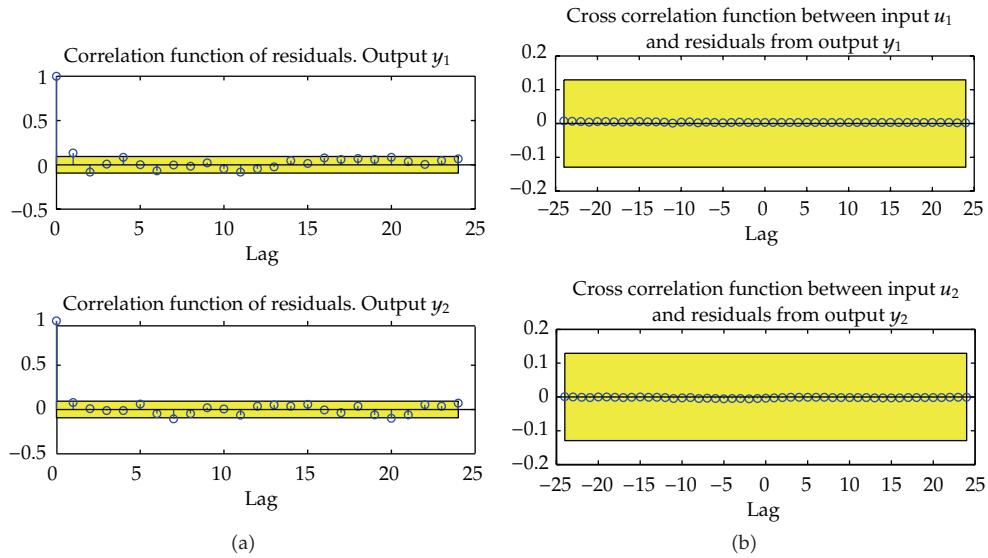

Figure 8: Traditional residual analysis: (a) auto- and (b) cross-correlation functions with uncertainty regions for both pools.

Table 1: Selection of the best subspace-based algorithm in the full operation point range.

Algorithm	Percentage of accuracy with MRSE in the full operation range		Percentage of accuracy with MVAF in the full operation range	
	Output y_1	Output y_2	Output y_1	Output y_2
N4SID1	89.45	74.85	79.71	83.73
N4SID2	90.98	73.12	88.19	81.57
MOESP	85.00	72.31	87.67	78.74
CVA	81.16	71.09	88.09	79.25

It is usual to plot these estimates as a function of τ and compare with their standard deviations to check if they are significantly different from zero. If not, there is no significant influence of input in ε, so it is not possible to say the estimated model has not picked up all the influence of u on y (the input on the output). It is supposed the assumption that ε is a white noise with variance λ and zero mean. The result is typically presented as a plot of the autocorrelation of the residuals and a plot of the cross-correlation between the inputs and the residuals. In Figure 8, auto- and cross-correlation functions with uncertainty regions for both pools are presented. It can be observed that the auto- and cross-correlation are within the regressors standard deviations providing a model that reproduces pretty well the main characteristics of dynamics of the pilot canal complex process.

Finally, the LPV canal global model is obtained by the use of N4SID2 method. The local models obtained with this algorithm are combined by interpolation to create the global model. Therefore, the parameters of the estimated model, that is, the matrices A_i, B_i, C_i, and D_i are interpolated by Nearest Neighbor Interpolation algorithm obtaining the (2.2). This algorithm is a numerical method widely extended by the scientific community [10, 25]. This method sets the value of an interpolated point to the value of the nearest data point. The

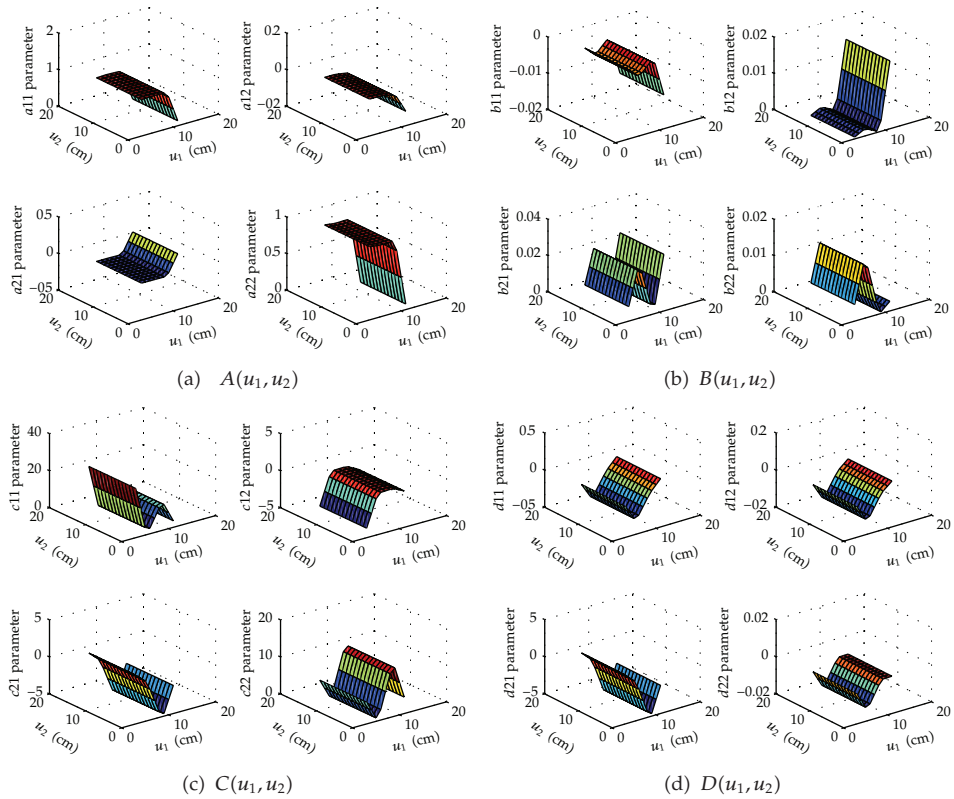

(a) $A(u_1, u_2)$ (b) $B(u_1, u_2)$

(c) $C(u_1, u_2)$ (d) $D(u_1, u_2)$

Figure 9: Interpolation of the parameters of the model: $A(u_1, u_2)$, $B(u_1, u_2)$, $C(u_1, u_2)$, and $D(u_1, u_2)$.

results of this interpolation can be seen in Figure 9. It can be observed that each parameter of the system depends on the operating point, the gate openings (u_1, u_2).

5. Conclusions

This paper introduces an approach for approximate modeling of distributed parameter processes using LPV identification. The use of LPV models allows the system to be approximated by multiple local low-order models combined by interpolation. Here, specifically an LPV MIMO state-space model for an irrigation canal is identified. The LPV identification is carried out with several subspace-based algorithms (N4SID, robust N4SID, MOESP, and CVA) in a local way. These methods have been compared and the most accurate in the full operation range has been selected. The model has been validated in a laboratory pilot multi-reach canal obtaining very good results.

Acknowledgment

This work has been funded by the Spanish Ministry of Science Project DPI2010-17112.

References

[1] Y. Bolea, V. Puig, J. Blesa, M. Gómez, and J. Rodellar, "A quasi-LPV Model for Gain-scheduling Canal Control," *Archives of Control Sciences*, vol. 14, no. 3/4, pp. 299–313, 2005.

[2] N. R. Draper and H. Smith, *Applied Regression Analysis*, John Wiley & Sons, New York, NY, USA, 3rd edition, 1998.

[3] V. T. Chow, *Open-Channel Hydraulics*, McGraw-Hill, 1959.

[4] O. A. Z. Sotomayor, S. W. Park, and C. Garcia, "Multivariable identification of an activated sludge process with subspace-based algorithms," *Control Engineering Practice*, vol. 11, no. 8, pp. 961–969, 2003.

[5] H. Dong, Z. Wang, and H. Gao, "H-infinity fuzzy control for systems with repeated scalar nonlinearities and random packet losses," *IEEE Transactions on Fuzzy Systems*, vol. 17, no. 2, pp. 440–450, 2009.

[6] J. Hu, Z. Wang, H. Gao, and L. K. Stergioulas, "Robust sliding mode control for discrete stochastic systems with mixed time-delays, randomly occurring uncertainties and randomly occurring nonlinearities," *IEEE Transactions on Industrial Electronics*, vol. 59, no. 7, pp. 3008–3015, 2012.

[7] J. Hu, Z. Wang, and H. Gao, "A delay fractioning approach to robust sliding mode control for discrete-time stochastic systems with randomly occurring non-linearities," *IMA Journal of Mathematical Control and Information*, vol. 28, no. 3, pp. 345–363, 2011.

[8] J. Hu, Z. Wang, H. Gao, and L. K. Stergioulas, "Robust H_∞ sliding mode control for discrete time-delay systems with stochastic nonlinearities," *Journal of the Franklin Institute*, vol. 349, no. 4, pp. 1459–1479, 2011.

[9] J. Hu, Z. Wang, H. Gao, and L. K. Stergioulas, "Robust H_∞ sliding mode control for discrete time-delay systems with stochastic nonlinearities," *Journal of the Franklin Institute*, vol. 349, no. 4, pp. 1459–1479, 2012.

[10] O. Bretscher, *Linear Algebra with Applications*, Pearson Prentice Hall, 5th edition, 2012.

[11] X. Litrico and V. Fromion, "Simplified modeling of irrigation canals for controller design," *Journal of Irrigation and Drainage Engineering*, vol. 130, no. 5, pp. 373–383, 2004.

[12] K. Eurén and E. Weyer, "System identification of open water channels with undershot and overshot gates," *Control Engineering Practice*, vol. 15, no. 7, pp. 813–824, 2007.

[13] L. Ljung, *System Identification: Theory for the User*, Prentice-Hall, 2nd edition, 1999.

[14] D. J. Leith and W. E. Leithead, "Survey of gain-scheduling analysis and design," *International Journal of Control*, vol. 73, no. 11, pp. 1001–1025, 2000.

[15] J. S. Shamma and M. Athans, "Guaranteed properties of gain scheduled control for linear parameter-varying plants," *Automatica*, vol. 27, no. 3, pp. 559–564, 1991.

[16] Murray-Smith, Roderick, and T. A. Johansen, *Multiple Model Approaches to Modelling and Control*, Taylor & Francis, London, UK, 1997.

[17] B. Bamieh and L. Giarré, "Identification of linear parameter varying models," *International Journal of Robust and Nonlinear Control*, vol. 12, no. 9, pp. 841–853, 2002.

[18] M. Pottmann, H. Unbehauen, and D. E. Seborg, "Application of a general multi-model approach for identification of highly nonlinear processes—a case study," *International Journal of Control*, vol. 57, no. 1, pp. 97–120, 1993.

[19] J. D. Caigny, J. F. Camino, and J. Swevers, "Identification of MIMO LPV models based on interpolation," in *Proceedings of the International Conference on Noise and Vibration Engineering (ISMA '08)*, 2008.

[20] J. Abonyi and R. Babuska, "Local and global identification and interpretation of parameters in Takagi-Sugeno fuzzy models," in *Proceedings of the 9th IEEE International Conference on Fuzzy Systems (FUZZ-IEEE '00)*, pp. 835–840, May 2000.

[21] T. A. Johansen and R. Murray-Smith, *The Operating Regime To Nonlinear Modelling and Control, Multiple Model Approaches Modelling and Control*, Taylor & Francis, 1996.

[22] B. L. Ho and R. E. Kalman, "Efficient construction of linear state variable models from input/output functions," *Regelungstechnik*, vol. 14, pp. 545–548, 1966.

[23] K. Zhou, J. C. Doyle, and K. Glover, *Robust and Optimal Control*, Prentice-Hall, 1996.

[24] V. Verdult, *Nonlinear system identification: a state-space approach [Ph.D. thesis]*, University of Twente, 2002.

[25] J. Stoer and R. Bulirsch, *Introduction To Numerical Analysis*, Springer Science + Business Media, New York, USA, 2002.

[26] E. F. Camacho, *Model Predictive Control*, Springer, New York, NY, USA, 1999.
[27] J. Schuurmans, O. H. Bosgra, and R. Brouwer, "Open-channel flow model approximation for controller design," *Applied Mathematical Modelling*, vol. 19, no. 9, pp. 525–530, 1995.
[28] M. Pinelli, P. R. Spina, and M. Venturini, "Optimized operating point selection for gas turbine health state analysis by using a multi-point technique," in *Proceedings of the ASME Turbo Expo*, pp. 43–51, Atlanta, Ga, USA, June 2003.
[29] X. Litrico and D. Georges, "Robust continuous-time and discrete-time flow control of a dam-river system. (I) Modelling," *Applied Mathematical Modelling*, vol. 23, no. 11, pp. 809–827, 1999.

Hindawi Publishing Corporation
Mathematical Problems in Engineering
Volume 2012, Article ID 240476, 14 pages
doi:10.1155/2012/240476

Research Article

Robot Navigation Control Based on Monocular Images: An Image Processing Algorithm for Obstacle Avoidance Decisions

William Benn and Stanislao Lauria

Department of Information Systems and Computing, Brunel University, Uxbridge UB8 3PH, UK

Correspondence should be addressed to Stanislao Lauria, stasha.lauria@brunel.ac.uk

Received 21 June 2012; Accepted 10 August 2012

Academic Editor: Zidong Wang

This paper covers the use of monocular vision to control autonomous navigation for a robot in a dynamically changing environment. The solution focused on using colour segmentation against a selected floor plane to distinctly separate obstacles from traversable space: this is then supplemented with canny edge detection to separate similarly coloured boundaries to the floor plane. The resulting binary map (where white identifies an obstacle-free area and black identifies an obstacle) could then be processed by fuzzy logic or neural networks to control the robot's next movements. Findings show that the algorithm performed strongly on solid coloured carpets, wooden, and concrete floors but had difficulty in separating colours in multicoloured floor types such as patterned carpets.

1. Introduction

Autonomous mobile robots need the capability to navigate along the hallway avoiding walls in indoor environments. A number of methods have been proposed to solve the navigation problems, based on different sensor technologies such as odometry, laser scanners, inertial sensors, sonar, and vision. Missing information due to sensor temporal failure or communication delay is one of the critical aspects when dealing with sensory data for robot navigation. In [1, 2] some solutions to tackle the missing information and filtering problems have been proposed. Also a multisensor architecture could be used to design robots. While combining different sensor types, such as ultrasound, vision, and infrared, may collectively result in a more accurate decision, it could also pose increasing costs and complexity [3].

This paper will be focusing on how effective vision alone can be used as a tool for navigation and collision avoidance. One notable challenge is providing autonomous

navigation in a dynamic environment, which Saffiotti [4] describes as *real world environments that have not been specifically engineered for the robot*.

Vision is one of the most important senses to a human being and in the past decade there has been an increased interest to use images in robotics. Machines may lack the vast knowledge of object recognition that a human brain can provide but the amount of computational power available in modern times make such machine vision a viable choice of input, and unlike a human eye, machine vision does not degrade over time providing consistent image capture. Images from a coloured web camera are used here as the source of information for this task. Visual sensors can provide plenty of information, however the environment they capture is often very dynamic and elements and features to be detected can change with the environment (i.e., the floor, door colour). Still to navigate successfully, a robot needs to distinguish between what is and is not navigable. By analysing each image frame, the system should be able to identify (if any) the available navigable areas.

Broadly speaking, there are two navigation strategies: *map-based navigation* and *map-less navigation*. In this paper, we focus on the latter. In indoor environments, the robot has often to navigate along the hallway while avoiding obstacles. Then, the navigation strategies are determined by capturing and extracting relevant information about the elements in the environment. These elements can be the walls, edges, doorways, and so forth and it is not necessary to calculate the absolute positions of these elements of the environment. The navigation problem is well studied (see, e.g., [5]). Whereas, [6, 7] are some examples of strategies developed for the detection of obstacles or edge detection using vision systems. However, often these methods are dependent on the environment around a robot. For example, in [7] it is not clear how the system would react to changes in the floor patterns, whereas in [6] Neural Networks strategies are considered during the camera calibration phase to tackle this issue. References [8, 9] have investigated the use of optical flow to identify a dominant ground plane. However, their assumption is that the floor is the dominant plane.

In our paper, we extend these ideas on using the floor to calculate the correct values for the parameters necessary to extract the required information from each image. Then, to identify the obstacles, the sequential use of *colour iImage segmentation* and then *edge detection* strategies has been investigated. That is, a two steps strategy has been used.

Step 1: Image Segmentation

Step 2: Edge Detection

Each of the steps above is based on one of two basic properties of intensity values: discontinuity and similarity. Once the image has been processed in this way, fuzzy logic, neural networks, and so forth could then be considered to optimise decisions and control the robot navigation strategies.

Colour segmentation will determine obstacles from the floor while canny edge detection supplements the colour segmentation by finding sharp changes in colour gradients. Colour image Segmentation is based on partitioning an image into regions that are similar according to a predefined criteria. Whereas the aim of the edge detection stage is to partition an image based on abrupt changes in intensity. In similar research, these two steps are not always applied independently or only one of the two is applied (see, e.g., [10, 11]). In our paper both steps are applied as a consecutive sequence to the image. A measure on the effect on the success rate of each step is also investigated. Each of the steps mentioned above is discussed in detail below. Then, results are presented and discussed.

1.1. Image Colour Segmentation

For robot navigation, image segmentation is the process of decomposing an image into parts which should be meaningful to identify obstacle-free areas.

A more formal definition of segmentation can be given in the following way [12]. Let I denote an image and let H define a certain homogeneity predicate. Then the segmentation of I is a partition P of I into a set of N regions R_n, $n = 1, \ldots, N$, such that

(1) $\bigcup_{n=1}^{N} R_n = I$ with $R_n \bigcup R_m \neq 0; n \neq m$,

(2) $H(R_n) =$ true for all n,

(3) $H(R_n \cup R_m) =$ false if R_n and R_m adjacent.

Condition (1) states that the partition has to cover the whole image, condition (2) states that each region has to be homogeneous with respect to the predicate H, and condition (3) states that the two adjacent region cannot be merged into a single regions that satisfies the predicate H. The desirable characteristics that a good image segmentation should exhibit have been defined in [13].

Several colour representations are currently in use in colour image processing. The most common is the RGB space where colors are represented by their red, green, and blue components in an orthogonal Cartesian space. Most cameras will capture an image using the RGB colour space.

However, colour is better represented in terms of hue, saturation, and intensity. An example of such a kind of representation is the HSV space. HSV rearranges the geometry of RGB in an attempt to be more intuitive and perceptually relevant (see e.g., [14]).

The main approaches in image colour segmentation are based on partitioning an image into regions that are similar according to a set of predefined criteria. These segmentation methods are based on sets of features that can be extracted from the images such as pixel intensities. Thresholding, clustering, and region growing are examples of such approaches. Extensive work has been done in this area (see e.g., [10]).

Thresholding is one of the simplest and most popular techniques for image segmentation. The threshold can be specified using a heuristic technique based on visual inspection of the histogram but this approach is operator-dependent. If the image is noisy, the selection of the threshold is not trivial. Thus, more sophisticated methods have been proposed. The Balanced Histogram Thresholding (BHT), see for example [15], is a histogram-based thresholding method. The BHT approach assumes that the image is divided in two main classes: the background and the foreground. The BHT method tries to find the optimum threshold level that divides the histogram in two classes. In general, thresholding creates binary images from grey-level ones by turning all pixels below some threshold to 0 and all pixels about that threshold to 1.

In this paper, a pre-defined area of the image (red area in Figure 5) has been used to calculate the threshold values. The selected rectangular area used is located at the bottom of the image because this area is likely to contain the floor. Within this area of selection colour thresholds are calculated to define the criteria to process in a meaningful way each pixel of the image during the successive phases of the segmentation process discussed below. Further details of the thresholding step are discussed in Section 3.

There is extensive work investigating different algorithms to segment regions by identifying common properties in order to separate an image into regions corresponding to objects. (see e.g., [16]).

In [17] a multiphase image segmentation model for color images is discussed. It mainly focuses on homogeneous multiphase images. It only considers the global information of the given image, thus it cannot deal with images with inhomogeneity.

Refernce [18] applies relative values for R, G, and B components on each pixel for image segmentation. He observed traffic signs in an open environment and segmented the red color in such a way that if green and blue colors in a pixel are summed up and compared with red color, it gives relatively 1.5 times higher values for the red component in pixel. If the pixel has relatively higher red component, it determines as the featured pixel. A binary segmented image is then created using the known coordinates of the featured pixels.

Refernce [19] proposed a detection and recognition algorithm for certain road signs. Signs have the red border for warning signs and a blue background for information signs. A car has a mounted camera that gets images. Colour information can be changed due to poor lighting and weather conditions such as dark illumination and rainy and foggy weather. To overcome these problems they proposed two algorithms by using RGB color image segmentation.

Refernce [20] focused on identifying similar colour domains from human skin and vegetables. The advantage of this solution is that it does not require converting from the RGB colour space (allowing the source of the captured image to be worked on directly) and was robust against various illumination. To avoid converting RGB to other colour spaces such as HSV, [20] devised a method which uses 5 constant threshold variables (α, $\beta 1$, $\beta 2$, $\gamma 1$, and $\gamma 2$) to determine whether an RGB pixel is within a specific colour zone. Assuming the following variable values:

r = Red value of the pixel
g = Green value of the pixel
b = Blue value of the pixel
α = Minimum red threshold value (0–255)
$\beta 1$ = Minimum red-green component value (0–255)
$\beta 2$ = Maximum red-green component value (0–255)
$\gamma 1$ = Minimum red-blue component value (0–255)
$\gamma 2$ = Maximum red-blue component value (0–255).

The algorithm considers a pixel to be within a certain colour range if

(1) $r > \alpha$,

(2) $\beta 1 < r - g < \beta 2$,

(3) $\gamma 1 < r - b < \gamma 2$.

Some initial evaluations of the [20] technique applied to indoor navigation domains have shown that it captured a too broader amount of the threshold from the target floor surface. Therefore, in the present paper a modification of the above algorithm has been investigated. In particular, an additional constant ($\alpha^{\max}$) has been added to hold the maximum red threshold while the existing red constant ($\alpha^{\min}$) was used to hold the minimum red threshold. The first rule was then modified as follows:

(1) $\alpha^{\min} < r < \alpha^{\max}$.

After a few tests, the optimal settings found for the α parameters were the following. In higher illuminated conditions and pastel coloured environments $\alpha^{\max}$ is most efficient at being set to higher values such as a range between 170 and 200. $\alpha^{\min}$ is best set to a midrange value between the 75 to 90 range. In low illumination conditions $\alpha^{\max}$ is most

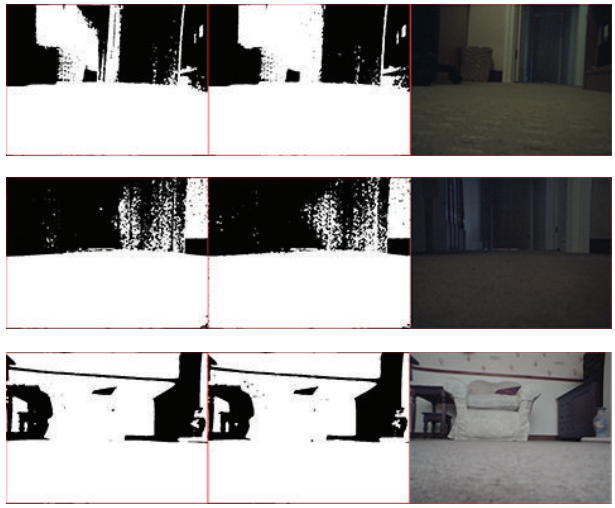

Figure 1: Comparison of original colour segmentation technique against modified rule set. Left image modified rule set, middle image original rule set, and right image raw capture.

efficient between low midrange values such as 60 to 80. $\alpha^{\min}$ should be set to a low range between 20 to 40. A higher broader range is needed under high illumination as it is most likely that obstacles will reside in the lower colour ranges. This broad range can be a downfall when obstacles are of a similar colour to the surrounding environment, which is where the edge supplementation is expected be of a great aid.

Figure 1 shows that the modified rule set investigated in the present paper picks up less noise from the image. It is also better at picking up colours that are similar to the floor plane, although the effect of this varies depending on the difference of change. From some initial tests, there is evidence that the modified algorithm keeps the floor threshold values correct when there are some small illumination changes caused by the robot's movement.

1.2. Edge Detection

Colour segmentation alone is not enough to fully segment an image, gaps were left by noise and areas of a similar colour to the floor plane were misinterpreted as traversable space. To eliminate this issue a separate edge map was produced from the captured image which was then processed by a probabilistic Hough algorithm to identify strong lines in an image.

It was decided that the best edge detection method for the project was the canny edge implementation. It excels in identifying strong edges with a lower number of line disconnections, it also picks out major details from an object [21, 22], while it is weaker at identifying minor details, we are only interested in the silhouette of an obstacle.

Once the canny edge map has been generated the probabilistic Hough transform can be applied to the image. The principle of this procedure is to scan through each pixel in a binary image finding all lines that could fit through this point. If a line fits through enough points then it is considered significant enough to keep [23]. Each point is picked randomly and once enough points have been passed through by a line, then they are removed from any subsequent scanning. This is then repeated until all points are eliminated or there are not enough points left to identify a significant line. The implementations used for this solution are

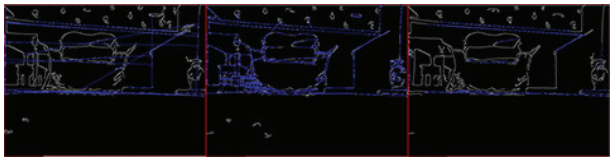

Figure 2: Comparison of Hough line parameters. Left image large maximum pixel gap value, middle image low line votes, and segment length value, right image optimal found settings.

from the OpenCv library, there are various parameters that can be passed to the probabilistic Hough transform.

Line votes number: of points a line must pass through to be considered significant

Minimum segment: length Minimum length a line must be to be selected

Maximum pixel gap: The biggest gap between points on a line that there can be.

After a few tests, the optimal settings found for the above parameters were the following:

Line votes = 80 lines

Minimum segment length = 20 pixels

Maximum pixel gap: Minimum pixel gap value.

In Figure 2 it is possible to note that when a large pixel gap is allowed lines will often extend across multiple disjointed edges from the canny map. This is not desirable for our purposes as it could fill legitimate gaps that a robot would be able to pass through. However, when a small segment length value and a low line vote count is set we end up with many short lines that could easily be combined into a single long line, this again is not desirable as the more lines there are, the larger the processing time that is required to apply the line information to the colour segmentation map. See Figure 3 for a list of images with the optimal found probabilistic Hough line parameters (with blue lines indicating the Hough lines).

Output of the probabilistic Hough transform was an array of lines. To apply this information to the colour segmentation map, a polygon was drawn from the start and end points of each line to the top of the image. Figure 4 shows a comparison between edge supplemented and nonedge supplemented segmentation maps.

2. Implementation

The algorithms have been implemented in `C++` because of the high-performance libraries available for this language. Additional processing was completed using the OpenCV library.

To calculate thresholds for the rules defined in Section 1.1, a rectangular area is selected from the image (Figure 5). Within this *mask*, thresholds are calculated as shown in Listing 1. In particular, each pixel is iterated, updating a colour threshold only when it is less than or bigger than the current threshold (depending on if it is a minimum or maximum threshold). Once the minimum and maximum thresholds have been calculated they can be compared against all the pixels in the captured image. If a pixel's RGB value is between the desired threshold, then the pixel can be marked as white otherwise as black as shown in Listing 2. To apply the Hough line information from the line array is simply a matter of drawing a black area onto the existing binary map, this is achieved by plotting a 4 sided polygon. Care must be taken to determine the correct winding order to avoid a twisted hourglass like shape; this

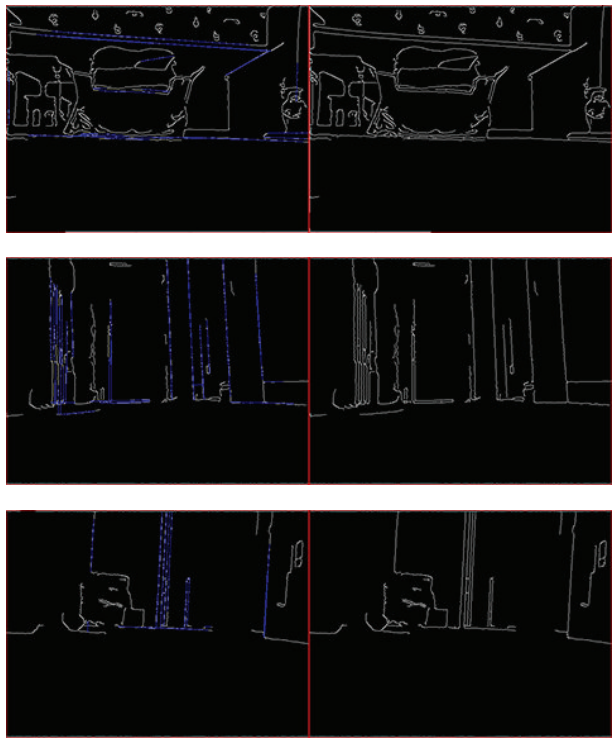

Figure 3: Optimal Hough line parameters applied to canny edge map.

is easily rectified by checking whether the first point of the line is to left or right of the end point and changing the point drawing order as shown in Listing 3.

3. Results

The algorithm discussed above has been tested using images from an indoor environment. The same set of images has been used to test different settings. For each setting, every image has been processed by a different combination of algorithms. The following four different settings have been tested:

Original. The image segmentation algorithm [20].

Original and edge. The original and the edge detection algrithms.

Modified. The modified image segmentation algorithm presented in this paper.

Modified and edge. The modified and the edge detection algorithms.

Once the image has been processed following one of the settings listed above, a decision algorithm has been applied to the produced binary map (*produced result*). The same decision algorithm (based on a fuzzy logic algorithm) has been applied irrespective of the setting used to obtain the binary image. Then, the *produced result* has been compared with the decision that humans would produce in those situations (*expected result*).

A match between the *produced result* and the *expected result* has been considered correct, whereas a discrepancy between the *produced result* and the *expected result* has been counted as an error. Six different possible outputs have been defined as the range of the possible

```
(1) for (int i = start Y; i < height; ++i)
(2) {
(3)             for (int j = start X; j < width; ++j)
(4)         {
(5)             unsigned char blue = pixel Data [i ∗ step + j ∗ channels];
(6)             unsigned char green = pixel Data [i ∗ step + j ∗ channels + 1];
(7)             unsigned char red = pixel Data [i ∗ step + j ∗ channels + 2];
(8)
(9)             if (red == 0 && green == 0 && blue == 0)
(10)            {
(11)                    continue;
(12)            }
(13)
(14)        //Find thersholds
(15)        if (red < mMinimumRed)
(16)        {
(17)            mMinimumRed = Red;
(18)        }
(19)
(20)        if (red > mMaximumRed)
(21)        {
(22)                mMaximumRed = Red;
(23)        }
(24)
(25)        int redGreenRange = red − green;
(26)        int redBlueRange = red − blue;
(27)
(28)        if (redGreenRange < mRedGreenRangeMin)
(29)        {
(30)                mRedGreenRangeMin = redGreenRange;
(31)        }
(32)
(33)        if (redGreenRange > mRedGreenRangeMax)
(34)        {
(35)            mRedGreenRangeMax = redGreenRange;
(36)        }
(37)
(38)        if (redBlueRange < mRedBlueRangeMin)
(39)        {
(40)            mRedBlueRangeMin = redBlueRange;
(41)        }
(42)
(43)        if (redBlueRange > mRedBlueRangeMax)
(44)        {
(45)                mRedBlueRangeMax = redBlueRange;
(46)        }
(47)    }
(48) }
```

Listing 1: Threshold. The code calculating the thresholds for the Image Segmentatation step.

```
(1) for (int i = 0; i < inImage − > height; ++i)
(2) {
(3)         for (int j = 0; j < inImage − > width; ++j)
(4)         {
(5)                 int bluePos = i ∗ step + j ∗ channels;
(6)                 int greenPos = i ∗ step + j ∗ channels + 1;
(7)                 int redPos = i ∗ step + j ∗ channels + 2;
(8)
(9)                 unsigned char red = inPixel Data [redPos];
(10)                unsigned char green = inPixel Data [greenPos];
(11)                unsigned char blue = inPixel Data [bluePos];
(12)                int redGreen = red − green;
(13)                int redBlue = red − blue;
(14)
(15)                if ((red > mMinimumRed && red < mMaximumRed)
(16)                        && (redGreen >= mRedGreenRangeMin
(17)                                && redGreen <= mRedGreenRangeMax)
(18)                    &&(redBlue >= mRedBlueRangeMin
(19)                                && redBlue <= mRedBlueRangeMax))
(20)                {
(21)                    //pixel is within floor range set to white
(22)                    outPixelData [redPos] = 255;
(23)                    outPixelData [greenPos] = 255;
(24)                    outPixelData [bluePos] = 255;
(25)                    ++total Pixels;
(26)                }
(27)                else
(28)                {
(29)                    outPixelData [redPos] = 0;
(30)                    outPixelData [greenPos] = 0;
(31)                    outPixelData [bluePos] = 0;
(32)                }
(33)        }
(34)}
```

LISTING 2: Image Segmentation. The code applying the thresholds.

decisions. `move forward` or `turn left` are examples of some of the six *produced, expected results* output.

Results in Table 1 show that both the use of the modified algorithm and the two steps strategy are very significant ($\chi^2(3,\ N = 21) = 12.4,\ p = 0.006$). That is, when the performance of the modified red threshold rule is compared with the original rule in both settings (*original* versus *modified* and *original and edge* versus *modified and edge*) a higher correct success rate is obtained for the modified algorithm. Moreover, the discrepancy between *produced result* and *expected result* is reduced with the introduction of the *edge step* when the image is processed.

Different floor patterns have also been tested to investigate the modified algorithm under different conditions. Figure 6 shows the outcome of using, respectively, the *modified* in (a) and the *original* in (b) for a given floor pattern raw image in (c). From Figure 6 it is possible to conclude that the modified rule set seems to perform specifically strongly with white colours compared to the original rule set. Moreover, the modified rule set handles the nonuniform floor patterns better. That is, with the introduction of the $\alpha^{\max}$ value it is possible

```
for (auto it = Filtered Lines. Begin (); it != Filtered Lines. end (); ++it)
{
        CvPoint poly Points [4];

        //First point is to the left of the right point
        if ((* it) [0] <= (* it) [2])
        {
                polyPoints [0] = cvPoint ((* it) [0], 0);
                polyPoints [1] = cvPoint ((* it) [2], 0);
                polyPoints [2] = cvPoint ((* it) [2], (* it) [3]);
                polyPoints [3] = cvPoint ((* it) [0], (* it) [1]);
        }
        else //First point is to the right of the right point
        {
                polyPoints [0] = cvPoint ((* it) [2], 0);
                polyPoints [1] = cvPoint ((* it) [0], 0);
                polyPoints [2] = cvPoint ((* it) [0], (* it) [1]);
                polyPoints [3] = cvPoint ((* it) [2], (* it) [3]);
        }

        cv Fill ConvexPoly (inImage, &polyPoints [0], 4, cvScalar (0, 0, 0));
}
```

LISTING 3: Edge Segmentation. The code implementing the Edge Segmentation algorithm.

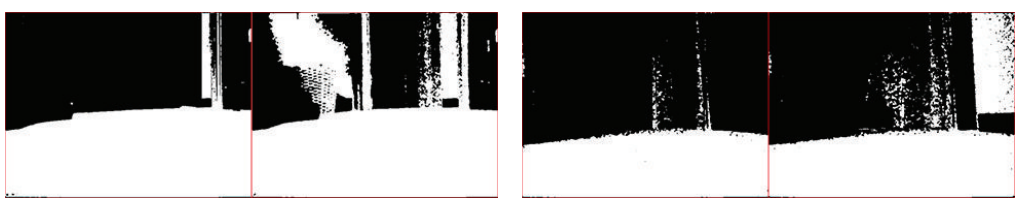

(a) (b)

Figure 4: Comparison of applied edge supplementation to colour segmentation map. In both (a) and (b), left image applied edge supplementation, right image nonapplied.

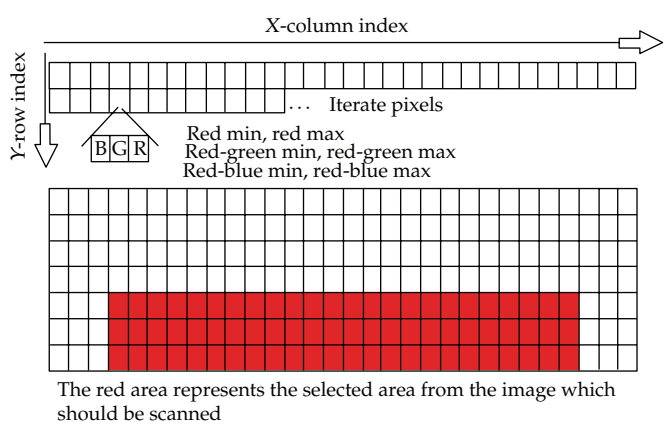

Figure 5: Selecting area for colour thresholds.

Table 1: Algorithm testing. Correct matching results between the *produced result* and the *expected result* for the different settings.

Setting	Success rate (%)
Original	42
Original and Edge	76
Modified	57
Modified and Edge	90

Table 2: Algorithm processing time. Processing time values (in ms) for the *image segmentation* and *edge detection* settings.

Setting	Processing time (ms)
Modified	25.6
Modified and Edge	27.6

to notice that the algorithm performs particularly strongly against white colours compared to the original algorithm (see, e.g., Figure 6). The original algorithm would have a much larger threshold, based on our tests the original algorithm has a threshold range 38.75% greater than that of the modified algorithm under highly illuminated environments.

Table 2 shows the processing time for the different settings described at the beginning of the section. The time difference between the image segmentation algorithm [20] (i.e., *original*) and the modified version presented in this paper (*modified*) is too negligible to show in the results, therefore only results for the *Modified* configuration have been shown.

The CPU used for all tests was a *Phenom II X4 955* and CPU clock was set to 3.6 GHz. The time without edge detection step and the time with the edge detection step has been measured, respectively, in row 1 and 2. The values in the table indicate the time in milliseconds it took to apply the algorithms indicated in the *Setting* column to the image and then to generate the binary collision map. In all cases the mean was taken from a sample of 10 measurements.

Results in Table 2 show that the modified algorithm does not increase the processing time (since as stated above *modified* and *original* settings produce similar processing time). Further, it shows a percentage increase of 7.8% over the no edge configuration. That is, as expected, the time to extract the required information increases by including the edge detection step in the algorithm. However, from Table 2 it is possible to observe that a percentage increase of 7.8% in processing time has produced a percentage increase of 57.9% in the success rate for the algorithm.

4. Discussions and Conclusions

The sequential use of *colour image segmentation* and then *edge detection* strategies has been investigated. A novel color image segmentation algorithm and a probabilistic Hough algorithm have been implemented and tested. The novelty introduced here has been demonstrated to improve an existing algorithm for image processing.

In particular, the modified red threshold rule considered for the image segmentation algorithm helped in keeping the learnt thresholds stable. Moreover, the use of both colour segmentation and edge detection techniques complemented each other by removing the weaknesses that each method separately presented. In particular, with the colour

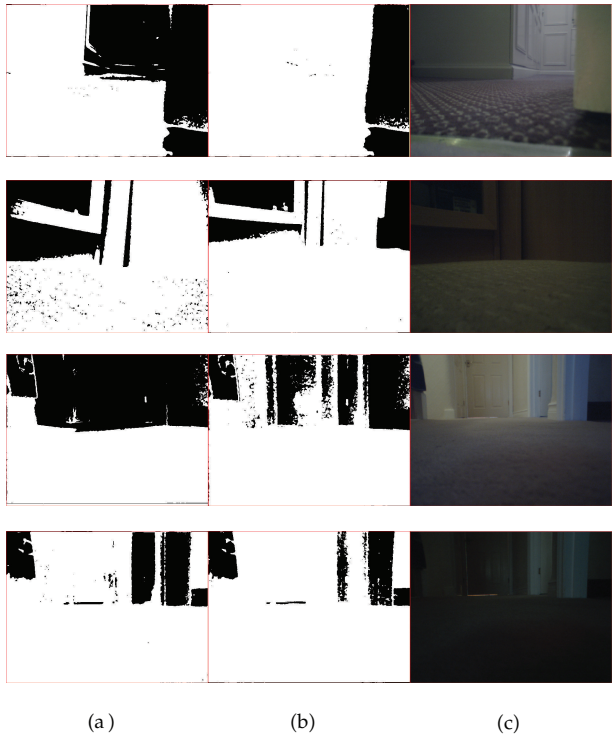

Figure 6: Comparisons between the 2 different image segmentation algorithms under different floor patterns. Columns (a) and (b) show the outcome of the processing for the raw image in (c).

segmentation technique identifying the main obstacle-free area and the edge detection filling any remaining gaps in the detected segments in the output binary map.

Although the approach discussed in this paper has been demonstrated to be independent of floor changes, further development is needed to cope with patterned floor surfaces. This is because the edges detected from the patterns and the wider colour thresholds that are learnt from such floors make it difficult to produce an accurate binary map. A possible solution could be to make use of the canny edge map to identify the patterned areas in the floor surface and combine that with the information from the threshold learning algorithm so that it would ignore colours within that area of the image. As a consequence the learnt colour thresholds would be narrower and would not erroneously detect obstacles as obstacle free areas.

The scalability of this algorithm for a distributed architecture (with several robots involved) is another aspect that could be investigate further. Each robot will produce a (slight) different image of the same environment to extract the required features. Therefore each robot can receive not only its own information but also the information from its neighboring robot according to the topology of the given robot network. Then to deal with the complicated coupling between one sensor and its neighbors, a filtering approach such as the ones in [24, 25] could be considered. However, some further investigation is required to analyse how these paradigms would perform with these types of data.

References

[1] H. Dong, Z. Wang, and H. Gao, "Distributed filtering for a class of time-varying systems over sensor networks with quantization errors and successive packet dropouts," *IEEE Transactions on Signal Processing*, vol. 60, no. 6, Article ID Article number6168290, pp. 3164–3173, 2012.

[2] Z. Wang, B. Shen, H. Shu, and G. Wei, "Quantized H_∞ control for nonlinear stochastic time-delay systems with missing measurements," *IEEE Transactions on Automatic Control*, vol. 57, no. 6, Article ID Article number6082385, pp. 1431–1444, 2012.

[3] J. Esteban, A. Starr, R. Willetts, P. Hannah, and P. Bryanston-Cross, "A review of data fusion models and architectures: towards engineering guidelines," *Neural Computing and Applications*, vol. 14, no. 4, pp. 273–281, 2005.

[4] A. Saffiotti, "The uses of fuzzy logic in autonomous robot navigation," *Soft Computing*, vol. 1, no. 4, pp. 180–197, 1997, http://aass.oru.se/~asaffio/.

[5] G. N. DeSouza and A. C. Kak, "Vision for mobile robot navigation: a survey," *IEEE Transactions on Pattern Analysis and Machine Intelligence*, vol. 24, no. 2, pp. 237–267, 2002.

[6] A. M. Zou, Z. G. Hou, M. Tan, and D. Liu, "Vision-guided mobile robot navigation," in *Proceedings of the IEEE International Conference on Networking, Sensing and Control (ICNSC '06)*, pp. 209–213, April 2006.

[7] W. Shi and J. Samarabandu, "Corridor line detection for vision based indoor robot navigation," in *Proceedings of the Canadian Conference on Electrical and Computer Engineering (CCECE '06)*, pp. 1988–1991, May 2006.

[8] N. Ohnishi and A. Imiya, "Dominant plane detection from optical flow for robot navigation," *Pattern Recognition Letters*, vol. 27, no. 9, pp. 1009–1021, 2006.

[9] K. Van Workum and R. Green, "Smart wheelchair guidance using optical flow," in *Proceedings of the 24th International Conference Image and Vision Computing New Zealand (IVCNZ '09)*, pp. 7–11, November 2009.

[10] N. Senthilkumaran and R. Rajesh, "Edge detection techniques for image segmentation a survey of soft computing approaches," *International Journal of Recent Trends in Engineering*, vol. 1, no. 2, pp. 844–846, 2009.

[11] S. Al-amri, N. V. Kalyankar, and S. D. Khamitkar, "Image segmentation by using edge detection," *International Journal on Computer Science and Engineering*, vol. 2, no. 3, pp. 804–807, 2010.

[12] L. Lucchese and S. K. Mitra, "Color image segmentation : a state-of-the-art survey," *Citeseer*, vol. 67, no. 2, pp. 207–221, 2001.

[13] R. M. Haralick and L. G. Shapiro, "Image segmentation techniques," *Computer Vision, Graphics, & Image Processing*, vol. 29, no. 1, pp. 100–132, 1985.

[14] R. C. Gonzales and R. Woods, *Digital Image Processing*, Addison-Wesley, Reading, Mass, USA, 1992.

[15] N. Otsu, "A threshold selection method from gray-level histograms," *IEEE Transactions on Systems, Man, and Cybernetics*, vol. 9, no. 1, pp. 62–66, 1979.

[16] H. D. Cheng, X. H. Jiang, Y. Sun, and J. Wang, "Color image segmentation: advances and prospects," *Pattern Recognition*, vol. 34, no. 12, pp. 2259–2281, 2001.

[17] Y. Yang and B. Wu, "A new and fast multiphase image segmentation model for color images," *Mathematical Problems in Engineering*, vol. 2012, Article ID 494761, 20 pages, 2012.

[18] S. Varun, S. Singh, R. Sanjeev Kunte, R. D. Sudhaker Samuel, and B. Philip, "A road traffic signal recognition system based on template matching employing tree classifier," in *Proceedings of the International Conference on Computational Intelligence and Multimedia Applications (ICCIMA '07)*, pp. 360–365, December 2007.

[19] V. Andrey and K. H. Jo, "Automatic detection and recognition of traffic signs using geometric structure analysis," in *Proceedings of the International Joint Conference (SICE-ICASE '06)*, pp. 1451–1456, October 2006.

[20] C. Lin, C. H. Su, H. S. Huang, and K. C. Fan, "Colour image segmentation in various illumination circumstances," in *Proceedings of the 9th WSEAS International Conference on Circuits, Systems, Electronics, Control and Signal Processing (CSECS '10)*, pp. 179–184, Stevens Point, Wis, USA, December 2010.

[21] E. Nadernejad, S. Sharifzadeh, and H. Hassanpour, "Edge detection techniques: evaluations and comparisons," *Applied Mathematical Sciences*, vol. 2, no. 29–32, pp. 1507–1520, 2008.

[22] D. Ziou and S. Tabbone, "Edge detection techniques - an overview," *International Journal of Pattern Recognition and Image Analysis*, vol. 8, pp. 537–559, 1998.

[23] R. Laganiére, *OpenCV 2 Computer Vision Application Programming Cookbook*, Packt, 2001.

[24] Z. Wang, B. Shen, and X. Liu, "H_∞ filtering with randomly occurring sensor saturations and missing measurements," *Automatica*, vol. 48, no. 3, pp. 556–562, 2012.

[25] B. Shen, Z. Wang, and X. Liu, "A stochastic sampled-data approach to distributed H_∞ filtering in sensor networks," *IEEE Transactions on Circuits and Systems. I. Regular Papers*, vol. 58, no. 9, pp. 2237–2246, 2011.

Hindawi Publishing Corporation
Mathematical Problems in Engineering
Volume 2012, Article ID 964742, 28 pages
doi:10.1155/2012/964742

Research Article

MPC Schemes Guaranteeing ISDS and ISS for Nonlinear (Time-Delay) Systems

Sergey Dashkovskiy[1] and Lars Naujok[2]

[1] *Department of Civil Engineering, University of Applied Sciences Erfurt, P.O. Box 450155, 99051 Erfurt, Germany*
[2] *Centre of Industrial Mathematics, University of Bremen, P.O. Box 330440, 28334 Bremen, Germany*

Correspondence should be addressed to Lars Naujok, larsnaujok@gmx.de

Received 22 June 2012; Accepted 3 October 2012

Academic Editor: Hamid Reza Karimi

New directions in model predictive control (MPC) are introduced. On the one hand, we combine the input-to-state dynamical stability (ISDS) with MPC for single and interconnected systems. On the other hand, we introduce MPC schemes guaranteeing input-to-state stability (ISS) of single systems and networks with time delays. In both directions, recent results of the stability analysis from the mentioned areas are applied using Lyapunov function(al)s to show that the corresponding cost function(al) of the MPC scheme is a Lyapunov function(al). For networks, we show that under a small-gain condition and with an optimal control obtained by an MPC scheme for networks, it has the ISDS property or ISS property, respectively.

1. Introduction

The approach of MPC started in the late 1970s and spread out in the 1990s by an increasing usage of automation processes in the industry. It has a wide range of applications, see the survey papers [1, 2].

The aim of MPC is to control a system to follow a certain trajectory or to steer the solution of a system into an equilibrium point under constraints and unknown disturbances. Additionally, the control should be optimal in view of defined goals, for example, optimal regarding effort. An overview about MPC can be found in the books [3–5] and the Ph.D. theses [6–8], for example.

We consider systems with disturbances of the form,

$$\dot{x}(t) = f(x(t), w(t), u(t)), \tag{1.1}$$

where $w \in \mathcal{W} \subseteq L_\infty(\mathbb{R}_+, \mathbb{R}^P)$ is the unknown disturbance and $\mathcal{W}$ is a compact and convex set containing the origin. The input u is a measurable and essentially bounded control subject to input constraints $u \in \mathcal{U}$, where $\mathcal{U} \subseteq \mathbb{R}^m$ is a compact and convex set containing the origin in its interior. The function f is assumed to be locally Lipschitz in x uniformly in w and u to guarantee that a unique solution of (1.1) exists, which is denoted by $x(t; x_0, w, u)$ or $x(t)$ in short.

The control input is obtained by an MPC scheme and applied to the system. We are interested in stability of MPC. It was shown in [9] that the application of the control obtained by an MPC scheme to a system does not guarantee that a system without disturbances is asymptotically stable. For stability of a system in applications, it is desired to analyze under which conditions stability of a system can be achieved using an MPC scheme. An overview about existing results regarding stability and MPC for systems without disturbances can be found in [10] and recent results are included in [5–8]. To design stabilizing MPC controllers for nonlinear systems, a general framework can be found in [11].

Taking the unknown disturbance $w \in \mathcal{W}$ into account, MPC schemes which guarantee input-to-state stability (ISS) were developed. First results can be found in [12] regarding ISS for MPC of nonlinear discrete-time systems. Furthermore, results using the ISS property with initial states from a compact set, namely, regional-ISS, are given in [6, 13]. In [14, 15], an MPC scheme that guarantees ISS using the so-called *min-max approach* was given. The approach uses a closed-loop formulation of the optimization problem to compensate the effect of the unknown disturbance.

Stable MPC schemes for interconnected systems were investigated in [6, 16, 17], where in [6, 16] conditions to assure ISS of the whole system were derived and in [17] asymptotically stable MPC schemes without terminal constraints were provided. Note that in [17], the subsystems are not directly connected, but they exchange information over the network to control themselves according to state constraints.

One research topic of this paper provides a new direction in MPC: we combine the input-to-state dynamical stability (ISDS) property, introduced in [18], with MPC for single and interconnected systems. The provided MPC scheme uses the min-max approach (see [14, 15]). Conditions are derived such that single closed-loop systems and whole closed-loop networks with an optimal control obtained by an MPC scheme have the ISDS property. The results of [18] for single systems and the ISDS small-gain theorem for networks (see [19]) are applied to prove the main results of the corresponding section.

The advantage of the usage of ISDS over ISS for MPC is that the ISDS estimation takes only recent values of the disturbance into account due to the memory fading effect, see [18, 19]. In particular, if the disturbance tends to zero, then the ISDS estimation tends to zero, for example. Moreover, the decay rate can be derived using ISDS-Lyapunov functions. This information can be useful for applications of MPC.

In practice, there are problems, where the advantages of ISDS over ISS, in particular the memory fading effect of the ISDS estimation, lead to more efficient controllers with respect to costs. Examples are the control of air planes, robots, or automatic transportation vehicles.

A second research topic of this paper is the stability analysis of MPC schemes for systems with time-delays. In many applications, there occur time-delays, for example, in communication networks, logistic networks, or biological systems. The presence of time-delays can lead to instability of a network, see [9], where it was shown that the application of the control obtained by an MPC scheme to a system does not guarantee that a system without disturbances is asymptotically stable.

Therefore, we are interested in the analysis of networks with time-delays in view of input-to-state stability (ISS). In [2, 20], tools based on the Lyapunov-Razumikhin and

Lyapunov-Krasovskii approaches were developed to check, whether a single system with time-delays has the ISS property. Considering networks with time-delays recent results regarding ISS were given in [21] using a small-gain condition.

Considering time-delay systems (TDSs) and MPC, recent results for asymptotically stable MPC schemes of single systems can be found in [22, 23]. In these works, continuous-time TDSs were investigated and conditions were derived, which guarantee asymptotic stability of a TDS using a Lyapunov-Krasovskii approach. Moreover, by the help of Lyapunov-Razumikhin arguments it was shown, how to determine the terminal cost and terminal region, and to compute a locally stabilizing controller.

As a second part of this paper, we investigate the ISS property for MPC of single systems and networks with time-delays. Conditions are derived such that single closed-loop TDSs and whole closed-loop time-delay networks with an optimal control obtained by an MPC scheme have the ISS property. The results of the Lyapunov-Krasovskii approach, introduced in [20] for single systems and the corresponding small-gain theorem proved in [21] for networks with time-delays, are applied to prove the main results of the corresponding section.

Since time-delays and disturbances appear in many problems, the results of the second part of this paper regarding ISS for MPC of time-delay systems can be applied to a huge range of practical problems. Classical examples are not only communication networks, transportation, or production systems, but also biological networks or chemical networks.

In comparison to existing results in the literature, where only ISS for MPC for single systems (see [6, 13–15]) and networks (see [6, 16]) without time-delays was investigated, we use, on the one hand, the advantages of ISDS for MPC, in particular the memory fading effect. On the other hand, we use the stability notion ISS for MPC of systems with time-delays and disturbances, where in the literature only MPC schemes for single time-delay systems without disturbances were investigated in view of asymptotic stability (see [22, 23]). Both approaches presented in this paper were never done before, and this paper is a first theoretical step in the mentioned directions.

This paper is organized as follows: the preliminaries are given in Section 2. In Section 3.1, an MPC scheme of single systems guaranteeing ISDS is provided. ISDS for MPC of networks is investigated in Section 3.2, where we prove that each subsystem has the ISDS property and the whole network has the ISDS property using the control obtained by an MPC scheme. In Section 4.1, the ISS property for MPC of single systems is investigated. Networks with time-delays are considered in Section 4.2. Finally, the conclusions and an outlook for future research possibilities can be found in Section 5.

2. Preliminaries

By x^T we denote the transposition of a vector $x \in \mathbb{R}^n$, $n \in \mathbb{N}$; furthermore, $\mathbb{R}_+ := [0, \infty)$ and $\mathbb{R}^n_+$ denotes the positive orthant $\{x \in \mathbb{R}^n : x \geq 0\}$, where we use the standard partial order for $x, y \in \mathbb{R}^n$ given by

$$\begin{aligned} x \geq y &\Longleftrightarrow x_i \geq y_i, \quad i = 1, \ldots, n, \\ x \ngeq y &\Longleftrightarrow \exists i : x_i < y_i, \\ x > y &\Longleftrightarrow x_i > y_i, \quad i = 1, \ldots, n. \end{aligned} \tag{2.1}$$

$|\cdot|$ denotes the Euclidean norm in $\mathbb{R}^n$. The essential supremum norm of a (Lebesgue-) measurable function $f : \mathbb{R} \to \mathbb{R}^n$ is denoted by $\|f\|$. We denote the set of essentially bounded (Lebesgue-) measurable functions u from $\mathbb{R}$ to $\mathbb{R}^m$ by

$$L_\infty(\mathbb{R}, \mathbb{R}^m) := \{u : \mathbb{R} \longrightarrow \mathbb{R}^m \text{ measurable} \mid \exists K > 0 : |u(t)| \leq K, \text{ for almost all (f.a.a.) } t\}. \tag{2.2}$$

∇V is the gradient of a function $V : \mathbb{R}^n \to \mathbb{R}_+$.

For $t_1, t_2 \in \mathbb{R}$, $t_1 < t_2$, let $C([t_1, t_2]; \mathbb{R}^N)$ denotes the Banach space of continuous functions defined on $[t_1, t_2]$ equipped with the norm $\|\phi\|_{[t_1,t_2]} := \sup_{t_1 \leq s \leq t_2} |\phi(s)|$ and values in $\mathbb{R}^N$. Let $\theta \in \mathbb{R}_+$. The function $x^t \in C([-\theta, 0]; \mathbb{R}^N)$ is given by $x^t(\tau) := x(t + \tau), \tau \in [-\theta, 0]$.

For a function $v : \mathbb{R}_+ \to \mathbb{R}^m$, we define its restriction to the interval $[s_1, s_2]$ by

$$v_{[s_1,s_2]}(t) := \begin{cases} v(t) & \text{if } t \in [s_1, s_2], \\ 0 & \text{otherwise,} \end{cases} \quad t, s_1, s_2 \in \mathbb{R}_+. \tag{2.3}$$

Definition 2.1. We define the following classes of functions:

$$\begin{gathered}
\mathcal{P} := \{f : \mathbb{R}^n \longrightarrow \mathbb{R}_+ \mid f(0) = 0,\ f(x) > 0,\ x \neq 0\}, \\
\mathcal{K} := \{\gamma : \mathbb{R}_+ \to \mathbb{R}_+ \mid \gamma \text{ is continuous}, \gamma(0) = 0 \text{ and strictly increasing}\}, \\
\mathcal{K}_\infty := \{\gamma \in \mathcal{K} \mid \gamma \text{ is unbounded}\}, \\
\mathcal{L} := \left\{\gamma : \mathbb{R}_+ \to \mathbb{R}_+ \mid \gamma \text{ is continuous and decreasing with} \lim_{t \to \infty} \gamma(t) = 0\right\}, \\
\mathcal{KL} := \{\beta : \mathbb{R}_+ \times \mathbb{R}_+ \to \mathbb{R}_+ \mid \beta \text{ is continuous},\ \beta(\cdot, t) \in \mathcal{K},\ \beta(r, \cdot) \in \mathcal{L},\ \forall t, r \geq 0\}, \\
\mathcal{KLD} := \{\mu \in \mathcal{KL} \mid \mu(r, t + s) = \mu(\mu(r, t), s),\ \forall r, t, s \geq 0\}.
\end{gathered} \tag{2.4}$$

We will call functions of class $\mathcal{P}$ *positive definite*.

Now, we recall some results related to ISDS. Therefore, we consider systems of the form

$$\dot{x}(t) = f(x(t), u(t)), \tag{2.5}$$

where $t \in \mathbb{R}_+$ is the (continuous) time, $\dot{x}$ denotes the derivative of the state $x \in \mathbb{R}^N$, and $u \in L_\infty(\mathbb{R}_+, \mathbb{R}^m)$ is the input. The function $f : \mathbb{R}^{N+m} \to \mathbb{R}^N$, $N, m \in \mathbb{N}$, is assumed to be locally Lipschitz continuous in x uniformly in u to have existence and uniqueness of the solution, denoted by $x(t; x_0, u)$ or $x(t)$ for short, for the given initial value $x(0) = x_0$.

The notion of ISDS was introduced in [18].

Definition 2.2 (Input-to-state dynamical stability (ISDS)). The system (2.5) is called input-to-state dynamically stable (ISDS) if there exist $\mu \in \mathcal{KLD}$, $\eta, \gamma \in \mathcal{K}_\infty$ such that for all initial

values x_0 and all inputs u, it holds that

$$|x(t)| \leq \max\left\{\mu(\eta(|x_0|),t), \operatorname*{ess\,sup}_{\tau\in[0,t]} \mu(\gamma(|u(\tau)|),t-\tau)\right\}, \tag{2.6}$$

for all $t \in \mathbb{R}_+$. μ is called *decay rate*, η is called *overshoot gain,* and γ is called *robustness gain*.

A useful tool to check whether a system has the ISDS property is the following.

Definition 2.3 (ISDS-Lyapunov function). Given $\varepsilon > 0$, a function $V : \mathbb{R}^N \to \mathbb{R}_+$, which is locally Lipschitz on $\mathbb{R}^N \setminus \{0\}$, is called an ISDS-Lyapunov function of the system (2.5) if there exist $\eta, \gamma \in \mathcal{K}_\infty$, $\mu \in \mathcal{KLD}$ such that

$$\frac{|x|}{1+\varepsilon} \leq V(x) \leq \eta(|x|), \quad \forall x \in \mathbb{R}^N, \tag{2.7}$$

$$V(x) > \gamma(|u|) \Longrightarrow \nabla V(x) f(x,u) \leq -(1-\varepsilon) g(V(x)) \tag{2.8}$$

holds, for almost all $x \in \mathbb{R}^N \setminus \{0\}$ and all u, where μ solves

$$\frac{d}{dt}\mu(r,t) = -g(\mu(r,t)), \quad r,t > 0, \tag{2.9}$$

for a locally Lipschitz continuous function $g : \mathbb{R}_+ \to \mathbb{R}_+$.

The equivalence of ISDS and the existence of an ISDS-Lyapunov function were proved in [18].

Theorem 2.4. *The system* (2.5) *is ISDS with $\mu \in \mathcal{KLD}$ and $\eta, \gamma \in \mathcal{K}_\infty$ if and only if for each $\varepsilon > 0$ there exists an ISDS-Lyapunov function V.*

Remark 2.5. Note that for a system, which possesses the ISDS property, it holds that the decay rate μ and gains η, γ in Definition 2.2 are exactly the same as in Definition 2.3.

Now, consider networks of the form

$$\dot{x}_i(t) = f_i(x_1(t), \ldots, x_n(t), u_i(t)), \quad i = 1, \ldots, n, \tag{2.10}$$

where $n \in \mathbb{N}$, $x_i \in \mathbb{R}^{N_i}$, $N_i \in \mathbb{N}$, $u_i \in L_\infty(\mathbb{R}_+, \mathbb{R}^{M_i})$, and $f_i : \mathbb{R}^{\sum_{j=1}^n N_j + M_i} \to \mathbb{R}^{N_i}$ are locally Lipschitz in $x = (x_1^T, \ldots, x_n^T)^T$ uniformly in u_i, $i = 1, \ldots, n$. If we define $N := \sum N_i$, $m = \sum M_i$, and $f := (f_1^T, \ldots, f_n^T)^T$, then (2.10) can be written as a system of the form (2.5), which we call the whole system.

The ith *subsystem of* (2.10) *is called ISDS* if there exists a $\mathcal{KLD}$-function μ_i and functions η_i, γ_i, and $\gamma_{ij} \in \mathcal{K}_\infty \cup \{0\}$ such that the solution $x_i(t; x_i^0, u_i) = x_i(t)$ for all initial values x_i^0, all inputs x_j, $j \neq i$, u_i, and for all $t \in \mathbb{R}_+$ satisfies

$$\begin{gathered}
|x_i(t)| \leq \max\left\{\mu_i\left(\eta_i\left(\left|x_i^0\right|\right), t\right), \max_{j\neq i} v_{ij}(x_j, t), v_i(u_i, t)\right\}, \\
v_i(u_i, t) := \operatorname*{ess\,sup}_{\tau\in[0,t]} \mu_i(\gamma_i(|u_i(\tau)|), t-\tau), \\
v_{ij}(x_j, t) := \sup_{\tau\in[0,t]} \mu_i(\gamma_{ij}(|x_j(\tau)|), t-\tau)
\end{gathered} \tag{2.11}$$

$i, j = 1, \ldots, n$, $i \neq j$. γ_{ij} are called gains.

We collect all the gains in a matrix Γ, defined by $\Gamma := (\gamma_{ij})_{n\times n}$ with $\gamma_{ii} \equiv 0$, $i, j = 1, \ldots, n$. This defines a map $\Gamma : \mathbb{R}_+^n \to \mathbb{R}_+^n$ for $s \in \mathbb{R}_+^n$ by

$$\Gamma(s) := \left(\max_j \gamma_{1j}(s_j), \ldots, \max_j \gamma_{nj}(s_j)\right)^T. \tag{2.12}$$

In view of ISDS of the whole network, we say that Γ satisfies the *small-gain condition (SGC)* (see [24]) if

$$\Gamma(s) \not\geq s, \quad \forall s \in \mathbb{R}_+^n \setminus \{0\}. \tag{2.13}$$

To recall the Lyapunov version of the small-gain theorem for ISDS, we need the following.

Definition 2.6. A continuous path $\sigma \in \mathcal{K}_\infty^n$ is called an Ω-path with respect to Γ if

(i) for each i, the function σ_i^{-1} is locally Lipschitz continuous on $(0, \infty)$;

(ii) for every compact set $P \subset (0, \infty)$, there are constants $0 < K_1 < K_2$ such that for all points of differentiability of σ_i^{-1} and $i = 1, \ldots, n$ we have

$$0 < K_1 \leq \left(\sigma_i^{-1}\right)'(r) \leq K_2, \quad \forall r \in P; \tag{2.14}$$

(iii) it holds that $\Gamma(\sigma(r)) < \sigma(r)$, for all $r > 0$.

More details about an Ω-path can be found in [24–26].

The following proposition is useful for the construction of an ISDS-Lyapunov function for the whole system.

Proposition 2.7. *Let $\Gamma \in (\mathcal{K}_\infty \cup \{0\})^{n\times n}$ be a gain-matrix. If Γ satisfies the small-gain condition* (2.13)*, then there exists an Ω-path σ with respect to Γ.*

The proof can be found in [24], for example.

We assume that for each subsystem of (2.10) there exists a function $V_i : \mathbb{R}^{N_i} \to \mathbb{R}_+$, which is locally Lipschitz continuous and positive definite. Given $\varepsilon_i > 0$, a function $V_i : \mathbb{R}^{N_i} \to \mathbb{R}_+$, which is locally Lipschitz continuous on $\mathbb{R}^{N_i} \setminus \{0\}$, is an *ISDS-Lyapunov function of the ith subsystem in* (2.10) if it satisfies the following:

(i) there exists a function $\eta_i \in \mathcal{K}_\infty$ such that for all $x_i \in \mathbb{R}^{N_i}$ it holds

$$\frac{|x_i|}{1+\varepsilon_i} \le V_i(x_i) \le \eta_i(|x_i|); \tag{2.15}$$

(ii) there exist functions $\mu_i \in \mathcal{KLD}$, $\gamma_i \in \mathcal{K}_\infty \cup \{0\}$, $\gamma_{ij} \in \mathcal{K}_\infty \cup \{0\}$, $j = 1, \ldots, n$, $i \neq j$ such that for almost all $x_i \in \mathbb{R}^{N_i} \setminus \{0\}$, all inputs x_j, $j \neq i$, and u_i it holds that

$$V_i(x_i) > \max\left\{\max_{j\neq i} \gamma_{ij}\left(V_j\left(x_j\right)\right), \gamma_i(|u_i|)\right\} \Longrightarrow \nabla V_i(x_i) f_i(x,u) \le -(1-\varepsilon_i) g_i(V_i(x_i)), \tag{2.16}$$

where $\mu_i \in \mathcal{KLD}$ solves $(d/dt)\mu_i(r,t) = -g_i(\mu_i(r,t))$, $r,t > 0$ for some locally Lipschitz function $g_i : \mathbb{R}_+ \to \mathbb{R}_+$.

Now, we recall the main result of [19], which establishes ISDS for networks using Lyapunov functions.

Theorem 2.8. *Assume that each subsystem of* (2.10) *has the ISDS property. This means that for each subsystem and for each $\varepsilon_i > 0$ there exists an ISDS-Lyapunov function V_i, which satisfies* (2.15) *and* (2.16). *Let Γ be given by* (2.12), *satisfying the small-gain condition* (2.13), *and let $\sigma \in \mathcal{K}_\infty^n$ be an Ω-path from Proposition 2.7 with respect to Γ. Then, the whole system* (2.5) *has the ISDS property and its ISDS-Lyapunov function is given by*

$$V(x) = \psi^{-1}\left(\max_i\left\{\sigma_i^{-1}(V_i(x_i))\right\}\right), \tag{2.17}$$

where $\psi(|x|) = \min_i \sigma_i^{-1}(|x|/\sqrt{n})$.

As a second topic of this paper, we are going to establish ISS with the help of MPC for TDSs of the form

$$\begin{aligned} \dot{x}(t) &= f\left(x^t, u(t)\right), \quad t \in \mathbb{R}_+, \\ x^0(\tau) &= \xi(\tau), \quad \tau \in [-\theta, 0], \end{aligned} \tag{2.18}$$

where $x \in \mathbb{R}^N$, $u \in L_\infty(\mathbb{R}_+, \mathbb{R}^m)$, and "$\cdot$" represents the right-hand side derivative. θ is the maximum involved delay, and $f : C([-\theta,0];\mathbb{R}^N) \times \mathbb{R}^m \to \mathbb{R}^N$ is locally Lipschitz continuous on any bounded set. This guarantees that the system (2.18) admits a unique solution on a maximal interval $[-\theta, T_{\max})$, $0 < T_{\max} \le +\infty$, which is locally absolutely continuous, see [27, Section 2.6]. We denote the solution by $x(t;\xi,u)$ or $x(t)$ for short, satisfying the initial condition $x^0 \equiv \xi$ for any $\xi \in C([-\theta,0],\mathbb{R}^N)$.

The notion of ISS for TDSs reads as follows.

Definition 2.9 (ISS for TDSs). The system (2.18) is called ISS if there exist $\beta \in \mathcal{KL}$ and $\gamma \in \mathcal{K}$ such that for all ξ, all u, and all $t \in \mathbb{R}_+$ it holds that

$$|x(t)| \leq \max\left\{\beta\left(\|\xi\|_{[-\theta,0]}, t\right), \gamma(\|u\|)\right\}. \tag{2.19}$$

In [20], ISS-Lyapunov-Krasovskii functionals are introduced to check whether a TDS has the ISS property. Given a locally Lipschitz continuous functional $V : C([-\theta,0];\mathbb{R}^N) \to \mathbb{R}_+$, the upper right-hand side derivate D^+V of the functional V along the solution $x(t;\xi,u)$ is defined according to [27, Chapter 5.2]

$$D^+V(\phi,u) := \limsup_{h\to 0^+} \frac{1}{h}\left(V\left(x^{t+h}\right) - V(\phi)\right), \tag{2.20}$$

where $x^{t+h} \in C([-\theta,0];\mathbb{R}^N)$ is generated by the solution $x(t;\phi,u)$ of $\dot{x}(t) = f(x^t, u(t))$, and $t \in (t_0, t_0+h)$ with $x^{t_0} := \phi \in C([-\theta,0];\mathbb{R}^N)$.

Remark 2.10. Note that in contrast to (2.20), the definition of D^+V in [20] is slightly different, since there the functional is assumed to be only continuous and in that case, D^+V can take infinite values. Nevertheless, the results in [20] also hold true if the functional is chosen to be locally Lipschitz, according to the results in [28] and using (2.20).

By $\|\cdot\|_a$, we indicate any norm in $C([-\theta,0];\mathbb{R}^N)$ such that for some $c_1, c_2 \in \mathbb{R}_+ \setminus \{0\}$ the following inequalities hold:

$$c_1|\phi(0)| \leq \|\phi\|_a \leq c_2\|\phi\|_{[-\theta,0]}, \quad \forall \phi \in C\left([-\theta,0];\mathbb{R}^N\right). \tag{2.21}$$

Definition 2.11 (ISS-Lyapunov-Krasovskii functional). A locally Lipschitz continuous functional $V : C([-\theta,0];\mathbb{R}^N) \to \mathbb{R}_+$ is called an ISS-Lyapunov-Krasovskii functional for the system (2.18) if there exist functions $\varphi_1, \varphi_2 \in \mathcal{K}_\infty$ and functions $\chi, \alpha \in \mathcal{K}$ such that

$$\varphi_1(|\phi(0)|) \leq V(\phi) \leq \varphi_2(\|\phi\|_a), \tag{2.22}$$

$$V(\phi) \geq \chi(|u|) \implies D^+V(\phi,u) \leq -\alpha(V(\phi)), \tag{2.23}$$

for all $\phi \in C([-\theta,0];\mathbb{R}^N)$, $u \in L_\infty(\mathbb{R}_+,\mathbb{R}^m)$.

The next theorem was proved in [20].

Theorem 2.12. *If there exists an ISS-Lyapunov-Krasovskii functional V for the system* (2.18), *then the system* (2.18) *has the ISS property.*

Now, we investigate networks with time-delays: we consider $n \in \mathbb{N}$ interconnected TDSs of the form

$$\dot{x}_i(t) = f_i\left(x_1^t, \ldots, x_n^t, u_i(t)\right), \quad i = 1, \ldots, n, \tag{2.24}$$

where $x_i^t \in C([-\theta,0];\mathbb{R}^{N_i})$, $x_i^t(\tau) := x_i(t+\tau)$, $\tau \in [-\theta,0]$, $x_i \in \mathbb{R}^{N_i}$, and $u_i \in L_\infty(\mathbb{R}_+,\mathbb{R}^{M_i})$. θ denotes the maximal involved delay and x_j^t, $j \neq i$ can be interpreted as internal inputs of

the ith subsystem. The functionals $f_i : C([-\theta,0];\mathbb{R}^{N_1}) \times \cdots \times C([-\theta,0];\mathbb{R}^{N_n}) \times \mathbb{R}^{M_i} \to \mathbb{R}^{N_i}$ are locally Lipschitz continuous on any bounded set. We denote the solution of a subsystem by $x_i(t;\xi_i,u)$ or $x_i(t)$ for short, satisfying the initial condition $x_i^0 \equiv \xi_i$ for any $\xi_i \in C([-\theta,0],\mathbb{R}^{N_i})$.

The ISS property for a subsystem of (2.24) reads as follows: the *i subsystem of* (2.24) *is ISS* if there exist $\beta_i \in \mathcal{KL}$, $\gamma_{ij}, \gamma_i \in \mathcal{K}_\infty \cup \{0\}$, $j = 1,\ldots,n$, $j \neq i$ such that for all $t \in \mathbb{R}_+$ it holds

$$|x_i(t)| \leq \max\left\{\beta_i\left(\|\xi_i\|_{[-\theta,0]},t\right), \max_{j,j\neq i}\gamma_{ij}\left(\|x_j\|_{[-\theta,t]}\right), \gamma_i(\|u_i\|)\right\}. \tag{2.25}$$

If we define $N := \sum N_i$, $m := \sum M_i$, $x := (x_1^T,\ldots,x_n^T)^T$, $u = (u_1^T,\ldots,u_n^T)^T$, and $f := (f_1^T, \ldots, f_n^T)^T$, then (2.24) can be written as a system of the form (2.18), which we call the whole system. The Krasovskii functionals for subsystems are as follows.

A locally Lipschitz continuous functional $V_i : C([-\theta,0];\mathbb{R}^{N_i}) \to \mathbb{R}_+$ is an *ISS-Lyapunov-Krasovskii functional of the ith subsystem* of (2.24) if there exist functionals V_j, $j = 1,\ldots,n$, which are positive definite and locally Lipschitz continuous on $C([-\theta,0];\mathbb{R}^{N_j})$, functions $\psi_{1i}, \psi_{2i} \in \mathcal{K}_\infty$, $\tilde{\chi}_{ij}, \tilde{\chi}_i \in \mathcal{K} \cup \{0\}$, and $\tilde{\alpha}_i \in \mathcal{K}$, $j = 1,\ldots,n$, $i \neq j$ such that for all $\phi_i \in C([-\theta,0],\mathbb{R}^{N_i})$

$$\begin{gathered}\psi_{1i}(|\phi_i(0)|) \leq V_i(\phi_i) \leq \psi_{2i}(\|\phi_i\|_a), \\ V_i(\phi_i) \geq \max\left\{\max_{j,j\neq i}\tilde{\chi}_{ij}(V_j(\phi_j)), \tilde{\chi}_i(|u_i|)\right\} \Longrightarrow D^+V_i(\phi_i,u) \leq -\tilde{\alpha}_i(V_i(\phi_i)),\end{gathered} \tag{2.26}$$

for all $\phi_i \in C([-\theta,0],\mathbb{R}^{N_i})$, $u \in L_\infty(\mathbb{R}_+,\mathbb{R}^m)$.

The gain-matrix is defined by $\Gamma := (\chi_{ij})_{n\times n}$, $\chi_{ii} \equiv 0$, $i = 1,\ldots,n$, which defines a map $\Gamma : \mathbb{R}_+^n \to \mathbb{R}_+^n$ as in (2.12).

The next theorem is one of the main results of [21] and provides a construction for an ISS-Lyapunov-Krasovskii functional of the whole system.

Theorem 2.13 (ISS-Lyapunov-Krasovskii theorem for general networks with time-delays). *Consider an interconnected system of the form* (2.24). *Assume that each subsystem has an ISS-Lyapunov-Krasovskii functional V_i, which satisfies the conditions* (2.26), $i = 1,\ldots,n$. *If the corresponding gain-matrix Γ satisfies the small-gain condition* (2.13), *then*

$$V(\phi) := \max_i\left\{\sigma_i^{-1}(V_i(\phi_i))\right\} \tag{2.27}$$

is the ISS-Lyapunov-Krasovskii functional for the whole system of the form (2.18), *which is ISS, where $\sigma = (\sigma_1,\ldots,\sigma_n)^T$ is an Ω-path as in Definition 2.6 and $\phi = (\phi_i,\ldots,\phi_n)^T \in C([-\theta,0];\mathbb{R}^N)$. The Lyapunov gain is given by $\chi(r) := \max_i\sigma_i^{-1}(\chi_i(r))$, $r > 0$.*

Now, we present the new directions in MPC: ISDS and ISS for single and interconnected systems with and without time-delays. We start with MPC schemes guaranteeing ISDS.

3. MPC and ISDS

In this section, we combine ISDS and MPC for nonlinear single and interconnected systems. Conditions are derived, which assure ISDS of a system is obtained by application of the control to the system (1.1), and calculated by an MPC scheme.

3.1. Single Systems

We consider systems of the form (1.1) and we use the min-max approach to calculate an optimal control: to compensate the effect of the disturbance w, we apply a *feedback control law* $\pi(t, x(t))$ to the system. An optimal control law is obtained by solving the finite horizon optimal control problem (FHOCP), which consists of minimization of the cost function J with respect to $\pi(t, x(t))$ and maximization of the cost function J with respect to the disturbance w. The following definition is taken from [14, 15] with a slightly adjustment using ε here to apply the ISDS property to the FHOCP.

Definition 3.1 (Finite horizon optimal control problem (FHOCP)). Let $1 > \varepsilon > 0$ be given. Let $T > 0$ be the prediction horizon and $u(t) = \pi(t, x(t))$ a feedback control law. The finite horizon optimal control problem for a system of the form (1.1) is formulated as

$$\begin{aligned}
&\min_{\pi}\max_{w} \quad J(\overline{x}_0, \pi, w; t, T) \\
&:= \min_{\pi}\max_{w} \quad (1-\varepsilon)\int_t^{t+T} \left(l\left(x(t'), \pi(t', x(t'))\right) - l_w\left(w(t')\right)\right)dt' + V_f(x(t+T)) \\
&\text{subject to} \\
&\qquad \dot{x}(t') = f\left(x(t'), w(t'), u(t')\right), \qquad x(t) = \overline{x}_0, \quad t' \in [t, t+T], \\
&\qquad x \in \mathcal{X}, \\
&\qquad w \in \mathcal{W}, \\
&\qquad \pi \in \Pi, \\
&\qquad x(t+T) \in \Omega \subseteq \mathbb{R}^N,
\end{aligned} \tag{3.1}$$

where $\overline{x}_0 \in \mathbb{R}^N$ is the initial value of the system at time t, the terminal region Ω is a compact and convex set with the origin in its interior, and $\pi(t, x(t))$ is essentially bounded, locally Lipschitz in x and measurable in t. $l - l_w$ is the stage cost, where $l : \mathbb{R}^N \times \mathbb{R}^m \to \mathbb{R}_+$ penalizes the distance of the state from the equilibrium point 0 of the system and it penalizes the control effort. $l_w : \mathbb{R}^P \to \mathbb{R}_+$ penalizes the disturbance, which influences the systems behavior. l and l_w are locally Lipschitz continuous with $l(0,0) = 0$, $l_w(0) = 0$, and $V_f : \Omega \to \mathbb{R}_+$ is the terminal penalty.

The FHOCP will be solved at the sampling instants $t = k\Delta$, $k \in \mathbb{N}, \Delta \in \mathbb{R}_+$. The optimal solution is denoted by $\pi^*(t', x(t'); t, T)$ and $w^*(t')$, $t' \in [t, t+T]$. The optimal cost function is

denoted by $J^*(\overline{x}_0, \pi^*, w^*; t, T)$. The control input to the system (1.1) is defined in the usual receding horizon fashion as

$$u(t') = \pi^*(t', x(t'); t, T), \quad t' \in [t, t+\Delta]. \tag{3.2}$$

In the following, we need some definitions, which can be found, for example, in [5].

Definition 3.2. (i) A feedback control π is called a feasible solution of the FHOCP at time t, if for a given initial value $\overline{x}_0$ at time t the feedback $\pi(t', x(t')), t' \in [t, t+T]$ controls the state of the system (1.1) into Ω at time $t+T$, that is, $x(t+T) \in \Omega$, for all $w \in \mathcal{W}$.

(ii) A set $\Omega \subseteq \mathbb{R}^N$ is called positively invariant if for all $x_0 \in \Omega$ a feedback control π keeps the trajectory of the system (1.1) in Ω, that is,

$$x(t; x_0, w, \pi) \in \Omega, \quad \forall t \in (0, \infty), \tag{3.3}$$

for all $w \in \mathcal{W}$.

To prove that the system (1.1) with the control obtained by solving the FHOCP has the ISDS property, we need the following assumption.

Assumption 3.3. (1) There exist functions α_l, $\alpha_w \in \mathcal{K}_\infty$, where α_l is locally Lipschitz continuous such that

$$\begin{gathered} l(x, \pi) \geq \alpha_l(|x|), \quad x \in \mathcal{X},\ \pi \in \Pi, \\ l_w(w) \leq \alpha_w(|w|), \quad w \in \mathcal{W}. \end{gathered} \tag{3.4}$$

(2) The FHOCP in Definition 3.1 admits a feasible solution at the initial time $t = 0$.

(3) There exists a controller $u(t) = \pi(t, x(t))$ such that the system (1.1) has the ISDS property.

(4) For each $1 > \varepsilon > 0$, there exists a locally Lipschitz continuous function $V_f(x)$ such that the terminal region Ω is a positively invariant set and we have

$$V_f(x) \leq \eta(|x|), \quad \forall x \in \Omega, \tag{3.5}$$

$$\dot{V}_f(x) \leq -(1-\varepsilon) l(x, \pi) + (1-\varepsilon) l_w(w), \quad \text{f.a.a. } x \in \Omega, \tag{3.6}$$

where $\eta \in \mathcal{K}_\infty$, $w \in \mathcal{W}$, and $\dot{V}_f$ denotes the derivative of V_f along the solution of system (1.1) with the control $u \equiv \pi$ from point 3 of this assumption.

(5) For each sufficiently small $\varepsilon > 0$, it holds that

$$(1-\varepsilon) \int_t^{t+T} l(x(t'), \pi(t', x(t'))) dt' \geq \frac{|x(t)|}{1+\varepsilon}. \tag{3.7}$$

(6) The optimal cost function $J^*(\overline{x}_0, \pi^*, w^*; t, T)$ is locally Lipschitz continuous.

Remark 3.4. In [6], it is discussed that a different stage cost, for example, by the definition of $l_s := l - l_w$, can be used for the FHOCP. In view of stability, the stage cost l_s has to fulfill some additional assumptions, see [6, Chapter 3.4].

Remark 3.5. The assumption (3.7) is needed to assure that the cost function satisfies the lower estimation in (2.7). However, we did not investigated whether this condition is restrictive or not. In case of discrete-time systems and the according cost function, the assumption (3.7) is not necessary, see the proofs in [6, 12–15].

The following theorem establishes ISDS of the system (1.1), using the optimal control input $u \equiv \pi^*$ obtained from solving the FHOCP.

Theorem 3.6. *Consider a system of the form* (1.1). *Under Assumption 3.3, the system resulting from the application of the predictive control strategy to the system, namely,* $\dot{x}(t) = f(x(t), w(t), \pi^*(t, x(t))), t \in \mathbb{R}_+, x(0) = x_0$, *possesses the ISDS property.*

Remark 3.7. Note that the gains and the decay rate of the definition of the ISDS property, Definition 2.2, can be calculated using Assumption 3.3, as it is partially displayed in the following proof.

Proof. We show that the optimal cost function $J^*(\overline{x}_0, \pi^*, w^*; t, T) =: V(\overline{x}_0)$ is an ISDS-Lyapunov function, following the steps:

(i) the control problem admits a feasible solution π for all times $t > 0$;

(ii) $J^*(\overline{x}_0, \pi^*, w^*; t, T)$ satisfies the conditions (2.7) and (2.8).

Then, by application of Theorem 2.4, the ISDS property follows.

Let us prove the following feasibility: we suppose that a feasible solution $\widetilde{\pi}(t', x(t'))$, $t' \in [t, t+T]$ at time t exists. For $\Delta > 0$, we construct a control by

$$\widehat{\pi}(t', x(t')) = \begin{cases} \widetilde{\pi}(t', x(t')), & t' \in [t+\Delta,\, t+T], \\ \pi(t', x(t')), & t' \in (t+T,\, t+T+\Delta], \end{cases} \tag{3.8}$$

where π is the controller from Assumption 3.3, point 3. Since $\widetilde{\pi}$ controls $x(t+\Delta)$ into $x(t+T) \in \Omega$ and Ω is a positively invariant set, $\pi(t', x(t'))$ keeps the systems trajectory in Ω for $t+T < t' \leq t+T+\Delta$ under the constraints of the FHOCP. This means that from the existence of a feasible solution for the time t, we have a feasible solution for the time $t+\Delta$. Since we assume that a feasible solution for the FHOCP at the time $t = 0$ exists (Assumption 3.3, point 2), it follows that a feasible solution exists for every $t > 0$.

We replace $\widetilde{\pi}$ in (3.8) by π^*. Then, it follows from (3.6) that

$$\begin{aligned} &J^*(\overline{x}_0, \pi^*, w^*; t, T+\Delta) \\ &\quad \leq J(\overline{x}_0, \widehat{\pi}, w^*; t, T+\Delta) \\ &\quad = (1-\varepsilon)\int_t^{t+T} \left(l\left(x(t'), \pi^*(t', x(t'); t, T)\right) - l_w(w^*(t'))\right) dt' \\ &\qquad + (1-\varepsilon)\int_{t+T}^{t+T+\Delta} \left(l\left(x(t'), \pi(t', x(t'))\right) - l_w(w^*(t'))\right) dt' \\ &\qquad + V_f(x(t+T+\Delta)) \end{aligned}$$

$$
\begin{aligned}
&= J^*(\overline{x}_0, \pi^*, w^*; t, T) - V_f(x(t+T)) + V_f(x(t+T+\Delta)) \\
&\quad + (1-\varepsilon)\int_{t+T}^{t+T+\Delta} \left(l\left(x(t'), \pi(t', x(t'))\right) - l_w\left(w^*(t')\right)\right) dt' \\
&\le J^*(\overline{x}_0, \pi^*, w^*; t, T)
\end{aligned}
\tag{3.9}
$$

holds. From this and with (3.5), it holds that

$$
J^*(\overline{x}_0, \pi^*, w^*; t, T) \le J^*(\overline{x}_0, \pi^*, w^*; t, 0) = V_f(\overline{x}_0) \le \eta(|\overline{x}_0|). \tag{3.10}
$$

Now, with Assumption 3.3, point 5, we have

$$
V(\overline{x}_0) \ge J(\overline{x}_0, \pi^*, 0; t, T) \ge (1-\varepsilon)\int_t^{t+T} l\left(x(t'), \pi^*(t', x(t'))\right) dt' \ge \frac{|\overline{x}_0|}{1+\varepsilon}. \tag{3.11}
$$

This shows that J^* satisfies (2.7). Now, denote $\tilde{x}_0 := x(t+h)$. From $J^*(\overline{x}_0, \pi^*, w^*; t, T + \Delta) \le J^*(\overline{x}_0, \pi^*, w^*; t, T)$, we get

$$
\begin{aligned}
&(1-\varepsilon)\int_t^{t+h} \left(l\left(x(t'), \pi^*(t', x(t'); t, T)\right) - l_w\left(w^*(t')\right)\right) dt' + J^*(\tilde{x}_0, \pi^*, w^*; t+h, T+\Delta-h) \\
&\quad \le (1-\varepsilon)\int_t^{t+h} \left(l\left(x(t'), \pi^*(t', x(t'); t, T)\right) - l_w\left(w^*(t')\right)\right) dt' \\
&\qquad + J^*(\tilde{x}_0, \pi^*, w^*; t+h, T-h),
\end{aligned}
\tag{3.12}
$$

and therefore

$$
J^*(\tilde{x}_0, \pi^*, w^*; t+h, T+\Delta-h) \le J^*(\tilde{x}_0, \pi^*, w^*; t+h, T-h). \tag{3.13}
$$

Now, we show that J^* satisfies the condition (2.8). Note that by Assumption 3.3, point 6, J^* is locally Lipschitz continuous. With (3.13), it holds that

$$
\begin{aligned}
&J^*(\overline{x}_0, \pi^*, w^*; t, T) \\
&\quad = (1-\varepsilon)\int_t^{t+h} \left(l\left(x(t'), \pi^*(t', x(t'); t, T)\right) - l_w\left(w^*(t')\right)\right) dt' \\
&\qquad + J^*(\tilde{x}_0, \pi^*, w^*; t+h, T-h) \\
&\quad \ge (1-\varepsilon)\int_t^{t+h} \left(l\left(x(t'), \pi^*(t', x(t'); t, T)\right) - l_w\left(w^*(t')\right)\right) dt' \\
&\qquad + J^*(\tilde{x}_0, \pi^*, w^*; t+h, T).
\end{aligned}
\tag{3.14}
$$

This leads to

$$\begin{aligned}&\frac{J^*(\tilde{x}_0,\pi^*,w^*;t+h,T)-J^*(\overline{x}_0,\pi^*,w^*;t,T)}{h}\\&\quad\le-\frac{1}{h}(1-\varepsilon)\int_t^{t+h}\left(l\left(x(t'),\pi^*(t',x(t');t,T)\right)-l_w\left(w^*(t')\right)\right)dt'.\end{aligned}\tag{3.15}$$

For $h \to 0$ and using the first point of Assumption 3.3, we obtain

$$\dot{V}(\overline{x}_0) \le -(1-\varepsilon)\alpha_l(|\overline{x}_0|) + (1-\varepsilon)\alpha_w(|w^*|), \quad \text{f.a.a. } \overline{x}_0 \in \mathcal{X},\ \forall w \in \mathcal{W}. \tag{3.16}$$

By definition of $\gamma(r) := \eta(\alpha_l^{-1}(2\alpha_w(r)))$ and $g(r) := (1/2)\alpha_l(\eta^{-1}(r)), r \ge 0$, this implies

$$V(\overline{x}_0) > \gamma(|w^*|) \Longrightarrow \dot{V}(\overline{x}_0) \le -(1-\varepsilon)g(V(\overline{x}_0)), \tag{3.17}$$

where the function g is locally Lipschitz continuous. We conclude that J^* is an ISDS-Lyapunov function for the system

$$\dot{x}(t) = f(x(t), w(t), \pi^*(t, x(t))), \tag{3.18}$$

and by application of Theorem 2.4 the system has the ISDS property. □

In the next subsection, we transform the analysis of ISDS for MPC of single systems to interconnected systems.

3.2. Interconnected Systems

We consider interconnected systems with disturbances of the form

$$\dot{x}_i(t) = f_i(x_1(t), \ldots, x_n(t), w_i(t), u_i(t)), \quad i = 1, \ldots, n, \tag{3.19}$$

where $u_i \in \mathbb{R}^{M_i}$, measurable and essentially bounded, are the control inputs and $w_i \in \mathbb{R}^{P_i}$ are the unknown disturbances. We assume that the states, disturbances, and inputs fulfill the constraints

$$x_i \in \mathcal{X}_i, \quad w_i \in \mathcal{W}_i, \quad u_i \in \mathcal{U}_i, \quad i = 1, \ldots, n, \tag{3.20}$$

where $\mathcal{X}_i \subseteq \mathbb{R}^{N_i}$, $\mathcal{W}_i \subseteq L_\infty(\mathbb{R}_+, \mathbb{R}^{P_i})$, and $\mathcal{U}_i \subseteq \mathbb{R}^{M_i}$ are compact and convex sets containing the origin in their interior.

Now, we are going to determine an MPC scheme for interconnected systems. An overview of existing distributed and hierarchical MPC schemes can be found in [29]. The used scheme in this work is inspired by the min-max approach for single systems as in Definition 3.1, see [14, 15].

At first, we determine the cost function of the ith subsystem by

$$\begin{aligned} J_i\left(\overline{x}_i^0, (x_j)_{j\neq i}, \pi_i, w_i; t, T\right) &:= (1-\varepsilon_i)\int_t^{t+T}\left(l_i(x_i(t'), \pi_i(t', x(t'))) - (l_w)_i(w_i(t')) - \sum_{j\neq i} l_{ij}(x_j(t'))\right)dt' \\ &\quad + (V_f)_i(x_i(t+T)), \end{aligned} \tag{3.21}$$

where $1 > \varepsilon_i > 0$, $\overline{x}_i^0 \in \mathcal{X}_i$ is the initial value of the ith subsystem at time t and $\pi_i \in \Pi_i$ is a feedback, essentially bounded, locally Lipschitz in x and measurable in t, where $\Pi_i \subseteq \mathbb{R}^{M_i}$ is a compact and convex set containing the origin in its interior. $l_i - (l_w)_i - \sum l_{ij}$ is the stage cost, where $l_i : \mathbb{R}^{N_i} \times \mathbb{R}^{M_i} \to \mathbb{R}_+$. $(l_w)_i : \mathbb{R}^{P_i} \to \mathbb{R}_+$ penalizes the disturbance and $l_{ij} : \mathbb{R}^{N_j} \to \mathbb{R}_+$ penalizes the internal input for all $j = 1, \ldots, n$, $j \neq i$. l_i, $(l_w)_i$ and l_{ij} are locally Lipschitz continuous functions with $l_i(0,0) = 0$, $(l_w)_i(0) = 0$, $l_{ij}(0) = 0$, and $(V_f)_i : \Omega_i \to \mathbb{R}_+$ is the terminal penalty of the ith subsystem, $\Omega_i \subseteq \mathbb{R}^{N_i}$.

In contrast to single systems, we add the terms $l_{ij}(x_j)$, $j \neq i$, to the cost function due to the interconnected structure of the subsystems. Here, two problems arise: the formulation of an optimal control problem for each subsystem and the calculation/determination of the internal inputs x_j, $j \neq i$.

We conserve the minimization of J_i with respect to π_i and the maximization of J_i with respect to w_i as in Definition 3.1 for single systems. In the spirit of ISS/ISDS, which treat the internal inputs as "disturbances," we maximize the cost function with respect to x_j, $j \neq i$ (worst-case approach). Since we assume that $x_j \in \mathcal{X}_j$, we get an optimal solution π_i^*, w_i^*, x_j^*, $j \neq i$, of the control problem.

The drawbacks of this approach are that, on the one hand, we do not use the systems equations (3.19) to predict x_j, $j \neq i$ and, on the other hand, the computation of the optimal solution could be numerically inefficient, especially if the number of subsystems n is "huge" or/and the sets $\mathcal{X}_i$ are "large." Moreover, taking into account the worst-case approach, the maximization over x_j, the obtained optimal control π_i^* for each subsystem could be extremely conservative, which leads to extremely conservative ISS or ISDS estimations.

To avoid these drawbacks of the maximization of J_i with respect to x_j, $j \neq i$, one could use the system equation (3.19) to predict x_j, $j \neq i$ instead.

A numerically efficient way to calculate the optimal solutions π_i^*, w_i^* of the subsystems is a parallel calculation. Due to interconnected structure of the system, the information about systems states of the subsystems should be exchanged. But this exchange of information causes that an optimal solution π_i^*, w_i^* could not be calculated. To the best of our knowledge, no theorem is proved that provides the existence of an optimal solution of the optimal control problem using such a parallel strategy. We conclude that a parallel calculation cannot help in our case.

Another approach of an MPC scheme for networks is inspired by the hierarchical MPC scheme in [30]. One could use the predictions of the internal inputs x_j, $j \neq i$, as follows: at sampling time $t = k\Delta$, $k \in \mathbb{N}$, $\Delta > 0$ all subsystems calculate the optimal solution iteratively. This means that for the calculation of the optimal solution for the ith subsystem,the currently "optimized" trajectories of the subsystems $1, \ldots, i-1$ will be used, denoted by $x_p^{\mathrm{opt},k\Delta}$, $p = 1, \ldots, i-1$, and the "optimal" trajectories of the subsystems $i+1, \ldots, n$ of the optimization at sampling time $t = (k-1)\Delta$ will be used, denoted by $x_p^{\mathrm{opt},(k-1)\Delta}$, $p = i+1, \ldots, n$.

The advantage of this approach would be that the optimal solution is not that much conservative as the min-max approach and the calculation of the optimal solution could be performed in a numerically efficient way, due to the usage of the model to predict the "optimal" trajectories and that the maximization over x_j, $j \neq i$ will be avoided. The drawback is that the optimal cost function of each subsystem depends on the trajectories $x_j^{\mathrm{opt},\cdot}$, $j \neq i$ using this hierarchical approach. Then, to the best of our knowledge, it is not possible to show that the optimal cost functions are ISDS-Lyapunov functions of the subsystems, which is a crucial step for proving ISDS of a subsystem or the whole network, because no helpful estimations for the Lyapunov function properties can be performed due to the dependence of the optimal cost functions of the trajectories $x_j^{\mathrm{opt},\cdot}$, $j \neq i$.

The FHOCP for the ith subsystem reads as follows:

$$\begin{aligned}
&\min_{\pi_i} \max_{w_i} \max_{(x_j)_{j\neq i}} \quad J_i\left(\overline{x}_i^0, (x_j)_{j\neq i}, \pi_i, w_i; t, T\right) \\
&\quad \text{subject to} \\
&\qquad \dot{x}_i(t') = f_i(x_1(t'), \ldots, x_n(t'), w_i(t'), u_i(t')), \quad t' \in [t, t+T], \\
&\qquad x_i(t) = \overline{x}_i^0, \\
&\qquad x_j \in \mathcal{X}_j, \quad j = 1, \ldots, n, \\
&\qquad w_i \in \mathcal{W}_i, \\
&\qquad \pi_i \in \Pi_i, \\
&\qquad x_i(t+T) \in \Omega_i \subseteq \mathbb{R}^{N_i},
\end{aligned} \tag{3.22}$$

where the terminal region Ω_i is a compact and convex set with the origin in its interior.

The resulting optimal control of each subsystem is a feedback control law, that is, $u_i^*(t) = \pi_i^*(t, x(t))$, where $x = (x_1^T, \ldots, x_n^T)^T \in \mathbb{R}^N$, $N = \sum_i N_i$, and $\pi_i^*(t, x^{*i}(t))$ is essentially bounded, locally Lipschitz in x, and measurable in t, for all $i = 1, \ldots, n$.

To show that each subsystem and the whole system have the ISDS property using the mentioned distributed MPC scheme, we suppose the following assumption for the ith subsystem of (3.19).

Assumption 3.8. (1) There exist functions $\alpha_i^l, \alpha_i^w, \alpha_{ij} \in \mathcal{K}_\infty$, $j = 1, \ldots, n$, $j \neq i$ such that

$$\begin{gathered}
l_i(x_i, \pi_i) \geq \alpha_i^l(|x_i|), \quad x_i \in \mathcal{X}_i,\ \pi_i \in \Pi_i, \\
(l_w)_i(w_i) \leq \alpha_i^w(|w_i|), \quad w_i \in \mathcal{W}_i, \\
l_{ij}(x_j) \leq \alpha_{ij}(V_j(x_j)), \quad x_j \in \mathcal{X}_j,\ j = 1, \ldots, n,\ j \neq i.
\end{gathered} \tag{3.23}$$

(2) The FHOCP admits a feasible solution at the initial time $t = 0$.

(3) There exists a controller $u_i(t) = \pi_i(t, x(t))$ such that the ith subsystem of (3.19) has the ISDS property.

(4) For each $1 > \varepsilon_i > 0$, there exists a locally Lipschitz continuous function $(V_f)_i(x_i)$ such that the terminal region Ω_i is a positively invariant set and we have

$$\begin{gathered}(V_f)_i(x_i) \leq \eta_i(|x_i|), \quad \forall x_i \in \Omega_i, \\ (\dot{V}_f)_i(x_i) \leq -(1-\varepsilon_i)l_i(x_i,\pi_i) + (1-\varepsilon_i)(l_w)_i(w_i) + (1-\varepsilon_i)\sum_{j\neq i} l_{ij}(x_j),\end{gathered} \tag{3.24}$$

for almost all $x_i \in \Omega_i$, where $\eta_i \in \mathcal{K}_\infty$, $w_i \in \mathcal{W}_i$, and $(\dot{V}_f)_i$ denotes the derivative of $(V_f)_i$ along the solution of the ith subsystem of (3.19) with the control $u_i \equiv \pi_i$ from point 3 of this assumption.

(5) For each sufficiently small $\varepsilon_i > 0$ it holds that

$$(1-\varepsilon_i)\int_t^{t+T} l_i(x_i(t'),\pi_i^*(t',x(t'))) - \sum_{j\neq i} l_{ij}(x_j(t'))dt' \geq \frac{|x(t)|}{1+\varepsilon_i}. \tag{3.25}$$

(6) The optimal cost function $J_i^*(\overline{x}_i^0,(x_j)_{j\neq i}^*,\pi_i^*,w_i^*;t,T)$ is locally Lipschitz continuous.

Now, we can state that each subsystem possesses the ISDS property using the mentioned MPC scheme.

Theorem 3.9. *Consider an interconnected system of the form* (3.19). *Let Assumption 3.8 be satisfied for each subsystem. Then, each subsystem resulting from the application of the control obtained by the FHOCP for each subsystem to the system, namely,*

$$\dot{x}_i(t) = f_i(x_1(t),\ldots,x_n(t),w_i(t),\pi_i^*(t,x(t))), \quad t\in\mathbb{R}_+,\ x_i^0 = x_i(0), \tag{3.26}$$

possesses the ISDS property.

Proof. Consider the ith subsystem. We show that the optimal cost function $V_i(\overline{x}_i^0) := J_i^*(\overline{x}_i^0, (x_j)_{j\neq i}^*,\pi_i^*,w_i^*;t,T)$ is an ISDS-Lyapunov function for the ith subsystem. We abbreviate $x_j = (x_j)_{j\neq i}^*$.

By following the steps of the proof of Theorem 3.6, we conclude that there exists a feasible solution for all times $t > 0$ and that by (3.25) the functional $V_i(\overline{x}_i^0)$ satisfies the condition

$$\frac{\left|\overline{x}_i^0\right|}{(1+\varepsilon_i)} \leq V_i\left(\overline{x}_i^0\right) \leq \eta_i\left(\left|\overline{x}_i^0\right|\right), \tag{3.27}$$

using $|\overline{x}_0| \geq |\overline{x}_i^0|$. Note that by Assumption 3.8, point 6, J_i^* is locally Lipschitz continuous. We have that it holds

$$\dot{V}_i\left(\overline{x}_i^0\right) \leq -(1-\varepsilon_i)\alpha_i^l\left(\eta_i^{-1}\left(V_i\left(\overline{x}_i^0\right)\right)\right) + (1-\varepsilon_i)\alpha_i^w(|w_i^*|) + (1-\varepsilon_i)\sum_{j\neq i}\alpha_{ij}\left(V_j\left(\left(\overline{x}_j^0\right)\right)\right), \tag{3.28}$$

and equivalently

$$\dot{V}_i\left(\overline{x}_i^0\right) \leq -(1-\varepsilon_i)\alpha_i^l\left(\eta_i^{-1}\left(V_i\left(\overline{x}_i^0\right)\right)\right) + (1-\varepsilon_i)\max\left\{n\alpha_i^w(|w_i^*|), \max_{j\neq i} n\alpha_{ij}\left(V_j\left(\left(\overline{x}_j^0\right)\right)\right)\right\}, \tag{3.29}$$

which implies

$$V_i\left(\overline{x}_i^0\right) > \max\left\{\gamma_i(|w_i^*|), \max_{j\neq i}\gamma_{ij}\left(V_j\left(\left(\overline{x}_i^0\right)\right)\right)\right\} \Longrightarrow \dot{V}_i\left(\overline{x}_i^0\right) \leq -(1-\varepsilon_i)g_i\left(V_i\left(\overline{x}_i^0\right)\right), \tag{3.30}$$

for almost all $\overline{x}_i^0 \in \mathcal{X}_i$ and all $w_i^* \in \mathcal{W}_i$, where $\gamma_i(r) := \eta_i((\alpha_i^l)^{-1}(2n\alpha_i^w(r)))$, $\gamma_{ij}(r) := \eta_i((\alpha_i^l)^{-1}(2n\alpha_{ij}(r)))$ and $g_i(r) := (1/2)\alpha_i^l(\eta_i^{-1}(r))$, where g_i is locally Lipschitz continuous.

Since i can be chosen arbitrarily, we conclude that each subsystem has an ISDS-Lyapunov function. It follows that each subsystem has the ISDS property. □

To investigate whether the whole system has the ISDS property, we collect all functions γ_{ij} in a matrix $\Gamma := (\gamma_{ij})_{n\times n}$, $\gamma_{ii} \equiv 0$, which defines a map as in (2.12).

Using the small-gain condition for Γ, the ISDS property for the whole system can be guaranteed.

Corollary 3.10. *Consider an interconnected system of the form* (3.19). *Let Assumption 3.8 be satisfied for each subsystem. If* Γ *satisfies the small-gain condition* (2.13), *then the whole system possesses the ISDS property.*

Proof. Each subsystem has an ISDS-Lyapunov function with gains γ_{ij}. This follows from Theorem 3.9. The matrix Γ satisfies the SGC, and all assumptions of Theorem 2.8 are satisfied. It follows that with $x = (x_1^T, \ldots, x_n^T)^T$, $w = (w_1^T, \ldots, w_n^T)^T$, and $\pi^*(\cdot, x(\cdot)) = ((\pi_1^*(\cdot, x(\cdot)))^T, \ldots, (\pi_n^*(\cdot, x(\cdot)))^T)^T$, the whole system of the form

$$\dot{x}(t) = f(x(t), w(t), \pi^*(t, x(t))) \tag{3.31}$$

has the ISDS property. □

In the next section, we investigate the ISS property for MPC of TDS.

4. MPC and ISS for Time-Delay Systems

Now, we introduce the ISS property for MPC of TDS. We derive conditions to assure that a single system, a subsystem of a network, and the whole system possess the ISS property applying the control obtained by an MPC scheme for TDS.

4.1. Single Systems

We consider systems of the form (2.18) with disturbances,

$$\begin{aligned} \dot{x}(t) &= f\left(x^t, w(t), u(t)\right), \quad t \in \mathbb{R}_+, \\ x_0(\tau) &= \xi(\tau), \quad \tau \in [-\theta, 0], \end{aligned} \tag{4.1}$$

where $w \in \mathcal{W} \subseteq L_\infty(\mathbb{R}_+, \mathbb{R}^P)$ is the unknown disturbance and $\mathcal{W}$ is a compact and convex set containing the origin. The input u is an essentially bounded and measurable control subject to input constraints $u \in \mathcal{U}$, where $\mathcal{U} \subseteq \mathbb{R}^{\Updownarrow}$ is a compact and convex set containing the origin in its interior. The functional f has to satisfy the same conditions as in the previous section to assure that a unique solution exists, which is denoted by $x(t; \xi, w, u)$ or $x(t)$ in short.

The aim is to find an (optimal) control u such that the system (4.1) has the ISS property.

Due to the presence of disturbances, we apply a feedback control structure, which compensates the effect of the disturbance. This means that we apply a *feedback control law* $\pi(t, x^t)$ to the system. In the rest of this section, we assume that $\pi(t, x^t) \in \Pi$ is essentially bounded, locally Lipschitz in x^t, and measurable in t. The set $\Pi \subseteq \mathbb{R}^m$ is assumed to be compact and convex containing the origin in its interior. We obtain an MPC control law by solving the control problem.

Definition 4.1 (Finite horizon optimal control problem with time-delays (FHOCPTD)). Let T be the prediction horizon and $\pi(t, x^t)$ a feedback control law. The finite horizon optimal control problem with time-delays for a system of the form (4.1) is formulated as

$$\begin{aligned} &\min_{\pi} \max_{w} \quad \left(\bar{\xi}, \pi, w; t, T\right) \\ &:= \min_{\pi} \max_{w} \quad \int_t^{t+T} \left(l\left(x(t'), \pi\left(t', x^{t'}\right)\right) - l_w(w(t'))\right) dt' + V_f\left(x^{t+T}\right) \\ &\text{subject to} \\ &\qquad \dot{x}(t') = f\left(x^{t'}, w(t'), u(t')\right), \quad t' \in [t, t+T], \\ &\qquad x(t+\tau) = \bar{\xi}(\tau), \quad \tau \in [-\theta, 0], \\ &\qquad x^{t'} \in \mathcal{X}, \\ &\qquad w \in \mathcal{W}, \\ &\qquad \pi \in \Pi, \\ &\qquad x^{t+T} \in \Omega \subseteq C\left([-\theta, 0], \mathbb{R}^N\right), \end{aligned} \tag{4.2}$$

where $\bar{\xi} \in C([-\theta, 0], \mathbb{R}^N)$ is the initial function of the system at time t, and the terminal region Ω and the state constraint set $\mathcal{X} \subseteq C([-\theta, 0], \mathbb{R}^N)$ are compact and convex sets with the origin in their interior. $l - l_w$ is the stage cost, where $l : \mathbb{R}^N \times \mathbb{R}^m \to \mathbb{R}_+$ and $l_w : \mathbb{R}^P \to \mathbb{R}_+$ are locally Lipschitz continuous with $l(0,0) = 0$, $l_w(0) = 0$, and $V_f : \Omega \to \mathbb{R}_+$ is the terminal penalty.

The control problem will be solved at the sampling instants $t = k\Delta$, $k \in \mathbb{N}$, and $\Delta \in \mathbb{R}_+$. The optimal solution is denoted by $\pi^*(t', x^{t'}; t, T)$ and $w^*(t')$, $t' \in [t, t+T]$ and the optimal cost functional is denoted by $J^*(\bar{\xi}, \pi^*, w^*; t, T)$. The control input to the system (4.1) is defined in the usual receding horizon fashion as

$$u(t') = \pi^*\left(t', x^{t'}; t, T\right), \quad t' \in [t, t+\Delta]. \tag{4.3}$$

Definition 4.2. (i) A feedback control π is called a feasible solution of the FHOCPTD at time t if for a given initial function $\bar{\xi}$ at time t the feedback $\pi(t', x^{t'})$, $t' \in [t, t+T]$ controls the state of the system (4.1) into Ω at time $t+T$, that is, $x^{t+T} \in \Omega$, for all $w \in \mathcal{W}$.

(ii) A set $\Omega \subseteq C([-\theta, 0], \mathbb{R}^N)$ is called positively invariant if for all initial functions $\bar{\xi} \in \Omega$ a feedback control π keeps the trajectory of the system (4.1) in Ω, that is,

$$x^t \in \Omega, \quad \forall t \in (0, \infty), \tag{4.4}$$

for all $w \in \mathcal{W}$.

For the goal of this section, establishing ISS of TDS with the help of MPC, we need the following.

Assumption 4.3. (1) There exist functions $\alpha_l, \alpha_w \in \mathcal{K}_\infty$ such that

$$\begin{gathered} l(\phi(0), \pi) \geq \alpha_l(|\phi|_a), \quad \phi \in \mathcal{X},\ \pi \in \Pi, \\ l_w(w) \leq \alpha_w(|w|), \quad w \in \mathcal{W}. \end{gathered} \tag{4.5}$$

(2) The FHOCPTD in Definition 4.1 admits a feasible solution at the initial time $t = 0$.

(3) There exists a controller $u(t) = \pi(t, x^t)$ such that the system (4.1) has the ISS property.

(4) There exists a locally Lipschitz continuous functional $V_f(\phi)$ such that the terminal region Ω is a positively invariant set and for all $\phi \in \Omega$ we have

$$V_f(\phi) \leq \varphi_2(|\phi|_a), \tag{4.6}$$

$$D^+V_f(\phi, w) \leq -l(\phi(0), \pi) + l_w(w), \tag{4.7}$$

where $\varphi_2 \in \mathcal{K}_\infty$, $w \in \mathcal{W}$, and D^+V_f denotes the upper right-hand side derivate of the functional V along the solution of (4.1) with the control $u \equiv \pi$ from point 3 of this assumption.

(5) There exists a $\mathcal{K}_\infty$ function φ_1 such that for all $t > 0$ it holds

$$\int_t^{t+T} l\left(x(t'), \pi\left(t', x^{t'}\right)\right) dt' \geq \varphi_1\left(\left|\bar{\xi}(0)\right|\right), \quad \bar{\xi}(0) = x(t). \tag{4.8}$$

(6) The optimal cost functional $J^*(\bar{\xi}, \pi^*, w^*; t, T)$ is locally Lipschitz continuous.

Now, we can state a theorem that assures ISS of MPC for a single time-delay system with disturbances.

Theorem 4.4. *Let Assumption 4.3 be satisfied. Then, the system resulting from the application of the predictive control strategy to the system, namely,* $\dot{x}(t) = f(x^t, w(t), \pi^*(t, x^t))$, $t \in \mathbb{R}_+$, $x_0(\tau) = \xi(\tau)$, $\tau \in [-\theta, 0]$, *possesses the ISS property.*

Proof. The proof goes along the lines of the proof of Theorem 3.6 with changes according to time-delays and functionals, that is, we show that the optimal cost functional $V(\bar{\xi}) := J^*(\bar{\xi}, \pi^*, w^*; t, T)$ is an ISS-Lyapunov-Krasovskii functional.

For a feasible solution for all times $t > 0$, we suppose that a feasible solution $\pi(t', x^{t'})$, $t' \in [t, t+T]$ at time t exists. We construct a control by

$$\hat{\pi}\left(t', x^{t'}\right) = \begin{cases} \tilde{\pi}\left(t', x^{t'}\right), & t' \in [t+\Delta,\, t+T], \\ \pi\left(t', x^{t'}\right), & t' \in (t+T,\, t+T+\Delta], \end{cases} \tag{4.9}$$

where π is the controller from Assumption 4.3, point 3, and $\Delta > 0$. $\tilde{\pi}$ steers $x^{t+\Delta}$ into $x^{t+T} \in \Omega$ and Ω is a positively invariant set. This means that $\pi(t', x^{t'})$ keeps the system trajectory in Ω for $t + T < t' \leq t + T + \Delta$ under the constraints of the FHOCPTD. This implies that from the existence of a feasible solution for the time t, we have a feasible solution for the time $t + \Delta$. From Assumption 4.3, point 2, there exists a feasible solution for the FHOCPTD at the time $t = 0$ and it follows that a feasible solution exists for every $t > 0$.

Replacing $\tilde{\pi}$ in (4.9) by π^*, it follows from (4.7) that

$$\begin{aligned} &J^*\left(\bar{\xi}, \pi^*, w^*; t, T+\Delta\right) \\ &\quad \leq J\left(\bar{\xi}, \hat{\pi}, w^*; t, T+\Delta\right) \\ &\quad = \int_t^{t+T} \left(l\left(x(t'), \pi^*\left(t', x^{t'}; t, T\right)\right) - l_w(w^*(t'))\right) dt' \\ &\qquad + \int_{t+T}^{t+T+\Delta} \left(l\left(x(t'), \pi\left(t', x^{t'}\right)\right) - l_w(w^*(t'))\right) dt' + V_f\left(x^{t+T+\Delta}\right) \\ &\quad = J^*\left(\bar{\xi}, \pi^*, w^*; t, T\right) - V_f\left(x^{t+T}\right) + V_f\left(x^{t+T+\Delta}\right) \\ &\qquad + \int_{t+T}^{t+T+\Delta} \left(l\left(x(t'), \pi\left(t', x^{t'}\right)\right) - l_w(w^*(t'))\right) dt' \\ &\quad \leq J^*\left(\bar{\xi}, \pi^*, w^*; t, T\right) \end{aligned} \tag{4.10}$$

hold, and with (4.6) this implies

$$J^*\left(\bar{\xi}, \pi^*, w^*; t, T\right) \leq J^*\left(\bar{\xi}, \pi^*, w^*; t, 0\right) = V_f\left(\bar{\xi}\right) \leq \varphi_2\left(\left|\bar{\xi}\right|_a\right). \tag{4.11}$$

For the lower bound, it holds that

$$V\left(\bar{\xi}\right) \geq J\left(\bar{\xi}, \pi^*, 0; t, T\right) \geq \int_t^{t+T} l\left(x(t'), \pi^*\left(t', x^{t'}\right)\right) dt', \tag{4.12}$$

and by (4.8) we have $V(\bar{\xi}) \geq \varphi_1(|\bar{\xi}(0)|)$. This shows that J^* satisfies (2.22). Now, we use the notation $x^t(\tau) := \bar{\xi}(\tau),\ \tau \in [-\theta + t, t]$. With $J^*(x^t, \pi^*, w^*; t, T + \Delta) \leq J^*(x^t, \pi^*, w^*; t, T)$, we have

$$\begin{aligned}
&\int_t^{t+h} \left(l\left(x(t'), \pi^*\left(t', x^{t'}; t, T\right)\right) - l_w(w^*(t'))\right) dt' \\
&\qquad + J^*\left(x^{t+h}, \pi^*, w^*; t+h, T + \Delta - h\right) \\
&\quad \leq \int_t^{t+h} \left(l\left(x(t'), \pi^*\left(t', x^{t'}; t, T\right)\right) - l_w(w^*(t'))\right) dt' \\
&\qquad + J^*\left(x^{t+h}, \pi^*, w^*; t+h, T - h\right).
\end{aligned} \tag{4.13}$$

This implies

$$J^*\left(x^{t+h}, \pi^*, w^*; t+h, T + \Delta - h\right) \leq J^*\left(x^{t+h}, \pi^*, w^*; t+h, T - h\right). \tag{4.14}$$

Note that by Assumption 4.3, point 6, J^* is locally Lipschitz continuous. With (4.14) it holds

$$\begin{aligned}
&J^*(x^t, \pi^*, w^*; t, T) \\
&\quad = \int_t^{t+h} \left(l\left(x(t'), \pi^*\left(t', x^{t'}; t, T\right)\right) - l_w(w^*(t'))\right) dt' + J^*\left(x^{t+h}, \pi^*, w^*; t+h, T - h\right) \\
&\quad \geq \int_t^{t+h} \left(l\left(x(t'), \pi^*\left(t', x^{t'}; t, T\right)\right) - l_w(w^*(t'))\right) dt' + J^*\left(x^{t+h}, \pi^*, w^*; t+h, T\right),
\end{aligned} \tag{4.15}$$

which leads to

$$\begin{aligned}
&\frac{J^*(x^{t+h}, \pi^*, w^*; t+h, T) - J^*(x^t, \pi^*, w^*; t, T)}{h} \\
&\qquad \leq -\frac{1}{h} \int_t^{t+h} \left(l\left(x(t'), \pi^*\left(t', x^{t'}; t, T\right)\right) - l_w(w^*(t'))\right) dt'.
\end{aligned} \tag{4.16}$$

Let $h \to 0^+$, and using the first point of Assumption 4.3 we get

$$D^+V(x^t, w^*) \leq -\alpha_l(|x^t|_a) + \alpha_w(|w^*|). \tag{4.17}$$

By definition of $\chi(r) := \psi_2(\alpha_l^{-1}(2\alpha_w(r)))$ and $\alpha(r) := (1/2)\alpha_l(\psi_2^{-1}(r))$, $r \geq 0$, this implies

$$V(x^t) \geq \chi(|w^*|) \Longrightarrow D^+V(x^t, w^*) \leq -\alpha(V(x^t)), \tag{4.18}$$

that is, J^* satisfies the condition (2.23).

We conclude that J^* is an ISS-Lyapunov-Krasovskii functional for the system

$$\dot{x}(t) = f(x^t, w(t), \pi^*(t, x^t)), \tag{4.19}$$

and by application of Theorem 2.12 the system has the ISS property. □

Now, we consider that interconnections of TDS and provide conditions such that the whole network with an optimal control obtained from an MPC scheme has the ISS property.

4.2. Interconnected Systems

We consider interconnected systems with time-delays and disturbances of the form

$$\dot{x}_i(t) = \tilde{f}_i(x_1^t, \ldots, x_n^t, w_i(t), u_i(t)), \quad i = 1, \ldots, n, \tag{4.20}$$

where $u_i \in \mathbb{R}^{M_i}$ are the essentially bounded and measurable control inputs and $w_i \in \mathbb{R}^{P_i}$ are the unknown disturbances. We assume that the states, disturbances, and inputs fulfill the constraints

$$x_i \in \mathcal{X}_i, \quad w_i \in \mathcal{W}_i, \quad u_i \in \mathcal{U}_i, \quad i = 1, \ldots, n, \tag{4.21}$$

where $\mathcal{X}_i \subseteq C([-\theta, 0], \mathbb{R}^{N_i})$, $\mathcal{W}_i \subseteq L_\infty(\mathbb{R}_+, \mathbb{R}^{P_i})$, and $\mathcal{U}_i \subseteq \mathbb{R}^{M_i}$ are compact and convex sets containing the origin in their interior.

We assume the same MPC strategy for interconnected TDS as in Section 3.2. The FHOCPTD for the ith subsystem of (4.20) reads as

$$\begin{aligned}
&\min_{\pi_i} \max_{w_i} \max_{(x_j)_{j\neq i}} \quad J_i\left(\bar{\xi}_i, (x_j)_{j\neq i}, \pi_i, w_i; t, T\right) \\
&:= \min_{\pi_i} \max_{w_i} \max_{(x_j)_{j\neq i}} \quad \int_t^{t+T} \left(l_i\left(x_i(t'), \pi_i\left(t', x_i^{t'}\right)\right) - (l_w)_i(w_i(t')) - \sum_{j\neq i} l_{ij}(x_j(t')) \right) dt' \\
&\qquad + (V_f)_i\left(x_i^{t+T}\right)
\end{aligned}$$

subject to

$$\dot{x}_i(t') = f_i\left(x_1^{t'}, \ldots, x_n^{t'}, w_i(t'), u_i(t')\right), \quad t' \in [t, t+T],$$

$$
\begin{aligned}
&x_i(t+\tau) = \bar{\xi}_i(\tau), \quad \tau \in [-\theta, 0], \\
&x_j \in \mathcal{X}_j, \quad j = 1, \ldots, n, \\
&w_i \in \mathcal{W}_i, \\
&\pi_i \in \Pi_i, \\
&x_i^{t+T} \in \Omega_i \subseteq C\left([-\theta, 0], \mathbb{R}^{N_i}\right),
\end{aligned}
\tag{4.22}
$$

where $\bar{\xi}_i \in \mathcal{X}_i$ is the initial function of the ith subsystem at time t and the terminal region Ω is a compact and convex set with the origin in its interior. $\pi_i(t, x^t)$ is essentially bounded, locally Lipschitz in x, and measurable in t and $\Pi_i \subseteq \mathbb{R}^{M_i}$ is a compact and convex sets containing the origin in its interior. $l_i - (l_w)_i - \sum l_{ij}$ is the stage cost, where $l_i : \mathbb{R}^{N_i} \times \mathbb{R}^{M_i} \to \mathbb{R}_+$. $(l_w)_i : \mathbb{R}^{P_i} \to \mathbb{R}_+$ penalizes the disturbance and $l_{ij} : \mathbb{R}^{N_j} \to \mathbb{R}_+$ penalizes the internal input for all $j = 1, \ldots, n,\ j \neq i$. l_i, $(l_w)_i$, and l_{ij} are locally Lipschitz continuous functions with $l_i(0,0) = 0$, $(l_w)_i(0) = 0$, $l_{ij}(0) = 0$, and $(V_f)_i : \Omega_i \to \mathbb{R}_+$ is the terminal penalty of the ith subsystem.

We obtain an optimal solution $\pi_i^*, (x_j)_{j \neq i}^*, w_i^*$, where the control of each subsystem is a feedback control law, which depends on the current states of the whole system, that is, $u_i(t) = \pi_i^*(t, x^t)$, where $x^t = ((x_1^t)^T, \ldots, (x_n^t)^T)^T \in C([-\theta, 0], \mathbb{R}^N)$, $N = \sum_i N_i$.

For the ith subsystem of (4.20), we suppose the following assumption.

Assumption 4.5. (1) There exist functions $\alpha_i^l, \alpha_i^w, \alpha_{ij} \in \mathcal{K}_\infty$, $j = 1, \ldots, n,\ j \neq i$ such that

$$
\begin{gathered}
l_i(\phi_i(0), \pi_i) \geq \alpha_i^l(|\phi_i|_a), \quad \phi_i \in C\left([-\theta, 0], \mathbb{R}^{N_i}\right),\ \pi_i \in \Pi_i, \\
(l_w)_i(w_i) \leq \alpha_i^w(|w_i|), \quad w_i \in \mathcal{W}_i, \\
l_{ij}(\phi_j(0)) \leq \alpha_{ij}(V_j(\phi_j)), \quad \phi_j \in C\left([-\theta, 0], \mathbb{R}^{N_j}\right), \quad j = 1, \ldots, n,\ j \neq i.
\end{gathered}
\tag{4.23}
$$

(2) The FHOCPTD admits a feasible solution at the initial time $t = 0$.

(3) There exists a controller $u_i(t) = \pi_i(t, x^t)$ such that the ith subsystem of (4.20) has the ISS property.

(4) There exists a locally Lipschitz continuous functional $(V_f)_i(\phi_i)$ such that the terminal region Ω_i is a positively invariant set and for all $\phi_i \in \Omega_i$ we have

$$
\begin{gathered}
(V_f)_i(\phi_i) \leq \varphi_{2i}(|\phi_i|_a), \\
D^+(V_f)_i(\phi_i, w_i) \leq -l_i(\phi_i(0), \pi_i) + (l_w)_i(w_i) + \sum_{j \neq i} l_{ij}(\phi_j(0)),
\end{gathered}
\tag{4.24}
$$

where $\varphi_{2i} \in \mathcal{K}_\infty$, $\phi_j \in C([-\theta, 0], \mathbb{R}^{N_j})$, $j = 1, \ldots, n$ and $w_i \in \mathcal{W}_i$. $D^+(V_f)_i$ denotes the upper right-hand side derivate of the functional $(V_f)_i$ along the solution of the ith subsystem of (4.20) with the control $u_i \equiv \pi_i$ from point 3. of this assumption.

(5) For each i, there exists a $\mathcal{K}_\infty$ function ψ_{1i} such that for all $t > 0$ it holds

$$\int_t^{t+T} l_i\left(x_i(t'), \pi_i\left(t', x^{t'}\right)\right) dt' \geq \psi_{1i}\left(\left|\bar{\xi}(0)\right|\right), \quad \bar{\xi}(0) = x(t). \tag{4.25}$$

(6) The optimal cost functional $J_i^*(\bar{\xi}_i, (x_j)^*_{j\neq i}, \pi_i^*, w_i^*; t, T)$ is locally Lipschitz continuous.

Now, we state that each subsystem of (4.20) has the ISS property by application of the optimal control obtained by the FHOCPTD.

Theorem 4.6. *Consider an interconnected system of the form* (4.20). *Let Assumption 4.5 be satisfied for each subsystem. Then, each subsystem resulting from the application of the predictive control strategy to the system, namely,* $\dot{x}_i(t) = f_i(x_1^t, \ldots, x_n^t, w_i(t), \pi_i^*(t, x^t))$, $t \in \mathbb{R}_+$, $x_i^0(\tau) = \xi_i(\tau), \tau \in [-\theta, 0]$, *possesses the ISS property.*

Proof. Consider the ith subsystem. We show that the optimal cost functional $V_i(\bar{\xi}_i) := J_i^*(\bar{\xi}_i, (x_j)^*_{j\neq i}, \pi_i^*, w_i^*; t, T)$ is an ISS-Lyapunov-Krasovskii functional for the ith subsystem. We abbreviate $x_j^t = ((x_j)^t_{j\neq i})^*$.

Following the lines of the proof of Theorem 4.4, we have that there exists a feasible solution of the ith subsystem for all times $t > 0$ and that the functional $V_i(\bar{\xi}_i)$ satisfies the condition

$$\psi_{1i}\left(\left|\bar{\xi}_i(0)\right|\right) \leq V_i\left(\bar{\xi}_i\right) \leq \psi_{2i}\left(\left|\bar{\xi}_i\right|_a\right), \tag{4.26}$$

using (4.25) and $|\bar{\xi}(0)| \geq |\bar{\xi}_i(0)|$. Note that by Assumption 4.5, point 6, J_i^* is locally Lipschitz continuous. We arrive that the following equation holds:

$$D^+V_i(x_i^t, w_i^*) \leq -\alpha_i^l\left(\psi_{2i}^{-1}(V_i(x_i^t))\right) + \alpha_i^w(|w_i^*|) + \sum_{j\neq i}\alpha_{ij}\left(V_j\left(x_j^t\right)\right). \tag{4.27}$$

This is equivalent to

$$D^+V_i(x_i^t, w_i^*) \leq -\alpha_i^l\left(\psi_{2i}^{-1}(V_i(x_i^t))\right) + \max\left\{n\alpha_i^w(|w_i^*|), \max_{j\neq i} n\alpha_{ij}\left(V_j\left(x_j^t\right)\right)\right\}, \tag{4.28}$$

which implies

$$V_i(x_i^t) \geq \max\left\{\tilde{\chi}_i(|w_i^*|), \max_{j\neq i}\tilde{\chi}_{ij}\left(V_j\left(x_j^t\right)\right)\right\} \Longrightarrow D^+V_i(x_i^t, w_i^*) \leq -\bar{\alpha}_i^l(V_i(x_i^t)), \tag{4.29}$$

where

$$\begin{aligned}
\widetilde{\chi}_i(r) &:= \psi_{2i}\left(\left(\alpha_i^l\right)^{-1}\left(2n\alpha_i^w(r)\right)\right),\\
\widetilde{\chi}_{ij}(r) &:= \psi_{2i}\left(\left(\alpha_i^l\right)^{-1}\left(2n\alpha_{ij}(r)\right)\right),\\
\overline{\alpha}_i^l(r) &:= \frac{1}{2}\alpha_i^l\left(\psi_{2i}^{-1}(r)\right).
\end{aligned} \tag{4.30}$$

This can be shown for each subsystem and we conclude that each subsystem has an ISS-Lyapunov-Krasovskii functional. It follows that the ith subsystem is ISS in maximum formulation. □

We collect all functions $\widetilde{\chi}_{ij}$ in a matrix $\Gamma := (\widetilde{\chi}_{ij})_{n\times n}$, $\widetilde{\chi}_{ii} \equiv 0$, which defines a map as in (2.12).

Using the small-gain condition for Γ, the following corollary from Theorem 4.6.

Corollary 4.7. *Consider an interconnected system of the form* (4.20)*. Let Assumption 4.5 be satisfied for each subsystem. If* Γ *satisfies the small-gain condition* (2.13)*, then the whole system possesses the ISS property.*

Proof. We know from Theorem 4.6 that each subsystem of (4.20) has an ISS-Lyapunov-Krasovskii functional with gains $\widetilde{\chi}_{ij}$. Since the matrix Γ satisfies the SGC, all assumptions of Theorem 2.13 are satisfied and it follows that the whole system of the form

$$\dot{x}(t) = f\left(x^t, w(t), \pi^*\left(t, x^t\right)\right) \tag{4.31}$$

is ISS in maximum formulation, where $x^t = ((x_1^t)^T, \ldots, (x_n^t)^T)^T$, $w = (w_1^T, \ldots, w_n^T)^T$, and $\pi^*(t, x^t) = ((\pi_1^*(t, x^t))^T, \ldots, (\pi_n^*(t, x^t))^T)^T$. □

5. Conclusions

We have combined the ISDS property with MPC for nonlinear continuous-time systems with disturbances. For single systems, we have derived conditions such that by application of the control obtained by an MPC scheme to the system, it has the ISDS property, see Theorem 3.6. Considering interconnected systems, we have proved that each subsystem possesses the ISDS property using the control of the proposed MPC scheme, which is Theorem 3.9. Using a small-gain condition, we have shown in Corollary 3.10 that the whole network has the ISDS property.

Considering single systems with time-delays, we have proved in Theorem 4.4 that a TDS has the ISS property using the control obtained by an MPC scheme, where we have used ISS-Lyapunov-Krasovskii functionals. For interconnected TDSs, we have established a theorem, that guarantees that each closed-loop subsystem obtained by application of the control obtained by a decentralized MPC scheme has the ISS property, see Theorem 4.6. From this result and using Theorem 2.13, we have shown that the whole network with time-delays has the ISS property under a small-gain condition, see Corollary 4.7.

In future research, we are going to derive conditions for open-loop MPC schemes to assure ISDS and ISS of TDSs, respectively. The differences of both schemes, closed-loop, and open-loop, will be analyzed and applied in practice.

Note that the results presented here are first steps of the approaches of ISDS for MPC and ISS for MPC with time-delays. More detailed studies should be done in these directions, especially in applications of these approaches. Therefore, numerical algorithms for the implementation of the proposed schemes, as in [5, 7], for example, should be developed. It could be analyzed if and how other existing algorithms could be used or how they should be adapted for implementation for the results presented in this work. The advantages of the usage of ISDS for MPC in contrast to ISS for MPC could be investigated and applied in practice.

Furthermore, one can investigate ISDS and ISS for unconstrained nonlinear MPC, as it was done in [17, 31], for example.

Acknowledgment

This research is funded by the German Research Foundation (DFG) as part of the Collaborative Research Centre 637 "Autonomous Cooperating Logistic Processes: A Paradigm Shift and its Limitations" (SFB 637).

References

[1] S. J. Qin and T. A. Badgwell, "An overview of nonlinear model predictive control applications," in *Nonlinear Predictive Control*, F. Allgöwer and A. Zheng, Eds., pp. 369–392, Birkhäuser, Berlin, Germany, 2000.

[2] S. J. Qin and T. A. Badgwell, "A survey of industrial model predictive control technology," *Control Engineering Practice*, vol. 11, pp. 733–764, 2003.

[3] J. Maciejowski, *Predictive Control with Constraints*, Prentice-Hall, 2001.

[4] E. F. Camacho and C. Bordons Alba, *Model Predictive Control*, Springer, 2004.

[5] L. Grüne and J. Pannek, *Nonlinear Model Predictive Control*, Springer, London, UK, 2011.

[6] D. M. Raimondo, *Nonlinear model predictive control [Ph.D. thesis]*, University of Pavia, Pavia, Italy, 2008.

[7] J. Pannek, *Receding horizon control: a suboptimality-based approach [Ph.D. thesis]*, University of Bayreuth, Germany, 2009.

[8] M. Lazar, *Predictive control algorithms for nonlinear systems [Ph.D. thesis]*, Technical University of Iasi, Romania, 2009.

[9] T. Raff, S. Huber, Z. K. Nagy, and F. Allgöwer, "Nonlinear model predicitve control of a four tank system: an experimental stability study," in *Proceedings of the IEEE Conference on Control in Applications*, pp. 237–242, 2006.

[10] D. Q. Mayne, J. B. Rawlings, C. V. Rao, and P. O. M. Scokaert, "Constrained model predictive control: stability and optimality," *Automatica*, vol. 36, no. 6, pp. 789–814, 2000.

[11] F. A. C. C. Fontes, "A general framework to design stabilizing nonlinear model predictive controllers," *Systems & Control Letters*, vol. 42, no. 2, pp. 127–143, 2001.

[12] D. L. Marruedo, T. Alamo, and E. F. Camacho, "Input-to-state stable MPC for constrained discrete-time nonlinear systems with bounded additive uncertainties," in *Proceedings of the 41st IEEE Conference on Decision and Control*, pp. 4619–4624, Las Vegas, Nev, USA, December 2002.

[13] L. Magni, D. M. Raimondo, and R. Scattolini, "Regional input-to-state stability for nonlinear model predictive control," *IEEE Transactions on Automatic Control*, vol. 51, no. 9, pp. 1548–1553, 2006.

[14] D. Limon, T. Alamo, F. Salas, and E. F. Camacho, "Input to state stability of min-max MPC controllers for nonlinear systems with bounded uncertainties," *Automatica*, vol. 42, no. 5, pp. 797–803, 2006.

[15] M. Lazar, D. Muñoz de la Peña, W. P. M. H. Heemels, and T. Alamo, "On input-to-state stability of min-max nonlinear model predictive control," *Systems & Control Letters*, vol. 57, no. 1, pp. 39–48, 2008.

[16] D. M. Raimondo, L. Magni, and R. Scattolini, "Decentralized MPC of nonlinear systems: an input-to-state stability approach," *International Journal of Robust and Nonlinear Control*, vol. 17, no. 17, pp. 1651–1667, 2007.

[17] L. Grüne and K. Worthmann, "A distributed NMPC scheme without stabilizing terminal constraints," in *Distributed Decision Making and Control*, R. Johansson and A. Rantzer, Eds., pp. 259–285, Springer, 2010.

[18] L. Grüne, "Input-to-state dynamical stability and its Lyapunov function characterization," *IEEE Transactions on Automatic Control*, vol. 47, no. 9, pp. 1499–1504, 2002.

[19] S. Dashkovskiy and L. Naujok, "ISDS small-gain theorem and construction of ISDS Lyapunov functions for interconnected systems," *Systems & Control Letters*, vol. 59, no. 5, pp. 299–304, 2010.

[20] P. Pepe and Z.-P. Jiang, "A Lyapunov-Krasovskii methodology for ISS and iISS of time-delay systems," *Systems & Control Letters*, vol. 55, no. 12, pp. 1006–1014, 2006.

[21] S. Dashkovskiy and L. Naujok, "Lyapunov-Razumikhin and Lyapunov-Krasovskii theorems for interconnected ISS time-delay systems," in *Proceedings of the 19th International Symposium on Mathematical Theory of Networks and Systems (MTNS '10)*, pp. 1179–1184, Budapest, Hungary, July 2010.

[22] R. M. Esfanjani, M. Reble, U. Münz, S. K. Y. Nikravesh, and F. Allgöwer, "Model predictive control of constrained nonlinear time-delay systems," in *Proceedings of the 48th IEEE Conference on Decision and Control*, pp. 1324–1329, 2009.

[23] M. Reble, F. D. Brunner, and F. Allgöwer, "Model predictive control for nonlinear time-delay systems without terminal constraint," in *Proceedings of the 18th World Congress of the International Federation of Automatic Control (IFAC '11)*, pp. 9254–9259, Milano, Italy, August 2011.

[24] B. Rüffer, *Monotone dynamical systems, graphs, and stability of large-scale interconnected systems [Ph.D. thesis]*, University of Bremen, Germany, 2007.

[25] B. S. Rüffer, "Monotone inequalities, dynamical systems, and paths in the positive orthant of Euclidean n-space," *Positivity*, vol. 14, no. 2, pp. 257–283, 2010.

[26] S. N. Dashkovskiy, B. S. Rüffer, and F. R. Wirth, "Small gain theorems for large scale systems and construction of ISS Lyapunov functions," *SIAM Journal on Control and Optimization*, vol. 48, no. 6, pp. 4089–4118, 2010.

[27] J. K. Hale and S. M. Verduyn Lunel, *Introduction to Functional-Differential Equations*, vol. 99 of *Applied Mathematical Sciences*, Springer, New York, NY, USA, 1993.

[28] P. Pepe, "On Liapunov-Krasovskii functionals under Carathéodory conditions," *Automatica*, vol. 43, no. 4, pp. 701–706, 2007.

[29] R. Scattolini, "Architectures for distributed and hierarchical model predictive control—a review," *Journal of Process Control*, vol. 19, pp. 723–731, 2009.

[30] A. Richards and J. P. How, "Robust distributed model predictive control," *International Journal of Control*, vol. 80, no. 9, pp. 1517–1531, 2007.

[31] L. Grüne, "Analysis and design of unconstrained nonlinear MPC schemes for finite and infinite dimensional systems," *SIAM Journal on Control and Optimization*, vol. 48, no. 2, pp. 1206–1228, 2009.

Hindawi Publishing Corporation
Mathematical Problems in Engineering
Volume 2012, Article ID 830154, 25 pages
doi:10.1155/2012/830154

Research Article

Robust Finite-Time H_∞ Control for Impulsive Switched Nonlinear Systems with State Delay

Jian Guo, Chao Liu, and Zhengrong Xiang

School of Automation, Nanjing University of Science and Technology, Nanjing 210094, China

Correspondence should be addressed to Zhengrong Xiang, xiangzr@mail.njust.edu.cn

Received 20 June 2012; Revised 9 September 2012; Accepted 10 September 2012

Academic Editor: Zidong Wang

This paper investigates robust finite-time H_∞ control for a class of impulsive switched nonlinear systems with time-delay. Firstly, using piecewise Lyapunov function, sufficient conditions ensuring finite-time boundedness of the impulsive switched system are derived. Then, finite-time H_∞ performance analysis for impulsive switched systems is developed, and a robust finite-time H_∞ state feedback controller is proposed to guarantee that the resulting closed-loop system is finite-time bounded with H_∞ disturbance attenuation. All the results are given in terms of linear matrix inequalities (LMIs). Finally, two numerical examples are provided to show the effectiveness of the proposed method.

1. Introduction

A switched system is a hybrid dynamical system consisting of a family of continuous-time or discrete-time subsystems and a switching law that orchestrates the switching between them [1]. In the last decades, in the stability analysis and stabilization for switched systems, lots of valuable results are established (see [2–5]). Most recently, on the basis of Lyapunov functions and other analysis tools, the stability problem of linear and nonlinear switched systems with time-delay has been further investigated (see [6–15]), and lots of valuable results are established for H_∞ control problems (see [16–22]).

It is well known that impulsive dynamical behaviors inevitably exist in some practical systems like physical, biological, engineering, and information science systems due to abrupt changes at certain instants during the dynamical process. Although hybrid system and switched system are important models for dealing with complex real systems, there is little work concerned with the above impulsive phenomena. Such a phenomenon can be modeled

as an impulsive switched system, it is characteristic that their states change during the switching because of the occurrence of impulses [23].

In recent years, the impulsive switched systems have drawn more and more attention and many useful conclusions have been obtained. Multiple Krasovskii-Lyapunov function approach is employed to study the problem of ISS stability of a class of impulsive switched systems with time-delay in [24]. By the Lyapunov-Razumikhin technique, a delay-independent criterion of the exponential stability is established on the minimum dwell time in [25]. The problem of robust H_∞ stabilization of nonlinear impulsive switched system with time-delays is studied in [23].

Usually, the stability of a system is defined over an infinite-time interval. But in many practical systems, we focus on the dynamical behavior of a system over a fixed finite-time interval. Based on this, finite-time stability is first proposed by Dorato in 1961 [26]. Compared with the classical Lyapunov stability, finite-time stability is proposed for the study of the transient performance of the system, which is a totally different concept. The so-called finite-time stability means the boundedness of the state of a system over a fixed finite-time interval. Finite-time stability problems can be found in [27–32]. The finite-time stability of linear impulsive systems is analyzed in [33], the finite-time stability and stabilization of impulsive dynamic systems are carried out in [34–36]. The finite-time stability and stabilization of switched systems are investigated in [37].

Recently, robust finite-time control of switched systems is studied in [38, 39]. However, to the best of our knowledge, there are very few results on finite-time boundedness and robust H_∞ control of the impulsive switched systems, which motivates the present study. The paper is organized as follows. In Section 2, problem formulation and some necessary lemmas are given. In Section 3, based on the dwell time approach, finite-time boundedness and finite-time H_∞ performance for switched impulsive systems are addressed, and sufficient conditions for the existence of a robust finite-time H_∞ state feedback controller are proposed in terms of a set of matrix inequalities. Numerical examples are provided to show the effectiveness of the proposed approach in Section 4. Concluding remarks are given in Section 5.

Notations. The notations used in this paper are standard. The notation $P > 0$ means that P is a real positive definite matrix; $\operatorname{diag}\{\cdots\}$ stands for a block-diagonal matrix; $\lambda_{\max}(P)$ and $\lambda_{\min}(P)$ denote the maximum and minimum eigenvalues of matrix P, respectively; $\|x(t)\| = \sqrt{x^T(t)x(t)}$ and $\|x(t)\|_2 = (\int_0^\infty \|x(t)\|^2 dt)^{1/2}$.

2. Problem Formulation and Preliminaries

Consider the following impulsive switched system:

$$\dot{x}(t) = \widehat{A}_{\sigma(t)}x(t) + \widehat{A}_{d\sigma(t)}x(t-h) + \widehat{B}_{1\sigma(t)}u_1(t) + f_{\sigma(t)}(x(t)) + B_{2\sigma(t)}w(t), \quad t \neq t_k \tag{2.1a}$$

$$\Delta x = E_{\sigma(t)}x(t) + u_2(t), \quad t = t_k, \quad k = 1, 2, 3, \ldots \tag{2.1b}$$

$$z(t) = C_{\sigma(t)}x(t) + D_{\sigma(t)}u_1(t), \tag{2.1c}$$

$$x(t) = \varphi(t), \quad t \in [t_0 - h, t_0], \tag{2.1d}$$

where $x(t) \in R^n$ is the state vector, $z(t) \in R^r$ is the controlled output, $w(t) \in R^p$ is the disturbance input which belongs to $L_2[0,\infty)$, $u_1(t) \in R^m$, $t \neq t_k$ is the switched control input, $u_2(t_k) \in R^n$ is the impulsive control input at t_k, on the other hand, $u_2(t) = 0$, $t \neq t_k$, $k = 1,2,3,\ldots$. $\sigma(t) : [t_0,+\infty) \to \overline{N} = \{1,2,\ldots,N\}$ is a switching signal. $t \in (t_k,t_{k+1}]$, $\sigma(t) = i_k$, $i_k \in \overline{N}$, $k = 0,1,2,3,\ldots$. $\Delta x(t) = x(t^+) - x(t^-)$, $x(t^+) = \lim_{h\to 0^+} x(t+h)$, $x(t) = x(t^-) = \lim_{h\to 0^+} x(t-h)$. t_k, $k = 0,1,2,3,\ldots$ are the impulsive jumping points or switching points. t_0 is the initial time, $t_0 < t_1 < \cdots < t_k < \cdots$, and $\lim_{k\to\infty} t_k = +\infty$. $h > 0$ is the time-delay which is a positive constant. $f_i(\cdot) : R^n \to R^n$, $i \in \overline{N}$ is nonlinear vector-valued function. $\varphi(t)$, $t \in [t_0 - h, t_0]$ is a continuous vector-valued initial function. $\widehat{A}_i$, $\widehat{A}_{di}$, $\widehat{B}_{1i}$, $i \in \overline{N}$ are uncertain real-valued matrices with appropriate dimensions, B_{2i}, E_i, C_i, D_i, $i \in \overline{N}$ are known real constant matrices with appropriate dimensions.

Assumption 2.1. For each $i \in \overline{N}$, $\widehat{A}_i$, $\widehat{A}_{di}$, $\widehat{B}_{1i}$ are uncertain real-valued matrices with appropriate dimensions. We assume that the uncertainties are of the form

$$\widehat{A}_i = A_i + \Delta A_i, \qquad \widehat{A}_{di} = A_{di} + \Delta A_{di}, \qquad \widehat{B}_{1i} = B_{1i} + \Delta B_{1i}, \tag{2.2a}$$

$$\begin{bmatrix} \Delta A_i & \Delta A_{di} & \Delta B_{1i} \end{bmatrix} = H_i F_i(t) \begin{bmatrix} E_{Ai} & E_{Adi} & E_{Bi} \end{bmatrix}, \tag{2.2b}$$

where A_i, A_{di}, B_{1i}, H_i, E_{Ai}, E_{Adi}, and E_{Bi} are known real-valued constant matrices with appropriate dimensions, $F_i(t)$ is the uncertain matrix satisfying

$$F_i^T(t) F_i(t) \leq I. \tag{2.3}$$

Assumption 2.2. For each $i \in \overline{N}$, nonlinear vector-valued function f_i satisfies Lipschitz condition

$$\left\| f_i(x(t)) \right\| \leq \| U_i x(t) \|, \tag{2.4}$$

where U_i is the Lipschitz constant matrix.

Assumption 2.3. For a given time constant $T_f > t_0$, the external disturbance $w(t)$ satisfies

$$\int_0^{T_f} w^T(t) w(t) dt \leq d^2. \tag{2.5}$$

Assumption 2.4. For system (2.1a)–(2.1d), the impulsive jump matrices E_i satisfy that $(I + E_i)$ are invertible.

Definition 2.5 (see [32]). For a given time constant $T_f > t_0$, impulsive switched system (2.1a), (2.1b), (2.1c) and (2.1d) with $u_1(t) \equiv 0$, $u_2(t) \equiv 0$, and $w(t) \equiv 0$, is said to be finite-time stable with respect to $(c_1^2, c_2^2, T_f, R, \sigma(t))$ if the following inequality holds:

$$\sup_{t_0 - h \leq \tau \leq t_0} x^T(\tau) R x(\tau) \leq c_1^2 \Longrightarrow x^T(t) R x(t) < c_2^2, \quad t \in \left(t_0, T_f\right], \tag{2.6}$$

where $c_2 > c_1 > 0$, R is a positive definite matrix, and $\sigma(t)$ is a switching signal.

Remark 2.6. Equation (2.6) stands for the boundedness of the state of a system over a fixed finite-time interval $(t_0, T_f]$, when the initial state is bounded.

Definition 2.7 (see [40]). For a given time constant T_f, impulsive switched system (2.1a)–(2.1d) with $u_1(t) \equiv 0$, $u_2(t) \equiv 0$, and $w(t)$ satisfying (2.5), is said to be finite-time bounded with respect to $(c_1^2, c_2^2, T_f, d^2, R, \sigma(t))$ if the condition (2.6) holds, where $c_2 > c_1 > 0$, R is a positive definite matrix and $\sigma(t)$ is a switching signal.

Definition 2.8. For any $T_2 > T_1 > 0$, let $N_{\sigma(t)}(T_1, T_2)$ denote the switching number of $\sigma(t)$ on an interval (T_1, T_2). If $N_{\sigma(t)}(T_1, T_2) \leq N_0 + (T_2 - T_1)/\tau_a$ holds for given $N_0 \geq 0$, $\tau_a > 0$, then the constant τ_a is called the average dwell time. In this paper we let $N_0 = 0$.

Definition 2.9. For a given time constant T_f, impulsive switched system (2.1a)–(2.1d) with $u_1(t) \equiv 0$, $u_2(t) \equiv 0$ is said to have finite-time H_∞ performance with respect to $(0, c_2^2, T_f, d^2, \gamma, R, \sigma(t))$ if the system is finite-time bounded and the following inequality holds:

$$\|z(t)\|_2 \leq \gamma \|w(t)\|_2, \quad \forall w(t) \in L_2[0, \infty), \tag{2.7}$$

where $c_2 > 0$, $\gamma > 0$, R is a positive definite matrix and $\sigma(t)$is a switching signal.

Definition 2.10. For a given time constant T_f, impulsive switched system (2.1a)–(2.1d) is said to be robust finite-time stabilization with H_∞ disturbance attenuation level γ, if there exists a switched controller $u_1(t) = K_{\sigma(t)}x(t)$, $t \neq t_k$ and an impulsive controller $u_2(t_k) = \overline{K}_{\sigma(t)}x(t_k)$, $t = t_k$, where $t \in (t_0, T_f]$ such that

(i) the corresponding closed-loop system is finite-time bounded with respect to $(0, c_2^2, T_f, d^2, R, \sigma(t))$;

(ii) under zero initial condition, inequality (2.7) holds for any $w(t)$ satisfying (2.5).

Lemma 2.11. *Let U, V, W, and X be real matrices of appropriate dimensions with X satisfying $X = X^T$, then for all $V^T V \leq I$,*

$$X + UVW + W^T V^T U^T < 0, \tag{2.8}$$

if and only if there exists a scalar $\varepsilon > 0$ such that

$$X + \varepsilon UU^T + \varepsilon^{-1} W^T W < 0. \tag{2.9}$$

3. Main Results

3.1. Finite-Time Boundedness Analysis

In this subsection, we focus on the finite-time boundedness of the following impulsive switched system:

$$\dot{x}(t) = A_{\sigma(t)}x(t) + A_{d\sigma(t)}x(t-h) + f_{\sigma(t)}(x(t)) + B_{2\sigma(t)}w(t), \quad t \neq t_k \tag{3.1a}$$

$$\Delta x = E_{\sigma(t)}x(t), \quad t = t_k, \quad k = 1, 2, 3, \ldots \tag{3.1b}$$

$$x(t) = \varphi(t), \quad t \in [t_0 - h, t_0]. \tag{3.1c}$$

Before proceeding to Lemma 3.2, we first introduce a function $v(t)$. For given positive definite matrices $Q_{i_k}, i_k \in \overline{N}$, by Assumption 2.4, there exists a real number $\rho_{i_k} \geq 1$, $\rho^* = \max\{\rho_{i_k}, i_k \in \overline{N}\}$ such that

$$Q_{i_{k-1}} \leq \rho_{i_k}(I + E_{i_{k-1}})^T Q_{i_k}(I + E_{i_{k-1}}). \tag{3.2}$$

Furthermore, we define the following function

$$v_k(t) = \rho_{i_k} - \frac{(t - t_k)^2}{(t_{k+1} - t_k)^2}(\rho_{i_k} - 1), \quad t \in (t_k, t_{k+1}]. \tag{3.3}$$

Finally, a piecewise continuous function $v(t)$ is as follows:

$$v(t) = v_k(t), \quad t \in (t_k, t_{k+1}]. \tag{3.4}$$

Consider the function $v(t)$, for each interval $(t_k, t_{k+1}]$, $v(t_k^+) = \rho_{i_k}$, $v(t_{k+1}) = 1$, and $v(t)$ is monotonically nonincreasing and bounded function, $v(t_{k+1}) \leq v(t) \leq v(t_k^+)$.

Remark 3.1. Note that the previous works require the condition $Q_{i_{k-1}} \leq (I + E_{i_{k-1}})^T Q_{i_k}(I + E_{i_{k-1}})$ (see [23, 41]), which can be obtained by setting $\rho_{i_k} = 1$ in (3.2). Thus, the proposed approach may provide more relaxed conditions.

Lemma 3.2. *Consider the following Lyapunov functional candidate:*

$$V(t) = x^T(t)P_{\sigma(t)}x(t) + \int_{t-h}^{t} v(s)x^T(s)e^{\alpha(t-s)}Q_{\sigma(s)}x(s)ds \tag{3.5}$$

for system (3.1a), (3.1b), *and* (3.1c), *where P_i and Q_i, $i \in \overline{N}$ are symmetric positive definite matrices with appropriate dimensions.*

The following inequality is derived:

$$\begin{aligned}\dot{V}(t) \le{}& 2x^T(t)P_{i_k}\dot{x}(t) + \alpha\int_{t-h}^{t} v(s)x^T(s)e^{\alpha(t-s)}Q_{\sigma(s)}x(s)ds \\ &+ v(t)x^T(t)Q_{i_k}x(t) - v(t-h)x^T(t-h)Q_{i_{k-m}}x(t-h)e^{\alpha h} \\ &t\in(t_k,t_{k+1}],\quad t-h\in(t_{k-m},t_{k-m+1}],\quad m\in\{0,1,2,3,\ldots\}.\end{aligned} \tag{3.6}$$

Proof. (i) When $t_k + h \ge t_{k+1}$,

$$\begin{aligned}V(t) &= x^T(t)P_{\sigma(t)}x(t) + \int_{t-h}^{t} v(s)x^T(s)e^{\alpha(t-s)}Q_{\sigma(s)}x(s)ds \\ &= x^T(t)P_{i_k}x(t) + \int_{t-h}^{t_{k-m+1}} v(s)x^T(s)e^{\alpha(t-s)}Q_{i_{k-m}}x(s)ds \\ &\quad + \int_{t_{k-m+1}}^{t_{k-m+2}} v(s)x^T(s)e^{\alpha(t-s)}Q_{i_{k-m+1}}x(s)ds\cdots + \int_{t_k}^{t} v(s)x^T(s)e^{\alpha(t-s)}Q_{i_k}x(s)ds, \\ \dot{V}(t) &= 2x^T(t)P_{i_k}\dot{x}(t) + \alpha\int_{t-h}^{t} v(s)x^T(s)e^{\alpha(t-s)}Q_{\sigma(s)}x(s)ds \\ &\quad + v(t_{k-m+1})x^T(t_{k-m+1})e^{\alpha(t-t_{k-m+1})}Q_{i_{k-m}}x(t_{k-m+1}) \\ &\quad - v(t-h)x^T(t-h)e^{\alpha h}Q_{i_{k-m}}x(t-h) \\ &\quad + v(t_{k-m+2})x^T(t_{k-m+2})e^{\alpha(t-t_{k-m+2})}Q_{i_{k-m+1}}x(t_{k-m+2}) \\ &\quad - v(t_{k-m+1}^+)x^T(t_{k-m+1}^+)e^{\alpha(t-t_{k-m+1})}Q_{i_{k-m+1}}x(t_{k-m+1}^+)\cdots + v(t_k)x^T(t_k)e^{\alpha(t-t_k)}Q_{i_{k-1}}x(t_k) \\ &\quad - v(t_{k-1}^+)x^T(t_{k-1}^+)e^{\alpha(t-t_k)}Q_{i_{k-1}}x(t_{k-1}^+) + v(t)x^T(t)Q_{i_k}x(t) \\ &\quad - v(t_k^+)x^T(t_k^+)e^{\alpha(t-t_k)}Q_{i_k}x(t_k^+), \\ \dot{V}(t) &= 2x^T(t)P_{i_k}\dot{x}(t) + \alpha\int_{t-h}^{t} v(s)x^T(s)e^{\alpha(t-s)}Q_{\sigma(s)}x(s)ds \\ &\quad + v(t)x^T(t)Q_{i_k}x(t) - v(t-h)x^T(t-h)e^{\alpha h}Q_{i_{k-m}}x(t-h) \\ &\quad + x^T(t_{k-m+1})e^{\alpha(t-t_{k-m+1})}\left[Q_{i_{k-m}} - \rho_{i_{k-m+1}}(I+E_{i_{k-m}})^TQ_{i_{k-m+1}}(I+E_{i_{k-m}})\right]x(t_{k-m+1})\ldots \\ &\quad + x^T(t_k)e^{\alpha(t-t_k)}\left[Q_{i_{k-1}} - \rho_{i_k}(I+E_{i_{k-1}})^TQ_{i_k}(I+E_{i_{k-1}})\right]x(t_k).\end{aligned} \tag{3.7}$$

From (3.2), we can obtain that

$$\begin{aligned} &Q_{i_{k-m}} - \rho_{i_{k-m+1}}(I + E_{i_{k-m}})^T Q_{i_{k-m+1}}(I + E_{i_{k-m}}) \le 0 \\ &\qquad\qquad \vdots \\ &Q_{i_{k-1}} - \rho_{i_k}(I + E_{i_{k-1}})^T Q_{i_k}(I + E_{i_{k-1}}) \le 0. \end{aligned} \tag{3.8}$$

Combining (3.7) and (3.8), (3.6) is obtained.

(ii) When $t_k + h < t_{k+1}$,

(1) $t \in (t_k, t_k + h]$, the proof is similar to the proof line in the situation (i).

(2) $t \in (t_k + h, t_{k+1}]$,

$$\begin{aligned} V(t) &= x^T(t)P_{\sigma(t)}x(t) + \int_{t-h}^{t} v(s)x^T(s)e^{\alpha(t-s)}Q_{\sigma(s)}x(s)ds \\ &= x^T(t)P_{i_k}x(t) + \int_{t-h}^{t} v(s)x^T(s)e^{\alpha(t-s)}Q_{i_k}x(s)ds. \end{aligned} \tag{3.9}$$

The proof for this situation is omitted.

The proof is completed. □

Lemma 3.3. *Consider the following Lyapunov function:*

$$V(t) = x^T(t)P_{\sigma(t)}x(t) + \int_{t-h}^{t} v(s)x^T(s)e^{\alpha(t-s)}Q_{\sigma(s)}x(s)ds \tag{3.10}$$

for system (3.1a), (3.1b), *and* (3.1c), *where* P_i *and* Q_i, $i \in \{1, 2, \ldots, N\}$ *are symmetric positive definite matrices with appropriate dimensions. Under the condition*

$$\begin{bmatrix} -e^{\alpha h}\rho^* P_j & I + E_j^T & E_i^T \\ * & -P_i^{-1} & 0 \\ * & * & -e^{-\alpha h}(\rho^*)^{-1}Q_i^{-1} \end{bmatrix} < 0, \quad \forall i, j \in \overline{N}, \tag{3.11}$$

we have

$$V(t_k^+) < e^{\alpha h}\rho^* V(t_k), \tag{3.12}$$

where $\rho^* = \max\{\rho_{i_k}, i_k \in \overline{N}\}$.

Proof. Without loss of generality, let $\sigma(t_k^+) = i,\ \sigma(t_k) = j$. Then, we have

$$\begin{aligned}
V(t_k^+) &= x^T(t_k^+)P_{\sigma(t_k^+)}x(t_k^+) + \int_{t_k^+-h}^{t_k^+} v(s)x^T(s)e^{\alpha(t_k^+-s)}Q_{\sigma(s)}x(s)ds \\
&\le x^T(t_k^+)P_{\sigma(t_k^+)}x(t_k^+) + e^{\alpha h}\rho^* \int_{t_k^+-h}^{t_k^+} x^T(s)Q_{\sigma(s)}x(s)ds \\
&\le x^T(t_k)(I+E_j)^T P_i(I+E_j)x(t_k) + e^{\alpha h}\rho^* x^T(t_k)E_j^T Q_i E_j x(t_k) \\
&\quad + e^{\alpha h}\rho^* \int_{t_k-h}^{t_k} v(s)x^T(s)e^{\alpha(t_k-s)}Q_{\sigma(s)}x(s)ds,
\end{aligned} \tag{3.13}$$

$$V(t_k) = x^T(t_k)P_j x(t_k) + \int_{t_k-h}^{t_k} v(s)x^T(s)e^{\alpha(t_k-s)}Q_{\sigma(s)}x(s)ds. \tag{3.14}$$

Combining (3.13) with (3.14), we have

$$\begin{aligned}
V(t_k^+) - e^{\alpha h}\rho^* V(t_k) &\le x^T(t_k)(I+E_j)^T P_i(I+E_j)x(t_k) \\
&\quad + e^{\alpha h}\rho^* x^T(t_k)E_j^T Q_i E_j x(t_k) - e^{\alpha h}\rho^* x^T(t_k)P_j x(t_k) \\
&= x^T(t_k)\Sigma_{ij}x(t_k),
\end{aligned} \tag{3.15}$$

where

$$\sum_{ij} = (I+E_j)^T P_i(I+E_j) + e^{\alpha h}\rho^* E_j^T Q_i E_j - e^{\alpha h}\rho^* P_j. \tag{3.16}$$

Using Schur complement, (3.11) is equivalent to

$$\Sigma_{ij} < 0 \quad \text{or} \quad V(t_k^+) - e^{\alpha h}\rho^* V(t_k) < 0. \tag{3.17}$$

The proof is completed. □

Theorem 3.4. *R is a positive definite matrix. Let $\widetilde{P}_i = R^{-1/2}P_iR^{-1/2}$, $\widetilde{Q}_i = R^{-1/2}Q_iR^{-1/2}$, For all $i \in \overline{N}$, if there exist positive scalars $\rho_i \geq 1$, $i \in \overline{N}$, $\rho^* = \max\{\rho_i, i \in \overline{N}\}$, α, λ_1, λ_2, λ_3 and symmetric positive matrices P_i, P_j, Q_i, T_i, $i, j \in \overline{N}$ such that*

$$\frac{1}{\rho^*}(I+E_i)^{-1}\widetilde{Q}_j(I+E_i)^{-T} - \widetilde{Q}_i \leq 0, \quad \forall i, j \in \overline{N} \tag{3.18}$$

$$\begin{bmatrix} \widetilde{P}_iA_i^T + A_i\widetilde{P}_i - \alpha\widetilde{P}_i + I & A_{di}\widetilde{Q}_i & B_{2i} & \widetilde{P}_i \\ * & -e^{\alpha h}\widetilde{Q}_j & 0 & 0 \\ * & * & -T_i & 0 \\ * & * & * & -\left(\rho^{*-1}\widetilde{Q}_i + U_{i_k}^TU_{i_k}\right) \end{bmatrix} < 0, \quad \forall i, j \in \overline{N} \tag{3.19}$$

$$\begin{bmatrix} -e^{\alpha h}\rho^*\widetilde{P}_j & \widetilde{P}_j\left(I+E_j^T\right) & \widetilde{P}_jE_j^T \\ * & -\widetilde{P}_i & 0 \\ * & * & -e^{-\alpha h}\left(\rho^*\right)^{-1}\widetilde{Q}_i \end{bmatrix} < 0, \quad \forall i, j \in \overline{N} \tag{3.20}$$

$$\lambda_1R^{-1} < \widetilde{P}_i < R^{-1}, \quad \lambda_2R^{-1} < \widetilde{Q}_i, \quad T_i < \lambda_3I, \quad \forall i \in \overline{N} \tag{3.21}$$

$$\begin{bmatrix} -c_2^2e^{-\alpha T_f} + d^2\lambda_3 & c_1 & c_1 \\ * & -\lambda_1 & 0 \\ * & * & -\dfrac{1}{\rho^*h}e^{-\alpha h}\lambda_2 \end{bmatrix} < 0 \tag{3.22}$$

hold, under the average dwell time scheme

$$\tau_a > \tau_a^* = \frac{T_f\left(\alpha h + \ln\rho^*\right)}{\ln\left(c_2^2e^{-\alpha T_f}\right) - \ln\left[\left(1/\lambda_1 + h\rho^*e^{\alpha h}/\lambda_2\right)c_1^2 + d^2\lambda_3\right]}, \tag{3.23}$$

system (3.1a)–(3.1c) *is finite-time bounded with respect to* $(c_1^2, c_2^2, T_f, d^2, R, \sigma(t))$.

Proof. Assuming that when $t \in (t_k, t_{k+1}]$, $\sigma(t) = i_k$, $i_k \in \overline{N}$, $k = 0, 1, 2, 3, \ldots$.

Choose the following Lyapunov functional candidate:

$$V(t) = x^T(t)\widetilde{P}_{\sigma(t)}^{-1}x(t) + \int_{t-h}^{t} v(s)x^T(s)e^{\alpha(t-s)}\widetilde{Q}_{\sigma(s)}^{-1}x(s)ds. \tag{3.24}$$

When $t \in (t_k, t_{k+1}]$, according to (3.18) and Lemma 3.2, we have

$$\begin{aligned}
\dot{V}(t) &\le 2x^T(t)\tilde{P}_{i_k}^{-1}\dot{x}(t) + \alpha\int_{t-h}^{t} v(s)x^T(s)e^{\alpha(t-s)}\tilde{Q}_{\sigma(s)}^{-1}x(s)ds \\
&\quad + v(t)x^T(t)\tilde{Q}_{i_k}^{-1}x(t) - v(t-h)x^T(t-h)\tilde{Q}_{i_{k-m}}^{-1}x(t-h)e^{\alpha h}, \\
\dot{V}(x(t)) - \alpha V(x(t)) - w^T(t)T_{i_k}w(t) &\le 2x^T(t)\tilde{P}_{i_k}^{-1}\dot{x}(t) + \alpha\int_{t-h}^{t} v(s)x^T(s)e^{\alpha(t-s)}\tilde{Q}_{\sigma(s)}^{-1}x(s)ds \\
&\quad + v(t)x^T(t)\tilde{Q}_{i_k}^{-1}x(t) - v(t-h)x^T(t-h)\tilde{Q}_{i_{k-m}}^{-1}x(t-h)e^{\alpha h} \\
&\quad - \alpha x^T(t)\tilde{P}_{i_k}^{-1}x(t) - \alpha\int_{t-h}^{t} v(s)x^T(s)e^{\alpha(t-s)}\tilde{Q}_{\sigma(s)}^{-1}x(s)ds \\
&\quad - w^T(t)T_{i_k}w(t) \\
&\le 2x^T(t)\tilde{P}_{i_k}^{-1}\dot{x}(t) + \rho^* x^T(t)\tilde{Q}_{i_k}^{-1}x(t) \\
&\quad - x^T(t-h)\tilde{Q}_{i_{k-m}}^{-1}x(t-h)e^{\alpha h} - \alpha x^T(t)\tilde{P}_{i_k}^{-1}x(t) \\
&\quad - w^T(t)T_{i_k}w(t).
\end{aligned} \tag{3.25}$$

According to (3.1a)–(3.1c), and (3.25), Assumption 2.2, and the fallowing inequality:

$$\begin{aligned}
2x^T(t)\tilde{P}_{i_k}^{-1}f(x(t)) &\le f_{i_k}^T(x(t))f_{i_k}(x(t)) + x^T(t)\tilde{P}_{i_k}^{-1}\tilde{P}_{i_k}^{-1}x(t) \\
&\le x^T(t)U_{i_k}^T U_{i_k}x(t) + x^T(t)\tilde{P}_{i_k}^{-1}\tilde{P}_{i_k}^{-1}x(t),
\end{aligned} \tag{3.26}$$

we have

$$\dot{V}(x(t)) - \alpha V(x(t)) - w^T(t)T_{i_k}w(t) \le X^T(t)\Xi_k X(t), \tag{3.27}$$

where $X^T(t) = (x^T(t)x^T(t-h)w^T(t))$,

$$\begin{gathered}
\Xi_k = \begin{bmatrix} \Delta_k & \tilde{P}_{i_k}^{-1}A_{di_k} & \tilde{P}_{i_k}^{-1}B_{2i_k} \\ * & -e^{\alpha h}\tilde{Q}_{i_{k-m}}^{-1} & 0 \\ * & * & -T_{i_k} \end{bmatrix}, \\
\Delta_k = A_{i_k}^T\tilde{P}_{i_k}^{-1} + \tilde{P}_{i_k}^{-1}A_{i_k} + \rho^*\tilde{Q}_{i_k}^{-1} - \alpha\tilde{P}_{i_k}^{-1} + U_{i_k}^T U_{i_k} + \tilde{P}_{i_k}^{-1}\tilde{P}_{i_k}^{-1}.
\end{gathered} \tag{3.28}$$

Using Schur complement, we obtain from (3.19) that

$$\begin{bmatrix} O_i & \tilde{P}_i^{-1}A_{di} & \tilde{P}_i^{-1}B_{2i} \\ * & -e^{\alpha h}\tilde{Q}_j^{-1} & 0 \\ * & * & -T_i \end{bmatrix} < 0, \tag{3.29}$$

where

$$O_i = A_i^T \widetilde{P}_i^{-1} + \widetilde{P}_i^{-1} A_i + \rho^* \widetilde{Q}_i^{-1} - \alpha \widetilde{P}_i^{-1} + U_i^T U_i + \widetilde{P}_i^{-1} \widetilde{P}_i^{-1}. \tag{3.30}$$

Noticing that the above inequality holds for all $i, j \in \overline{N}$, then we have $\Xi_k < 0$ for $i_k, i_{k-1} \in \overline{N}$. Thus,

$$\dot{V}(x(t)) - \alpha V(x(t)) - w^T(t) T_{i_k} w(t) < 0. \tag{3.31}$$

When $t \in (t_k, t_{k+1}]$, according to Lemma 3.3, we can obtain (3.12) from condition (3.20).

Combining (3.31) and (3.12), we can obtain that

$$\begin{aligned}
V(t) &< e^{\alpha(t-t_k)} V(t_k^+) + \int_{t_k}^{t} e^{\alpha(t-s)} w^T(s) T_{i_k} w(s) ds \\
&< e^{\alpha(t-t_k)} e^{\alpha h} \rho^* V(t_k) + \int_{t_k}^{t} e^{\alpha(t-s)} w^T(s) T_{i_k} w(s) ds \\
&< e^{\alpha(t-t_k)} e^{\alpha h} \rho^* \left[e^{\alpha(t_k - t_{k-1})} V(t_{k-1}^+) + \int_{t_{k-1}}^{t_k} e^{\alpha(t_k - s)} w^T(s) T_{i_{k-1}} w(s) ds \right] \\
&\quad + \int_{t_k}^{t} e^{\alpha(t-s)} w^T(s) T_{i_k} w(s) ds \\
&< \cdots \\
&< e^{\alpha(t-t_0)} \left(e^{\alpha h} \rho^* \right)^{N_\sigma(t_0,t)} V(t_0) + \left(e^{\alpha h} \rho^* \right)^{N_\sigma(t_0,t)} \int_{t_0}^{t_1} e^{\alpha(t-s)} w^T(s) T_{i_0} w(s) ds \\
&\quad + \left(e^{\alpha h} \rho^* \right)^{N_\sigma(t_1,t)} \int_{t_1}^{t_2} e^{\alpha(t-s)} w^T(s) T_{i_1} w(s) ds \\
&\quad + \cdots + e^{\alpha h} \rho^* \int_{t_{k-1}}^{t_k} e^{\alpha(t-s)} w^T(s) T_{i_{k-1}} w(s) ds + \int_{t_k}^{t} e^{\alpha(t-s)} w^T(s) T_{i_k} w(s) ds \\
&= e^{\alpha(t-t_0)} \left(e^{\alpha h} \rho^* \right)^{N_\sigma(t_0,t)} V(t_0) + \int_{t_0}^{t} e^{\alpha(t-s)} \left(e^{\alpha h} \rho^* \right)^{N_\sigma(s,t)} w^T(s) T_{i_k} w(s) ds \\
&< e^{\alpha t} \left(e^{\alpha h} \rho^* \right)^{N_\sigma(t_0,t)} V(t_0) + \left(e^{\alpha h} \rho^* \right)^{N_\sigma(t_0,t)} e^{\alpha t} \int_{t_0}^{t} w^T(s) T_{i_k} w(s) ds \\
&< e^{\alpha T_f} \left(e^{\alpha h} \rho^* \right)^{N_\sigma(t_0,t)} \left[V(t_0) + \int_{t_0}^{T_f} w^T(s) T_{i_k} w(s) ds \right] \\
&< e^{\alpha T_f} \left(e^{\alpha h} \rho^* \right)^{N_\sigma(t_0,t)} \left[V(t_0) + \lambda_{\max}(T_{i_k}) d^2 \right].
\end{aligned} \tag{3.32}$$

Noticing that $N_\sigma(t_0, T_f) < T_f/\tau_a$ and according to (3.21), we have

$$\begin{aligned} V(t) &< e^{(\alpha+\alpha h/\tau_a)T_f}\left(\rho^*\right)^{T_f/\tau_a}\left[V(t_0) + \lambda_3 d^2\right], \\ V(t) &\geq x^T(t)\widetilde{P}_{i_k}^{-1}x(t) = x^T(t)R^{1/2}P_{i_k}^{-1}R^{1/2}x(t) \\ &\geq \lambda_{\min}\left(P_{i_k}^{-1}\right)x^T(t)Rx(t) = \frac{1}{\lambda_{\max}(P_{i_k})}x^T(t)Rx(t). \end{aligned} \tag{3.33}$$

Because $\lambda_1 R^{-1} < \widetilde{P}_i < R^{-1}$, we have

$$V(t) > x^T(t)Rx(t). \tag{3.34}$$

According to the Lyapunov function that we have chosen, we have

$$\begin{aligned} V(t_0) &= x^T(t_0)\widetilde{P}_i^{-1}x(t_0) + \int_{t_0-h}^{t_0} v(s)x^T(s)e^{-\alpha(t_0-s)}\widetilde{Q}_i^{-1}x(s)ds \\ &\leq \max_{i\in\overline{N}}\lambda_{\max}\left(P_i^{-1}\right)x^T(t_0)Rx(t_0) \\ &\quad + he^{\alpha h}\rho^*\max_{i\in\overline{N}}\lambda_{\max}\left(Q_i^{-1}\right)\sup_{t_0-h\leq\theta\leq t_0}x^T(\theta)Rx(\theta) \\ &\leq \left(\frac{1}{\min_{i\in\overline{N}}\lambda_{\min}(P_i)} + \frac{\rho^* he^{\alpha h}}{\min_{i\in\overline{N}}\lambda_{\min}(Q_i)}\right)\sup_{t_0-h\leq\theta\leq t_0}x^T(\theta)Rx(\theta). \end{aligned} \tag{3.35}$$

According to (3.21), the following inequality is derived:

$$V(t_0) < \left(\frac{1}{\lambda_1} + \frac{\rho^* he^{\alpha h}}{\lambda_2}\right)c_1^2. \tag{3.36}$$

Combining (3.33), (3.34), and (3.36), we can obtain that

$$x^T(t)Rx(t) < V(t) < e^{(\alpha+\alpha h/\tau_a)T_f}\left(\rho^*\right)^{T_f/\tau_a}\left[\left(\frac{1}{\lambda_1} + \frac{\rho^* he^{\alpha h}}{\lambda_2}\right)c_1^2 + \lambda_3 d^2\right]. \tag{3.37}$$

Using Schur complement, (3.22) is equivalent to

$$\left(\frac{1}{\lambda_1} + \frac{\rho^* he^{\alpha h}}{\lambda_2}\right)c_1^2 + \lambda_3 d^2 < c_2^2 e^{-\alpha T_f}. \tag{3.38}$$

From (3.38), we can obtain that $\tau_a > 0$.

Substituting (3.23) into (3.37) leads to

$$x^T(t)Rx(t) < c_2^2. \tag{3.39}$$

Thus, system (3.1a)–(3.1c) is finite-time bounded with respect to $(c_1^2, c_2^2, T_f, d^2, R, \sigma(t))$.

The proof is completed. □

Corollary 3.5. *R is a positive definite matrix, let $w(t) \equiv 0$, $\widetilde{P}_i = R^{-1/2}P_iR^{-1/2}$, $\widetilde{Q}_i = R^{-1/2}Q_iR^{-1/2}$ for all $i \in \overline{N}$. If there exist positive scalars $\rho_i \geq 1$, $i \in \overline{N}$, $\rho^* = \max\{\rho_i, i \in \overline{N}\}$, $\alpha, \lambda_1, \lambda_2$ and symmetric positive matrices P_i, P_j, Q_i for all $i, j \in \overline{N}$ with appropriate dimensions such that*

$$\begin{gathered}
\frac{1}{\rho^*}(I+E_i)^{-1}\widetilde{Q}_j(I+E_i)^{-T} - \widetilde{Q}_i \leq 0, \quad \forall i, j \in \overline{N} \\
\begin{bmatrix} \widetilde{P}_iA_i^T + A_i\widetilde{P}_i - \alpha\widetilde{P}_i + I & A_{di}\widetilde{Q}_i & \widetilde{P}_i \\ * & -e^{\alpha h}\widetilde{Q}_j & 0 \\ * & * & -\left(\rho^{*-1}\widetilde{Q}_i + U_{i_k}^TU_{i_k}\right) \end{bmatrix} < 0, \quad \forall i, j \in \overline{N} \\
\begin{bmatrix} -e^{\alpha h}\rho^*\widetilde{P}_j & \widetilde{P}_j\left(I + E_j^T\right) & \widetilde{P}_jE_j^T \\ * & -\widetilde{P}_i & 0 \\ * & * & -e^{-\alpha h}\left(\rho^*\right)^{-1}\widetilde{Q}_i \end{bmatrix} < 0, \quad \forall i, j \in \overline{N} \\
\lambda_1R^{-1} < \widetilde{P}_i < R^{-1}, \quad \lambda_2R^{-1} < \widetilde{Q}_i, \quad \forall i \in \overline{N} \\
\begin{bmatrix} -c_2^2e^{-\alpha T_f} & c_1 & c_1 \\ * & -\lambda_1 & 0 \\ * & * & -\dfrac{1}{\rho^*h}e^{-\alpha h}\lambda_2 \end{bmatrix} < 0
\end{gathered} \tag{3.40}$$

hold with average dwell time

$$\tau_a > \tau_a^* = \frac{T_f\left(\alpha h + \ln\rho^*\right)}{\ln\left(c_2^2e^{-\alpha T_f}\right) - \ln\left[\left(1/\lambda_1 + \rho^*he^{\alpha h}/\lambda_2\right)c_1^2\right]}. \tag{3.41}$$

System (3.1a)–(3.1c) *with $w(t) \equiv 0$ is finite-time stable with respect to $(c_1^2, c_2^2, T_f, R, \sigma(t))$.*

3.2. H_∞ Performance Analysis

In this subsection, H_∞ performance of the following system is investigated:

$$\dot{x}(t) = A_{\sigma(t)}x(t) + A_{d\sigma(t)}x(t-h) + f_{\sigma(t)}(x(t)) + B_{2\sigma(t)}w(t), \quad t \neq t_k \tag{3.42a}$$

$$\Delta x = E_{\sigma(t)}x(t), \quad t = t_k, \quad k = 1,2,3,\ldots \tag{3.42b}$$

$$z(t) = C_{\sigma(t)}x(t), \tag{3.42c}$$

$$x(t) = \varphi(t), \quad t \in [t_0 - h, t_0] \tag{3.42d}$$

Theorem 3.6. *R is a positive definite matrix. Let $\widetilde{P}_i = R^{-1/2}P_iR^{-1/2}$, $\widetilde{Q}_i = R^{-1/2}Q_iR^{-1/2}$ for all $i \in \overline{N}$. Suppose that there exist positive scalars $\rho_i \geq 1, i \in \overline{N}$, $\rho^* = \max\{\rho_i, i \in \overline{N}\}$, $\alpha, \gamma, \varepsilon$ and symmetric positive matrices P_i, P_j, Q_i for all $i, j \in \overline{N}$ such that*

$$\frac{1}{\rho^*}(I+E_i)^{-1}\widetilde{Q}_j(I+E_i)^{-T} - \widetilde{Q}_i \leq 0, \quad \forall i,j \in \overline{N} \tag{3.43}$$

$$\begin{bmatrix} \widetilde{P}_iA_i^T + A_i\widetilde{P}_i - \alpha\widetilde{P}_i + I & A_{di}\widetilde{Q}_i & B_{2i} & \widetilde{P}_i & \widetilde{P}_iC_i^T \\ * & -e^{\alpha h}\widetilde{Q}_j & 0 & 0 & 0 \\ * & * & -\gamma^2 & 0 & 0 \\ * & * & * & -\left(\rho^{*-1}\widetilde{Q}_i + U_{i_k}^TU_{i_k}\right) & 0 \\ * & * & * & * & -I \end{bmatrix} < 0, \quad \forall i,j \in \overline{N} \tag{3.44}$$

$$\begin{bmatrix} -e^{\alpha h}\rho^*\widetilde{P}_j & \widetilde{P}_j\left(I+E_j^T\right) & \widetilde{P}_jE_j^T \\ * & -\widetilde{P}_i & 0 \\ * & * & -e^{-\alpha h}(\rho^*)^{-1}\widetilde{Q}_i \end{bmatrix} < 0, \quad \forall i,j \in \overline{N} \tag{3.45}$$

$$\widetilde{P}_i < R^{-1}, \quad \forall i \in \overline{N} \tag{3.46}$$

$$-c_2^2 + e^{\alpha T_f}\gamma^2d^2 < 0 \tag{3.47}$$

hold with average dwell time

$$\tau_a > \tau_a^* = \max\left\{\frac{T_f(\alpha h + \ln\rho^*)}{\ln(c_2^2) - \ln(e^{\alpha T_f}\gamma^2d^2)}, \frac{h}{\varepsilon}\right\}. \tag{3.48}$$

Then, system (3.42a)–(3.42d) *is finite-time bounded and has H_∞ performance with respect to $(0, c_2^2, T_f, d^2, \overline{\gamma}, R, \sigma(t))$, where $\overline{\gamma}^2 = e^{(1+\varepsilon)\alpha T_f}(\rho^*)^{\varepsilon T_f/h}\gamma^2$.*

Proof. When $t \in (t_k, t_{k+1}]$, $\sigma(t) = i_k$, $i_k \in \overline{N}$, $k = 0,1,2,3,\ldots$. Choose the following Lyapunov functional candidate for system (3.42a)–(3.42d)

$$V(t) = x^T(t)\widetilde{P}_{\sigma(t)}^{-1}x(t) + \int_{t-h}^{t} v(s)x^T(s)e^{\alpha(t-s)}\widetilde{Q}_{\sigma(s)}^{-1}x(s)ds. \tag{3.49}$$

When $t \in (t_k, t_{k+1}]$,

$$\dot{V}(x(t)) - \alpha V(x(t)) + z^T(t)z(t) - \gamma^2 w^T(t)w(t) \leq X^T(t)\Psi_k X(t), \tag{3.50}$$

where $X^T(t) = (x^T(t) \quad x^T(t-h) \quad w^T(t))$,

$$\Psi_k = \begin{bmatrix} \Delta_k & \widetilde{P}_{i_k}^{-1} A_{di_k} & \widetilde{P}_{i_k}^{-1} B_{2i_k} \\ * & -e^{\alpha h}\widetilde{Q}_{i_{k-m}}^{-1} & 0 \\ * & * & -\gamma^2 I \end{bmatrix},$$
$$\Delta_k = A_{i_k}^T \widetilde{P}_{i_k}^{-1} + \widetilde{P}_{i_k}^{-1} A_{i_k} + \rho^* \widetilde{Q}_{i_k}^{-1} - \alpha \widetilde{P}_{i_k}^{-1} + U_{i_k}^T U_{i_k} + \widetilde{P}_{i_k}^{-1}\widetilde{P}_{i_k}^{-1} + C_{i_k}^T C_{i_k}. \tag{3.51}$$

Using Schur complement, we obtain from (3.44) that

$$\begin{bmatrix} E_i & \widetilde{P}_i^{-1} A_{di} & \widetilde{P}_i^{-1} B_{2i} \\ * & -e^{\alpha h}\widetilde{Q}_j^{-1} & 0 \\ * & * & -\gamma^2 I \end{bmatrix} < 0, \tag{3.52}$$

where $E_i = A_i^T \widetilde{P}_i^{-1} + \widetilde{P}_i^{-1} A_i + \rho^* \widetilde{Q}_i^{-1} - \alpha \widetilde{P}_i^{-1} + U_i^T U_i + \widetilde{P}_i^{-1}\widetilde{P}_i^{-1} + C_i^T C_i$.

Noticing that the above inequality holds for all $i, j \in \overline{N}$, then we have $\Psi_k < 0$, for $i_k, i_{k-m} \in \overline{N}$.

Thus,

$$\dot{V}(x(t)) - \alpha V(x(t)) + z^T(t)z(t) - \gamma^2 w^T(t)w(t) < 0, \tag{3.53}$$

Let $\gamma^2 w^T(s)w(s) - z^T(s)z(s) = \Delta(s)$, from (3.32), we have

$$V(t) < e^{\alpha(t-t_0)}\left(e^{\alpha h}\rho^*\right)^{N_\sigma(t_0,t)} V(t_0) + \int_{t_0}^{t} e^{\alpha(t-s)}\left(e^{\alpha h}\rho^*\right)^{N_\sigma(s,t)} \Delta(s)ds. \tag{3.54}$$

Under zero initial condition, we have

$$0 < \int_{t_0}^{t} e^{\alpha(t-s)}\left(e^{\alpha h}\rho^*\right)^{N_\sigma(s,t)} \Delta(s)ds, \tag{3.55}$$

that is,

$$\int_{t_0}^{t} e^{\alpha(t-s)}\left(e^{\alpha h}\rho^*\right)^{N_\sigma(s,t)} z^T(s)z(s)ds < \int_{t_0}^{t} e^{\alpha(t-s)}\left(e^{\alpha h}\rho^*\right)^{N_\sigma(s,t)} \gamma^2 w^T(s)w(s)ds. \tag{3.56}$$

Noticing that

$$\int_{t_0}^{t} e^{\alpha(t-s)}\left(e^{\alpha h}\rho^*\right)^{N_\sigma(s,t)} z^T(s)z(s)ds > \int_{t_0}^{t} z^T(s)z(s)ds. \tag{3.57}$$

Then, we have

$$\int_{t_0}^{t} e^{\alpha(t-s)}\left(e^{\alpha h}\rho^*\right)^{N_\sigma(s,t)}\gamma^2 w^T(s)w(s)ds < e^{\alpha t}\left(e^{\alpha h}\rho^*\right)^{N_\sigma(t_0,t)}\int_{t_0}^{t}\gamma^2 w^T(s)w(s)ds. \tag{3.58}$$

Let $t = T_f$, because $\tau_a > h/\varepsilon$, we have

$$\int_{t_0}^{T_f} z^T(s)z(s)ds < e^{(1+\varepsilon)\alpha T_f}(\rho*)^{\varepsilon T_f/h}\gamma^2\int_{t_0}^{T_f} w^T(s)w(s)ds, \tag{3.59}$$

then

$$\int_{t_0}^{T_f} z^T(s)z(s)ds < \overline{\gamma}^2\int_{t_0}^{T_f} w^T(s)w(s)ds. \tag{3.60}$$

Thus, system (3.42a)–(3.42d) is finite-time bounded and has H_∞ performance with respect to $(0, c_2^2, T_f, d^2, \overline{\gamma}, R, \sigma(t))$, where $\overline{\gamma}^2 = e^{(1+\varepsilon)\alpha T_f}(\rho^*)^{\varepsilon T_f/h}\gamma^2$.

The proof is completed. □

Remark 3.7. When $\rho^* = 1$, Theorem 3.6 degenerates to the result of [41], which cannot guarantee the finite-time boundedness of the addressed system if $\rho^* > 1$.

3.3. Robust Finite-Time H_∞ Control

Consider system (2.1a)–(2.1d), under the switching controller $u_1(t) = K_{\sigma(t)}x(t)$, $t \neq t_k$ and impulsive controller $u_2(t_k) = \overline{K}_{\sigma(t)}x(t_k)$, $t = t_k$, the corresponding closed-loop system is given by

$$\dot{x}(t) = \left(\widehat{A}_{\sigma(t)} + \widehat{B}_{1\sigma(t)}K_{\sigma(t)}\right)x(t) + \widehat{A}_{d\sigma(t)}x(t-h) + f_{\sigma(t)}(x(t)) + B_{2\sigma(t)}w(t), \quad t \neq t_k \tag{3.61a}$$

$$\Delta x = \left(E_{\sigma(t)} + \overline{K}_{\sigma(t)}\right)x(t), \quad t = t_k,\ k = 1,2,3,\ldots \tag{3.61b}$$

$$z(t) = \left(C_{\sigma(t)} + D_{\sigma(t)}K_{\sigma(t)}\right)x(t), \tag{3.61c}$$

$$x(t) = \varphi(t), \quad t \in [t_0 - h, t_0]. \tag{3.61d}$$

Theorem 3.8. *Consider impulsive switched system* (2.1a)–(2.1d), *let* $\widetilde{P}_i = R^{-1/2}P_iR^{-1/2}$, $\widetilde{Q}_i = R^{-1/2}Q_iR^{-1/2}$*for all* $i \in \overline{N}$. *If there exist positive scalars* $\rho_i \geq 1$, $i \in \overline{N}$, $\rho^* = \max\{\rho_i, i \in \overline{N}\}$ $\alpha, \gamma, \varepsilon, \delta_i$ *and positive definite symmetric matrices* P_i, Q_i, *and matrices* Y_i, $i \in \overline{N}$, *with appropriate dimensions, such that the following inequalities hold*

$$\frac{1}{\rho^*}(I+E_i)^{-1}\tilde{Q}_j(I+E_i)^{-T}-\tilde{Q}_i\le 0,\quad \forall i,j\in\overline{N} \tag{3.62}$$

$$\begin{bmatrix} \Gamma_i & A_{di}\tilde{Q}_i & B_{2i} & \tilde{P}_i & \tilde{P}_iC_i^T+Y_i^TD_i^T & Y_i^TE_{Bi}^T+\tilde{P}_iE_{Ai}^T \\ * & -e^{\alpha h}\tilde{Q}_j & 0 & 0 & 0 & \tilde{Q}_iE_{Adi}^T \\ * & * & -\gamma^2 & 0 & 0 & 0 \\ * & * & * & -\left(\rho^{*-1}\tilde{Q}_i+U_{i_k}^TU_{i_k}\right) & 0 & 0 \\ * & * & * & * & -I & 0 \\ * & * & * & * & * & -\delta_i \end{bmatrix}<0,\quad \forall i,j\in\overline{N}, \tag{3.63}$$

where

$$\Gamma_i=\tilde{P}_iA_i^T+Y_i^TB_{1i}^T+A_i\tilde{P}_i+B_{1i}Y_i-\alpha\tilde{P}_i+I+\delta_iH_iH_i^T,$$

$$\begin{bmatrix} -e^{\alpha h}\rho^*\tilde{P}_j & \tilde{P}_j \\ * & -\tilde{P}_i \end{bmatrix}<0,\quad \forall i,j\in\overline{N} \tag{3.64}$$

$$\tilde{P}_i<R^{-1},\quad i\in\overline{N}, \tag{3.65}$$

$$-c_2^2+e^{\alpha T_f}\gamma^2d^2<0. \tag{3.66}$$

Then, under the controller $K_i=Y_i\tilde{P}_i^{-1}$, $\overline{K}_i=-E_i$, *and the following average dwell time scheme*

$$\tau_a>\tau_a^*=\max\left\{\frac{T_f(\alpha h+\ln\rho^*)}{\ln(c_2^2)-\ln(e^{\alpha T_f}\gamma^2d^2)},\frac{h}{\varepsilon}\right\}, \tag{3.67}$$

the corresponding closed-loop system is finite-time bounded with H_∞ *performance with respect to* $(0,c_2^2,T_f,d^2,\overline{\gamma},R,\sigma(t))$ *and* $\overline{\gamma}^2=e^{(1+\varepsilon)\alpha T_f}(\rho^*)^{\varepsilon T_f/h}\gamma^2$.

Proof. According to Assumption 2.1, we have

$$\widehat{A}_i+\widehat{B}_{1i}K_i=(A_i+B_{1i}K_i)+H_iF_i(E_{Ai}+E_{Bi}K_i),\qquad \widehat{A}_{di}=A_{di}+H_iF_iE_{Adi}. \tag{3.68}$$

Now replacing A_i, A_{di}, C_i in the left side of (3.44) with $\widehat{A}_i+\widehat{B}_{1i}K_i$, $\widehat{A}_{di}$, $C_i+D_iK_i$, we can obtain that

$$\Theta_{ij}=\begin{bmatrix} \Omega_i & (A_{di}+H_iF_iE_{Adi})\tilde{Q}_i & B_{2i} & \tilde{P}_i & \tilde{P}_i(C_i+D_iK_i)^T \\ * & -e^{\alpha h}\tilde{Q}_j & 0 & 0 & 0 \\ * & * & -\gamma^2 & 0 & 0 \\ * & * & * & -\left(\rho^{*-1}\tilde{Q}_i+U_{i_k}^TU_{i_k}\right) & 0 \\ * & * & * & * & -I \end{bmatrix}, \tag{3.69}$$

where

$$\Omega_i = [(A_i + B_{1i}K_i) + H_iF_i(E_{Ai} + E_{Bi}K_i)]\tilde{P}_i + \tilde{P}_i[(A_i + B_{1i}K_i) + H_iF_i(E_{Ai} + E_{Bi}K_i)]^T - \alpha\tilde{P}_i + I. \tag{3.70}$$

From (3.69), we know that

$$\Theta_{ij} = \Pi_{1ij} + \Pi_{2ij}, \tag{3.71}$$

where

$$\Pi_{1ij} = \begin{bmatrix} \Upsilon_{1i} & A_{di}\tilde{Q}_i & B_{2i} & \tilde{P}_i & \tilde{P}_i(C_i + D_iK_i)^T \\ * & -e^{\alpha h}\tilde{Q}_j & 0 & 0 & 0 \\ * & * & -\gamma^2 & 0 & 0 \\ * & * & * & -\left(\rho^{*-1}\tilde{Q}_i + U_{i_k}^T U_{i_k}\right) & 0 \\ * & * & * & * & -I \end{bmatrix},$$
$$\Pi_{2ij} = \begin{bmatrix} \Upsilon_{2i} & H_iF_iE_{Adi}\tilde{Q}_i & 0 & 0 & 0 \\ * & 0 & 0 & 0 & 0 \\ * & * & 0 & 0 & 0 \\ * & * & * & 0 & 0 \\ * & * & * & * & 0 \end{bmatrix}, \tag{3.72}$$

with

$$\begin{aligned} \Upsilon_{1i} &= \tilde{P}_i(A_i + B_{1i}K_i)^T + (A_i + B_{1i}K)\tilde{P}_i - \alpha\tilde{P}_i + I, \\ \Upsilon_{2i} &= \tilde{P}_i(E_{A_i} + E_{B_i}K_i)^T F_i^T H_i^T + H_iF_i(E_{Ai} + E_{Bi}K_i)\tilde{P}_i, \end{aligned} \tag{3.73}$$

let $Y_i = K_i\tilde{P}_i$, then

$$\begin{aligned} \Upsilon_{1i} &= \tilde{P}_iA_i^T + Y_i^TB_{1i}^T + A_i\tilde{P}_i + B_{1i}Y_i - \alpha\tilde{P}_i + I, \\ \Upsilon_{2i} &= \left(Y_i^TE_{Bi}^T + \tilde{P}_iE_{Ai}^T\right)F_i^TH_i^T + H_iF_i\left(E_{Ai}\tilde{P}_i + E_{Bi}Y_i\right). \end{aligned} \tag{3.74}$$

From Lemma 2.11, we can obtain that

$$\begin{aligned}
\Theta_{ij} &= \Pi_{1ij} + \begin{bmatrix} H_i \\ 0 \\ 0 \\ 0 \\ 0 \end{bmatrix} F_i \begin{bmatrix} E_{Ai}\tilde{P}_i + E_{Bi}Y_i & E_{Adi}\tilde{Q}_i & 0 & 0 & 0 \end{bmatrix} \\
&\quad + \begin{bmatrix} Y_i^T E_{Bi}^T + \tilde{P}_i E_{Ai}^T \\ \tilde{Q}_i E_{Adi}^T \\ 0 \\ 0 \\ 0 \end{bmatrix} F_i \begin{bmatrix} H_i^T & 0 & 0 & 0 & 0 \end{bmatrix} \\
&\le \Pi_{1ij} + \delta_i \begin{bmatrix} H_i \\ 0 \\ 0 \\ 0 \\ 0 \end{bmatrix} \begin{bmatrix} H_i^T & 0 & 0 & 0 & 0 \end{bmatrix} \\
&\quad + \frac{1}{\delta_i} \begin{bmatrix} Y_i^T E_{Bi}^T + \tilde{P}_i E_{Ai}^T \\ \tilde{Q}_i E_{Adi}^T \\ 0 \\ 0 \\ 0 \end{bmatrix} \begin{bmatrix} E_{Ai}\tilde{P}_i + E_{Bi}Y_i & E_{Adi}\tilde{Q}_i & 0 & 0 & 0 \end{bmatrix}.
\end{aligned} \tag{3.75}$$

Using Schur complement lemma, we get from (3.63) that

$$\Theta_{ij} < 0. \tag{3.76}$$

Now we choose $\overline{K}_i = -E_i$, and replacing E_i in (3.45) with $E_i + \overline{K}_i$, we know that

$$\begin{bmatrix} -e^{\alpha h}\rho^* \tilde{P}_j & \tilde{P}_j & 0 \\ * & -\tilde{P}_i & 0 \\ * & * & -e^{-\alpha h}(\rho^*)^{-1}\tilde{Q}_i \end{bmatrix} < 0, \tag{3.77}$$

by (3.64), we know that the condition(3.45) hold.

Then, system (2.1a)–(2.1d) is robust finite-time bounded with H_∞ performance with respect to $(0, c_2^2, T_f, d^2, \overline{\gamma}, R, \sigma(t))$, and $\overline{\gamma}^2 = e^{(1+\varepsilon)\alpha T_f}(\rho^*)^{\varepsilon T_f/h}\gamma^2$.

The proof is completed. □

Remark 3.9. In order to eliminate the impulsive jump, we design an impulsive feedback controller $\overline{K}_i = -E_i$, $t = t_k$. Then the system becomes a switched system with continuous states.

4. Numerical Examples

In this section, we present two examples to illustrate the effectiveness of the proposed approach.

Example 4.1. Consider system (2.1a)–(2.1d) with the following parameters.

Subsystem 1

$$A_1 = \begin{bmatrix} -8 & 1 \\ 2 & -7 \end{bmatrix}, \quad A_{d1} = \begin{bmatrix} -1.3 & 0.1 \\ 0.2 & -1 \end{bmatrix}, \quad H_1 = \begin{bmatrix} -0.1 & 0.3 \\ 0.2 & 0.4 \end{bmatrix}, \quad E_{Ad1} = \begin{bmatrix} 0.2 & 0.1 \\ 0.3 & -0.2 \end{bmatrix},$$
$$E_1 = \begin{bmatrix} 0.43 & 0 \\ 0 & 0.15 \end{bmatrix}, \quad U_1 = \begin{bmatrix} 0.1 & 0 \\ 0 & 0.1 \end{bmatrix}, \quad B_{11} = \begin{bmatrix} 3 & -3 \\ 0 & 4 \end{bmatrix},$$
$$E_{B1} = \begin{bmatrix} 0.2 & 0.1 \\ 0 & -0.3 \end{bmatrix}, \quad B_{21} = \begin{bmatrix} 1 & -1 \\ 2 & 1 \end{bmatrix},$$
$$C_1 = \begin{bmatrix} 1 & 1 \\ 0 & 2 \end{bmatrix}, \quad D_1 = \begin{bmatrix} 0.8 & 0 \\ 0 & 0.2 \end{bmatrix}, \quad E_{A1} = \begin{bmatrix} -0.3 & -0.1 \\ 0.2 & -0.1 \end{bmatrix}, \tag{4.1}$$

$f_1(x(t)) = 0.1 \sin x(t)$, where $\|f_1(x(t))\| < \|U_1 x(t)\|$.

Subsystem 2

$$A_2 = \begin{bmatrix} -7 & 2 \\ 1 & -6 \end{bmatrix}, \quad A_{d2} = \begin{bmatrix} -1.2 & 0.1 \\ 0.3 & -1.1 \end{bmatrix}, \quad H_2 = \begin{bmatrix} -0.1 & 0.2 \\ -0.2 & -0.1 \end{bmatrix}, \quad E_{Ad2} = \begin{bmatrix} -0.3 & 0.1 \\ 0.2 & -0.3 \end{bmatrix},$$
$$E_2 = \begin{bmatrix} 0.15 & 0 \\ 0 & 0.4 \end{bmatrix}, \quad U_2 = \begin{bmatrix} 0.2 & 0 \\ 0 & 0.18 \end{bmatrix}, \quad B_{12} = \begin{bmatrix} 4 & -1 \\ 1 & 6 \end{bmatrix}, \quad E_{B2} = \begin{bmatrix} -0.3 & 0.1 \\ 0 & 0.2 \end{bmatrix},$$
$$B_{22} = \begin{bmatrix} -1 & 0 \\ 2 & 0.8 \end{bmatrix}, \quad C_2 = \begin{bmatrix} 2 & 1 \\ 0 & 3 \end{bmatrix}, \quad D_2 = \begin{bmatrix} 0.8 & 0 \\ 1 & -1 \end{bmatrix}, \quad E_{A2} = \begin{bmatrix} 0.1 & 0.3 \\ 0.2 & -0.2 \end{bmatrix}, \tag{4.2}$$

$f_2(x(t)) = 0.18 \cos x(t)$, where $\|f_2(x(t))\| < \|U_2 x(t)\|$.

Choosing $T_f = 12, h = 0.2, d^2 = 10, R = I,\ \alpha = 0.1, C_2^2 = 2,\ \varepsilon = 0.1,\ \gamma^2 = 0.5441,\ \rho^* = 1$, solving the LMIs in (3.62)–(3.66) leads to

$$\tilde{Q}_1 = \begin{bmatrix} 1.3506 & -0.1265 \\ -0.1265 & 0.7891 \end{bmatrix}, \quad \tilde{Q}_2 = \begin{bmatrix} 0.5042 & 0.0525 \\ 0.0525 & 0.3221 \end{bmatrix}, \quad Y_1 = \begin{bmatrix} 0.0234 & -0.3577 \\ 0.1631 & 0.2680 \end{bmatrix},$$

$$Y_2 = \begin{bmatrix} -0.0001 & -0.5221 \\ 0.1109 & 0.0371 \end{bmatrix}, \quad \tilde{P}_1 = \begin{bmatrix} 0.9887 & 0.0011 \\ 0.0011 & 0.9921 \end{bmatrix}, \quad \tilde{P}_2 = \begin{bmatrix} 0.9995 & -0.0001 \\ -0.0001 & 1.0006 \end{bmatrix},$$

$$K_1 = \begin{bmatrix} 0.0241 & -0.3605 \\ 0.1647 & 0.2699 \end{bmatrix}, \quad K_2 = \begin{bmatrix} -0.0001 & -0.5218 \\ 0.1109 & 0.0371 \end{bmatrix},$$

$$\begin{aligned} &\tilde{Q}_1^{-1} - (I + E_1)^T \tilde{Q}_1^{-1} (I + E_1) \leq 0, \\ &\tilde{Q}_2^{-1} - (I + E_2)^T \tilde{Q}_1^{-1} (I + E_2) \leq 0, \\ &\tilde{Q}_2^{-1} - (I + E_2)^T \tilde{Q}_2^{-1} (I + E_2) \leq 0, \\ &\tilde{Q}_1^{-1} - (I + E_1)^T \tilde{Q}_2^{-1} (I + E_1) \leq 0, \end{aligned} \tag{4.3}$$

$\tau_a > \tau_a^* = 1.2049$, we choose $\tau_a = 2$, $\bar{\gamma}^2 = e^{(1+\varepsilon)\alpha T_f} (\rho^*)^{\varepsilon \alpha T_f} \gamma^2 = 2.0368$, then the system is finite-time bounded according to [41, Theorem 3].

Example 4.2. Consider system (2.1a)–(2.1d) with the following parameters.

Subsystem 1

$$\begin{aligned} &A_1 = \begin{bmatrix} -8 & 1 \\ 2 & -7 \end{bmatrix}, \quad A_{d1} = \begin{bmatrix} -1.3 & 0.1 \\ 0.2 & -1 \end{bmatrix}, \quad H_1 = \begin{bmatrix} -0.1 & 0.3 \\ 0.2 & 0.4 \end{bmatrix}, \quad E_{Ad1} = \begin{bmatrix} 0.2 & 0.1 \\ 0.3 & -0.2 \end{bmatrix}, \\ &E_1 = \begin{bmatrix} -0.1 & 0 \\ 0 & -0.1 \end{bmatrix}, \quad U_1 = \begin{bmatrix} 0.01 & 0 \\ 0 & 0.01 \end{bmatrix}, \quad B_{11} = \begin{bmatrix} 3 & -3 \\ 0 & 4 \end{bmatrix}, \quad E_{B1} = \begin{bmatrix} 0.2 & 0.1 \\ 0 & -0.3 \end{bmatrix}, \\ &B_{21} = \begin{bmatrix} 1 & -1 \\ 2 & 1 \end{bmatrix}, \quad C_1 = \begin{bmatrix} -3 & 1 \\ 0 & -2 \end{bmatrix}, \quad D_1 = \begin{bmatrix} 8 & 0 \\ 0 & 2 \end{bmatrix}, \quad E_{A1} = \begin{bmatrix} -3 & -0.1 \\ 0.2 & -1 \end{bmatrix}, \end{aligned} \tag{4.4}$$

$f_1(x(t)) = 0.01 \sin x(t)$.

Subsystem 2

$$\begin{aligned} &A_2 = \begin{bmatrix} -7 & 2 \\ 1 & -6 \end{bmatrix}, \quad A_{d2} = \begin{bmatrix} -1.2 & 0.1 \\ 0.3 & -1.1 \end{bmatrix}, \quad H_2 = \begin{bmatrix} -0.1 & 0.2 \\ -0.2 & -0.1 \end{bmatrix}, \quad E_{Ad2} = \begin{bmatrix} -0.3 & 0.1 \\ 0.2 & -0.3 \end{bmatrix}, \\ &E_2 = \begin{bmatrix} -0.1 & 0 \\ 0 & -0.1 \end{bmatrix}, \quad U_2 = \begin{bmatrix} 0.02 & 0 \\ 0 & 0.08 \end{bmatrix}, \quad B_{12} = \begin{bmatrix} 4 & -1 \\ 1 & 6 \end{bmatrix}, \quad E_{B2} = \begin{bmatrix} -0.3 & 0.1 \\ 0 & 0.2 \end{bmatrix}, \\ &B_{22} = \begin{bmatrix} -1 & 0 \\ 2 & 0.8 \end{bmatrix}, \quad C_2 = \begin{bmatrix} -2 & 1 \\ 0 & -3 \end{bmatrix}, \quad D_2 = \begin{bmatrix} 8 & 0 \\ 1 & 8 \end{bmatrix}, \quad E_{A2} = \begin{bmatrix} -1 & 0.3 \\ 0.2 & -2 \end{bmatrix}, \end{aligned} \tag{4.5}$$

$f_2(x(t)) = 0.02 \cos x(t)$.

(1) Let $h = 0.2, T_f = 12, d^2 = 10, R = I$, $\alpha = 0.001$, $C_2^2 = 21$, $\rho^* = 1.3$, $\gamma^2 = 0.9344$. By solving the LMIs in (3.62)–(3.66), we can get

$$\tilde{Q}_1 = \begin{bmatrix} 0.4252 & 0.0387 \\ 0.0387 & 1.2272 \end{bmatrix}, \quad \tilde{Q}_2 = \begin{bmatrix} 0.4352 & 0.0470 \\ 0.0470 & 1.2369 \end{bmatrix}, \quad Y_1 = \begin{bmatrix} 0.0866 & -0.4834 \\ -0.0863 & 0.5554 \end{bmatrix},$$
$$Y_2 = \begin{bmatrix} 0.1064 & -0.2575 \\ -0.1260 & 0.2934 \end{bmatrix}, \quad \tilde{P}_1 = \begin{bmatrix} 0.4606 & 0.0418 \\ 0.0418 & 0.9965 \end{bmatrix}, \quad \tilde{P}_2 = \begin{bmatrix} 0.5364 & -0.0611 \\ -0.0611 & 0.9884 \end{bmatrix}, \tag{4.6}$$
$$K_1 = \begin{bmatrix} 0.2329 & -0.4949 \\ -0.2389 & 0.5673 \end{bmatrix}, \quad K_2 = \begin{bmatrix} 0.1699 & -0.2500 \\ -0.2024 & 0.2844 \end{bmatrix},$$

and $\tau_a > \tau_a^* = 3.8340$. We choose $\tau_a = 4$, $\varepsilon = 0.05$, $\overline{\gamma}^2 = 0.9464$, the initial condition $x(t) = 0, t \in [-h, 0]$, the switching signal is shown in Figure 1, and state trajectories of the closed-loop system are shown in Figure 2.

We can see from Figure 2 that the states of the system are continuous due to the feedback $\overline{K}_i$ in impulsive instants.

(2) Let $h = 0.2, T_f = 12, d^2 = 10, R = I$, and $\alpha = 0.001$. By solving the LMIs of [41, Theorem 3], we can get

$$\tilde{Q}_1 = \begin{bmatrix} 0.4015 & 0.0359 \\ 0.0359 & 1.0563 \end{bmatrix}, \quad \tilde{Q}_2 = \begin{bmatrix} 0.5224 & 0.1104 \\ 0.1104 & 1.0717 \end{bmatrix}, \quad Y_1 = \begin{bmatrix} 0.1245 & -0.6523 \\ -0.0998 & 0.5952 \end{bmatrix},$$
$$Y_2 = \begin{bmatrix} 0.1279 & -0.2380 \\ -0.1006 & 0.2699 \end{bmatrix}, \quad \tilde{P}_1 = \begin{bmatrix} 0.5577 & 0.0099 \\ 0.0099 & 0.9992 \end{bmatrix}, \quad \tilde{P}_2 = \begin{bmatrix} 0.5577 & 0.0099 \\ 0.0099 & 0.9992 \end{bmatrix},$$
$$K_1 = \begin{bmatrix} 0.2349 & -0.6552 \\ -0.1896 & 0.5976 \end{bmatrix}, \quad K_2 = \begin{bmatrix} 0.2336 & -0.2405 \\ -0.1852 & 0.2720 \end{bmatrix},$$
$$\tilde{Q}_1^{-1} - (I + E_1)^T \tilde{Q}_1^{-1} (I + E_1) > 0,$$
$$\tilde{Q}_2^{-1} - (I + E_2)^T \tilde{Q}_1^{-1} (I + E_2) > 0,$$
$$\tilde{Q}_2^{-1} - (I + E_2)^T \tilde{Q}_2^{-1} (I + E_2) > 0,$$
$$\tilde{Q}_1^{-1} - (I + E_1)^T \tilde{Q}_2^{-1} (I + E_1) > 0. \tag{4.7}$$

Obviously, the above inequalities do not satisfy the conditions of [41, Theorem 3]. Thus, we cannot draw the conclusion that the closed-loop system is finite-time bounded from Theorem 3 in [41].

5. Conclusions

This paper has investigated robust finite-time H_∞ control for a class of impulsive switched nonlinear systems with time-delay. Based on piecewise Lyapunov function, sufficient conditions which guarantee finite-time boundedness of the impulsive switched system are

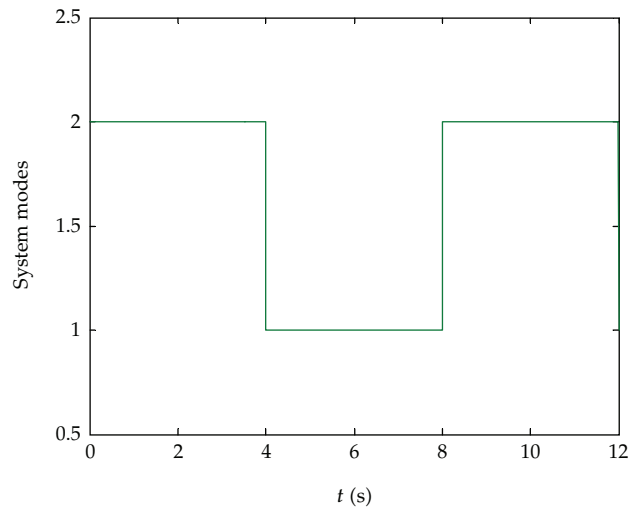

Figure 1: Switching signal.

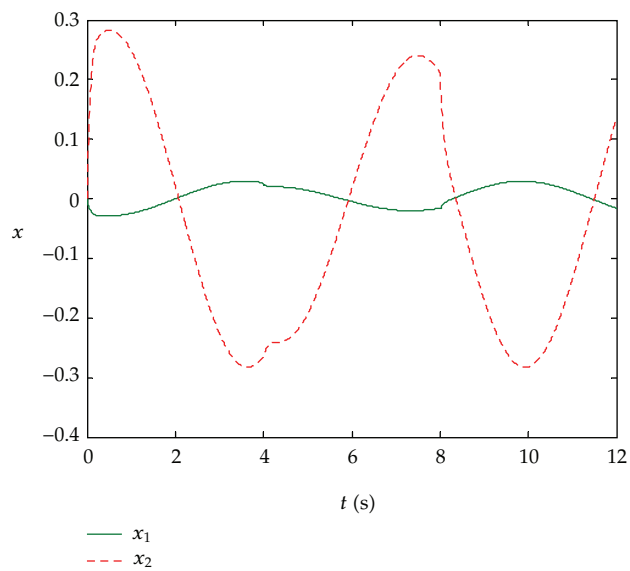

Figure 2: State trajectories of the closed-loop system.

derived. Then, a feedback control scheme consisting of an impulsive feedback controller and a switching controller is proposed, and the proposed control strategy can guarantee that the closed-loop system is finite-time bounded with H_∞ disturbance attenuation level. Finally, the results are illustrated by means of two numerical examples.

Acknowledgment

This work was supported by the National Natural Science Foundation of China under Grant nos. 61074023, 60974027, and 61273120.

References

[1] D. J. Leith, R. N. Shorten, W. E. Leithead, O. Mason, and P. Curran, "Issues in the design of switched linear control systems: a benchmark study," *International Journal of Adaptive Control and Signal Processing*, vol. 17, no. 2, pp. 103–118, 2003.

[2] D. Liberzon and A. S. Morse, "Basic problems in stability and design of switched systems," *IEEE Control Systems Magazine*, vol. 19, no. 5, pp. 59–70, 1999.

[3] D. Liberzon, J. P. Hespanha, and A. S. Morse, "Stability of switched systems: a Lie-algebraic condition," *Systems & Control Letters*, vol. 37, no. 3, pp. 117–122, 1999.

[4] H. Lin and P. J. Antsaklis, "Stability and stabilizability of switched linear systems: a survey of recent results," *IEEE Transactions on Automatic Control*, vol. 54, no. 2, pp. 308–322, 2009.

[5] R. A. Decarlo, M. S. Branicky, S. Pettersson, and B. Lennartson, "Perspectives and results on the stability and stabilizability of hybrid systems," *Proceedings of the IEEE*, vol. 88, no. 7, pp. 1069–1082, 2000.

[6] S. Kim, S. A. Campbell, and X. Liu, "Stability of a class of linear switching systems with time delay," *IEEE Transactions on Circuits and Systems. I*, vol. 53, no. 2, pp. 384–393, 2006.

[7] D. Liberzon, *Switching in Systems and Control*, Birkhäuser, Boston, Mass, USA, 2003.

[8] F. Blanchini and S. Miani, *Set-theoretic Methods in Control*, Birkhäuser, Boston, Mass, USA, 2008.

[9] R. Yuan, Z. Jing, and L. Chen, "Uniform asymptotic stability of hybrid dynamical systems with delay," *IEEE Transactions on Automatic Control*, vol. 48, no. 2, pp. 344–348, 2003.

[10] P. Colaneri, J. C. Geromel, and A. Astolfi, "Stabilization of continuous-time switched nonlinear systems," *Systems & Control Letters*, vol. 57, no. 1, pp. 95–103, 2008.

[11] M. da la Sen, "Quadratic stability and stabilization of switched dynamic systems with uncommensurate internal point delays," *Applied Mathematics and Computation*, vol. 185, no. 1, pp. 508–526, 2007.

[12] O. M. Abou Al-Ola, K. Fujimoto, and T. Yoshinaga, "Common Lyapunov function based on Kullback-Leibler divergence for a switched nonlinear system," *Mathematical Problems in Engineering*, vol. 2011, Article ID 723509, 12 pages, 2011.

[13] M. de la Sen and A. Ibeas, "Stability results for switched linear systems with constant discrete delays," *Mathematical Problems in Engineering*, vol. 2008, Article ID 543145, 28 pages, 2008.

[14] C. Gökçek, "Stability analysis of periodically switched linear systems using Floquet theory," *Mathematical Problems in Engineering*, vol. 2044, no. 1, pp. 1–10, 2004.

[15] M. de la Sen, "Sufficiency-type stability and stabilization criteria for linear time-invariant systems with constant point delays," *Lithuanian Mathmatical Journal*, vol. 43, no. 3, pp. 235–256, 2003.

[16] H. Dong, Z. Wang, D. W. C. Ho, and H. Gao, "Robust H_∞ filtering for Markovian jump systems with randomly occurring nonlinearities and sensor saturation: the finite-horizon case," *IEEE Transactions on Signal Processing*, vol. 59, no. 7, pp. 3048–3057, 2011.

[17] H. Dong, Z. Wang, and H. Gao, "Observer-based H_∞ control for systems with repeated scalar nonlinearities and multiple packet losses," *International Journal of Robust and Nonlinear Control*, vol. 20, no. 12, pp. 1363–1378, 2010.

[18] H. Dong, Z. Wang, and H. Gao, "Robust H_∞ filtering for a class of nonlinear networked systems with multiple stochastic communication delays and packet dropouts," *IEEE Transactions on Signal Processing*, vol. 58, no. 4, pp. 1957–1966, 2010.

[19] B. Shen, Z. Wang, and X. Liu, "Bounded H_∞ synchronization and state estimation for discrete time-varying stochastic complex networks over a finite horizon," *IEEE Transactions on Neural Networks*, vol. 22, no. 1, pp. 145–157, 2011.

[20] B. Shen, Z. Wang, Y. S. Hung, and G. Chesi, "Distributed H_∞ filtering for polynomial nonlinear stochastic systems in sensor networks," *IEEE Transactions on Industrial Electronics*, vol. 58, no. 5, pp. 1971–1979, 2011.

[21] B. Shen, Z. Wang, and Y. S. Hung, "Distributed H_∞-consensus filtering in sensor networks with multiple missing measurements: the finite-horizon case," *Automatica*, vol. 46, no. 10, pp. 1682–1688, 2010.

[22] Z. Xiang, Y.-N. Sun, and M. S. Mahmoud, "Robust finite-time H_∞ control for a class of uncertain switched neutral systems," *Communications in Nonlinear Science and Numerical Simulation*, vol. 17, no. 4, pp. 1766–1778, 2012.

[23] G. Zong, S. Xu, and Y. Wu, "Robust H_∞ stabilization for uncertain switched impulsive control systems with state delay: an LMI approach," *Nonlinear Analysis: Hybrid Systems*, vol. 2, no. 4, pp. 1287–1300, 2008.

[24] J. Liu, X. Liu, and W.-C. Xie, "Input-to-state stability of impulsive and switching hybrid systems with time-delay," *Automatica*, vol. 47, no. 5, pp. 899–908, 2011.
[25] X. Liu, S. Zhong, and X. Ding, "Robust exponential stability of impulsive switched systems with switching delays: a Razumikhin approach," *Communications in Nonlinear Science and Numerical Simulation*, vol. 17, no. 4, pp. 1805–1812, 2012.
[26] P. Dorato, "Short time stability in linear time-varying systems," in *Proceedings of the IRE International Convention Record Part 4*, pp. 83–87, 1961.
[27] F. Amato, M. Ariola, and P. Dorato, "Finite-time control of linear systems subject to parametric uncertainties and disturbances," *Automatica*, vol. 37, no. 9, pp. 1459–1463, 2001.
[28] S. Zhao, J. Sun, and L. Liu, "Finite-time stability of linear time-varying singular systems with impulsive effects," *International Journal of Control*, vol. 81, no. 11, pp. 1824–1829, 2008.
[29] E. Moulay and W. Perruquetti, "Finite time stability conditions for non-autonomous continuous systems," *International Journal of Control*, vol. 81, no. 5, pp. 797–803, 2008.
[30] F. Amato, M. Ariola, and C. Cosentino, "Finite-time control of discrete-time linear systems: analysis and design conditions," *Automatica*, vol. 46, no. 5, pp. 919–924, 2010.
[31] F. Amato, M. Ariola, and C. Cosentino, "Finite-time stability of linear time-varying systems: analysis and controller design," *IEEE Transactions on Automatic Control*, vol. 55, no. 4, pp. 1003–1008, 2010.
[32] L. Weiss and E. F. Infante, "Finite time stability under perturbing forces and on product spaces," *IEEE Transactions on Automatic Control*, vol. 12, pp. 54–59, 1967.
[33] L. Liu and J. Sun, "Finite-time stabilization of linear systems via impulsive control," *International Journal of Control*, vol. 81, no. 6, pp. 905–909, 2008.
[34] F. Amato, R. Ambrosino, M. Ariola, and C. Cosentino, "Finite-time stability of linear time-varying systems with jumps," *Automatica*, vol. 45, no. 5, pp. 1354–1358, 2009.
[35] R. Ambrosino, F. Calabrese, C. Cosentino, and G. De Tommasi, "Sufficient conditions for finite-time stability of impulsive dynamical systems," *IEEE Transactions on Automatic Control*, vol. 54, no. 4, pp. 861–865, 2009.
[36] F. Amato, R. Ambrosino, C. Cosentino, and G. De Tommasi, "Finite-time stabilization of impulsive dynamical linear systems," *Nonlinear Analysis: Hybrid Systems*, vol. 5, no. 1, pp. 89–101, 2011.
[37] H. Du, X. Lin, and S. Li, "Finite-time stability and stabilization of switched linear systems," in *Proceedings of the 28th Chinese Control Conference (CCC '09)*, pp. 1938–1943, December 2009.
[38] W. Xiang and J. Xiao, "H_∞ finite-time control for switched nonlinear discrete-time systems with norm-bounded disturbance," *Journal of the Franklin Institute*, vol. 348, no. 2, pp. 331–352, 2011.
[39] Z. Hualin and S. Hongfei, "The design of switching law of linear switched systems of finite-time stability," in *Proceedings of the International Conference on Electrical and Control Engineering (ICECE '10)*, pp. 2318–2320, June 2010.
[40] F. Amato, M. Ariola, C. T. Abdallah, and P. Dorato, "Finite-time control for uncertain linear systems with disturbance inputs," in *Proceedings of the American Control Conference (ACC '99)*, pp. 1776–1780, June 1999.
[41] C. Liu and Z. R. Xiang, "Robust H_∞ finite-time stabilization of nonlinear impulsive switched system with time-delays," in *Proceedings of the 24th Chinese Control and Decision Conference*, pp. 264–269, 2012.

Hindawi Publishing Corporation
Mathematical Problems in Engineering
Volume 2012, Article ID 616507, 18 pages
doi:10.1155/2012/616507

Research Article

Robust $\mathcal{H}_\infty$ Dynamic Output Feedback Control Synthesis with Pole Placement Constraints for Offshore Wind Turbine Systems

Tore Bakka and Hamid Reza Karimi

Department of Engineering, Faculty of Engineering and Science, University of Agder, 4879 Grimstad, Norway

Correspondence should be addressed to Hamid Reza Karimi, hamid.r.karimi@uia.no

Received 7 June 2012; Accepted 21 September 2012

Academic Editor: Zidong Wang

The problem of robust $\mathcal{H}_\infty$ dynamic output feedback control design with pole placement constraints is studied for a linear parameter-varying model of a floating wind turbine. A nonlinear model is obtained and linearized using the FAST software developed for wind turbines. The main contributions of this paper are threefold. Firstly, a family of linear models are represented based on an affine parameter-varying model structure for a wind turbine system. Secondly, the bounded parameter-varying parameters are removed using upper bounded inequalities in the control design process. Thirdly, the control problem is formulated in terms of linear matrix inequalities (LMIs). The simulation results show a comparison between controller design based on a constant linear model and a controller design for the linear parameter-varying model. The results show the effectiveness of our proposed design technique.

1. Introduction

Wind energy is nowadays one of the fastest growing renewable industries. As a consequence of the oil crises in the early 1970s and a general interest of renewable energy, the wind energy sector has had a tremendous growth over the last decades. With Europe leading the global market, the turbine capacity has had an annual growth rate of up to 30% [1].

Wind turbines are complex mechanical systems, and they are highly nonlinear due to the conversion of wind energy to mechanical torque. This makes the wind turbine a challenging task both to model and control. In literature, linear and nonlinear controllers have been extensively used for power regulation through the control of blade pitch angle (see, for instance, [2–14] and the references therein). More recently, the problem of gain scheduling and output feedback $\mathcal{H}_\infty$ control design for an offshore floating wind turbine was studied in [15, 16]. Furthermore, a mixed $\mathcal{H}_2/\mathcal{H}_\infty$ control design was proposed for an offshore floating

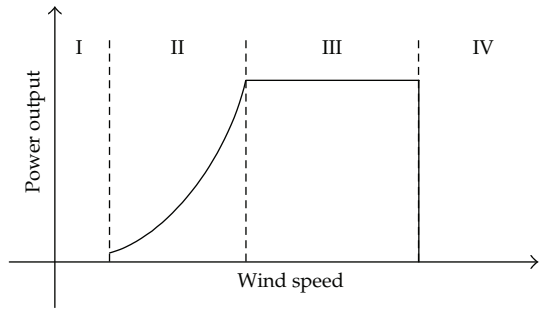

Figure 1: Operating region of a typical wind turbine.

wind turbine system investigated in [17]. However, the performance of these controllers is limited by the highly nonlinear characteristics of the wind turbine. These controllers are designed on the basis of one operating condition and therefor can only guarantee performance and stability at this point. By designing the controller on the basis of a linear-parameter-varying (LPV) model, it is possible to overcome these limitations. So, in order to sustain the growth in the wind industry sector, design of advanced control methodologies is one research area where such improvements can be achieved. In recent years, several advanced wind turbine simulation softwares have emerged, such as HAWC2 [18], FAST [19], and Cp-Lambda [20]. In this paper we will use FAST interfaced with MATLAB for all the simulations. The operation region of a wind turbine is often divided into four regions (Figure 1).

In region I ($v < v_{\text{cut-in}}$) the wind speed is lower than the cut-in wind speed and no power can be produced. In region II ($v_{\text{cut-in}} \leq v < v_{\text{rated}}$) the pitch is usually kept constant while the generator torque is the controlling variable. In region III ($v_{\text{rated}} \leq v < v_{\text{cut-out}}$) the main concern is to keep the rated power and to limit loads on critical parts of the structure by pitching the blades. In region IV ($v \leq v_{\text{cut-out}}$) the wind speed is too high, and the turbine is shut down. In this paper we will focus on the above rated wind speed scenario, that is, region III.

This paper makes three specific contributions. First, it suggests a family of linear models for a wind turbine system based on an affine parameter-varying model structure. Second, robust stabilization and disturbance attenuation of such parameter-varying models are investigated using $\mathscr{H}_\infty$ method such that the bounded parameter-varying parameters are removed using upper bounded inequalities in the control design procedure. Third, the control problem is formulated in terms of linear matrix inequalities (LMIs) and a dynamic output feedback controller is computed. Finally, the simulation results show that the obtained controller can achieve the robust stability and disturbance attenuation, simultaneously.

This paper is organized as follows. Section 2 describes the model under consideration and how to include the parameter-varying terms in the closed loop system. Section 3 is devoted to the control design technique. Simulation results are presented in Section 4. Finally, concluding remarks and suggestions to future works are discussed in Section 5.

The notations used throughout the paper are fairly standard. I and 0 represent identity matrix and zero matrix; the superscript T stands for matrix transposition; $\Re^n$ denotes the n-dimensional Euclidean space; $\Re^{n\times m}$ is the set of all real m by n matrices. $\|\cdot\|$ refers to the Euclidean vector norm or the induced matrix 2-norm. $\text{diag}\{\cdots\}$ represents a block diagonal matrix. The operator $\text{sym}(A)$ denotes $A + A^T$, and $\otimes$ denotes the Kronecker product. The notation $P > 0$ means that P is real symmetric and positive definite; the symbol $*$ denotes

the elements below the main diagonal of a symmetric block matrix. Finally given a signal $x(z)$, $\|x(z)\|_2$ denotes the L_2 norm of $x(z)$, that is, $\|x(z)\|_2^2 = \int_0^\infty x^T(z)x(z)dt$.

2. Wind Turbine Model

The wind turbine model is obtained from the wind turbine simulation software FAST [19]. The simulation model is an upscaled version of Statoil's Hywind 2.3 (MW) turbine, which is located off the Norwegian west coast. This upscaled version is also a floating turbine and has the capacity 5 (MW). For specifications, see [21].

FAST provides a fully nonlinear wind turbine model with up to 24 degrees of freedom (DOF). For the controller design, we need a linear model and we want the linear model to be as simple as possible. All the DOFs available cannot be included, so we choose the ones we think will represent the most important dynamics. Linearization routines are available in the FAST package. The model is now linearized at each desired azimuth angle. We find this angle in the plane of rotor rotation. One linear model at each 10th angle is obtained, that is, the total amount of 36 models are obtained. The models is of the following standard state space form:

$$\begin{aligned} \dot{x} &= A_i x + B_i u, \\ y &= C_i x, \quad i = 1, 2, \ldots, 36, \end{aligned} \tag{2.1}$$

where x is the state vector with dimensions $\mathcal{R}^{n\times 1}$, u is the control signal with dimensions $\mathcal{R}^{p\times 1}$, y is the model outputs with dimensions $\mathcal{R}^{m\times 1}$, and A, B, C are the system matrices with dimensions $\mathcal{R}^{n\times n}$, $\mathcal{R}^{n\times p}$, $\mathcal{R}^{m\times n}$, and $\mathcal{R}^{m\times p}$, respectively. The states in this linear model are tower fore-aft displacement (x_1), generator position (x_2), rotor position (x_3), and the last three states are the first derivative of x_{1-3}. The model input u, which will eventually be calculated by the controller, is the blade pitch angle. The model outputs in y are tower fore-aft displacement, generator speed, and rotor speed.

A common way to simplify these models is to take the average of all the 36 models and use this as basis for the controller design. By doing this simplification, important information is easily lost. This is why in this paper we will try to do the controller design based on a model representation which tries to include as much as possible of the information in the 36 models. The matrices A and B are behaving in a periodic way, and the matrix values depend on the rotor azimuth angle. Several things are the cause of this periodic behavior, that is, aerodynamic loads, tower shadow, gravitational loads, and deflections of the tower due to thrust loading. The matrix associated with the output y is not varying, since this C-matrix only handles the measurements. In (2.2) we define the varying matrices in an affine way, and $A(z)$ and $B(z)$ vary in a continuous manner:

$$\begin{aligned} A(z) &= A_n + \Delta A(z), \\ B(z) &= B_{2n} + \Delta B(z), \end{aligned} \tag{2.2}$$

where A_n and B_{2n} are the nominal plant matrices, $\Delta A(z)$ and $\Delta B(z)$ contributes with the varying terms, and z represents the rotor azimuth angle. We are looking to represent the parameter-varying terms in this way: $\Delta A(z) = F\Delta(z)E$, and a similar expression for $\Delta B(z)$. After analyzing the 36 models we find appropriate matrices F and E, but we also find out

that more than one scheduling parameter is needed. The periodic matrices $A(z)$ and $B(z)$ can now be represented in a continuous way with the use of sine and cosine functions. The parameter-varying terms in (2.2) are defined in the following way:

$$\begin{aligned} \Delta A(z) &= \sum_{i=1}^{2}\sum_{j=1}^{2} F_i \Delta_j(z) E_{jia}, \\ \Delta B(z) &= \sum_{i=1}^{2}\sum_{j=1}^{2} F_i \Delta_j(z) E_{jib}, \end{aligned} \tag{2.3}$$

where the vectors F and E have appropriate dimensions, and the scheduling variables $\Delta_1(z)$ and $\Delta_2(z)$ are found to be $\sin(\omega t)$, and $\cos(\omega t)$ respectively. A plot which shows what the different parameters are in the original matrices $A_{1,\ldots,36}$ and $B_{1,\ldots,36}$ and in the new representation $A_n + \Delta A(z)$ and $B_{2n} + \Delta B(z)$ is found in the appendix.

3. Control Design

The purpose of $\mathcal{H}_\infty$ control is to minimize the effect of disturbances on the controlled output. The control design is formulated in terms of LMIs. After manipulating the linear model obtained from FAST, we end up with a state space system with parameter-varying A and B matrices. This model is more accurate than if we just took the average of all the 36 models. By using a LPV model of the system we are able to catch some of the dynamics that are lost under the linearization. The challenge is now to incorporate these additional terms into the control design.

These robust control designs mostly deal with frequency domain aspects of the closed loop system, but it is well known that the location of the closed loop poles play a large role in the transient behavior of the controlled system. By adding pole placement to the list of constraints we can prevent large poles and end up with a system which can respond in a realistic way. The controller we are searching for will try to keep the generator speed at its rated value while mitigating oscillations in the drive train and in the tower.

The LMIs for the control design are solved using YALMIP [22] interfaced with MATLAB, and we are using the solver SeDuMi. This solver is searching for two positive definite matrices X and Y which stabilizes the system. If these matrices exist, we can calculate the controller. The next sections present how to obtain the LMIs for the controller design and also how to incorporate the parameter-varying part of the state space system.

3.1. System Representation

Figure 2 shows the output feedback control scheme, where $P(s)$ is the generalized plant and $K(s)$ is the controller. The two blocks represent in the equations (3.1) and (3.2). $P(s)$ includes the wind turbine model and the signals of interest:

$$\begin{aligned} \dot{x} &= Ax + B_1 w + B_2 u, \\ z_\infty &= C_{1i} x + D_{1i} w + D_{2i} u, \\ y &= C_2 x + D_{21} w, \end{aligned} \tag{3.1}$$

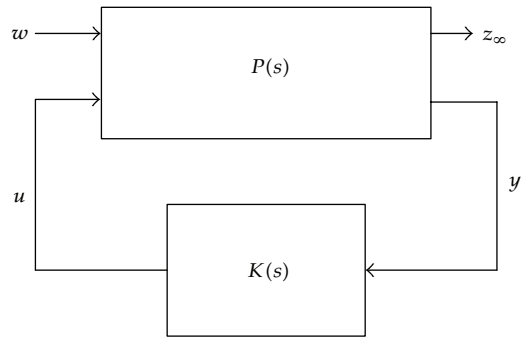

Figure 2: Output feedback block diagram.

where A, B_2, and C_2 represent the matrices from the standard state space form in (2.1). To include the parameter-varying matrices, A is substituted with $A(z)$ and B_2 with $B(z)$. The other matrices are considered with appropriate dimensions. u is the control input, w is the disturbance signal, and y is the measured output. The signal z_∞ is the controlled output for $\mathscr{H}_\infty$ performance measure. For system (3.1), the dynamic output feedback, $u(s) = K(s)y(s)$, is of the following form:

$$K(s)\begin{cases}\dot{\zeta} = A_k\zeta + B_k y,\\ u = C_k\zeta + D_k y.\end{cases} \tag{3.2}$$

The closed loop system is given in (3.3) with the states $x_{\mathrm{cl}} = [\,x\ \zeta\,]^T$:

$$\begin{aligned}\dot{x}_{\mathrm{cl}} &= A_{\mathrm{cl}}x + B_{\mathrm{cl}}w,\\ z_\infty &= C_{\mathrm{cl}}x + D_{\mathrm{cl}}w.\end{aligned} \tag{3.3}$$

The closed loop system is divided into two parts, one with constant state space matrices and one where the parameter-varying matrices are

$$\begin{aligned}\left(\begin{array}{c|c} A_{\mathrm{cl}} & B_{\mathrm{cl}}\\ \hline C_{\mathrm{cl}} & D_{\mathrm{cl}}\end{array}\right) &= \left(\begin{array}{c|c} A_{\mathrm{cl}\,1} & B_{\mathrm{cl}\,1}\\ \hline C_{\mathrm{cl}\,1} & D_{\mathrm{cl}\,1}\end{array}\right) + \left(\begin{array}{c|c} A_{\mathrm{cl}\,2}(z) & B_{\mathrm{cl}\,2}(z)\\ \hline 0 & 0\end{array}\right)\\ &= \left(\begin{array}{cc|c} A_n + B_{2n}D_kC_2 & B_{2n}C_k & B_1 + B_{2n}D_kD_{21}\\ B_kC_2 & A_k & B_kD_{21}\\ \hline C_{1i} + D_{2i}D_kC_2 & D_{2i}C_k & D_{1i} + D_{2i}D_kD_{21}\end{array}\right)\\ &\quad + \left(\begin{array}{cc|c} \Delta A(z) + \Delta B(z)D_kC_2 & \Delta B(z)C_k & \Delta B(z)D_kD_{21}\\ 0 & 0 & 0\\ \hline 0 & 0 & 0\end{array}\right).\end{aligned} \tag{3.4}$$

3.2. $\mathscr{H}_\infty$ Control

Because of the parameter-varying state space system we now get an additional term to the standard Bounded Real Lemma (BRL). This additional term is the second part of the summation in constraint (3.5). We want to make sure that the closed loop $\mathscr{H}_\infty$ norm of the closed loop transfer function does not exceed γ. This is true if and only if there exists a symmetric matrix X such that

$$\begin{pmatrix} A_{\mathrm{cl}\,1}^T X + X A_{\mathrm{cl}\,1} & X B_{\mathrm{cl}\,1} & C_{\mathrm{cl}\,1}^T \\ * & -\gamma I & D_{\mathrm{cl}\,1}^T \\ * & * & -\gamma I \end{pmatrix} + \begin{pmatrix} A_{\mathrm{cl}\,2}^T(z) X + X A_{\mathrm{cl}\,2}(z) & X B_{\mathrm{cl}\,2}(z) & 0 \\ * & 0 & 0 \\ * & * & 0 \end{pmatrix} < 0$$
$$X > 0. \tag{3.5}$$

3.3. Change of Variables

Obviously, the $\mathscr{H}_\infty$ constraint (3.5) is not an LMI because of the nonlinear terms which occur when we close the loop. In order to transform these nonlinear terms into proper LMIs we need to do two things. First, we need to linearize them with the use of change of variables. Second, we need to remove the parameter-varying terms. The linearization part is not as straight forward as for the state feedback case, additional information about this can be found in [23].

The new Lyapunov matrix is partitioned in the following form:

$$\mathcal{X} = \begin{bmatrix} Y & N \\ N^T & \# \end{bmatrix}, \qquad \mathcal{X}^{-1} = \begin{bmatrix} X & M \\ M^T & \# \end{bmatrix}, \tag{3.6}$$

where X and Y are symmetric matrices of dimension $n \times n$. It is not necessary to know the matrices noted as #.

In addition, we define the following two matrices:

$$\Pi_1 = \begin{bmatrix} X & I \\ M^T & 0 \end{bmatrix}, \qquad \Pi_2 = \begin{bmatrix} I & Y \\ 0 & N^T \end{bmatrix}, \tag{3.7}$$

that, as can be inferred from the identity $\mathcal{X}\mathcal{X}^{-1} = I$, satisfy

$$\mathcal{X}\Pi_1 = \Pi_2. \tag{3.8}$$

Then, the following change of controller variables are defined:

$$\begin{aligned}\widehat{A} &= NA_kM^T + NB_kC_2X + YB_{2n}C_kM^T + Y(A_n + B_{2n}D_kC_2)X,\\ \widehat{B} &= NB_k + YB_{2n}D_k,\\ \widehat{C} &= C_kM^T + D_kC_2X,\\ \widehat{D} &= D_k.\end{aligned} \tag{3.9}$$

Now we are ready to convert our nonlinear matrix inequalities into LMIs. By performing congruence transformation with $\operatorname{diag}(\Pi_1, I, I)$ on the obtained inequality (3.5), we end up with following matrix inequality:

$$\begin{aligned}&\Sigma_1 + \operatorname{sym}(G_1\Delta_1(z)H_1) + \operatorname{sym}(G_2\Delta_1(z)H_1)\\ &\quad + \operatorname{sym}(G_1\Delta_1(z)H_2) + \operatorname{sym}(G_2\Delta_1(z)H_2)\\ &\quad + \operatorname{sym}(G_3\Delta_2(z)H_3) + \operatorname{sym}(G_4\Delta_2(z)H_3)\\ &\quad + \operatorname{sym}(G_3\Delta_2(z)H_4) + \operatorname{sym}(G_4\Delta_2(z)H_4) < 0,\end{aligned} \tag{3.10}$$

where the matrix Σ_1 and the vectors G_i and H_i are defined in the appendix.

Lemma 3.1 (see [24]). *Given $\Sigma = \Sigma^T$, G, Δ, and H of appropriate dimensions with $\Delta^T\Delta \le I$, then the matrix inequality*

$$\Sigma + (G\Delta H) < 0 \tag{3.11}$$

holds for all Σ if and only if there exists a scalar $\epsilon > 0$ such that

$$\Sigma + \epsilon GG^T + \epsilon^{-1}H^TH < 0. \tag{3.12}$$

By using Lemma 3.1 we are able to remove the parameter-varying parts $\Delta_i(z)$ in the matrix inequality (3.10). We end up with a new LMI which contains the constants ϵ_1 and ϵ_2:

$$\begin{aligned}&\Sigma_1 + 2\epsilon_1G_1G_1^T + 2\epsilon_1^{-1}H_1^TH_1 + 2\epsilon_1G_2G_2^T + 2\epsilon_1^{-1}H_2^TH_2\\ &\quad + 2\epsilon_2G_3G_3^T + 2\epsilon_2^{-1}H_3^TH_3 + 2\epsilon_2G_2G_4^T + 2\epsilon_2^{-1}H_4^TH_4 < 0.\end{aligned} \tag{3.13}$$

By using the Schur complement we can convert (3.13) into the following LMIs:

$$\begin{pmatrix}\Sigma_1 & \Sigma_2\\ * & \Sigma_3\end{pmatrix} < 0, \tag{3.14}$$

$$\begin{pmatrix}X & I\\ I & Y\end{pmatrix} > 0, \tag{3.15}$$

where

$$\Sigma_2 = \begin{bmatrix} G_1 & H_1^T & G_2 & H_2^T & G_3 & H_3^T & G_4 & H_4^T \end{bmatrix}$$
$$\Sigma_3 = \operatorname{diag}\left\{ -\frac{1}{2}\epsilon_1^{-1}, -\frac{1}{2}\epsilon_1, -\frac{1}{2}\epsilon_1^{-1}, -\frac{1}{2}\epsilon_1, -\frac{1}{2}\epsilon_2^{-1}, -\frac{1}{2}\epsilon_2, -\frac{1}{2}\epsilon_2^{-1}, -\frac{1}{2}\epsilon_2 \right\}. \tag{3.16}$$

3.4. LMI Region

An LMI region is any convex subset $\mathfrak{D}$ of the complex plane that can be characterized as an LMI in z and $\overline{z}$ [25] as follows:

$$D = \left\{ z \in C : \overline{L} + \overline{M}z + \overline{M}^T\overline{z} < 0 \right\}, \tag{3.17}$$

for some fixed real matrices $\overline{M}$ and $\overline{L} = \overline{L}^T$, where $\overline{z}$ is a complex number. This class of regions encompasses half planes, strips, conic sectors, disks, ellipses, and any intersection of the above. From [25], we find that all eigenvalues of the matrix A are in the LMI region $\{z \in C : [\overline{l}_{ij} + \overline{m}_{ij}z + \overline{m}_{ji}\overline{z}]_{i,j} < 0\}$ if and only if there exists a symmetric matrix X such that

$$\left[\overline{l}_{ij}X + \overline{m}_{ij}A^TX + \overline{m}_{ji}XA\right]_{i,j} < 0, \quad X > 0. \tag{3.18}$$

Also, here we need to include the change of variables and remove the parameter-varying terms, this is done in (3.19). The LMI is obtained in a manner similar to the one that was used for the $\mathcal{H}_\infty$ constraint:

$$\begin{pmatrix} \Sigma_4 & \Sigma_5 \\ * & \Sigma_3 \end{pmatrix} < 0, \tag{3.19}$$

where

$$\Sigma_5 = \begin{bmatrix} \epsilon_1 P_1 & N_1^T & \epsilon_1 P_2 & N_2^T & \epsilon_2 P_3 & N_3^T & \epsilon_2 P_4 & N_4^T \end{bmatrix} \tag{3.20}$$

and Σ_4 and the other terms in Σ_5 are defined in the appendix.

Remark 3.2. It is observed that the inequalities (3.14), (3.15), and (3.19) are linear in $(X, Y, \widehat{A}, \widehat{B}, \widehat{C}, \widehat{D})$ and thus the standard LMI techniques can be exploited to find the LMI solutions. It is also seen from the above results that there exists much freedom contained in the design of control law, such as the choices of appropriate ϵ_1 and ϵ_2. This design freedom can be exploited to achieve other desired closed loop properties.

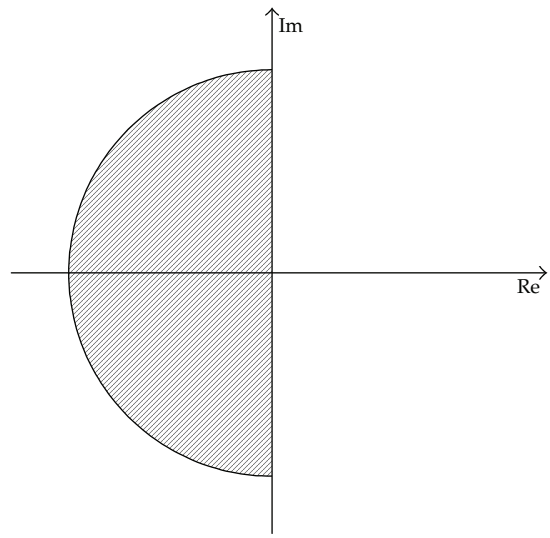

Figure 3: LMI region $\mathfrak{D}$.

The desired region $\mathfrak{D}$ is a disk (Figure 3), with center located along the x-axis (distance q from the origin) and radius r. This determines the region

$$\mathfrak{D} = \begin{pmatrix} -r & q+z \\ q+\overline{z} & -r \end{pmatrix}. \tag{3.21}$$

From this we can find the matrices $\overline{L}$ and $\overline{M}$, which are the two matrices that determine the LMI region.

All constraints in (3.14), (3.15), and (3.19) are now subjected to the minimization of the objective function, which is the $\mathscr{H}_\infty$ norm. They need to be solved in terms of $(X, Y, \widehat{A}, \widehat{B}, \widehat{C}, \widehat{D})$.

Once all these matrices are obtained, the controller matrices are computed in the following way. First we obtain M and N from the factorization problem

$$MN^T = I - XY. \tag{3.22}$$

Second, the controller matrices are computed from the following relationship:

$$\begin{gathered} D_k = \widehat{D}, \\ C_k = \left(\widehat{C} - D_k C_2 X\right)\left(M^T\right)^{-1}, \\ B_k = N^{-1}\left(\widehat{B} - Y B_{2n} D_k\right), \\ A_k = N^{-1}\left(\widehat{A} - N B_k C_2 X - Y B_{2n} C_k M^T - Y(A_n + B_{2n} D_k C_2) X\right)\left(M^T\right)^{-1}. \end{gathered} \tag{3.23}$$

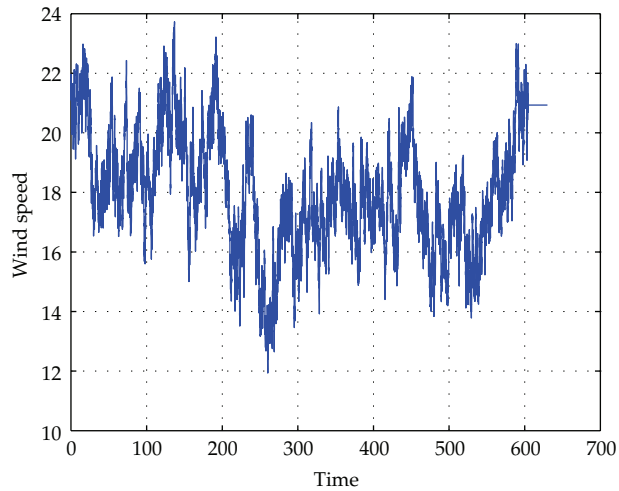

Figure 4: Wind profile.

4. Simulation Results

The simulations are carried out with FAST software interfaced with MATLAB/Simulink. The controllers are tested on the fully nonlinear system with 22 out of 24 DOFs enabled. Yaw and platform surge-motion are left out. The wind turbine system is subjected to extreme wind conditions. The wind profile is a 50-year extreme case with an average speed of 18 [m/s] (Figure 4) and a turbulence intensity of 17%. Significant wave hight is 6 [m] with a peak wave period of 10 [s]. The wind profile is obtained from the software Turbsim [26].

Suitable results are found with the following $\mathscr{H}_\infty$ performance measure:

$$z_\infty = x_1 + x_2 + x_6 + u. \tag{4.1}$$

The blue line in the plots is the result where the parameter-varying terms are taken into consideration in the controller design. The red line shows the result where the parameter-varying terms are left out. We also show NREL's PI gain scheduled controller (cyan colored line) as a reference plot. Our two controllers are designed and tested on exactly the same operating conditions, that is, same performance measure, same pole placement constraint, and same wind condition. From Figures 5 and 6 we see that the blue line is operating more steady around the rated values for the rotor and generator, which are 12.1 [rpm] and 1173.7 [rpm], respectively. This will in turn result in a smoother torque output, as seen in Figure 7.

Our two controller designs show a large increment in pitching activity, see Figure 8. If we inspect the pitching rate, we see that it is not more than 5–10 [deg/s] and hence should be within the wind turbine's limit. The blue line in Figure 9 shows that the amplitude of the oscillations is lower in the fore-aft direction than in the other two plots. From these plots we see that the results are according to the controller objectives.

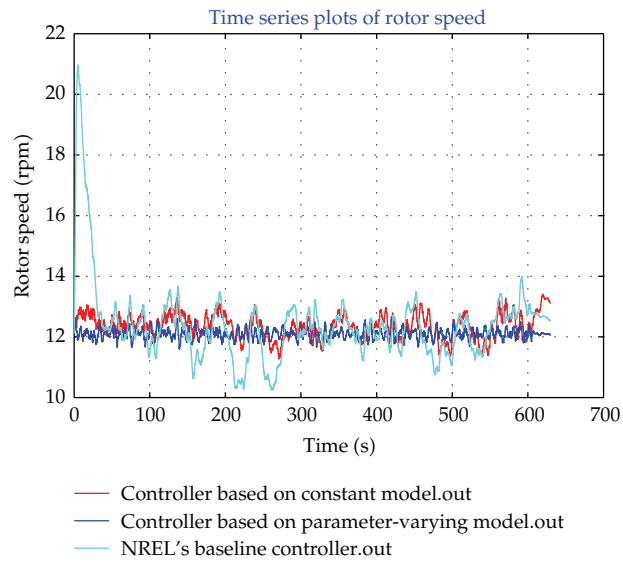

Figure 5: Rotor speed.

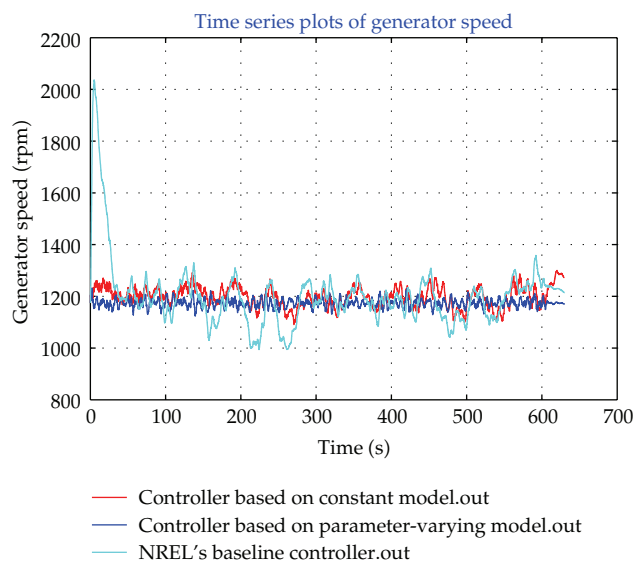

Figure 6: Generator speed.

5. Conclusions

In this paper we have obtained and linearized a wind turbine model using the commercial software FAST. The output from the linearization is a family of models describing the turbine system at each 10th azimuth angle. This family of models is converted into one parameter-varying model. The new model is dependent on the azimuth angle. In this way we can make the control design based on a model consisting of more information than if we had done it the conventional way, which is to use the average of the family of models. The controller is tested

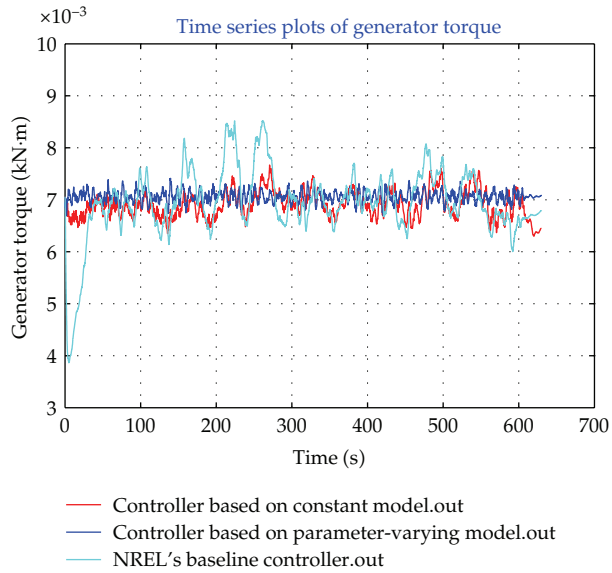

Figure 7: Generator torque.

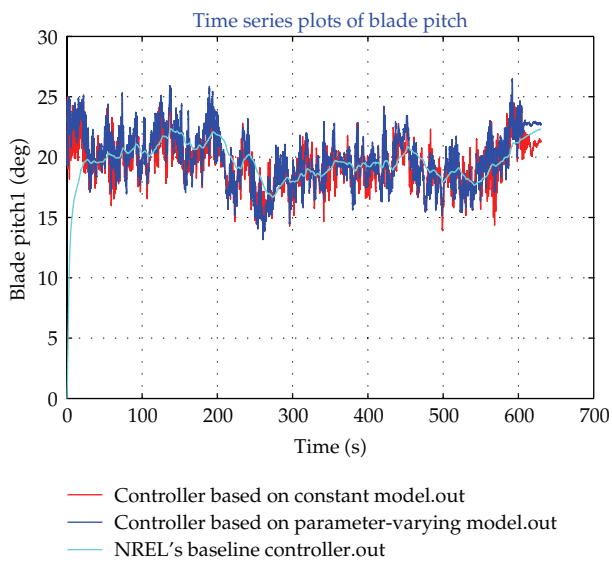

Figure 8: Blade pitch.

on the fully nonlinear system subjected to 50-year extreme wind conditions. The simulation results show a comparison between controller design done with the new method and done the conventional way. The plots show that the simulation results meet our control objectives.

Based on the results in this paper, interesting future research may be prospective as follows.

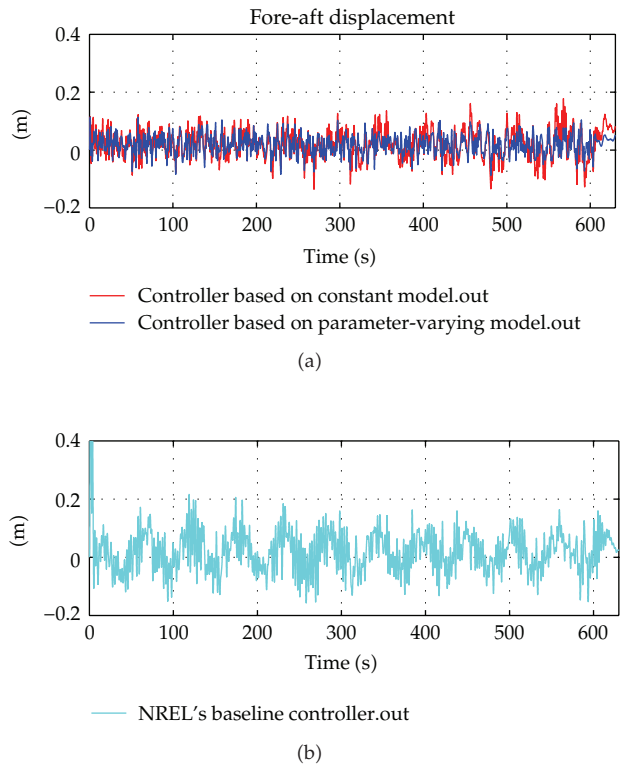

Figure 9: Tower fore-aft.

(1) It is worth noting that in this paper a constant controller is designed for a parameter-varying model. A next step could be to design a parameter-varying controller, where the scheduling parameter is the azimuth angle.

(2) The methods presented in [27, 28] can be used for a stochastic model of a wind turbine system with constrained information exchange and a partial knowledge of the state variables.

(3) Fault detection and control design for wind turbine systems over a network (see, for instance, [29, 30]) can be studied in the framework of this paper.

(4) Though the addressed issue is the control problem, the methods proposed in the paper can be extended to filtering problems (see, for instance, [31]).

Appendix

The size of the A matrix is 6×6, and the B matrix has size 6×1. Only the last three rows are shown in Figures 10 and 11, respectively. The first three rows contain either constant or zero values. The blue line shows how the 36 linear models are distributed along the 360

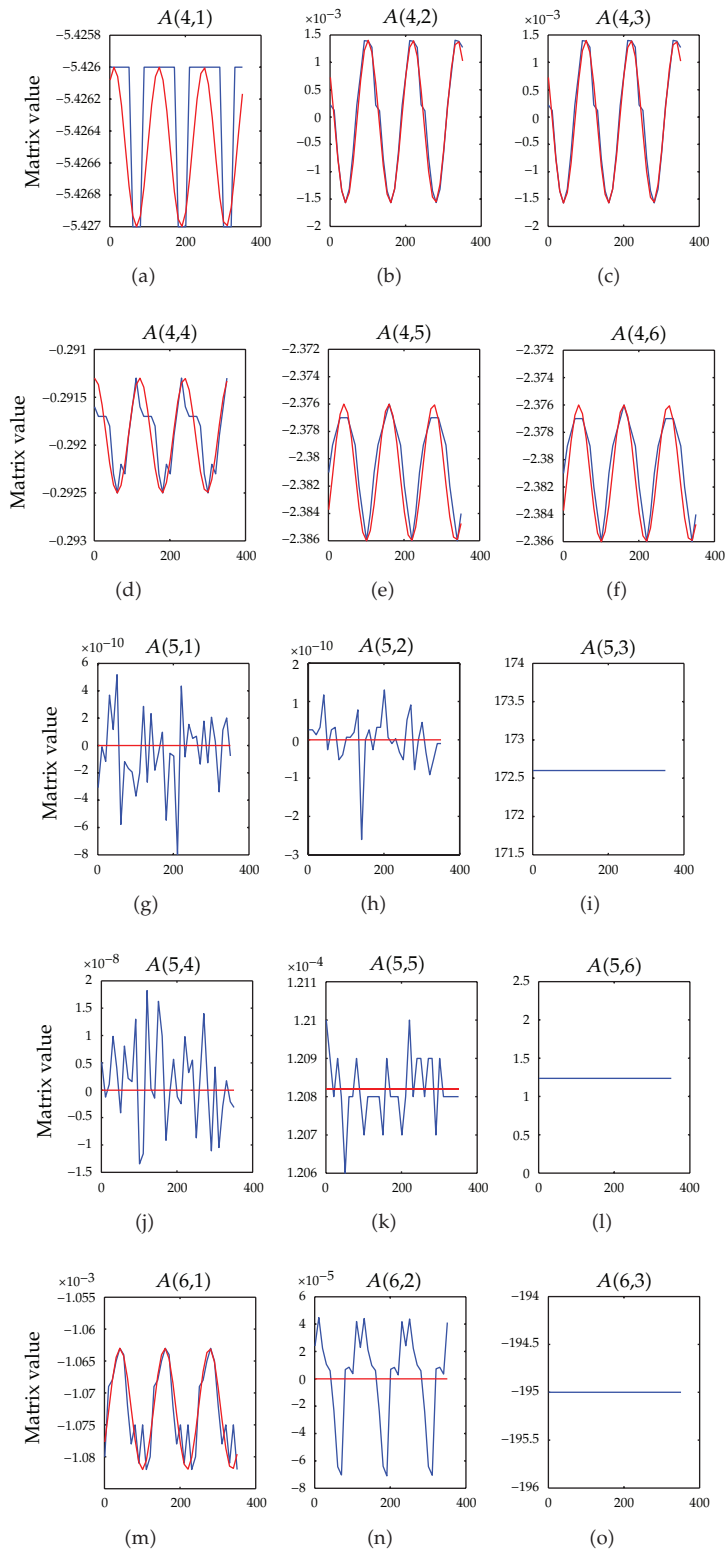

Figure 10: Continued.

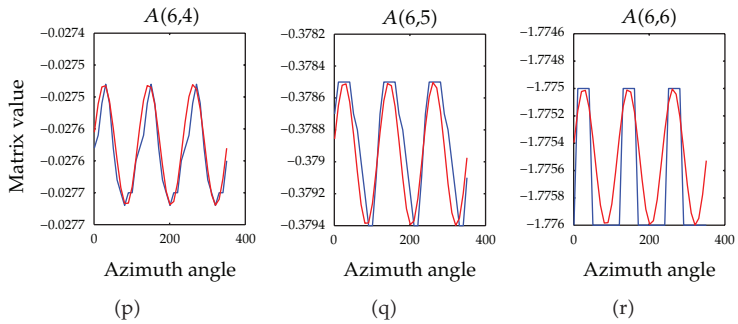

Figure 10: Parameters in A matrix rows 4–6.

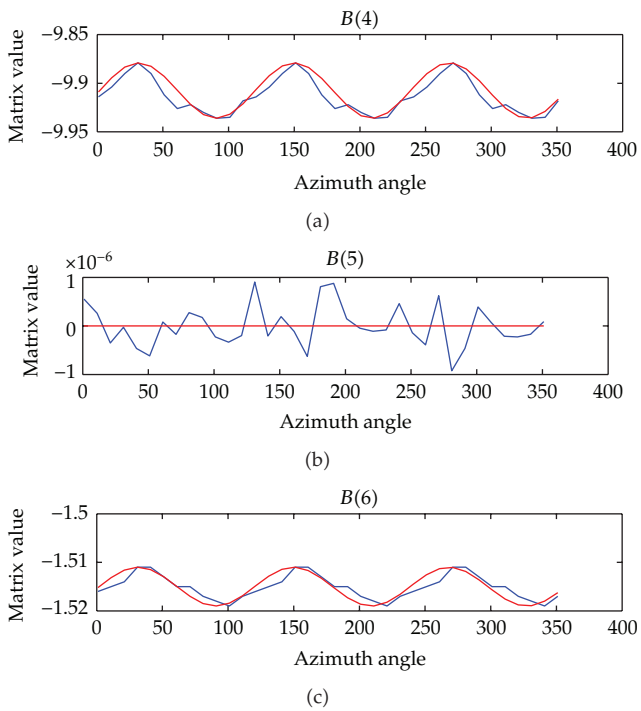

Figure 11: Parameters in B-matrix rows 4–6.

azimuth angles. The red line shows our attempt to emulate these periodic matrix values with a function on the form $A_n + \Delta A(z)$ for the A matrix and $B_{2n} + \Delta B(z)$ for the B matrix

$$\Sigma_1 = \begin{pmatrix} \operatorname{sym}\left(AX + B_2\widehat{C}\right) & \widehat{A}^T + A + B_2\widehat{D}C_2 & B_1 + B_2\widehat{D}D_{21} & XC_{1i}^T + \widehat{C}^T D_{21}^T \\ * & \operatorname{sym}\left(\Upsilon A + \widehat{B}C_2\right) & \Upsilon B_1 + \widehat{B}D_{21} & C_{1i}^T + C_2^T\widehat{D}^T + D_{2i}^T \\ * & * & -\gamma I & D_{1i}^T + D_{21}^T\widehat{D}D_{2i}^T \\ * & * & * & -\gamma I \end{pmatrix}, \tag{A.1}$$

$$
\begin{aligned}
&G_1 = \left[F_1 \;\; 0_{1\times 8}\right]^T, \qquad G_2 = \left[0_{1\times 6} \;\; YF_1 \;\; 0_{1\times 2}\right]^T,\\
&G_3 = \left[F_2 \;\; 0_{1\times 8}\right]^T, \qquad G_4 = \left[0_{1\times 6} \;\; YF_2 \;\; 0_{1\times 2}\right]^T,\\
&H_1 = \left[E_{11a}X + E_{11b}\widehat{C} \;\; E_{11a} + E_{11b}\widehat{D}C_2 \;\; E_{11b}\widehat{D}D_{21}0\right],\\
&H_2 = \left[E_{12a}X + E_{12b}\widehat{C} \;\; E_{12a} + E_{12b}\widehat{D}C_2 \;\; E_{12b}\widehat{D}D_{21}0\right],\\
&H_3 = \left[E_{21a}X + E_{21b}\widehat{C} \;\; E_{21a} + E_{21b}\widehat{D}C_2 \;\; E_{21b}\widehat{D}D_{21}0\right],\\
&H_4 = \left[E_{22a}X + E_{22b}\widehat{C} \;\; E_{22a} + E_{22b}\widehat{D}C_2 \;\; E_{22b}\widehat{D}D_{21}0\right],
\end{aligned}
\tag{A.2}
$$

$$
\begin{aligned}
\Sigma_4 = \Bigg(&\overline{L} \otimes \begin{pmatrix} X & I \\ I & Y \end{pmatrix} + \overline{M} \otimes \begin{pmatrix} AX + B\widehat{C} & A + B\widehat{D}C \\ \widehat{A} & YA + \widehat{B}C \end{pmatrix}\\
&+\overline{M}^T \otimes \begin{pmatrix} AX + B\widehat{C} & A + B\widehat{D}C \\ \widehat{A} & YA + \widehat{B}C \end{pmatrix}^T\Bigg),
\end{aligned}
\tag{A.3}
$$

$$
\begin{aligned}
&G_1 = \left[F_1 \;\; 0_{1\times 6}\right]^T, \qquad G_2 = \left[0_{1\times 6} \;\; YF_1\right]^T, \qquad G_3 = \left[F_2 \;\; 0_{1\times 6}\right]^T, \qquad G_4 = \left[0_{1\times 6} \;\; YF_2\right]^T,\\
&H_{1-2} = \left[E_{11a}X + E_{11b}\widehat{C} \;\; E_{11a} + E_{11b}\widehat{D}C_2\right], \qquad H_{2-2} = \left[E_{12a}X + E_{12b}\widehat{C} \;\; E_{12a} + E_{12b}\widehat{D}C_2\right],\\
&H_{3-2} = \left[E_{21a}X + E_{21b}\widehat{C} \;\; E_{21a} + E_{21b}\widehat{D}C_2\right], \qquad H_{4-2} = \left[E_{22a}X + E_{22b}\widehat{C} \;\; E_{22a} + E_{22b}\widehat{D}C_2\right],\\
&N_1 = I_{2\times 2} \otimes H_{1-2}, \qquad N_2 = I_{2\times 2} \otimes H_{2-2}, \qquad N_3 = I_{2\times 2} \otimes H_{3-2}, \qquad N_4 = I_{2\times 2} \otimes H_{4-2},\\
&H_1 = M \otimes G_{1-2}, \qquad H_2 = M \otimes G_{2-2}, \qquad H_3 = M \otimes G_{3-2}, \qquad H_4 = M \otimes G_{4-2}.
\end{aligned}
\tag{A.4}
$$

Acknowledgments

This work has been (partially) funded by Norwegian Centre for Offshore Wind Energy (NORCOWE) under Grant 193821/S60 from Research Council of Norway (RCN). NORCOWE is a consortium with partners from industry and science, hosted by Christian Michelsen Research.

References

[1] EWEA, "Wind Industry Factsheet," Tech. Rep., European Wind Energy Association (EWEA), 2004.
[2] Y. D. Song, B. Dhinakaran, and X. Y. Bao, "Variable speed control of wind turbines using nonlinear and adaptive algorithms," *Journal of Wind Engineering and Industrial Aerodynamics*, vol. 85, no. 3, pp. 293–308, 2000.
[3] R. Melcioa, V. M. F. Mendesc, and J. P. S. Cataloa, "Comparative study of power converter topologies and control strategies for the harmonic performance of variable-speed wind turbine generator systems," *Energy*, vol. 36, no. 1, pp. 520–529, 2011.
[4] A. Kusiak, W. Li, and Z. Song, "Dynamic control of wind turbines," *Renewable Energy*, vol. 35, no. 2, pp. 456–463, 2010.
[5] A. Kusiak and Z. Zhang, "Control of wind turbine power and vibration with a data-driven approach," *Renewable Energy*, vol. 43, pp. 73–82, 2012.

[6] R. Eide and H. R. Karimi, "Control design methodologies for vibration mitigation on wind turbine systems," in *Vibration Control*, F. Beltran-carbajal, Ed., pp. 217–242, INTECH.
[7] H. R. Karimi and T. Bakka, "Stochastic Analysis and H_∞ Control ofWind Turbine Systems with Wireless Sensor Networks," in *Proceedings of the 24th International Congress on Condition Monitoring and Diagnostics Engineering Management*, pp. 1086–1095, 2011.
[8] H. R. Karimi, "Wavelet-based optimal control of a wind turbine system: a computational approach," *Journal of Advanced Mechanical Design, Systems, and Manufacturing*, vol. 5, no. 3, pp. 171–186, 2011.
[9] F. D. Bianchi, H. de Battista, and R. J. Mantz, *Wind Turbine Control Systems*, Springer, 2007.
[10] C. W. Taylor, F. R. Nassief, and R. L. Cresap, "Northwest power pool transient stability and load shedding controls for generation-load imbalances," *IEEE transactions on power apparatus and systems*, vol. 100, no. 7, pp. 3486–3495, 1981.
[11] A. Mullane, G. Lightbody, and R. Ya, "Adaptive control of variable speed wind turbines," *Revue Des Energies Renouveables: Power Engineering*, pp. 101–110, 2001.
[12] F. Valenciaga, P. F. Puleston, P. E. Battaiotto, and R. J. Mantz, "An adaptive feedback linearization strategy for variable speed wind energy conversion systems," *International Journal of Energy Research*, vol. 24, no. 2, pp. 151–161, 2000.
[13] M. Steinbuch and O. H. Bosqra, "Optimal output feedback of a wind energy conversion system," in *Proceedings of the Power Systems Modelling and Control Applications*, A. J. Calvaer, Ed., IFAC Proceeding series, pp. 313–319, September 1988.
[14] R. Rocha, L. S. Martins Filho, and M. V. Bortolus, "Optimal multivariable control for wind energy conversion system - A comparison between H_2 and H_∞ controllers," in *Proceedings of the 44th IEEE Conference on Decision and Control, and the European Control Conference, (CDC-ECC '05)*, pp. 7906–7911, December 2005.
[15] T. Bakka, H. R. Karimi, and N. A. Duffie, "Gain scheduling for output $\mathscr{H}_\infty$ control of offshore wind turbine," in *Proceedings of the 22nd International Offshore and Polar Engineering Conference*, pp. 496–501, Rhodes, Greece, June 2012.
[16] T. Bakka and H. R. Karimi, "Robust output feedback $\mathscr{H}_\infty$ control synthesis with pole placement for offshore wind turbine system: an LMI approach," in *IEEE International Conference on Control Applications (CCA '12)*, Dubrovnik, Croatia, October 2012.
[17] T. Bakka and H. R. Karimi, "Mixed H_2/H_∞ control design for wind turbine system with pole placement constraints," in *Proceedings of the 31st Chinese Control Conference*, pp. 4775–4780, Hefei, China, July 2012.
[18] T. J. Larsen, "How 2 HAWC2, the users manual," Ris-R-1597(ver. 3–9)(EN), 2009.
[19] J. Jonkman and M. L. Buhl Jr., "FAST Users Guide," Tech. Rep. NREL/EL-500-38230, National Renewable Energy Laboratory, 2005.
[20] C. L. Bottasso and A. Croce, *Cp-Lambda User Manual*, Dipartimento di Ingnegneria Aerospaziale, Politecnico di Milano, Milano, Italy, 2009.
[21] J. Jonkman, S. Butterfield, W. Musial, and G. Scott, "Definition of a 5-MW referencewind turbine for offshore system development," Tech. Rep. NREL/TP-500-38060, National Renewable Energy Laboratory, 2009.
[22] J. Lfberg, "YALMIP: a toolbox for modeling and optimization in MATLAB," in *Proceedings of the IEEE International Symposium on Computer Aided Control Systems Design, (CACSD '04)*, pp. 284–289, Taipei, Taiwan, 2004.
[23] C. Scherer, P. Gahinet, and M. Chilali, "Multiobjective output-feedback control via LMI optimization," *IEEE Transactions on Automatic Control*, vol. 42, no. 7, pp. 896–911, 1997.
[24] P. P. Khargonekar, I. R. Petersen, and K. Zhou, "Robust stabilization of uncertain linear systems: quadratic stabilizability and H∞ control theory," *IEEE Transactions on Automatic Control*, vol. 35, no. 3, pp. 356–361, 1990.
[25] M. Chilali and P. Gahinet, "H_∞ design with pole placement constraints: an LMI approach," *IEEE Transactions on Automatic Control*, vol. 41, no. 3, pp. 358–367, 1996.
[26] B. J. Jonkman, "TurbSim User's Guide: Version 1.50," Tech. Rep. NREL/EL-500-46198, National Renewable Energy Laboratory, 2009.
[27] Z. Wang, D. W. C. Ho, H. Dong, and H. Gao, "Robust H_∞ finite-horizon control for a class of stochastic nonlinear time-varying systems subject to sensor and actuator saturations," *IEEE Transactions on Automatic Control*, vol. 55, no. 7, pp. 1716–1722, 2010.
[28] H. Dong, Z. Wang, D. W. C. Ho, and H. Gao, "Robust H_∞ fuzzy output-feedback control with multiple probabilistic delays and multiple missing measurements," *IEEE Transactions on Fuzzy Systems*, vol. 18, no. 4, pp. 712–725, 2010.

[29] H. Dong, Z. Wang, and H. Gao, "Robust H_∞ filtering for a class of nonlinear networked systems with multiple stochastic communication delays and packet dropouts," *IEEE Transactions on Signal Processing*, vol. 58, no. 4, pp. 1957–1966, 2010.

[30] B. Shen, Z. Wang, H. Shu, and G. Wei, "Robust H_∞ finite-horizon filtering with randomly occurred nonlinearities and quantization effects," *Automatica*, vol. 46, no. 11, pp. 1743–1751, 2010.

[31] B. Shen, Z. Wang, H. Shu, and G. Wei, "H_∞ filtering for nonlinear discrete-time stochastic systems with randomly varying sensor delays," *Automatica*, vol. 45, no. 4, pp. 1032–1037, 2009.

Hindawi Publishing Corporation
Mathematical Problems in Engineering
Volume 2012, Article ID 832836, 21 pages
doi:10.1155/2012/832836

Research Article

Data-Driven Adaptive Observer for Fault Diagnosis

Shen Yin,[1] Xuebo Yang,[1] and Hamid Reza Karimi[2]

[1] *Research Institute of Intelligent Control and Systems, Harbin Institute of Technology, Harbin 150001, China*
[2] *Faculty of Engineering and Science, University of Agder, 4898 Grimstad, Norway*

Correspondence should be addressed to Shen Yin, shen.yin2011@gmail.com

Received 25 June 2012; Accepted 12 August 2012

Academic Editor: Bo Shen

This paper presents an approach for data-driven design of fault diagnosis system. The proposed fault diagnosis scheme consists of an adaptive residual generator and a bank of isolation observers, whose parameters are directly identified from the process data without identification of complete process model. To deal with normal variations in the process, the parameters of residual generator are online updated by standard adaptive technique to achieve reliable fault detection performance. After a fault is successfully detected, the isolation scheme will be activated, in which each isolation observer serves as an indicator corresponding to occurrence of a particular type of fault in the process. The thresholds can be determined analytically or through estimating the probability density function of related variables. To illustrate the performance of proposed fault diagnosis approach, a laboratory-scale three-tank system is finally utilized. It shows that the proposed data-driven scheme is efficient to deal with applications, whose analytical process models are unavailable. Especially, for the large-scale plants, whose physical models are generally difficult to be established, the proposed approach may offer an effective alternative solution for process monitoring.

1. Introduction

During the last two decades, diagnostic observers and parity space-based fault detection and isolation (FDI) schemes for linear time invariant (LTI) systems are intensively studied [1–6]. The core of the parity space FDI technique is, based on state space representation of the system, construction of residual generator by means of the so-called parity vector, which is the null space of the observability matrix. As pointed out in Ding [6], the design of an observer-based residual generator can be equivalently formulated as a similar problem.

Since the majority of observer and parity space-based FDI schemes involve rigorous development of process models based on the first principles, later identification techniques that extracts transfer function [7] or state space model become a necessary step prior to

the design. For this purpose, subspace identification methods (SIM) that identify the complete state space matrices have been successfully implemented see Overschee and Moor [8], Favoreel et al. [9], and Qin [10]. Provided the process model is known *a priori*, observer and parity space-based FDI systems can be designed with a large number of applications [11–13]. The approaches of filtering and control for such complex systems have been well studied in the literature; see Shen et al. [14], Shen et al. [15], and Dong et al. [16], Dong et al. [17]. Recently, an alternative data-driven approach has been proposed that does not require the identification of complete set of process model but only the so-called primary form of the residual generator from the process data; see Ding et al. [18]. Based on it, the advanced observer-based FDI system can be designed in an efficient way [19–23]. Thanks to its simple forms and less requirements on the design and engineering efforts, the data-driven FDI approach becomes more efficient in many industry sectors, especially for large-scale industry applications [24]. Recent survey given by Ding et al. [22, 23] provided the reader with a comprehensive overview on the basic and advanced data-driven FDI schemes.

Our study is motivated by the aforementioned data-driven FDI approach, in that we also recognize the wide existence of systems with uncertain or normal variation parameters in practice, which have not been paid enough attention in research study. Extension of the data-driven FDI scheme to such processes will improve the safety and reliability of these applications and further reduce the complexity to perform FDI especially on the large-scale systems. For this purpose, a data-driven fault diagnosis approach was proposed in this paper, in which the issues of fault isolation and threshold setting were studied to complete the earlier work given by Ding et al. [19, 20]. The structure of the fault diagnosis scheme consists of an adaptive residual generator and a bank of isolation observers, whose parameters are directly updated from the plant data with standard adaptive technique to cope with normal variations in the process. The threshold for fault detection can be determined either analytically or by probability density function estimation technique. When a fault is detected, the fault isolation scheme is activated, in which each isolation observer indicates the occurrence of a particular type of fault in the process. Fault isolation is successfully achieved when all the isolation indices, except the one responsible for the fault, exceed the thresholds. For the realization of the isolation scheme, the standard projection algorithm is implemented [25, 26]. The sufficient condition of fault isolability is also analyzed in this work.

The rest of the paper is organized as follows. In Section 2, the mathematical preliminaries and problem formulation are presented. Section 3 addresses the theoretical core of the proposed fault diagnosis scheme, in which both fault detection and isolation issues will be analyzed in detail. In Section 4, the simulation of laboratory-scale three-tank system is used to illustrate the performance of the proposed scheme. The paper ends with concluding remarks in the last section.

2. Preliminaries and Problem Formulation

2.1. Preliminaries of Model-Based Residual Generator

Consider a discrete-time LTI system which is described by

$$x_{k+1} = Ax_k + Bu_k, \tag{2.1}$$

$$y_k = Cx_k, \tag{2.2}$$

where $x_k \in \mathcal{R}^n$, $u_k \in \mathcal{R}^l$, and $y_k \in \mathcal{R}^m$ represent the vector of state variables and process input and output, respectively. A, B, and C are system matrices with appropriate dimensions. Reformulate (2.1)-(2.2) into

$$Z = \begin{bmatrix} Y \\ U \end{bmatrix} = \begin{bmatrix} \Gamma_s & H_{s,u} \\ 0 & I \end{bmatrix} \begin{bmatrix} X_i \\ U \end{bmatrix} \in \mathcal{R}^{(s+1)(m+l)\times N}, \tag{2.3}$$

where $X_i = [x_i \; x_{i+1} \; \cdots \; x_{i+N-1}] \in \mathcal{R}^{n\times N}$, $U = [u_{s,k} \; \cdots \; u_{s,k+N-1}] \in \mathcal{R}^{(s+1)l\times N}$, $Y = [y_{s,k} \; \cdots \; y_{s,k+N-1}] \in \mathcal{R}^{(s+1)m\times N}$, and

$$y_{s,k} = \begin{bmatrix} y_{k-s} \\ \vdots \\ y_k \end{bmatrix}, \qquad u_{s,k} = \begin{bmatrix} u_{k-s} \\ \vdots \\ u_k \end{bmatrix}, \qquad \Gamma_s = \begin{bmatrix} C \\ CA \\ \vdots \\ CA^s \end{bmatrix}, \qquad H_{s,u} = \begin{bmatrix} 0 & 0 & \cdots & 0 \\ CB & 0 & \cdots & 0 \\ \vdots & \ddots & \ddots & \vdots \\ CA^{s-2}B & \cdots & CB & 0 \end{bmatrix}, \tag{2.4}$$

and $s(\geq n)$ and $N(\gg s)$ are integers. On the assumption of known A, B, and C, the design of a parity space-based residual generator consists in solving

$$\alpha_s \Gamma_s = 0, \tag{2.5}$$

for the so-called parity vector $\alpha_s[\alpha_{s,0} \; \alpha_{s,1} \; \cdots \; \alpha_{s,s}] \in \mathcal{R}^{1\times(s+1)m}$. The design of an observer-based residual generator is achieved by solving the so-called Luenberger equations

$$TA - A_z T = LC, \qquad c_z T = gC, \qquad B_z = TB, \tag{2.6}$$

$$A_z \in \mathcal{R}^{s\times s}, \qquad T \in \mathcal{R}^{s\times n}, \qquad c_z \in \mathcal{R}^{1\times s}, \qquad g \in \mathcal{R}^{1\times m} \tag{2.7}$$

for A_z (should be stable), B_z, c_z, g, L together with a transformation matrix T. It follows then the construction of the parity space-based residual generator

$$r_k = \alpha_s(y_{s,k} - H_{s,u}u_{s,k}), \tag{2.8}$$

and the observer-based residual generation

$$z_{k+1} = A_z z_k + B_z u_k + L y_k \in \mathcal{R}^s, \tag{2.9}$$

$$r_k = g y_k - c_z z_k \in \mathcal{R}. \tag{2.10}$$

In the above equations, r_k is called residual signal and s the order of the parity space or the observer-based residual generator. The following lemma given by Ding [6] describes the one-to-one mapping between the parity vector and the solutions of Luenberger equations.

Lemma 2.1 (see Ding [6]). *Given any parity vector* $\alpha_s = [\alpha_{s,0}\ \alpha_{s,1}\ \cdots\ \alpha_{s,s}]$, *with* $\alpha_{s,i} \in \mathcal{R}^{1\times m}$, $i = 0, 1, \ldots, s$ *and process model* (2.1)-(2.2), *then*

$$A_z = \begin{bmatrix} 0 & 0 & \cdots & 0 \\ 1 & 0 & \cdots & 0 \\ \vdots & \ddots & \ddots & \vdots \\ 0 & \cdots & 1 & 0 \end{bmatrix} \in \mathcal{R}^{s\times s}, \qquad L = -\begin{bmatrix} \alpha_{s,0} \\ \alpha_{s,1} \\ \vdots \\ \alpha_{s,s-1} \end{bmatrix}, \qquad T = \begin{bmatrix} \alpha_{s,1} & \alpha_{s,2} & \cdots & \alpha_{s,s} \\ \alpha_{s,2} & \cdots & \alpha_{s,s} & 0 \\ \vdots & \ddots & \ddots & \vdots \\ \alpha_{s,s} & 0 & \cdots & 0 \end{bmatrix} \begin{bmatrix} C \\ CA \\ \vdots \\ CA^{s-1} \end{bmatrix}, \tag{2.11}$$

$$c_z = [0\ \cdots\ 0\ \ 1] \in \mathcal{R}^{1\times s}, \qquad g = \alpha_{s,s} \in \mathcal{R}^{1\times m}, \tag{2.12}$$

solve the Luenberger equations (2.6).

2.2. Preliminaries of Data-Driven Residual Generator Design

It is assumed that system matrices A, B, and C and system order n are *unknown a priori*; Ding et al. [19, 20] proposed an approach for data-driven design of observer-based residual generator, which briefly consists of two algorithms, that is,

(i) *Algorithm D2PS* (from data to parity subspace),

(ii) *Algorithm PS2DO* (from parity vector to diagnostic observer (DO)).

Algorithm 2.2. D2PS (from data to parity subspace).

Step 1. Generate data sets Z and construct $(1/N)ZZ^T$.
Step 2. Compute the SVD of $(1/N)ZZ^T$

$$\begin{gathered} \frac{1}{N}ZZ^T = U_z \begin{bmatrix} \Sigma_{z,1} & 0 \\ 0 & \Sigma_{z,2} \end{bmatrix} U_z^T, \\ U_z = \begin{bmatrix} U_{z,11} & U_{z,12} \\ U_{z,21} & U_{z,22} \end{bmatrix}, \qquad \Sigma_{z,2} = 0 \in \mathcal{R}^{((s-1)m-n)\times((s-1)m-n)}, \\ U_{z,11} \in \mathcal{R}^{(s+1)m\times((s+1)l+n)}, \qquad U_{z,12}^T \in \mathcal{R}^{((s+1)m-n)\times(s+1)m}. \end{gathered} \tag{2.13}$$

Step 3. Set $\Gamma_s^{\perp} = U_{z,12}^T$, $\Gamma_s^{\perp} H_{s,u} = -U_{z,22}^T$.

Note that any row of matrix $\Gamma_s^{\perp}$ is a parity vector. For a system with multiple output $(m > 1)$, $(s+1)m$ may be significantly larger than n. In order to reduce the online computation, an order reduction algorithm is given by Ding et al. [19, 20] to achieve a reduced order $s \le n$. For multiple output systems, s may be significantly smaller than n.

Algorithm 2.3. PS2DO (from parity vector to DO).

Step 1. Select $\alpha_s \in \Gamma_s^{\perp}$ and corresponding row $\beta_s \in \Gamma_s^{\perp} H_{s,u}$ and form them as

$$\begin{gathered} \alpha_s = [\alpha_{s,0}\ \ \alpha_{s,1}\ \ \cdots\ \ \alpha_{s,s}], \quad \alpha_{s,i} \in \mathcal{R}^{1\times m}, \\ \beta_s = [\beta_{s,0}\ \ \beta_{s,1}\ \ \cdots\ \ \beta_{s,s}], \quad \beta_{s,i} \in \mathcal{R}^{1\times l}. \end{gathered} \tag{2.14}$$

Step 2. Set A_z, c_z, L, g according to (2.11)-(2.12) and $B_z^T = [\beta_{s,0}^T \cdots \beta_{s,s-1}^T]$.
Step 3. Construct the DO according to (2.9)-(2.10).

2.3. Problem Formulation

So far in our study, the data-driven fault detection scheme has been developed for LTI systems. However, The wide existence of systems with uncertain or normal variation parameters has not been considered enough in the literatures. In order to develop an efficient data-driven fault diagnosis scheme for such systems, it is necessary to

(i) propose an efficient residual generator to deal with normal parameter variations in the process,

(ii) determine proper threshold for fault detection purpose,

(iii) develop related fault isolation strategy to complete the diagnosis task.

Without loss of generality, in the remaining part of this paper, the parameter variation rate is assumed bound in term of l^2-norm. In addition, the persistent excitation condition for identification methods is assumed to be satisfied.

3. Data-Driven Design of Fault Diagnosis Scheme

3.1. Adaptive Residual Generator-Based Fault Detection Scheme

According to Lemma 2.1, the system (2.1)-(2.2) can be represented in following form:

$$z_{k+1} = \overline{A}_z z_k + Q(u_k, y_k)\theta, \tag{3.1}$$

where $z_k = Tx_k$, $\overline{A}_z = A_z - L_0 c_z$, L_0 is a design parameter vector to ensure that the eigenvalues of $\overline{A}_z$ lie in the unit circle and

$$\begin{gathered}
Q(u_k, y_k) = \left[\overline{Q}(u_k, y_k) \quad L_0 y_k^T\right] \in \mathcal{R}^{s\times[s(m+l)+m]}, \\
\overline{Q}(u_k, y_k) = \left[\mathcal{U}_k \quad \mathcal{Y}_k\right] \in \mathcal{R}^{s\times s(m+l)}, \\
\mathcal{U}_k = \left[u_{1,k} \times I_{s\times s} \quad \cdots \quad u_{l,k} \times I_{s\times s}\right], \qquad \mathcal{Y}_k = \left[y_{1,k} \times I_{s\times s} \quad \cdots \quad y_{m,k} \times I_{s\times s}\right], \\
\theta = \begin{bmatrix} \overline{\theta} \\ g^T \end{bmatrix} \in \mathcal{R}^{s(m+l)+m}, \qquad \overline{\theta} = \begin{bmatrix} \mathrm{col}(B_z) \\ \mathrm{col}(L) \end{bmatrix} \in \mathcal{R}^{s(m+l)},
\end{gathered} \tag{3.2}$$

with col(•) denotes a column-wise reordering of a matrix; that is,

$$P = \left[p_1 \quad \cdots \quad p_\alpha\right] \in \mathcal{R}^{\beta\times\alpha}, \qquad \mathrm{col}(P) = \begin{bmatrix} p_1 \\ \vdots \\ p_\alpha \end{bmatrix} \in \mathcal{R}^{\beta\alpha\times 1}. \tag{3.3}$$

In the following study, set $L_0 = 0$ for the purpose of simplicity.

Note that in (3.1) the system matrices A, B, and C are integrated into vector θ, and the input and output signals are included in $Q(u_k, y_k)$. Any parameter variation in the original system can be reflected through the parameter variation rate defined as $\Delta_k = \theta_{k+1} - \theta_k$, which is bounded by

$$\|\Delta_k\| \leq v, \tag{3.4}$$

where $\|\bullet\|$ denotes l^2-norm. Let us firstly consider the basic case, that is, a constant parameter θ; the adaptive residual generator is stated in the following theorem.

Theorem 3.1. *Given the following adaptive residual generator which consists of three subsystems.*

(i) Residual generator:

$$\widehat{z}_{k+1} = \overline{A}_z \widehat{z}_k + Q(u_k, y_k)\widehat{\theta}_k + V_{k+1}\left(\widehat{\theta}_{k+1} - \widehat{\theta}_k\right), \tag{3.5}$$

$$r_k = \widehat{g}_k y_k - c_z \widehat{z}_k. \tag{3.6}$$

(ii) Auxiliary filter

$$V_{k+1} = \overline{A}_z V_k + Q(u_k, y_k) \in \mathcal{R}^{s\times[s(m+l)+m]}, \tag{3.7}$$

$$\varphi_k = c_z V_k - \begin{bmatrix} 0 & \cdots & 0 & y_k^T \end{bmatrix} \in \mathcal{R}^{s(m+l)+m}. \tag{3.8}$$

(iii) Parameter estimator

$$\widehat{\theta}_{k+1} = \gamma_k \varphi_k^T r_k + \widehat{\theta}_k \in \mathcal{R}^{s(m+l)+m}, \tag{3.9}$$

$$\gamma_k = \frac{\mu}{\delta + \varphi_k \varphi_k^T}, \quad \delta > 0,\ 0 < \mu < 2, \tag{3.10}$$

$$\widehat{\theta}_k = \begin{bmatrix} \widehat{\overline{\theta}}_k \\ (\widehat{g}_k)^T \end{bmatrix}, \quad \widehat{\overline{\theta}}_k \in \mathcal{R}^{s(m+l)},\ \widehat{g}_k \in \mathcal{R}^{1\times m}. \tag{3.11}$$

it follows that the adaptive residual generator is stable and in the fault-free case the residual signal satisfies

$$\lim_{k\to\infty} r_k = 0. \tag{3.12}$$

Moreover, if the persistent excitation condition is satisfied; that is, there exist positive constants β_1, β_2 and integer Π such that for all k

$$0 < \beta_1 I \leq \sum_{i=k}^{k+\Pi-1} \varphi_i^T \varphi_i \leq \beta_2 I < \infty, \tag{3.13}$$

the adaptive residual generator is exponentially stable, and the parameter estimation $\widehat{\theta}_k$ converges to the true value θ with an exponential convergence rate:

$$\lim_{k\to\infty} \widehat{\theta}_k = \theta. \tag{3.14}$$

Proof. The proof can be found in the earlier study by Ding et al. [19, 20]. □

Until now, the unknown parameter θ has been assumed constant. We would like to further consider the behavior of the adaptive residual generator (3.5)–(3.10) in case θ is a time-varying parameter and bounds by (3.4). To simplify the notations, define

$$\eta_k = \widetilde{z}_k - V_k\widetilde{\theta}_k, \qquad \widetilde{z}_k = z_k - \widehat{z}_k, \qquad \widetilde{\theta}_k = \theta_k - \widehat{\theta}_k. \tag{3.15}$$

After a straightforward calculation, it follows that

$$\eta_{k+1} = \overline{A}_z\eta_k + \epsilon_k, \tag{3.16}$$

$$\widetilde{\theta}_{k+1} = \left(I - \gamma_k\varphi_k^T\varphi_k\right)\widetilde{\theta}_k + \overline{\epsilon}_k, \tag{3.17}$$

$$r_k = c_z\eta_k + \varphi_k\widetilde{\theta}_k, \tag{3.18}$$

with $\Theta_k = -\gamma_k\varphi_k^T c_z$, $\Delta_k = \theta_{k+1} - \theta_k$, $\overline{\epsilon}_k = \Theta_k\eta_k + \Delta_k$, and $\epsilon_k = -V_{k+1}\Delta_k$. According to (3.18), the residual r_k has a nonzero value since $\Delta_k \neq 0$. Assume that persistent excitation condition (3.13) is satisfied, the properties of adaptive residual generator (3.5)–(3.10) can be generalized in the following theorem.

Theorem 3.2. *In case of $\Delta_k \neq 0$ and bounded by* (3.4)*, the adaptive residual generator* (3.5)–(3.10) *ensures the following:*

(i) the estimation error $\widetilde{\theta}_k$ converges exponentially to the set

$$\mathcal{B} = \left\{\widetilde{\theta}_k \mid \left\|\widetilde{\theta}_k\right\| \le \alpha_1^{k-k_0}\left\|\widetilde{\theta}_{k_0}\right\| + \frac{1-\alpha_1^{k-k_0}}{1-\alpha_1}\overline{\epsilon}\right\}, \quad 0 < \alpha_1 < 1, \tag{3.19}$$

where $\overline{\epsilon}$ is a positive scalar such that $\|\overline{\epsilon}_k\| < \overline{\epsilon}$ and k_0 denotes the initial time sample;

(ii) the residual signal r_k converges exponentially to the set

$$\mathcal{R} = \left\{r_k \mid |r_k| \le \epsilon + \|\varphi_k\|\alpha_1^{k-k_0}\left\|\widetilde{\theta}_{k_0}\right\| + \|\varphi_k\|\frac{1-\alpha_1^{k-k_0}}{1-\alpha_1}\overline{\epsilon}\right\}, \tag{3.20}$$

where ϵ is a positive scalar such that $\|\epsilon_k\| < \epsilon$;

(iii) based on the assumption of the zero initial condition, that is, $\widetilde{\theta}_{k_0} = 0$, the normalized residual signal $\overline{r}_k$ satisfies

$$|\overline{r}_k| \le \sqrt{s}v + \frac{1+\sqrt{s}}{1-\alpha_1}v, \tag{3.21}$$

where $\overline{r}_k = r_k/\sqrt{\delta + \varphi_k\varphi_k^T}$. *Furthermore, if the process corrupted by noise/disturbance, the residual signal can be formulated as*

$$r_k = c_z\eta_k + \varphi_k\widetilde{\theta}_k + p_k, \tag{3.22}$$

where p_k *represents the influence of noise/disturbance on the residual signal. It follows that*

$$|\overline{r}_k| \le \sqrt{s}v + \frac{1+\sqrt{s}}{1-\alpha_1}v + p, \tag{3.23}$$

with $p = \sup_{\forall k}(p_k/\sqrt{\delta + \varphi_k\varphi_k^T})$.

Proof. According to (3.17), for all $k > k_0$, we have

$$\widetilde{\theta}_k = S_{k,k_0}\widetilde{\theta}_{k_0} + \sum_{i=k_0}^{k-1} S_{k,i+1}\overline{\epsilon}_k, \tag{3.24}$$

where S_{k,k_0} is the transition matrix of the linear time-varying system (3.17). Since (3.13) is satisfied, the system (3.17) is exponentially stable; and Astrom and Wittenmark [27]. Therefore, there exists a positive constant $0 < \alpha_1 < 1$ such that $\|S_{k,k_0}\| \le \alpha_1^{k-k_0}$. Consequently, from (3.17), we have

$$\left\|\widetilde{\theta}_k\right\| \le \alpha_1^{k-k_0}\left\|\widetilde{\theta}_{k_0}\right\| + \left\|\sum_{i=k_0}^{k-1} S_{k\cdot i+1}\overline{\epsilon}_k\right\| \le \alpha_1^{k-k_0}\left\|\widetilde{\theta}_{k_0}\right\| + \frac{1-\alpha_1^{k-k_0}}{1-\alpha_1}\overline{\epsilon}. \tag{3.25}$$

Since $L_0 = 0$, $\overline{A}_z = A_z$, and all the eigenvalues of $\overline{A}_z$ are zero, it follows from (3.16) that

$$\|\eta_k\| \le \epsilon. \tag{3.26}$$

The bound of residual signal can be straightforwardly obtained

$$|r_k| \le \|c_z\eta_k\| + \left\|\varphi_k\widetilde{\theta}_k\right\| \le \epsilon + \|\varphi_k\|\alpha_1^{k-k_0}\left\|\widetilde{\theta}_{k_0}\right\| + \|\varphi_k\|\frac{1-\alpha_1^{k-k_0}}{1-\alpha_1}\overline{\epsilon}. \tag{3.27}$$

It is easier to prove that

$$\begin{gathered}\frac{\|\varepsilon_k\|}{\sqrt{\delta + \varphi_k\varphi_k^T}} \le \sqrt{s}\|\Delta_k\| \le \sqrt{s}v, \\ \|\overline{\varepsilon}_k\| \le \left(1+\sqrt{s}\right)\|\Delta_k\| \le \left(1+\sqrt{s}\right)v.\end{gathered} \tag{3.28}$$

Thus, set

$$\frac{\varepsilon}{\sqrt{\delta + \varphi_k \varphi_k^T}} = \sqrt{s}v, \qquad \bar{\epsilon} = \left(1 + \sqrt{s}\right)v, \tag{3.29}$$

the normalized residual becomes

$$|\bar{r}_k| \leq \sqrt{s}v + \frac{1 + \sqrt{s}}{1 - \alpha_1}v. \tag{3.30}$$

Equations (3.22)-(3.23) can be easily proved, and thus they are omitted here. □

According to Theorem 3.2, in case θ is a time-varying parameter and bounds by (3.4) the residual $\bar{r}_k$ is bounded and the threshold J_{th} can be set as the right-hand side presented by (3.23); that is,

$$J_{\text{th}} = \sqrt{s}v + \frac{1 + \sqrt{s}}{1 - \alpha_1}v + p. \tag{3.31}$$

The fault detection logic is given by

$$\begin{aligned} &|\bar{r}_k| \leq J_{\text{th}}, \quad \text{fault free}, \\ &|\bar{r}_k| > J_{\text{th}}, \quad \text{alarm for fault}. \end{aligned} \tag{3.32}$$

Remark 3.3. It is of great interest to detect the faults that cause abnormal changes on physical parameters of the process. Although the identified parameter θ is physically meaningless, any abnormal physical parameters variations can influence θ and should be finally discovered by the residual signal. In practice, the bound of normal variation rate of θ given by (3.4) can be determined through the offline test data. The related threshold of residual signal is designed for the detection of abnormal parameter change, which is supposed to be faster than the normal parameter variation.

Remark 3.4. The order of residual generator s could be significantly smaller than system order n in multiple output systems ($m > 1$): $s = (n+1)/m - 1$. An algorithm is proposed in Ding et al. [19, 20] for constructing the reduced order residual generator. Thus, if persistent excitation condition is satisfied, the estimation error $\tilde{\theta}_k$ converges exponentially to a set determined by Δ_k. For industrial process, the excitation mainly comes from the variation of process variables and measurement noise.

Remark 3.5. Another efficient way to determine the threshold for residual signal is based on statistical methods. Without special assumption on process data, the so-called kernel density estimation (KDE) is widely used in practice for estimating the probability density function of residual signals. Based on a large number of offline test data, a proper threshold can be chosen under given confidence level. More detailed description on KDE can be found in Silverman [28] and Martin and Morris [29].

3.2. Fault Isolation Scheme Design

In this subsection, the fault isolation scheme will be further introduced in the framework of adaptive residual generator.

Suppose that there exist S classes of faults in the process including all potential abnormalities in sensors and actuators. Under the influence of ith class of fault, $i = 1, \ldots, S$, the unknown parameter becomes θ_f^i, which is assumed to belong to a known compact and convex set $\Theta_f^i \in \mathcal{R}^{s(m+l)+m}$. Note that, the set Θ_f^i could be offline identified by using the faulty data within the framework of adaptive scheme (3.5)–(3.10).

The proposed fault isolation strategy can be developed by integrating the fault information, that is, Θ_f^i. Based on it, S fault isolation observers are constructed, in which the ith observer is only responsible for the ith set of fault. According to the fault detection scheme discussed in the last subsection, after a fault is detected at time t_d, the fault isolation scheme is activated, such that the ith isolator is insensitive to the ith type of fault, but sensitive to other faults; see Zhang et al. [30]. In order to realize these requirements, the parameter projection method is utilized and the ith fault isolation observer has the following form:

$$\hat{z}_{k+1}^i = \overline{A}_z \hat{z}_k^i + Q(u_k, y_k)\hat{\theta}_k^i + V_{k+1}^i\left(\hat{\theta}_{k+1}^i - \hat{\theta}_k^i\right), \tag{3.33}$$

$$r_k^i = \hat{g}_k^i y_k - c_z \hat{z}_k^i,$$

$$V_{k+1}^i = \overline{A}_z V_k^i + Q(u_k, y_k) \in \mathcal{R}^{s\times[s(m+l)+m]}, \tag{3.34}$$

$$\varphi_k^i = c_z V_k^i - \begin{bmatrix} 0 & \cdots & 0 & y_k^T \end{bmatrix} \in \mathcal{R}^{s(m+l)+m},$$

$$\hat{\theta}_{k+1}^{i*} = \hat{\theta}_k^i + \frac{(\varphi_k^i)^T r_k^i}{\delta + \varphi_k^i (\varphi_k^i)^T} \in \mathcal{R}^{s(m+l)+m}, \tag{3.35}$$

$$\hat{\theta}_{k+1}^i = \mathcal{P}_{\Theta_f^i}\left[\hat{\theta}_{k+1}^{i*}\right], \tag{3.36}$$

where

$$\hat{\theta}_k^i = \begin{bmatrix} \overline{\theta}_k^i \\ (\hat{g}_k^i)^T \end{bmatrix}, \quad \overline{\theta}_k^i \in \mathcal{R}^{s(m+l)}, \ \hat{g}_k^i \in \mathcal{R}^m, \tag{3.37}$$

the $\delta > 0$, $\mathcal{P}_{\Theta_f^i}$ denotes a projection operator that ensures $\hat{\theta}_{k+1}^i$ lies in a known bounded convex subset $\Theta_f^i \in \mathcal{R}^{s(m+l)+m}$. Details on the projection operator can be founded in Tao [26]. The following theorem states the properties of the ith isolation observer in case of the ith type of fault occurred.

Theorem 3.6. *Given the ith fault isolation observer in the form* (3.33)–(3.36), *suppose that there is a positive constant d_i, such that for all $\theta_1, \theta_2 \in \Theta_f^i$, it follows that*

$$d_i = \sup_{\theta_1,\theta_2\in\Theta_f^i} \|\theta_1 - \theta_2\|. \tag{3.38}$$

In case of the ith type of fault occurs, one has the following:

(i) the ith fault isolation observer is stable and

$$\left\|\tilde{\theta}_{k+1}^{i}\right\| \leq d_i, \qquad \left\|\hat{\theta}_{k+1}^{i} - \hat{\theta}_{k}^{i}\right\| \leq \left|\bar{r}_k^i\right|, \tag{3.39}$$

where $\bar{r}_k^i = r_k^i / \sqrt{\delta + \varphi_k^i (\varphi_k^i)^T}$, $\tilde{\theta}_{k+1}^i = \theta_{k+1}^i - \hat{\theta}_{k+1}^i$,

(ii) based on the assumption of the zero initial condition, the normalized residual signal satisfies

$$\left(\bar{r}_k^i\right)^2 \leq d_i^2 + \left(2s + 2\sqrt{s} + 1\right) v_i^2 + \left(2 + 2\sqrt{s}\right) v_i d_i, \tag{3.40}$$

where v_i *is a positive scalar such that* $\|\Delta_k^i\| \leq v_i$ *with* $\Delta_k^i = \theta_{k+1}^i - \theta_k^i$.

Proof. According to the property of the projection operator, it follows that $\hat{\theta}_{k+1}^i \in \Theta_f^i$. From (3.38), we have

$$\left\|\tilde{\theta}_{k+1}^{i}\right\| = \left\|\theta_{k+1}^{i} - \hat{\theta}_{k+1}^{i}\right\| \leq d_i. \tag{3.41}$$

It is evident that for all k,

$$\left\|\hat{\theta}_{k+1}^{i} - \theta_{k+1}^{i}\right\| \leq \left\|\hat{\theta}_{k+1}^{i*} - \theta_{k+1}^{i}\right\|, \tag{3.42}$$

and consequently,

$$\left\|\hat{\theta}_{k+1}^{i} - \hat{\theta}_{k}^{i}\right\| \leq \left\|\hat{\theta}_{k+1}^{i*} - \hat{\theta}_{k}^{i}\right\| \leq \frac{\left\|(\varphi_k^i)^T\right\| \left|\bar{r}_k^i\right|}{\delta + \varphi_k^i (\varphi_k^i)^T} \leq \left|\bar{r}_k^i\right|. \tag{3.43}$$

Now, define a new parameter

$$\tilde{\theta}_{k+1}^{i*} = \hat{\theta}_{k+1}^{i*} - \theta_{k+1}^{i}. \tag{3.44}$$

Using (3.42), we get

$$\left\|\tilde{\theta}_{k+1}^{i}\right\|^2 - \left\|\tilde{\theta}_{k}^{i}\right\|^2 \leq \left\|\tilde{\theta}_{k+1}^{i*}\right\|^2 - \left\|\tilde{\theta}_{k}^{i}\right\|^2. \tag{3.45}$$

The right-hand side of (3.45) becomes

$$\left\|\tilde{\theta}_{k+1}^{i*}\right\|^2 - \left\|\tilde{\theta}_{k}^{i}\right\|^2 = \left(\theta_{k+1}^{i} - \hat{\theta}_{k+1}^{i*} - \theta_{k}^{i} + \hat{\theta}_{k}^{i}\right)^T \left(\theta_{k+1}^{i} - \hat{\theta}_{k+1}^{i*} + \theta_{k}^{i} - \hat{\theta}_{k}^{i}\right). \tag{3.46}$$

Note that, (3.35) can be reformulated as

$$\widehat{\theta}_{k+1}^{i*} = \widehat{\theta}_k^i + \left(\overline{\varphi}_k^i\right)^T \overline{r}_k^i, \tag{3.47}$$

where

$$\left(\overline{\varphi}_k^i\right)^T = \frac{\left(\varphi_k^i\right)^T}{\sqrt{\delta + \varphi_k^i \left(\varphi_k^i\right)^T}}. \tag{3.48}$$

For the normalized residual signal $\overline{r}_k^i$, it is known that

$$\overline{r}_k^i = \overline{\varphi}_k^i \widetilde{\theta}_k^i + \overline{\eta}_k^i, \tag{3.49}$$

with

$$\begin{gathered} \overline{\eta}_k^i = \frac{c_z \eta_k^i}{\sqrt{\delta + \varphi_k^i \left(\varphi_k^i\right)^T}}, \\ \eta_k^i = \overline{A}_z \eta_{k-1}^i - V_k^i \Delta_{k-1}^i, \\ \Delta_{k-1}^i = \theta_k^i - \theta_{k-1}^i, \quad 0 \le \overline{\varphi}_k \overline{\varphi}_k^T \le 1. \end{gathered} \tag{3.50}$$

Combining (3.46), (3.47), and (3.49), we have

$$\left\|\widetilde{\theta}_{k+1}^i\right\|^2 - \left\|\widetilde{\theta}_k^i\right\|^2 \le -\left(\overline{r}_k^i\right)^2 + 2\overline{r}_k^i \overline{\eta}_k^i + \left(-2\overline{\varphi}_k^i \overline{r}_k^i + 2\left(\widetilde{\theta}_k^i\right)^T + \left(\theta_{k+1}^i\right)^T - \left(\theta_k^i\right)^T\right) \Delta_k^i. \tag{3.51}$$

Equation (3.51) can be reformulated as

$$\left(\overline{r}_k^i\right)^2 \le -\left\|\widetilde{\theta}_{k+1}^i\right\|^2 + \left\|\widetilde{\theta}_k^i\right\|^2 + 2\left(\overline{\eta}_k^i\right)^2 + 2\left|\overline{\eta}_k^i\right| \left\|\widetilde{\theta}_k^i\right\| \tag{3.52}$$

$$+ \left\|\theta_{k+1}^i - \theta_k^i\right\| \left(2\left\|\widetilde{\theta}_k^i\right\| + 2\left|\overline{\eta}_k^i\right| + \left\|\theta_{k+1}^i - \theta_k^i\right\|\right). \tag{3.53}$$

Since

$$\left|\overline{\eta}_k^i\right| \le \frac{\left\|\eta_k^i\right\|}{\sqrt{\delta + \varphi_k^i \left(\varphi_k^i\right)^T}} \le \sqrt{s} v_i, \tag{3.54}$$

according to (3.52), the result represented by (3.40) can be easily proved. □

For the ith isolation observer, define the fault isolation index

$$J_k^i = \overline{r}_k^i, \tag{3.55}$$

and the related threshold $J_{\text{th}}^{i,\text{iso}}$. Based on Theorem 3.6, we have the following corollary.

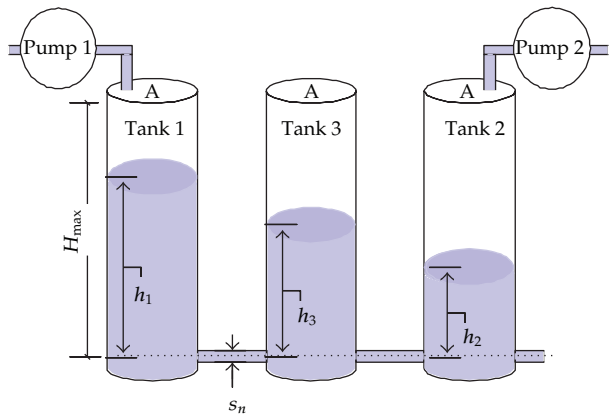

Figure 1: Structure of TTS.

Corollary 3.7. *For the ith isolation observer, the fault isolation threshold $J_{th}^{i,iso}$ can be determined by*

$$J_{th}^{i,iso} = \sqrt{d_i^2 + (2s + 2\sqrt{s} + 1)v_i^2 + (2 + 2\sqrt{s})v_i d_i}. \tag{3.56}$$

Moreover, if the process corrupted by disturbance and/or noise, the normalized residual is

$$\overline{r}_k^i = \overline{\varphi}_k^i \widetilde{\theta}_k^i + \overline{\eta}_k^i + \overline{p}_k^i, \tag{3.57}$$

where $\overline{p}_k^i$ represents the influence of noise/disturbance on the normalized residual signal. In this case, the threshold for fault isolation purpose is given by

$$J_{th}^{i,iso} = \sqrt{d_i^2 + (2s + 2\sqrt{s} + 1)v_i^2 + cv_i d_i + c\overline{p}^i v_i}, \tag{3.58}$$

with

$$\overline{p}^i = \sup_{\forall k}\left(\overline{p}_k^i\right), \qquad c = 2 + 2\sqrt{s}. \tag{3.59}$$

Proof. The proof is straightforward based on Theorem 3.6 and omitted here. □

The fault isolation logic can be described as the following:

(i) for the ith isolation observer, if $\exists t_a > t_d$ such that $|J_{t_a}^i| > J_{\text{th}}^{i,\text{iso}}$, then the occurrence of the ith type of fault is excluded;

(ii) otherwise, if $|J_{t_a}^i| < J_{\text{th}}^{i,\text{iso}}$ for $\forall t_a > t_d$, the ith type of fault is occurred.

The sufficient condition of fault isolability is given by the following theorem.

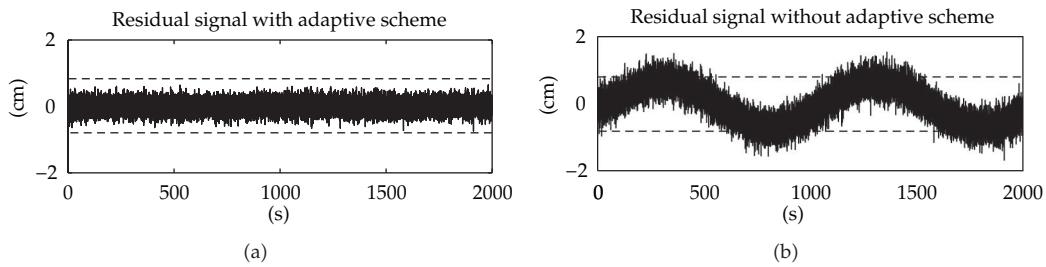

Figure 2: Residual signal.

Theorem 3.8. *Based on the fault isolation observer* (3.33)–(3.36), *the* i*th type of fault, which detected at time* t_d, *is isolable, if for the other* $S-1$ *fault isolation observers,* $\exists t_a > t_d$ *such that the following inequality is satisfied*

$$\left|\overline{\varphi}_{t_a}^{r}\tilde{\theta}_{t_a}^{r}\right| > \sqrt{s}v_r + \sqrt{sv_r^2 + \left(J_{th}^{r,iso}\right)^2}, \tag{3.60}$$

where

$$J_{\text{th}}^{r,iso} = \sqrt{d_r^2 + (2s + 2\sqrt{s} + 1)v_r^2 + (2 + 2\sqrt{s})v_r d_r}, \quad r = 1, \ldots, S,\ r \neq i. \tag{3.61}$$

Furthermore, if $s = 1$, $L_0 = 0$, *it follows that*

$$\left|\overline{\varphi}_{t_a}^{r}\tilde{\theta}_{t_a}^{r}\right| > v_r + \sqrt{d_r^2 + 6v_r^2 + 4v_r d_r}. \tag{3.62}$$

Proof. For the rth fault isolation observer, we have

$$\begin{aligned}\left(J_{t_a}^{r}\right)^2 &= \left(\overline{\varphi}_{t_a}^{r}\tilde{\theta}_{t_a}^{r}\right)^2 + \left(\overline{\eta}_{t_a}^{r}\right)^2 + 2\overline{\varphi}_{t_a}^{r}\tilde{\theta}_{t_a}^{r}\overline{\eta}_{t_a}^{r} \\ &\geq \left(\overline{\varphi}_{t_a}^{r}\tilde{\theta}_{t_a}^{r}\right)^2 - 2\sqrt{s}v_r\left|\overline{\varphi}_{t_a}^{r}\tilde{\theta}_{t_a}^{r}\right|.\end{aligned} \tag{3.63}$$

Straightforwardly, if for all $r = 1, \ldots, S,\ r \neq i$, $\exists t_a > t_d$ such that

$$\left(\overline{\varphi}_{t_a}^{r}\tilde{\theta}_{t_a}^{r}\right)^2 - 2\sqrt{s}v_r\left|\overline{\varphi}_{t_a}^{r}\tilde{\theta}_{t_a}^{r}\right| > \left(J_{\text{th}}^{r,\text{iso}}\right)^2, \tag{3.64}$$

the ith type of fault is isolable and directly (3.60) is proofed. In the case of $s = 1$ and $L_0 = 0$, (3.62) is straightforward. □

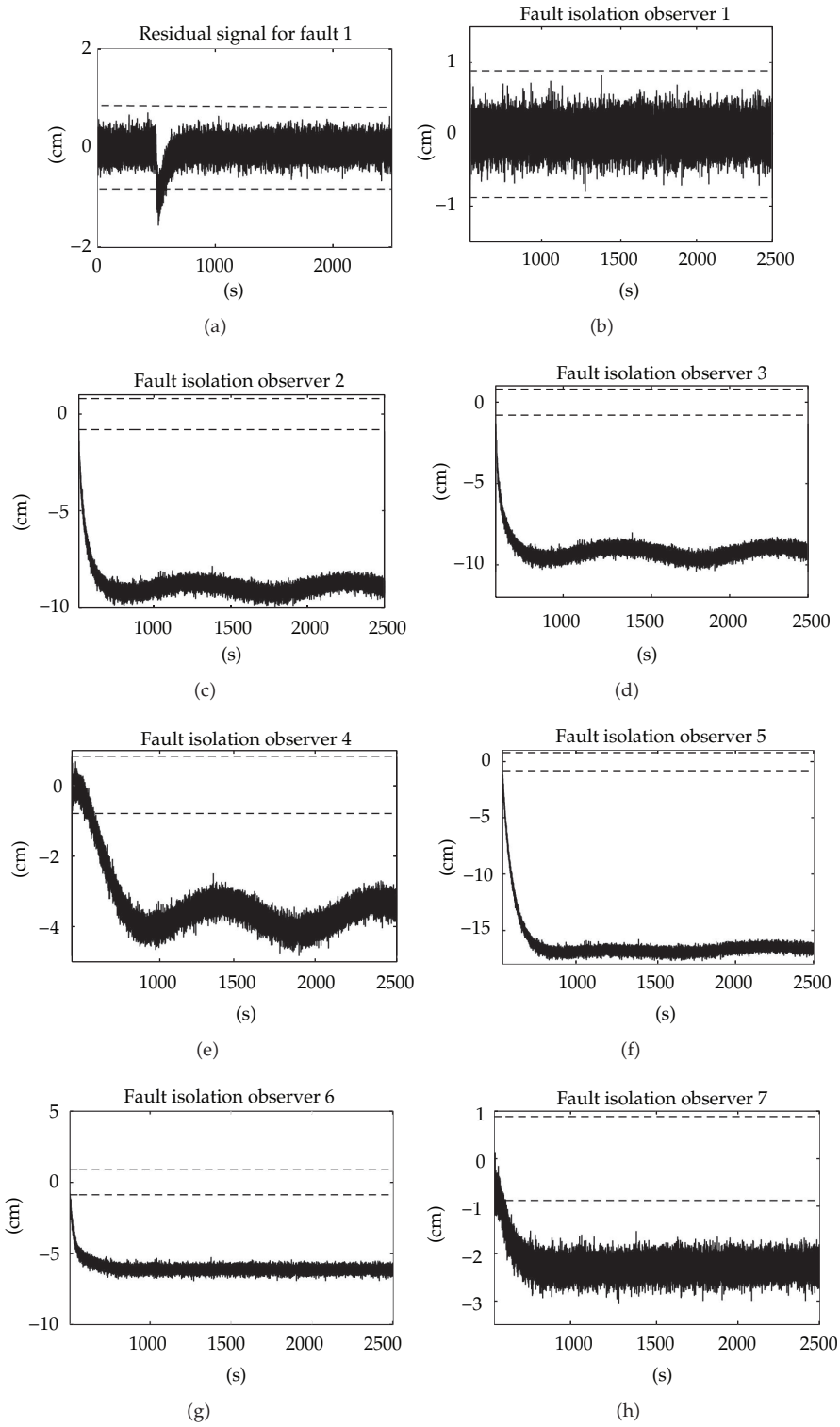

Figure 3: Continued.

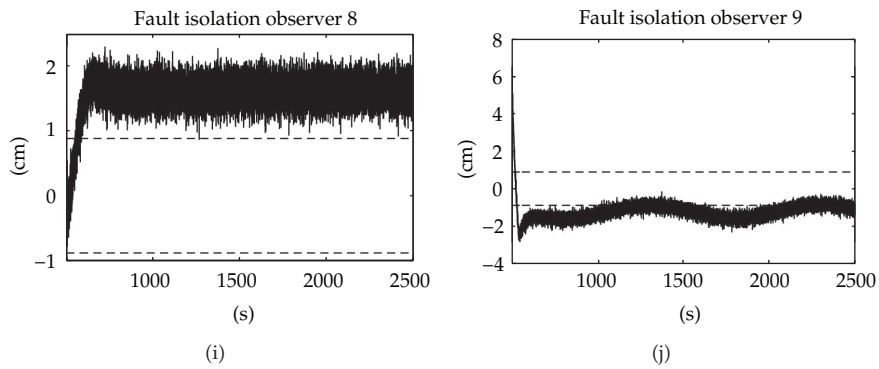

Figure 3: Fault diagnosis for fault 1.

4. Application to Three-Tank System

The three-tank system (TTS) considered in our study is a laboratory setup located in the laboratory of Institute for Automatic Control and Complex Systems, University of Duisburg-Essen. The sketch is shown in Figure 1, which has typical characteristics of tanks, pipelines, and pumps used in the chemical industry and thus often serves as benchmark process for many control and monitoring relevant studies.

The plant consists of three cylindrical tanks which are serially interconnected with each other by cylindrical pipes with the cross-section of S_n. The outflowing water is collected in a reservoir, which supplies pumps 1 and 2. $H_{\max}$ denotes the maximal height of tanks. The flow rates and water levels of tanks, represented by h_i, $i = 1, 2, 3$, are measured throughout the process. By integrating a nonlinear controller, water levels h_1 and h_2 can be controlled. The detailed description of TTS can be found in Ding [6].

It is well known that the system matrices of TTS, which are achieved from linearization at different operation points, are different. In our experiment, the operation point of water level h_1 is periodically changed in order to simulate the normal parameter variations in the process. An experiment including the following steps has been performed.

(i) Place TTS at the operating point $h_1 = 35 + \sin(0.002t)$ cm, $h_2 = 25$ cm, in which sin signal added to h_1 leads to normal parameter variations.

(ii) Use the adaptive scheme (3.5)–(3.10) to identify θ through the data collected at the operating point $h_1 = 35$ cm, $h_2 = 25$ cm with reduced order $s = 1$ and $L_0 = 0$. Note that the system order $n = 3$ can be determined by Algorithm D2PS, and based on it the reduced order s is calculated according to the relationship $s = (n+1)/m - 1$ with two system outputs; that is, $m = 2$.

(iii) Construct two residual generators: (a) an adaptive residual generator (3.5)–(3.10) (b) a standard one without adaptive scheme.

(iv) Both the residual generators run for 2000 s (seconds). The threshold $J_{\text{th}} = 0.78$ is determined according to (3.23) with the parameters $\mu = 0.01$, $\alpha_1 = 0.9997$, $v = 7.3668 \times 10^{-5}$, and $p = 0.55$, which are chosen according to the offline test data.

Figure 2 shows the residual signals with and without the adaptive scheme. It is clear that the standard process monitoring method is unsuitable to monitor TTS with normal parameters variations that is apparent by the numerous false alarms.

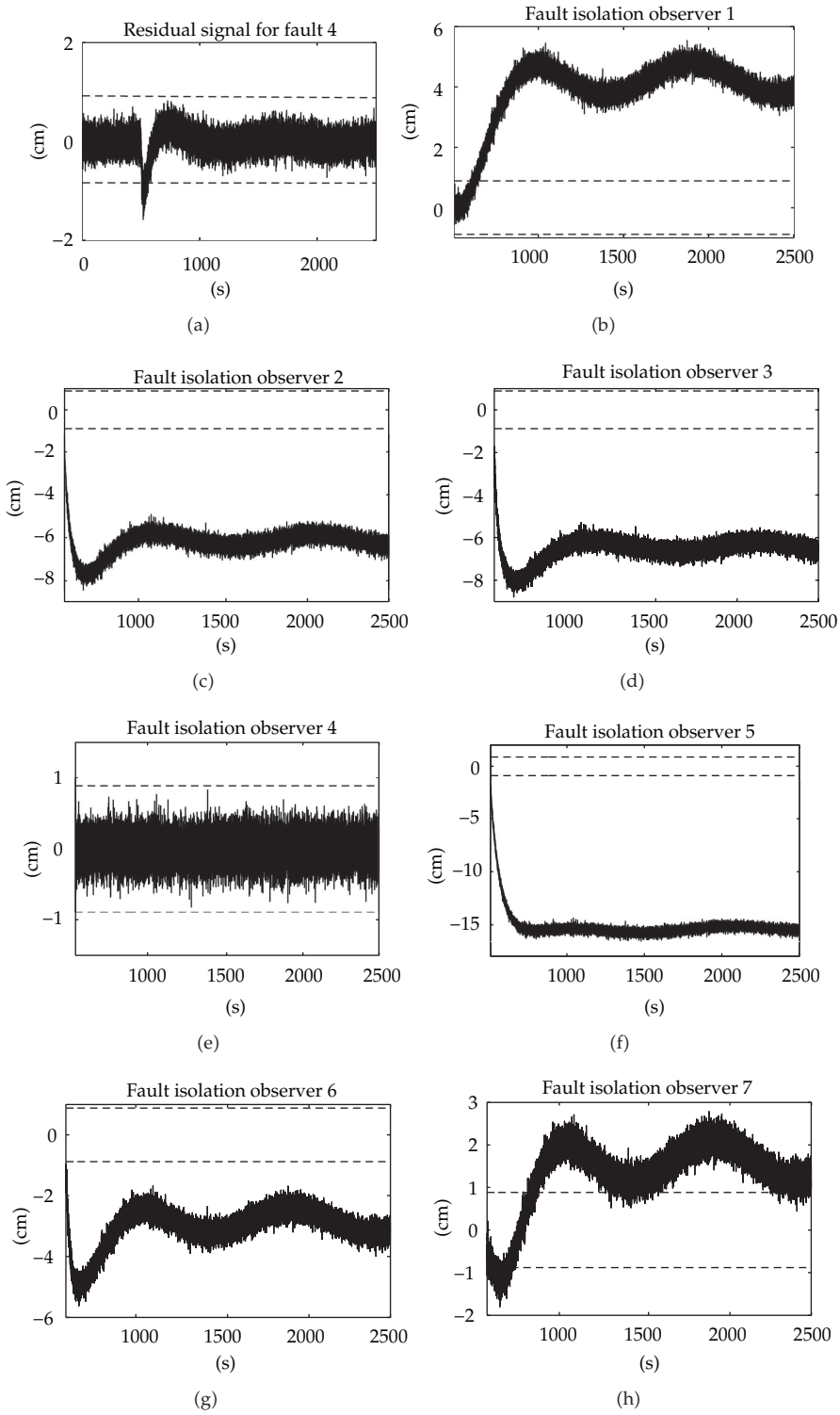

Figure 4: Continued.

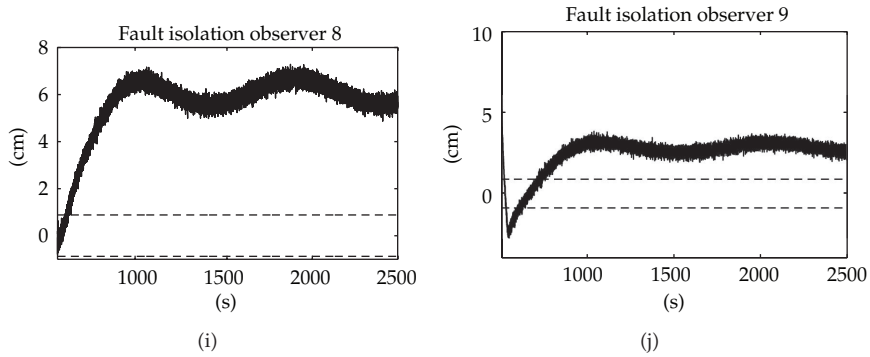

Figure 4: Fault diagnosis for fault 4.

Table 1: The faults existed in TTS.

Fault number	Description	Type
Faults 1–3	Leaking in tank 1, 2, 3	Process fault
Faults 4-5	Offset of actuator Q_1, Q_2	Actuator fault
Faults 6–8	Plugging in tank 1, 2, 3	Process fault
Fault 9	Offset of sensor h_1	Sensor fault

The faults occurred in TTS can be classified as process fault, sensor fault, and actuator fault, which are shown in Table 1. To verify the performance of the proposed fault diagnosis scheme, the following experiment is carried out.

(i) Offline: apply adaptive scheme (3.5)–(3.10) to identify Θ_f^i through the ith type of faulty data with $s = 1$ and $L_0 = 0$.

(ii) Online: use adaptive residual generator (3.5)–(3.10) for fault detection purpose. If there exists time t_d such that $|\overline{r}_k| > J_{th}$, the alarm is released. Simultaneously, the $S-1$ fault isolation observers (3.33)–(3.36) are activated, and the threshold $J_{\text{iso}}^i = 0.8822$ is determined according to (3.58) with the parameters $v_i = 1 \times 10^{-2}$, $d_i = 0.85$, and $\overline{p}_i = 0.55$.

The fault diagnosis results of faults 1, 4, and 9, which represent the process, actuator, and sensor fault, are mainly presented in the following study. All these faults occur at the 500th second. The sensor fault 9 has 30% offset compared to the normal value and the actuator fault 4 represents 100% offset to the desired value. Figures 3(a), 4(a), and 5(a) show the residual signal from adaptive residual generator for fault detection purpose. It can be seen that the faults are successfully detected at the 505 s, the 507 s, and the 501 s, respectively.

In the meanwhile, the fault isolation observers are activated, and the related fault isolation indices are shown in Figures 3(b)–3(j), 4(b)–4(j), and 5(b)–5(j) for faults 1, 4, 9, respectively. It is evident that the fault isolation indices from the 1st isolation observer (Figure 3(b)), the 4th isolation observer (Figure 4(e)), and the 9th isolation observer (Figure 5(j)) are consistently maintained under respective thresholds which indicate occurrence of these faults. On the other hand, the other subfigures show the isolation indices associated to other isolation observers. It is obvious that all of them exceed the related thresholds, which indicate the absence of these faults in the process.

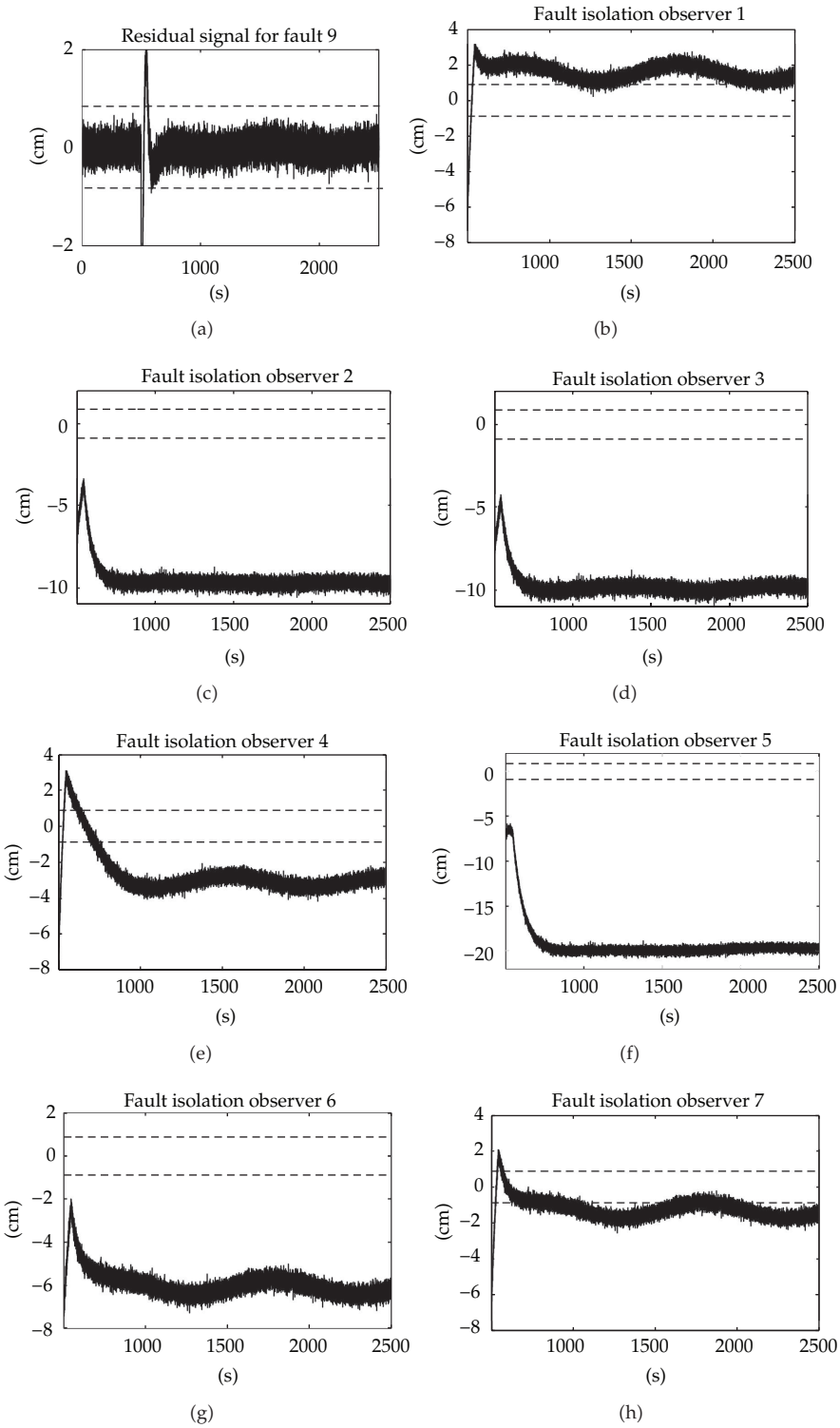

Figure 5: Continued.

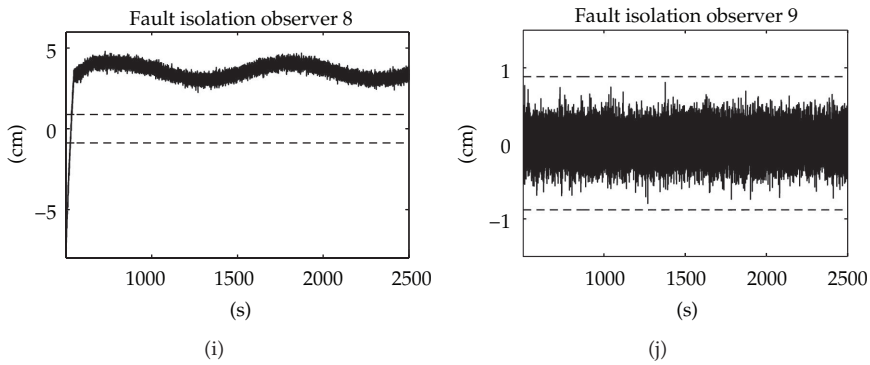

Figure 5: Fault diagnosis for fault 9.

5. Conclusion

In this paper, we have proposed an approach for data-driven design of fault diagnosis system, which consists of an adaptive residual generator and a bank of observers for fault detection and isolation purposes. Analytical results regarding the issues of adaptive observers, threshold calculation, and fault isolation strategy are discussed. The proposed design scheme is demonstrated on the simulation of laboratory-scale three-tank system, which shows satisfactory fault diagnosis performance.

References

[1] J. Gertler, *Fault Detection and Diagnosis in Engineering Systems*, Marcel Dekker, New York, NY, USA, 1998.

[2] J. Chen and R. Patton, *Robust Model-Based Fault Diagnosis for Dynamic Systems*, Kluwer Academic, Norwell, Mass, USA, 1999.

[3] R. Patton, P. Frank, and R. Clark, *Issues of Fault Diagnosis for Dynamic Systems*, Springer, Berlin, Germany, 2000.

[4] M. Blanke, M. Kinnaert, J. Lunze, M. Staroswiecki, and J. Schröder, *Diagnosis and Fault-Tolerant Control*, Springer, Berlin, Germany, 2006.

[5] R. Isermann, *Fault Diagnosis Systems: An Introduction from Fault Detection to Fault Tolerance*, Springer, Berlin, Germany, 2006.

[6] S. Ding, *Model-Based Fault Diagnosis Techniques*, Springer, Berlin, Germany, 2008.

[7] L. Ljung, *System Identification: Theory for the User*, Prentice Hall, Englewood Cliffs, NJ, USA, 1987.

[8] P. V. Overschee and B. D. Moor, *Subspace Identification for Linear Systems*, Kluwer Academic, Dordrecht, The Netherlands, 1996.

[9] W. Favoreel, B. De Moor, and P. Van Overschee, "Subspace state space system identification for industrial processes," *Journal of Process Control*, vol. 10, no. 2-3, pp. 149–155, 2000.

[10] S. Qin, "An overview of subspace identification," *Computers and Chemical Engineering*, vol. 30, no. 10–12, pp. 1502–1513, 2006.

[11] I. Hwang, S. Kim, Y. Kim, and C. E. Seah, "A survey of fault detection, isolation, and reconfiguration methods," *IEEE Transactions on Control Systems Technology*, vol. 18, no. 3, pp. 636–653, 2010.

[12] V. Venkatasubramanian, R. Rengaswamy, K. Yin, and S. Kavuri, "A review of process fault detection and diagnosis. Part I: Quantitative model-based methods," *Computers and Chemical Engineering*, vol. 27, pp. 293–311, 2003.

[13] P. Zhang and S. Ding, "On fault detection in linear discrete-time, periodic, and sampled-data systems (survey)," *Journal of Control Science and Engineering*, vol. 2008, Article ID 849546, 19 pages, 2008.

[14] B. Shen, Z. Wang, H. Shu, and G. Wei, "Robust $H\infty$ finite-horizon filtering with randomly occurred nonlinearities and quantization effects," *Automatica*, vol. 46, no. 11, pp. 1743–1751, 2010.

[15] B. Shen, Z. Wang, and Y. S. Hung, "Distributed $H\infty$-consensus filtering in sensor networks with multiple missing measurements: the finite-horizon case," *Automatica*, vol. 46, no. 10, pp. 1682–1688, 2010.

[16] H. Dong, Z. Wang, D. W. C. Ho, and H. Gao, "Robust $H\infty$ filtering for Markovian jump systems with randomly occurring nonlinearities and sensor saturation: the finite-horizon case," *IEEE Transactions on Signal Processing*, vol. 59, no. 7, pp. 3048–3057, 2011.

[17] H. Dong, Z. Wang, J. Lam, and H. Gao, "Fuzzy-model-based robust fault detection with stochastic mixed time-delays and successive packet dropouts," *IEEE Transactions on Systems, Man, and Cybernetics*, vol. 42, no. 3, part B, pp. 365–376, 2012.

[18] S. X. Ding, P. Zhang, B. Huang, and E. L. Ding, "Subspace method aided data-driven design of observer based fault detection systems," in *Proceedings of the 16th Triennial World Congress of International Federation of Automatic Control (IFAC '05)*, pp. 167–172, Prague, Czech Republic, July 2005.

[19] S. Ding, S. Yin, P. Zhang, E. Ding, and A. Naik, "An approach to data-driven adaptive residual generator design and implementation," in *Proceedings of the 7th IFAC Symposium on Fault Detection and Supervision and Safety of Technical Processes*, Barcelona, Spain, 2009.

[20] S. X. Ding, P. Zhang, A. Naik, E. L. Ding, and B. Huang, "Subspace method aided data-driven design of fault detection and isolation systems," *Journal of Process Control*, vol. 19, no. 9, pp. 1496–1510, 2009.

[21] S. Yin, A. Naik, and S. Ding, "Data-driven design of fault diagnosis scheme for periodic systems," in *Proceedings of the 7th Workshop on Advanced Control and Diagnosis*, Zielona Gora, Poland, 2009.

[22] S. Ding, S. Yin, Y. Wang, Y. Wang, Y. Yang, and B. Ni, "Data-driven design of observers and its applications," in *Proceedings of the 18th IFAC World Congress*, Milano, Italy, 2011.

[23] S. Ding, P. Zhang, E. Ding, P. Engel, and W. Gui, "A survey of the application of basic data-driven and model-based methods in process monitoring and fault diagnosis," in *Proceedings of the 18th IFAC World Congress*, Milano, Italy, 2011.

[24] L. Chiang, E. Russell, and R. Braatz, *Fault Detection and Diagnosis in Industrial Systems*, Springer, London, UK, 2001.

[25] P. Ioannou and J. Sun, *Robust Adaptive Control*, Prentice Hall, 1996.

[26] G. Tao, *Adaptive Control Design and Analysis*, Wiley-Interscience, Hoboken, NJ, USA, 2003.

[27] K. Astrom and B. Wittenmark, *Adaptive Control*, Addison-Wesley, 1995.

[28] B. W. Silverman, *Density Estimation for Statistics and Data Analysis*, Chapman & Hall, London, UK, 1986.

[29] E. Martin and A. Morris, "Non-parametric confidence bounds for process performance monitoring charts," *Journal of Process Control*, vol. 6, no. 6, pp. 349–358, 1996.

[30] X. Zhang, M. Polycarpou, and T. Parisini, "Design and analysis of fault isolation scheme for a class of uncertain nonlinear systems," *Annual Reviews in Control*, vol. 32, pp. 107–121, 2008.

Hindawi Publishing Corporation
Mathematical Problems in Engineering
Volume 2012, Article ID 636878, 20 pages
doi:10.1155/2012/636878

Research Article

Discrete-Time Multioverlapping Controller Design for Structural Vibration Control of Tall Buildings under Seismic Excitation

Francisco Palacios-Quiñonero,[1] Josep Rubió-Massegú,[1] Josep M. Rossell,[1] and Hamid Reza Karimi[2]

[1] *Departament de Matemàtica Aplicada III, Universitat Politècnica de Catalunya (UPC), Avinguda Bases de Manresa 61-73, 08242 Manresa, Barcelona, Spain*
[2] *Department of Engineering, Faculty of Engineering and Science, University of Agder (UiA), 4898 Grimstad, Norway*

Correspondence should be addressed to Francisco Palacios-Quiñonero, francisco.palacios@upc.edu

Received 22 June 2012; Revised 9 September 2012; Accepted 10 September 2012

Academic Editor: Jun Hu

In this paper, a computationally effective strategy to obtain multioverlapping controllers via the Inclusion Principle is applied to design discrete-time state-feedback multioverlapping LQR controllers for seismic protection of tall buildings. To compute the corresponding control actions, the proposed semidecentralized controllers only require state information from neighboring stories. This particular configuration of information exchange allows introducing a dramatic reduction in the transmission range required for a wireless implementation of the communication system. To investigate the behavior of the proposed semidecentralized multioverlapping controllers, a proper simulation model has been designed. This model includes semiactive actuation devices with limited force capacity, control sampling times consistent with the communication latency, time-delayed state information, and communication failures. The performance of the proposed multioverlapping controllers has been assessed through numerical simulations of the seismic response of a 20-story building with positive results.

1. Introduction

Over the last decades, problems of ever increasing complexity have been considered in the field of Structural Vibration Control (SVC). Current SVC systems for seismic protection of tall buildings can involve a large number of sensors and actuation devices and a wide and sophisticated communication network [1–3]. Semidecentralized control strategies, which can operate using only state information from neighboring stories, are especially relevant for

wireless implementations of the communication system. Semidecentralized state-feedback LQR controllers were proposed by Wang and Lynch in [4], and the study was extended to state-feedback H_∞ controllers by Wang et al. in [5]. The numerical and experimental results obtained in these works clearly indicate that the proposed semidecentralized control strategies are specially suitable for SVC of tall buildings with wireless communications. It should be highlighted, however, that important computational difficulties can arise when applying these control design strategies to large buildings. The LQR controller design presented in [4] uses a variant of the heuristic iterative procedure proposed by Lunze in [6], and the H_∞ controller design in [5] is based on a Linear Matrix Inequality formulation (LMI). For large-dimensional problems, a great computational effort is required by the iterative procedure used in the LQR design. Analogously, solving large-dimensional convex optimization problems with LMI constraints is also a costly computational task.

In this context, the design of semidecentralized controllers using multioverlapping decompositions based on the *Inclusion Principle* (IP) is a very interesting option [7–12]. Broadly speaking, the IP allows decomposing the original large-dimensional problem into a set of low-dimensional decoupled problems. This decomposition takes advantage of the particular structure of the original system and can help to significantly reduce the computational effort. Examples of successful applications of the IP to SVC can be found in [13–15]. Recently, an effective computational strategy to design semidecentralized multioverlapping controllers based on a sequential application of the IP was presented by Palacios-Quiñonero et al. in [16]. In that work, semidecentralized multioverlapping LQR controllers are designed for seismic protection of a four-story building with positive results. However, it has to be noted that all these applications of the IP to SVC have been conducted using small buildings, continuous-time models, and assuming highly idealized conditions, such as active force actuators with unrestricted force capacity and communication systems with no failures nor delays.

The main contribution of the present paper is to present a large-scale application of the IP to the design of semidecentralized controllers for SVC, paying special attention to some aspects of practical relevance. More specifically, the computational strategy proposed in [16] is applied to design discrete-time state-feedback multioverlapping LQR controllers to mitigate the seismic response of a 20-story building. Moreover, to gain a meaningful insight into the behavior of the proposed multioverlapping controllers, the models used in the numerical simulations include some factors of practical relevance such as control sampling rates, realistic implementation of the control actions, time-delayed state information, and communication latency and failures. One of the main difficulties encountered when applying the IP to discrete-time controller design is that the natural structure of the continuous-time model is lost in the discretization process. To overcome this difficulty, the discretization process has been carried out on the expanded decoupled subsystems. The results obtained in the numerical simulations confirm the excellent characteristics of the proposed semidecentralized multioverlapping controllers for SVC of large buildings.

The organization of the paper is as follows: In Section 2, a detailed derivation of the continuous-time state-space model for an n-story building is presented. Section 3 begins with a summary discussion on the design of discrete-time state-feedback centralized LQR controllers. Next, the main ideas involved in the design of discrete-time state-feedback multioverlapping LQR controllers are briefly presented. In Section 4, three mathematical models used to conduct the numerical simulations of the building seismic response are presented: (i) *Basic building model*, which consists in a discrete-time approximation of the continuous-time state-space model with a small sampling time and no control action.

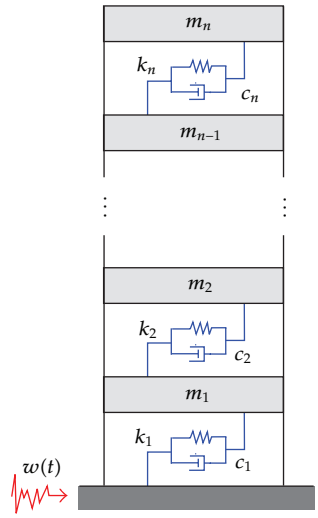

Figure 1: Building lumped-mass model.

(ii) *Centralized control model*, which implements the discrete-time centralized LQR controller with perfect state knowledge, small sampling time, and ideal semiactive force actuators with limited force capacity. (iii) *Multioverlapping control model*. This case implements a discrete-time multioverlapping controller considering semiactive actuation devices with limited force capacity, a control sampling time consistent with the communication latency, time-delayed state information, and communication failures. Finally, in Section 5, the control design methodology presented in Section 3 and the simulation models introduced in Section 4 are applied to a particular 20-story building to assess the performance of the proposed multioverlapping controllers.

2. Continuous-Time Building Model

Let us consider the n-story building schematically displayed in Figure 1, which is modeled as a lumped-mass planar system with displacements in the direction of the ground motion. The building motion can be described by the second-order differential equation:

$$M\ddot{q}(t) + C\dot{q}(t) + Kq(t) = T_u u(t) + T_\omega \omega(t), \tag{2.1}$$

where

$$q(t) = \left[q_1(t), \ldots, q_n(t)\right]^T \tag{2.2}$$

is the vector of story displacements with respect to the ground, and $q_i(t)$ represents the displacement of the ith story. M, C, K are the *mass*, *damping*, and *stiffness* matrices, respectively. The vector of control actions is

$$u(t) = \left[u_1(t), \ldots, u_n(t)\right]^T, \tag{2.3}$$

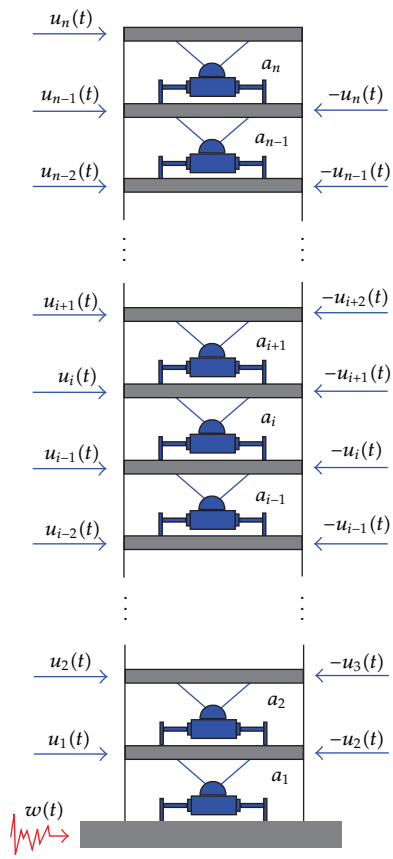

Figure 2: Actuation scheme.

where $u_i(t)$ represents the control force exerted by the actuation device a_i (see Figure 2), and T_u is the control location matrix. The seismic ground acceleration is $\omega(t)$, and T_ω denotes the disturbance input matrix. The mass and stiffness matrices have the following structures:

$$M = \begin{bmatrix} m_1 & & & \\ & \cdots & & \\ & & \cdots & \\ & & & m_n \end{bmatrix}, \tag{2.4}$$

$$K = \begin{bmatrix} k_1 + k_2 & -k_2 & & & & \\ -k_2 & k_2 + k_3 & -k_3 & & & \\ & \cdots & \cdots & \cdots & & \\ & & \cdots & \cdots & \cdots & \\ & & & -k_{n-1} & k_{n-1} + k_n & -k_n \\ & & & & -k_n & k_n \end{bmatrix}, \tag{2.5}$$

where m_i and k_i represent, respectively, the mass and stiffness of the ith story. When the values of the story damping coefficients c_i, $1 \leq i \leq n$, are known, a damping matrix C with

the same structure as K can be obtained by replacing k_i by c_i in (2.5). Alternatively, a tridiagonal damping matrix in the form

$$C = \alpha_0 M + \alpha_1 K \tag{2.6}$$

can be computed following the *Rayleigh damping* approach by setting the damping ratio values for two selected natural frequencies [17]. For the actuation system schematically depicted in Figure 2, the control location matrix has dimensions $n \times n$ and the following structure:

$$T_u = \begin{cases} [T_u]_{i,i} = 1, & \text{for } 1 \le i \le n, \\ [T_u]_{i,i+1} = -1, & \text{for } 1 \le i < n, \\ [T_u]_{i,j} = 0, & \text{otherwise}, \end{cases} \tag{2.7}$$

where $[T_u]_{i,j}$ denotes the element in the ith row and jth column of T_u. Finally, the disturbance input matrix is

$$T_w = -M[1]_{n\times 1}, \tag{2.8}$$

where $[1]_{n\times 1}$ is a column vector of dimension n with all its entries equal to 1.

Now, we take the state vector

$$x_I(t) = \begin{bmatrix} q(t) \\ \dot{q}(t) \end{bmatrix} \tag{2.9}$$

and derive a first-order state-space model

$$S_I : \dot{x}_I(t) = A_I x_I(t) + B_I u(t) + E_I \omega(t). \tag{2.10}$$

The state, control, and disturbance input matrices are, respectively,

$$A_I = \begin{bmatrix} [0]_{n\times n} & I_n \\ -M^{-1}K & -M^{-1}C \end{bmatrix}, \qquad B_I = \begin{bmatrix} [0]_{n\times n} \\ M^{-1}T_u \end{bmatrix}, \qquad E_I = \begin{bmatrix} [0]_{n\times 1} \\ -[1]_{n\times 1} \end{bmatrix}, \tag{2.11}$$

where $[0]_{r\times s}$ represents a zero matrix of dimensions $r \times s$, and I_n is the identity matrix of dimension n. Next, we consider a new state vector

$$x(t) = [x_1(t), \ldots, x_{2n}(t)]^T, \tag{2.12}$$

which groups together the interstory drifts and interstory velocities in increasing order

$$x(t) = \begin{cases} x_1(t) = q_1(t), \\ x_2(t) = \dot{q}_1(t), \\ x_{2i-1}(t) = q_i(t) - q_{i-1}(t), & \text{for } 1 < i \leq n, \\ x_{2i}(t) = \dot{q}_i(t) - \dot{q}_{i-1}(t), & \text{for } 1 < i \leq n. \end{cases} \tag{2.13}$$

Using the change of basis

$$x(t) = P x_I(t), \tag{2.14}$$

defined by the $2n \times 2n$ matrix

$$P = \begin{cases} p_{1,1} = 1, \ p_{2,n+1} = 1, \\ p_{2i-1,i-1} = -1, \ p_{2i-1,i} = 1, & \text{for } 1 < i \leq n, \\ p_{2i,n+i-1} = -1, \ p_{2i,n+i} = 1, & \text{for } 1 < i \leq n, \\ p_{i,j} = 0, & \text{otherwise}, \end{cases} \tag{2.15}$$

we obtain the new state space model:

$$S : \dot{x}(t) = Ax(t) + Bu(t) + E\omega(t), \tag{2.16}$$

where

$$A = PA_I P^{-1}, \qquad B = PB_I, \qquad E = PE_I. \tag{2.17}$$

In this work, we restrict our attention to the interstory drifts as output variables. The output vector can then be obtained as

$$y(t) = \left[y_1(t), \ldots, y_n(t)\right]^T = C_y x(t), \tag{2.18}$$

where C_y is a matrix of dimensions $n \times 2n$ with the following structure:

$$C_y = \begin{cases} \left[C_y\right]_{i,2i-1} = 1, & \text{for } 1 \leq i \leq n, \\ \left[C_y\right]_{i,j} = 0, & \text{otherwise}. \end{cases} \tag{2.19}$$

3. Control Design

To design a discrete-time centralized state-feedback LQR controller for the n-story building model presented in the previous section, we begin by considering the continuous-time system:

$$S_c : \dot{x}(t) = Ax(t) + Bu(t), \tag{3.1}$$

obtained from (2.16) by removing the disturbance term $E\omega(t)$. The discrete-time system corresponding to the zero-hold approximation of (3.1) with sampling time τ is

$$\{S_c\}_\tau : x[k+1] = A_\tau x[k] + B_\tau u[k], \tag{3.2}$$

where

$$A_\tau = e^{A\tau}, \qquad B_\tau = \int_0^\tau e^{At} B\, dt. \tag{3.3}$$

Next, we consider the discrete-time state-feedback controller:

$$u[k] = -G_\tau x[k] \tag{3.4}$$

and the quadratic index:

$$J(x,u) = \sum_{k=0}^{k=\infty} x[k]^T Q x[k] + u[k]^T R u[k], \tag{3.5}$$

where Q is a symmetric positive semidefinite matrix, and R is a symmetric positive definite matrix. The control gain matrix G_τ that minimizes (3.5) under constraints (3.2) and (3.4) can be computed as

$$G_\tau = \left(R + B_\tau^T P B_\tau\right)^{-1} B_\tau^T P A_\tau, \tag{3.6}$$

where P is the solution of the discrete-time Riccati equation:

$$A_\tau^T P A_\tau - P + Q - A_\tau^T P B_\tau \left(R + B_\tau^T P B_\tau\right)^{-1} B_\tau^T P A_\tau = 0. \tag{3.7}$$

To design a multioverlapping controller that is able to compute the control actions $u_i[k]$ using only state information corresponding to neighboring stories, we consider the n-story building decomposed into a sequence of $n-1$ two-story overlapped subsystems

$$S^{(i)} = [s_i, s_{i+1}], \quad 1 \le i \le n-1, \tag{3.8}$$

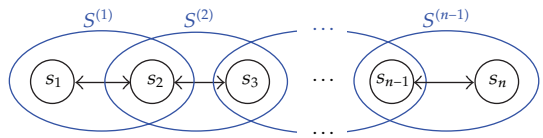

Figure 3: Decomposition in two-story overlapping subsystems.

where s_i represents the ith story. This overlapping decomposition is schematically depicted in Figure 3. Following the sequential multioverlapping decomposition strategy proposed in [16], the initial continuous-time system (3.1) can be conveniently expanded to form a new continuous-time system:

$$\widetilde{S} : \dot{\widetilde{x}}(t) = \widetilde{A}\widetilde{x}(t) + \widetilde{B}\widetilde{u}(t), \tag{3.9}$$

where the state matrix $\widetilde{A}$ and the control input matrix $\widetilde{B}$ are block diagonal. The expanded system $\widetilde{S}$ can then be decomposed into a sequence of decoupled continuous-time subsystems:

$$\widetilde{S}^{(i)} : \dot{\widetilde{x}}^{(i)}(t) = \widetilde{A}^{(i)}\widetilde{x}^{(i)}(t) + \widetilde{B}^{(i)}\widetilde{u}^{(i)}(t), \quad 1 \le i \le n-1. \tag{3.10}$$

For the continuous-time subsystems $\widetilde{S}^{(i)}$, we compute discrete-time zero-hold approximations with sampling time $\widehat{\tau}$:

$$\left\{\widetilde{S}^{(i)}\right\}_{\widehat{\tau}} : \widetilde{x}^{(i)}[k+1] = \widetilde{A}^{(i)}_{\widehat{\tau}}\widetilde{x}^{(i)}[k] + \widetilde{B}^{(i)}_{\widehat{\tau}}\widetilde{u}^{(i)}[k], \quad 1 \le i \le n-1, \tag{3.11}$$

where

$$\widetilde{A}^{(i)}_{\widehat{\tau}} = e^{\widetilde{A}^{(i)}\widehat{\tau}}, \qquad \widetilde{B}^{(i)}_{\widehat{\tau}} = \int_0^{\widehat{\tau}} e^{\widetilde{A}^{(i)}t}\ \widetilde{B}^{(i)}\ dt \tag{3.12}$$

and consider the local quadratic indexes:

$$\widetilde{J}^{(i)}\left(\widetilde{x}^{(i)}, \widetilde{u}^{(i)}\right) = \sum_{k=0}^{k=\infty}\left\{\widetilde{x}^{(i)}[k]\right\}^T Q^{(i)}\widetilde{x}^{(i)}[k] + \left\{\widetilde{u}^{(i)}[k]\right\}^T R^{(i)}\widetilde{u}^{(i)}[k], \quad 1 \le i \le n-1, \tag{3.13}$$

to compute local discrete-time LQR controllers

$$\widetilde{u}^{(i)}[k] = -\widetilde{G}^{(i)}_{\widehat{\tau}}\widetilde{x}^{(i)}[k], \quad 1 \le i \le n-1, \tag{3.14}$$

which minimize the indexes (3.13) under constraints (3.11) and (3.14). Finally, the sequence of expanded local control matrices $\widetilde{G}_{\widehat{\tau}}^{(i)}$ is contracted back to a control gain matrix $\widehat{G}_{\widehat{\tau}}$ in order to define a discrete-time multioverlapping controller:

$$\widehat{u}[k] = -\widehat{G}_{\widehat{\tau}} x[k] \tag{3.15}$$

for the original discrete-time system (3.2).

Remark 3.1. The expansion-contraction procedure associated to the design of multioverlapping controllers for large buildings is only outlined in this section. For clarity and simplicity, a detailed account of this procedure has not been included in the paper. However, a complete presentation of this background material together with some practical applications to SVC of small buildings can be found in [15, 16].

Remark 3.2. The expanded block-diagonal system (3.9) can only be computed when the matrices of the initial state-space system have a suitable zero-nonzero block structure. For the building model (2.1), the initial state-space system (3.1) has a proper structure. However, this structure is lost in the discretization process and the expansion-decoupling process can no longer be applied to the discrete-time state-space system (3.2). To overcome this difficulty, the expansion-decoupling process is first completed for the continuous-time system and, after that, the discretization process is carried out on the continuous-time expanded decoupled subsystems (3.10) to obtain the discrete-time expanded decoupled subsystems (3.11).

Remark 3.3. It should be noted that the control gain matrix $G_\tau = [(g_\tau)_{i,j}]$ given in (3.6) is a full matrix of size $n \times 2n$, and the full state is required to compute the control action for the actuation device a_i:

$$u_i[k] = \sum_{j=1}^{j=2n} (g_\tau)_{i,j} x_j[k], \quad 1 \le i \le n. \tag{3.16}$$

In contrast, the multioverlapping control matrix $\widehat{G}_{\widehat{\tau}} = [(\widehat{g}_{\widehat{\tau}})_{i,j}]$ has a block-tridiagonal structure and only requires a reduced number of 4–6 states to compute the control action for each actuation device. More specifically, we have

$$\widehat{u}[k] = \begin{cases} \widehat{u}_1[k] = \displaystyle\sum_{j=1}^{j=4} (\widehat{g}_{\widehat{\tau}})_{1,j} x_j[k], \\ \widehat{u}_i[k] = \displaystyle\sum_{j=2i-3}^{j=2i+2} (\widehat{g}_{\widehat{\tau}})_{i,j} x_j[k], \quad \text{for } 1 < i < n, \\ \widehat{u}_n[k] = \displaystyle\sum_{j=2n-3}^{j=2n} (\widehat{g}_{\widehat{\tau}})_{n,j} x_j[k]. \end{cases} \tag{3.17}$$

Remark 3.4. For clarity and simplicity, the controllers presented in this section have been computed following an LQR approach. However, it has to be highlighted that other control strategies are also possible. For example, an application of the IP to the design of semi-decentralized static output-feedback controllers for SVC can be found in [14].

4. Simulation Models

One of the main objectives of the present work is to gain a meaningful insight into the behavior of semidecentralized multioverlapping controllers through numerical simulations. To this end, the simulation models have to include some relevant factors such as sampling rates, realistic implementation of the control actions, time-delayed state information, and communication latency and failures. Trying to achieve a proper balance between simplicity and accuracy, we have considered a simulation framework formed by three different models: (i) *Basic building model*, which consists in a discrete-time approximation of the continuous-time state-space model (3.1) with a small basic sampling time τ and no control action. (ii) *Centralized control model*, which implements the discrete-time LQR controller given in (3.4) with perfect state knowledge and the basic sampling time τ. The actuation devices, however, are assumed to be ideal semiactive force actuators with limited force capacity. (iii) *Multioverlapping control model*. This case implements the discrete-time multioverlapping controller given in (3.15) considering semiactive actuation devices with limited force capacity, a control sampling time $\widehat{\tau} > \tau$ consistent with the communication latency, time-delayed state information, and communication failures. In all the cases, the interstory drifts are taken as output variables.

The basic building model is:

$$\mathcal{M}_\tau : \begin{cases} x[k+1] = A_\tau x[k] + E_\tau \omega_\tau[k], \\ y[k] = C_y x[k], \end{cases} \tag{4.1}$$

where A_τ is the discrete-time state matrix in (3.3); E_τ is the discrete-time disturbance input matrix, which can be computed as

$$E_\tau = \int_0^\tau e^{At} E \, dt, \tag{4.2}$$

with A and E representing, respectively, the state and disturbance input continuous-time matrices; and $\omega_\tau[k] = \omega(k\tau)$ is the sampled disturbance. The vector of interstory drifts is computed with the output matrix C_y given in (2.19). A good approximation of the uncontrolled seismic response of the building can be obtained using the basic building model $\mathcal{M}_\tau$ with a small sampling time τ.

The centralized control model is:

$$\overline{\mathcal{M}}_\tau : \begin{cases} u[k] = -G_\tau x[k], \\ x[k+1] = A_\tau x[k] + B_\tau \sigma(u[k]) + E_\tau \omega_\tau[k], \\ y[k] = C_y x[k], \end{cases} \tag{4.3}$$

where the sampling time τ, the matrices A_τ, E_τ, and C_y, and the sampled disturbance $\omega_\tau[k]$ are the same as those used in (4.1); and B_τ is the discrete-time input-control matrix defined in (3.3). The vector of control actions

$$u[k] = [u_1[k], \ldots, u_n[k]]^T, \tag{4.4}$$

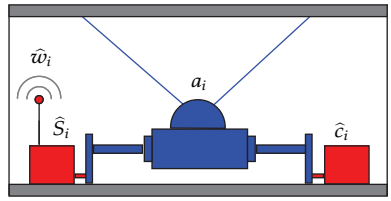

Figure 4: Actuation-communication system for the multioverlapping control model.

is computed using the discrete-time centralized control gain matrix G_τ given in (3.6), and the vector of control forces is

$$\sigma(u[k]) = [\sigma(u_1[k]), \ldots, \sigma(u_n[k])]^T. \tag{4.5}$$

In this section, the actuation devices a_i are modeled as ideal semiactive force actuators with maximum actuation force $[f_{\max}]_i$. For a given control action $u_i[k]$, the actual control force exerted by the actuation device a_i is

$$\sigma(u_i[k]) = \begin{cases} u_i[k] & \text{if } u_i[k] \cdot v_i[k] < 0, \text{ and } |u_i[k]| \leq [f_{\max}]_i \\ \operatorname{sgn}(u_i[k]) \cdot [f_{\max}]_i & \text{if } u_i[k] \cdot v_i[k] < 0, \text{ and } |u_i[k]| > [f_{\max}]_i \\ 0 & \text{if } u_i[k] \cdot v_i[k] \geq 0, \end{cases} \tag{4.6}$$

where $v_i[k]$ is the corresponding interstory velocity, and $\operatorname{sgn}(x) = x/|x|$ is the *signum function*. In the centralized control model, we assume an ideal communication system, which can provide a perfect knowledge of the full state vector $x[k]$. This model is used as a reference in the performance assessment of the multioverlapping controller.

In the multioverlapping control model, we consider the actuation-communication system schematically depicted in Figure 4, consisting in an actuation device a_i, a sensor unit $\widehat{s}_i$, a local control unit $\widehat{c}_i$, and a wireless communication unit $\widehat{w}_i$. The actuation device a_i produces the semiactive implementation of the control actions defined in (4.6). The sensor unit $\widehat{s}_i$ is an ideal sensor that provides an exact measurement of the local state

$$\widehat{x}_i[k] = \begin{bmatrix} y_i[k] \\ v_i[k] \end{bmatrix}, \tag{4.7}$$

where $y_i[k]$ and $v_i[k]$ denote the local interstory drift and velocity, respectively. To model the operation of the local control unit, we introduce the controller sampling tim

$$\widehat{\tau} = \widehat{r}\tau, \quad \widehat{r} > 1, \tag{4.8}$$

where τ is the basic sampling time used in (4.1) and (4.3), and $\widehat{r}$ can be understood as the maximum number of sampling steps that can be spent by $\widehat{c}_i$ to collect state information from

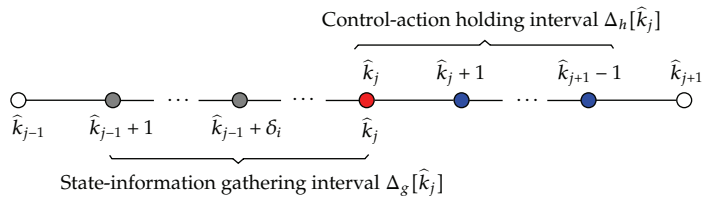

Figure 5: Time intervals for state information gathering and control action holding.

neighboring stories through the communication unit $\widehat{w}_i$. We also consider the update-control times

$$\widehat{k}_j = j\widehat{r}, \quad j \geq 1, \tag{4.9}$$

and define the interval of state-information gathering

$$\Delta_g\left[\widehat{k}_j\right] = \left[\widehat{k}_{j-1} + 1, \ldots, \widehat{k}_j\right], \tag{4.10}$$

and the interval of control-action holding

$$\Delta_h\left[\widehat{k}_j\right] = \left[\widehat{k}_j, \ldots, \widehat{k}_{j+1} - 1\right], \tag{4.11}$$

which are schematically represented in Figure 5. The operation of the local control unit $\widehat{c}_i$ has been modeled in accordance with the following set of basic principles:

(P.1) The local control action $\widehat{u}_i[k]$ is updated at the sampling times $k = \widehat{k}_j$, $j \geq 1$.

(P.2) The local controller unit $\widehat{c}_i$ has direct access to the sensing unit $\widehat{s}_i$; consequently the local state $\widehat{x}_i[\widehat{k}_j]$ is assumed to be always available.

(P.3) The state information of neighboring stories obtained through the wireless communication unit $\widehat{w}_i$ has the form $\widehat{x}_{i'}[k - \delta_{i'}[\widehat{k}_j]]$, where $i' = i \pm 1$ and the time delay satisfies $0 \leq \delta_{i'}[\widehat{k}_j] < \widehat{r}$.

(P.4) For a given time interval I with length $\widehat{\tau}$, the events $E_{i,i'}(I, \widehat{\tau}) = [\widehat{c}_{\mathrm{i}}$ obtains the neighboring state $\widehat{x}_{\mathrm{i}'}$ in the time interval I of length $\widehat{\tau}]$ are independent random events with common probability

$$\mathrm{Prob}[E_{i,i'}(I, \widehat{\tau})] = p_{\widehat{\tau}}. \tag{4.12}$$

(P.5) If I, I' are non-overlapping time intervals with respective lengths $\widehat{\tau}$ and $\widehat{\tau}'$, then $E_{i,i'}(I, \widehat{\tau})$ and $E_{i,i'}(I', \widehat{\tau}')$ are independent random events.

(P.6) Through the time interval $\Delta_g[\widehat{k}_j]$, the local control unit $\widehat{c}_i$ tries to collect the state information required to compute the control action. If this state information is

successfully acquired, the flag variable $\phi_i[\widehat{k}_j]$ is set to 1 and the new control action $\widehat{u}_i[\widehat{k}_j]$ is computed; otherwise, the flag variable $\phi_i[\widehat{k}_j]$ and the control action $\widehat{u}_i[\widehat{k}_j]$ are both set to 0.

(P.7) The control action computed at the sampling time $k = \widehat{k}_j$ is held through the time interval $\Delta_h[\widehat{k}_j]$.

According to the previous principles, the vector of control actions

$$\widehat{u}[k] = [\widehat{u}_1[k], \ldots, \widehat{u}_n[k]]^T \tag{4.13}$$

can be computed by setting the initial value

$$\widehat{u}[0] = [0]_{n\times 1}, \tag{4.14}$$

and, for $k > 0$, using the expression

$$\widehat{u}[k] = \begin{cases} -F_\phi[k]\left(D_{\widehat{G}_{\widehat{\tau}}} x[k] + L_{\widehat{G}_{\widehat{\tau}}} x[k-\delta[k]]\right) & \text{if } \mod(k,\widehat{r}) = 0, \\ \widehat{u}[k-1], & \text{otherwise}, \end{cases} \tag{4.15}$$

where $\mathrm{mod}(k,\widehat{r})$ represents the integer remainder after division, $F_\phi[k]$ is the diagonal matrix

$$F_\phi[k] = \begin{bmatrix} \phi_1[k] & & \\ & \ddots & \\ & & \phi_n[k] \end{bmatrix}, \tag{4.16}$$

$D_{\widehat{G}_{\widehat{\tau}}}$ is the block-diagonal matrix

$$D_{\widehat{G}_{\widehat{\tau}}} = \begin{bmatrix} \left[\widehat{G}_{\widehat{\tau}}\right]_{1,1} & & \\ & \ddots & \\ & & \left[\widehat{G}_{\widehat{\tau}}\right]_{n,n} \end{bmatrix} \tag{4.17}$$

formed by the diagonal blocks of $\widehat{G}_{\widehat{\tau}}$

$$\left[\widehat{G}_{\widehat{\tau}}\right]_{i,i} = \left[\{\widehat{g}_{\widehat{\tau}}\}_{i,2i-1}, \{\widehat{g}_{\widehat{\tau}}\}_{i,2i}\right], \quad 1 \le i \le n, \tag{4.18}$$

and the matrix

$$L_{\widehat{G}_{\widehat{\tau}}} = \widehat{G}_{\widehat{\tau}} - D_{\widehat{G}_{\widehat{\tau}}} \tag{4.19}$$

contains the out-of-diagonal blocks of the block-tridiagonal multioverlapping control matrix $\widehat{G}_{\widehat{\tau}}$. The notation $x[k-\delta[k]]$ represents the delayed state

$$x[k-\delta[k]] = \begin{bmatrix} \widehat{x}_1[k-\delta_1[k]] \\ \vdots \\ \widehat{x}_n[k-\delta_n[k]] \end{bmatrix}, \tag{4.20}$$

where $\delta_i[k]$ is the delay in the local state $\widehat{x}_i$.

The multioverlapping control model can now be obtained by completing (4.14) and (4.15) with the state and output equations

$$\begin{gathered} x[k+1] = A_\tau x[k] + B_\tau \sigma(\widehat{u}[k]) + E_\tau \omega_\tau[k], \\ y[k] = C_y x[k]. \end{gathered} \tag{4.21}$$

It should be noted that expressions (4.16) and (4.20) are only evaluated at the update-control times $\widehat{k}_j = j\widehat{r}$. Moreover, according to (P.1), (P.4) and (P.6), the information-state flag variables $\phi_i[\widehat{k}_j]$ are independent random variables with Bernoulli distributions $\mathcal{B}(p)$. In particular $\phi_1[\widehat{k}_j]$ and $\phi_n[\widehat{k}_j]$ have a Bernoulli distribution $\mathcal{B}(p_{\widehat{\tau}})$, and $\phi_i[\widehat{k}_j]$ has distribution $\mathcal{B}(p_{\widehat{\tau}}^2)$ for $1 < i < n$. Finally, it should also be noted that the probability of gathering the neighboring state information $\widehat{x}_{i'}$ by the controller unit $\widehat{c}_i$ in a time interval I' of length $2\widehat{\tau}$ is

$$\operatorname{Prob}\left[E_{i,i'}(I', 2\widehat{\tau})\right] = 2p_{\widehat{\tau}} - p_{\widehat{\tau}}^2. \tag{4.22}$$

This formula can be easily obtained by writing the time interval I' as union of two non-overlapping intervals $I' = I'_1 \cup I'_2$ of length $\widehat{\tau}$. According to (P.5), $E_{i,i'}(I'_1, \widehat{\tau})$ and $E_{i,i'}(I'_2, \widehat{\tau})$ are independent random events, and the probability of failing to acquire the state $\widehat{x}_{i'}$ in the whole interval I' is $(1-p_{\widehat{\tau}})^2$. Analogously, it can be shown that the corresponding probability for a time interval I'' of length $(1/2)\widehat{\tau}$ is

$$\operatorname{Prob}\left[E_{i,i'}\left(I'', \frac{1}{2}\widehat{\tau}\right)\right] = 1 - \sqrt{1-p_{\widehat{\tau}}}. \tag{4.23}$$

5. Numerical Simulations

In this section, the behavior of discrete-time multioverlapping LQR controllers is investigated through numerical simulations of the seismic response of a 20-story building. The parameter values for this particular building are collected in Table 1 and are similar to those used in [5]. The damping matrix has been computed as a Rayleigh damping matrix by setting a 5% of damping ratio for the 1st and 18th natural frequencies. The actuation system a_i implemented between the $(i-1)$th and ith stories (see Figure 2) is assumed to be formed by a number of identical actuation devices that work coordinately as a single device. The force saturation level of a single actuation device has been taken as 1.2×10^6 N. The total number of actuation devices and the maximum actuation force for the actuation systems a_i, $1 \leq i \leq n$, is also presented in Table 1.

Table 1: Particular parameter values for the 20-story building.

	Story					
	1–5	6–11	12–14	15–17	18-19	20
Mass ($\times 10^6$ Kg)	1.10	1.10	1.10	1.10	1.10	1.10
Stiffness ($\times 10^6$ N/m)	8.62	5.54	4.54	2.91	2.56	1.72
Number of actuation devices	4	2	2	1	1	1
Max. actuation force ($\times 10^6$ N)	4.8	2.4	2.4	1.2	1.2	1.2
Natural damping	5%					

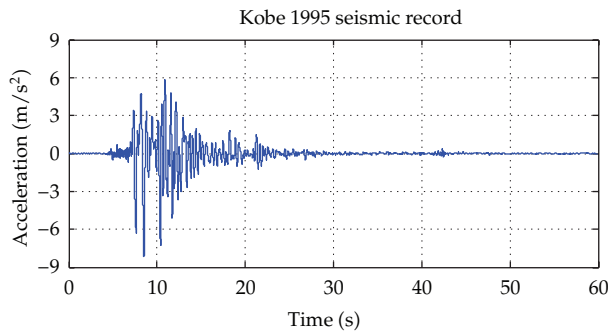

Figure 6: Full scale Kobe 1995 North-South seismic record.

For this 20-story building, three different discrete-time LQR controllers are designed: a centralized controller G_τ, which has been obtained using the basic sampling time $\tau = 10^{-3}$ s; and two multioverlapping controllers $\widehat{G}_{\widehat{\tau}}$ and $\widehat{G}_{\widehat{\tau}'}$, computed with sampling times $\widehat{\tau} = 40\ \tau$, and $\widehat{\tau}' = 20\ \tau$, respectively. The particular values of the weighting matrices in (3.5) used to design the centralized controller are $Q = I_{40}$ and $R = 10^{-17.5} \times I_{20}$. For the multioverlapping controllers, the weighting matrices in (3.13) used to compute the local expanded LQR controllers $\widetilde{G}^{(i)}_{\widehat{\tau}}$ and $\widetilde{G}^{(i)}_{\widehat{\tau}'}$, $1 \leq i < 20$, have been taken as $Q^{(i)} = I_4$ and $R^{(i)} = 10^{-17.5} \times I_2$, for $1 \leq i < 20$.

In the numerical simulations, the maximum absolute interstory drifts have been computed for different control configurations. The basic building model given in (4.1) with sampling time $\tau = 10^{-3}$ s has been used to compute the uncontrolled seismic response. The controlled response corresponding to the centralized controller G_τ has been obtained with the centralized control model presented in (4.3). Finally, the multioverlapping control model defined in (4.14), (4.15), and (4.21) has been used to compute the controlled response for the multioverlapping controllers $\widehat{G}_{\widehat{\tau}}$ and $\widehat{G}_{\widehat{\tau}'}$. In all the cases, the full scale 1995 Kobe North-South seismic record has been taken as ground acceleration (see Figure 6). This seismic record, obtained at the Kobe Japanese Meteorological Agency station during the Hyogoken-Nanbu earthquake of January 17, 1995, is a near-field record that presents large acceleration peaks which are extremely destructive to tall structures [18, 19]. In the multioverlapping control model, the reference value of $p_{\widehat{\tau}} = 0.95$ has been set for the probability of obtaining state information from neighboring stories in a time interval of length $\widehat{\tau} = 40$ ms. According to (4.23), for the multioverlapping controller $\widehat{G}_{\widehat{\tau}'}$ with control sampling time $\widehat{\tau}' = 20$ ms, the probability of successfully gathering state information from neighboring stories can be taken as $p_{\widehat{\tau}'} = 0.78$.

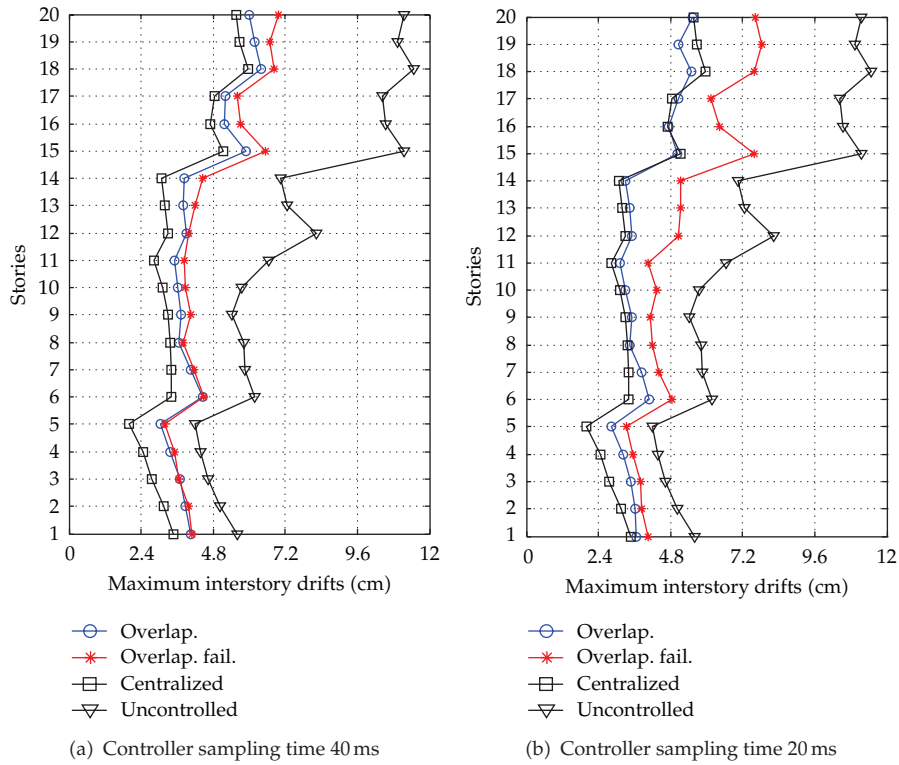

Figure 7: Maximum absolute interstory drifts for the 1995 Kobe North-South seismic record. Simulations with maximum state delay.

In Figure 7(a), the red line with asterisks (*Overlap. fail* in the legend) presents the maximum absolute interstory drifts corresponding to the multioverlapping controller $\widehat{G}_{\widehat{\tau}}$ with controller sampling time $\widehat{\tau} = 40$ ms, probability of successful communication $p_{\widehat{\tau}} = 0.95$, and state delay $\delta = 39$ ms. The blue line with circles (*Overlap.* in the legend), displays the values obtained with no communication failures, that is, with $p_{\widehat{\tau}} = 1$. The interstory drifts peak values corresponding to the multioverlapping controller $\widehat{G}_{\widehat{\tau}'}$ with controller sampling time $\widehat{\tau}' = 20$ ms, and state delay $\delta = 19$ ms are presented in Figure 7(b). Here, the red line with asterisks corresponds to the probability $p_{\widehat{\tau}'} = 0.78$, and the blue line with circles presents again the results for $p_{\widehat{\tau}'} = 1$. In both cases, the graphics corresponding to the uncontrolled response (black line with triangles), and the controlled response for the centralized controller G_{τ}, with controller sampling time $\tau = 1$ ms, with no communication failures nor delays (black line with squares) have been included as reference. In Figure 8, the red line with asterisks (*Over. delay* in the legend) displays the maximum absolute interstory drifts corresponding to the multioverlapping controller $\widehat{G}_{\widehat{\tau}}$ with $\widehat{\tau} = 40$ ms, $p_{\widehat{\tau}} = 0.95$, and state delay $\delta = 39$ ms, while the green line with circles (*Over. no delay* in the legend) presents the response obtained with null state delay.

The graphics in Figure 7(a) show the excellent performance of the proposed multi-overlapping controller for controller sampling times $\widehat{\tau}$ compatible with moderate values of communication latency and also compatible with moderate rates of communication failures. Moreover, the graphics in Figure 7(b) clearly illustrate the trade-off between the controller

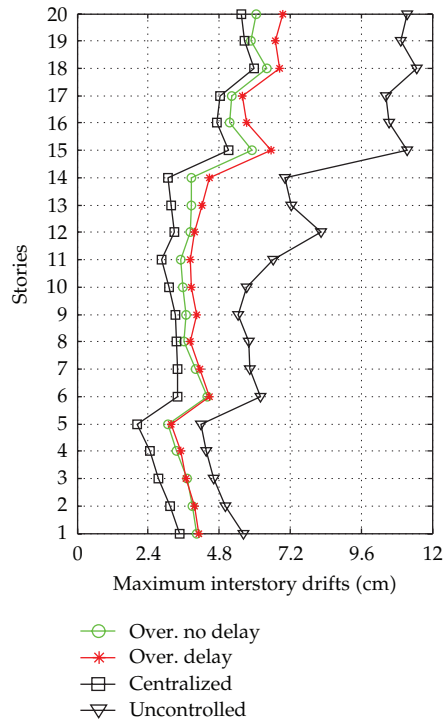

Figure 8: Maximum absolute interstory drifts for maximum and minimum state delays (controller sampling time 40 ms).

sampling time $\widehat{\tau}$ and the probability of successful communication $p_{\widehat{\tau}}$. Certainly, taking a smaller sampling time $\widehat{\tau}$ allows a more accurate implementation of the control actions; however, this also implies a reduction of the probability $p_{\widehat{\tau}}$ which, in the end, may result in an overall loss of performance.

Finally, the graphics in Figure 8 show the moderate influence of the state delay δ in the multioverlapping controller performance for reasonable values of the controller sampling time $\widehat{\tau}$.

Remark 5.1. It is worth to be mentioned that the behavior of the ideal discrete-time centralized controller G_τ is very similar to the behavior exhibited by an ideal continuous-time centralized LQR controller. As mentioned in Remark 3.3, full state information is required by centralized controllers and this fact makes them unsuitable for SVC of large buildings with wireless communication systems. A detailed discussion of this point can be found in [5].

Remark 5.2. The proposed semidecentralized controllers can operate using only state information from neighboring stories. This fact makes it possible for them to successfully collect the required state information in a relatively small time interval. As a side effect, state delays are also small and have no significant impact on the controller performance.

Remark 5.3. Force saturation is an important issue in SVC. For large seismic excitations, the required control actions frequently exceed the force capacity of the actuation devices. Consequently, force actuation constraints should be considered when studying the controllers

behavior. All the numerical simulations of the controlled responses presented in this paper have been conducted using the force saturation values displayed in Table 1.

6. Conclusions and Future Directions

In this paper, a computationally effective strategy has been used to design discrete-time state-feedback multioverlapping LQR controllers for seismic protection of tall buildings. This strategy, based on a sequential application of the Inclusion Principle, produces a block-tridiagonal control gain matrix that allows computing the corresponding control actions using only state information from neighboring stories. Due to this particular information exchange configuration of the multioverlapping controllers, the transmission range and the control sampling frequency in wireless implementations of the communication system can be dramatically improved. To investigate the behavior of the proposed semidecentralized multioverlapping controllers, a proper simulation model has been designed, which allows including semiactive actuation devices with limited force capacity, control sampling times consistent with the communication latency, time-delayed state information, and communication failures. To assess the performance of the proposed multioverlapping controllers, numerical simulations of the seismic response for a 20-story building model have been conducted with positive results.

For clarity and simplicity, the controllers presented in this paper have been designed following an LQR approach. In future works, further research effort should be addressed at exploring the effectiveness of the proposed control design strategy in more complex scenarios, which can involve issues of practical interest such as structural information constraints [20], actuator saturation [21], actuation and sensor failures [22], and limited frequency domain [23]. Other natural extensions of the present work should include a deeper treatment of some important practical aspects related to the communication system such as missing measurements [24–28], stochastic uncertainties [29], and stochastic nonlinearities [30–33].

Acknowledgments

This work has been partially supported by the Spanish Ministry of Economy and Competitiveness through the Grant DPI2011-25567-C02 and by the Norwegian Center of Offshore Wind Energy (NORCOWE) under Grant 193821/S60 from the Research Council of Norway (RCN).

References

[1] B. F. Spencer and S. Nagarajaiah, "State of the art of structural control," *Journal of Structural Engineering*, vol. 129, no. 7, pp. 845–856, 2003.

[2] R. A. Swartz and J. P. Lynch, "Strategic network utilization in a wireless structural control system for seismically excited structures," *Journal of Structural Engineering*, vol. 135, no. 5, pp. 597–608, 2009.

[3] H. Li and L. Huo, "Advances in structural control in civil engineering in China," *Mathematical Problems in Engineering*, vol. 2010, Article ID 936081, 23 pages, 2010.

[4] Y. Wang and J. Lynch, "Wireless sensing and decentralized control for civil structures: theory and implementation," Tech. Rep. 167, J. A. Blume Engineering Center, Department of Civil and Environmental Engineering, Stanford University, Stanford, Calif, USA, 2007.

[5] Y. Wang, J. P. Lynch, and K. H. Law, "Decentralized H_∞ controller design for large-scale civil structures," *Earthquake Engineering and Structural Dynamics*, vol. 38, no. 3, pp. 377–401, 2009.

[6] J. Lunze, *Feedback Control of Large-Scale Systems*, Prentice Hall, Upper Saddle River, NJ, USA, 1992.

[7] D. D. Šiljak, *Decentralized Control of Complex Systems*, vol. 184 of *Mathematics in Science and Engineering*, Academic Press, Boston, Mass, USA, 1991.

[8] L. Bakule, J. Rodellar, and J. M. Rossell, "Generalized selection of complementary matrices in the inclusion principle," *IEEE Transactions on Automatic Control*, vol. 45, no. 6, pp. 1237–1243, 2000.

[9] L. Bakule, J. Rodellar, and J. M. Rossell, "Structure of expansion-contraction matrices in the inclusion principle for dynamic systems," *SIAM Journal on Matrix Analysis and Applications*, vol. 21, no. 4, pp. 1136–1155, 2000.

[10] A. I. Zečević and D. D. Šiljak, "A decomposition-based control strategy for large, sparse dynamic systems," *Mathematical Problems in Engineering*, no. 1, pp. 33–48, 2005.

[11] X.-B. Chen and S. S. Stanković, "Decomposition and decentralized control of systems with multi-overlapping structure," *Automatica*, vol. 41, no. 10, pp. 1765–1772, 2005.

[12] A. I. Zečević and D. D. Šiljak, "Control of Complex Systems," *Structural Constraints and Uncertainty*, Springer, 2010.

[13] L. Bakule, F. Paulet-Crainiceanu, J. Rodellar, and J. M. Rossell, "Overlapping reliable control for a cable-stayed bridge benchmark," *IEEE Transactions on Control Systems Technology*, vol. 13, no. 4, pp. 663–669, 2005.

[14] J. M. Rossell, F. Palacios-Quiñonero, and J. Rodellar, "Semi-decentralized output feedback H_∞ control strategy for large building structures," in *Proceedings of the 5th World Conference on Structural Control and Monitoring*, Tokyo, Japan, 2010.

[15] F. Palacios-Quiñonero, J. M. Rossell, and H. R. Karimi, "Semi-decentralized strategies in structural vibration control," *Modeling Identification and Control*, vol. 32, no. 2, pp. 57–77, 2011.

[16] F. Palacios-Quiñonero, J. Rodellar, and J. M. Rossell, "Sequential design of multi-overlapping controllers for longitudinal multi-overlapping systems," *Applied Mathematics and Computation*, vol. 217, no. 3, pp. 1170–1183, 2010.

[17] A. K. Chopra, *Dynamics of Structures: Theory and Applications to Earthquake Engineering*, Prentice Hall, Upper Saddle River, NJ, USA, 3rd edition, 2007.

[18] Y. Ohtori, R. E. Christenson, B. F. Spencer, and S. J. Dyke, "Benchmark control problems for seismically excited nonlinear buildings," *Journal of Engineering Mechanics*, vol. 130, no. 4, pp. 366–385, 2004.

[19] C. T. Huang and S. S. Chen, "Near-field characteristics and engineering implications of the 1999 Chi-Chi earthquake," *Earthquake Engineering and Engineering Sysmology*, vol. 2, no. 1, pp. 23–41, 2000.

[20] J. Rubió-Massegú, F. Palacios-Quiñonero, and J. M. Rossell, "Decentralized static output-feedback H_∞ controller design for buildings under seismic excitation," *Earthquake Engineering and Structural Dynamics*, vol. 41, no. 7, pp. 1199–1205, 2012.

[21] H. Du and J. Lam, "Energy-to-peak performance controller design for building via static output feedback under consideration of actuator saturation," *Computers & Structures*, vol. 84, no. 31-32, pp. 2277–2290, 2006.

[22] W. Zhang, Y. Cheng, and H. Gao, "Energy-to-peak control for seismic-excited buildings with actuator faults and parameter uncertainties," *Journal of Sound and Vibration*, vol. 330, no. 4, pp. 581–602, 2011.

[23] Y. Chen, W. Zhan, and H. Gao, "Finite frequency H_∞ control for building under earthquake excitation," *Mechatronics*, vol. 20, no. 1, pp. 128–142, 2010.

[24] H. Dong, Z. Wang, and H. Gao, "H_∞ fuzzy control for systems with repeated scalar nonlinearities and random packet losses," *IEEE Transactions on Fuzzy Systems*, vol. 17, no. 2, pp. 440–450, 2009.

[25] B. Shen, Z. Wang, and Y. S. Hung, "Distributed H_∞ consensus filtering in sensor networks with multiple missing measurements: the finite-horizon case," *Automatica*, vol. 46, no. 10, pp. 1682–1688, 2010.

[26] H. Dong, Z. Wang, and H. Gao, "Distributed filtering for a class of time-varying systems over sensor networks with quantization errors and successive packet dropouts," *IEEE Transactions on Signal Processing*, vol. 60, no. 6, pp. 3164–3173, 2012.

[27] Z. Wang, B. Shen, H. Shu, and G. Wei, "Quantized H_∞ control for nonlinear stochastic time-delay systems with missing measurements," *IEEE Transactions on Automatic Control*, vol. 57, no. 6, pp. 1431–1444, 2012.

[28] Z. Wang, B. Shen, and X. Liu, "H_∞ filtering with randomly occurring sensor saturations and missing measurements," *Automatica*, vol. 48, no. 3, pp. 556–562, 2012.

[29] J. Hu, Z. Wang, H. Gao, and L. K. Stergioulas, "Robust sliding mode control for discrete stochastic systems with mixed time delays, randomly occurring uncertainties, and randomly occurring nonlinearities," *IEEE Transactions on Industrial Electronics*, vol. 59, no. 7, pp. 3008–3015, 2012.

[30] J. Hu, Z. Wang, Y. Niu, and L. K. Stergioulas, "H_∞ sliding mode observer design for a class of nonlinear discrete time-delay systems: a delay-fractioning approach," *International Journal of Robust and Nonlinear Control*, vol. 22, no. 16, pp. 1806–1826, 2012.

[31] J. Hu, Z. Wang, and H. Gao, "A delay fractioning approach to robust sliding mode control for discrete-time stochastic systems with randomly occurring non-linearities," *IMA Journal of Mathematical Control and Information*, vol. 28, no. 3, pp. 345–363, 2011.

[32] J. Hu, Z. Wang, H. Gao, and L. K. Stergioulas, "Robust H_∞ sliding mode control for discrete time-delay systems with stochastic nonlinearities," *Journal of the Franklin Institute*, vol. 349, no. 4, pp. 1459–1479, 2012.

[33] J. Hu, Z. Wang, H. Gao, and L. K. Stergioulas, "Probability-guaranteed H_∞ finite-horizon filtering for a class of nonlinear time-varying systems with sensor saturations," *Systems & Control Letters*, vol. 61, no. 4, pp. 477–484, 2012.

Hindawi Publishing Corporation
Mathematical Problems in Engineering
Volume 2012, Article ID 942910, 23 pages
doi:10.1155/2012/942910

Research Article

Structural Vibration Control for a Class of Connected Multistructure Mechanical Systems

Francisco Palacios-Quiñonero,[1] Josep M. Rossell,[1] Josep Rubió-Massegú,[1] and Hamid R. Karimi[2]

[1] *Departament de Matemàtica Aplicada III, Universitat Politècnica de Catalunya (UPC), Av. Bases de Manresa 61-73, Manresa 08242, Barcelona, Spain*
[2] *Department of Engineering, Faculty of Engineering and Science, University of Agder (UiA), 4898 Grimstad, Norway*

Correspondence should be addressed to Francisco Palacios-Quiñonero, francisco.palacios@upc.edu

Received 16 June 2012; Accepted 8 August 2012

Academic Editor: Zidong Wang

A mathematical model to compute the overall vibrational response of connected multistructure mechanical systems is presented. Using the proposed model, structural vibration control strategies for seismic protection of multibuilding systems can be efficiently designed. Particular attention is paid to the design of control configurations that combine passive interbuilding dampers with local feedback control systems implemented in the buildings. These hybrid active-passive control strategies possess the good properties of passive control systems and also have the high-performance characteristics of active control systems. Moreover, active-passive control configurations can be properly designed for multibuilding systems requiring different levels of seismic protection and are also remarkably robust against failures in the local feedback control systems. The application of the main ideas is illustrated by means of a three-building system, and numerical simulations are conducted to assess the performance of the proposed structural vibration control strategies.

1. Introduction

Over the last years, seismic protection of adjacent buildings has been attracting an increasing interest. For this kind of systems, the action of seismic excitations can produce interbuilding collisions (pounding), which can cause severe damage to the buildings structure and contents [1–5]. Consequently, structural vibration control (SVC) strategies for multibuilding systems must aim at mitigating not only the vibrational response of individual buildings, but also the negative interbuilding interactions.

The connected control method (CCM) is a SVC strategy for multibuilding systems that consists in linking adjacent buildings by coupling devices to provide appropriate reaction control forces. The application of the CCM using different types of passive [6–16], active [17–19], and semiactive [20–23] linking devices has been extensively investigated with positive results. Recently, more complex control configurations combining passive interbuilding dampers with local feedback control systems implemented in the buildings have been proposed [24, 25]. These active-passive SVC strategies combine the good properties of passive control systems and the high-performance characteristics of active control systems [26–28]. It should be highlighted, however, that most of the research effort undertaken to date has been directed at the two-building case, while more complex multibuilding problems still remain virtually unexplored. Obtaining a suitable formulation for the dynamical response of certain classes of connected multistructure mechanical systems is one of the major obstacles that has to be overcome in order to design SVC strategies for multibuilding systems. A preliminary work in this line presenting an active-passive SVC strategy for seismic protection of a three-building system can be found in [29].

The main contribution of the present paper is twofold: (i) a mathematical model to compute the overall vibrational response of connected multistructure mechanical systems is provided. (ii) Active-passive SVC strategies for seismic protection of multibuilding systems are designed using the proposed model and the CCM approach.

The paper is organized as follows: in Section 2, a general second-order model for the unforced response of connected multistructure mechanical systems is provided. The forced response is also studied for some particular cases of special relevance in SVC. In Section 3, passive, active, and active-passive SVC strategies for seismic protection of multibuilding systems are discussed. The main ideas are presented by means of a three-building system. Finally, in Section 4, a set of numerical simulations is conducted to assess the effectiveness of the proposed control strategies.

2. Multistructure Connected System

In this section, we present a mathematical model to compute the dynamical response of the multistructure system $\mathcal{S}$ schematically depicted in Figure 1. The overall system $\mathcal{S}$ consists of p parallel substructures $\mathcal{S}^{(1)}, \ldots, \mathcal{S}^{(p)}$. Each substructure $\mathcal{S}^{(j)}$ is a mass-spring-damper system with n_j degrees of freedom, and between adjacent substructures $\mathcal{S}^{(j)}$ and $\mathcal{S}^{(j+1)}$, there is a linking system $\mathcal{L}^{(j)}$ formed by a maximum number of $r_j = \min(n_j, n_{j+1})$ spring-damper elements. The aim of this section is to obtain a proper formulation of the second-order equation that describes the overall motion of system $\mathcal{S}$ in the form

$$M\ddot{q}(t) + C\dot{q}(t) + Kq(t) = f(t), \tag{2.1}$$

where M is the global mass matrix; C and K are the total damping and stiffness matrices, respectively, including the internal stiffness and damping coefficients of the substructures $\mathcal{S}^{(j)}$ as well as the stiffness and damping coefficients of the linking systems $\mathcal{L}^{(j)}$; $f(t)$ is the vector of external forces.

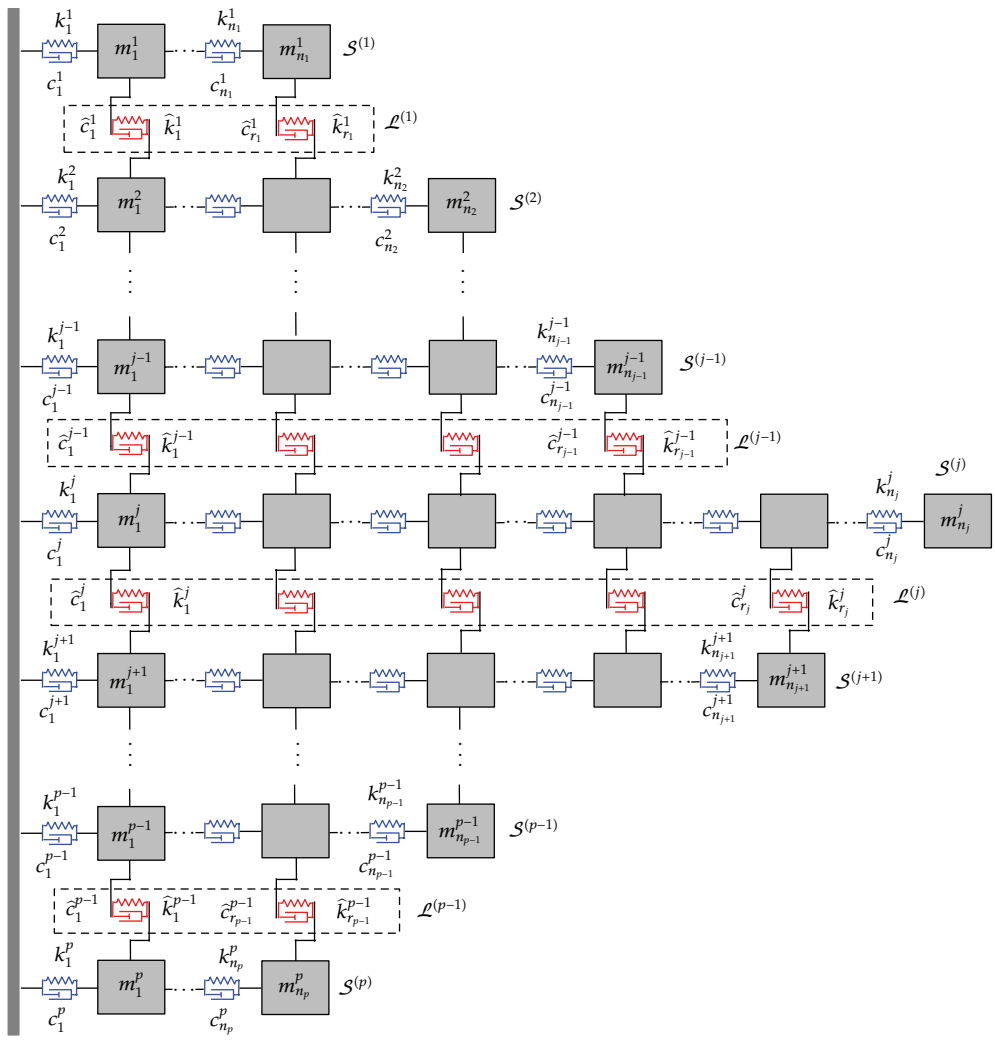

Figure 1: Multistructure system $\mathcal{S}$ formed by interconnected multiple-degree-of-freedom mass-spring-damper systems $\mathcal{S}^{(j)}$.

2.1. Unforced Response

Let us consider the jth substructure displayed in Figure 2. The vector of relative displacements is

$$q^{(j)}(t) = \left[q_1^j(t), \ldots, q_{n_j}^j(t)\right]^T, \tag{2.2}$$

where $q_i^j(t)$ represents the relative displacement of the mass m_i^j with respect to the fixed reference O, which in this subsection is assumed to be an inertial frame.

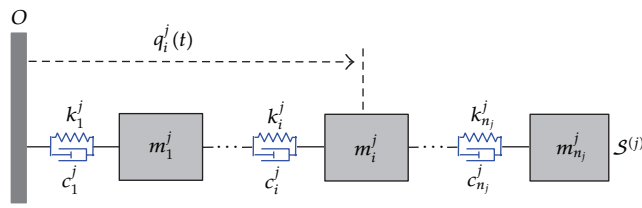

Figure 2: Multi-degree-of-freedom mass-spring-damper subsystem $\mathcal{S}^{(j)}$.

A second-order model for the substructure $\mathcal{S}^{(j)}$ can be written in the form

$$M^{(j)}\ \ddot{q}^{(j)}(t) + C^{(j)}\ \dot{q}^{(j)}(t) + K^{(j)}\ q^{(j)}(t) = f_{\ell}^{(j)}(t), \tag{2.3}$$

where $f_{\ell}^{(j)}(t)$ denotes the vector of interstructure forces resulting from the interaction between adjacent substructures through the linking elements. The mass matrix is a diagonal matrix

$$M^{(j)} = \operatorname{diag}\left[m_1^j, \ldots, m_{n_j}^j\right], \tag{2.4}$$

and the damping matrix has the following tridiagonal structure:

$$C^{(j)} = \begin{bmatrix} c_1^j + c_2^j & -c_2^j & & & \\ -c_2^j & c_2^j + c_3^j & -c_3^j & & \\ & \ddots & \ddots & \ddots & \\ & & -c_{n_j-1}^j & c_{n_j-1}^j + c_{n_j}^j & -c_{n_j}^j \\ & & & -c_{n_j}^j & c_{n_j}^j \end{bmatrix}. \tag{2.5}$$

The stiffness matrix $K^{(j)}$ has an analogous structure and can be obtained by replacing entries c_i^j by k_i^j in (2.5). We also define the damping and stiffness matrices of the linking system $\mathcal{L}^{(j)}$ as follows:

$$\widehat{C}^{(j)} = \operatorname{diag}\left[\widehat{c}_1^j, \ldots, \widehat{c}_{r_j}^j\right], \qquad \widehat{K}^{(j)} = \operatorname{diag}\left[\widehat{k}_1^j, \ldots, \widehat{k}_{r_j}^j\right], \qquad r_j = \min\left(n_j, n_{j+1}\right). \tag{2.6}$$

The main difficulty in obtaining a simple formulation for the overall second-order model (2.1) arises from the fact that adjacent substructures have, in general, different number of masses. This problem can be conveniently solved by extending the damping and stiffness matrices of the linking systems with a proper number of zero rows and columns. The benefits of this simple resource are twofold: (*i*) a plain and elegant matrix formulation of equation (2.1), and (*ii*) an extremely easy computational implementation. Next, we introduce the zero-extension of matrices and provide a simple Matlab function to compute it.

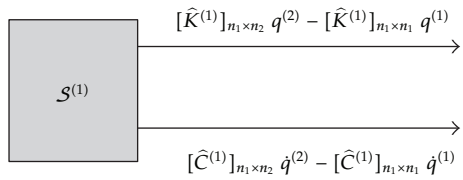

Figure 3: Force diagram for the initial substructure $\mathcal{S}^{(1)}$.

Definition 2.1. Given an $m \times n$ matrix A and two integers $m' \geq m$ and $n' \geq n$, we define the $m' \times n'$ zero-extension of A as the matrix

$$[A]_{m'\times n'} = \left[\begin{array}{c|c} A & [\mathbf{0}]_{m\times(n'-n)} \\ \hline [\mathbf{0}]_{(m'-m)\times n} & [\mathbf{0}]_{(m'-m)\times(n'-n)} \end{array}\right], \tag{2.7}$$

obtained from A by adding $m' - m$ final zero-rows and $n' - n$ final zero-columns.

The following Matlab function computes the matrix zero-extension:

```
Function M=zex(A,m1,n1)
[m,n]=size(A);
M=[A zeros(m,n1-n)
zeros(m1-m,n1)].
```

For the matrix

$$A = \begin{bmatrix} 1 & 2 \\ 3 & 4 \end{bmatrix}, \tag{2.8}$$

the 3×5 zero-extension can be computed with the command `zex(A,3,5)`, resulting

$$[A]_{3\times 5} = \begin{bmatrix} 1 & 2 & 0 & 0 & 0 \\ 3 & 4 & 0 & 0 & 0 \\ 0 & 0 & 0 & 0 & 0 \end{bmatrix}. \tag{2.9}$$

To obtain the expression for the vector of linking interstructure forces $f_\ell^{(j)}(t)$, we consider three different cases corresponding to the relative position of the substructure $\mathcal{S}^{(j)}$: (a) initial substructure $\mathcal{S}^{(1)}$, (b) interior substructure $\mathcal{S}^{(j)}$, $1 < j < p$, and (c) final substructure $\mathcal{S}^{(p)}$. For the initial substructure $\mathcal{S}^{(1)}$, from the force diagram in Figure 3, we have

$$f_\ell^{(1)} = \left[\widehat{C}^{(1)}\right]_{n_1\times n_2} \dot{q}^{(2)} - \left[\widehat{C}^{(1)}\right]_{n_1\times n_1} \dot{q}^{(1)} + \left[\widehat{K}^{(1)}\right]_{n_1\times n_2} q^{(2)} - \left[\widehat{K}^{(1)}\right]_{n_1\times n_1} q^{(1)}. \tag{2.10}$$

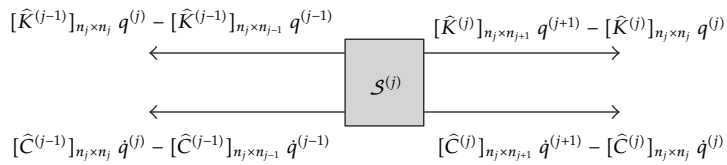

Figure 4: Force diagram for interior substructures $\mathcal{S}^{(j)}$, $1 < j < p$.

Equation (2.3) for $\mathcal{S}^{(1)}$ takes now the form

$$\begin{aligned} M^{(1)}\ \ddot{q}^{(1)} &+ \left\{ C^{(1)} + \left[\widehat{C}^{(1)}\right]_{n_1\times n_1} \right\} \dot{q}^{(1)} - \left[\widehat{C}^{(1)}\right]_{n_1\times n_2} \dot{q}^{(2)} \\ &+ \left\{ K^{(1)} + \left[\widehat{K}^{(1)}\right]_{n_1\times n_1} \right\} q^{(1)} - \left[\widehat{K}^{(1)}\right]_{n_1\times n_2} q^{(2)} = 0. \end{aligned} \tag{2.11}$$

Note that, for simplicity, the explicit dependence on time has been omitted in (2.10), (2.11), and Figure 3, and notations like $f_\ell^{(1)}$ and $q^{(1)}$ have been used instead of $f_\ell^{(1)}(t)$ and $q^{(1)}(t)$. The same will be done in the sequel when convenient.

Analogously, from the force diagram in Figure 4, it results

$$\begin{aligned} f_\ell^{(j)} = &\left[\widehat{C}^{(j-1)}\right]_{n_j\times n_{j-1}} \dot{q}^{(j-1)} - \left\{ \left[\widehat{C}^{(j-1)}\right]_{n_j\times n_j} + \left[\widehat{C}^{(j)}\right]_{n_j\times n_j} \right\} \dot{q}^{(j)} + \left[\widehat{C}^{(j)}\right]_{n_j\times n_{j+1}} \dot{q}^{(j+1)} \\ &+ \left[\widehat{K}^{(j-1)}\right]_{n_j\times n_{j-1}} q^{(j-1)} - \left\{ \left[\widehat{K}^{(j-1)}\right]_{n_j\times n_j} + \left[\widehat{K}^{(j)}\right]_{n_j\times n_j} \right\} q^{(j)} + \left[\widehat{K}^{(j)}\right]_{n_j\times n_{j+1}} q^{(j+1)}, \end{aligned} \tag{2.12}$$

and the second-order model for $\mathcal{S}^{(j)}$ can be written as

$$\begin{aligned} M^{(j)}\ \ddot{q}^{(j)} &- \left[\widehat{C}^{(j-1)}\right]_{n_j\times n_{j-1}} \dot{q}^{(j-1)} + \left\{ C^{(j)} + \left[\widehat{C}^{(j-1)}\right]_{n_j\times n_j} + \left[\widehat{C}^{(j)}\right]_{n_j\times n_j} \right\} \dot{q}^{(j)} \\ &- \left[\widehat{C}^{(j)}\right]_{n_j\times n_{j+1}} \dot{q}^{(j+1)} - \left[\widehat{K}^{(j-1)}\right]_{n_j\times n_{j-1}} q^{(j-1)} + \\ &+ \left\{ K^{(j)} + \left[\widehat{K}^{(j-1)}\right]_{n_j\times n_j} + \left[\widehat{K}^{(j)}\right]_{n_j\times n_j} \right\} q^{(j)} - \left[\widehat{K}^{(j)}\right]_{n_j\times n_{j+1}} q^{(j+1)} = 0. \end{aligned} \tag{2.13}$$

Finally, from Figure 5, we get

$$\begin{aligned} f_\ell^{(p)} = &- \left[\widehat{C}^{(p-1)}\right]_{n_p\times n_p} \dot{q}^{(p)} + \left[\widehat{C}^{(p-1)}\right]_{n_p\times n_{p-1}} \dot{q}^{(p-1)} \\ &- \left[\widehat{K}^{(p-1)}\right]_{n_p\times n_p} q^{(p)} + \left[\widehat{K}^{(p-1)}\right]_{n_p\times n_{p-1}} q^{(p-1)}, \end{aligned} \tag{2.14}$$

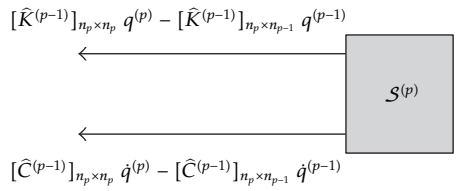

Figure 5: Force diagram for the final substructure $\mathcal{S}^{(p)}$.

and the corresponding second-order model is

$$\begin{aligned} M^{(p)}\,\ddot{q}^{(p)} &- \left[\widehat{C}^{(p-1)}\right]_{n_p\times n_{p-1}} \dot{q}^{(p-1)} + \left\{C^{(p)} + \left[\widehat{C}^{(p-1)}\right]_{n_p\times n_p}\right\}\dot{q}^{(p)} \\ &- \left[\widehat{K}^{(p-1)}\right]_{n_p\times n_{p-1}} q^{(p-1)} + \left\{K^{(p)} + \left[\widehat{K}^{(p-1)}\right]_{n_p\times n_p}\right\} q^{(p)} = 0. \end{aligned} \tag{2.15}$$

From (2.11), (2.13), and (2.15), we can now obtain an overall second-order model for the unforced response of the multibuilding coupled system in the form

$$M\,\ddot{q}(t) + C\,\dot{q}(t) + K\,q(t) = 0, \tag{2.16}$$

where

$$q(t) = \left[\{q^{(1)}(t)\}^T, \ldots, \{q^{(p)}(t)\}^T\right]^T, \tag{2.17}$$

is the overall vector of displacements. To this end, we express the global damping and stiffness matrices in the form

$$C = \overline{C} + \widehat{C}, \quad K = \overline{K} + \widehat{K}, \tag{2.18}$$

where matrices $\overline{C}$ and $\overline{K}$ correspond to the internal damping and stiffness of the substructures, respectively, and have the following block diagonal form:

$$\overline{C} = \operatorname{diag}\left[C^{(1)}, \ldots, C^{(p)}\right], \qquad \overline{K} = \operatorname{diag}\left[K^{(1)}, \ldots, K^{(p)}\right], \tag{2.19}$$

and matrices $C^{(j)}$, $K^{(j)}$ have the form given in (2.5). The damping matrix $\widehat{C}$ corresponds to the linking systems and has the tridiagonal block structure shown in Figure 6, the stiffness

$$\begin{bmatrix} [\widehat{C}^{(1)}]_{n_1\times n_1} & -[\widehat{C}^{(1)}]_{n_1\times n_2} & & & & \\ -[\widehat{C}^{(1)}]_{n_2\times n_1} & [\widehat{C}^{(1)}]_{n_2\times n_2} + [\widehat{C}^{(2)}]_{n_2\times n_2} & -[\widehat{C}^{(2)}]_{n_2\times n_3} & & & \\ \cdots & \cdots & \cdots & \cdots & \cdots & \cdots \\ & -[\widehat{C}^{(p-2)}]_{n_{p-1}\times n_{p-2}} & [\widehat{C}^{(p-2)}]_{n_{p-1}\times n_{p-1}} + [\widehat{C}^{(p-1)}]_{n_{p-1}\times n_{p-1}} & & -[\widehat{C}^{(p-1)}]_{n_{p-1}\times n_p} \\ & & -[\widehat{C}^{(p-1)}]_{n_p\times n_{p-1}} & & [\widehat{C}^{(p-1)}]_{n_p\times n_p} \end{bmatrix}$$

Figure 6: Damping matrix $\widehat{C}$ for the overall linking system.

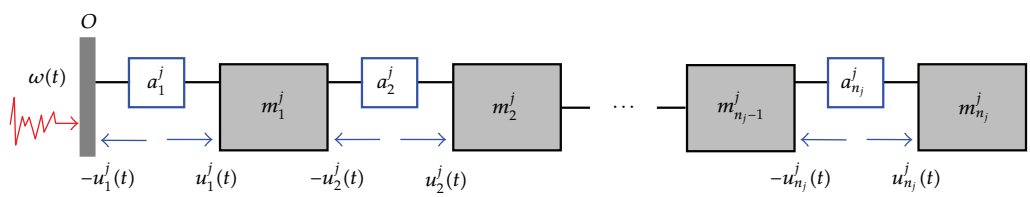

Figure 7: External excitations acting upon substructure $\mathcal{S}^{(j)}$.

matrix $\widehat{K}$ has the same structure as $\widehat{C}$ and can be obtained by replacing the entries $[\widehat{C}^{(j)}]_{n\times n'}$ by $[\widehat{K}^{(j)}]_{n\times n'}$. Finally, the global mass matrix M is the block diagonal matrix

$$M = \operatorname{diag}\left[M^{(1)}, \ldots, M^{(p)}\right], \tag{2.20}$$

where $M^{(j)}$, $1 \le j \le p$ are the substructure mass matrices given in (2.4).

2.2. Forced Response

Now, we assume that some external excitations are acting upon the substructures $\mathcal{S}^{(j)}$. Specifically, we will turn out our attention to the particular case schematically depicted in Figure 7, where $\omega(t)$ represents the acceleration of the reference frame O, and the element a_i^j is a force actuation device implemented between the adjacent masses m_{i-1}^j and m_i^j that produces a pair of opposite forces of magnitude $|u_i^j(t)|$ as indicated in the figure. This case is particularly relevant for structural vibration control of seismically excited buildings, where the external acceleration corresponds to the seismic ground acceleration, and the actuation devices a_i^j are interstory force actuators that implement suitable control forces to mitigate the vibrational response of the building.

A second-order model for the vibrational response of the substructure $\mathcal{S}^{(j)}$ can now be written in the form

$$M^{(j)}\ \ddot{q}^{(j)} + C^{(j)}\ \dot{q}^{(j)} + K^{(j)}\ q^{(j)} - f_{\ell}^{(j)}(t) = f_u^{(j)}(t) + f_{\omega}^{(j)}(t), \tag{2.21}$$

where the term $f_u^{(j)}(t)$ is the vector of control forces acting on $\mathcal{S}^{(j)}$, and $f_\omega^{(j)}(t)$ contains the inertial forces resulting from the fact that O is now an accelerated reference frame. Denoting by $[1]_{n_j\times 1}$ the column vector with n_j entries equal to 1, the vector of inertial forces can be written as

$$f_\omega^{(j)}(t) = -M^{(j)}[1]_{n_j\times 1}\ \omega(t). \tag{2.22}$$

For the vector of control actions, we consider the control location matrix of size $n_j \times n_j$

$$T_u^{(j)} = \begin{bmatrix} 1 & -1 & & & \\ & 1 & -1 & & \\ & & \ddots & \ddots & \\ & & & 1 & -1 \\ & & & & 1 \end{bmatrix}, \tag{2.23}$$

and the vector of control actions

$$u^{(j)}(t) = \left[u_1^j(t), \ldots, u_{n_j}^j(t)\right]^T, \tag{2.24}$$

to obtain

$$f_u^{(j)}(t) = T_u^{(j)}\ u^{(j)}(t). \tag{2.25}$$

Finally, considering (2.21), (2.22), (2.25), and the results presented in the previous subsection, we can derive a second-order model for the overall vibrational response of the multistructure system $\mathcal{S}$ in the following form:

$$M\ \ddot{q}(t) + C\ \dot{q}(t) + K\ q(t) = T_u u(t) + T_\omega\ \omega(t), \tag{2.26}$$

where $q(t)$ is the overall displacement vector defined in (2.17); matrices M, C, K are given in (2.18), (2.19), (2.20), and Figure 6; $\omega(t)$ is the external acceleration, and $T_\omega = -M[1]_{n\times 1}$ is the external disturbance matrix; $u(t)$ represents the overall vector of actuation forces

$$u(t) = \left[\left\{u^{(1)}(t)\right\}^T, \ldots, \left\{u^{(p)}(t)\right\}^T\right]^T, \tag{2.27}$$

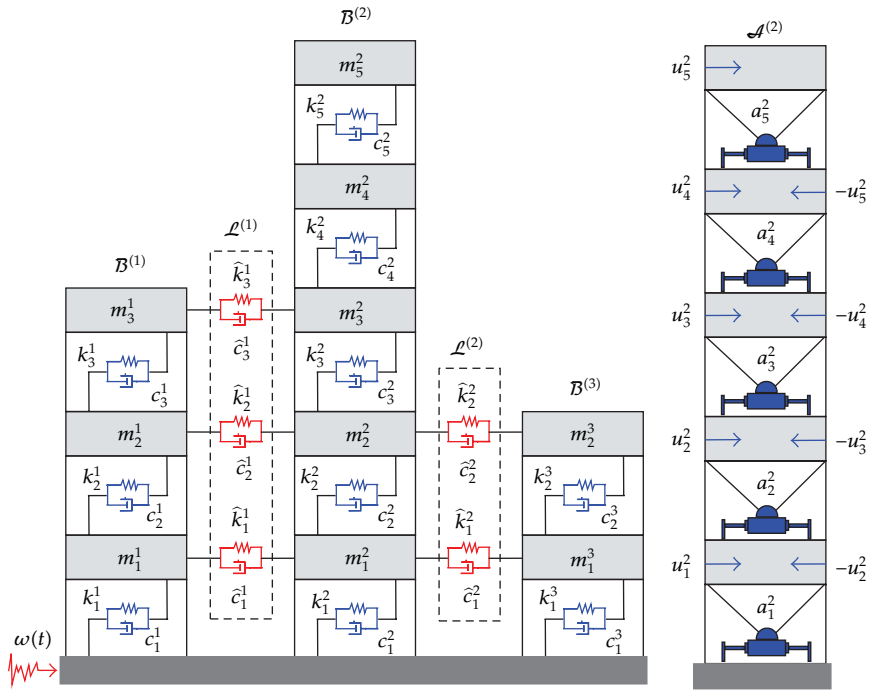

(a) Connected multibuilding model

(b) Actuation scheme in $\mathcal{B}^{(2)}$

Figure 8: Connected three-building system.

and T_u is the overall location control matrix defined as

$$T_u = \operatorname{diag}\left[T_u^{(1)}, \ldots, T_u^{(p)}\right], \tag{2.28}$$

$n = n_1 + \cdots + n_p$ is the total number of degrees of freedom, and p is the number of substructures. If no active control system has been implemented in the subsystem $\mathcal{S}^{(j)}$, $u^{(j)}(t)$ can be taken as a zero vector and $T_u^{(j)}$ as a zero matrix of appropriate dimensions. The proposed model includes the action of external acceleration disturbance and active control systems implemented in the substructures and, moreover, is formally analogous to the usual formulation used in single-structure SVC problems.

3. Structural Vibration Control Strategies for Multibuilding Systems

In this section, we are interested in designing SVC strategies for seismic protection of multibuilding systems. For clarity and simplicity, the main ideas are presented through the three-story building system schematically depicted in SubFigure 8(a), where the central five-story building is assumed to require a special level of seismic protection. For this particular multibuilding system, four control configurations are considered: (a) active-passive, (b) passive, (c) uncoupled-active, and (d) uncontrolled. In the active-passive control configuration (see SubFigure 9(a)), an active local state-feedback control system with the

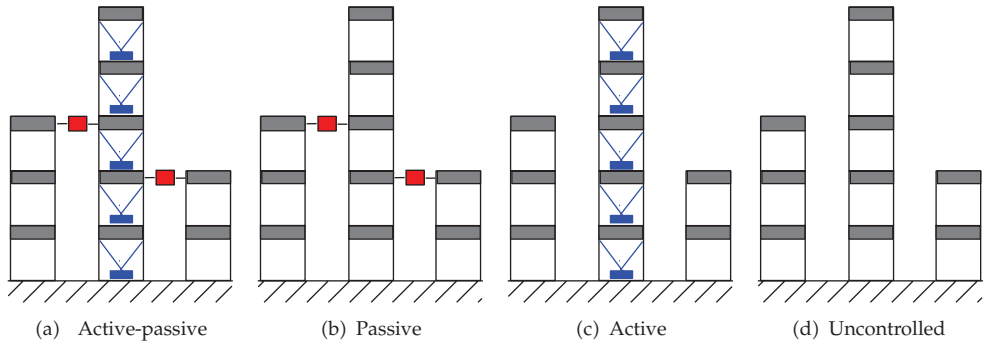

Figure 9: Control configurations for the three-building system.

actuation scheme presented in SubFigure 8(b) has been implemented in the central building. Moreover, two passive dampers have been placed as interbuilding linking elements: one at the third-floor level between buildings 1 and 2 and the other at the second-floor level between building 2 and building 3. The passive control configuration (SubFigure 9(b)) only comprises the interbuilding passive dampers. In the uncoupled-active control configuration (SubFigure 9(c)), an active local feedback system has been implemented in the central building, but no passive interbuilding elements have been installed. Finally, no seismic protection is provided in the uncontrolled control configuration (SubFigure 9(d)), which will be used as a reference in the performance assessments.

The section has been structured in three parts. First, the results presented in Section 2 are applied to obtain a second-order model for the three-building system. Next, suitable state-space models are derived. Finally, a state-feedback LQR controller is designed to drive the active local feedback control system implemented in building 2.

To compute the LQR local controller, the following particular values of the building parameters have been used: $m_i^j = 1.3 \times 10^6$ kg, $c_i^j = 10^5$ Ns/m, $k_i^1 = 2.0 \times 10^9$ N/m, $k_i^2 = 4 \times 10^9$ N/m, $k_i^3 = 2.0 \times 10^9$ N/m, for $1 \leq j \leq 3$, $1 \leq i \leq n_j$, $n_1 = 3$, $n_2 = 5$, $n_3 = 2$. The linking elements are considered as pure dampers with a damping constant $\hat{c}_i^j$=3.0 $\times$ 10^6 Ns/m and null stiffness; the value $\hat{c}_i^j$=0 indicates that no linking element exists at the ith level between buildings $\mathcal{B}^{(j)}$ and $\mathcal{B}^{(j+1)}$. The actuation elements a_i^2, $1 \leq i \leq 5$ are assumed to be ideal force actuation devices, which are able to implement exactly the control actions $u_i^2(t)$ producing the opposite pairs of control forces represented in Figure 8(b). These values will also be used in the numerical simulations conducted in Section 4.

3.1. Second-Order Model

Let us consider the three-story building system displayed in Figure 8(a) as a lumped-mass planar system with displacements in the direction of the ground motion. In this case, the multibuilding system can be represented by the connected multistructure system shown in Figure 10. Using the results presented in the previous section, a second-order model in the form

$$M\ \ddot{q}(t) + C\ \dot{q}(t) + K\ q(t) = T_u\ u(t) + T_\omega\ \omega(t), \tag{3.1}$$

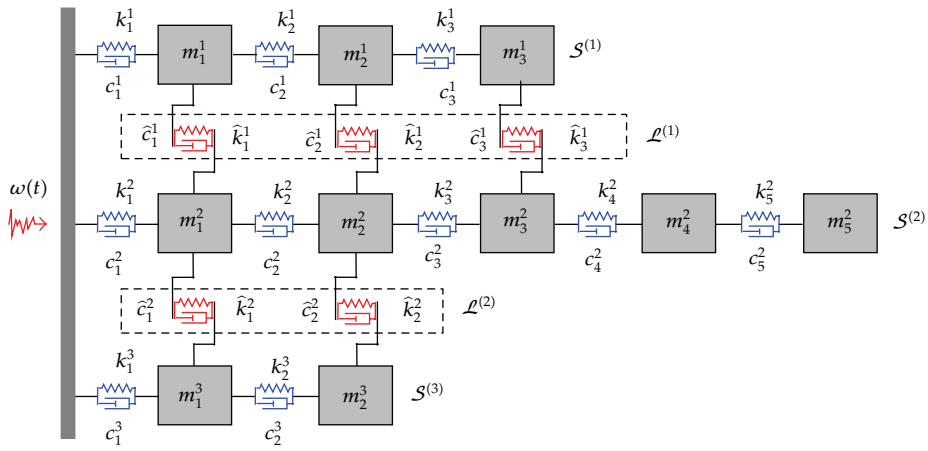

Figure 10: Connected three-building system.

to describe the buildings motion can be easily obtained. The overall vector of story displacements with respect to the ground is

$$q(t) = \left[q_1^1(t), q_2^1(t), q_3^1(t), q_1^2(t), q_2^2(t), q_3^2(t), q_4^2(t), q_5^2(t), q_1^3(t), q_2^3(t)\right]^T, \tag{3.2}$$

where $q_i^j(t)$ represents the displacement of the ith story in the jth building. The mass matrix is

$$M = \begin{bmatrix} M^{(1)} & [0]_{3\times5} & [0]_{3\times2} \\ [0]_{5\times3} & M^{(2)} & [0]_{5\times2} \\ [0]_{2\times3} & [0]_{2\times5} & M^{(3)} \end{bmatrix}, \tag{3.3}$$

with

$$M^{(1)} = \begin{bmatrix} m_1^1 & 0 & 0 \\ 0 & m_2^1 & 0 \\ 0 & 0 & m_3^1 \end{bmatrix}, \qquad M^{(2)} = \begin{bmatrix} m_1^2 & 0 & 0 & 0 & 0 \\ 0 & m_2^2 & 0 & 0 & 0 \\ 0 & 0 & m_3^2 & 0 & 0 \\ 0 & 0 & 0 & m_4^2 & 0 \\ 0 & 0 & 0 & 0 & m_5^2 \end{bmatrix}, \qquad M^{(3)} = \begin{bmatrix} m_1^3 & 0 \\ 0 & m_2^3 \end{bmatrix}. \tag{3.4}$$

The total damping matrix can be written in the form

$$C = \overline{C} + \widehat{C}, \tag{3.5}$$

where

$$\overline{C} = \begin{bmatrix} C^{(1)} & [0]_{3\times5} & [0]_{3\times2} \\ [0]_{5\times3} & C^{(2)} & [0]_{5\times2} \\ [0]_{2\times3} & [0]_{2\times5} & C^{(3)} \end{bmatrix}, \tag{3.6}$$

$$C^{(1)} = \begin{bmatrix} c_1^1 + c_2^1 & -c_2^1 & 0 \\ -c_2^1 & c_2^1 + c_3^1 & -c_3^1 \\ 0 & -c_3^1 & c_3^1 \end{bmatrix}, \qquad C^{(3)} = \begin{bmatrix} c_1^3 + c_2^3 & -c_2^3 \\ -c_2^3 & c_2^3 \end{bmatrix}, \tag{3.7}$$

$$C^{(2)} = \begin{bmatrix} c_1^2 + c_2^2 & -c_2^2 & 0 & 0 & 0 \\ -c_2^2 & c_2^2 + c_3^2 & -c_3^2 & 0 & 0 \\ 0 & -c_3^2 & c_3^2 + c_4^2 & -c_4^2 & 0 \\ 0 & 0 & -c_4^2 & c_4^2 + c_5^2 & -c_5^2 \\ 0 & 0 & 0 & -c_5^2 & c_5^2 \end{bmatrix}, \tag{3.8}$$

and the matrix corresponding to the linking elements $\widehat{C}$ has the following block tridiagonal structure:

$$\widehat{C} = \begin{bmatrix} \left[\widehat{C}^{(1)}\right]_{3\times3} & -\left[\widehat{C}^{(1)}\right]_{3\times5} & [0]_{3\times2} \\ -\left[\widehat{C}^{(1)}\right]_{5\times3} & \left[\widehat{C}^{(1)}\right]_{5\times5} + \left[\widehat{C}^{(2)}\right]_{5\times5} & -\left[\widehat{C}^{(2)}\right]_{5\times2} \\ [0]_{2\times3} & -\left[\widehat{C}^{(2)}\right]_{2\times5} & \left[\widehat{C}^{(2)}\right]_{2\times2} \end{bmatrix}, \tag{3.9}$$

$$\widehat{C}^{(1)} = \begin{bmatrix} \widehat{c}_1^1 & 0 & 0 \\ 0 & \widehat{c}_2^1 & 0 \\ 0 & 0 & \widehat{c}_3^1 \end{bmatrix}, \qquad \widehat{C}^{(2)} = \begin{bmatrix} \widehat{c}_1^2 & 0 \\ 0 & \widehat{c}_2^2 \end{bmatrix}, \tag{3.10}$$

where $[\widehat{C}^{(j)}]_{r\times s}$ denotes the $r \times s$ zero-extension of $\widehat{C}^{(j)}$, for example

$$\left[\widehat{C}^{(1)}\right]_{5\times5} = \begin{bmatrix} \widehat{c}_1^1 & 0 & 0 & 0 & 0 \\ 0 & \widehat{c}_2^1 & 0 & 0 & 0 \\ 0 & 0 & \widehat{c}_3^1 & 0 & 0 \\ 0 & 0 & 0 & 0 & 0 \\ 0 & 0 & 0 & 0 & 0 \end{bmatrix}, \qquad \left[\widehat{C}^{(2)}\right]_{5\times2} = \begin{bmatrix} \widehat{c}_1^2 & 0 \\ 0 & \widehat{c}_2^2 \\ 0 & 0 \\ 0 & 0 \\ 0 & 0 \end{bmatrix}. \tag{3.11}$$

To obtain the total stiffness matrix

$$K = \overline{K} + \widehat{K}, \tag{3.12}$$

matrices $\overline{K}$, $\widehat{K}$ can be computed replacing the damping coefficients c_i^j, $\widehat{c}_i^j$ by the corresponding stiffness coefficients k_i^j, $\widehat{k}_i^j$ in (3.7), (3.8), (3.10), and matrices $C^{(j)}$, $\widehat{C}^{(j)}$ by $K^{(j)}$, $\widehat{K}^{(j)}$ in (3.6), (3.9). For the active-passive control configuration depicted in Figure 9(a), the vector of control actions is

$$u(t) = \left[0, 0, 0, u_1^2(t), u_2^2(t), u_3^2(t), u_4^2(t), u_5^2(t), 0, 0\right]^T, \tag{3.13}$$

and the control location matrix T_u to produce the corresponding control forces can be written as follows:

$$T_u = \begin{bmatrix} [0]_{3\times3} & [0]_{3\times5} & [0]_{3\times2} \\ [0]_{5\times3} & T_u^{(2)} & [0]_{5\times2} \\ [0]_{2\times3} & [0]_{2\times5} & [0]_{2\times2} \end{bmatrix}, \qquad T_u^{(2)} = \begin{bmatrix} 1 & -1 & 0 & 0 & 0 \\ 0 & 1 & -1 & 0 & 0 \\ 0 & 0 & 1 & -1 & 0 \\ 0 & 0 & 0 & 1 & -1 \\ 0 & 0 & 0 & 0 & 1 \end{bmatrix}. \tag{3.14}$$

Finally, the disturbance input matrix is

$$T_w = -M\ [1]_{10\times1}\ . \tag{3.15}$$

3.2. *First-Order State-Space Model*

Now, we take the state vector

$$x(t) = \begin{bmatrix} q(t) \\ \dot{q}(t) \end{bmatrix}, \tag{3.16}$$

and derive the first-order state-space model

$$\begin{aligned} \dot{x}(t) &= Ax(t) + Bu(t) + E\omega(t), \\ y(t) &= C_y x(t), \end{aligned} \tag{3.17}$$

where the state, control, and disturbance input matrices are, respectively,

$$A = \begin{bmatrix} [0]_{10\times10} & I_{10} \\ -M^{-1}K & -M^{-1}C \end{bmatrix}, \qquad B = \begin{bmatrix} [0]_{10\times10} \\ M^{-1}T_u \end{bmatrix}, \qquad E = \begin{bmatrix} [0]_{10\times1} \\ -[1]_{10\times1} \end{bmatrix}. \tag{3.18}$$

Regarding the output, we consider two different cases: interstory drifts and interbuilding approaches. The *interstory drifts* represent the relative displacements between consecutive stories in the jth building and are defined by

$$\begin{aligned} \{y_s\}_1^j(t) &= q_1^j(t), \\ \{y_s\}_i^j(t) &= q_i^j(t) - q_{i-1}^j(t), \quad 1 < i \le n_j, \end{aligned} \tag{3.19}$$

where n_j is the number of stories in building $\mathcal{B}^{(j)}$. The vector of interstory drifts

$$y_s(t) = \left[\{y_s\}_1^1, \{y_s\}_2^1, \{y_s\}_3^1, \{y_s\}_1^2, \{y_s\}_2^2, \{y_s\}_3^2, \{y_s\}_4^2, \{y_s\}_5^2, \{y_s\}_1^3, \{y_s\}_2^3\right]^T \tag{3.20}$$

can be obtained with the output matrix

$$C_{y_s} = \begin{bmatrix} C_{y_s}^{(1)} & [0]_{3\times5} & [0]_{3\times2} & [0]_{3\times10} \\ [0]_{5\times3} & C_{y_s}^{(2)} & [0]_{5\times2} & [0]_{5\times10} \\ [0]_{2\times3} & [0]_{2\times5} & C_{y_s}^{(3)} & [0]_{2\times10} \end{bmatrix}, \tag{3.21}$$

where

$$C_{y_s}^{(1)} = \begin{bmatrix} 1 & 0 & 0 \\ -1 & 1 & 0 \\ 0 & -1 & 1 \end{bmatrix}, \qquad C_{y_s}^{(2)} = \begin{bmatrix} 1 & 0 & 0 & 0 & 0 \\ -1 & 1 & 0 & 0 & 0 \\ 0 & -1 & 1 & 0 & 0 \\ 0 & 0 & -1 & 1 & 0 \\ 0 & 0 & 0 & -1 & 1 \end{bmatrix},$$
$$C_{y_s}^{(3)} = \begin{bmatrix} 1 & 0 \\ -1 & 1 \end{bmatrix}. \tag{3.22}$$

The *interbuilding approaches* describe the approaching between the stories placed at the ith level in the adjacent buildings $\mathcal{B}^{(j)}$, $\mathcal{B}^{(j+1)}$ and are defined by

$$\{y_a\}_i^j(t) = -\left(q_i^{j+1}(t) - q_i^j(t)\right), \quad 1 \le i \le r_j,\ 1 \le j \le 2, \tag{3.23}$$

where $r_j = \min(n_j, n_{j+1})$. The vector of interbuilding approaches

$$y_a(t) = \left[\{y_a\}_1^1(t), \{y_a\}_2^1(t), \{y_a\}_3^1(t), \{y_a\}_1^2(t), \{y_a\}_2^2(t)\right]^T, \tag{3.24}$$

can be computed with the output matrix

$$C_{y_a} = \begin{bmatrix} I_3 & -[I_3]_{3\times5} & [0]_{3\times2} & [0]_{3\times10} \\ [0]_{2\times3} & [I_2]_{2\times5} & -I_2 & [0]_{2\times10} \end{bmatrix}. \tag{3.25}$$

Finally, let us suppose that the state-feedback controller

$$u^{(j)}(t) = G^{(j)} x^{(j)}(t) \tag{3.26}$$

has been computed to drive a local active control system in $\mathcal{B}^{(j)}$. We write the local vector of control actions as

$$u^{(j)}(t) = G^{(j)}x^{(j)}(t) = \left[\, G_1^{(j)} \,\middle|\, G_2^{(j)} \,\right] \begin{bmatrix} q^{(j)}(t) \\ \dot{q}^{(j)}(t) \end{bmatrix}, \tag{3.27}$$

where matrices $G_1^{(j)}$, $G_2^{(j)}$ are obtained by splitting the control matrix $G^{(j)}$ after the n_j-th column. The seismic response of the overall three-building system for different active-passive control configurations can be computed using the closed-loop state-space model as follows:

$$\begin{aligned} \dot{x}(t) &= \overline{A}x(t) + Ew(t), \\ y(t) &= C_y x(t), \end{aligned} \tag{3.28}$$

where the state matrix $\overline{A} = A + BG$ can be obtained using the matrices A, B, E given in (3.18), and the overall control matrix

$$G = \begin{bmatrix} \overline{G}_1^{(1)} & [0]_{3\times5} & [0]_{3\times2} & \overline{G}_2^{(1)} & [0]_{3\times5} & [0]_{3\times2} \\ [0]_{5\times3} & \overline{G}_1^{(2)} & [0]_{5\times2} & [0]_{5\times3} & \overline{G}_2^{(2)} & [0]_{5\times2} \\ [0]_{2\times3} & [0]_{2\times5} & \overline{G}_1^{(3)} & [0]_{2\times3} & [0]_{2\times5} & \overline{G}_2^{(3)} \end{bmatrix}, \tag{3.29}$$

with

$$\overline{G}_i^{(j)} = \begin{cases} G_i^{(j)}, & \text{if } \mathcal{B}^{(j)} \text{ is actively controlled,} \\ [0]_{n_j\times n_j}, & \text{otherwise.} \end{cases} \tag{3.30}$$

In particular, for the active-passive control configuration depicted in Figure 9(a), the overall control matrix has the form

$$G = \begin{bmatrix} [0]_{3\times3} & [0]_{3\times5} & [0]_{3\times2} & [0]_{3\times3} & [0]_{3\times5} & [0]_{3\times2} \\ [0]_{5\times3} & \overline{G}_1^{(2)} & [0]_{5\times2} & [0]_{5\times3} & \overline{G}_2^{(2)} & [0]_{5\times2} \\ [0]_{2\times3} & [0]_{2\times5} & [0]_{2\times2} & [0]_{2\times3} & [0]_{2\times5} & [0]_{2\times2} \end{bmatrix}. \tag{3.31}$$

3.3. Local State-Feedback Controller Design

To compute a local state-feedback LQR controller [30] for the actuation system in building $\mathcal{B}^{(2)}$, we consider the local second-order model

$$M^{(2)}\ \ddot{q}^{(2)}(t) + C^{(2)}\ \dot{q}^{(2)}(t) + K^{(2)}\ q^{(2)}(t) = T_u^{(2)}\ u^{(2)}(t), \tag{3.32}$$

where

$$q^{(2)}(t) = \left[q_1^2(t), q_2^2(t), q_3^2(t), q_4^2(t), q_5^2(t)\right]^T \tag{3.33}$$

is the vector of story displacements relative to the ground,

$$u^{(2)}(t) = \left[u_1^2(t), u_2^2(t), u_3^2(t), u_4^2(t), u_5^2(t)\right]^T \tag{3.34}$$

is the vector of control actions, and matrices $M^{(2)}$, $C^{(2)}$, $K^{(2)}$, $T_u^{(2)}$ have been given in the previous subsection. From (3.32), we obtain the first-order state-space model

$$\begin{aligned} \dot{x}^{(2)}(t) &= A^{(2)}x^{(2)}(t) + B^{(2)}u^{(2)}(t), \\ \{y_s\}^{(2)}(t) &= C_{y_s}^{(2)}\ x^{(2)}(t), \end{aligned} \tag{3.35}$$

with local state vector

$$x^{(2)}(t) = \begin{bmatrix} q^{(2)}(t) \\ \dot{q}^{(2)}(t) \end{bmatrix}, \tag{3.36}$$

state matrix

$$A^{(2)} = \begin{bmatrix} [0]_{5\times5} & I_5 \\ -\{M^{(2)}\}^{-1}K^{(2)} & -\{M^{(2)}\}^{-1}C^{(2)} \end{bmatrix}, \tag{3.37}$$

and control input matrix

$$B^{(2)} = \begin{bmatrix} [0]_{5\times5} \\ \{M^{(2)}\}^{-1}T_u^{(2)} \end{bmatrix}. \tag{3.38}$$

To obtain the local vector of interstory drifts

$$\{y_s\}^{(2)}(t) = \left[\{y_s\}_1^2(t), \{y_s\}_2^2(t), \{y_s\}_3^2(t), \{y_s\}_4^2(t), \{y_s\}_5^2(t)\right]^T, \tag{3.39}$$

we take the matrix $C_{y_s}^{(2)}$ given in (3.22) and define the local output matrix

$$\overline{C}_{y_s}^{(2)} = \left[C_{y_s}^{(2)}\ [0]_{5\times5}\ \right]. \tag{3.40}$$

Next, we consider the weighting matrices

$$Q^{(2)} = \left\{\overline{C}_{y_s}^{(2)}\right\}^T \overline{C}_{y_s}^{(2)}, \qquad R^{(2)} = 10^{-17.5} \times I_5, \tag{3.41}$$

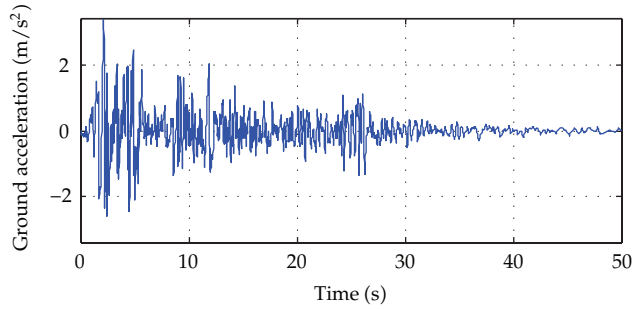

Figure 11: North-South El Centro 1940 seismic record.

and define the quadratic cost function

$$\begin{aligned} J^{(2)}\left(x^{(2)}, u^{(2)}\right) &= \int_0^\infty \left[\left\{x^{(2)}(t)\right\}^T Q^{(2)} x^{(2)}(t) + \left\{u^{(2)}(t)\right\}^T R^{(2)} u^{(2)}(t)\right] dt \\ &= \int_0^\infty \left[\left\{y_s^{(2)}(t)\right\}^T y_s^{(2)}(t) + \left\{u^{(2)}(t)\right\}^T R^{(2)} u^{(2)}(t)\right] dt, \end{aligned} \tag{3.42}$$

to compute a local state-feedback LQR controller

$$u^{(2)}(t) = G^{(2)} x^{(2)}(t) \tag{3.43}$$

with the following control gain matrix:

$$G^{(2)} = 10^7 \times \begin{bmatrix} -3.9335 & 0.0000 & 0.0000 & 0.0000 & 0.0000 & -0.8574 & -0.3617 & -0.2497 & -0.2051 & -0.1878 \\ 3.9335 & -3.9335 & 0.0000 & 0.0000 & 0.0000 & 0.4957 & -0.7454 & -0.3171 & -0.2323 & -0.2051 \\ 0.0000 & 3.9335 & -3.9335 & 0.0000 & 0.0000 & 0.1120 & 0.5403 & -0.7280 & -0.3171 & -0.2497 \\ 0.0000 & 0.0000 & 3.9335 & -3.9335 & 0.0000 & 0.0446 & 0.1294 & 0.5403 & -0.7454 & -0.3617 \\ 0.0000 & 0.0000 & 0.0000 & 3.9335 & -3.9335 & 0.0173 & 0.0446 & 0.1120 & 0.4957 & -0.8574 \end{bmatrix}. \tag{3.44}$$

4. Numerical Simulations

In this section, the vibrational response of the three-building system presented in Section 3 is computed for several control configurations. Specifically, the maximum absolute interstory drifts and maximum interbuilding approaches are computed for three control configurations: (a) *active-passive*, (b) *passive*, and (c) *uncoupled-active*, which are schematically depicted in Figures 9(a), 9(b), and 9(c). The vibrational response of the *uncontrolled* system (SubFigure 9(d)) is also computed, and it is used as a natural reference in the performance assessment. In all the cases, the full-scale North-South El Centro 1940 seismic record obtained at the Imperial Valley Irrigation District substation in El Centro, CA, during the Imperial Valley earthquake of May 18, 1940, has been used as a ground acceleration input (see Figure 11).

The maximum absolute interstory drifts are displayed in Figure 12. Looking at the central graphic, the excellent behavior of the active-passive (black asterisks) and the

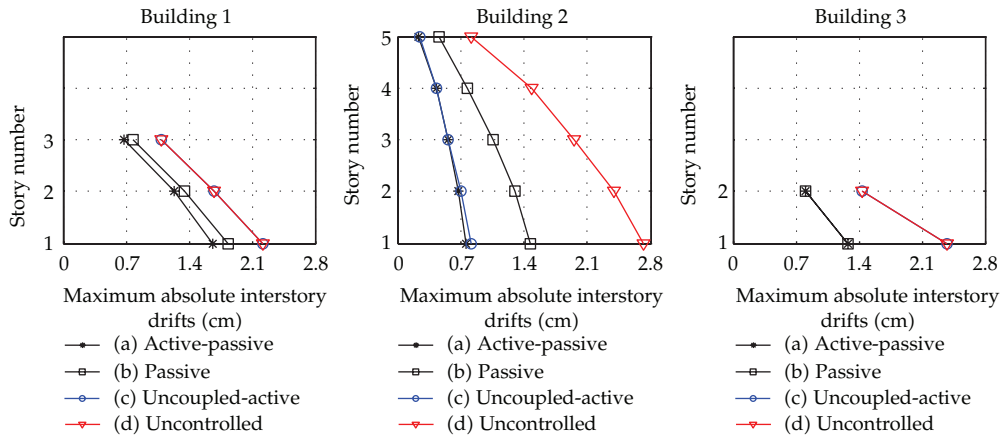

Figure 12: Maximum absolute interstory drifts for the North-South El Centro 1940 seismic excitation.

Table 1: Percentages of reduction in maximum absolute interstory drifts with respect to the uncontrolled response.

	Building 1			Building 2					Building 3	
	$\{y_s\}_1^1$	$\{y_s\}_2^1$	$\{y_s\}_3^1$	$\{y_s\}_1^2$	$\{y_s\}_2^2$	$\{y_s\}_3^2$	$\{y_s\}_4^2$	$\{y_s\}_5^2$	$\{y_s\}_1^3$	$\{y_s\}_2^3$
(a) Active-passive	24.7	26.7	37.4	72.4	71.7	71.3	71.1	71.5	43.3	43.7
(b) Passive	17.3	19.3	27.9	40.1	45.5	45.8	47.3	43.2	46.4	44.0
(c) Uncoupled-active	0	0	0	70.1	70.3	71.0	70.3	69.9	0	0

uncoupled-active (blue circles) control configurations can be clearly appreciated. In fact, the data in Table 1 indicate that these active control configurations attain reductions of about 70% in the peak interstory drift values with respect to the uncontrolled response. For the lateral buildings, however, the situation is totally different. In this case, the active-passive control configuration produces a lower but still significant reduction of the interstory drifts, while no seismic protection is provided by the uncoupled-active configuration.

Regarding the interbuilding approaches, we can see in Figure 13 that interbuilding separations of about 7.5 cm would have resulted in interbuilding collisions for the uncontrolled configuration. In contrast, interbuilding separations of about 2.5 cm can be considered safe for the active-passive control configuration. An important reduction in the interbuilding approaches is also achieved by the uncoupled-active configuration, but the data in Table 2 indicate that the percentages of reduction obtained by this configuration are about 25 points inferior to those obtained by the active-passive control configuration.

To complete the comparison between the active-passive and the uncoupled-active configurations, the corresponding maximum absolute control efforts are presented in Table 3. The values in the table indicate that the active-passive configuration requires a slightly higher level of control effort. However, considering the superior performance exhibited by the active-passive configuration, the extra cost is certainly small.

The behavior of the passive control configuration is also remarkable. Despite its simplicity and null power consumption, percentages of reduction in the interstory drifts peak values of about 45% are achieved in buildings 2 and 3 and around 20% in building 1. Reductions of about 60% are also produced for the interbuilding approaches.

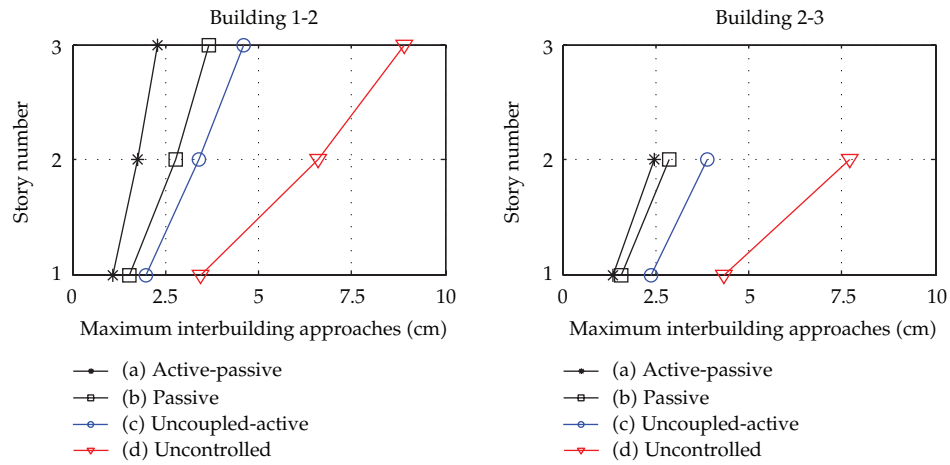

Figure 13: Maximum interbuilding approaches for the North-South El Centro 1940 seismic excitation.

Table 2: Percentages of reduction in maximum interbuilding approaches with respect to the uncontrolled response.

	Buildings 1-2			Buildings 2-3	
	$\{y_a\}_1^1$	$\{y_a\}_2^1$	$\{y_a\}_3^1$	$\{y_a\}_1^2$	$\{y_a\}_2^2$
(a) Active-passive	68.3	73.1	74.2	68.7	68.3
(b) Passive	55.4	57.8	58.6	63.8	63.7
(c) Uncoupled-active	43.3	48.6	48.5	45.5	49.9

Table 3: Maximum absolute control forces exerted by actuation devices in building 2.

	Control actions in $\mathcal{B}^{(2)}$ ($\times 10^6$ N)				
	a_1^2	a_2^2	a_3^2	a_4^2	a_5^2
(a) Active-passive	4.64	4.22	3.48	2.49	1.30
(c) Uncoupled-active	4.33	3.88	3.14	2.27	1.26

Finally, it should be highlighted the robustness of the active-passive control configuration against failures in the local active control system. Actually, in case of a full failure of the active control system, the passive level of seismic protection can still be guaranteed by the passive-active control configuration. In contrast, the same kind of failure in the uncoupled-active configuration would produce a total loss of seismic protection.

5. Final Remarks and Conclusions

In this work, a mathematical model to compute the overall vibrational response of connected multistructure mechanical systems has been presented. Using the proposed model and following the connected control method approach, structural vibration control strategies for seismic protection of multibuilding systems can be efficiently designed. As a practical

application of the new ideas, different control configurations for seismic protection of a particular three-building system have been designed. For these control configurations, numerical simulations of the three-building system vibrational response have been conducted using the full-scale North-South 1940 seismic record as a seismic excitation. The simulation results come to confirm the excellent properties of control configurations that combine passive interbuilding dampers with local feedback control systems implemented in the buildings. These hybrid active-passive control strategies possess the good properties of passive control systems and also have the high-performance characteristics of active control systems. Moreover, active-passive control configurations can be properly designed for multibuilding systems that require different levels of seismic protection and are also remarkably robust against failures in the local feedback control systems. Finally, it is worth highlighting that the proposed active-passive control strategy is compatible with practically any control design methodology of the local feedback control systems and also with semiactive implementations of the actuation systems. Consequently, further research effort needs to be aimed at exploring more complex scenarios involving issues of practical interest such as wireless implementation of the communications systems [31], actuator saturation [32], actuation and sensor failures [33], structural information constraints [34, 35], uncertain stochastic networked systems [36–38], or limited frequency domain [39].

Acknowledgments

This work has been partially supported by the Spanish Ministry of Economy and Competitiveness through the Grant DPI2011-25567-C02 and by the Norwegian Center of Offshore Wind Energy (NORCOWE) under Grant 193821/S60 from the Research Council of Norway (RCN).

References

[1] S. A. Anagnostopoulos, "Building pounding re-examined: how serious a problem is it?" *In Eleventh World Conference of Earthquake Engineering*, Elsevier Science, 1996.

[2] K. T. Chau, X. X. Wei, X. Guo, and C. Y. Shen, "Experimental and theoretical simulations of seismic poundings between two adjacent structures," *Earthquake Engineering and Structural Dynamics*, vol. 32, no. 4, pp. 537–554, 2003.

[3] P. Komodromos, P. C. Polycarpou, L. Papaloizou, and M. C. Phocas, "Response of seismically isolated buildings considering poundings," *Earthquake Engineering and Structural Dynamics*, vol. 36, no. 12, pp. 1605–1622, 2007.

[4] D. Lopez-Garcia and T. T. Soong, "Assessment of the separation necessary to prevent seismic pounding between linear structural systems," *Probabilistic Engineering Mechanics*, vol. 24, no. 2, pp. 210–223, 2009.

[5] P. C. Polycarpou and P. Komodromos, "Earthquake-induced poundings of a seismically isolated building with adjacent structures," *Engineering Structures*, vol. 32, no. 7, pp. 1937–1951, 2010.

[6] Y. L. Xu, Q. He, and J. M. Ko, "Dynamic response of damper-connected adjacent buildings under earthquake excitation," *Engineering Structures*, vol. 21, no. 2, pp. 135–148, 1999.

[7] W. S. Zhang and Y. L. Xu, "Dynamic characteristics and seismic response of adjacent buildings linked by discrete dampers," *Earthquake Engineering and Structural Dynamics*, vol. 28, pp. 1163–1185, 1999.

[8] Y. Q. Ni, J. M. Ko, and Z. G. Ying, "Random seismic response analysis of adjacent buildings coupled with non-linear hysteretic dampers," *Journal of Sound and Vibration*, vol. 246, no. 3, pp. 403–417, 2001.

[9] Z. Yang, Y. L. Xu, and X. L. Lu, "Experimental seismic study of adjacent buildings with fluid dampers," *Journal of Structural Engineering*, vol. 129, no. 2, pp. 197–205, 2003.

[10] V. A. Matsagar and R. S. Jangid, "Viscoelastic damper connected to adjacent structures involving seismic isolation," *Journal of Civil Engineering and Management*, vol. 11, no. 4, pp. 309–322, 2005.

[11] A. V. Bhaskararao and R. S. Jangid, "Seismic response of adjacent buildings connected with friction dampers," *Bulletin of Earthquake Engineering*, vol. 4, no. 1, pp. 43–64, 2006.
[12] J. Kim, J. Ryu, and L. Chung, "Seismic performance of structures connected by viscoelastic dampers," *Engineering Structures*, vol. 28, no. 2, pp. 183–195, 2006.
[13] M. Basili and M. De Angelis, "Optimal passive control of adjacent structures interconnected with nonlinear hysteretic devices," *Journal of Sound and Vibration*, vol. 301, no. 1-2, pp. 106–125, 2007.
[14] K. Makita, R. E. Christenson, K. Seto, and T. Watanabe, "Optimal design strategy of connected control method for two dynamically similar structures," *Journal of Engineering Mechanics*, vol. 133, no. 12, pp. 1247–1257, 2007.
[15] C. C. Patel, "Dynamic response of viscous damper connected similar multi-degree of freedom structures," *International Journal of Earth Sciences and Engineering*, vol. 4, no. 6, pp. 1068–1071, 2011.
[16] H. P. Zhu, D. D. Ge, and X. Huang, "Optimum connecting dampers to reduce the seismic responses of parallel structures," *Journal of Sound and Vibration*, vol. 330, no. 9, pp. 1931–1949, 2011.
[17] R. E. Christenson, B. F. Spencer, N. Hori, and K. Seto, "Coupled building control using acceleration feedback," *Computer-Aided Civil and Infrastructure Engineering*, vol. 18, no. 1, pp. 4–18, 2003.
[18] Z. G. Ying, Y. Q. Ni, and J. M. Ko, "Stochastic optimal coupling-control of adjacent building structures," *Computers and Structures*, vol. 81, no. 30-31, pp. 2775–2787, 2003.
[19] R. E. Christenson, B. F. Spencer, E. A. Johnson, and K. Seto, "Coupled building control considering the effects of building/connector configuration," *Journal of Structural Engineering*, vol. 132, no. 6, pp. 853–863, 2006.
[20] H. Zhu, Y. Wen, and H. Iemura, "A study on interaction control for seismic response of parallel structures," *Computers and Structures*, vol. 79, no. 2, pp. 231–242, 2001.
[21] R. E. Christenson, B. F. Spencer, and E. A. Johnson, "Semiactive connected control method for adjacent multidegree-of-freedom buildings," *Journal of Engineering Mechanics*, vol. 133, no. 3, pp. 290–298, 2007.
[22] S. D. Bharti, S. M. Dumne, and M. K. Shrimali, "Seismic response analysis of adjacent buildings connected with MR dampers," *Engineering Structures*, vol. 32, no. 8, pp. 2122–2133, 2010.
[23] M. S. Shahidzadeh, H. Tarzi, and M. Dorfeshan, "Takagi-Sugeno fuzzy control of adjacent structures using MR dampers," *Journal of Applied Sciences*, vol. 11, no. 15, pp. 2816–2822, 2011.
[24] F. Palacios-Quiñonero, J. Rodellar, J. M. Rossell, and H. R. Karimi, "Active-passive control strategy for adjacent buildings," in *Proceedings of the American Control Conference*, San Francisco, Calif, USA, 2011.
[25] F. Palacios-Quiñonero, J. M. Rossell, J. Rodellar, and H. R. Karimi, "Active-passive decentralized H_∞ control for adjacent buildings under seismic excitation," in *Proceedings of the 18th IFAC World Congress*, Milano, Italy, 2011.
[26] B. F. Spencer and S. Nagarajaiah, "State of the art of structural control," *Journal of Structural Engineering*, vol. 129, no. 7, pp. 845–856, 2003.
[27] Y. Ikeda, "Active and semi-active control of buildings in Japan," *Journal of Japan Association for Earthquake Engineering*, vol. 4, no. 3, pp. 278–282, 2004.
[28] H. Li and L. Huo, "Advances in structural control in civil engineering in China," *Mathematical Problems in Engineering*, Article ID 936081, pp. 1–23, 2010.
[29] F. Palacios-Quiñonero, J. M. Rossell, J. Rodellar, and R. Pons-López, "Passive-active vibration control for connected multi-building structures," in *Proceedings of the 8th International Conference on Structural Dynamics (Eurodyn)*, pp. 1931–1938, 2011.
[30] K. Ogata, *Modern Control Engineering*, Prentice Hall, Upper Saddle River, NJ USA, 3rd edition, 1997.
[31] R. A. Swartz and J. P. Lynch, "Strategic network utilization in a wireless structural control system for seismically excited structures," *Journal of Structural Engineering*, vol. 135, no. 5, pp. 597–608, 2009.
[32] H. Du and J. Lam, "Energy-to-peak performance controller design for building via static output feedback under consideration of actuator saturation," *Computers & Structures*, vol. 84, no. 31-32, pp. 2277–2290, 2006.
[33] W. Zhang, Y. Chen, and H. Gao, "Energy-to-peak control for seismic-excited buildings with actuator faults and parameter uncertainties," *Journal of Sound and Vibration*, vol. 330, no. 4, pp. 581–602, 2011.
[34] F. Palacios-Quiñonero, J. M. Rossell, and H. R. Karimi, "Semi-decentralized strategies in structural vibration control," *Modeling Identification and Control*, vol. 32, no. 2, pp. 57–77, 2011.
[35] J. Rubió-Massegú, F. Palacios-Quiñonero, and J. M. Rossell, "Decentralized static output-feedback H_∞ controller design for buildings under seismic excitation," *Earthquake Engineering and Structural Dynamics*, vol. 41, no. 7, pp. 1199–1205, 2012.
[36] H. Dong, Z. Wang, and H. Gao, "Distributed filtering for a class of time-varying systems over sensor networks with quantization errors and successive packet dropouts," *IEEE Transactions on Signal Processing*, vol. 60, no. 6, pp. 3164–3173, 2012.

[37] Z. Wang, B. Shen, H. Shu, and G. Wei, "Quantized H_∞ control for nonlinear stochastic time-delay systems with missing measurements," *IEEE Transactions on Automatic Control*, vol. 57, no. 6, pp. 1431–1444, 2012.

[38] Z. Wang, B. Shen, and X. Liu, "H_∞ filtering with randomly occurring sensor saturations and missing measurements," *Automatica*, vol. 48, no. 3, pp. 556–562, 2012.

[39] Y. Chen, W. Zhang, and H. Gao, "Finite frequency H_∞ control for building under earthquake excitation," *Mechatronics*, vol. 20, no. 1, pp. 128–142, 2010.

Hindawi Publishing Corporation
Mathematical Problems in Engineering
Volume 2012, Article ID 929503, 16 pages
doi:10.1155/2012/929503

Research Article

L_∞ Control with Finite-Time Stability for Switched Systems under Asynchronous Switching

Ronghao Wang,[1] Jianchun Xing,[1] Ping Wang,[1] Qiliang Yang,[1] and Zhengrong Xiang[2]

[1] *Institute of National Defense Engineering, PLA University of Science and Technology, Nanjing 210007, China*
[2] *School of Automation, Nanjing University of Science and Technology, Nanjing 210094, China*

Correspondence should be addressed to Ronghao Wang, wrh1985@yahoo.com.cn

Received 19 July 2012; Revised 23 September 2012; Accepted 23 September 2012

Academic Editor: Hamid Reza Karimi

This paper is concerned with the problem of controller design for switched systems under asynchronous switching with exogenous disturbances. The attention is focused on designing the feedback controller that guarantees the finite-time bounded and L_∞ finite-time stability of the dynamic system. Firstly, when there exists asynchronous switching between the controller and the system, a sufficient condition for the existence of stabilizing switching law for the addressed switched system is derived. It is proved that the switched system is finite-time stabilizable under asynchronous switching satisfying the average dwell-time condition. Furthermore, the problem of L_∞ control for switched systems under asynchronous switching is also investigated. Finally, a numerical example is given to illustrate the effectiveness of the proposed method.

1. Introduction

Switched systems are a class of hybrid systems consisting of subsystems and a switching law, which defines a specific subsystem being activated during a certain interval of time. Many real-world processes and systems can be modeled as switched systems such as chemical processes and computer controlled systems. Besides, switched systems are widely applied in many domains, including mechanical systems, automotive industry, aircraft and air traffic control, and many other fields [1–3].

At early time, the issue of stability of switched systems which has attracted most of the attention is one basic research topic. Lyapunov stability theory and its variations or generalizations had played an important role in this research field. Common Lyapunov function method and multiple Lyapunov functions method for switched system are

presented by researchers [4–8]. For most switched systems, it is hard to find a common Lyapunov function; however, we can guarantee the switched system is still stable under some properly chosen switching signals which are found by using the multiple Lyapunov functions technique. In addition, more researchers pay attention to average dwell-time control of switched systems [9, 10]. In particular, the average dwell-time approach is employed to deal with the control, observe, and filtering problem of switched delay systems or network control systems [11–14].

As we know, a large number of literatures related to stability of switched systems focus on Lyapunov asymptotic stability, which is defined over an infinite time interval. In many practical applications, however, the main concern is the behavior of the system over a fixed finite-time interval, for instance to avoid saturations or the excitation of nonlinear dynamics. It should be clear that a finite-time stable system may not be Lyapunov asymptotical stable, and a Lyapunov asymptotical stable system may not be finite-time stable since the transient of a system response may exceed the bound. Recently, there have been some literatures discussing the finite-time stability analysis of switched systems [15–17]. In [18], finite-time bounded and finite-time weighted L_2-gain for a class of switched delay systems with time-varying external disturbances is addressed. Reference [19] investigated finite-time control for switched discrete-time system. Considering the potential faults in a system, [20] studied fault-tolerant control with finite-time stability for switched linear systems. Delay-dependent observer-based H_∞ finite-time control for switched systems with time-varying delay was studied in [21]. In [22], the problems of finite-time stability analysis and stabilization for switched nonlinear discrete-time systems are investigated, and then the results are extended to H_∞ finite-time bounded. However, in many applications, external disturbance is always persistent bounded with infinite energy. H_∞ control cannot be employed to deal with a system with persistent bounded disturbance. In this situation, it is more appealing to develop L_∞ control for switched systems with disturbances of this type. So far, however, compared with research results on H_∞ finite-time stability, few results on L_∞ finite-time stability of switched systems have been given in the literature.

Additionally, in actual operation, there inevitably exists asynchronous switching between the controllers and the practical subsystems, that is, the real switching time of controllers exceeds or lags behind that of the practical subsystems, which will deteriorate performance of systems, even makes system out of control. Up to now, there have been a number of literatures on asynchronous switching control research of switched system [23–28]. But it is worth to point that all of these studies focus on designing the controller to guarantee the Lyapunov asymptotical stable or exponential stable of the system. To the best of our knowledge, the finite-time stabilization issue of switched system under asynchronous switching has not been fully investigated, which is quite an important issue for the switched system. This motivates us to carry out present work. In this paper, we deal with the problem of L_∞ finite-time stabilization for switched systems under asynchronous switching.

The main contributions of this paper are that several sufficient conditions ensuring the finite-time bounded and L_∞ finite-time stability are proposed with asynchronous switching between the controllers and the practical subsystems. The result shows that it is unnecessary to guarantee each subsystem can be finite-time stabilizable with L_∞ performance by the designed asynchronous switching controller. During the finite-time interval, the switching frequency only needs to be limited in some value, then the switched system is finite-time stable with L_∞ performance by the designed controller despite of the asynchronous switching between the controllers and the practical subsystems.

This paper is organized as follows. In Section 2, some preliminary definitions are provided, and the problem we deal with is precisely stated. Section 3 provides, the main results of this paper: a sufficient condition for the existence of a state feedback controller guaranteeing the finite-time stability under asynchronous switching between the controllers and the practical subsystems. Moreover, L_∞ control with finite-time stability for switched systems under asynchronous switching is provided in Section 4. Finally, a numerical example is presented by using LMI toolbox to illustrate the efficiency of the proposed method in Section 5. Our conclusions are drawn in Section 6.

Notation. Throughout this paper, A^T denotes transpose of matrix A, L_∞ denotes space of functions with bounded amplitude, $\|x(t)\|$ denotes the usually 2-norm. $\lambda_{\max}(P)$, and $\lambda_{\min}(P)$ denote the maximum and minimum eigenvalues of matrix P, respectively, I is an identity matrix with appropriate dimension. $S > 0$ denotes S is a positive definite symmetric matrix. Z denotes the integer set and Z^+ denotes the positive integer set.

2. Problem Formulation and Preliminary

A switched system is considered as follows:

$$\dot{x}(t) = A_{\sigma(t)}x(t) + B_{\sigma(t)}u(t) + G_{\sigma(t)}w(t), \tag{2.1}$$

where $x(t) \in R^n$ is the system state. $u(t) \in R^p$ is the control input, $x(t_0) = x_0$ is the initial state of the system. $w(t) \in R^q$ is the measurement noise over the interval $[t_0, T_f]$, which satisfies $\sup_{t\in[t_0,T_f]}\|w(t)\| < \infty$, $\sigma(t) : Z^+ \to \underline{N} = \{1, 2, \ldots, N\}$ is a switching signal which is a piecewise constant function depending on time t or state $x(t)$, and N denotes the number of subsystems. Moreover, $\sigma(t) = i$ means that the ith subsystem is activated. $A_i \in R^{n\times n}$, $B_i \in R^{n\times p}$, $G_i \in R^{n\times q}$ for $i \in \underline{N}$ are real-valued matrices with appropriate dimensions.

Assume that the state of the switched system (2.1) does not jump at the switching instants, that is, the trajectory $x(t)$ is everywhere continuous. The switching law $\sigma(t) : Z^+ \to \underline{N} = \{1, 2, \ldots, N\}$ discussed in this paper is time dependent, that is, $\sigma(t) : \{(t_0, \sigma(t_0)), (t_1, \sigma(t_1)), \ldots, (t_k, \sigma(t_k))\}$, $k \in Z$, where t_0 is the initial switching instant, and t_k denotes the kth switching instant.

Owing to asynchronous switching, the practical switching instant of controller is different from that of systems. For convenience, $\sigma'(t)$ is used to denote the practical switching signal of controller, $\sigma'(t)$ can be written as $\sigma'(t) : \{(t_0 + \Delta_0, \sigma(t_0)), (t_1 + \Delta_1, \sigma(t_1)), \ldots, (t_k + \Delta_k, \sigma(t_k))\}$, $k \in Z$, where $|\Delta_k| < \inf_{k\geq 0}(t_{k+1} - t_k)$, $\Delta_k > 0$ (or $|\Delta_k| < \inf_{k\geq 0}(t_k - t_{k-1})$, $\Delta_k < 0$); Δ_k represents the delayed period of the controller switching (or the exceeded period of the controller switching). In both cases, the period Δ_k is said to be the mismatched period between the controller and the system.

Remark 2.1. Mismatched period Δ_k guarantees that there always exists a period that the controller and the system operate synchronously, which makes it possible to design the stabilizable controller for the system.

Under the asynchronous switching, the switched controller can be written as

$$u(t) = K_{\sigma'(t)}x(t). \tag{2.2}$$

If we substitute the $u(t) = K_{\sigma'(t)}x(t)$ into system (2.1), we can obtain that

$$\dot{x}(t) = \left(A_{\sigma(t)} + B_{\sigma(t)}K_{\sigma'(t)}\right)x(t) + G_{\sigma(t)}w(t). \tag{2.3}$$

The following lemma will be useful for the design of controller.

Lemma 2.2 (see [29]). *If a real scalar function $\varphi(t), v(t)$ satisfies the following differential inequality:*

$$\dot{\varphi}(t) \leq \varsigma\varphi(t) + \kappa v(t), \tag{2.4}$$

then we have

$$\varphi(t) \leq e^{\varsigma(t-t_0)}\varphi(t_0) + \kappa\int_0^{t-t_0} e^{\varsigma\tau}v(t-\tau)d\tau, \tag{2.5}$$

where $\varsigma \in R,\ \kappa \in R,\ t \geq t_0$.

Let us review the definition of average dwell-time, which will be useful in designing the stabilization controller to guarantee the system finite-time stable.

Definition 2.3 (see [30]). For any $T_2 > T_1 \geq 0$, let $N_\sigma(T_1, T_2)$ denote the switching number of $\sigma(t)$ on an interval (T_1, T_2), if

$$N_\sigma(T_1, T_2) \leq N_0 + \frac{T_2 - T_1}{\tau_a} \tag{2.6}$$

holds for given $N_0 \geq 0,\ \tau_a > 0$. Then the constant τ_a is called the average dwell time, and N_0 is the chatter bound.

For switched system, the general conception of finite-time stability concerns the boundness of continuous state $x(t)$ over finite-time interval $[t_0, T_f]$ with respect to given initial condition x_0. This conception can be formulized through following definition.

Definition 2.4. The switched linear system (2.1) with $G_{\sigma(t)} \equiv 0$ is said to be finite-time stabilizable under the asynchronous switching control mode with respect to $(c_1, c_2, T_f, \sigma(t), \sigma'(t))$ with $c_1 < c_2$ and a given switching signal $\sigma(t)$, if $\|x(t)\| \leq c_2$, for all $t \in [t_0, T_f]$, whenever $\|x_0\| \leq c_1$.

Definition 2.5. Switched system (2.1) is said to be L_∞ finite-time stabilizable with respect to $(c_1, c_2, T_f, \sigma(t), \sigma'(t))$ where $c_1 < c_2$, $\sigma(t)$ is a switching signal of the system, and $\sigma'(t)$ is a switching signal of the controller, the following conditions should be satisfied.

(i) Switched linear system (2.1) with $G_{\sigma(t)} \equiv 0$ is finite-time stabilizable.

(ii) Under zero-initial condition $x(t_0) = 0$, the following inequality holds:

$$\sup_{t\in[t_0,T_f]} \|x(t)\| \leq \gamma \sup_{t\in[t_0,T_f]} \|w(t)\|, \quad \forall w(t) : \sup_{t\in[t_0,T_f]} \|w(t)\| < \infty. \tag{2.7}$$

The main issue in this paper is given as follows.

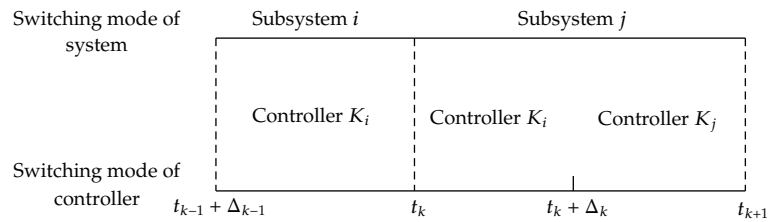

Figure 1: Asynchronous switching mode.

Given switched system (2.1), find a sufficient condition ensuring the finite-time stability with respect to $(c_1, c_2, T_f, \sigma(t), \sigma'(t))$ under the asynchronous switching control mode, then the result will be extended to the L_∞ controller design for system (2.1).

3. Finite-Time Stabilization under the Asynchronous Switching

It is assumed that the ith subsystem switched to the jth subsystem at the switching instant t_k. Owing to asynchronous switching, the switching instant of ith controller is $t_k + \Delta_k$, then there exists mismatched period at time interval $[t_k, t_k + \Delta_k)$, $\Delta_k > 0$ (or $(t_k + \Delta_k, t_k)$, $\Delta_k < 0$). In this period, the controller K_i affected the jth subsystem (or the controller K_j affected the ith subsystem).

Remark 3.1. We consider the case of $\Delta_k > 0$, that is to say, the switching time of the controller is lag of the switching time of the system. Figure 1, illustrates the asynchronous switching mode between the controller and the subsystems. From Figure 1, we can see that the controller K_i of the ith subsystem affects the ith subsystem in the matched period $[t_{k-1} + \Delta_{k-1}, t_k)$ and affects the jth subsystem in the mismatched period $[t_k, t_k + \Delta_k)$.

The following theorem presents the finite-time stabilization design method of the system (2.1) under asynchronous switching.

Theorem 3.2. *If there exist matrices $P_i > 0$, $P_{ij} > 0$, K_i and scalars $\mu_1 > 1$, $\mu_2 > 1$, $\lambda^+ > 0$, $\lambda^- > 0$ such that*

$$P_i < \mu_1 P_{ij}, \qquad P_{ij} < \mu_2 P_i, \tag{3.1}$$

$$(A_i + B_i K_i)^T P_i + P_i (A_i + B_i K_i) < \lambda^- P_i, \tag{3.2}$$

$$(A_j + B_j K_i)^T P_{ij} + P_{ij} (A_j + B_j K_i) < \lambda^+ P_{ij}, \tag{3.3}$$

$$\tau_a > \frac{(T_f - t_0)\ln(\mu_1\mu_2)}{\ln\left((\varepsilon^2/\delta^2)\cdot \mathcal{B}\cdot\left(\mu_2/(\mu_1\mu_2)^{N_0}\right)\right) - \lambda^+ T^+(t_0, T_f) - \lambda^- T^-(t_0, T_f)}, \tag{3.4}$$

where $\mathcal{B}$ denotes $\inf_{i,j\in\underline{N}}\{\lambda_{\min}(P_i), \lambda_{\min}(P_{ij})\}/\sup_{i,j\in\underline{N}}\{\lambda_{\max}(P_i), \lambda_{\max}(P_{ij})\}$, then switched system (2.1) is finite-time stabilizable with respect to $(\delta, \varepsilon, T_f, \overline{\sigma}(t), \sigma'(t))$ under the feedback controller $u(t) = K_{\sigma'(t)}x(t)$, where $T^-(t_0, T_f)$ and $T^+(t_0, T_f)$ denote the matched period and the mismatched period in finite-time interval $[t_0, T_f]$, respectively.

Proof. Here, we only discuss the situation of $\Delta_k > 0$. For $\Delta_k < 0$, the proof method is similar, and we can reach the same conclusion.

When $t \in [t_{k-1} + \Delta_{k-1}, t_k)$, for the ith subsystem, the state feedback controller $u(t) = K_i x(t)$. So the state equation of closed-loop system can be written as

$$\dot{x}(t) = (A_i + B_i K_i)x(t). \tag{3.5}$$

Choose a switching Lyapunov function as follows:

$$V_i(t) = x^T(t)P_i x(t). \tag{3.6}$$

By (3.2), it implies that

$$\dot{V}_i(t) < \lambda^- V_i(t). \tag{3.7}$$

When $t \in [t_k, t_k + \Delta_k)$, for the jth subsystem, the state feedback controller is still $u(t) = K_i x(t)$. So the closed-loop system can be described as

$$\dot{x}(t) = \left(A_j + B_j K_i\right)x(t). \tag{3.8}$$

Consider the Lyapunov function candidate as follows:

$$V_{ij}(t) = x^T(t)P_{ij}x(t). \tag{3.9}$$

By (3.3), we can obtain that

$$\dot{V}_{ij}(t) < \lambda^+ V_{ij}(t). \tag{3.10}$$

Notice that the Lyapunov function (3.6) and (3.9) can be rewritten as

$$\begin{aligned} V_i(t) &= x^T(t)P_i x(t), \quad t \in [t_{k-1} + \Delta_{k-1}, t_k),\ k = 1, 2, \ldots, \\ V_i(t) &= x^T(t)P_{ij}x(t), \quad t \in [t_k, t_k + \Delta_k),\ k = 0, 1, \ldots. \end{aligned} \tag{3.11}$$

Let $t_0 < t_1 < t_2 < \cdots < t_k = T_f$ is the switching time in the period $[t_0, T_f]$, we define the following piecewise Lyapunov function:

$$V(t) = \begin{cases} x^T(t)P_i x(t), & t \in [t_r + \Delta_r, t_{r+1}),\ r = 0, 1, \ldots, k-1, \\ x^T(t)P_{ij}x(t), & t \in [t_r, t_r + \Delta_r), \quad r = 0, 1, \ldots, k-1. \end{cases} \tag{3.12}$$

By (3.7) and (3.10), we can obtain that

$$\begin{aligned}
V(t) &< e^{\lambda^-(t-t_{k-1}-\Delta_{k-1})}V(t_{k-1}+\Delta_{k-1}) \\
&< \mu_1 e^{\lambda^-(t-t_{k-1}-\Delta_{k-1})}V\left((t_{k-1}+\Delta_{k-1})^-\right) \\
&< \mu_1 e^{\lambda^+\Delta_{k-1}}e^{\lambda^-(t-t_{k-1}-\Delta_{k-1})}V(t_{k-1}) \\
&< \mu_1\mu_2 e^{\lambda^+\Delta_{k-1}}e^{\lambda^-(t-t_{k-1}-\Delta_{k-1})}V\left(t_{k-1}^-\right) \\
&< \mu_1\mu_2 e^{\lambda^+\Delta_{k-1}}e^{\lambda^-(t-t_{k-1}-\Delta_{k-1})}e^{\lambda^-(t_{k-1}-t_{k-2}-\Delta_{k-2})}V(t_{k-2}+\Delta_{k-2}) \\
&< \mu_1^2\mu_2 e^{\lambda^+\Delta_{k-1}}e^{\lambda^-(t-t_{k-1}-\Delta_{k-1})}e^{\lambda^-(t_{k-1}-t_{k-2}-\Delta_{k-2})}V\left((t_{k-2}+\Delta_{k-2})^-\right) \\
&< \mu_1^2\mu_2 e^{\lambda^+\Delta_{k-1}}e^{\lambda^+\Delta_{k-2}}e^{\lambda^-(t-t_{k-1}-\Delta_{k-1})}e^{\lambda^-(t_{k-1}-t_{k-2}-\Delta_{k-2})}V(t_{k-2}) \\
&= \mu_1^2\mu_2 e^{\lambda^+(\Delta_{k-1}+\Delta_{k-2})+\lambda^-[(t-t_{k-1}-\Delta_{k-1})+(t_{k-1}-t_{k-2}-\Delta_{k-2})]}V(t_{k-2}) \\
&\cdots \\
&< \mu_1^k\mu_2^{k-1}e^{\lambda^+(\Delta_{k-1}+\cdots+\Delta_0)+\lambda^-[(t-t_{k-1}-\Delta_{k-1})+(t_{k-1}-t_{k-2}-\Delta_{k-2})+\cdots+(t_1-t_0-\Delta_0)]}V(t_0) \\
&< \mu_2^{-1}(\mu_1\mu_2)^{k_{[t_0,T_f]}}e^{\lambda^+T^+(t_0,T_f)+\lambda^-T^-(t_0,T_f)}V(t_0),
\end{aligned} \tag{3.13}$$

where $T^+(t_0,T_f)$ denotes the sum of the mismatched period between the controllers and subsystem in (t_0,T_f). $T^-(t_0,T_f)$ denotes the sum of the matched period between the controllers and subsystem in $[t_0,T_f]$.

And from (3.12) we have

$$V(t) \geq \inf_{i,j\in\underline{N}}\left\{\lambda_{\min}(P_i),\lambda_{\min}(P_{ij})\right\}\|x(t)\|^2. \tag{3.14}$$

On the other hand, for $i \in \underline{N}$, we have

$$V(t_0) \leq \sup_{i,j\in\underline{N}}\left\{\lambda_{\max}(P_i),\lambda_{\max}(P_{ij})\right\}\|x(t_0)\|^2. \tag{3.15}$$

Using the fact

$$\|x(t_0)\| \leq \delta, \tag{3.16}$$

we get

$$V(t_0) \leq \sup_{i,j\in\underline{N}}\left\{\lambda_{\max}(P_i),\lambda_{\max}(P_{ij})\right\}\delta^2. \tag{3.17}$$

Altogether (3.13)–(3.17), the following inequality can be derived

$$\|x(t)\|^2 \leq \mu_2^{-1}(\mu_1\mu_2)^{k_{[t_0,T_f]}} e^{\lambda^+T^+(t_0,T_f)+\lambda^-T^-(t_0,T_f)} \frac{\sup_{i,j\in\underline{N}}\{\lambda_{\max}(P_i),\lambda_{\max}(P_{ij})\}}{\inf_{i,j\in\underline{N}}\{\lambda_{\min}(P_i),\lambda_{\min}(P_{ij})\}}\delta^2. \tag{3.18}$$

From the Definition 2.3, we know that $k_{[t_0,T_f]} = N_\sigma$, then we have the relation

$$k_{[t_0,T_f]} \leq N_0 + \frac{T_f - t_0}{\tau_a}. \tag{3.19}$$

From (3.4) and (3.19), we get

$$\mu_2^{-1}(\mu_1\mu_2)^{k_{[t_0,T_f]}} e^{\lambda^+T^+(t_0,T_f)+\lambda^-T^-(t_0,T_f)} \frac{\sup_{i,j\in\underline{N}}\{\lambda_{\max}(P_i),\lambda_{\max}(P_{ij})\}}{\inf_{i,j\in\underline{N}}\{\lambda_{\min}(P_i),\lambda_{\min}(P_{ij})\}}\delta^2 < \varepsilon^2. \tag{3.20}$$

According to (3.18) and (3.20), we have

$$\|x(t)\| < \varepsilon. \tag{3.21}$$

The proof is completed. □

Remark 3.3. From (3.2) and (3.3), we know that for finite-time stabilization issue, the subsystem needs not to be stabilized in finite-time interval, that is to say, the designed asynchronous switching controller needs not to stabilize the subsystem in the matched period and the mismatched period in finite-time interval $[t_0, T_f]$, but the whole system is finite-time stabilizable. Reference [31] gives the exponential stabilization condition under asynchronous switching, which requests that the subsystem can be exponentially stabilized in the matched period. But as to the problem of finite-time stabilization, it is unnecessary to request that the subsystem can be stabilized in the matched period or mismatched period. In particular, when $\lambda^+ = \lambda^- = \lambda$ in (3.2) and (3.3), (3.4) becomes

$$\tau_a > \frac{(T_f - t_0)\ln(\mu_1\mu_2)}{\ln\left((\varepsilon^2/\delta^2)\cdot\mathcal{B}\cdot\left(\mu_2/(\mu_1\mu_2)^{N_0}\right)\right) - \lambda(T_f - t_0)} \tag{3.22}$$

which is independent of $T^+(t_0, T_f)$ and $T^-(t_0, T_f)$.

Remark 3.4. In fact, (3.4) in Theorem 3.2 implies that if switching sequence $\sigma(t) : \{(t_0, \sigma(t_0)), (t_1, \sigma(t_1)), \ldots, (t_k, \sigma(t_k))\}$ of the system can be prespecified, that is, τ_a is a known constant,

the matched period $T^-(t_0, T_f)$ and the mismatched period $T^+(t_0, T_f)$ should satisfy the following relation:

$$\lambda^+ T^+(t_0, T_f) + \lambda^- T^-(t_0, T_f) < \ln\left(\frac{\varepsilon^2}{\delta^2} \cdot \frac{\inf_{i,j\in\underline{N}}\{\lambda_{\min}(P_i), \lambda_{\min}(P_{ij})\}}{\sup_{i,j\in\underline{N}}\{\lambda_{\max}(P_i), \lambda_{\max}(P_{ij})\}} \cdot \frac{\mu_2}{(\mu_1\mu_2)^{N_0}}\right) - \frac{(T_f - t_0)\ln(\mu_1\mu_2)}{\tau_a}. \tag{3.23}$$

Remark 3.5. Reference [31] gives the design method of exponential stabilization controller under asynchronous switching. The condition implies that the ratio of the mismatched period and the matched period should be less than some value which means that the matched period should be large enough to stabilize the subsystem. However, from the condition of Theorem 3.2, we know that when the switching sequence is unknown, the ratio of the mismatched period and the matched period can be designed freely to guarantee the finite-time stability of the system by the asynchronous switched controller. But if switching sequence of the system is prespecified, the ratio of the mismatched period and the matched period may need to be limited. On the other hand, the average dwell-time scheme with Lyapunov stability limits the dwell-time τ_a and the ratio of $T^+(t_0, T_f)$ and $T^-(t_0, T_f)$ to satisfy the proposed condition in [31] at the same time. But for the average dwell-time scheme with finite-time stability, we can predetermine one value among two parameters of the dwell-time τ_a and the ratio of $T^+(t_0, T_f)$ and $T^-(t_0, T_f)$, then the other value can be determined by the condition (3.4).

Remark 3.6. In order to get the solution of the asynchronous switched controller K_i, we denote $X_i = P_i^{-1}$, $X_{ij} = P_{ij}^{-1}$, $W_i = K_i P_i^{-1}$, then (3.1) to (3.3) can be written as

$$\mu_1 X_i > X_{ij}, \qquad \mu_2 X_{ij} > X_i, \tag{3.24}$$

$$(A_i X_i + B_i W_i)^T + (A_i X_i + B_i W_i) < \lambda^- X_i, \tag{3.25}$$

$$X_{ij}\left(A_j + B_j W_i X_i^{-1}\right)^T + \left(A_j + B_j W_i X_i^{-1}\right) X_{ij} < \lambda^+ X_{ij}. \tag{3.26}$$

It is noticed that the matrix inequalities (3.24), (3.25), and(3.26) are coupled. Therefore, we can firstly solve the linear matrix inequality (3.25) to obtain the solution to matrices X_i and W_i. Then we solve the matrix inequality (3.24), (3.26) by substituting X_i and W_i into (3.24), (3.26). By adjusting the parameter μ_1, μ_2, and λ^+ appropriately, we seek the feasible solutions X_i, W_i and X_{ij} such that the matrix inequalities (3.24) and (3.26) hold. If the chosen parameters μ_1, μ_2, and λ^+ have no feasible solution, we can adjust μ_1, μ_2, or λ^+ to be larger. Following this guideline, the solution to the matrix inequalities (3.24)to (3.26) will be found.

4. L_∞ Finite-Time Stabilization under the Asynchronous Switching

Now, we are in a position to investigate L_∞ finite-time stabilization design method of the system (2.1) under asynchronous switching.

Theorem 4.1. *If there exist matrices $P_i > 0$, $P_{ij} > 0$, K_i and scalars $\mu_1 > 1$, $\mu_2 > 1$, $\lambda^+ > 0$, $\lambda^- > 0$ such that*

$$P_i < \mu_1 P_{ij}, \qquad P_{ij} < \mu_2 P_i, \tag{4.1}$$

$$\begin{bmatrix} (A_i + B_i K_i)^T P_i + P_i (A_i + B_i K_i) - \lambda^- P_i & P_i G_i \\ G_i^T P_i & -\varepsilon_i I \end{bmatrix} < 0, \tag{4.2}$$

$$\begin{bmatrix} (A_j + B_j K_i)^T P_{ij} + P_{ij} (A_j + B_j K_i) - \lambda^+ P_{ij} & P_{ij} G_j \\ G_j^T P_{ij} & -\varepsilon_{ij} I \end{bmatrix} < 0, \tag{4.3}$$

$$\tau_a > \frac{(T_f - t_0)\ln(\mu_1\mu_2)}{\ln\left((\varepsilon^2/\delta^2)\cdot \mathcal{B}\cdot\left(\mu_2/(\mu_1\mu_2)^{N_0}\right)\right) - \lambda^+ T^+(t_0, T_f) - \lambda^- T^-(t_0, T_f)}. \tag{4.4}$$

L_∞ disturbance attenuation performance $\gamma^- \le \sqrt{\varepsilon_i (e^{\lambda^- T^-(t_0,T_f)} - 1)/\lambda^- \lambda_{\min}(P_i)}$ during the matched period and $\gamma^+ \le \sqrt{\varepsilon_{ij} (e^{\lambda^+ T^+(t_0,T_f)} - 1)/\lambda^+ \lambda_{\min}(P_{ij})}$ during the mismatched period, then switched system (2.1) *is finite-time stabilizable of L_∞ disturbance attenuation performance with respect to $(\delta, \varepsilon, T_f, \sigma(t), \sigma'(t))$ under the feedback controller $u(t) = K_{\sigma'(t)} x(t)$, where $T^-(t_0, T_f)$ and $T^+(t_0, T_f)$ denote the matched period and the mismatched period in finite-time interval $[t_0, T_f]$, respectively.*

Proof. It can be concluded from Theorem 4.1 that system (2.1) is finite-time stable under the feedback controller $u(t) = K_{\sigma'(t)} x(t)$.

When $t \in [t_{k-1} + \Delta_{k-1}, t_k)$, for the ith subsystem, the state feedback controller $u(t) = K_i x(t)$. So the state equation of closed-loop system can be written as

$$\dot{x}(t) = (A_i + B_i K_i) x(t) + G_i w(t). \tag{4.5}$$

Choose a switching Lyapunov function as follows:

$$V_i(t) = x^T(t) P_i x(t), \quad t \in [t_{k-1} + \Delta_{k-1}, t_k),\ k = 1, 2, \ldots. \tag{4.6}$$

By (4.2), it implies that

$$\dot{V}_i(t) \le \lambda^- V_i(t) + \varepsilon_i w^T(t) w(t). \tag{4.7}$$

With zero initial conditions, by Lemma 2.2, we have

$$V_i(t) \le \varepsilon_i \int_0^{t - t_{k-1} - \Delta_{k-1}} e^{\lambda^- \tau} w^T(t - \tau) w(t - \tau) d\tau. \tag{4.8}$$

Note that

$$V_i(t) \ge \lambda_{\min}(P_i) \|x(t)\|^2. \tag{4.9}$$

From (4.8) and (4.9), we can obtain

$$\lambda_{\min}(P_i) \sup_{t\in[t_{k-1}+\Delta_{k-1},t_k)} \|x(t)\|^2 \le \frac{\varepsilon_i\left(e^{\lambda^- T^-(t_0,T_f)}-1\right)}{\lambda^-} \sup_{t\in[t_{k-1}+\Delta_{k-1},t_k)} \|w(t)\|^2. \tag{4.10}$$

From (4.10), we have

$$\frac{\sup_{t\in[t_{k-1}+\Delta_{k-1},t_k)}\|x(t)\|}{\sup_{t\in[t_{k-1}+\Delta_{k-1},t_k)}\|w(t)\|} \le \sqrt{\frac{\varepsilon_i\left(e^{\lambda^- T^-(t_0,T_f)}-1\right)}{\lambda^-\lambda_{\min}(P_i)}}. \tag{4.11}$$

When $t \in [t_k, t_k+\Delta_k)$, for the jth subsystem, the state feedback controller is still $u(t) = K_i x(t)$. So the closed-loop system can be described as

$$\dot{x}(t) = \left(A_j + B_j K_i\right)x(t) + G_j w(t). \tag{4.12}$$

Consider the Lyapunov function candidate as follows:

$$V_{ij}(t) = x^T(t)P_{ij}x(t), \quad t \in [t_k, t_k+\Delta_k),\ k = 0,1,\ldots. \tag{4.13}$$

By (4.3), it implies that

$$\dot{V}_{ij}(t) \le \lambda^+ V_{ij}(t) + \varepsilon_{ij} w^T(t)w(t). \tag{4.14}$$

With zero initial conditions, by Lemma 2.2, we have

$$V_{ij}(t) \le \varepsilon_{ij}\int_0^{t-t_k} e^{\lambda^+\tau} w^T(t-\tau)w(t-\tau)d\tau. \tag{4.15}$$

Notice that

$$V_{ij}(t) \ge \lambda_{\min}\left(P_{ij}\right)\|x(t)\|^2\ . \tag{4.16}$$

From (4.15) and (4.16), we can obtain

$$\lambda_{\min}\left(P_{ij}\right) \sup_{t\in[t_k,t_k+\Delta_k)} \|x(t)\|^2 \le \frac{\varepsilon_{ij}\left(e^{\lambda^+ T^+(t_0,T_f)}-1\right)}{\lambda^+} \sup_{t\in[t_k,t_k+\Delta_k)} \|w(t)\|^2. \tag{4.17}$$

From (4.17), we have

$$\frac{\sup_{t\in[t_k,t_k+\Delta_k)}\|x(t)\|}{\sup_{t\in[t_k,t_k+\Delta_k)}\|w(t)\|} \le \sqrt{\frac{\varepsilon_{ij}\left(e^{\lambda^+ T^+(t_0,T_f)}-1\right)}{\lambda^+\lambda_{\min}\left(P_{ij}\right)}}\ . \tag{4.18}$$

By (4.11) and (4.18), during the finite-time $[t_0, T_f] = \bigcup_{r=0}^{k-1}[t_r, t_r + \Delta_r) \cup [t_r + \Delta_r, t_{r+1})$, we can obtain

$$\frac{\sup_{t\in[t_0,T_f)}\|x(t)\|}{\sup_{t\in[t_0,T_f)}\|w(t)\|} \leq \max\left(\sqrt{\frac{e^{\lambda^- T^-(t_0,T_f)}-1}{\lambda^-}\max_{i\in\underline{N}}\left(\frac{\varepsilon_i}{\lambda_{\min}(P_i)}\right)}, \sqrt{\frac{e^{\lambda^+ T^+(t_0,T_f)}-1}{\lambda^+}\max_{i,j\in\underline{N}}\left(\frac{\varepsilon_{ij}}{\lambda_{\min}(P_{ij})}\right)}\right) \tag{4.19}$$

By the definition of L_∞ finite-time stabilization, we can obtain that the designed controller $u(t) = K_{\sigma'(t)}x(t)$ can guarantee the finite-time stability of L_∞ disturbance attenuation performance. This completes the proof. □

Remark 4.2. Theorem 4.1 represents that if each subsystem satisfies L_∞ disturbance attenuation performance during the mismatched period and the matched period, the designed asynchronous switched controller $u(t) = K_{\sigma'(t)}x(t)$ can guarantee the whole system has L_∞ disturbance attenuation performance. However, the condition of each subsystem satisfying L_∞ disturbance attenuation performance during the mismatched period and the matched period seems to be more conservative, and in fact through the following theorem, this condition is not essential.

Remark 4.3. Although Theorem 4.1 gives the method of finite-time stabilization with L_∞ disturbance attenuation performance, the matched period $T^-(t_0, T_f)$ and the mismatched period $T^+(t_0, T_f)$ need to be prespecified in order to obtain L_∞ disturbance attenuation performance of the system. However, in practical engineering it is difficult to obtain the matched period $T^-(t_0, T_f)$ and the mismatched period $T^+(t_0, T_f)$ before designing the controller. Based on these, the following result can be derived.

Theorem 4.4. *If there exist matrices $P_i > 0$, $P_{ij} > 0, K_i$ and scalars $\mu_1 > 1$, $\mu_2 > 1, \lambda^+ > 0, \lambda^- > 0$ such that*

$$P_i < \mu_1 P_{ij}, \qquad P_{ij} < \mu_2 P_i, \tag{4.20}$$

$$\begin{bmatrix} (A_i + B_i K_i)^T P_i + P_i(A_i + B_i K_i) - \lambda^- P_i & P_i G_i \\ G_i^T P_i & -\varepsilon_i I \end{bmatrix} < 0, \tag{4.21}$$

$$\begin{bmatrix} (A_j + B_j K_i)^T P_{ij} + P_{ij}(A_j + B_j K_i) - \lambda^+ P_{ij} & P_{ij} G_j \\ G_j^T P_{ij} & -\varepsilon_{ij} I \end{bmatrix} < 0\ , \tag{4.22}$$

$$\tau_a > \frac{(T_f - t_0)\ln(\mu_1\mu_2)}{\ln\left((\varepsilon^2/\delta^2)\cdot\mathcal{B}\cdot\left(\mu_2/(\mu_1\mu_2)^{N_0}\right)\right) - \lambda^+ T^+(t_0, T_f) - \lambda^- T^-(t_0, T_f)} \tag{4.23}$$

and in finite-time interval $[t_0, T_f]$ the measurement noise $w(t)$ satisfies $\sup_{t\in[t_0,T_f]}\|w(t)\| < \infty$, then switched system (2.1) is finite-time stabilizable of L_∞ disturbance attenuation performance $\gamma = \sqrt{\max_{i,j\in\underline{N}}(\varepsilon_i, \varepsilon_{ij})(e^{\max(\lambda^+,\lambda^-)(T_f-t_0)} - 1)/\max(\lambda^+, \lambda^-)\min_{i,j\in\underline{N}}(\lambda_{\min}(P_i), \lambda_{\min}(P_{ij}))}$ with respect to $(\delta, \varepsilon, T_f, \sigma(t), \sigma'(t))$ under the feedback controller $u(t) = K_{\sigma'(t)}x(t)$, where $T^-(t_0, T_f)$ and $T^+(t_0, T_f)$ denote the matched period and the mismatched period in finite-time interval $[t_0, T_f]$, respectively.

Proof. At first, from Theorem 4.4, system (2.1) is finite-time stable under the feedback controller $u(t) = K_{\sigma'(t)}x(t)$.

Then following the proof line of Theorem 4.1 and considering (4.6) and (4.13), we can define piecewise Lyapunov function

$$V(t) = \begin{cases} x^T(t)P_i x(t), & t \in [t_r + \Delta_r, t_{r+1}), \ r = 0, 1, \ldots, k-1, \\ x^T(t)P_{ij} x(t), & t \in [t_r, t_r + \Delta_r), \quad r = 0, 1, \ldots, k-1. \end{cases} \tag{4.24}$$

By (4.21) and (4.22), it implies that

$$\dot{V}(t) \leq \max(\lambda^+, \lambda^-)V(t) + \max_{i,j\in\underline{N}}(\varepsilon_i, \varepsilon_{ij})w^T(t)w(t). \tag{4.25}$$

With zero initial conditions, by Lemma 2.2, we have

$$V(t) \leq \max_{i,j\in\underline{N}}(\varepsilon_i, \varepsilon_{ij}) \int_0^{T_f - t_0} e^{\max(\lambda^+,\lambda^-)\tau} w^T(t-\tau)w(t-\tau)d\tau. \tag{4.26}$$

Notice that

$$V(t) \geq \min_{i,j\in\underline{N}}(\lambda_{\min}(P_i), \lambda_{\min}(P_{ij}))\|x(t)\|^2 \ . \tag{4.27}$$

From (4.26) and (4.27), we can obtain

$$\min_{i,j\in\underline{N}}(\lambda_{\min}(P_i), \lambda_{\min}(P_{ij})) \sup_{t\in[t_0,T_f]} \|x(t)\|^2 \leq \frac{\max_{i,j\in\underline{N}}(\varepsilon_i, \varepsilon_{ij})\left(e^{\max(\lambda^+,\lambda^-)(T_f - t_0)} - 1\right)}{\max(\lambda^+, \lambda^-)} \sup_{t\in[t_0,T_f]} \|w(t)\|^2. \tag{4.28}$$

From (4.28), we have

$$\frac{\sup_{t\in[t_0,T_f]}\|x(t)\|}{\sup_{t\in[t_0,T_f]}\|w(t)\|} \leq \sqrt{\frac{\max_{i,j\in\underline{N}}(\varepsilon_i, \varepsilon_{ij})\left(e^{\max(\lambda^+,\lambda^-)(T_f - t_0)} - 1\right)}{\max(\lambda^+, \lambda^-)\min_{i,j\in\underline{N}}(\lambda_{\min}(P_i), \lambda_{\min}(P_{ij}))}}. \tag{4.29}$$

By the definition of L_∞ finite-time stabilization, we can obtain that the designed controller $u(t) = K_{\sigma'(t)}x(t)$ can guarantee the finite-time stability of L_∞ disturbance attenuation performance. This completes the proof. □

Remark 4.5. It should be pointed out that the conditions in Theorems 4.4 are not standard LMIs conditions. However, through the variable substitution, (4.20) to (4.22) can be solved following the method proposed in Remark 3.6.

Remark 4.6. Theorem 4.4 presents that if the measurement noise $w(t)$ is magnitude bounded during finite-time interval $[t_0, T_f]$, then we can design the asynchronous switching controller

such that the system has L_∞ disturbance attenuation performance. However, it is unnecessary to guarantee L_∞ disturbance attenuation performance during the mismatched period and the matched period by the designed controller which is less conservative than Theorem 4.1.

5. Numerical Example

We consider an example to illustrate the main result. Consider the switched linear system given by the system (2.1) with $u(t) = K_{\sigma'(t)}x(t)$,

$$\dot{x}(t) = \left(A_{\sigma(t)} + B_{\sigma(t)}K_{\sigma'(t)}\right)x(t) + G_{\sigma(t)}w(t), \tag{5.1}$$

where $A_1 = \left[\begin{smallmatrix} -1 & 0 \\ 0 & 0.1 \end{smallmatrix}\right]$, $A_2 = \left[\begin{smallmatrix} 2.1 & 1 \\ 0 & 0.3 \end{smallmatrix}\right]$, $B_1 = \left[\begin{smallmatrix} 0.2 & 0.14 \\ 0 & 2 \end{smallmatrix}\right]$, $B_2 = \left[\begin{smallmatrix} 1 & 0 \\ 0.3 & 0.1 \end{smallmatrix}\right]$, $G_1 = \left[\begin{smallmatrix} 0.2 & 0 \\ 0.3 & 0.1 \end{smallmatrix}\right]$, $G_2 = \left[\begin{smallmatrix} 0.1 & 0.2 \\ 0.4 & 0 \end{smallmatrix}\right]$.

Applying Theorem 4.4 and solving corresponding matrix inequalities lead to feasible solutions, when $\delta = 0.1$, $\varepsilon = 10$, $\varepsilon_1 = \varepsilon_2 = 100$, $\varepsilon_{12} = \varepsilon_{21} = 10$, $\mu_1 = \mu_2 = 20$, $\lambda^+ = 100$, $\lambda^- = 10$, $T_f = 0.005$, $t_0 = 0, N_0 = 0$, $\tau_a = 0.00375$.

$$\begin{gathered} K_1 = \begin{bmatrix} 9.6364 & 1.4424 \\ -10.3539 & 0.4207 \end{bmatrix}, \qquad K_2 = \begin{bmatrix} 2.1337 & 0.4083 \\ -0.6623 & 3.5807 \end{bmatrix}, \\ X_1 = \begin{bmatrix} 8.2146 & -14.6028 \\ -14.6028 & 86.9322 \end{bmatrix}, \qquad X_2 = \begin{bmatrix} 92.6569 & 14.6028 \\ 14.6028 & 13.9393 \end{bmatrix}, \\ X_{12} = \begin{bmatrix} 7.9844 & -0.3851 \\ -0.3851 & 9.9854 \end{bmatrix}, \qquad X_{21} = \begin{bmatrix} 10.1766 & 0.1461 \\ 0.1461 & 8.7611 \end{bmatrix}. \end{gathered} \tag{5.2}$$

Then from (3.23), we know that the matched period $T^-(t_0, T_f)$ and the mismatched period $T^+(t_0, T_f)$ satisfy the following relation:

$$100T^+\left(t_0, T_f\right) + 10T^-\left(t_0, T_f\right) < 0.36. \tag{5.3}$$

Notice that $T^+(t_0, T_f) + T^-(t_0, T_f) = 0.005$, then we have

$$\begin{gathered} T^+\left(t_0, T_f\right) < 0.003, \\ 0.003 < T^-\left(t_0, T_f\right) < 0.005. \end{gathered} \tag{5.4}$$

the L_∞ state feedback controller K_1, K_2 can guarantee that system (5.1) is finite-time stabilizable with respect to $(0.1, 10, 0.005, \sigma(t), \sigma'(t))$ under the asynchronous switching where L_∞ disturbance attenuation performance $\gamma = 7.8$.

6. Conclusions

The L_∞ finite-time stabilization problems for switched linear system are addressed in this paper. When there exists asynchronous switching between the controller and the system, a sufficient condition for the existence of stabilizing switching law for the addressed

switched system is derived. It is proved that the switched system is finite-time stabilizable under asynchronous switching satisfying the average dwell-time condition. Furthermore, the problem of L_∞ control for switched systems under asynchronous switching is also investigated. At last, a numerical example is given to illustrate the effectiveness of the proposed method.

Acknowledgments

This work was supported by the Pre-Research Foundation of PLA University of Science and Technology under Grant no. 20110316 and the National Natural Science Foundation of China under Grants nos. 60974027 and 61273120.

References

[1] P. Varaiya, "Smart cars on smart roads: problems of control," *IEEE Transactions on Automatic Control*, vol. 38, no. 2, pp. 195–207, 1993.
[2] W. S. Wong and R. W. Brockett, "Systems with finite communication bandwidth constraints. I. State estimation problems," *IEEE Transactions on Automatic Control*, vol. 42, no. 9, pp. 1294–1299, 1997.
[3] C. Tomlin, G. J. Pappas, and S. Sastry, "Conflict resolution for air traffic management: a study in multiagent hybrid systems," *IEEE Transactions on Automatic Control*, vol. 43, no. 4, pp. 509–521, 1998.
[4] D. Liberzon and A. S. Morse, "Basic problems in stability and design of switched systems," *IEEE Control Systems Magazine*, vol. 19, no. 5, pp. 59–70, 1999.
[5] J. Zhao and D. J. Hill, "Vector L_2-gain and stability of feedback switched systems," *Automatica*, vol. 45, no. 7, pp. 1703–1707, 2009.
[6] X.-M. Sun, J. Zhao, and D. J. Hill, "Stability and L_2-gain analysis for switched delay systems: a delay-dependent method," *Automatica*, vol. 42, no. 10, pp. 1769–1774, 2006.
[7] M. S. Branicky, "Multiple Lyapunov functions and other analysis tools for switched and hybrid systems," *IEEE Transactions on Automatic Control*, vol. 43, no. 4, pp. 475–482, 1998.
[8] Y. G. Sun, L. Wang, and G. Xie, "Stability of switched systems with time-varying delays: delay-dependent common Lyapunov functional approach," in *Proceedings of the American Control Conference*, pp. 1544–1549, Minneapolis, Minn, USA, June 2006.
[9] G. Zhai, B. Hu, K. Yasuda, and A. N. Michel, "Stability analysis of switched systems with stable and unstable subsystems: an average dwell time approach," in *Proceedings of the American Control Conference*, pp. 200–204, June 2000.
[10] J. P. Hespanha and A. S. Morse, "Stability of switched systems with average dwell-time," in *Proceedings of the 38th IEEE Conference on Decision and Control (CDC '99)*, pp. 2655–2660, December 1999.
[11] M. Liu, D. W. C. Ho, and Y. Niu, "Stabilization of Markovian jump linear system over networks with random communication delay," *Automatica*, vol. 45, no. 2, pp. 416–421, 2009.
[12] D. Wang, P. Shi, J. Wang, and W. Wang, "Delay-dependent exponential H∞ filtering for discrete-time switched delay systems," *International Journal of Robust and Nonlinear Control*, vol. 22, no. 13, pp. 1522–1536, 2012.
[13] D. Wang, W. Wang, and P. Shi, "Delay-dependent exponential stability for switched delay systems," *Optimal Control Applications & Methods*, vol. 30, no. 4, pp. 383–397, 2009.
[14] J. Lian, Z. Feng, and P. Shi, "Observer design for switched recurrent neural networks: an average dwell time approach," *IEEE Transactions on Neural Networks*, vol. 22, no. 10, pp. 1547–1556, 2011.
[15] W. M. Xiang, J. Xiao, and C. Y. Xiao, "Finite-time stability analysis for switched linear systems," in *Proceedings of the Chinese Control and Decision Conference*, pp. 3115–3120, Mianyang, China, 2011.
[16] X. Lin, H. Du, and S. Li, "Set finite-time stability of a class of switched systems," in *Proceedings of the 8th World Congress on Intelligent Control and Automation (WCICA '10)*, pp. 7073–7078, Jinan, China, July 2010.
[17] H. Du, X. Lin, and S. Li, "Finite-time stability and stabilization of switched linear systems," in *Proceedings of the 48th IEEE Conference on Decision and Control Held Jointly with 28th Chinese Control Conference (CDC/CCC '09)*, pp. 1938–1943, Shanghai, China, December 2009.

[18] X. Lin, H. Du, and S. Li, "Finite-time boundedness and L_2-gain analysis for switched delay systems with norm-bounded disturbance," *Applied Mathematics and Computation*, vol. 217, no. 12, pp. 5982–5993, 2011.

[19] W. M. Xiang and Y. C. Zhao, "Finite-time control for switched discrete-time system," *Energy Procedia*, vol. 13, pp. 4486–4491, 2011.

[20] S. Gao and X. L. Zhang, "Fault-tolerant control with finite-time stability for switched linear systems," in *Proceedings of the 6th International Conference on Computer Science & Education*, pp. 923–927, 2011.

[21] H. Liu, Y. Shen, and X. D. Zhao, "Delay-dependent observer-based H_∞ finite-time control for switched systems with time-varying delay," *Nonlinear Analysis: Hybrid Systems*, vol. 6, pp. 885–898, 2012.

[22] W. Xiang and J. Xiao, "H_∞ finite-time control for switched nonlinear discrete-time systems with norm-bounded disturbance," *Journal of the Franklin Institute*, vol. 348, no. 2, pp. 331–352, 2011.

[23] Z. R. Xiang and R. H. Wang, "Robust control for uncertain switched non-linear systems with time delay under asynchronous switching," *IET Control Theory & Applications*, vol. 3, no. 8, pp. 1041–1050, 2009.

[24] L. Zhang and P. Shi, "Stability, L_2-gain and asynchronous H_∞ control of discrete-time switched systems with average dwell time," *IEEE Transactions on Automatic Control*, vol. 54, no. 9, pp. 2192–2199, 2009.

[25] L. Zhang and H. Gao, "Asynchronously switched control of switched linear systems with average dwell time," *Automatica*, vol. 46, no. 5, pp. 953–958, 2010.

[26] Z. Xiang and Q. Chen, "Robust reliable control for uncertain switched nonlinear systems with time delay under asynchronous switching," *Applied Mathematics and Computation*, vol. 216, no. 3, pp. 800–811, 2010.

[27] J. Lin, S. Fei, and Z. Gao, "Stabilization of discrete-time switched singular time-delay systems under asynchronous switching," *Journal of the Franklin Institute*, vol. 349, no. 5, pp. 1808–1827, 2012.

[28] D. Xie, Q. Wang, and Y. Wu, "Average dwell-time approach to L_2 gain control synthesis of switched linear systems with time delay in detection of switching signal," *IET Control Theory & Applications*, vol. 3, no. 6, pp. 763–771, 2009.

[29] C. S. Tseng and B. S. Chen, "L_∞ gain fuzzy control for nonlinear dynamic systems with persistent bounded disturbances," in *Proceedings of the IEEE International Conference on Fuzzy Systems*, vol. 2, pp. 783–788, Budapest, Hungary, July 2004.

[30] D. Liberzon, *Switching in Systems and Control*, Birkhäauser, Boston, Mass, USA, 2003.

[31] Z. R. Xiang and R. H. Wang, "Robust stabilization of switched non-linear systems with time-varying delays under asynchronous switching," *Proceedings of the Institution of Mechanical Engineers I*, vol. 223, no. 8, pp. 1111–1128, 2009.

Hindawi Publishing Corporation
Mathematical Problems in Engineering
Volume 2012, Article ID 260236, 10 pages
doi:10.1155/2012/260236

Research Article

Semistability of Nonlinear Impulsive Systems with Delays

Xiaowu Mu[1] and Yongliang Gao[1,2]

[1] *Department of Mathematics, Zhengzhou University, Zhengzhou 450052, China*
[2] *College of Science, Zhongyuan University of Technology, Zhengzhou 450007, China*

Correspondence should be addressed to Yongliang Gao, gaoy973@163.com

Received 22 June 2012; Revised 23 August 2012; Accepted 15 September 2012

Academic Editor: Bo Shen

This paper is concerned with the stability analysis and semistability theorems for delay impulsive systems having a continuum of equilibria. We relate stability and semistability to the classical concepts of system storage functions to impulsive systems providing a generalized hybrid system energy interpretation in terms of storage energy. We show a set of Lyapunov-based sufficient conditions for establishing these stability properties. These make it possible to deduce properties of the Lyapunov functional and thus lead to sufficient conditions for stability and semistability. Our proposed results are evaluated using an illustrative example to show their effectiveness.

1. Introduction

Due to their numerous applications in various fields of sciences and engineering, impulsive differential systems have become a large and growing interdisciplinary area of research. In recent years, the issues of stability in impulsive differential equations with time delays have attracted increasing interest in both theoretical research and practical applications [1–9], while difficulties and challenges remain in the area of impulsive differential equations [10], especially those involving time delays [11]. Various mathematical models in the study of biology, population dynamics, ecology and epidemic, and so forth can be expressed by impulsive delay differential equations. These processes and phenomena, for which the adequate mathematical models are impulsive delay differential equations, are characterized by the fact that there is sudden change of their state and that the processes under consideration depend on their prehistory at each moment of time. In the transmission of the impulse information, input delays are often encountered. Control and synchronization of chaotic systems are considered in [12, 13]. By utilizing impulsive feedback control, all the solutions of the Lorenz chaotic system will converge to an equilibrium point. The application

of networked control systems is considered in [14–17], while in [14], when analyzing the asymptotic stability for discrete-time neural networks, the activation functions are not required to be differentiable or strictly monotonic. The existence of the equilibrium point is first proved under mild conditions. By constructing a new Lyapnuov-Krasovskii functional, a linear matrix inequality (LMI) approach is developed to establish sufficient conditions for the discrete-time neural networks to be globally asymptotically stable. In [18], Razumikhin-type theorems are established which guarantee ISS/iISS for delayed impulsive systems with external input affecting both the continuous dynamics and the discrete dynamics. It is shown that when the delayed continuous dynamics are ISS/iISS but the discrete dynamics governing the impulses are not, the ISS/iISS property of the impulsive system can be retained if the length of the impulsive interval is large enough. Conversely, when the delayed continuous dynamics are not ISS/iISS but the discrete dynamics governing the impulses are, the impulsive system can achieve ISS/iISS. In [19, 20], the authors consider linear time invariant uncertain sampled-data systems in which there are two sources of uncertainty: the values of the process parameters can be unknown while satisfying a polytopic condition and the sampling intervals can be uncertain and variable. They model such systems as linear impulsive systems and they apply their theorem to the analysis and state-feedback stabilization. They find a positive constant which determines an upper bound on the sampling intervals for which the stability of the closed loop is guaranteed. Population growth and biological systems are considered in [21, 22]. Stochastic systems are considered in [23–25], and so forth. However, the corresponding theory for impulsive systems with time delays having a continuum of equilibria has been relatively less developed.

The purpose of this paper is to study the stability and semistability properties for nonlinear delayed impulsive systems with continuum of equilibria. Examples of such systems include mechanical systems having rigid-body modes and isospectral matrix dynamical systems [26]. Such systems also arise in chemical kinetics, compartmental modeling, and adaptive control. Since every neighborhood of a nonisolated equilibrium contains another equilibrium, a nonisolated equilibrium cannot be asymptotically stable. Thus asymptotic stability is not the appropriate notion of stability for systems having a continuum of equilibria. Two notions that are of particular relevance to such systems are convergence and semistability. Convergence is the property whereby every solution converges to a limit point that may depend on the initial condition. Semistability is the additional requirement that all solutions converge to limit points that are Lyapunov stable. More precisely, an equilibrium is semistable if it is Lyapunov stable, and every trajectory starting in a neighborhood of the equilibrium converges to a (possibly different) Lyapunov stable equilibrium. It can be seen that, for an equilibrium, asymptotic stability implies semistability, while semistability implies Lyapunov stability. We will employ the method of Lyapunov function for the study of stability and semistability of impulsive systems with time delays. Several stability criteria are established. A set of Lyapunov-based sufficient conditions is provided for stability criteria, then we extend the notion of stability to develop the concept of semistability for delay impulsive systems. Finally, an example illustrates the effectiveness of our approach.

2. Preliminaries

Let $\mathbb{N}$ denote the set of positive integer numbers. Let PC_t denote the set of piecewise right continuous functions $\phi : [t-r, t] \to \mathbb{R}^n$ with the norm defined by $\|\phi\|_r^t = \sup_{-r\le s\le 0}\|\phi(t+s)\|$. For simplicity, define $\|\phi\|_r = \|\phi\|_r^0$, for $\phi \in \mathrm{PC}_0$. For given $r > 0$, if $x \in \mathrm{PC}([t_0 - r, +\infty), \mathbb{R}^n)$,

then for each $t \geq t_0$, we define $x_t, x_{t^-} \in \mathrm{PC}_0$ by $x_t(s) = x(t+s)$ $(-r \leq s \leq 0)$ and $x_{t^-}(s) = x(t+s)$ $(-r \leq s < 0)$, respectively. A function $\alpha : \mathbb{R}^+ \to \mathbb{R}^+$ is of class $\mathcal{K}$, if α is continuous, strictly increasing, and $\alpha(0) = 0$. For a given scalar $\rho \geq 0$, let $\mathcal{B}(\rho) = \{x \in \mathbb{R}^n;\ \|x\| \leq \rho\}$.

Let $\Omega \in \mathbb{R}^n$ be an open set and $\mathfrak{B}(\rho) \subset \Omega$ for some $\rho > 0$. Given functionals $f : \mathbb{R}^+ \times \mathrm{PC}([-r,0],\Omega) \to \mathbb{R}^n$, $g : \mathbb{R}^+ \times \Omega \to \mathbb{R}^n$, satisfying $f(t,0) = 0$, $g(0,0) = 0$. Considering the following nonlinear time-delay impulsive system Σ_t described by the state equation

$$\dot{x}(t) = f(t, x_t), \quad t > t_0,\ t \neq t_k,\ k \in \mathbb{N}, \tag{2.1}$$

$$x(t^+) = g(t, x(t)), \quad t = t_k,\ k \in \mathbb{N}, \tag{2.2}$$

$$x(t_0 + \theta) = \phi(\theta), \quad \theta \in [-r, 0], \tag{2.3}$$

where $x(t) \in \mathbb{R}^n$ is the system state, $\dot{x}(t)$ denotes the right-hand derivative of $x(t)$, $x(t^+)$ and $x(t^-)$ denote the limit from the right and the limit from the left at point t, respectively. t_0 is the initial time. Here we assume that the solutions of system Σ_t are right continuous, that is, $x(t^+) = x(t)$. $\{t_k\}$, $k \in \mathbb{N}$ is a strictly increasing sequence of impulse times in (t_0, ∞) where $\lim_{k\to\infty} t_k = \infty$.

Definition 2.1. The function $f : \mathbb{R} \times \mathrm{PC} \to \mathbb{R}^n$ is said to be composite-PC, if for each $t_0 \in \mathbb{R}$ and $\alpha > 0$, $x \in \mathrm{PC}([t_0 - r, t_0 + \alpha], \mathbb{R}^n)$ and x is continuous at each $t \neq t_k$ in $[t_0, t_0 + \alpha]$, then the composite function $h(x) = f(t, x_t) \in \mathrm{PC}([t_0 - r, t_0 + \alpha], \mathbb{R}^n)$.

Definition 2.2. The function $f : \mathbb{R} \times \mathrm{PC} \to \mathbb{R}^n$ is said to be quasi-bounded, if for each $t_0 \in \mathbb{R}^+$, $\alpha > 0$, and for each compact set $F \in \mathbb{R}^n$, there exists some $M > 0$, such that $\|f(t,\varphi)\| \leq M$ for all $(t,\varphi) \in [t_0, t_0 + \alpha] \times \mathrm{PC}([-r,0], F)$.

Definition 2.3. The function $x : [t_0 - r, t_0 + \alpha] \to \mathbb{R}^n$ with $\alpha > 0$ is said to be a solution of Σ_t if

(i) x is continuous at each $t \neq t_k$ in $(t_0, t_0 + \alpha]$;

(ii) the derivative of x exists and is continuous at all but at most a finite number of points t in $t \in [t_0, t_0 + \alpha)$;

(iii) the right-hand derivative of x exists and satisfies (2.1) in $t \in [t_0, t_0 + \alpha]$, while for each $t_k \in [t_0, t_0 + \alpha]$, (2.2) holds;

(iv) Equation (2.3) holds, that is, $x(t_0 + \theta) = \phi(\theta)$, $\theta \in [-r, 0]$.

We denote by $x(t, t_0, \phi)$ (or $x(t)$, if in not confusing) the solution of Σ_t. $x(t)$ is said to be a solution defined on $[t_0 - r, \infty)$ if all above conditions hold for any $\alpha > 0$.

We make the following assumptions on system Σ_t.

(A1) $f(t,\varphi)$ is composite-PC, quasi-bounded and locally Lipschitzian in φ.

(A2) For each fixed $t \in \mathbb{R}^+$, $f(t,\varphi)$ is a continuous function of φ on $\mathrm{PC}([-\tau, 0], \mathbb{R}^n)$.

Under the assumptions above, it was shown in [11] that for any $\phi \in \mathrm{PC}([-r,0], \mathbb{R}^n)$, system Σ_t admits a solution $x(t, t_0, \phi)$ that exists in a maximal interval $[t_0 - r, t_0 + b)$ $(0 < b \leq +\infty)$ and the zero solution of the system exists.

Definition 2.4. An equilibrium point of Σ_t is a point $x_e \in \mathrm{PC}([t_0 - r, t_0 + \alpha], \mathbb{R}^n)$ satisfying $x(t, t_0, \phi) = x_e$ for all $t \geq 0$ where $x(t, t_0, \phi)$ is the solution of Σ_t. Let $\mathcal{E}$ denote the set of equilibrium points of Σ_t.

Definition 2.5. Consider the delay impulsive system Σ_t.

(i) An equilibrium point $x(t) \equiv x_e$ of Σ_t is Lyapunov stable if for any $\varepsilon > 0$ there exists $\delta(\varepsilon, t_0)$, such that $\|\phi - \phi_e\|_r < \delta$ implies $\|x(t) - x_e\| < \varepsilon$ for all $t \geq t_0$, where ϕ_e is the initial function for x_e. An equilibrium point x is uniformly Lyapunov stable, if, in addition, the number δ is independent of t_0.

(ii) An equilibrium point x of Σ_t is semistable if it is Lyapunov stable and there exists an open subset of Ω containing x such that for all initial conditions in Ω the trajectory of Σ_t converges to a Lyapunov stable equilibrium point, that is, $\lim_{t\to\infty} x(t, t_0, \phi) = y,\ \phi \in \Omega$, where y is a Lyapunov stable equilibrium point.

(iii) System Σ_t is said to be uniformly asymptotically stable in the sense of Lyapunov with respect to the zero solution, if it is uniformly stable and $\lim_{t\to\infty}\|x(t)\| = 0$.

Definition 2.6. The function $V : [t_0, +\infty) \times \mathrm{PC}([-\tau, 0], \mathcal{B}(\rho)) \to \mathbb{R}^+$ is said to belong to the class $\mathcal{V}_0$ if

(i) V is continuous in each of the sets $[t_{k-1}, t_k) \times \mathrm{PC}([-\tau, 0], \mathcal{B}(\rho))$ and for each $k \in \mathbb{N}$, $\lim_{(t,y)\to(t_k^-,x)} V(t, y) = V(t_k^-, x)$ exists;

(ii) $V(t, x)$ is locally Lipschitzian in $x \in \mathrm{PC}([-\tau, 0], \mathcal{B}(\rho))$, and for all $t \geq t_0$, $V(t, 0) \equiv 0$.

Definition 2.7. Let $V \in \mathcal{V}_0$. For any $(t, \psi) \in [t_0, +\infty) \times \mathrm{PC}([-\tau, 0], \mathcal{B}(\rho))$, the upper right-hand derivative of V with respect to system Σ_t is defined by

$$D^+V(t, \psi(0)) := \limsup_{h\to 0^+} \frac{1}{h}\{V(t + h, \psi(0) + hf(t, \psi)) - V(t, \psi(0))\}. \tag{2.4}$$

3. Main Results

In the following, we will establish several sufficient conditions for Lyapunov stability and semistability for impulsive differential system Σ_t with time delays.

Theorem 3.1. *System Σ_t is uniformly stable, and the zero solution of Σ_t is asymptotically stable if there exists a Lyapunov function $V \in \mathcal{V}_0$ which satisfies the following.*

(i) $\exists a, b \in \mathcal{K}$ *such that*

$$a(\|x\|) \leq V(t, x) \leq b(\|x\|). \tag{3.1}$$

(ii) *For any $t \in [t_0, +\infty)$, $t \neq t_k$ and $\psi \in PC([-r, 0], \mathbb{R}^n)$, there exists $c > 0$, such that*

$$D^+V(t, \psi(0)) \leq -cV(t, \psi(0)). \tag{3.2}$$

(iii) *There exist a μ $(0 < \mu < 1)$ and a subsequence $\{t_{k_j}\}$ of the impulsive moments $\{t_k\}$ such that*

$$\left\|V\left(t_{k_{j+1}}, x\right)\right\|_r \leq \mu\left\|V\left(t_{k_j}, x\right)\right\|_r. \tag{3.3}$$

(iv) *For any* m, $0 \le m \le k_0$, *for all* $x_e \in \mathcal{E}$ *there exists a function* $\alpha \in \mathcal{K}$, *such that*

$$\|V(t_m, x - x_e)\|_r \le \alpha(\|\phi - \phi_e\|_r). \tag{3.4}$$

(v) *For any* $m \in \mathbb{N}$, $k_j \le m < k_{j+1}$, $j = 0, 1, 2, \ldots$, *there exists a function* $\beta \in \mathcal{K}$ *such that*

$$\|V(t_m, x - x_e)\|_r \le \beta \left\| V\left(t_{k_j}, x - x_e\right) \right\|_r. \tag{3.5}$$

Proof. Let x_e be an equilibrium point of the system Σ_t. We first prove that x_e is uniformly stable, that is, for for all $\varepsilon > 0$, there exists $\delta = \delta(\varepsilon) > 0$ such that $\|\phi - \phi_e\|_r < \delta$ implies $\|x(t) - x_e\| < \varepsilon$ for all $t \ge t_0$.

For all $\varepsilon > 0$, let $0 < \delta < \varepsilon$ such that

$$a(\varepsilon) > \max\{\alpha(\delta), \beta(\alpha(\delta))\}. \tag{3.6}$$

For any $\|\phi - \phi_e\|_r < \delta$, by condition (3.4), we get

$$\|V(t_m, x - x_e)\|_r \le \alpha(\|\phi - \phi_e\|_r) \le \alpha(\delta), \quad 0 \le m \le k_0. \tag{3.7}$$

By (3.3), it is clear that $\|V(t, x)\|_r$ is nonincreasing along the subsequence $\{t_{k_j}\}$, so we have

$$\left\| V\left(t_{k_j}, x - x_e\right) \right\|_r \le \|V(t_{k_0}, x - x_e)\|_r \le \alpha(\delta), \quad j = 0, 1, 2, \ldots. \tag{3.8}$$

For any m, $k_j \le m < k_{j+1}$, $j = 0, 1, 2, \ldots$, by (3.5), we get

$$\|V(t_m, x - x_e)\|_r \le \beta(\alpha(\delta)). \tag{3.9}$$

Combining (3.7), (3.8), and (3.9), we conclude that

$$\|V(t_k, x - x_e)\|_r < a(\varepsilon), \quad k = 1, 2, \ldots. \tag{3.10}$$

By condition (3.2), for any $t \in [t_k, t_{k+1})$, $k = 0, 1, 2 \ldots$, we have

$$V(t, x - x_e) \le V(t_k, x - x_e) < a(\varepsilon), \tag{3.11}$$

and then, by (3.10), for any $t \ge t_0$ we derive that $V(t, x - x_e) < a(\varepsilon)$. Hence, by (3.1) we obtain that $a(\|x - x_e\|) \le V(t, x - x_e) < a(\varepsilon)$. Since $a \in \mathcal{K}$, we get

$$\|x(t) - x_e\| < \varepsilon, \quad t \ge t_0, \tag{3.12}$$

which implies that system Σ_t is uniformly Lyapunov stable.

Next, we will prove that the zero solution of Σ_t is asymptotically stable.

Since system Σ_t is uniformly stable, from (3.1), there must exist a real number $M > 0$ such that $\|V(t,x)\|_r \leq M,\ t \geq t_0$. Hence, there exists a $v \geq 0$ such that

$$\lim_{t\to\infty}\sup\|V(t,x)\|_r = v \leq M. \tag{3.13}$$

In the following, we will show that $v = 0$. Without loss of generality, we can suppose that there exists a sequence $\{t_n\} \subset [t_0,\infty),\ n = 1,2,\ldots$, such that

$$\lim_{n\to\infty}\|V(t_n,x)\|_r = \lim_{n\to\infty}\sup\|V(t,x)\|_r = v. \tag{3.14}$$

From (3.3) we get

$$\left\|V\left(t_{k_j},x\right)\right\|_r < \mu^j\|v(t_{k_0},x)\|_r. \tag{3.15}$$

Since $0 < \mu < 1$, we obtain

$$\lim_{j\to\infty}\left\|V\left(t_{k_j},x\right)\right\|_r = 0. \tag{3.16}$$

If the sequence $\{t_n\} \subset [t_0,\infty),\ n = 1,2,\ldots$ is the same as the sequence $\{t_{k_j}\},\ j = 0,1,2,\ldots$, then it is obvious that $v = 0$. If $0 \leq n < k_0$, it follows from the assumptions above that (3.16) holds. Otherwise, we assume that $n \geq k_0$; there exists a $j \in \mathbb{N}$ such that $k_j \leq n < k_{j+1}$. Then from condition (3.5) we get

$$\|V(t_n,x)\|_r \leq \beta\left(\left\|V\left(t_{k_j},x\right)\right\|_r\right). \tag{3.17}$$

So

$$\lim_{n\to\infty}\|V(t_n,x)\|_r \leq \lim_{j\to\infty}\beta\left(\left\|V\left(t_{k_j},x\right)\right\|_r\right) = 0, \tag{3.18}$$

which implies $v = 0$.

Hence, we derive that $\lim_{t\to\infty}\|V(t,x)\| = 0$. Finally, by (3.1), we have $\lim_{t\to\infty}\|x(t)\| = 0$ which implies that the zero solution of the system Σ_t is asymptotically stable. The proof is completed. □

Next, we present a sufficient condition for semistability for system Σ_t.

Let $\mathfrak{L}_1 := \{f : [0,\infty) \to \mathbb{R}; f$ is measurable and $\int_0^\infty |f(t)|dt < \infty\}$.

Theorem 3.2. *Consider the system Σ_t; assume that there exists nonnegative-definite continuous function $W : \mathbb{R}\times\mathbb{R}^n \to \mathbb{R}$ such that*

$$D^+V(t,\varphi(0)) \leq -W(t,\varphi(0)). \tag{3.19}$$

Let $W^{-1}(0) := \{x \mid W(t,x) \equiv 0,$ for all $t \geq t_0\}$. If every equilibrium point of system Σ_t is Lyapunov stable, then every point in $W^{-1}(0)$ is semistable.

Proof. Define

$$\varphi(t) := \begin{cases} W(t, \psi(0)), & t \neq t_k,\ k \in \mathbb{N}, \\ 0, & t = t_k,\ k \in \mathbb{N}. \end{cases} \tag{3.20}$$

It follows from (3.19) and (3.3) that

$$\int_0^t \varphi(s)ds \leq V(x(t_1)) - V(x(t)) \leq V(x(t_1)) \ . \tag{3.21}$$

Since $\varphi(\cdot)$ is nonnegative, it follows that $\varphi(\cdot) \in \mathfrak{L}_1$. Next, we show that $\varphi(t) \to 0$ as $t \to \infty$.

If it is not true, then there exists $\varepsilon > 0$ and an infinite sequence of times $\tau_1, \tau_2, \ldots$ such that $|\varphi(\tau_i)| \geq \varepsilon$. By definition of $\varphi(\cdot)$ we have $\tau_i,\ i = 1, 2 \ldots$ that does not belong to the set of impulsive times $\{t_k\}$.

Note that from (3.19), it follows from Proposition 3.1 of [26] that $x(t)$ is bounded for all $t \geq 0$. Hence, it follows from the Lipschitz continuity of $f(\cdot)$ that $\dot{x}(t)$ is bounded for all $t \geq 0$; thus, $\varphi(\cdot)$ is uniformly continuous on $[t_0, +\infty) \setminus \{t_n\}$. So, there exists $\delta > 0$ such that every τ_i is contained in some interval of $I_i,\ \tau_i \in I_i$ of length δ on which $\varphi(t) \geq \varepsilon/2,\ t \in I_i$. This contradicts $\varphi(\cdot) \in \mathfrak{L}_1$. Hence $\varphi(t) \to 0$ as $t \to \infty$. It follows that $W(t, \psi(0)) \to 0$ as $t \to \infty$. Since $x(t)$ is bounded, we get $x(t) \to W^{-1}(0)$ (as $t \to \infty$).

Next, let $x_e \in W^{-1}(0)$. For every open neighborhood U and $x_0 \in U$, $x(t) \to W^{-1}(0)$ (as $t \to \infty$), it follows from Proposition 5.1 of [26] that there exists $y \in W^{-1}(0)$ such that $\lim_{t\to\infty} x(t) = y$. Since every point in $\mathcal{E}$ is Lyapunov stable, and hence y is a Lyapunov stable equilibrium of Σ_t, it follows that x_e is semistable. Finally, since $x_e \in W^{-1}(0)$ is arbitrary, this implies every point in $W^{-1}(0)$ is semistable. The proof is completed. □

4. Numerical Example

In this section, we give an example about compartmental systems to illustrate the effectiveness of the proposed method. Compartmental systems involve dynamical models that are characterized by conservation laws (e.g., mass and energy) capturing the exchange of material between coupled macroscopic subsystems known as compartments. Each compartment is assumed to be kinetically homogeneous, that is, any material entering the compartment is instantaneously mixed with the material of the compartment.

Example 4.1. Consider the nonlinear two-compartment time-delay impulsive systems given by

$$\begin{gathered} \dot{x}_1(t) = -x_1(t) + x_2(t)\{1 - \sin(x_1(t-r))\} + x_2^3(t) - x_1^3(t), \quad t \neq t_k,\ k \in \mathbb{N}, \\ \dot{x}_2(t) = -x_2(t) + x_1(t)\{1 + \sin(x_1(t-r))\} + x_1^3(t) - x_2^3(t), \quad t \neq t_k,\ k \in \mathbb{N}, \\ x_1(t^+) = 0.8x_1(t), \quad t = t_k,\ k \in \mathbb{N}, \\ x_2(t^+) = 0.9x_2(t), \quad t = t_k,\ k \in \mathbb{N}, \\ x(t_0 + \theta) = \phi(\theta) = \begin{pmatrix} \cos\theta \\ \sin\theta \end{pmatrix}, \quad \theta \in [-0.2, 0], \end{gathered} \tag{4.1}$$

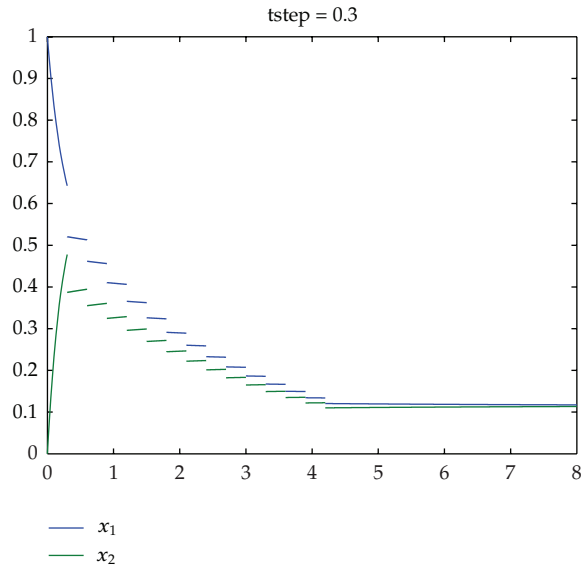

Figure 1: State trajectory: semistable.

where $r \geq 0$. Let Lyapunov function $V(\psi(0)) = (1/2)\psi_1^2(0) + (1/2)\psi_2^2(0)$, then for any $\psi \in \mathrm{PC}([-r,0],\mathcal{B}(\rho))$ we have

$$\begin{aligned} D^+V(\psi(0)) &= -\frac{1}{2}\left(x_1^2+x_2^2\right) - \frac{1}{2}(x_1-x_2)^2\left(x_1^2+x_1x_2+x_2^2\right) \\ &\leq -\frac{1}{2}\left(x_1^2+x_2^2\right) = -V(\psi(0)). \end{aligned} \tag{4.2}$$

Let $c = 1$, $a(\|x\|) = b(\|x\|) = (1/2)\|x\|$, $\mu = 0.9$, and $\beta(\|x\|) = \|x\|$, then the conditions of Theorem 3.1 are satisfied, which means the equilibrium points of the system are Lyapunov stable, and

$$\begin{aligned} D^+V(\psi(0)) &= -\frac{1}{2}(x_1-x_2)^2\left[1+\frac{3}{4}x_1^2+\left(\frac{1}{2}x_1+x_2\right)^2\right] \\ &\leq -\frac{1}{2}(x_1-x_2)^2. \end{aligned} \tag{4.3}$$

Let $W(x_1,x_2) = (1/2)(x_1-x_2)^2$ then we derive that $D^+V(\psi(0)) \leq -W(\psi(0))$; it follows from Theorem 3.2 that every point in $W^{-1}(0)$ is semistable.

The simulation result is depicted in Figure 1, where the length of the impulsive intervals is $T = 0.3$ second and the time delay $r = 0.1$ second.

Acknowledgments

The authors would like to thank the Editor and the anonymous reviewers for their valuable comments and suggestions that improved the overall quality of this paper. This work was supported by Grants of NSFC-60874006.

References

[1] G. Ballinger and X. Liu, "Existence, uniqueness and boundedness results for impulsive delay differential equations," *Applicable Analysis*, vol. 74, no. 1-2, pp. 71–93, 2000.

[2] X. Liu and G. Ballinger, "Existence and continuability of solutions for differential equations with delays and state-dependent impulses," *Nonlinear Analysis*, vol. 51, no. 4, pp. 633–647, 2002.

[3] X. Liu, X. Shen, Y. Zhang, and Q. Wang, "Stability criteria for impulsive systems with time delay and unstable system matrices," *IEEE Transactions on Circuits and Systems. I*, vol. 54, no. 10, pp. 2288–2298, 2007.

[4] J. S. Yu, "Stability for nonlinear delay differential equations of unstable type under impulsive perturbations," *Applied Mathematics Letters*, vol. 14, no. 7, pp. 849–857, 2001.

[5] X. Liu and Q. Wang, "The method of Lyapunov functionals and exponential stability of impulsive systems with time delay," *Nonlinear Analysis*, vol. 66, no. 7, pp. 1465–1484, 2007.

[6] Z. Luo and J. Shen, "Stability of impulsive functional differential equations via the Liapunov functional," *Applied Mathematics Letters*, vol. 22, no. 2, pp. 163–169, 2009.

[7] J. Liu, X. Liu, and W. C. Xie, "Input-to-state stability of impulsive and switching hybrid systems with time-delay," *Automatica*, vol. 47, no. 5, pp. 899–908, 2011.

[8] W. Zhu, "Stability analysis of switched impulsive systems with time delays," *Nonlinear Analysis: Hybrid Systems*, vol. 4, no. 3, pp. 608–617, 2010.

[9] Q. Wu, J. Zhou, and L. Xiang, "Global exponential stability of impulsive differential equations with any time delays," *Applied Mathematics Letters*, vol. 23, no. 2, pp. 143–147, 2010.

[10] V. Lakshmikantham, D. D. Baĭnov, and P. S. Simeonov, *Theory of Impulsive Differential Equations*, vol. 6 of *Series in Modern Applied Mathematics*, World Scientific, Teaneck, NJ, USA, 1989.

[11] G. Ballinger and X. Liu, "Existence and uniqueness results for impulsive delay differential equations," *Dynamics of Continuous, Discrete and Impulsive Systems*, vol. 5, no. 1–4, pp. 579–591, 1999.

[12] C. Li, X. Liao, X. Yang, and T. Huang, "Impulsive stabilization and synchronization of a class of chaotic delay systems," *Chaos*, vol. 15, no. 4, Article ID 043103, p. 9, 2005.

[13] X. Liu, "Impulsive stabilization and control of chaotic system," *Nonlinear Analysis*, vol. 47, no. 2, pp. 1081–1092, 2001.

[14] Y. Liu, Z. Wang, and X. Liu, "Asymptotic stability for neural networks with mixed time-delays: the discrete-time case," *Neural Networks*, vol. 22, no. 1, pp. 67–74, 2009.

[15] Y. K. Li and P. Liu, "Existence and stability of positive periodic solution for BAM neural networks with delays," *Mathematical and Computer Modelling*, vol. 40, no. 7-8, pp. 757–770, 2004.

[16] Z. Yang and D. Xu, "Stability analysis of delay neural networks with impulsive effects," *IEEE Transactions on Circuits and Systems II*, vol. 52, no. 8, pp. 517–521, 2005.

[17] M. Tan and Y. Tan, "Global exponential stability of periodic solution of neural network with variable coefficients and time-varying delays," *Applied Mathematical Modelling*, vol. 33, no. 1, pp. 373–385, 2009.

[18] W. H. Chen and W. X. Zheng, "Input-in-state stability and integral input-to-state stability of nonlinear impulsive systems with delays," *Automatica*, vol. 45, no. 6, pp. 1481–1488, 2009.

[19] P. Naghshtabrizi, J. P. Hespanha, and A. R. Teel, "Exponential stability of impulsive systems with application to uncertain sampled-data systems," *Systems & Control Letters*, vol. 57, no. 5, pp. 378–385, 2008.

[20] N. van de Wouw, P. Naghshtabrizi, M. B. G. Cloosterman, and J. P. Hespanha, "Tracking control for sampled-data systems with uncertain time-varying sampling intervals and delays," *International Journal of Robust and Nonlinear Control*, vol. 20, no. 4, pp. 387–411, 2010.

[21] X. Liu, "Impulsive stabilization and applications to population growth models," *The Rocky Mountain Journal of Mathematics*, vol. 25, no. 1, pp. 381–395, 1995.

[22] X. Liu and K. Rohlf, "Impulsive control of a Lotka-Volterra system," *IMA Journal of Mathematical Control and Information*, vol. 15, no. 3, pp. 269–284, 1998.

[23] Z. Wang, B. Shen, H. Shu, and G. Wei, "Quantized H_∞ control for nonlinear stochastic time-delay systems with missing measurements," *IEEE Transactions on Automatic Control*, vol. 57, no. 6, pp. 1431–1444, 2012.

[24] Z. Wang, B. Shen, and X. Liu, "H_∞ filtering with randomly occurring sensor saturations and missing measurements," *Automatica*, vol. 48, no. 3, pp. 556–562, 2012.

[25] H. Dong, Z. Wang, and H. Gao, "Distributed filtering for a class of time-varying systems over sensor networks with quantization errors and successive packet dropouts," *IEEE Transactions on Signal Processing*, vol. 60, no. 6, pp. 3164–3173, 2012.

[26] S. P. Bhat and D. S. Bernstein, "Nontangency-based Lyapunov tests for convergence and stability in systems having a continuum of equilibria," *SIAM Journal on Control and Optimization*, vol. 42, no. 5, pp. 1745–1775, 2003.

Hindawi Publishing Corporation
Mathematical Problems in Engineering
Volume 2012, Article ID 890512, 15 pages
doi:10.1155/2012/890512

Research Article

Estimation for Stochastic Nonlinear Systems with Randomly Distributed Time-Varying Delays and Missing Measurements

Yan Che,[1,2] Huisheng Shu,[1] and Xiu Kan[1]

[1] *School of Information Science and Technology, Donghua University, Shanghai 201620, China*
[2] *Department of Electronics and Information Engineering, Putian University, Putian 351100, China*

Correspondence should be addressed to Huisheng Shu, hsshu@dhu.edu.cn

Received 21 June 2012; Accepted 6 September 2012

Academic Editor: Zidong Wang

The estimation problem is investigated for a class of stochastic nonlinear systems with distributed time-varying delays and missing measurements. The considered distributed time-varying delays, stochastic nonlinearities, and missing measurements are modeled in random ways governed by Bernoulli stochastic variables. The discussed nonlinearities are expressed by the statistical means. By using the linear matrix inequality method, a sufficient condition is established to guarantee the mean-square stability of the estimation error, and then the estimator parameters are characterized by the solution to a set of LMIs. Finally, a simulation example is exploited to show the effectiveness of the proposed design procedures.

1. Introduction

In the past decades, estimation techniques have been extensively investigated in many complex dynamical processes of networks such as target tracking [1], advanced aircrafts, and manufacturing processes. A number of estimation methods have been proposed in the literature, most of them are under the assumption that the measurements always contain true signals with the disturbances and the noises, see for example, [2–9]. But, in practical applications, the measurements may contain missing measurements due to many reasons such as the sensor temporal failures, network congestion, multipath fading, and high maneuverability of the tracked targets. Because of the clear engineering signification, the estimation problems with missing measurements have received attention, see for example [10–22].

Recently, with the rapid development of networks, novel methods and flexible models have been devoted, but the research of missing measurements is still a challenge, and the Bernoulli-based distributed model has still been a hot approach to modeling the missing observation cases. For example, in [10], the missing probability for each sensor is governed by an individual random variable satisfying a certain probabilistic distribution over the interval [0 1]. Packet dropouts and communication delays are considered simultaneously in [12]. The variance-constrained dissipative control problem for a class of stochastic nonlinear systems with multiple degraded measurements in [13], where the degraded probability for each sensor is governed by an individual random variable satisfying a certain probabilistic distribution over a given interval. The H_∞ filtering problem has been addressed in [20] for a class of nonlinear systems with randomly occurring incomplete information, where the considered incomplete information includes both the sensor saturations and the missing measurements, a regional sensor model has been designed to account for both the randomly occurring sensor saturation and missing measurement in a unified representation, based on this sensor model, a newfangled H_∞ filter with a certain ellipsoid constraint has been researched such that the filtering error dynamics is locally mean-square asymptotically stable and the H_∞-norm requirement is satisfied.

On the other hand, time delays are frequently encountered in real-world application such as communications, engineering, and biological systems. The occurrence of time delays may induce instability, oscillation, and poor performance. Consequently, research on time-delay systems has been a topic of recurring interest over the past decades. Current efforts can be classified into several categories, for example, simple delay and multiple delays [12], delay-independence [23, 24] and delay-dependence [5, 8, 25–30], time-varying delays [31, 32] and constant delays, retarded-type delay and neutral-type delay [30, 33], and mixed delays [34, 35]. However, in some applications, such as these systems connected over a wireless networks/or neural networks, as pointed out in [36], networks usually have a spatial extent due of the presence of a multitude of parallel pathways with a variety of axon sizes and lengths, and therefore the propagation delays can be distributed over a period of time, so it is essential to describe the distributed time delay under the probability framework as possible as. In this paper, the probability distribution of the time-vary delays are described for Itô type discrete-time stochastic distribution by a binary switching sequence satisfying the Bernoulli-distributed model.

Motivated by the aforementioned discussions, in this paper, we model the stochastic nonlinearities, the missing measurements, and the distributed time-vary delays by Bernoulli distributed white sequence with known conditional probability distribution. We aim at designing a estimator such that, for all possible measurements missing and distributed time-vary delays to obtain the estimation error system mean-square stable. The solvability of the addressed estimation problem can be expressed as the feasibility of a set of LMIs. Finally, a numerical simulation example is exploited to show the effectiveness of the results derived. The main contributions of this paper are summarized as the following: (1) a new estimation problem is studied for the stochastic nonlinear systems with both distributed time-vary delays and measurements missing phenomenon; (2) a mean-square stable performance is taken into consideration for the addressed stochastic nonlinear systems with distributed time-vary delays and missing measurements.

The rest of this paper is organized as follows. Section 2 briefly introduces the problem under consideration. In Section 3, a sufficient condition is established such that, for the missing measurements, the randomly distributed time-varying delays and nonlinearities,

the estimation error system is the mean-square stability. A numerical example is given in Section 4. This paper is concluded in Section 5.

Notations. The notation used here is fairly standard except where otherwise stated. $\mathbb{R}^n$, $\mathbb{R}^{n\times m}$, and $\mathbb{I}^+$ denote, respectively, the n-dimension Euclidean space, the set of all $n\times m$ real matrices, and the set of nonnegative integers. $(\Omega, \mathcal{F}, \{\mathcal{F}_k\}_{k\in\mathbb{I}^+}, \mathbb{P})$ is complete filtered probability space, Ω is the sample space, $\mathcal{F}$ is the σ-algebra of subsets of the sample space, and $\mathbb{P}$ is the probability measure on $\mathcal{F}$. $\mathbb{E}\{x\}$ stands for the expectation of the stochastic variable x. $\mathrm{Prob}\{\cdot\}$ is used for the occurrence probability of the event "$\cdot$". The superscript "T" stands for matrix transposition. $P > 0\,(P \geq 0)$ means that matrix P is real symmetric and positive definite (positive semi-definite). $\lambda_{\min}(\cdot)$ denotes the minimum eigenvalue of a matrix. I and 0 represent the identity matrix and the zero matrix with appropriate dimensions, respectively. $\mathrm{diag}\{X_1, X_2, \ldots, X_n\}$ stands for a block-diagonal matrix with matrices $X_1, X_2, \ldots, X_n$ on the diagonal. In symmetric block matrices or long matrix expressions, we use "$*$" to represent a term, that is, induced by symmetry. Matrices, if their dimensions are not explicitly stated, are assumed to be compatible for algebraic operations.

2. Problem Formulation and Preliminaries

Consider the following class of stochastic nonlinear system with distributed time-varying delays:

$$\begin{aligned} x(k+1) &= Ax(k) + \kappa_1(k)B\sum_{m=-\tau(k)}^{-1} x(k+m) + \kappa_2(k)f(x(k)) + E_1x(k)w(k), \\ y(k) &= \kappa_3(k)Cx(k) + E_2x(k)w(k), \\ z(k) &= H_1x(k), \end{aligned} \tag{2.1}$$

where $x(k) \in \mathbb{R}^n$ is the state vector, $y(k) \in \mathbb{R}^m$ is the measured output vector, $z(k) \in \mathbb{R}^q$ is the signal to be estimated, $w(k)$ is a one-dimensional, zero-mean, Gaussian white noise sequence on a probability space $(\Omega, \mathcal{F}, \{\mathcal{F}_k\}_{k\in\mathbb{I}^+}, \mathbb{P})$ with $\mathbb{E}\{\omega^2(k)\} = 1$, A, B, C, E_1, E_2, and H_1 are known real constant matrices with appropriate dimensions, $\tau(k)$ denoting time-varying delays are positive integers and bounded, namely, $0 < \tau_l \leq \tau(k) \leq \tau_u$, the stochastic variables $\kappa_1(k) \in \mathbb{R}$, $\kappa_2(k) \in \mathbb{R}$, and $\kappa_3(k) \in \mathbb{R}$ are Bernoulli distributed white sequence taking the values of 0 and 1 with

$$\mathrm{Prob}\{\kappa_1(k) = 1\} = \mathbb{E}\{\kappa_1(k)\} := \alpha_1, \tag{2.2}$$

$$\mathrm{Prob}\{\kappa_1(k) = 0\} := 1 - \alpha_1, \tag{2.3}$$

$$\mathrm{Prob}\{\kappa_2(k) = 1\} = \mathbb{E}\{\kappa_2(k)\} := \alpha_2, \tag{2.4}$$

$$\mathrm{Prob}\{\kappa_2(k) = 0\} := 1 - \alpha_2, \tag{2.5}$$

$$\mathrm{Prob}\{\kappa_3(k) = 1\} = \mathbb{E}\{\kappa_3(k)\} := \alpha_3, \tag{2.6}$$

$$\mathrm{Prob}\{\kappa_3(k) = 0\} := 1 - \alpha_3, \tag{2.7}$$

where $\alpha_1 \in [0\ 1]$, $\alpha_2 \in [0\ 1]$, and $\alpha_3 \in [0\ 1]$ are known positive scalars.

Remark 2.1. The nonlinear stochastic $f(x(k))$ is assumed to have the following for all $x(k)$:

$$\begin{gathered}\mathbb{E}\{f(x(k)) \mid x(k)\} = 0,\\ \mathbb{E}\{f(x(k)) \;\; f^T(x(k)) \mid x(k)\} = 0, \quad k \neq j,\\ \mathbb{E}\{f(x(k)) \;\; f^T(x(k)) \mid x(k)\} \leq \sum_{i=1}^{q} \Pi_i x^T(k) \Phi_i x(k),\end{gathered} \tag{2.8}$$

where q is a known nonnegative integer, $\Pi_i = \overline{\Pi}_i \overline{\Pi}_i^T$, Π_i, $\overline{\Pi}_i$, and Φ_i $(i = 1, \ldots, q)$ are known matrices with appropriate dimensions. For convenience, one assumes that $f(x(k))$ is unrelated with $\kappa_1(k)$, $\kappa_2(k)$, $\kappa_3(k)$, and $\omega(k)$.

In this paper, we aim at designing a linear estimator of the following structure:

$$x_f(k+1) = A_f x_f(k) + A_k y(k), \qquad \hat{z}(k) = H_2 x_f(k), \qquad \hat{z}(0) = 0, \tag{2.9}$$

where $x_f \in \mathbb{R}^n$ is the state estimate, $\hat{z}(k)$ is the estimate output, H_2 is a known real constant matrix with appropriate dimension, and A_f and A_k are estimator parameters to be determined.

By defining $\hat{x}(k) = [x^T(k) \;\; x_f^T(k)]^T$, we have the following augmented system:

$$\begin{aligned}\hat{x}(k+1) = {} & \mathcal{A}\hat{x}(k) + \overline{\mathcal{A}}\hat{x}(k) + \mathcal{B} \sum_{m=-\tau(k)}^{-1} \hat{x}(k+m) + \overline{\mathcal{B}} \sum_{m=-\tau(k)}^{-1} \hat{x}(k+m)\\ & + \mathcal{N}h(k) + \overline{\mathcal{N}}h(k) + \mathcal{E}\hat{x}(k)w(k),\end{aligned} \tag{2.10}$$

where

$$\begin{gathered}\mathcal{A} = \begin{bmatrix} A & 0 \\ \alpha_3 A_k C & A_f \end{bmatrix}, \qquad \overline{\mathcal{A}} = \begin{bmatrix} 0 & 0 \\ (\kappa_3(k) - \alpha_3) A_k C & 0 \end{bmatrix}, \qquad \mathcal{B} = \begin{bmatrix} \alpha_1 B & 0 \\ 0 & 0 \end{bmatrix},\\ \overline{\mathcal{B}} = \begin{bmatrix} (\kappa_1(k) - \alpha_1) B & 0 \\ 0 & 0 \end{bmatrix}, \qquad \hat{x}(k+i) = \begin{bmatrix} x(k+i) \\ x_f(k+i) \end{bmatrix}, \qquad h(k) = \begin{bmatrix} f(x(k)) \\ 0 \end{bmatrix},\\ \mathcal{E} = \begin{bmatrix} E_1 & 0 \\ A_k E_2 & 0 \end{bmatrix}, \qquad \widehat{\mathcal{N}} = \begin{bmatrix} I & 0 \\ 0 & 0 \end{bmatrix}, \qquad \mathcal{N} = \alpha_2 \widehat{\mathcal{N}}, \qquad \overline{\mathcal{N}} = (\kappa_2(k) - \alpha_2)\widehat{\mathcal{N}}.\end{gathered} \tag{2.11}$$

Observe the system (2.10) and let $\hat{x}(k;\varphi)$ denote the state trajectory from the initial data $\hat{x}(s) = \varphi(s)$ on $-\xi_M \leq s \leq -\xi_m$. Obviously, $\hat{x}(k;0) \equiv 0$ is the trivial solution of system (2.10) corresponding to the initial data $\varphi = 0$.

In what follows, we aim to design a linear estimator of the form (2.9) for system (2.1) such that, for all admissible randomly occurring distributed time-varying delays, missing measurements, stochastic nonlinearities, and estimation error system (2.10) is mean-square stable.

3. Main Results

The following lemmas are essential in establishing our main results.

Lemma 3.1 (Schur Complement). *There are constant matrices Υ_1, Υ_2, and Υ_3 where $\Upsilon_1 = \Upsilon_1^T$ and $\Upsilon_2 = \Upsilon_2^T > 0$, then $\Upsilon_1 + \Upsilon_3^T \Upsilon_2^{-1}\Upsilon_3 < 0$ if and only if $\begin{bmatrix} \Upsilon_1 & \Upsilon_3^T \\ \Upsilon_3 & -\Upsilon_2 \end{bmatrix} < 0$.*

Lemma 3.2. *Let $\mathcal{W} \in \mathbb{R}^{n\times n}$ be a positive semidefinite matrix, $x_i \in \mathbb{R}^n$ be a vector, and $a_i \geq 0$ $(i = 1, 2, \ldots)$ be scalars. If the series concerned are convergent, then the following inequality holds [35]*

$$\left(\sum_{i=1}^{+\infty} a_i x_i\right)^T \mathcal{W}\left(\sum_{i=1}^{+\infty} a_i x_i\right) \leq \left(\sum_{i=1}^{+\infty} a_i\right)\sum_{i=1}^{+\infty} a_i x_i^T \mathcal{W} x_i. \tag{3.1}$$

In the following theorem, Lyapunov stability theorem and a LMI-based method are combined together to deal with the stability analysis issue for the estimator design of the discrete-time stochastic nonlinear system with distributed time-varying delays and missing measurements. A sufficient condition is derived that ensures the solvability of the estimation problem.

Theorem 3.3. *Given the estimator parameters A_f and A_k consider the estimation error system* (2.10). *If there exist positive definite matrices $P = P^T > 0$, $Q = Q^T > 0$, and positive scalars $\varpi_i > 0$ $(i = 1, 2, \ldots, q)$ such that the following matrix inequalities,*

$$\begin{bmatrix} -P & * & * & * & * & * & * & * \\ 0 & -Q & * & * & * & * & * & * \\ P\mathcal{E} & 0 & -P & * & * & * & * & * \\ \beta_1 Q & 0 & 0 & -Q & * & * & * & * \\ P\mathcal{A} & P\mathcal{B} & 0 & 0 & -P & * & * & * \\ \beta_3 P & 0 & 0 & 0 & 0 & -P & * & * \\ \beta_4\widehat{\Phi} & 0 & 0 & 0 & 0 & 0 & -\Xi & * \\ 0 & \beta_2 P\mathcal{F} & 0 & 0 & 0 & 0 & 0 & -P \end{bmatrix} < 0, \tag{3.2}$$

$$\Delta = \begin{bmatrix} -\varpi_i I & * \\ P\widetilde{\mathcal{N}\Pi_i} & -P \end{bmatrix} < 0, \quad i = 1, 2, \ldots, q, \tag{3.3}$$

hold, where

$$\begin{gathered} \beta_1 = \left(\tau_u + \frac{1}{2}(\tau_u - \tau_l)(\tau_u + \tau_l - 1)\right)^{1/2}, \qquad \beta_2 = (\alpha_1(1-\alpha_1))^{1/2}, \\ \beta_3 = (\alpha_3(1-\alpha_3))^{1/2}, \qquad \beta_4 = (\alpha_2)^{1/2}, \qquad \widehat{\Phi} = \left[\varpi_1\overline{\Phi}_1^{1/2}, \ldots, \varpi_q\overline{\Phi}_q^{1/2}\right]^T, \\ \overline{\Phi}_i = \begin{bmatrix} \Phi_i & 0 \\ 0 & 0 \end{bmatrix}, \qquad \overline{\Pi}_i = \begin{bmatrix} \widehat{\pi}_i \\ \widehat{\pi}_i \end{bmatrix}, \qquad \Xi = \operatorname{diag}\{\varpi_1 I, \ldots, \varpi_q I\}, \qquad \mathcal{F} = \begin{bmatrix} B & 0 \\ 0 & 0 \end{bmatrix}, \end{gathered} \tag{3.4}$$

then the estimation error system (2.10) *is mean-square stable.*

Proof. Define the following Lyapunov functional candidate for system (2.10):

$$V(\hat{x}(k),k) = \hat{x}^T(k)P\hat{x}(k) + \sum_{i=-\tau(k)}^{-1}\sum_{j=k+i}^{k-1}\hat{x}^T(j)Q\hat{x}(j) + \sum_{i=-\tau_u}^{-\tau_l-1}\sum_{j=i+1}^{-1}\sum_{n=k+j}^{k-1}\hat{x}^T(n)Q\hat{x}(n). \tag{3.5}$$

By calculating the difference of the Lyapunov functional (3.5), based on Lemma 3.2, one has,

$$\begin{aligned}
&\mathbb{E}\{\triangle V(\hat{x}(k),k)\}\\
&\quad= \mathbb{E}\{V(\hat{x}(k+1),k+1) \mid \hat{x}(k)\} - V\{(\hat{x}(k),k)\}\\
&\quad= \left[\mathcal{A}\hat{x}(k) + \mathcal{B}\sum_{m=-\tau(k)}^{-1}\hat{x}(k+m)\right]^T P\left[\mathcal{A}\hat{x}(k) + \mathcal{B}\sum_{m=-\tau(k)}^{-1}\hat{x}(k+m)\right]\\
&\qquad+ \mathbb{E}\left\{\left[\overline{\mathcal{B}}\sum_{m=-\tau(k)}^{-1}\hat{x}(k+m)\right]^T P\left[\overline{\mathcal{B}}\sum_{m=-\tau(k)}^{-1}\hat{x}(k+m)\right]\right\} + \alpha_3(1-\alpha 3)\hat{x}^T(k)P\hat{x}(k)\\
&\qquad+ \hat{x}^T(k)\mathcal{E}^T P\mathcal{E}\hat{x}(k) + \alpha_2\mathbb{E}\left\{h^T(k)\widehat{\mathcal{N}}^T P\widehat{\mathcal{N}}h(k)\right\} - \hat{x}^T(k)P\hat{x}(k)\\
&\qquad+ \sum_{i=-\tau(k+1)}^{-1}\sum_{j=k+i+1}^{k}\hat{x}^T(j)Q\hat{x}(j) - \sum_{i=-\tau(k)}^{-1}\sum_{j=k+i}^{k-1}\hat{x}^T(j)Q\hat{x}(j)\\
&\qquad+ \sum_{i=-\tau_u}^{-\tau_l-1}\sum_{j=i+1}^{-1}\left[\sum_{n=k+j+1}^{k} - \sum_{n=k+j}^{k-1}\right]\hat{x}^T(n)Q\hat{x}(n)\\
&\quad= \left[\mathcal{A}\hat{x}(k) + \mathcal{B}\sum_{m=-\tau(k)}^{-1}\hat{x}(k+m)\right]^T P\left[\mathcal{A}\hat{x}(k) + \mathcal{B}\sum_{m=-\tau(k)}^{-1}\hat{x}(k+m)\right]\\
&\qquad+ \mathbb{E}\left\{\left[\overline{\mathcal{B}}\sum_{m=-\tau(k)}^{-1}\hat{x}(k+m)\right]^T P\left[\overline{\mathcal{B}}\sum_{m=-\tau(k)}^{-1}\hat{x}(k+m)\right]\right\} + \alpha_3(1-\alpha 3)\hat{x}^T(k)P\hat{x}(k)\\
&\qquad+ \hat{x}^T(k)\mathcal{E}^T P\mathcal{E}\hat{x}(k) + \alpha_2\mathbb{E}\left\{h^T(k)\widehat{\mathcal{N}}^T P\widehat{\mathcal{N}}h(k)\right\} - \hat{x}^T(k)P\hat{x}(k)\\
&\qquad+ \sum_{i=-\tau(k+1)}^{-1}\left[\sum_{j=k+i+1}^{k-1}\hat{x}^T(j)Q\hat{x}(j) + \hat{x}^T(k)Q\hat{x}(k)\right]\\
&\qquad- \sum_{i=-\tau(k)}^{-1}\left[\sum_{j=k+i+1}^{k-1}\hat{x}^T(j)Q\hat{x}(j) + \hat{x}^T(k+i)Q\hat{x}(k+i)\right]\\
&\qquad+ \sum_{i=-\tau_u}^{-\tau_l-1}\sum_{j=i+1}^{-1}\left[\hat{x}^T(k)Q\hat{x}(k) - \hat{x}^T(k+j)Q\hat{x}(k+j)\right]
\end{aligned}$$

$$
\begin{aligned}
&\leq \left[\mathcal{A}\hat{x}(k) + \mathcal{B}\sum_{m=-\tau(k)}^{-1}\hat{x}(k+m)\right]^T P \left[\mathcal{A}\hat{x}(k) + \mathcal{B}\sum_{m=-\tau(k)}^{-1}\hat{x}(k+m)\right] \\
&\quad + \mathbb{E}\left\{\left[\overline{\mathcal{B}}\sum_{m=-\tau(k)}^{-1}\hat{x}(k+m)\right]^T \left[\overline{\mathcal{B}}\sum_{m=-\tau(k)}^{-1}\hat{x}(k+m)\right]\right\} + \alpha_3(1-\alpha 3)\hat{x}^T(k)P\hat{x}(k) \\
&\quad + \hat{x}^T(k)\mathcal{E}^T P\mathcal{E}\hat{x}(k) + \alpha_2\mathbb{E}\left\{h^T(k)\widehat{\mathcal{N}}^T P\widehat{\mathcal{N}}h(k)\right\} - \hat{x}^T(k)P\hat{x}(k) \\
&\quad + \sum_{i=-\tau_u}^{-\tau_l-1}\sum_{j=k+i+1}^{k-1}\hat{x}^T(j)Q\hat{x}(j) + \sum_{i=-\tau_l}^{-1}\sum_{j=k+i+1}^{k-1}\hat{x}^T(j)Q\hat{x}(j) \\
&\quad + \tau_u\hat{x}^T(k)Q\hat{x}(k) - \sum_{i=-\tau_l}^{-1}\sum_{j=k+i+1}^{k-1}\hat{x}^T(j)Q\hat{x}(j) - \sum_{i=-\tau(k)}^{-1}\hat{x}^T(k+i)Q\hat{x}(k+j) \\
&\quad + \frac{1}{2}(\tau_u-\tau_l)(\tau_u+\tau_l-1)\hat{x}^T(k)Q\hat{x}(k) - \sum_{i=-\tau_u}^{-\tau_l-1}\sum_{j=k+i+1}^{k-1}\hat{x}^T(j)Q\hat{x}(j) \\
&= \left[\mathcal{A}\hat{x}(k) + \mathcal{B}\sum_{m=-\tau(k)}^{-1}\hat{x}(k+m)\right]^T P \left[\mathcal{A}\hat{x}(k) + \mathcal{B}\sum_{m=-\tau(k)}^{-1}\hat{x}(k+m)\right] \\
&\quad + \mathbb{E}\left\{\left[\overline{\mathcal{B}}\sum_{m=-\tau(k)}^{-1}\hat{x}(k+m)\right]^T P\left[\overline{\mathcal{B}}\sum_{m=-\tau(k)}^{-1}\hat{x}(k+m)\right]\right\} + \alpha_3(1-\alpha 3)\hat{x}^T(k)P\hat{x}(k) \\
&\quad + \hat{x}^T(k)\mathcal{E}^T P\mathcal{E}\hat{x}(k) + \alpha_2\mathbb{E}\left\{h^T(k)\widehat{\mathcal{N}}^T P\widehat{\mathcal{N}}h(k)\right\} - \hat{x}^T(k)P\hat{x}(k) \\
&\quad + \tau_u\hat{x}^T(k)Q\hat{x}(k) - \sum_{i=-\tau(k)}^{-1}\hat{x}^T(k+i)Q\hat{x}(k+i) \\
&\quad + \frac{1}{2}(\tau_u-\tau_l)(\tau_u+\tau_l-1)\hat{x}^T(k)Q\hat{x}(k) \\
&\leq \left[\mathcal{A}\hat{x}(k) + \mathcal{B}\sum_{m=-\tau(k)}^{-1}\hat{x}(k+m)\right]^T P \left[\mathcal{A}\hat{x}(k) + \mathcal{B}\sum_{m=-\tau(k)}^{-1}\hat{x}(k+m)\right] \\
&\quad + \mathbb{E}\left\{\left[\overline{\mathcal{B}}\sum_{m=-\tau(k)}^{-1}\hat{x}(k+m)\right]^T P\left[\overline{\mathcal{B}}\sum_{m=-\tau(k)}^{-1}\hat{x}(k+m)\right]\right\} + \alpha_3(1-\alpha 3)\hat{x}^T(k)P\hat{x}(k) \\
&\quad + \hat{x}^T(k)\mathcal{E}^T P\mathcal{E}\hat{x}(k) + \alpha_2\mathbb{E}\left\{h^T(k)\widehat{\mathcal{N}}^T P\widehat{\mathcal{N}}h(k)\right\} - \hat{x}^T(k)P\hat{x}(k) \\
&\quad + \tau_u\hat{x}^T(k)Q\hat{x}(k) + \frac{1}{2}(\tau_u-\tau_l)(\tau_u+\tau_l-1)\hat{x}^T(k)Q\hat{x}(k) \\
&\quad - \sum_{i=-\tau(k)}^{-1}\hat{x}^T(k+i)Q\hat{x}(k+i)
\end{aligned}
$$

$$
\begin{aligned}
&\leq \left[\mathcal{A}\hat{x}(k) + \mathcal{B}\sum_{m=-\tau(k)}^{-1}\hat{x}(k+m)\right]^T P\left[\mathcal{A}\hat{x}(k) + \mathcal{B}\sum_{m=-\tau(k)}^{-1}\hat{x}(k+m)\right] \\
&\quad + \mathbb{E}\left\{\left[\overline{\mathcal{B}}\sum_{m=-\tau(k)}^{-1}\hat{x}(k+m)\right]^T P\left[\overline{\mathcal{B}}\sum_{m=-\tau(k)}^{-1}\hat{x}(k+m)\right]\right\} + \alpha_3(1-\alpha 3)\hat{x}^T(k)P\hat{x}(k) \\
&\quad + \hat{x}^T(k)\mathcal{E}^T P\mathcal{E}\hat{x}(k) + \alpha_2\mathbb{E}\left\{h^T(k)\widehat{\mathcal{N}}^T P\widehat{\mathcal{N}}h(k)\right\} - \hat{x}^T(k)P\hat{x}(k) \\
&\quad + \tau_u\hat{x}^T(k)Q\hat{x}(k) + \frac{1}{2}(\tau_u-\tau_l)(\tau_u+\tau_l-1)\hat{x}^T(k)Q\hat{x}(k) \\
&\quad - \tau_u^{-1}\left(\sum_{i=-\tau(k)}^{-1}\hat{x}^T(k+i)\right)Q\left(\sum_{i=-\tau(k)}^{-1}\hat{x}(k+i)\right).
\end{aligned}
\tag{3.6}
$$

From (2.8), it can be seen that

$$
\mathbb{E}\left\{h^T(k)\widehat{\mathcal{N}}^T P\widehat{\mathcal{N}}h(k)\right\} \leq \sum_{i=1}^{q}\left[\hat{x}^T(k)\overline{\Phi}_i\hat{x}(k)\right]\operatorname{tr}\left(\widehat{\mathcal{N}}\Pi_i\widehat{\mathcal{N}}^T P\right), \tag{3.7}
$$

where $\Pi_i := \overline{\Pi}_i\overline{\Pi}_i^T$ with $\overline{\Phi}_i$ and $\overline{\Pi}_i$ defined in (3.4).

Furthermore,

$$
\begin{aligned}
&\mathbb{E}\left\{\left[\mathcal{B}\sum_{m=-\tau(k)}^{-1}\hat{x}(k+m)\right]^T P\left[\mathcal{B}\sum_{m=-\tau(k)}^{-1}\hat{x}(k+m)\right]\right\} \\
&\qquad \leq \beta_2^2\sum_{m=-\tau(k)}^{-1}\hat{x}^T(k+m)\mathcal{F}^T P\mathcal{F}\sum_{m=-\tau(k)}^{-1}\hat{x}(k+m),
\end{aligned}
\tag{3.8}
$$

where β_2 is defined in (3.4).

From (3.6)–(3.8), one has

$$
\mathbb{E}\{\Delta V(\hat{x}(k),k)\} \leq \mathbb{E}\left\{\eta^T(k)\Theta\eta(k)\right\}, \tag{3.9}
$$

where $\eta(k) = [\hat{x}^T(k), \sum_{i=-\tau(k)}^{-1}\hat{x}^T(k+i)]^T$ and

$$
\Theta = \begin{bmatrix}\Theta_1 & \mathcal{A}P\mathcal{B} \\ * & \Theta_2\end{bmatrix}, \tag{3.10}
$$

where $\Theta_1 = -P + \mathcal{E}^T P \mathcal{E} + (\tau_u + (1/2)(\tau_u - \tau_l)(\tau_u + \tau_l - 1))Q + \mathcal{A}^T P \mathcal{A} + \beta_4^2 \sum_{i=1}^{q} \overline{\Phi}_i \operatorname{tr}(\widehat{\mathcal{N}}\Pi_i \widehat{\mathcal{N}}^T P) + \beta_3^2 P, \Theta_2 = -(1/\tau_u)Q + \mathcal{B}^T P \mathcal{B} + \beta_2^2 \mathcal{F}^T P \mathcal{F}$, β_3, β_4, $\mathcal{F}$ are defined in (3.4).

From Lemma 3.1, (3.10) holds if and only if $\operatorname{tr}(\widehat{\mathcal{N}}\Pi_i \widehat{\mathcal{N}}^T P)$. Furthermore, by Lemma 3.1, one can obtain from (3.2), (3.3) that $\Theta < 0$ and, subsequently,

$$\mathbb{E}\{\triangle V(\hat{x}(k), k)\} < -\lambda_{\min}(\Theta)|\hat{x}(k)|^2. \tag{3.11}$$

Thus, the augmented estimation system (2.10) is mean-square stable. □

The following theorem is focused on the design of the desired estimation parameters A_f and A_k by using the results in Theorem 3.3.

Theorem 3.4. *Consider the augmented estimation system* (2.10) *with given estimator parameters. If there exist positive-definite matrices $S = S^T > 0$, $R = R^T > 0$, $Q = Q^T > 0$, matrices $\widetilde{A}_f$, $\widetilde{A}_k$, and positive scalars $\varpi_i > 0$, $(i = 1, 2, \ldots, q)$ such that the following linear matrix inequalities holds*

$$\Gamma = \begin{bmatrix} -S & * & * & * & * & * & * & * & * & * & * & * & * \\ -S & -R & * & * & * & * & * & * & * & * & * & * & * \\ 0 & 0 & -Q & * & * & * & * & * & * & * & * & * & * \\ SE_1 & E_1 & 0 & -S & * & * & * & * & * & * & * & * & * \\ \phi_1 & \phi_2 & 0 & -S & -R & * & * & * & * & * & * & * & * \\ \beta_1 Q & \beta_1 Q & 0 & 0 & 0 & -Q & * & * & * & * & * & * & * \\ SA & SA & \alpha_1 SB & 0 & 0 & 0 & -S & * & * & * & * & * & * \\ \phi_3 & \phi_4 & \alpha_1 RB & 0 & 0 & 0 & -S & -R & * & * & * & * & * \\ \beta_3 S & \beta_3 S & 0 & 0 & 0 & 0 & 0 & 0 & -S & * & * & * & * \\ \beta_3 S & \beta_3 R & 0 & 0 & 0 & 0 & 0 & 0 & -S & -R & * & * & * \\ \widetilde{\Phi} & \widetilde{\Phi} & 0 & 0 & 0 & 0 & 0 & 0 & 0 & 0 & -\Xi & * & * \\ 0 & 0 & \beta_2 SB & 0 & 0 & 0 & 0 & 0 & 0 & 0 & 0 & -R & * \\ 0 & 0 & \beta_2 RB & 0 & 0 & 0 & 0 & 0 & 0 & 0 & 0 & -S & -R \end{bmatrix} < 0, \tag{3.12}$$

$$\begin{bmatrix} -\varpi_i I & * & * \\ S\widehat{\pi}_i & -S & * \\ R\widehat{\pi}_i + \widetilde{A}_f \widehat{\pi}_i & -S & -R \end{bmatrix} < 0, \quad i = 1, 2, \ldots, q, \tag{3.13}$$

$$S - R < 0 \tag{3.14}$$

hold, where α_1 is defined in (2.2), *β_1, β_2, β_3, and β_4 are defined in* (3.4),

$$\begin{gathered} \widetilde{\Phi}^T = \left[\beta_4 \left[\varpi_1 \Phi_1^{1/2}\right]^T, \ldots, \beta_4 \left[\varpi_q \Phi_q^{1/2}\right]^T\right], \\ \phi_1 = RE_1 + \widetilde{A}_f E_2, \qquad \phi_2 = RE_1 + \widetilde{A}_f E_2, \\ \phi_3 = RA + \alpha_2 \widetilde{A}_f C + \widetilde{A}_k, \qquad \phi_4 = RA + \alpha_2 \widetilde{A}_f C, \end{gathered} \tag{3.15}$$

then the estimator parameters are designed as

$$A_k = X_{12}^{-1}\widetilde{A}_f, \qquad A_f = X_{12}^{-1}\widetilde{A}_k S^{-1}\left(Y_{12}^T\right)^{-1}, \tag{3.16}$$

where X_{12}, Y_{12} *are any square and nonsingular matrices satisfying* $X_{12}Y_{12}^T = I - RS^{-1} < 0$, *then the estimation error system* (2.10) *is mean-square stable.*

Proof. Recall that our goal is to derive the expression of the estimator parameters from (2.9). To do this, we partition P and P^{-1} as

$$P = \begin{bmatrix} R & X_{12} \\ X_{12}^T & X_{22} \end{bmatrix}, \qquad P^{-1} = \begin{bmatrix} S^{-1} & Y_{12} \\ Y_{12}^T & Y_{22} \end{bmatrix}, \tag{3.17}$$

where the partitioning of P and P^{-1} is compatible with that of $\mathcal{A}$ defined in (2.11), that is, $R \in R^{n\times n}$, $X_{12} \in R^{n\times n}$, $X_{22} \in R^{n\times n}$, $S \in R^{n\times n}$, $Y_{12} \in R^{n\times n}$, and $Y_{22} \in R^{n\times n}$. Define

$$T_1 = \begin{bmatrix} S^{-1} & I \\ Y_{12}^T & 0 \end{bmatrix}, \qquad T_2 = \begin{bmatrix} I & R \\ 0 & X_{12}^T \end{bmatrix} \tag{3.18}$$

which imply that $PT_1 = T_2$ and $T_1^T P T_1 = T_1^T T_2$.

By applying the congruence transformations $\operatorname{diag}\{T_1, I, T_1, I, T_1, T_1, I, \ldots, I, T_1\}$ and the congruence transformations $\operatorname{diag}\{S, I, I, S, I, I, S, I, S, I, I, \ldots, I, S, I\}$ to (3.2), we have (3.12).

Again, performing the congruence transformation $\operatorname{diag}\{I, T_1\}$ to (3.3) lead to (3.19)

$$\begin{bmatrix} -\varpi_i I & * & * \\ \widehat{\pi}_i & -S^{-1} & * \\ R\widehat{\pi}_i + X_{12}A_k\widehat{\pi}_i & -I & -R \end{bmatrix} < 0, \quad i = 1, 2, \ldots, q. \tag{3.19}$$

Then, one uses congruence transformation $\operatorname{diag}\{I, S, I\}$ to (3.19) and we have

$$\begin{bmatrix} -\varpi_i I & * & * \\ S\widehat{\pi}_i & -S & * \\ R\widehat{\pi}_i + X_{12}A_k\widehat{\pi}_i & -S & -R \end{bmatrix} < 0, \quad i = 1, 2, \ldots, q. \tag{3.20}$$

Furthermore, if (3.12) is feasible, we have $\left[\begin{smallmatrix} -S & -S \\ -S & -R \end{smallmatrix}\right] < 0$ or $\left[\begin{smallmatrix} -S^{-1} & I \\ I & R \end{smallmatrix}\right] > 0$.

It follows directly from $XX^{-1} = I$ that $I - RS^{-1} = X_{12}Y_{12}^T < 0$. Hence, one can always find square and nonsingular X_{12} and Y_{12} [37]. Therefore, this completes the proof. □

4. Numerical Example

In this section, an example is presented to illustrate the usefulness and flexibility of the estimator design method developed in this paper. The system data of (2.1)–(2.9) are the following:

$$A = \begin{bmatrix} 0.15 & 0 \\ 0.2 & 0.1 \end{bmatrix}, \qquad B = \begin{bmatrix} 0.09 & 0 \\ 0 & 0.09 \end{bmatrix}, \qquad C = \begin{bmatrix} 1.2 & 0 \\ 0 & 1.2 \end{bmatrix},$$
$$E_1 = \begin{bmatrix} 0.12 & 0 \\ 0 & 0.12 \end{bmatrix}, \qquad E_2 = \begin{bmatrix} 0.12 & 0 \\ 0 & 0.12 \end{bmatrix}, \qquad H_1 = H_2 = \begin{bmatrix} 0.6 & 0 \\ 0 & 0.6 \end{bmatrix}, \tag{4.1}$$

where $n = q = 2$, $\tau(k) = 1 + (1 + (-1)^k)$, $\tau_l = 1$, $\tau_u = 3$.

$f(x(k))$ describes the stochastic nonlinear function of the states in (2.1), which is bounded as follows:

$$\mathbb{E}\left\{ f(x(k)) f(x(k))^T \mid x(k) \right\} = \begin{bmatrix} 0.22 \\ 0.22 \end{bmatrix} \begin{bmatrix} 0.22 \\ 0.22 \end{bmatrix}^T x^T(k) \begin{bmatrix} 0.11 & 0 \\ 0 & 0.11 \end{bmatrix} x(k). \tag{4.2}$$

Let $\alpha_1 = 0.2$, $\alpha_2 = 0.3$, and $\alpha_3 = 0.9$. Using Matlab LMI Toolbox to solve the LMIs in (3.12)–(3.14), one has

$$S = \begin{bmatrix} 0.6726 & -0.0035 \\ -0.0035 & 0.6563 \end{bmatrix}, \qquad R = \begin{bmatrix} 1.8796 & -0.0041 \\ -0.0041 & 1.8411 \end{bmatrix},$$
$$Q = \begin{bmatrix} 0.0668 & -0.0013 \\ -0.0013 & 0.0693 \end{bmatrix}, \qquad \varpi_1 = 1.0776, \quad \varpi_2 = 1.3335. \tag{4.3}$$

Thus, we can calculate the estimator parameters as follows:

$$A_f = \begin{bmatrix} 0.1325 & 0.0486 \\ 0.0462 & -0.1465 \end{bmatrix}, \qquad A_k = \begin{bmatrix} -0.9144 & -0.1677 \\ -0.1684 & -0.8160 \end{bmatrix}. \tag{4.4}$$

Remark 4.1. Seldom of the estimation literature explicitly introduce the effects of the estimators by the digits in the graphs, for example [18]. In this paper, some digits are marked in Figures 1–4. Figures 1–2 show the actual measurements and ideal measurements. Figures 3–4 plot the estimation errors. From these digits in the graphs, it can be seen that the designed estimator performs well.

5. Conclusions

In this paper, we research the estimation problem for a class of stochastic nonlinear systems with both the probabilistic distributed time-varying delays and missing measurements. The distributed time-varying delays and missing measurements are assumed to occur in random ways, and the occurring probabilities are governed by Bernoulli stochastic variables. A linear estimator is designed such that, for the admissible random distributed delays, the

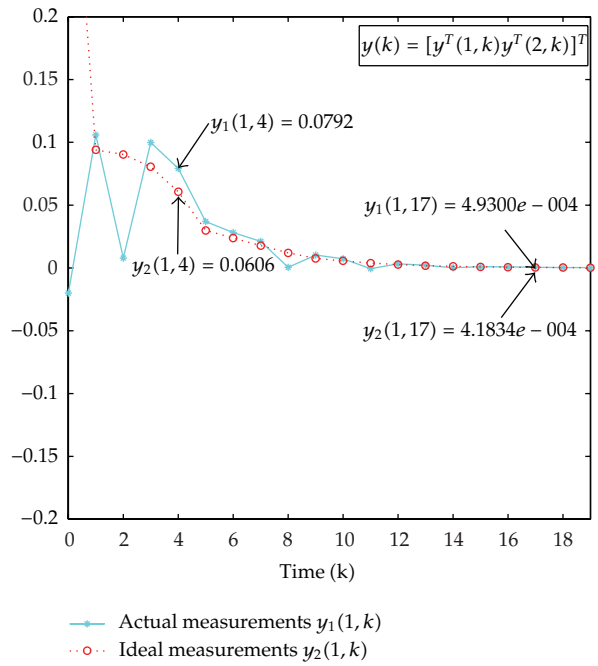

Figure 1: Actual Measurements $y_1(1,k)$ and ideal Measurements $y_2(1,k)$.

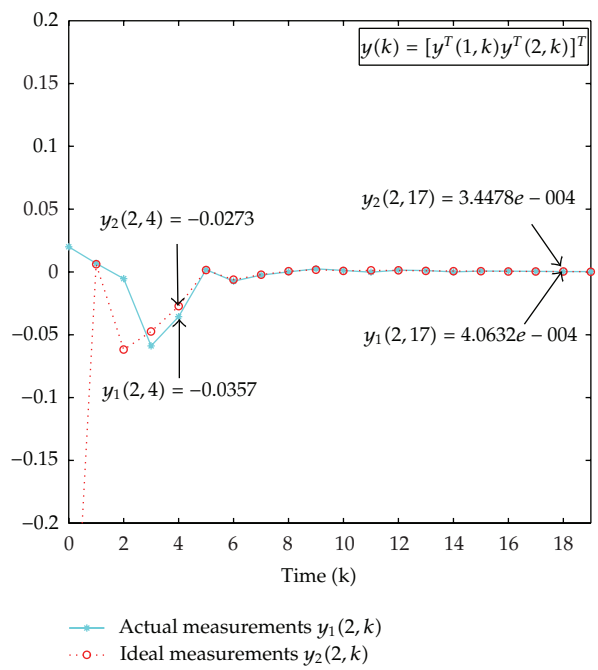

Figure 2: Actual Measurements $y_1(2,k)$ and ideal Measurements $y_2(2,k)$.

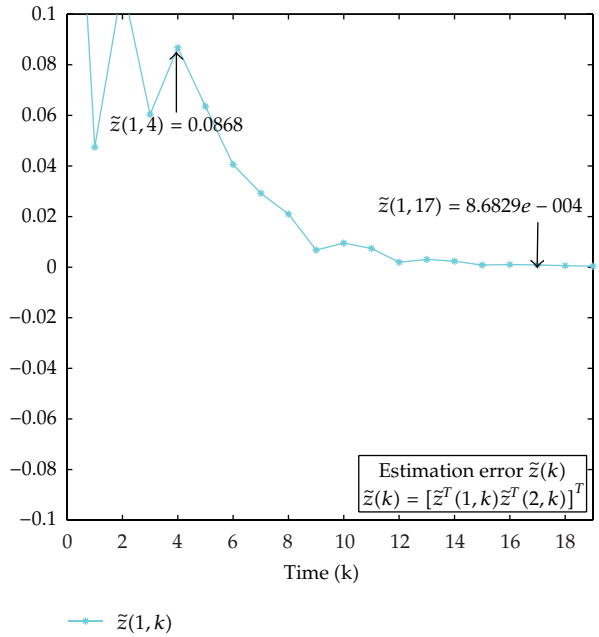

Figure 3: Estimation Errors $\tilde{z}(1,k)$.

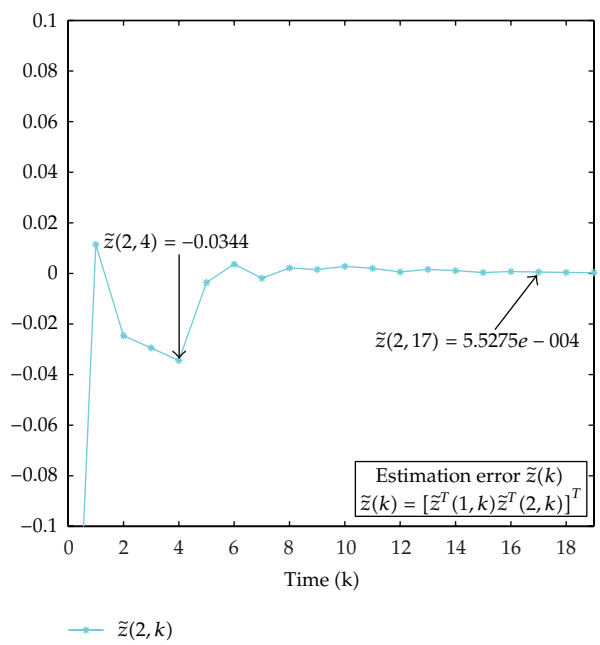

Figure 4: Estimation Errors $\tilde{z}(2,k)$.

stochastic disturbances, and the stochastic nonlinearities, the error dynamics of the estimation process is mean-square stable. At last, an illustrative example has been exploited to show the effectiveness of the proposed approach. In the future, we plan to consider the estimation problem with Markovian switching is in the finite-horizon case, and the nonlinearities are in more general forms.

Acknowledgments

This work was supported in part by the National Natural Science Foundation of China under Grant nos. 60974030 and 61104125, the Science and Technology Project of Education Department in Fujian Province under Grant no. JA11211, and the Science and Technology Innovation Platform "CAD/CAM Engineering Research Center of Universities of Fujian Province" which is set up in Putian University, Putian, Fujian Province, China.

References

[1] M. F. Bugallo and S. Xu, "Performance comparison of EKF and particle filtering methods for maneuvering targets," *Digital Signal Processing*, vol. 17, no. 4, pp. 774–786, 2007.

[2] C. Chen, H. Liu, and X. Guan, "H_∞ filtering of time-delay T-S fuzzy systems based on piecewise Lyapunov-Krasovskii functional," *Signal Processing*, vol. 89, no. 10, pp. 1998–2005, 2009.

[3] O. Costa, "Stationary filter for linear minimum means quare error estimator of discretetime markovian jump systems," *IEEE Transactions on Automatic Control*, vol. 48, no. 8, pp. 1351–1356, 2002.

[4] H. Gao, J. Lam, L. Xie, and C. Wang, "New approach to mixed H_2/H_∞ filtering for polytopic discrete-time systems," *IEEE Transactions on Signal Processing*, vol. 53, no. 8, pp. 3183–3192, 2005.

[5] H. Gao and C. Wang, "A delay-dependent approach to robust H_∞ filtering for uncertain discrete-time state-delayed systems," *IEEE Transactions on Signal Processing*, vol. 52, no. 6, pp. 1631–1640, 2004.

[6] H. Gao, J. Lam, C. Wang, and S. Xu, "Robust H_∞ filtering for 2D stochastic systems," *Circuits, Systems, and Signal Processing*, vol. 23, no. 6, pp. 479–505, 2004.

[7] H. Gao, J. Lam, and C. Wang, "Robust energy-to-peak filter design for stochastic time-delay systems," *Systems & Control Letters*, vol. 55, no. 2, pp. 101–111, 2006.

[8] W. Zhou, H. Su, and J. Chu, "Delay-dependent H1 filtering for singular Markovian jump time-delay systems," *Signal Processing*, vol. 90, no. 6, pp. 1815–1824, 2010.

[9] A. Subramanian and A. H. Sayed, "Multiobjective filter design for uncertain stochastic time-delay systems," *IEE E Transactions on Automatic Control*, vol. 49, no. 1, pp. 149–154, 2004.

[10] G. Wei, Z. Wang, and H. Shu, "Robust filtering with stochastic nonlinearities and multiple missing measurements," *Automatica*, vol. 45, no. 3, pp. 836–841, 2009.

[11] B. Shen, Z. Wang, H. Shu, and G. Wei, "On nonlinear H_∞ filtering for discrete-time stochastic systems with missing measurements," *IEEE Transactions on Automatic Control*, vol. 53, no. 9, pp. 2170–2180, 2008.

[12] G. Wei, Z. Wang, X. He, and H. Shu, "Filtering for networked stochastic time-delay systems with sector nonlinearity," *IEEE Transactions on Circuits and Systems-II*, vol. 56, no. 1, pp. 71–75, 2009.

[13] Z. Wang, J. Lam, L. Ma, Y. Bo, and Z. Guo, "Variance-constrained dissipative observer-based control for a class of nonlinear stochastic systems with degraded measurements," *Journal of Mathematical Analysis and Applications*, vol. 377, no. 2, pp. 645–658, 2011.

[14] Z. Wang, F. Yang, D. W. C. Ho, and X. Liu, "Robust H^∞ filtering for stochstic time-delay systems with missing measurements," *IEEE Transactions on Signal Processing*, vol. 54, no. 7, pp. 2579–2587, 2006.

[15] B. Shen, Z. Wang, and Y. S. Hung, "Distributed H_∞-consensus filtering in sensor networks with multiple missing measurements: the finite-horizon case," *Automatica*, vol. 46, no. 10, pp. 1682–1688, 2010.

[16] Q. Ling and M. D. Lemmon, "Optimal dropout compensation in networked control systems," in *Proceedings of the IEEE Conference on Decosion and Control*, pp. 670–675, Honolulu, Hawaii, USA, 2003.

[17] B. Sinopoli, L. Schenato, M. Franceschetti, K. Poolla, M. I. Jordan, and S. S. Sastry, "Kalman filtering with intermittent observations," *IEEE Transactions on Automatic Control*, vol. 49, no. 9, pp. 1453–1464, 2004.

[18] Y. Che, H. Shu, and Z. Wang, "Nonlinear systems filtering with missing measurements and randomly distributed delays," *Journal of Harbin University of Science and Technology*, vol. 16, no. 6, pp. 36–41, 2011.

[19] Z. Wang, B. Shen, H. Shu, and G. Wei, "Quantized H-infinity control for nonlinear stochastic time-delay systems with missing measurements," *IEEE Transactions on Automatic Control*, vol. 57, no. 6, pp. 1431–1444, 2012.

[20] Z. Wang, B. Shen, and X. Liu, "H_∞ filtering with randomly occurring sensor saturations and missing measurements," *Automatica*, vol. 48, no. 3, pp. 556–562, 2012.

[21] B. Shen, Z. Wang, J. Liang, and Y. Liu, "Recent advances on filtering and control for nonlinear stochastic complex systems with incomplete information: a survey," *Mathematical Problems in Engineering*, vol. 2012, Article ID 530759, 16 pages, 2012.

[22] H. Dong, Z. Wang, and H. Gao, "Distributed filtering for a class of time-varying systems over sensor networks with quantization errors and successive packet dropouts," *IEEE Transactions on Signal Processing*, vol. 60, no. 6, pp. 3164–3173, 2012.

[23] V. Kapila and W. M. Haddad, "Memoryless H1 controllers for discrete-time systems with time delay," *Automatica*, vol. 34, no. 8, pp. 1141–1144, 1998.

[24] J. H. Kim and H. B. Park, "H^∞ state feedback control for generalized continuous/discrete time-delay system," *Automatica*, vol. 35, no. 8, pp. 1443–1451, 1999.

[25] C. E. de Souza and X. Li, "Delay-dependent robust H_∞ control of uncertain linear state-delayed systems," *Automatica*, vol. 35, no. 7, pp. 1313–1321, 1999.

[26] E. Fridman and U. Shaked, "A descriptor system approach to H_∞ control of linear time-delay systems," *IEEE Transactions on Automatic Control*, vol. 47, no. 2, pp. 253–270, 2002.

[27] E. Fridman and U. Shaked, "An improved stabilization method for linear time-delay systems," *IEEE Transactions on Automatic Control*, vol. 47, no. 11, pp. 1931–1937, 2002.

[28] Y. S. Moon, P. Park, W. H. Kwon, and Y. S. Lee, "Delay-dependent robust stabilization of uncertain state-delayed systems," *International Journal of Control*, vol. 74, no. 14, pp. 1447–1455, 2001.

[29] Y. Zhang, S. Xu, Y. Zou, and J. Lu, "Delay-dependent robust stabilization for uncertain discrete-time fuzzy Markovian jump systems with mode-dependent time delays," *Fuzzy Sets and Systems*, vol. 164, no. 1, pp. 66–81, 2011.

[30] Z.-W. Liu and H.-G. Zhang, "Delay-dependent stability for systems with fast-varying neutral-type delays via a PTVD compensation," *Acta Automatica Sinica*, vol. 36, no. 1, pp. 147–152, 2010.

[31] D. Yue and H. Li, "Synchronization stability of continuous/discrete complex dynamical networks with interval time-varying delays," *Neurocomputing*, vol. 73, pp. 4809–6819, 2010.

[32] Y. Liu, Z. Wang, and X. Liu, "Robust H_∞ filtering for discrete nonlinear stochastic systems with time-varying delay," *Journal of Mathematical Analysis and Applications*, vol. 341, no. 1, pp. 318–336, 2008.

[33] S. Xu, J. Lam, and C. Yang, "H_∞ and positive-real control for linear neutral delay systems," *IEEE Transactions on Automatic Control*, vol. 46, no. 8, pp. 1321–1326, 2001.

[34] R. Rakkiyappan and P. Balasubramaniam, "Delay-probability-distribution-dependent stability of uncertain stochastic genetic regulatory networks with mixed time-varying delays: an LMI approach," *Nonlinear Analysis. Hybrid Systems*, vol. 4, no. 3, pp. 600–607, 2010.

[35] Y. Liu, Z. Wang, and X. Liu, "State estimation for discrete-time Markovian jumping neural networks with mixed mode-dependent delays," *Physics Letters A*, vol. 372, no. 48, pp. 7147–7155, 2008.

[36] H. Shu, Z. Wang, and Z. Lü, "Global asymptotic stability of uncertain stochastic bi-directional associative memory networks with discrete and distributed delays," *Mathematics and Computers in Simulation*, vol. 80, no. 3, pp. 490–505, 2009.

[37] C. Scherer, P. Gahinet, and M. Chilali, "Multiobjective output-feedback control via LMI optimization," *IEEE Transactions on Automatic Control*, vol. 42, no. 7, pp. 896–911, 1997.

Hindawi Publishing Corporation
Mathematical Problems in Engineering
Volume 2012, Article ID 750841, 16 pages
doi:10.1155/2012/750841

Research Article

Robust H_2/H_∞ Filter Design for a Class of Nonlinear Stochastic Systems with State-Dependent Noise

Weihai Zhang,[1] Bor-Sen Chen,[2] Li Sheng,[3] and Ming Gao[1]

[1] *College of Information and Electrical Engineering, Shandong University of Science and Technology, Qingdao 266590, China*
[2] *Department of Electrical Engineering, National Tsing Hua University, Hsinchu 30013, Taiwan*
[3] *College of Information and Control Engineering, China University of Petroleum (East China), Qingdao 266555, China*

Correspondence should be addressed to Weihai Zhang, w_hzhang@163.com

Received 17 June 2012; Accepted 24 August 2012

Academic Editor: Jun Hu

This paper investigates the problem of robust filter design for a class of nonlinear stochastic systems with state-dependent noise. The state and measurement are corrupted by stochastic uncertain exogenous disturbance and the dynamic system is modeled by Itô-type stochastic differential equations. For this class of nonlinear stochastic systems, the robust H_∞ filter can be designed by solving linear matrix inequalities (LMIs). Moreover, a mixed H_2/H_∞ filtering problem is also solved by minimizing the total estimation error energy when the worst-case disturbance is considered in the design procedure. A numerical example is provided to illustrate the effectiveness of the proposed method.

1. Introduction

Over the past decades, the robust H_∞ filtering problem has been investigated extensively since it is very useful in signal processing and engineering applications [1–5]. The so-called H_∞ filtering problem is to design an estimator to estimate the unknown state combination via measurement output, which guarantees the $\mathcal{L}_2$ gain (from the external disturbance to the estimation error) to be less than a prescribed level $\gamma > 0$. In contrast to classical Kalman filter, it is not necessary to know the exact statistic information about the external disturbance in the H_∞ filter design. Obviously, there may be more than one solution to H_∞ filtering problem with a desired robustness. Since the H_2 performance is appealing for engineering, it naturally leads to the mixed H_2/H_∞ filtering problem [6–8]. Compared with the sole H_∞ filter, the mixed H_2/H_∞ filter is more attractive in engineering practice, since the former is a worst-case

design which tends to be conservative whereas the latter minimizes the average performance with a guaranteed worst-case performance. The robust H_2/H_∞ filtering problem for linear perturbed systems with steady-state error variance constraints was investigated in [6], and the mixed H_2/H_∞ filter for polytopic discrete-time systems was discussed in [7].

On the other hand, stochastic H_∞ control and filtering problems for systems expressed by stochastic Itô-type differential equations have attracted a great deal of attention [9–13, 23]. A bounded real lemma was proposed for linear continuous-time stochastic systems [11], according to which full- and reduced-order robust H_∞ problems for linear stochastic systems were investigated by [12, 13], respectively. Most of the aforementioned works were limited to linear stochastic systems. Recently, the H_∞ filtering problem for nonlinear stochastic systems has become another popular research topic [14–20]. Wang et al. [14] studied the robust H_∞ filtering problem for a class of uncertain time-delay stochastic systems with sector-bounded nonlinearities. For general nonlinear stochastic systems, Zhang et al. [15] found that the H_∞ filter can be obtained by solving a second-order Hamilton-Jacobi inequality (HJI). Considering that it is difficult to solve the HJI, Tseng [17] designed the H_∞ fuzzy filter for nonlinear stochastic systems via solving LMIs instead of an HJI. However, there is little work dealing with the H_2/H_∞ filtering problem for nonlinear stochastic systems.

In this paper, we will deal with the robust filtering problem for a class of nonlinear stochastic systems. The state is corrupted not only by white noise but also by exogenous disturbance signal, and the measurement equation also includes noises. Our goal in this paper is to construct an asymptotically stable observer that leads to a mean square stable estimation error process whose $\mathcal{L}_2$ gain with respect to disturbance signal is less than a prescribed level. Moreover, a stochastic H_2/H_∞ filtering is designed for the nonlinear stochastic systems. Our main results are expressed in linear matrix inequalities (LMIs), which are more easily computed in practical application.

This paper is organized as follows: in Section 2, some definitions and notations are introduced; Section 3 treats with the H_∞ and mixed H_2/H_∞ filtering problems, and the main outcomes of this section are Theorems 3.2 and 3.6; a numerical example is presented to illustrate the effectiveness of the proposed filtering method in Section 4; Section 5 concludes this paper.

Notations. For convenience, we adopt the following notations. $\mathcal{S}_n$: the set of all $n\times n$ symmetric matrices; its components may be complex. A': the transpose of the corresponding matrix A. $A \geq 0$ ($A > 0$): A is positive semidefinite (positive definite) symmetric matrix. $|x| := (\sum_{i=1}^{n} x_i^2)^{1/2}$, that is, $|x|$ denotes the Euclidean 2-norm of x, where $x = (x_1, x_2, \ldots, x_n)' \in \mathcal{R}^n$. $\mathcal{L}^2(\mathcal{R}_+, \mathcal{R}^l)$: the space of nonanticipative stochastic processes $y(t)$ with respect to filter $\mathcal{F}_t$ satisfying $\|y(t)\|_{L_2}^2 := E\int_0^\infty |y(t)|^2 dt < \infty$. $C_2^0(\{t > 0\} \times U)$: class of functions $V(t,x)$ twice continuously differential with respect to $x \in U$ and once continuously differential with respect to $t > 0$ except possibly at the point $x = 0$.

2. Problem Setting

Consider the following nonlinear stochastic system governed by Itô differential equation:

$$dx(t) = \big(f(x(t)) + B_0 w(t)\big)dt + \sigma(x(t))dw_0(t), \tag{2.1}$$

with the following measurement equation:

$$dy(t) = (A_1 x(t) + B_1 w(t))dt + C_1 x(t) dw_1(t), \tag{2.2}$$

and the controlled output

$$z(t) = Dx(t). \tag{2.3}$$

In the above, $x(t) \in \mathcal{R}^n$ is called the system state, $y(t) \in \mathcal{R}^r$ is the measurement output, $z(t)$ is the state combination to be estimated. $w_0(t), w_1(t)$ are the standard Wiener processes defined on the probability space $(\Omega, \mathcal{F}, \mathcal{P})$ related to an increasing family $(\mathcal{F}_t)_{t\in\mathcal{R}_+}$ of σ-algebras $\mathcal{F}_t \subset \mathcal{F}$. Without loss of generality, we can suppose $w_0(t), w_1(t)$ are one-dimensional, mutually uncorrelated. B_0, A_1, B_1, C_1, D are constant matrices of suitable dimensions, $w \in \mathcal{L}^2(\mathcal{R}_+, \mathcal{R}^q)$ represents the exogenous disturbance signal. Under very general conditions on f and σ, stochastic systems (2.1)-(2.2) have, respectively, a unique strong solution $x_{s,\xi}(t)$ for any $t \geq s \geq 0$ and initial state $x(s) = \xi \in \mathcal{R}^n$; see [21].

Now, we first introduce the following definitions.

Definition 2.1 (see [9]). We say that the equilibrium point $x \equiv 0$ of system

$$dx(t) = f(x(t))dt + \sigma(x(t))dw_0(t) \tag{2.4}$$

is exponentially mean square stable, if for some positive constants ρ, ϱ,

$$E|x(t)|^2 \leq \rho|x(0)|^2 \exp(-\varrho t), \quad t \geq 0. \tag{2.5}$$

Remark 2.2. It is well known that for stochastic linear time-invariant systems, the exponential mean square stability is equivalent to asymptotical mean square stability [9].

Definition 2.3. Nonlinear stochastic uncertain system (2.1) is said to be internally stable at the origin, if (2.1) with $w = 0$ is exponentially mean square stable.

Lemma 2.4 (see [9]). *The trivial solution of* (2.4) *is exponentially mean square stable for* $t \geq 0$ *if there exists* $V(t,x) \in C_2^0(\{t > 0\} \times \mathcal{R}^n)$ *such that*

$$k_1|x|^2 \leq V(t,x) \leq k_2|x|^2, \qquad \mathcal{L}V(t,x) \leq -k_3|x|^2 \tag{2.6}$$

for some positive constants k_1, k_2, k_3, *where* $\mathcal{L}$ *is the so-called an infinitesimal generator of* (2.4).

Now, suppose $f(x)$ *and* $\sigma(x)$ *can be linearized, respectively, as*

$$\begin{aligned} f(x) &= Ax + F_0(x), \qquad F_0(0) = 0, \\ \sigma(x) &= Cx + F_1(x), \qquad F_1(0) = 0, \end{aligned} \tag{2.7}$$

then the linearized stochastic system of (2.1) *becomes*

$$dx = (Ax + B_0 w + F_0(x))dt + (Cx + F_1(x))dw_0, \tag{2.8}$$

where A *and* C *are constant matrices.*

Consider the following filter for the estimation of $z(t)$:

$$d\hat{x} = A_f\hat{x}dt + B_f dy, \qquad \hat{x}(0) = \hat{x}_0, \qquad \hat{z} = D\hat{x}, \tag{2.9}$$

where $\hat{x} \in \mathcal{R}^n$. Let $\xi' = [x' \;\; x' - \hat{x}']$, $\tilde{z} = z - \hat{z}$, then

$$d\xi = \tilde{A}\xi dt + \tilde{D}_1\xi dw_0 + \tilde{D}_2\xi dw_1 + \tilde{F}_1 dt + \tilde{F}_2 dw_0 + \tilde{F}_3 w dt, \tag{2.10}$$

where

$$\begin{gathered}\tilde{A} = \begin{bmatrix} A & 0 \\ A - B_f A_1 - A_f & -A_f \end{bmatrix}, \qquad \tilde{D}_1 = \begin{bmatrix} C & 0 \\ C & 0 \end{bmatrix}, \qquad \tilde{D}_2 = \begin{bmatrix} 0 & 0 \\ -B_f C_1 & 0 \end{bmatrix}, \\ \tilde{F}_1 = \begin{bmatrix} F_0(x) \\ F_0(x) \end{bmatrix}, \qquad \tilde{F}_2 = \begin{bmatrix} F_1(x) \\ F_1(x) \end{bmatrix}, \qquad \tilde{F}_3 = \begin{bmatrix} B_0 \\ B_0 - B_f B_1 \end{bmatrix}.\end{gathered} \tag{2.11}$$

For any given disturbance attenuation level $\gamma > 0$, one wants to find A_f, B_f, such that

$$\|\tilde{z}(t)\|_{L_2}^2 < \gamma^2 \|w(t)\|_{L_2}^2 \tag{2.12}$$

holds for any $w \in \mathcal{L}^2(\mathcal{R}_+, \mathcal{R}^q)$. Define the H_∞ performance index as

$$J_s = \|\tilde{z}(t)\|_{L_2}^2 - \gamma^2 \|w(t)\|_{L_2}^2. \tag{2.13}$$

Obviously, (2.12) *holds iff $J_s < 0$. As in [12], H_∞ and mixed H_2/H_∞-based robust state estimation problems are formulated as follows.*

(i) *Stochastic H_∞ filtering problem: given $\gamma > 0$, find an estimator $\hat{x}$ of the form* (2.9) *leading* (2.10) *to being internally stable; Moreover, $J_s < 0$ for all nonzero $w \in \mathcal{L}^2(\mathcal{R}_+, \mathcal{R}^n)$ with $\xi(0) = 0$.*

(ii) *Stochastic H_2/H_∞ filtering problem: of all the H_∞ filter of (i), one finds the one that minimizes the steady error variance*

$$\lim_{t\to\infty} E\left[\tilde{z}'(t)\tilde{z}(t)\right], \tag{2.14}$$

where in this case, $w(t) = \dot{\eta}$, η is taken as a standard Wiener process, independent of $w_0(t)$ and $w_1(t)$, so $w(t)$ is a white noise. (2.2) *and* (2.8) *can be written as (see, e.g., [22])*

$$\begin{gathered} dy(t) = A_1 x(t)dt + B_1 d\eta(t) + C_1 x(t) dw_1(t), \\ dx(t) = (Ax(t) + F_0(x(t)))dt + (Cx(t) + F_1(x(t)))dw_0(t) + B_0 d\eta(t), \end{gathered} \tag{2.15}$$

respectively.

3. Stochastic H_∞ and Mixed H_2/H_∞ Filter Design

In this section, we will discuss, respectively, stochastic H_∞ and mixed H_2/H_∞ filtering problems.

3.1. Stochastic H_∞ Filter Design

In this section, some sufficient conditions are given for H_∞ filter design; our main results are as follows.

Theorem 3.1. *Suppose there exists a scalar $\lambda > 0$, such that*

$$|F_i(x)| \leq \lambda |x|, \quad i = 0, 1, \ \forall x \in \mathcal{R}^n. \tag{3.1}$$

If the following matrix inequalities

$$P\tilde{A} + \tilde{A}'P + 2\tilde{D}_1'P\tilde{D}_1 + \tilde{D}_2'P\tilde{D}_2 + P + 6\lambda^2\alpha I + Q + \frac{1}{\gamma^2}P\tilde{F}_3\tilde{F}_3'P < 0, \tag{3.2}$$

$$0 < P \leq \alpha I \tag{3.3}$$

have a solution $P > 0$, $\alpha > 0$, then (2.10) *is internally stable and H_∞ filtering performance $J_s < 0$, where $Q = (0 \ D)'(0 \ D)$.*

Proof. We first show (2.10) to be internally stable, that is, the following system

$$d\xi = \tilde{A}\xi dt + \tilde{D}_1\xi dw_0 + \tilde{D}_2\xi dw_1 + \tilde{F}_1 dt + \tilde{F}_2 dw_0(t) \tag{3.4}$$

is asymptotically mean square stable. Let $\mathcal{L}_\xi$ be the infinitesimal operator of (3.4), $V(\xi) = \xi' P\xi$ with $\alpha I \geq P > 0$ to be determined. According to Lemma 2.4, in order to show (3.4) to be internally stable, we only need to show

$$\mathcal{L}_\xi V(\xi) \leq -k_3|\xi|^2 \tag{3.5}$$

for some $k_3 > 0$. Note that

$$\begin{aligned}\mathcal{L}_\xi V(\xi) &= \frac{\partial V'(\xi)}{\partial \xi}\left(\tilde{A}\xi + \tilde{F}_1\right) + \frac{1}{2}\left(\tilde{D}_1\xi + \tilde{F}_2\right)'\frac{\partial^2 V(\xi)}{\partial \xi^2}\left(\tilde{D}_1\xi + \tilde{F}_2\right) + \frac{1}{2}\left(\tilde{D}_2\xi\right)'\frac{\partial^2 V(\xi)}{\partial \xi^2}\left(\tilde{D}_2\xi\right) \\ &= \xi'\left(P\tilde{A} + \tilde{A}'P + \tilde{D}_1'P\tilde{D}_1 + \tilde{D}_2'P\tilde{D}_2\right)\xi + 2\tilde{F}_1'P\xi + \tilde{F}_2'P\tilde{F}_2 + 2\xi'\tilde{D}_1'P\tilde{F}_2.\end{aligned} \tag{3.6}$$

By condition (3.1), we have

$$\begin{aligned} 2\widetilde{F}_1'P\xi &\le \xi'P\xi + \widetilde{F}_1'P\widetilde{F}_1 \le \xi'P\xi + \alpha\widetilde{F}_1'\widetilde{F}_1 = \xi'P\xi + 2\alpha F_0'F_0 \\ &\le \xi'P\xi + 2\alpha|F_0|^2 \le \xi'P\xi + 2\alpha\lambda^2|\xi|^2. \end{aligned} \tag{3.7}$$

Similarly,

$$\begin{aligned} 2\xi'\widetilde{D}_1'P\widetilde{F}_2 &\le \xi'\widetilde{D}_1'P\widetilde{D}_1\xi + 2\alpha\lambda^2|\xi|^2, \\ \widetilde{F}_2'P\widetilde{F}_2 &\le 2\alpha\lambda^2|\xi|^2. \end{aligned} \tag{3.8}$$

Substituting (3.7), (3.8) into (3.6) and considering (3.2), it follows

$$\begin{aligned} \mathcal{L}_\xi V(\xi) &\le \xi'\left(P\widetilde{A} + \widetilde{A}'P + 2\widetilde{D}_1'P\widetilde{D}_1 + \widetilde{D}_2'P\widetilde{D}_2 + P + 6\alpha\lambda^2 I\right)\xi \\ &< -\xi'\left(Q + \frac{1}{\gamma^2}P\widetilde{F}_3\widetilde{F}_3'P\right)\xi \le 0. \end{aligned} \tag{3.9}$$

By Lemma 2.4, the internal stability of (2.10) is proved.

Secondly, we further show the H_∞ filtering performance $J_s < 0$. Let $\mathcal{L}_{\xi,w}$ be the infinitesimal generator of (2.10). For $V(\xi) = \xi'P\xi$, it is easy to show that

$$\mathcal{L}_{\xi,w}V(\xi) = \mathcal{L}_\xi V(\xi) + 2\xi'P\widetilde{F}_3 w. \tag{3.10}$$

For any $T > 0$ and $\xi(0) = 0$, we have

$$\begin{aligned} J_s(T) &:= E\int_0^T \left[|\widetilde{z}(t)|^2 - \gamma^2|w(t)|^2\right]dt \\ &= E\int_0^T \left\{\left[|\widetilde{z}(t)|^2 - \gamma^2|w(t)|^2\right]dt + d\left(\xi'P\xi\right)\right\} - E[\xi(T)P\xi(T)] \\ &\le E\int_0^T \left[|\widetilde{z}(t)|^2 - \gamma^2|w(t)|^2 + \mathcal{L}_{\xi,w}V(\xi)\right]dt. \end{aligned} \tag{3.11}$$

Note that

$$\begin{aligned} \mathcal{L}_{\xi,w}V(\xi) &\le \xi'\left(P\widetilde{A} + \widetilde{A}'P + 2\widetilde{D}_1'P\widetilde{D}_1 + \widetilde{D}_2'P\widetilde{D}_2 + P + 6\lambda^2\alpha I\right)\xi + 2\xi'P\widetilde{F}_3 w, \\ |\widetilde{z}(t)|^2 &= \xi'Q\xi. \end{aligned} \tag{3.12}$$

So

$$|\widetilde{z}(t)|^2 - \gamma^2|w(t)|^2 + \mathcal{L}_{\xi,w}V(\xi) \le \begin{bmatrix}\xi \\ w\end{bmatrix}' \begin{bmatrix}\Lambda_{11} & P\widetilde{F}_3 \\ \widetilde{F}_3'P & -\gamma^2 I\end{bmatrix}\begin{bmatrix}\xi \\ w\end{bmatrix} < 0, \tag{3.13}$$

where

$$\Lambda_{11} := P\tilde{A} + \tilde{A}'P + 2\tilde{D}_1'P\tilde{D}_1 + \tilde{D}_2'P\tilde{D}_2 + P + 6\lambda^2\alpha I + Q. \tag{3.14}$$

By the well-known Schur's complement and (3.2), there exists $\varepsilon > 0$, such that

$$\begin{bmatrix} \Lambda_{11} & P\tilde{F}_3 \\ \tilde{F}_3'P & -\gamma^2 I \end{bmatrix} < -\varepsilon I. \tag{3.15}$$

Summarizing the above analysis, (3.11) yields

$$J_s(T) \le -\varepsilon E \int_0^T \left(|\xi(t)|^2 + w(t)|^2\right) dt \le -\varepsilon E \int_0^T |w(t)|^2 dt. \tag{3.16}$$

So for any $T > 0$, $E\int_0^T |\tilde{z}(t)|^2 dt \le (\gamma^2 - \varepsilon) E \int_0^T |w(t)|^2 dt$.

Let $T \to \infty$, then

$$\|\tilde{z}(t)\|_{L_2}^2 \le \left(\gamma^2 - \varepsilon\right) \|w(t)\|_{L_2}^2 \tag{3.17}$$

which yields $J_s < 0$. This theorem is proved. □

Theorem 3.1 only has theoretical sense, because it is difficult to be used in designing H_∞ filter. The following result is of more important in practice.

Theorem 3.2. *Under the condition of Theorem 3.1, if the following LMIs*

$$\begin{bmatrix} P_{11} - \alpha I & 0 \\ 0 & P_{22} - \alpha I \end{bmatrix} < 0, \tag{3.18}$$

$$\begin{bmatrix} a_{11} & A'^{P_{22}} - A_1'Z_1' - Z' & \sqrt{2}C'^{P_{11}} & \sqrt{2}C'^{P_{22}} & -C_1'Z_1' & P_{11}B_0 \\ P_{22}A - Z_1A_1 - Z & a_{22} & 0 & 0 & 0 & P_{22}B_0 - Z_1B_1 \\ \sqrt{2}P_{11}C & 0 & -P_{11} & 0 & 0 & 0 \\ \sqrt{2}P_{22}C & 0 & 0 & -P_{22} & 0 & 0 \\ -Z_1C_1 & 0 & 0 & 0 & -P_{22} & 0 \\ B_0'P_{11} & B_0'P_{22} - B_1'Z_1' & 0 & 0 & 0 & -\gamma^2 I \end{bmatrix} < 0 \tag{3.19}$$

have solutions $P_{11} > 0, P_{22} > 0, \alpha > 0, Z_1 \in \mathcal{R}^{n\times r}$, $Z \in \mathcal{R}^{n\times n}$, *then* (2.10) *is internally stable and* $J_s < 0$.

Moreover,

$$d\hat{x} = P_{22}^{-1} Z\hat{x}dt + P_{22}^{-1} Z_1 dy \tag{3.20}$$

is the corresponding H_∞ *filter. In* (3.19), $a_{11} = P_{11}A + A'P_{11} + 6\lambda^2\alpha I + P_{11}$, $a_{22} = -Z - Z' + 6\lambda^2\alpha I + D'D + P_{22}$.

Proof. By Schur's complement, (3.2) is equivalent to

$$\begin{bmatrix} P\tilde{A} + \tilde{A}'P + P + 6\lambda^2\alpha I + Q & \sqrt{2}\tilde{D}_1'P & \tilde{D}_2'P & P\tilde{F}_3 \\ \sqrt{2}P\tilde{D}_1 & -P & 0 & 0 \\ P\tilde{D}_2 & 0 & -P & 0 \\ \tilde{F}_3'P & 0 & 0 & -\gamma^2 I \end{bmatrix} < 0. \tag{3.21}$$

Taking $P = \operatorname{diag}(P_{11}, P_{22})$ and substituting (2.11) into (3.21), we have

$$\begin{bmatrix} \Psi_{11} & \Psi_{12}' & \Psi_{13}' & \phi_{14}' \\ \Psi_{12} & \Psi_{22} & 0 & 0 \\ \Psi_{13} & 0 & \Psi_{33} & 0 \\ \Psi_{14} & 0 & 0 & \Psi_{44} \end{bmatrix} < 0, \tag{3.22}$$

where

$$\Psi_{11} = \begin{bmatrix} P_{11}A + A'P_{11} + 6\lambda^2\alpha I + P_{11} & (A - B_f A_1 - A_f)'P_{22} \\ P_{22}(A - B_f A_1 - A_f) & -P_{22}A_f - A_f'P_{22} + 6\lambda^2\alpha I + P_{22} + D'D \end{bmatrix},$$

$$\Psi_{22} = \Psi_{33} = -P = \begin{bmatrix} -P_{11} & 0 \\ 0 & -P_{22} \end{bmatrix}, \qquad \Psi_{44} = -\gamma^2 I, \tag{3.23}$$

$$\Psi_{12}' = \begin{bmatrix} \sqrt{2}C'P_{11} & \sqrt{2}C'P_{22} \\ 0 & 0 \end{bmatrix}, \qquad \Psi_{13}' = \begin{bmatrix} 0 & -C_1'B_f'P_{22} \\ 0 & 0 \end{bmatrix}, \qquad \Psi_{14}' = \begin{bmatrix} P_{11}B_0 \\ P_{22}(B_0 - B_f B_1) \end{bmatrix}.$$

(3.22) is equivalent to

$$\begin{bmatrix} \bar{a}_{11} & (A - B_f A_1 - A_f)'P_{22} & \sqrt{2}C'P_{11} & \sqrt{2}C'P_{22} & -C_1'B_f'P_{22} & P_{11}B_0 \\ P_{22}(A - B_f A_1 - A_f) & \bar{a}_{22} & 0 & 0 & 0 & P_{22}(B_0 - B_f B_1) \\ \sqrt{2}P_{11}C & 0 & -P_{11} & 0 & 0 & 0 \\ \sqrt{2}P_{22}C & 0 & 0 & -P_{22} & 0 & 0 \\ -P_{22}B_f C_1 & 0 & 0 & 0 & -P_{22} & 0 \\ B_0'P_{11} & (B_0 - B_f B_1)'P_{22} & 0 & 0 & 0 & -\gamma^2 I \end{bmatrix} < 0, \tag{3.24}$$

where $\bar{a}_{11} = P_{11}A + A'P_{11} + 6\lambda^2\alpha I + P_{11}$, $\bar{a}_{22} = -P_{22}A_f - A'_f P_{22} + 6\lambda^2\alpha I + P_{11}$. Let $P_{22}A_f = Z, P_{22}B_f = Z_1$, then (3.22) becomes (3.19). From our assumption, $A_f = P_{22}^{-1}Z, B_f = P_{22}^{-1}Z_1$, so an H_∞ filtering equation is constructed as in the form of (3.20). Theorem 3.2 is proved. □

3.2. Mixed H_2/H_∞ Filtering

To design the mixed stochastic H_2/H_∞ filter, we need to choose the one from the set of all H_∞ filters, which also minimizes the estimation error variance, or concretely speaking, minimizes the H_2 performance

$$\begin{aligned} J_2 &:= \lim_{t\to\infty} E\{\tilde{z}'(t)\tilde{z}(t)\} = \lim_{t\to\infty} E\{\xi'(t)(0\ I)'D'D(0\ I)\xi(t)\} \\ &= \lim_{t\to\infty} \operatorname{Tr}\{D(0\ I)E\xi(t)\xi'(t)(0\ I)'D'\}. \end{aligned} \tag{3.25}$$

Two performances J_s in (2.13) and J_2 in (3.25) associated with H_∞ robustness and H_2 optimization have constructed, respectively. Now, we need to design the mixed H_2/H_∞ filter to maximize J_s and minimize J_2. Consider the following linear stochastic constant system

$$d\xi = A_{11}\xi dt + \sum_{i=1}^{l} B_{ii}\xi dw_i, \tag{3.26}$$

where $\{w_i,\ i = 1,\ldots,l\}$ are independent, standard Wiener processes. The following lemma will be used in this section.

Lemma 3.3 (see [23]). *System* (3.26) *is exponentially mean square stable iff for any $R > 0$, the following Lyapunov-type equation*

$$PA_{11} + A_{11}'P + \sum_{i=1}^{l} B_{ii}'PB_{ii} = -R \tag{3.27}$$

has a unique positive definite solution $P > 0$.

In the next, for simplicity, when (3.26) *is exponentially stable, one also says $(A_{11}, B_{11}, \ldots, B_{ll})$ is stable.*

As we have pointed out before, at this stage, we assume $w(t) = \dot{\eta}(t)$; (2.10) *accordingly becomes*

$$d\xi = \tilde{A}\xi dt + \tilde{D}_1\xi dw_0 + \tilde{D}_2\xi dw_1 + \tilde{F}_1 dt + \tilde{F}_2 dw_0 + \tilde{F}_3 d\eta. \tag{3.28}$$

Let $X(t) = E[\xi(t)\xi'(t)]$ in (3.28)*, then by Itô's formula, we have*

$$\begin{aligned} \dot{X}(t) = {} & \tilde{A}X(t) + X(t)\tilde{A}' + E\left[\tilde{F}_1\xi' + \xi\tilde{F}_1'\right] + \tilde{D}_1X\tilde{D}_1' \\ & + E\left[\tilde{D}_1\xi\tilde{F}_2' + \tilde{F}_2\xi'\tilde{D}_1'\right] + E\left[\tilde{F}_2\tilde{F}_2'\right] + \tilde{D}_2X(t)\tilde{D}_2' + \tilde{F}_3\tilde{F}_3'. \end{aligned} \tag{3.29}$$

By means of

$$\begin{aligned} E\left[\tilde{F}_1\xi' + \xi\tilde{F}_1'\right] &\le E\left[\tilde{F}_1\tilde{F}_1'\right] + X(t), \\ E\left[\tilde{D}_1\xi\tilde{F}_2' + \tilde{F}_2\xi'\tilde{D}_1'\right] &\le \tilde{D}_1X\tilde{D}_1' + E\left[\tilde{F}_2\tilde{F}_2'\right], \end{aligned} \tag{3.30}$$

we have

$$\begin{aligned}\dot{X}(t) \le{}& \tilde{A}X(t) + X(t)\tilde{A}' + 2\tilde{D}_1X(t)\tilde{D}_1' + \tilde{D}_2X(t)\tilde{D}_2' \\ &+ X(t) + 2E\left[\tilde{F}_2\tilde{F}_2'\right] + E\left[\tilde{F}_1\tilde{F}_1'\right] + \tilde{F}_3\tilde{F}_3'.\end{aligned} \tag{3.31}$$

Now, we suppose $F_i(x)$ $(i = 0, 1)$ *satisfy*

$$F_i(x)F_i'(x) \le G_ixx'G_i', \quad i = 0, 1, \ \forall x \in \mathcal{R}^n, \tag{3.32}$$

where G_1, G_2 *are constant matrices of suitable dimensions. At this stage,*

$$\begin{aligned}\tilde{F}_i\tilde{F}_i' &= \begin{bmatrix} I & 0 \\ I & I \end{bmatrix}\begin{bmatrix} F_iF_i' & 0 \\ 0 & 0 \end{bmatrix}\begin{bmatrix} I & I \\ 0 & I \end{bmatrix} \\ &\le \begin{bmatrix} I & 0 \\ I & I \end{bmatrix}\begin{bmatrix} G_ixx'G_i' & 0 \\ 0 & 0 \end{bmatrix}\begin{bmatrix} I & I \\ 0 & I \end{bmatrix} \\ &= \begin{bmatrix} I & 0 \\ I & I \end{bmatrix}\begin{bmatrix} G_i & 0 \\ 0 & 0 \end{bmatrix}\xi\xi'\begin{bmatrix} G_i' & 0 \\ 0 & 0 \end{bmatrix}\begin{bmatrix} I & I \\ 0 & I \end{bmatrix} \\ &= \begin{bmatrix} G_i & 0 \\ G_i & 0 \end{bmatrix}\xi\xi'\begin{bmatrix} G_i' & G_i' \\ 0 & 0 \end{bmatrix} \\ &:= \tilde{G}_i\xi\xi'\tilde{G}_i', \quad i = 0, 1,\end{aligned} \tag{3.33}$$

where

$$\tilde{G}_i = \begin{bmatrix} G_i & 0 \\ G_i & 0 \end{bmatrix}. \tag{3.34}$$

So (3.31) *becomes*

$$\dot{X}(t) \le \tilde{A}X(t) + X(t)\tilde{A}' + 2\tilde{D}_1X(t)\tilde{D}_1' + \tilde{D}_2X(t)\tilde{D}_2' + X(t) + 2\tilde{G}_2X(t)\tilde{G}_2' + \tilde{G}_1X(t)\tilde{G}_1' + \tilde{F}_3\tilde{F}_3'. \tag{3.35}$$

In addition, if $X_1(t)$ *solves*

$$\begin{aligned}\dot{X}_1(t) &= \tilde{A}X_1(t) + X_1(t)\tilde{A}' + 2\tilde{D}_1X_1(t)\tilde{D}_1' + \tilde{D}_2X_1(t)\tilde{D}_2' + X_1(t) \\ &\quad + 2\tilde{G}_2X_1(t)\tilde{G}_2' + \tilde{G}_1X_1(t)\tilde{G}_1' + \tilde{F}_3\tilde{F}_3' \\ X_1(0) &= X(0)\end{aligned} \tag{3.36}$$

then it is easy to prove that $X(t) \le X_1(t)$. *Denoting* $\overline{X}_1 := \lim_{t\to\infty}X_1(t)$, *where* $\overline{X}_1$ *satisfies*

$$\tilde{A}\overline{X}_1 + \overline{X}_1\tilde{A}' + 2\tilde{D}_1\overline{X}_1\tilde{D}_1' + \tilde{D}_2\overline{X}_1\tilde{D}_2' + 2\tilde{G}_2\overline{X}_1\tilde{G}_2' + \tilde{G}_1\overline{X}_1\tilde{G}_1' + \overline{X}_1 + \tilde{F}_3\tilde{F}_3' = 0. \tag{3.37}$$

Obviously, $\lim_{t\to\infty} X(t) \le \overline{X}_1$*, accordingly,*

$$J_2 \le \operatorname{Tr}\left\{D(0\ I)\overline{X}_1(0\ I)'D'\right\} = \operatorname{Tr}\left\{\overline{X}_1 Q\right\}. \tag{3.38}$$

As in [12, 24], it is easily seen the following fact.

Lemma 3.4. *If* $\widehat{P}$ *is a solution of*

$$\widetilde{A}'\widehat{P} + \widehat{P}\widetilde{A} + 2\widetilde{D}_1'\widehat{P}\widetilde{D}_1 + \widetilde{D}_2'\widehat{P}\widetilde{D}_2 + 2\widetilde{G}_2'\widehat{P}\widetilde{G}_2 + \widetilde{G}_1'\widehat{P}\widetilde{G}_1 + Q + \widehat{P} = 0 \tag{3.39}$$

then $\operatorname{Tr}(\overline{X}_1 Q) = \operatorname{Tr}(\widehat{P}(\widetilde{F}_3\widetilde{F}_3'))$.

Secondly, suppose $P > 0$ *satisfies*

$$\widetilde{A}'P + P\widetilde{A} + 2\widetilde{D}_1'P\widetilde{D}_1 + \widetilde{D}_2'P\widetilde{D}_2 + Q + P + 2\widetilde{G}_2'P\widetilde{G}_2 + \widetilde{G}_1'P\widetilde{G}_1 < 0. \tag{3.40}$$

By means of Lemma 3.3, one can show $P > \widehat{P}$*. So we have the following lemma.*

Lemma 3.5. $P > \widehat{P}$*, where* P *and* $\widehat{P}$ *stand for the positive definite solutions of* (3.40) *and* (3.39)*, respectively.*

From Lemmas 3.4–3.5, it gives

$$\begin{aligned}
J_2 &= \lim_{t\to\infty} \operatorname{Tr}\left\{D(0\ I)X(t)(0\ I)'D'\right\} \\
&\le \lim_{t\to\infty} \operatorname{Tr}\left\{D(0\ I)X_1(t)(0\ I)'D'\right\} \\
&= \operatorname{Tr}\left\{D(0\ I)\overline{X}_1(0\ I)'D'\right\} \\
&= \operatorname{Tr}\left\{\overline{X}_1 Q\right\} = \operatorname{Tr}\left(\widehat{P}\widetilde{F}_3\widetilde{F}_3'\right) \\
&= \operatorname{Tr}\left(\widetilde{F}_3'\widehat{P}\widetilde{F}_3\right) \\
&\le \operatorname{Tr}\left(\widetilde{F}_3'P\widetilde{F}_3\right) := \widehat{J}_2.
\end{aligned} \tag{3.41}$$

Hence, to solve the mixed stochastic H_2/H_∞ *filtering problem, we seek to minimize an upper-bound on* $\widehat{J}_2$ *subject to* (3.2), (3.3)*, and*

$$P\widetilde{A} + \widetilde{A}'P + 2\widetilde{D}_1'P\widetilde{D}_1 + \widetilde{D}_2'P\widetilde{D}_2' + P + 2\widetilde{G}_2'P\widetilde{G}_2 + \widetilde{G}_1'P\widetilde{G}_1 + Q < 0. \tag{3.42}$$

(3.42) *having a positive definite solution* $P > 0$ *is equivalent to*

$$\begin{bmatrix} P\tilde{A} + \tilde{A}'P + P + Q & \sqrt{2}\tilde{D}_1'P & \tilde{D}_2'P & \tilde{G}_1'P & \sqrt{2}\tilde{G}_2'P \\ \sqrt{2}P\tilde{D}_1 & -P & 0 & 0 & 0 \\ P\tilde{D}_2 & 0 & -P & 0 & 0 \\ P\tilde{G}_1 & 0 & 0 & -P & 0 \\ \sqrt{2}P\tilde{G}_2 & 0 & 0 & 0 & -P \end{bmatrix} < 0. \tag{3.43}$$

A suboptimal H_2/H_∞ *filtering can be obtained by minimizing* $\mathrm{Tr}(H)$ *subject to* (3.2), (3.3), (3.43), *and*

$$H - \tilde{F}_3'P\tilde{F}_3 > 0. \tag{3.44}$$

(3.44) *is equivalent to*

$$\begin{bmatrix} H & \tilde{F}_3'P \\ P\tilde{F}_3 & P \end{bmatrix} > 0. \tag{3.45}$$

We still take $P = \mathrm{diag}(P_{11}, P_{22}) > 0$, $P_{22}B_f = Z_1$, $P_{22}A_f = Z$, *then* (3.3), (3.2), (3.43), *and* (3.45) *become, respectively, as* (3.18), (3.19),

$$\begin{bmatrix} \gamma_{11} & \gamma_{12} & \sqrt{2}C'P_{11} & \sqrt{2}C'P_{22} & -C_1'Z_1' & G_1'P_{11} & G_1'P_{22} & G_2'P_{11} & G_2'P_{22} \\ \gamma_{21} & \gamma_{22} & 0 & 0 & 0 & 0 & 0 & 0 & 0 \\ \sqrt{2}P_{11}C & 0 & -P_{11} & 0 & 0 & 0 & 0 & 0 & 0 \\ \sqrt{2}P_{22}C & 0 & 0 & -P_{22} & 0 & 0 & 0 & 0 & 0 \\ -Z_1C_1 & 0 & 0 & 0 & -P_{22} & 0 & 0 & 0 & 0 \\ P_{11}G_1 & 0 & 0 & 0 & 0 & -P_{11} & 0 & 0 & 0 \\ P_{22}G_1 & 0 & 0 & 0 & 0 & 0 & -P_{22} & 0 & 0 \\ P_{11}G_2 & 0 & 0 & 0 & 0 & 0 & 0 & -P_{11} & 0 \\ P_{22}G_2 & 0 & 0 & 0 & 0 & 0 & 0 & 0 & -P_{22} \end{bmatrix} < 0,$$

$$\begin{bmatrix} H & B_0'P_{11} & B_0'P_{22} - B_1'Z_1' \\ P_{11}B_0 & P_{11} & 0 \\ P_{22}B_0 - Z_1B_1 & 0 & P_{22} \end{bmatrix} > 0, \tag{3.46}$$

where $\gamma_{11} = P_{11}A + A'P_{11} + P_{11}$, $\gamma_{12} = A'P_{22} - A_1'Z_1' - Z'$, $\gamma_{21} = P_{22}A - Z_1A_1 - Z$, $\gamma_{22} = -Z - Z' + D'D + P_{22}$. *Therefore, we have the following theorem.*

Theorem 3.6. *Under the conditions of Theorem 3.2 and assumption* (3.32), *if there exists a solution* $(P_{11} > 0, P_{22} > 0, Z, Z_1, \alpha > 0)$ *to* (3.18), (3.19), (3.46), *then a suboptimal mixed stochastic* H_2/H_∞ *filtering is obtained by solving* P_{11} *and* P_{22} *from the following convex optimization problem:* $\min_{P_{11},P_{22},Z,Z_1,\alpha} \mathrm{Tr}(H)$ *subject to* (3.18),(3.19), (3.46), *and the corresponding filter is given by* (3.20).

Remark 3.7. In the proof of Theorems 3.2 and 3.6, the matrix P is chosen as $\mathrm{diag}(P_{11}, P_{22})$ for simplicity. In order to reduce the conservatism of the conditions, the matrix P can also be chosen as $\begin{bmatrix} P_{11} & P_{12} \\ P_{12}' & P_{22} \end{bmatrix}$. However, this case will increase the complexity of computation.

4. Numerical Example

Example 4.1. Consider the following nonlinear stochastic system governed by Itô differential equation

$$\begin{aligned} dx &= (Ax + B_0 w + F_0(x))dt + (Cx + F_1(x))dw_0, \\ dy &= (A_1 + B_1 w)dt + C_1 x dw_1, \qquad z = Dx, \end{aligned} \tag{4.1}$$

where

$$\begin{gathered} A = \begin{bmatrix} -3 & 1/2 \\ -1 & -3 \end{bmatrix}, \qquad B_0 = \begin{bmatrix} 1 \\ 0 \end{bmatrix}, \qquad C = \begin{bmatrix} 1 & 0 \\ 0 & 0 \end{bmatrix}, \\ F_0(x) = 0.3\tanh(x), \qquad F_1(x) = 0.3\sin(x), \\ A_1 = \begin{bmatrix} -1 & 1 \\ 1 & -1 \end{bmatrix}, \qquad B_1 = \begin{bmatrix} 0 \\ 1 \end{bmatrix}, \qquad C_1 = \begin{bmatrix} 1 & 0 \\ 0 & 1 \end{bmatrix}, \\ D = \begin{bmatrix} 0 \\ 1 \end{bmatrix}, \quad w = \frac{1}{1+2t}, \quad t \geq 0. \end{gathered} \tag{4.2}$$

Consider the following filter for the estimation of $z(t)$:

$$d\hat{x} = A_f \hat{x} dt + B_f dy, \qquad \hat{z} = D\hat{x}. \tag{4.3}$$

Setting $\gamma = 0.9$, and using the LMI control toolbox of Matlab, the estimation gains of H_∞ filter are derived from Theorem 3.2:

$$A_f = \begin{bmatrix} 5.6231 & 3.7259 \\ -0.1617 & 8.2289 \end{bmatrix}, \qquad B_f = \begin{bmatrix} 0.1812 & -1.8190 \\ -0.2525 & 0.4635 \end{bmatrix}. \tag{4.4}$$

From Theorem 3.6, the estimation gains of H_2/H_∞ filter are obtained as follows:

$$A_f = \begin{bmatrix} 4.1449 & 3.4665 \\ -0.2469 & 6.3382 \end{bmatrix}, \qquad B_f = \begin{bmatrix} 0.5270 & -1.2388 \\ -0.3693 & 0.3445 \end{bmatrix}. \tag{4.5}$$

The initial condition in the simulation is assumed to be $\xi_0 = [0.3\ 0.2\ -0.02\ -0.05]'$. Figures 1 and 2 show the trajectories of $x_1(t)$, $\hat{x}_1(t)$, $x_2(t)$, $\hat{x}_2(t)$ by using the proposed H_∞ and H_2/H_∞ filters, respectively. The trajectories of the estimation error $\tilde{z}(t)$ for H_∞ and H_2/H_∞ filters are shown in Figures 3 and 4, respectively. From Figures 3 and 4, it is obvious that the performance of the proposed H_2/H_∞ filter is better than that of the H_∞ filter.

In [15], the H_∞ and H_2/H_∞ filters for general nonlinear stochastic systems were obtained by solving a second-order nonlinear HJI. Generally, it is difficult to solve the HJI. In fact, for the special nonlinear stochastic system (4.1), the H_∞ and H_2/H_∞ filtering problems can be solved via the LMI technique instead of the HJI according to Theorems 3.2 and 3.6 in this paper. Simulation results show the effectiveness of the proposed method.

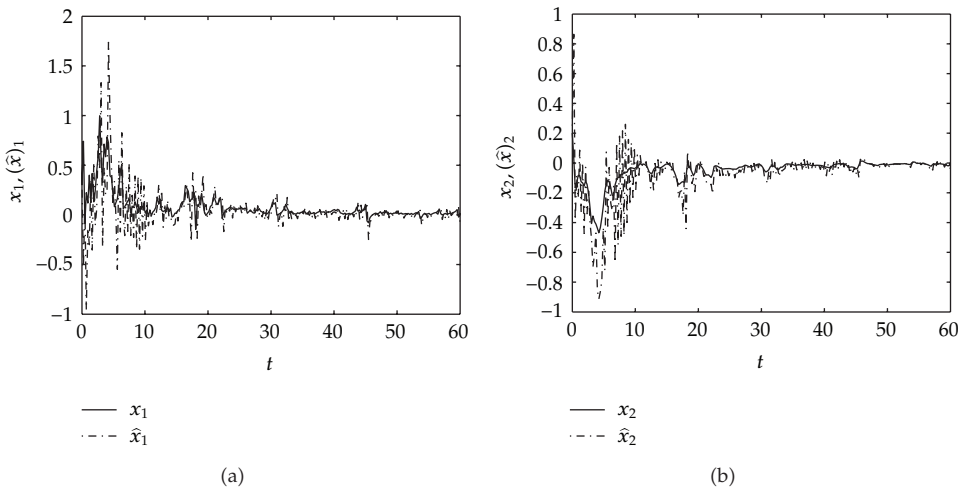

Figure 1: Trajectories of $x_1(t)$, $\widehat{x}_1(t)$ and $x_2(t)$, $\widehat{x}_2(t)$ for the proposed H_∞ filter.

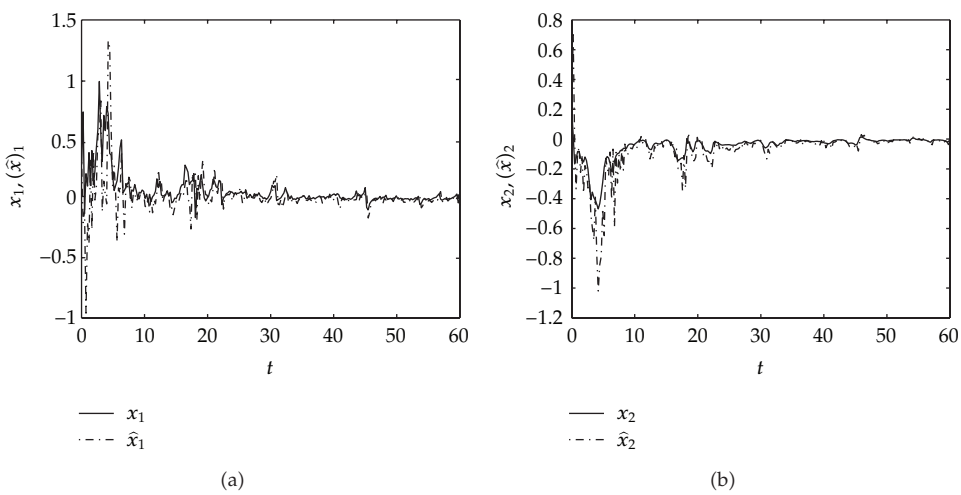

Figure 2: Trajectories of $x_1(t)$, $\widehat{x}_1(t)$ and $x_2(t)$, $\widehat{x}_2(t)$ for the proposed H_2/H_∞ filter.

5. Conclusions

In this paper, we have discussed the robust H_∞ filtering problem for a class of nonlinear stochastic systems. Meanwhile, the mixed H_2/H_∞ filtering analysis is also considered. Since the results can be solved by LMIs, the proposed method has much advantage in practical computation. Although we only demand the state equation to be nonlinear, one can tackle the case that when both the state and measurement equations are nonlinear.

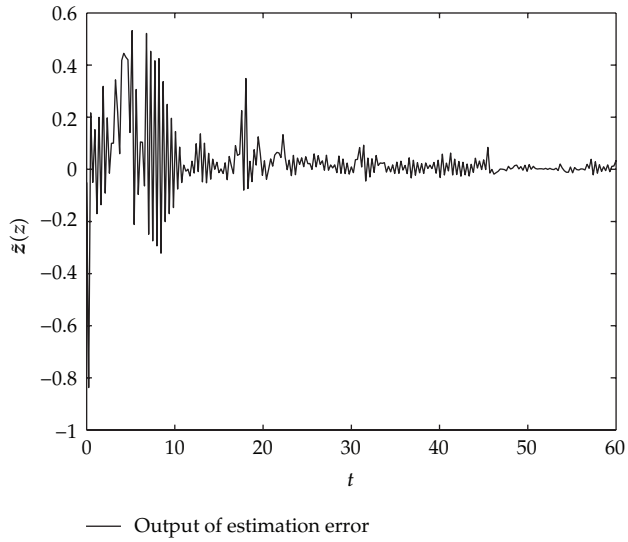

Figure 3: Trajectory of the estimation error $\tilde{z}(t)$ for the proposed H_∞ filter.

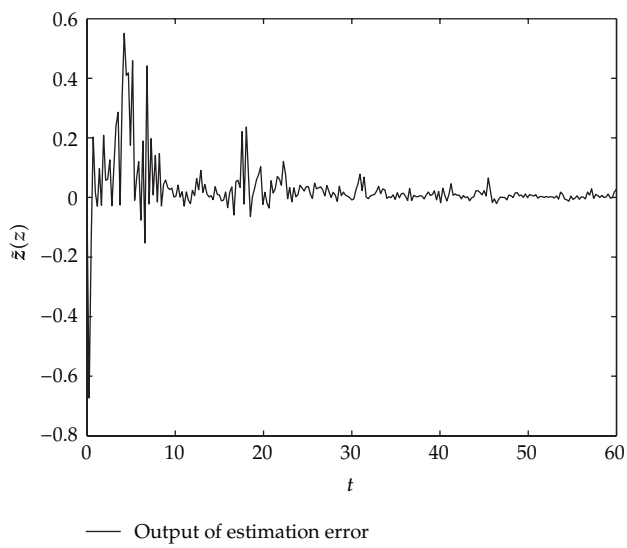

Figure 4: Trajectory of the estimation error $\tilde{z}(t)$ for the proposed H_2/H_∞ filter.

Acknowledgments

This work is supported by the National Natural Science Foundation of China (no. 61174078, 61203053), Natural Science Foundation of Shandong Province of China (no. ZR2011FL025), Fundamental Research Funds for the Central Universities (no. 11CX04042A), Research Fund for the Taishan Scholar Project of Shandong Province of China, and SDUST Research Fund.

References

[1] M. J. Grimble and A. Elsayed, "Solution of the H_∞ optimal linear filtering problem for discrete-time systems," *IEEE Transactions on Acoustics, Speech, and Signal Processing*, vol. 38, no. 7, pp. 1092–1104, 1990.

[2] W. M. McEneaney, "Robust/H_∞ filtering for nonlinear systems," *Systems & Control Letters*, vol. 33, no. 5, pp. 315–325, 1998.

[3] S. Xu, J. Lam, and Y. Zou, "H_∞ filtering for singular systems," *IEEE Transactions on Automatic Control*, vol. 48, no. 12, pp. 2217–2222, 2003.

[4] S. Xu, J. Lam, and X. Mao, "Delay-dependent H_∞ control and filtering for uncertain Markovian jump systems with time-varying delays," *IEEE Transactions on Circuits and Systems. I.*, vol. 54, no. 9, pp. 2070–2077, 2007.

[5] Z. Wang, B. Shen, and X. Liu, "H_∞ filtering with randomly occurring sensor saturations and missing measurements," *Automatica*, vol. 48, no. 3, pp. 556–562, 2012.

[6] Z. Wang and B. Huang, "Robust H_2/H_∞ filtering for linear systems with error variance constraints," *IEEE Transactions on Signal Processing*, vol. 48, no. 8, pp. 2463–2467, 2000.

[7] H. Gao, J. Lam, L. Xie, and C. Wang, "New approach to mixed H_2/H_∞ filtering for polytopic discrete-time systems," *IEEE Transactions on Signal Processing*, vol. 53, no. 8, part 2, pp. 3183–3192, 2005.

[8] B. S. Chen, C. L. Tsai, and Y. F. Chen, "Mixed H_2/H_∞ filtering design in multirate transmultiplexer system LMI approach," *IEEE Transactions on Signal Processing*, vol. 49, no. 11, pp. 2693–2701, 2001.

[9] R. Z. Has'minskii, *Stochastic Stability of Differential Equations*, vol. 7, Sijthoff & Noordhoff, Alphen aan den Rijn, The Netherlands, 1980.

[10] Z. Wang, F. Yang, D. W. C. Ho, and X. Liu, "Robust H_∞ filtering for stochastic time-delay systems with missing measurements," *IEEE Transactions on Signal Processing*, vol. 54, no. 7, pp. 2579–2587, 2006.

[11] D. Hinrichsen and A. J. Pritchard, "Stochastic H^∞," *SIAM Journal on Control and Optimization*, vol. 36, no. 5, pp. 1504–1538, 1998.

[12] E. Gershon, D. J. N. Limebeer, U. Shaked, and I. Yaesh, "Robust H_∞ filtering of stationary continuous-time linear systems with stochastic uncertainties," *IEEE Transactions on Automatic Control*, vol. 46, no. 11, pp. 1788–1793, 2001.

[13] S. Xu and T. Chen, "Reduced-order H_∞ filtering for stochastic systems," *IEEE Transactions on Signal Processing*, vol. 50, no. 12, pp. 2998–3007, 2002.

[14] Z. Wang, Y. Liu, and X. Liu, "H_∞ filtering for uncertain stochastic time-delay systems with sector-bounded nonlinearities," *Automatica*, vol. 44, no. 5, pp. 1268–1277, 2008.

[15] W. Zhang, B.-S. Chen, and C.-S. Tseng, "Robust H_∞ filtering for nonlinear stochastic systems," *IEEE Transactions on Signal Processing*, vol. 53, no. 2, part 1, pp. 589–598, 2005.

[16] W. Zhang, G. Feng, and Q. Li, "Robust H_∞ filtering for nonlinear stochastic state-delayed systems," in *Proceedings of the 7th World Congress on Intelligent Control and Automation (WCICA '08)*, pp. 2212–2217, Chongqing, China, June 2008.

[17] C. S. Tseng, "Robust fuzzy filter design for a class of nonlinear stochastic systems," *IEEE Transactions on Fuzzy Systems*, vol. 152, pp. 261–274, 2007.

[18] B. Shen, Z. Wang, H. Shu, and G. Wei, "On nonlinear H_∞ filtering for discrete-time stochastic systems with missing measurements," *IEEE Transactions on Automatic Control*, vol. 53, no. 9, pp. 2170–2180, 2008.

[19] H. Dong, Z. Wang, and H. Gao, "Robust H_∞ filtering for a class of nonlinear networked systems with multiple stochastic communication delays and packet dropouts," *IEEE Transactions on Signal Processing*, vol. 58, no. 4, pp. 1957–1966, 2010.

[20] J. Hu, Z. Wang, H. Gao, and L. K. Stergioulas, "Robust sliding mode control for discrete stochastic systems with mixed time-delays, randomly occurring uncertainties and randomly occurring nonlinearities," *IEEE Transactions on Industrial Electronics*, vol. 59, no. 7, pp. 3008–3015, 2012.

[21] B. Øksendal, *Stochastic Differential Equations*, Springer, Berlin, Germany, 5th edition, 1998.

[22] W. M. Wonham, "Random differential equations in control theory," in *Probabilistic Methods in Applied Mathematics*, vol. 2, pp. 131–212, Academic Press, New York, NY, USA, 1970.

[23] W. Zhang and B.-S. Chen, "On stabilizability and exact observability of stochastic systems with their applications," *Automatica*, vol. 40, no. 1, pp. 87–94, 2004.

[24] V. Drăgan, T. Morozan, and A. Halanay, "Optimal stabilizing compensator for linear systems with state-dependent noise," *Stochastic Analysis and Applications*, vol. 10, no. 5, pp. 557–572, 1992.

Hindawi Publishing Corporation
Mathematical Problems in Engineering
Volume 2012, Article ID 586279, 13 pages
doi:10.1155/2012/586279

Research Article

Robust Anti-Windup Control Considering Multiple Design Objectives

Dongming Ge,[1] Guanghui Sun,[2] and Hamid Reza Karimi[3]

[1] *Beijing Institute of Spacecraft System Engineering, Beijing 100094, China*
[2] *School of Astronautics, Harbin Institute of Technology, Harbin 150001, China*
[3] *Faculty of Engineering and Science, University of Agder, Grimstad 4879, Norway*

Correspondence should be addressed to Guanghui Sun, guanghuisun@hit.edu.cn

Received 20 April 2012; Accepted 31 July 2012

Academic Editor: Jun Hu

A new saturation control technique is proposed to design multiobjective and robust anti-windup controllers for linear systems with input saturations. Based on the characterization of saturation nonlinearities and modeling uncertainties via integral quadratic constraints (IQCs), this method considers a mixed H_2/H_∞ performance indexes while maintaining dynamic constraints on the controller. The analysis and synthesis conditions are presented in terms of scaled linear matrix inequalities (LMIs). The proposed control algorithm can improve the performance of the input-constrained system while also guaranteeing robustness with respect to the modeling uncertainties. Finally, a numerical example is given to illustrate the effectiveness of the developed techniques.

1. Introduction

Nonlinear control was one of the most active areas of control research. A number of different approaches have recently emerged to discuss this challenging problems, such as the fuzzy control [1–5] and robust sliding mode control [6–8]. Saturation nonlinearities are very common in feedback control systems [9], nearly all physical systems are subjected to some type of control input saturation. If input constraints are not taken into account, harmful effects on system performance and stability may appear. Numerous methods have been proposed to handle such nonlinearities, among which the anti-windup strategy is related to pratical use closely. The basic idea underlining anti-windup designs is to introduce control modifications in order to recover, as much as possible, the performance induced by a previous design carried out on the basis of the unsaturated system. First results on anti-windup consisted on

ad hoc methods intended to work with standard PID controllers, which are commonly used in present commercial controllers. Nonetheless, major improvements have been achieved in the last decade as it can be researched rigorousy in theory.

A general framework that unifies a large class of existing anti-windup control schemes in terms of two matrix parameters was proposed in [10]. In [11], a rigorous definition of anti-windup compensation was provided in terms of L_2 stability and performance. The rigorous stability analysis based on passivity concept was developed in [12]. The synthesis condition of static anti-windup controllers was formulated as an LMI problem in [13]. References [14, 15] further derived the dynamic anti-windup controller synthesis condition with linear matrix inequality (LMI) constraints. In addition, based on the linear fractional transformation (LFT)/linear parameter-varying (LPV) framework, extended anti-windup schemes were introduced in [16, 17]. In these contributions, the saturations are modeled as sector-bounded nonlinearities and the anti-windup control design is recast as a convex optimization problem by absolute stability theory provided that no uncertainty affects the plant.

The problems associated with robustness to plant uncertainty and the problems associated with actuator saturation have often been considered in isolation. There has been little literature which attempts to handle them simultaneously in the anti-windup framework. As noted in [18], nominal linear robustness is only a necessary, but not sufficient condition for the robustness of the overall anti-windup compensated system. Furthermore, [18] introduced an approach to synthesizing anti-windup compensators for input constrained systems subject to additive dynamic uncertainty. Reference [19] considered anti-windup design problem for a closed-loop LFT model whose structured perturbation block contains parametric uncertainties.

In this paper, we propose a unified synthesis method for the construction of multiobjective and robust anti-windup controller for linear systems with actuator saturations, time-varying parametric and dynamic uncertainties. Through an equivalent representation, actuator saturations are treated as sector-bounded nonlinear uncertainty and are included in a block-diagonal operator Δ together with the other uncertainties. Inspired by the research work in [20], the problems associated with robustness are handled within the integral quadratic constraints (IQCs) framework characterizing the properties and structure of Δ. The performance objectives are specified in terms of H_∞ norm, H_2 norm, and additional regional constraints on the closed-loop poles. Interestingly, the regional closed-loop poles placement also ensures the pole-placement constraints on the anti-windup controller in that the closed-loop poles exactly consist of the poles of nominal system and those of anti-windup controller. As observed in [21], this helps to prohibit the slow dynamics which remain visible on the plant outputs even when the saturations are no longer active. The overall analysis conditions are cast as an optimization over LMIs using S-procedure technique and a common quadratic Lyapunov function. The controller synthesis procedure requires solving scaled LMIs with a D/K-like iteration and provides a full-order dynamic anti-windup controller.

Notation. Let $\Lambda^{n\times n}$ denote n-dimensional diagonal matrix. For compact presentation, given a square matrix X we denote $\mathrm{He}\,X := X + X^T$. A block-diagonal structure with sub-blocks $X_1, X_2, \ldots, X_p$ in its diagonal will be denoted by diag $(X_1, X_2, \ldots, X_p)$. L_{2e}^n denotes n-dimensional functional space whose members only need to be square integrable on finite intervals. ϵ is a sufficiently small value. Other notations are standard.

Table 1: IQC characterization for specified Δ_i.

Type	$\Phi \in [0, K_\Phi]$	$\mathrm{diag}(\delta_1, \ldots, \delta_{n_i})$	$\delta_i(t) I_{n_i}$	$\lVert \Delta_i(s) \rVert_\infty < 1$
	$Q = -2V \in \Lambda^{n_i \times n_i}$	$Q \in \Lambda^{n_i \times n_i}$	$Q \in \Re^{n_i \times n_i}$	$Q = qI_{n_i}$, $q \in \Re$
Scalings	$S = VK_\Phi$	$S = 0$	$S + S^T = 0$	$S = 0$
	$R = \epsilon I$	$R = -Q$	$R = -Q$	$R = -Q$

2. Problem Statement

The anti-windup control problem is sketched in Figure 1(a). The block $P(s)$ denotes the stable nominal system and typically includes a model of the plant with uncertainties, nominal controller together with weighing functions specified by the user. Note that $\Phi = z - \Psi(z)$, where Ψ denotes the standard saturation operator. For clearness, the anti-windup control diagram in Figure 1(a) is equivalently reformulated as LFT structure in Figure 1(b) with $\widetilde{P}(s)$ described by

$$\begin{aligned}
\dot{x}_p &= A_p x_p + B_r w_r + B_p w_p + B_u u, \\
z_r &= C_r x_p + D_{rr} w_r + D_{rp} w_p + D_{ru} u, \\
z_\infty &= C_\infty x_p + D_{\infty r} w_r + D_{\infty p} w_p + D_{\infty u} u, \\
z_2 &= C_2 x_p + D_{2r} w_r + D_{2p} w_p + D_{2u} u, \\
w &= D_{wr} w_r, \\
w_r &= \Delta z_r.
\end{aligned} \tag{2.1}$$

Here, $x_p \in \Re^n$ are the states. The input/output channels associated with the robustness are $w_r, z_r \in \Re^{n_r}$. The input/output channels associated with the performance criterion are $w_p \in \Re^{n_p}$, $z_\infty \in \Re^{n_\infty}$, and $z_2 \in \Re^{n_2}$. $u \in \Re^{n_u}$ are the compensated controls, and $w \in \Re^{n_w}$ are the saturation error feedback. For well posedness, we will assume that $D_{2p} = 0$.

Δ is a causal operator from $L_{2e}^r[0, \infty]$ to $L_{2e}^r[0, \infty]$ with its inputs and outputs satisfying the following time-domain integral quadratic constraint

$$\int_0^t \begin{bmatrix} w_r(t) \\ z_r(t) \end{bmatrix}^T \begin{bmatrix} Q & S^T \\ S & R \end{bmatrix} \begin{bmatrix} w_r(t) \\ z_r(t) \end{bmatrix} dt \geq 0, \quad \forall t \geq 0. \tag{2.2}$$

Let Q, S, R be constant scaling matrices such that $Q < 0$, $R > 0$. We assume that Δ is block diagonal: $\Delta = \mathrm{diag}(\Delta_1, \ldots, \Delta_r)$, where Δ_i denotes a "troublemaking" component. The IQC characterizations for the typical cases considered here are listed in Table 1. Reference [20] provides a fairly complete overview of IQCs. For application, all of the individual IQC are collected in block-diagonal matrices $Q = \mathrm{diag}\ (Q_1, \ldots, Q_r)$, $R = \mathrm{diag}\ (R_1, \ldots, R_r)$, and $S = \mathrm{diag}\ (S_1, \ldots, S_r)$ to characterize the associated composition of Δ.

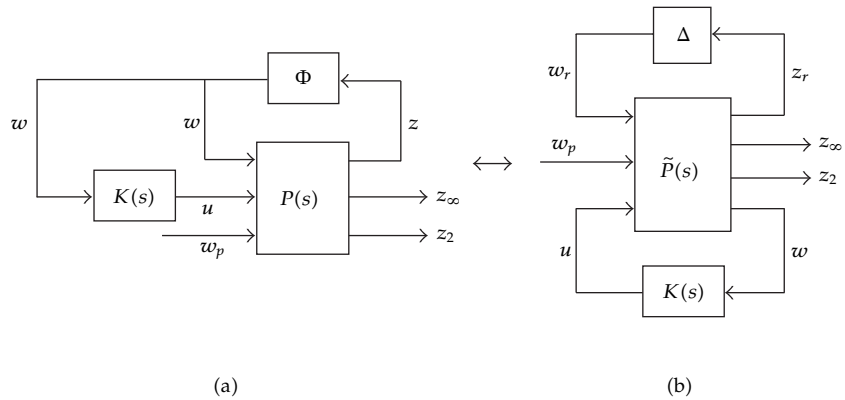

Figure 1: (a) Anti-windup control structure; (b) equivalent LFT formulation.

Considering system (2.1), we assume that a full-order dynamic anti-windup compensator is of the form

$$\begin{aligned} \dot{x}_k &= A_k x_k + B_k w, \\ u &= C_k x_k + D_k w, \end{aligned} \tag{2.3}$$

where $x_k \in \Re^n$ is the controller state, and A_k, B_k, C_k, D_k are constant matrices of appropriate dimensions. Then, the final closed-loop system admits the realization

$$\begin{aligned} \dot{x}_c &= \mathcal{A}_c x_c + \mathcal{B}_r w_r + \mathcal{B}_p w_p, \\ z_r &= \mathcal{C}_r x_c + \mathfrak{D}_{rr} w_r + \mathfrak{D}_{rp} w_p, \\ z_\infty &= \mathcal{C}_\infty x_c + \mathfrak{D}_{\infty r} w_r + \mathfrak{D}_{\infty p} w_p, \\ z_2 &= \mathcal{C}_2 x_c + \mathfrak{D}_{2r} w_r, \end{aligned} \tag{2.4}$$

where $x_c = [x_p^T \;\; x_k^T]^T$ and

$$\begin{bmatrix} \mathcal{A}_c & \mathcal{B}_i \\ \mathcal{C}_j & \mathfrak{D}_{ji} \end{bmatrix} = \left[\begin{array}{cc|c} A_p & B_u C_k & B_i + B_u D_k D_{\omega i} \\ 0 & A_k & B_k D_{\omega i} \\ \hline C_j & D_{ju} C_k & D_{ji} + D_{ju} D_k D_{\omega i} \end{array}\right] \tag{2.5}$$

with $i = r, p$ and $j = r, \infty, 2$.

Denoting by $T_\infty(s)$ and $T_2(s)$ the closed-loop transfer functions from w_p to z_∞ and z_2 respectively, we consider the following multiobjective synthesis problem: design an dynamic anti-windup controller (2.3) such that as follows.

(1) The closed-loop system (2.4) is robustly stable with respect to the perturbation block Δ.

(2) Minimize $\|T_2(s)\|_2$ subject to $\|T_\infty(s)\|_\infty < \gamma$.

(3) The closed-loop poles can be placed in the prescribed complex plane which is described by LMI region.

3. LMI Formulation of System Analysis

In this section, we will provide robust stability and performance analysis conditions for the closed-loop system (2.4) in the LMI framework. The specifications and objectives under consideration include H_∞ performance, H_2 performance. Additional regional constraints on the closed-loop poles can also be imposed.

Theorem 3.1 (robust H_∞ performance). *Given the closed-loop system* (2.4) *with perturbation block* Δ *satisfying the integral quadratic constraint* (2.2) *and a scalar* γ*, if there exist a positive-definite matrix* P_∞ *and scaling matrices* Q, S, R *such that*

$$\mathrm{He}\begin{bmatrix} P_\infty \mathcal{A}_c & P_\infty \mathcal{B}_r + \mathcal{C}_r^T S & P_\infty \mathcal{B}_p & 0 & 0 \\ 0 & \frac{1}{2}Q + S^T \mathfrak{D}_{rr} & S^T \mathfrak{D}_{rp} & 0 & 0 \\ 0 & 0 & -\frac{1}{2}\gamma I & 0 & 0 \\ R\mathcal{C}_r & R\mathfrak{D}_{rr} & R\mathfrak{D}_{rp} & -\frac{1}{2}R & 0 \\ \mathcal{C}_\infty & \mathfrak{D}_{\infty r} & \mathfrak{D}_{\infty p} & 0 & -\frac{1}{2}\gamma I \end{bmatrix} < 0 \tag{3.1}$$

then the closed-loop system is robustly stable against the perturbation block Δ*, and one has* $\|T_\infty(s)\|_\infty < \gamma$ *with zero-state initial conditions.*

Proof. Consider a Lyapunov function $V(x_c) = x_c^T P_\infty x_c$ for the closed-loop system (2.4). A sufficient condition for the robust H_∞ performance specification can be established from the inequality

$$\dot{V} + \begin{bmatrix} w_r \\ z_r \end{bmatrix}^T \begin{bmatrix} Q & S^T \\ S & R \end{bmatrix} \begin{bmatrix} w_r \\ z_r \end{bmatrix} + \frac{1}{\gamma} z_\infty^T z_\infty - \gamma w_p^T w_p < 0. \tag{3.2}$$

First, consider the robust stability with the performance channel removed, the inequality (3.2) is rewritten as

$$\frac{d}{dt}\left(V + \int_0^t \begin{bmatrix} w_r \\ z_r \end{bmatrix}^T \begin{bmatrix} Q & S^T \\ S & R \end{bmatrix} \begin{bmatrix} w_r \\ z_r \end{bmatrix} dt \right) < 0. \tag{3.3}$$

Note that the second term is always nonnegative. According to standard arguments from Lyapunov theory, the closed-loop system is stable. Here, the function V decreases to zero, but not necessarily monotonically. Next, consider robust performance, integrating (3.2) from 0 to ∞ with initial condition $x_c(0) = 0$ yields $\|z_\infty\|_2 < \gamma \|w_p\|_2$. As a result, robust H_∞ performance can be guaranteed. Inequality (3.2) is equivalent to the LMI condition (3.1) by Schur complement. □

Theorem 3.2 (robust H_2 performance). *Given the closed-loop system* (2.4) *with perturbation block* Δ *satisfying the integral quadratic constraint* (2.2) *and a scalar* ν, *if there exist a positive-definite matrix* P_2 *and scaling matrices* Q, S, R *such that*

$$\mathrm{He}\begin{bmatrix} P_2\mathcal{A}_c & P_2\mathcal{B}_r + \mathcal{C}_r^T S & 0 & 0 \\ 0 & \frac{1}{2}Q + S^T\mathfrak{D}_{rr} & 0 & 0 \\ R\mathcal{C}_r & R\mathfrak{D}_{rr} & -\frac{1}{2}R & 0 \\ \mathcal{C}_2 & \mathfrak{D}_{2r} & 0 & -\frac{1}{2}I \end{bmatrix} < 0,$$
$$\begin{bmatrix} P_2 & P_2\mathcal{B}_p \\ \mathcal{B}_p^T P_2 & W \end{bmatrix} > 0,$$
$$\mathrm{Tr}(W) < \nu^2 \tag{3.4}$$

then the closed-loop system is robustly stable against the perturbation block Δ, *and one has* $\|T_2(S)\|_2 < \nu$.

Proof. Let $\{e_1, \ldots, e_{n_p}\}$ be a basis of the input space $\Re^{n_p}$. Let $x_{c0\cdot i} = \mathcal{B}_p e_i$, $i = 1, \ldots, n_p$ be the initial conditions of the closed-loop system (2.4). Let $z_{2\cdot i}$ denote the output response subject to initial condition $x_{c0\cdot i}$ and $w_p = 0$. Then the H_2 norm $\|T_2(s)\|_2$ can be equivalently defined as [22]

$$\|T_2(s)\|_2^2 := \sum_{i=1}^{n_p} \|z_{2\cdot i}\|_2^2. \tag{3.5}$$

With these results, a Lyapunov function $V(x_c) = x_c^T P_2 x_c$ can be constructed to satisfy the following inequality

$$\dot{V} + \begin{bmatrix} w_r \\ z_r \end{bmatrix}^T \begin{bmatrix} Q & S^T \\ S & R \end{bmatrix} \begin{bmatrix} w_r \\ z_r \end{bmatrix} + z_2^T z_2 < 0. \tag{3.6}$$

The robust stability proof is the same as the one in Theorem 3.1. As for robust performance, integrating (3.6) from 0 to ∞ with $x_c(\infty) = 0$ guaranteed by stability, we can obtain $\|z_2\|_2^2 < V(x_c(0))$. As a result, the output energy is bounded by

$$\sum_{i=1}^{n_p} \|z_{2\cdot i}\|_2^2 < \sum_{i=1}^{n_p} e_i^T \mathcal{B}_p^T P_2 \mathcal{B}_p e_i = \mathrm{Tr}\left(\mathcal{B}_p^T P_2 \mathcal{B}_p\right). \tag{3.7}$$

With an auxiliary parameter W such that $\mathcal{B}_p^T P_2 \mathcal{B}_p < W$, the LMI conditions (9~11) can be obtained by Schur complement. □

Pole assignment in convex regions of the left-half plane can be expressed as LMI constraints on the Lyapunov matrix. An LMI region is any region D of the complex plane that can be defined as

$$D = \left\{ z \in C : L + Mz + M^T \overline{z} < 0 \right\} \tag{3.8}$$

with $L = L^T = \{\lambda_{ij}\}_{1\le i,j\le m}$ and $M = \{\mu_{ij}\}_{1\le i,j\le m}$ being constant real matrices. Reference [23] gives a thorough discussion for various types of the convex region.

Theorem 3.3 (see [23] (pole placement)). *The closed-loop state matrix $\mathcal{A}_c$ has all its eigenvalues in the LMI region D* (3.8) *if and only if there exists a positive definite matrix P_{pol} such that*

$$\left[\lambda_{ij} P_{\text{pol}} + \mu_{ij} \mathcal{A}_c^T P_{\text{pol}} + \mu_{ji} P_{\text{pol}} \mathcal{A}_c\right]_{1\le i,j\le m} < 0. \tag{3.9}$$

Note that the closed-loop poles of system (2.4) exactly consist of the poles of system (2.1) and those of controller (2.3); LMI region D should include the poles of system (2.1) to ensure the feasibility of the problem. Furthermore, the dynamics of the controller (2.3) can be constrained by the LMI region D.

4. LMI Approach to Multiobjective Synthesis

Based on the analysis results stated in the above section, in this section we aim to present a constructive procedure to design an anti-windup controller of the form (2.3), satisfying the multiobjective synthesis purposes proposed in Section 2. This procedure relies on a simple change of controller variables to map all LMIs of Section 3 into a set of affine constraints on the new controller variables and the closed-loop Lyapunov matrix.

For tractability in the LMI framework, we must seek a common Lyapunov matrix

$$P := P_\infty = P_2 = P_{\text{pol}} \tag{4.1}$$

that satisfies Theorems 3.1, 3.2, and 3.3. This restriction has been extensively used in multiobjective control problem such as [23, 24]. Partition P and P^{-1} as

$$P = \begin{bmatrix} Y & N \\ N^T & * \end{bmatrix}, \qquad P^{-1} = \begin{bmatrix} X & M \\ M^T & * \end{bmatrix}, \tag{4.2}$$

where $X, Y \in \Re^{n\times n}$ are symmetric. Factorizing P as

$$PX_1 = X_2, \qquad X_1 = \begin{bmatrix} X & I \\ M^T & 0 \end{bmatrix}, \qquad X_2 = \begin{bmatrix} I & Y \\ 0 & N^T \end{bmatrix} \tag{4.3}$$

we define the change of controller variables as follows:

$$\begin{aligned}
\mathcal{A}_k &:= YA_pX + YB_uC_kM^T + NA_kM^T,\\
\mathcal{B}_k &:= YB_uD_k + NB_k,\\
\mathcal{C}_k &:= C_kM^T,\\
\mathcal{D}_k &:= D_k.
\end{aligned} \tag{4.4}$$

For full-order design, one can always assume that M, N are $n \times n$ square and invertible matrices. Hence the controller variables A_k, B_k, C_k, D_k can be determined by $\mathcal{A}_k, \mathcal{B}_k, \mathcal{C}_k, \mathcal{D}_k, X, Y$ uniquely. Then through suitable congruence transformation, the analysis results of Section 3 are readily turned into inequality constraints on the variables $X, Y, \mathcal{A}_k, \mathcal{B}_k, \mathcal{C}_k, \mathcal{D}_k$ as well as auxiliary variable W and scaling matrices Q, S, R, and we arrive at Theorem 4.1.

Theorem 4.1 (multiobjective synthesis for robust anti-windup controller). *Given the generalized plant* (2.1) *with perturbation block* Δ *satisfies the integral quadratic constraint* (2.2) *and the LMI region* D (3.7). *There exists a controller* (2.3) *which robustly stabilizes plant* (2.1) *and enforces a tight upper bound* $\sqrt{\mathrm{Tr}(W)}$ *on* $\|T_2(s)\|_2$ *subject to* $\|T_\infty(s)\|_\infty < \gamma$ *and closed-loop poles constraints specified by* D, *if there exist matrices* $X, Y, \mathcal{A}_k, \mathcal{B}_k, \mathcal{C}_k, \mathcal{D}_k$ *as well as auxiliary variable* W *and scaling matrices* Q, S, R *such that the inequalities hold as shown in (20~22) at the top of the next page, together with*

$$\mathrm{He}\begin{bmatrix}
A_pX + B_u\mathcal{C}_k & A_p + \mathcal{A}_k^T & B_r + B_u\mathcal{D}_kD_{wr} + XC_r^TS + \mathcal{C}_k^TD_{ru}^TS & B_p & 0 & 0\\
0 & YA_p & YB_r + \mathcal{B}_kD_{wr} + C_r^TS & YB_p & 0 & 0\\
0 & 0 & \frac{1}{2}Q + S^TD_{rr} + S^TD_{ru}\mathcal{D}_kD_{wr} & S^TD_{rp} & 0 & 0\\
0 & 0 & 0 & -\frac{1}{2}\gamma I & 0 & 0\\
RC_rX + RD_{ru}\mathcal{C}_k & RC_r & RD_{rr} + RD_{ru}\mathcal{D}_kD_{wr} & RD_{rp} & -\frac{1}{2}R & 0\\
C_\infty X + D_{\infty u}\mathcal{C}_k & C_\infty & D_{\infty r} + D_{\infty u}\mathcal{D}_kD_{wr} & D_{\infty p} & 0 & -\frac{1}{2}\gamma I
\end{bmatrix} < 0,$$

$$\mathrm{He}\begin{bmatrix}
A_pX + B_u\mathcal{C}_k & A_p + \mathcal{A}_k^T & B_r + B_u\mathcal{D}_kD_{wr} + XC_r^TS + \mathcal{C}_k^TD_{ru}^TS & 0 & 0\\
0 & YA_p & YB_r + \mathcal{B}_kD_{wr} + C_r^TS & 0 & 0\\
0 & 0 & \frac{1}{2}Q + S^TD_{rr} + S^TD_{ru}\mathcal{D}_kD_{wr} & 0 & 0\\
RC_rX + RD_{ru}\mathcal{C}_k & RC_r & RD_{rr} + RD_{ru}\mathcal{D}_kD_{wr} & -\frac{1}{2}R & 0\\
C_2X + D_{2u}\mathcal{C}_k & C_2 & D_{2r} + D_{2u}\mathcal{D}_kD_{wr} & 0 & -\frac{1}{2}I
\end{bmatrix} < 0,$$

$$\left[\lambda_{ij}\begin{pmatrix} X & I\\ I & Y\end{pmatrix} + \mu_{ij}\begin{pmatrix} A_pX + B_u\mathcal{C}_k & A_p\\ \mathcal{A}_k & YA_p\end{pmatrix}^T + \mu_{ji}\begin{pmatrix} A_pX + B_u\mathcal{C}_k & A_p\\ \mathcal{A}_k & YA_p\end{pmatrix}\right]_{1\le i,j\le m} < 0,$$

$$\begin{bmatrix} X & I & B_p \\ I & Y & YB_p \\ B_p^T & B_p^T Y & W \end{bmatrix} > 0,$$
$$\text{Minimizing } \operatorname{Tr}(W). \tag{4.5}$$

Due to the fact that the matrix variables $X, Y, \mathcal{A}_k, \mathcal{B}_k, \mathcal{C}_k, \mathfrak{D}_k$ and scaling matrices Q, S, R enter the inequalities (21~22) in nonlinear fashion, synthesis conditions are no longer convex optimization problem. In order to overcome this difficulty, one will resort to the following iterative scheme based on LMI.

Step 1. Initialize scaling matrices Q, S, R.

Step 2. With fixed Q, S, R, perform control synthesis according to Theorem 4.1. Compute two invertible matrices $M, N \in \Re^{n\times n}$ such that

$$MN^T = I - XY. \tag{4.6}$$

Equation (4.4) can be solved for D_k, C_k, B_k, A_k in this order.

Step 3. Apply Theorems 3.1, 3.2, 3.3, and (4.1) to the closed-loop system (2.4) to solve scaling matrices Q, S, R minimizing $\operatorname{Tr}(W)$.

Step 4. Iterate over Step 2 to Step 3 until $\operatorname{Tr}(W)$ cannot be decreased significantly.

It is important to mention that the previously described iterative scheme, although not guaranteeing a global solution theoretically, has proven very efficient in practice.

5. Application Example

As an application, a missile benchmark problem [25] will be used to demonstrate the effectiveness of the results discussed. The model is linearized at $\alpha = 10\,\text{deg}$ (angle of attack) and $Ma = 3$ (Mach number), and admits the realization

$$\begin{bmatrix} \dot{\alpha} \\ \dot{q} \\ \dot{\vartheta} \end{bmatrix} = \begin{bmatrix} Z_\alpha & 1 & 0 \\ M_\alpha & 0 & 0 \\ 0 & 1 & 0 \end{bmatrix} \begin{bmatrix} \alpha \\ q \\ \vartheta \end{bmatrix} + \begin{bmatrix} Z_\delta \\ M_\delta \\ 0 \end{bmatrix} \delta, \tag{5.1}$$

where q, ϑ, and δ denote pitch rate, pitch angle, and elevator deflection, respectively. The measurement outputs are the flight path angle $r = \vartheta - \alpha$ and the pitch rate q. The parametric uncertainties originate from the aerodynamic force Z and moment M with uncertainty level of ±20%. The actuator dynamics are given by $G_{\text{act}}(s) = 150^2/(s^2 + 210s + 150^2)$ with saturation limit $\delta \in [-15, 15]$ deg.

Ignoring the saturation, a PID controller can be designed as $\delta_c = [1.5\int(r - r_c)dt + 2r + 0.3q]$. δ_c and r_c denote the commanded signal to the actuator and the commanded flight path angle, respectively. According to the analysis results in Section 3, the PID controller can

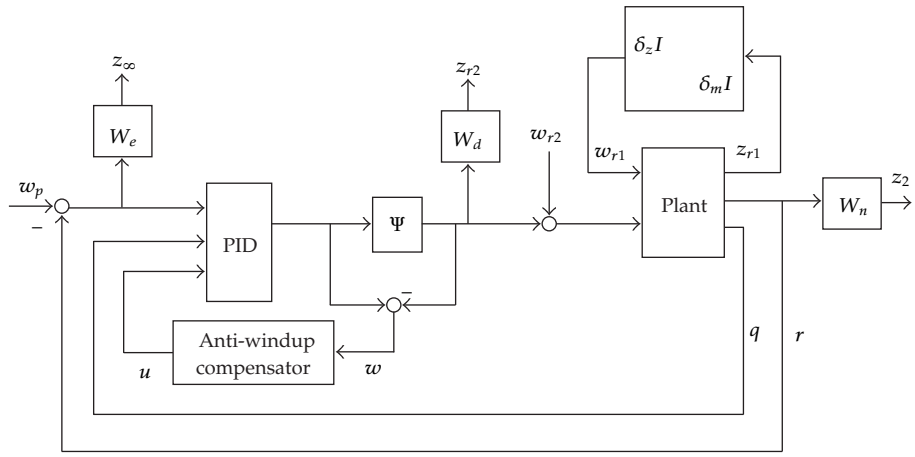

Figure 2: Interconnection structure for anti-windup design.

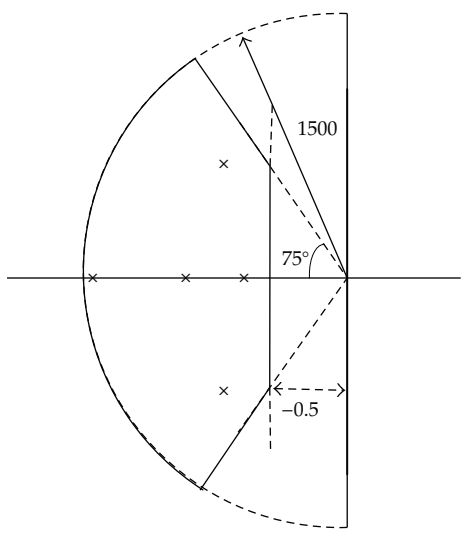

Figure 3: LMI region with poles $[-1346, -61, -1, -9.8 \pm 10.2i]$.

guarantee global stability for the saturated plant with $K_\Phi = 1$. Although the PID controller provides adequate stability and nominal performance, the tracking trajectory of the nominal system under saturation deteriorates and exhibits great overshoot (see Figure 4). This clearly necessitates the anti-windup compensation scheme.

In the anti-windup design, firstly parametric uncertainties in Z and M are extracted from the plant in a linear fractional way and rescaled to $[-1, 1]$. Secondly, to avoid excitation of unmodeled high-frequency dynamics, a multiplicative input uncertainty $\Delta_d(s)$ weighted by $W_d(s) = 1.5[(s+2)/(s+80)]$ is placed at the actuator. Finally, we end up with the control interconnection as shown in Figure 2. Constant weights $W_e = 1$ and $W_n = 0.001$ are used to reflect the tracking performance and measurements with noise.

We combine the sector-bounded nonlinearity $\Phi = I - \Psi$ with the modeling uncertainties as a block-diagonal uncertainty structure given by $\Delta = \text{diag}\,(\Phi, \delta_z I, \delta_m I, \Delta_d)$.

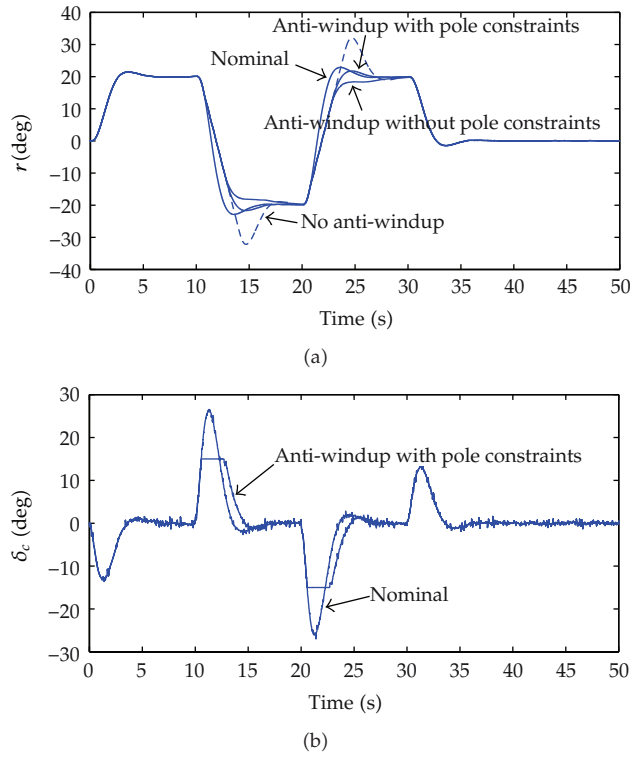

Figure 4: Time-domain responses to a double pulse reference.

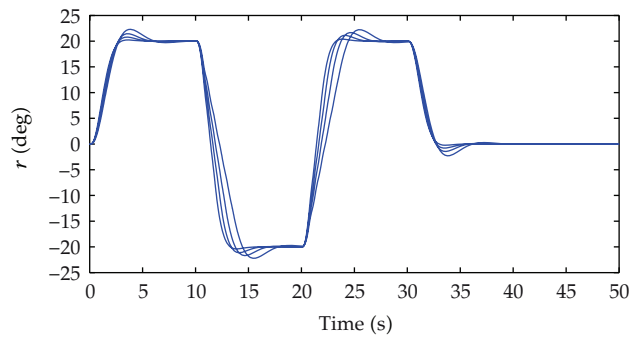

Figure 5: Time-domain responses for all combinations of perturbed aerodynamics.

Then, the anti-windup control diagram in Figure 2 is equivalently reformulated as LFT structure in Figure 1(b) for design. For low-order compensator, the actuator dynamics are ignored in design. This is justified by the fact that the bandwidth of the system is far below that of the actuator. The LMI region D specified in Figure 3 is used to constrain the dynamics of the compensator. We choose to minimize $\|T_2(s)\|_2$ subject to $\|T_\infty(s)\|_\infty < \gamma$. $K_\Phi = 0.8$ is used to allocate the partial design freedom for coping with robustness and performance at the cost of global stability. As a result, we achieve $\gamma = 38.6$ and $\|T_2(s)\|_2 = 4.2$. The control deflection should satisfy the condition $|\delta| \leq (1/(1 - K_\Phi))15\,\text{deg}$. The distribution of the poles of the compensator is shown in Figure 3.

For numerical simulations, the measurement noise is chosen as band-limited white noise of power 10^{-6} passed through a zero order holder with sampling time 10^{-3} s. The resulting anti-windup response almost coincides with the linear response (see Figure 4). We can see that the designed anti-windup controlled guarantees the stability and recovers the nominal performance when the actuator is saturated deeply. For comparison, the anti-windup response of the nondynamically constrained compensator become worse because of the existence of a slow compensator mode -0.002. Figure 5 shows the time-domain robust performance behaves. As expected from previous results, Figure 5 illustrated that the anti-windup performance of the obtained controller is robust with respect to the error in model parameters.

6. Conclusion

This paper presents a unified synthesis method for the construction of multiobjective and robust anti-windup compensator for linear systems with actuator saturations, time-varying parametric and dynamic uncertainties. Motivated by the capability of integral quadratic constraints in characterizing saturation nonlinearities and modeling uncertainties, the concerned anti-windup and robustness problems are addressed in the framework of IQCs. The performance objectives are specified in terms of a mixed H_2/H_∞ norm and additional constraints on the poles of the controller. The controller synthesis procedure requires solving scaled LMIs with a D/K-like iteration and provides dynamically constrained anti-windup compensators. Finally, simulation example demonstrates the effectiveness of the results.

Acknowledgments

This research was partially supported by the National Natural Science Foundation of China (No. 61104112), the Fundamental Research Funds for the Central Universities (No. HIT. NSRIF. 201162), and the China Postdoctoral Science Foundation (No. 2012M510960).

References

[1] X. Su, P. Shi, L. Wu, and Y.-D. Song, "A novel approach to filter design for T-S fuzzy discrete-time systems with time- varying delay," *IEEE Transactions on Fuzzy Systems*, vol. 20, no. 99, p. 1.

[2] X. Su, L. Wu, P. Shi, and Y. -D. Song, "H_∞ model reduction of T-S fuzzy stochasticsystems," *IEEE Transactions on Systems, Man, and Cybernetics*. In press.

[3] L. Wu, X. Su, P. Shi, and J. Qiu, "Model approximation for discrete-time state-delay systems in the TS fuzzy framework," *IEEE Transactions on Fuzzy Systems*, vol. 19, no. 2, pp. 366–378, 2011.

[4] L. Wu, X. Su, P. Shi, and J. Qiu, "A new approach to stability analysis and stabilization of discrete-time T-S fuzzy time-varying delay systems," *IEEE Transactions on Systems, Man, and Cybernetics*, vol. 41, no. 1, pp. 273–286, 2011.

[5] H. L. Dong, Z. D. Wang, and H. J. Gao, "H_∞ fuzzy control for systems with repeated scalar nonlinearities and random packet losses," *IEEE Transactions on Fuzzy Systems*, vol. 17, no. 2, pp. 440–450, 2009.

[6] L. Wu, X. Su, and P. Shi, "Sliding mode control with bounded L_2 gain performance of Markovian jump singular time-delay systems," *Automatica*, vol. 48, no. 8, pp. 1929–1933, 2012.

[7] J. Hu, Z. D. Wang, H. J. Gao, and L. K. Stergioulas, "Robust sliding mode control for discrete stochastic systems with mixed timedelays, randomly occurring uncertainties and randomly occurring nonlinearities," *IEEE Transactions on Industrial Electronics*, vol. 59, no. 7, pp. 3008–3015, 2012.

[8] J. Hu, Z. D. Wang, H. J. Gao, and L. K. Stergioulas, "Robust H_∞ sliding mode control for discrete time-delay systems with stochastic nonlinearities," *Journal of the Franklin Institute*, vol. 349, no. 4, pp. 1459–1479, 2012.

[9] J. Hu, Z. D. Wang, H. J. Gao, and L. K. Stergioulas, "Probabilityguaranteed H_∞ finite-horizon filtering for a class of nonlinear timevarying systems with sensor saturation," *System & Control Letters*, vol. 61, no. 4, pp. 477–484, 2012.

[10] M. V. Kothare, P. J. Campo, M. Morari, and C. N. Nett, "A unified framework for the study of anti-windup designs," *Automatica*, vol. 30, no. 12, pp. 1869–1883, 1994.

[11] A. R.. Teel and N. Kapoor, "The L_2 anti-windup problem: its definition and solution," in *Proceedings of the 4th European Control Conference*, 1997.

[12] M. V. Kothare and M. Morari, "Multiplier theory for stability analysis of anti-windup control systems," *Automatica*, vol. 35, no. 5, pp. 917–928, 1999.

[13] E. F. Mulder, M. V. Kothare, and M. Morari, "Multivariable anti-windup controller synthesis using linear matrix inequalities," *Automatica*, vol. 37, no. 9, pp. 1407–1416, 2001.

[14] G. Grimm, J. Hatfield, I. Postlethwaite, A. R. Teel, M. C. Turner, and L. Zaccarian, "Antiwindup for stable linear systems with input saturation: an LMI-based synthesis," *IEEE Transactions on Automatic Control*, vol. 48, no. 9, pp. 1509–1525, 2003.

[15] F. Wu and B. Lu, "Anti-windup control design for exponentially unstable LTI systems with actuator saturation," *Systems & Control Letters*, vol. 52, no. 3-4, pp. 305–322, 2004.

[16] B. Lu, F. Wu, and S. W. Kim, "Linear parameter-varying antiwindup compensation for enhanced flight control performance," *Journal of Guidance, Control, and Dynamics*, vol. 28, no. 3, pp. 494–505, 2005.

[17] M. Saeki and N. Wada, "Synthesis of a static anti-windup compensator via linear matrix inequalities," *International Journal of Robust and Nonlinear Control*, vol. 12, no. 10, pp. 927–953, 2002.

[18] M. C. Turner, G. Herrmann, and I. Postlethwaite, "Accounting for uncertainty in anti-windup synthesis," in *Proceedings of the American Control Conference*, pp. 5292–5297, IEEE Press, Piscataway, NJ, USA, July 2004.

[19] G. Ferreres and J.-M. Biannic, "Convex design of a robust antiwindup controller for an LFT model," *IEEE Transactions on Automatic Control*, vol. 52, no. 11, pp. 2173–2177, 2007.

[20] A. Megretski and A. Rantzer, "System analysis via integral quadratic constraints," *IEEE Transactions on Automatic Control*, vol. 42, no. 6, pp. 819–830, 1997.

[21] C. Roos and J.-M. Biannic, "A convex characterization of dynamically-constrained anti-windup controllers," *Automatica*, vol. 44, no. 9, pp. 2449–2452, 2008.

[22] D. Banjerdpongchai and J. How, "Parametric robust H_2 control design using LMI synthesis," in *Proceedings of the AIAA Guidance, Navigation and Control Conference and Exhibit*, pp. 3733–3744, AIAA, 1996.

[23] M. Chilali and P. Gahinet, "H_∞ design with pole placement constraints: an LMI approach," *IEEE Transactions on Automatic Control*, vol. 41, no. 3, pp. 358–367, 1996.

[24] C. Scherer, P. Gahinet, and M. Chilali, "Multiobjective output-feedback control via LMI optimization," *IEEE Transactions on Automatic Control*, vol. 42, no. 7, pp. 896–911, 1997.

[25] R. A. Nichols, R. T. Reichert, and W. J. Rugh, "Gain scheduling for H-infinity controllers: a flight control example," *IEEE Transactions on Control Systems Technology*, vol. 1, no. 2, pp. 69–78, 1993.

Hindawi Publishing Corporation
Mathematical Problems in Engineering
Volume 2012, Article ID 867847, 16 pages
doi:10.1155/2012/867847

Research Article

Distribution-Free Continuous Review Inventory Model with Controllable Lead Time and Setup Cost in the Presence of a Service Level Constraint

Wei-Min MA and Bing-Bing QIU

School of Economics and Management, Tongji University, Shanghai 200092, China

Correspondence should be addressed to Bing-Bing QIU, qiubb2005@163.com

Received 15 March 2012; Revised 3 June 2012; Accepted 4 July 2012

Academic Editor: Jun Hu

Based on the mean and the standard deviation of lead time demand, and also taking the difficulty in measuring shortage cost into consideration, we investigate the joint decision problem of continuous review inventory in which a service level constraint should be satisfied. Under the assumption of controllable lead time and setup cost, a mathematical programming model is established. The objective function of the proposed model is the total expected annual cost and the constraint guarantees that the service level requirement can be satisfied at the worst case. Subsequently, an equivalent nonlinear programming model is derived. By constructing Lagrange function, the analysis regarding the solution procedure is conducted, and a solution algorithm is then provided. Moreover, a numerical example is introduced to illustrate the proposed model and solution algorithm. Through sensitivity analysis, some observations and managerial implications are provided.

1. Introduction

In inventory management, the length of lead time has direct influence on customer service level and total inventory cost. With the increasing competition in today's business environment, plenty of enterprises have devoted their efforts to pursuing a short lead time to enhance market competition ability. It is no doubt that the achievement of a shortened lead time requires a number of capital investments. Thus, some researchers have paid their attentions to balancing benefits and costs resulting from the reduction of lead time, and developed some theoretical models for possible decision aid. For example, Liao and Shyu [1] regarded the lead time as a decision variable. By assuming that the lead time composes of several components and the crashing cost is a linear function in the length of lead time concerning each component, a mathematical programming model with controllable lead time

was constructed. Later, with the lead time crashing cost function proposed by Liao and Shyu [1], a lot of work has been done to develope some optimization models and algorithms in various decision environments for continuous inventory problems with variable lead time, such as Hariga and Ben-Daya [2], Ouyang and Chang [3], Wu and Ouyang [4], Yang et al. [5], Lee [6], Hoque and Goyal [7], and Annadurai and Uthayakumar [8]. However, the piecewise linear expression of lead time crashing cost has some deficiencies in application. Thus, Ben-Daya and Raouf [9] adopted negative exponential function to describe the lead time crashing cost and proposed a corresponding continuous review inventory model. Subsequently, Wu et al. [10] employed the negative exponential lead time crashing cost to develop a continuous review inventory model in which the lead time demand with the mixture of distributions was taken into account. Besides, Yang [11] proposed a supply chain integrated inventory model in the present of time value. In the proposed model, the lead time crashing cost was also assumed to be nonlinear in the length of lead time.

Likewise, in many real inventory problems, the setup cost could be reduced through increasing labor, improving facilities or adopting other relevant measures. In view of this point, Ouyang et al. [12] considered the partial backorder and proposed a modified continuous review inventory model with controllable lead time and setup cost. Taking the imperfect production process into account, Ouyang and Chang [13] constructed an inventory optimization model with controllable lead time and setup cost. In their research, both logarithmic and power investment functions were considered. With the assumption of controllable lead time and setup cost, Ouyang et al. [14] considered quality improvement in imperfect production process and investigated the associated inventory decision problem. Chuang et al. [15] assumed that the lead time demand is distribution-free in protection level and presented an inventory optimization model with variable lead time and setup cost. Taking the inconsistency between the receiving quantity and the ordering quantity into account, Wu and Lin [16] proposed an extended continuous review inventory model in which both lead time and ordering cost were variable. Subsequently, in supply chain setting, Chang et al. [17] proposed two integrated inventory models with the reductions of lead time and ordering cost. Considering the backorder discount, Lee et al. [18] developed a joint inventory decision model with variable lead time and ordering cost. In the research conducted by Uthayakumar and Parvathi [19], not only lead time and setup cost, but also yield variability was assumed to be variable. Besides, the backorder rate was assumed to be controllable through the amount of expected shortage. In their models, all the capital investments were assumed to be subject to logarithmic function. Annadurai and Uthayakumar [20] took the imperfect quality into account and developed a continuous review inventory model involving variable lead time and setup cost.

It is inevitable that shortage takes place with the assumption of stochastic lead time demand in continuous review inventory. However, in some practical situations, the shortage cost is difficult to estimate and therefore a service level constraint is announced by manager instead. Thus, based on different service level metrics, Aardal et al. [21] studied the optimal replenishment problem of continuous review inventory system. Moreover, some convex programming formulations were developed, and the associated solution algorithms were also given. With the normally distributed lead time demand, Ouyang and Wu [22] established a continuous review inventory model involving controllable lead time. In their research, a service level constraint was taken into account. Then, the assumption of normal distribution on lead time demand was relaxed and a distribution-free computational procedure was developed. By using the mixture of distributions to describe lead time demand, Lee et al. [23] proposed a continuous review inventory model with variable

backorder rate and service level constraint. Jha and Shanker [24] proposed a model to solve ordering quantity, length of lead time and number of shipments in supply chain environment. In the concerned problem, controllable lead time and service level constraint were taken into consideration. Tajbakhsh [25] studied a distribution-free inventory model with a fill rate constraint. By solving the proposed model, the closed-form expressions of ordering quantity and reorder point were derived. Hsu and Huang [26] developed a distribution-free continuous review inventory model with multi-retailer. Moreover, both controllable lead time and service level constraint were considered. In Annadurai and Uthayakumar [27], and Jaggi and Arneja [28], with a service level constraint, the continuous review inventory models involving controllable lead time and setup cost were investigated. The former focused on the demand with the mixture of distributions, while the latter focused on the demand with normal distribution. More recently, Lin [29] presented a continuous review inventory model with a service level constraint. In the proposed model, setup cost, backorder rate, and lead time were assumed to be controllable. One of the same features in the models proposed by Annadurai and Uthayakumar [27], Jaggi and Arneja [28], and Lin [29] is that the piecewise linear lead time crashing cost was adopted. Besides, they derived safety coefficient from the allowable stock-out probability during lead time and thus the safety coefficient is not a decision variable. In fact, safety coefficient could be optimized, such as in Hariga and Ben-Daya [2], Wu and Ouyang [4], Hoque and Go [7], Annadurai and Uthayakumar [8, 20], Ouyang et al. [12, 14], Ouyang and Chang [3, 13], Chang et al. [17], Aardal et al. [21] and Tajbakhsh [25].

In this paper, we develop a continuous review inventory model with controllable lead time and setup cost. The lead-time-dependent cost is assumed to be a power function in the length of lead time, and the capital investment in setup cost reduction is assumed to follow a logarithmic expression. Moreover, the safety coefficient is treated as a decision variable. This disposition definitely leads to a more complex procedure of analyzing and deriving the optimal solution. In consideration of the difficulty in providing a precise estimation on the probability density function (p.d.f.) due to the insufficiency of historical data, we propose a distribution-free model according to the mean and the standard deviation of lead time demand. By constructing Lagrange function, we develop a solution procedure to determine ordering quantity, reorder point, length of lead time, and setup cost. Furthermore, we resolve a numerical example by using the proposed solution procedure and analyze the effects of the lower bound of service level.

The rest of this paper is organized as follows. In Section 2, we list the basic notations and assumptions used throughout this paper. In Section 3, the expression of total expected annual cost is firstly provided, and then a mathematical model of the concerned problem is proposed. In Section 4, an equivalent nonlinear programming formulation is derived. Moreover, a Lagrange function is constructed to obtain the optimal solution of the proposed model, and a solution algorithm is given. In Section 5, we resolve a numerical example by using the proposed solution algorithm. Through sensitivity analysis, some observations and managerial implications are presented. Finally, in Section 6, we summarize the whole paper and point out the next research work.

2. Notations and Assumptions

Before further development, we list the following notations which will be used throughout the paper.

q: ordering quantity, a decision variable.

k: safety coefficient, $k \geq 0$, a decision variable.

L: length of lead time, a decision variable.

A: setup cost, a decision variable.

X: lead time demand, a random variable.

d: demand rate per year.

f_X: probability density function of lead time demand.

$\sigma\sqrt{L}$: standard derivation of lead time demand.

r: reorder point.

A_0: original setup cost.

SL: service level.

β: lower bound of service level.

$R(L)$: lead-time-dependent cost.

$I(A)$: capital investment in setup cost reduction.

γ: fractional opportunity cost per unit capital per year.

h: holding cost per unit item per year.

EAC: total expected annual cost.

Moreover, the present problem is based on the following assumptions.

(1) Inventory is continuously monitored. Whenever the inventory level drops to a target value, an order is placed.

(2) The probability density function with regard to lead time demand is unknown.

(3) The service level is scaled by the fill rate which is defined as the fraction of demand satisfied from stock. Mathematically,

$$SL = 1 - \frac{E(X - r)^+}{q}. \tag{2.1}$$

in which $E(\cdot)$ is the mathematical expectation and $x^+ = \max(x, 0)$.

(4) The reorder point is determined by $r = dL + k\sigma\sqrt{L}$, in which $k\sigma\sqrt{L}$ denotes safety inventory.

(5) The lead-time-dependent cost follows a power function. Mathematically,

$$R(L) = aL^{-b}, \tag{2.2}$$

in which $a > 0$ and $b > 0$ are constants.

(6) The capital investment in setup cost reduction follows a logarithmic function. Mathematically,

$$I(A) = \frac{1}{\delta}\ln\left(\frac{A_0}{A}\right), \quad 0 < A \leq A_0, \tag{2.3}$$

in which $\delta > 0$ is a constant.

(7) As in Tajbakhsh [25], we assume that the lower bound of service level satisfies $1/2 < \beta < 1$. This value range is quite reasonable in application.

3. The Mathematical Model

Herein, we intend to provide a feasible solution scheme for the joint decision problem in continuous review inventory with a service level constraint. For the present problem, it is assumed that both lead time and setup cost can be reduced through capital expenditures. Hence, the decision variables contain not only ordering quantity and safety coefficient, but also length of lead time and setup cost.

Based on the previous description, the length of cycle is q/d, and the setup cost per cycle is A. In continuous review inventory system, an order with size q is placed when the inventory level drops to the reorder point r, and the order is received at the end of lead time. Thus, the inventory holding cost per year is $(h)/(2)\ [q + 2(r - dL)]$, in which dL denotes the mean of lead time demand.

Taking the capital expenditures related to the reductions of lead time and setup cost into account, we can formulate the expression of total expected annual cost as follows:

$$\mathrm{EAC}(q, r, A, L) = \frac{d}{q}\left(A + aL^{-b}\right) + \frac{h}{2}\left[q + 2(r - dL)\right] + \frac{\gamma}{\delta}\ln\left(\frac{A_0}{A}\right). \tag{3.1}$$

Generally speaking, the precise estimation of probability density function on lead time demand requires enough adequate data, which is difficult to realize in application. Therefore, in the development of the proposed model, we do not make any assumptions on the distribution function of lead time demand. Namely, we focused on the case when the specific distribution of lead time demand is unavailable.

Denote the collection of probability density function f_X with the mean dL and the standard derivation $\sigma\sqrt{L}$ by F. Assuming the manager is conservative and expects that the service level constraint holds for all possible probability distributions, we get

$$\underset{f_X \in F}{\text{minimize}}\left\{1 - \frac{E(X - r)^+}{q}\right\} \geq \beta. \tag{3.2}$$

The above disposition to service level constraint is in line with Tajbakhsh [25] and reflects robustness. Similar philosophy was widely adopted in the control of complex systems, such as Bausoa et al. [30], Dong et al. [31], Jaśkiewicz and Nowak [32] and

Hu et al. [33]. Furthermore, taking the total expected annual cost as objective function, we can establish the following programming model for the present problem:

$$\begin{aligned} \underset{q,r,A,L}{\text{minimize}} \quad & \mathrm{EAC}(q,r,A,L) \\ \text{subject to} \ \underset{f_X \in F}{\text{maximize}} \quad & E(X-r)^+ \le (1-\beta)q \\ & q \ge 0, \quad r \ge dL, \quad 0 < A \le A_0, \quad L > 0. \end{aligned} \tag{3.3}$$

4. Solution Procedure

To facilitate further exploration, we introduce the following proposition to eliminate the max operator in the service level constraint of model (3.3).

Proposition 4.1. *Given the mean dL and the standard derivation $\sigma\sqrt{L}$ of lead time demand X, then*

$$E(X-r)^+ \le \frac{\sigma\sqrt{L}\left(\sqrt{k^2+1}-k\right)}{2}. \tag{4.1}$$

Moreover, there is at least a p.d.f. which makes the equal sign in (4.1) *holds.*

Proposition 4.1 is similar to Lemma 1 in Gallego and Moon [34]. Therefore, we omit the proof procedure. In light of Proposition 4.1, and substituting the relation $r = dL + k\sigma\sqrt{L}$ into the objective function of model (3.3), we get an equivalent nonlinear programming model:

$$\begin{aligned} \underset{q,k,A,L}{\text{minimize}} \ \mathrm{EAC}(q,k,A,L) &= \frac{d}{q}\left(A + aL^{-b}\right) + \frac{h}{2}\left(q + 2k\sigma\sqrt{L}\right) + \frac{\gamma}{\delta}\ln\left(\frac{A_0}{A}\right) \\ \text{subject to } \sigma\sqrt{L}\left(\sqrt{k^2+1}-k\right) - 2(1-\beta)q &\le 0 \\ q \ge 0, \quad k \ge 0, \quad 0 < A \le A_0, \quad L > 0. \end{aligned} \tag{4.2}$$

To solve model (4.2), a Lagrange function is constructed as follows:

$$\begin{aligned} F(q,k,A,L,\lambda) = {} & \frac{d}{q}\left(A + aL^{-b}\right) + \frac{h}{2}\left(q + 2k\sigma\sqrt{L}\right) + \frac{\gamma}{\delta}\ln\left(\frac{A_0}{A}\right) \\ & + \lambda\left[\sigma\sqrt{L}\left(\sqrt{k^2+1}-k\right) - 2(1-\beta)q\right], \end{aligned} \tag{4.3}$$

in which $\lambda \ge 0$ is a Lagrange multiplier.

Then, with the first order optimality condition $\partial F(q,k,A,L,\lambda)/\partial k = 0$, we get

$$\lambda = \frac{h\sqrt{k^2+1}}{\sqrt{k^2+1}-k}. \tag{4.4}$$

From (4.4), we conclude that the Lagrange multiplier should satisfy $\lambda \geq h$. This relationship manifests that the service level constraint is never inactive. Thus, the optimal solution should satisfy the following equation:

$$\sigma\sqrt{L}\left(\sqrt{k^2+1}-k\right)-2(1-\beta)q=0. \tag{4.5}$$

Equivalently,

$$q=\frac{\sigma\sqrt{L}\left(\sqrt{k^2+1}-k\right)}{2(1-\beta)}. \tag{4.6}$$

Let $\partial F(q,k,A,L,\lambda)/\partial L=0$ and yield:

$$2abd-\sigma qL^{b+1/2}\left[hk+\lambda\left(\sqrt{k^2+1}-k\right)\right]=0. \tag{4.7}$$

Substituting (4.4) and (4.6) into (4.7), after some algebraic manipulation, we get

$$L_{1*}=\left[\frac{4abd(1-\beta)}{h\sigma^2}\right]^{1/(b+1)}. \tag{4.8}$$

Furthermore, by letting $\partial F(q,k,A,L,\lambda)/(\partial A)=0$, we obtain

$$q=\frac{\delta dA}{\gamma}. \tag{4.9}$$

Combining (4.4), (4.6), and (4.9), we have

$$\lambda=\frac{hL\sigma^2\gamma^2}{8\delta^2d^2A^2(1-\beta)^2}+\frac{h}{2}. \tag{4.10}$$

Then, let $\partial F(q,k,A,L,\lambda)/\partial q=0$ and get

$$2d\left(A+aL^{-b}\right)+q^2\left[4(1-\beta)\lambda-h\right]=0. \tag{4.11}$$

Then, with the length of lead time from (4.8), and substituting (4.9) and (4.10) into (4.11), we get the following quadratic equation with respect to setup cost A:

$$A^2-\frac{2\gamma^2A}{dh\delta^2(2\beta-1)}-\frac{\gamma^2\left[h\sigma^2L_{1*}^{b+1}+4ad(1-\beta)\right]}{2h\delta^2d^2L_{1*}^{b}(1-\beta)(2\beta-1)}=0. \tag{4.12}$$

Again, with the assumption $1/2 < \beta < 1$, it is obvious that the above equation has a unique positive root. Due to the complex formulation of (4.12), we do not write the analytical expression of its solution. However, with the given parameters, it is easy to resolve (4.12) and get the value of setup cost. For the convenience of description in the sequel, we denote the unique positive solution of (4.12) by A_{1*}.

With the resultant setup cost A_{1*} and the length of lead time L_{1*}, we can determine the corresponding ordering quantity q_{1*} and the Lagrange multiplier λ_{1*},respectively, by using (4.9) and (4.10). Namely, $q_{1*} = \delta d A_{1*}/\gamma$ and $\lambda_{1*} = hL\sigma^2\gamma^2 \ /8\delta^2 d^2 \ A^2{}_{1*} \ (1-\beta)^2 + h/2$.

Subsequently, the safety coefficient can be obtained by the following formula:

$$k_{1*} = \frac{\lambda_{1*} - h}{\sqrt{h(2\lambda_{1*} - h)}}. \tag{4.13}$$

Then, we need to examine whether the solution $(q_{1*}, k_{1*}, A_{1*}, L_{1*})$ is a minimum. Although it is difficult to verify that the nonlinear programming model (4.2) is convex, we can demonstrate that the Hessian of Lagrangian is positive definition at point $(q_{1*}, k_{1*}, A_{1*}, L_{1*}, \lambda_{1*})$. To this end, the Hessian matrix is written as follows:

$$H = \begin{bmatrix} \dfrac{\partial^2 F(q,k,A,L,\lambda)}{\partial q^2} & \dfrac{\partial^2 F(q,k,A,L,\lambda)}{\partial q \partial k} & \dfrac{\partial^2 F(q,k,A,L,\lambda)}{\partial q \partial A} & \dfrac{\partial^2 F(q,k,A,L,\lambda)}{\partial q \partial L} \\ \dfrac{\partial^2 F(q,k,A,L,\lambda)}{\partial k \partial q} & \dfrac{\partial^2 F(q,k,A,L,\lambda)}{\partial k^2} & \dfrac{\partial^2 F(q,k,A,L,\lambda)}{\partial k \partial A} & \dfrac{\partial^2 F(q,k,A,L,\lambda)}{\partial k \partial L} \\ \dfrac{\partial^2 F(q,k,A,L,\lambda)}{\partial A \partial q} & \dfrac{\partial^2 F(q,k,A,L,\lambda)}{\partial A \partial k} & \dfrac{\partial^2 F(q,k,A,L,\lambda)}{\partial A^2} & \dfrac{\partial^2 F(q,k,A,L,\lambda)}{\partial A \partial L} \\ \dfrac{\partial^2 F(q,k,A,L,\lambda)}{\partial L \partial q} & \dfrac{\partial^2 F(q,k,A,L,\lambda)}{\partial L \partial k} & \dfrac{\partial^2 F(q,k,A,L,\lambda)}{\partial L \partial A} & \dfrac{\partial^2 F(q,k,A,L,\lambda)}{\partial L^2} \end{bmatrix}. \tag{4.14}$$

Moreover,

$$\frac{\partial^2 F(q_{1*}, k_{1*}, A_{1*}, L_{1*}, \lambda_{1*})}{\partial q^2} = \frac{2d\left(a + A_{1*}L_{1*}^b\right)}{q_{1*}^3 L_{1*}^b}, \tag{4.15}$$

$$\frac{\partial^2 F(q_{1*}, k_{1*}, A_{1*}, L_{1*}, \lambda_{1*})}{\partial k^2} = \frac{\lambda\sigma\sqrt{L_{1*}}}{\left(k_{1*}^2 + 1\right)^{3/2}}, \tag{4.16}$$

$$\begin{aligned} \frac{\partial^2 F(q_{1*}, k_{1*}, A_{1*}, L_{1*}, \lambda_{1*})}{\partial A^2} &= \frac{\gamma}{\delta A_{1*}^2} \\ &= \frac{d}{q_{1*}A_{1*}}, \end{aligned} \tag{4.17}$$

$$\begin{aligned} \frac{\partial^2 F(q_{1*}, k_{1*}, A_{1*}, L_{1*}, \lambda_{1*})}{\partial L^2} &= \frac{abd(b+1)}{q_{1*}L_{1*}^{b+2}} + \frac{\sigma\left[hk_{1*} + \lambda\left(\sqrt{k_{1*}^2 + 1} - k_{1*}\right)\right]}{4L_{1*}^{3/2}} \\ &= \frac{abd(2b+3)}{2q_{1*}L_{1*}^{b+2}}, \end{aligned} \tag{4.18}$$

$$\begin{aligned}\frac{\partial^2 F(q_{1*}, k_{1*}, A_{1*}, L_{1*}, \lambda_{1*})}{\partial q \partial k} &= \frac{\partial^2 F(q_{1*}, k_{1*}, A_{1*}, L_{1*}, \lambda_{1*})}{\partial k \partial q} \\ &= \frac{\partial^2 F(q_{1*}, k_{1*}, A_{1*}, L_{1*}, \lambda_{1*})}{\partial k \partial A} \\ &= \frac{\partial^2 F(q_{1*}, k_{1*}, A_{1*}, L_{1*}, \lambda_{1*})}{\partial A \partial k} \\ &= \frac{\partial^2 F(q_{1*}, k_{1*}, A_{1*}, L_{1*}, \lambda_{1*})}{\partial A \partial L} \\ &= \frac{\partial^2 F(q_{1*}, k_{1*}, A_{1*}, L_{1*}, \lambda_{1*})}{\partial L \partial A} \\ &= 0,\end{aligned} \tag{4.19}$$

$$\begin{aligned}\frac{\partial^2 F(q_{1*}, k_{1*}, A_{1*}, L_{1*}, \lambda_{1*})}{\partial q \partial A} &= \frac{\partial^2 F(q_{1*}, k_{1*}, A_{1*}, L_{1*}, \lambda_{1*})}{\partial A \partial q} \\ &= -\frac{d}{q_{1*}^2},\end{aligned} \tag{4.20}$$

$$\begin{aligned}\frac{\partial^2 F(q_{1*}, k_{1*}, A_{1*}, L_{1*}, \lambda_{1*})}{\partial q \partial L} &= \frac{\partial^2 F(q_{1*}, k_{1*}, A_{1*}, L_{1*}, \lambda_{1*})}{\partial L \partial q} \\ &= \frac{abd}{q_{1*}^2 L_{1*}^{b+1}},\end{aligned} \tag{4.21}$$

$$\begin{aligned}\frac{\partial^2 F(q_{1*}, k_{1*}, A_{1*}, L_{1*}, \lambda_{1*})}{\partial k \partial L} &= \frac{\partial^2 F(q_{1*}, k_{1*}, A_{1*}, L_{1*}, \lambda_{1*})}{\partial L \partial k} \\ &= \frac{\sigma\left[(h-\lambda_{1*})\sqrt{k_{1*}^2+1}+\lambda_{1*}k_{1*}\right]}{2\sqrt{L_{1*}(k_{1*}^2+1)}} \\ &= 0.\end{aligned} \tag{4.22}$$

It is worth mentioning that the second equal sign in (4.17) is based on (4.9), the second equal sign in (4.18) is based on (4.4), (4.6) and (4.8), and the third equal sign in (4.22) is based on (4.4).

In light of (4.15)–(4.22), the first and second principal minor determinants of matrix H at point $(q_{1*}, k_{1*}, A_{1*}, L_{1*}, \lambda_{1*})$ are obviously positive, which are shown as follows:

$$\begin{aligned}|H_{11}| &= \frac{2d\left(a + A_{1*}L_{1*}^b\right)}{q_{1*}^3 L_{1*}^b} \\ &\geq 0,\end{aligned} \tag{4.23}$$

$$|H_{22}| = \frac{2\lambda\sigma d\left(a + A_{1*}L_{1*}^{b}\right)}{q_{1*}^{3}L_{1*}^{b-1/2}\left(k_{1*}^{2}+1\right)^{3/2}} \geq 0. \tag{4.24}$$

And the third principal minor determinant of H at point $(q_{1*}, k_{1*}, A_{1*}, L_{1*}, \lambda_{1*})$ is computed as follows:

$$\begin{aligned} |H_{33}| &= \frac{2\lambda\sigma d^{2}\left(a + A_{1*}L_{1*}^{b}\right)}{A_{1*}q_{1*}^{4}L_{1*}^{b-1/2}\left(k_{1*}^{2}+1\right)^{3/2}} - \frac{\lambda\sigma d^{2}\sqrt{L_{1*}}}{q_{1*}^{4}\left(k_{1*}^{2}+1\right)^{3/2}} \\ &= \frac{\lambda\sigma d^{2}\left(2a + A_{1*}L_{1*}^{b}\right)}{A_{1*}q_{1*}^{4}L_{1*}^{b-1/2}\left(k_{1*}^{2}+1\right)^{3/2}} \\ &\geq 0. \end{aligned} \tag{4.25}$$

In addition, the fourth principal minor determinant of Hessian matrix H at point $(q_{1*}, k_{1*}, A_{1*}, L_{1*}, \lambda_{1*})$ is computed as follows:

$$\begin{aligned} |H_{44}| &= \frac{\lambda\sigma abd^{3}(2b+3)\left(a + A_{1*}L_{1*}^{b}\right)}{A_{1*}q_{1*}^{5}L_{1*}^{2b+3/2}\left(k_{1*}^{2}+1\right)^{3/2}} - \frac{\lambda\sigma abd^{3}(2b+3)}{2q_{1*}^{5}L_{1*}^{b+3/2}\left(k_{1*}^{2}+1\right)^{3/2}} \\ &= \frac{\lambda\sigma abd^{3}(2b+3)\left(2a + A_{1*}L_{1*}^{b}\right)}{2A_{1*}q_{1*}^{5}L_{1*}^{2b+3/2}\left(k_{1*}^{2}+1\right)^{3/2}} \\ &\geq 0. \end{aligned} \tag{4.26}$$

Therefore, according to the second order sufficient conditions (SOSCs) [35], $(q_{1*}, k_{1*}, A_{1*}, L_{1*})$ is a minimum.

Notice that the interval and nonnegative constraints of model (4.2) are ignored while constructing Lagrange function (4.3). Thus, if the setup cost derived using (4.12) does not make the inequality $A_{1*} \leq A_0$ hold, we need to take the following special case into account, that is, $A_{2*} = A_0$.

For the case of $A_{2*} = A_0$, it means that, to minimize the total expected annual cost, the manager need not adopt any actions to reduce the setup cost. Thus, similar to the above

deduction procedure, we can achieve the length of lead time and the ordering quantity through the following equations:

$$L_{2*} = \left[\frac{4abd(1-\beta)}{h\sigma^2}\right]^{1/(b+1)},$$
$$q_{2*} = \sqrt{\frac{4d(1-\beta)\left(a + A_{2*}L_{2*}^b\right) + h\sigma^2 L_{2*}^{b+1}}{2(1-\beta)(2\beta-1)hL_{2*}^b}}. \tag{4.27}$$

Then, the Lagrange multiplier is

$$\lambda_{2*} = \frac{h}{4(1-\beta)} - \frac{d\left(a + A_{2*}L_{2*}^b\right)}{2(1-\beta)q_{2*}^2 L_{2*}^b}. \tag{4.28}$$

Accordingly, the safety coefficient is

$$k_{2*} = \frac{\lambda_{2*} - h}{\sqrt{h(2\lambda_{2*} - h)}}. \tag{4.29}$$

In accordance with Aardal et al. [21], we confine the present discussion to the service level which yields $k > 0$. Actually, with a similar computational procedure, it is easy to determine the optimal values of ordering quantity, length of lead time, and setup cost for the case of $k = 0$. To keep compact, we do not provide the details.

According to the above analysis procedure, the solution algorithm for the proposed model is summarized as follows.

Step 1. Determine the values of L_{1*} and A_{1*}, respectively, by using (4.8) and (4.12).

Step 2. If $A_{1*} > A_0$, go to Step 3. Otherwise, determine the values of q_{1*}, λ_{1*}, and k_{1*}, respectively, by using (4.9), (4.10), and (4.13). Let $q^* = q_{1*}$, $k^* = k_{1*}$, $A^* = A_{1*}$, $L^* = L_{1*}$. Go to Step 4.

Step 3. Set $A_{2*} = A_0$ and determine the values of L_{2*} and q_{2*} by using (4.27) and (4.28). Then, determine the values of λ_{2*} and k_{2*}, respectively, by using (4.28) and (4.29). Let $q^* = q_{2*}$, $k^* = k_{2*}$, $A^* = A_{2*}$, $L^* = L_{2*}$.

Step 4. End.

5. Numerical Example

In this section, a numerical example is utilized to demonstrate the feasibility of the proposed solution procedure. Moreover, we will vary the lower bound of service level to perform

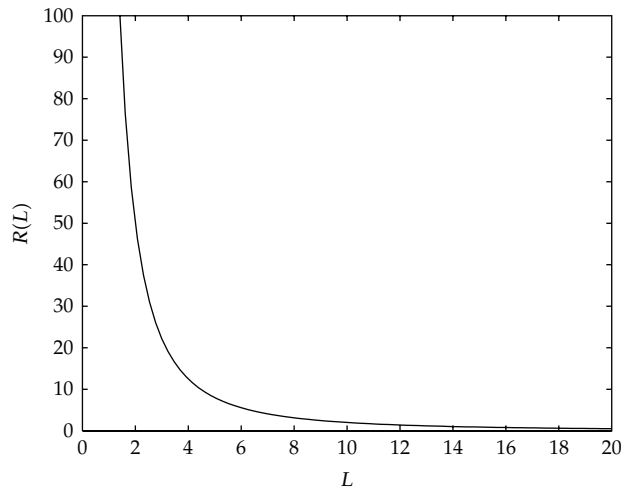

Figure 1: The lead-time-dependent cost.

sensitivity analysis and give some observations and managerial implications. The basic parameters are as follows:

$\beta = 0.975$,

$\gamma = 0.1/\text{dollar}/\text{year}$,

$d = 700$ units/year,

$\sigma = 15$ units/week,

$h = \$25/\text{year}/\text{unit}$,

$A_0 = \$300/\text{order}$.

The function expression of lead-time-dependent cost is $R(L) = 1000L^{-3}$ with $a = 1000$ and $b = 3$. Moreover, the function expression of capital investment in setup cost reduction is $I(A) = 10000\ln(300/A)$ with $\delta = 0.0001$. The curves of two capital investment functions are, respectively, depicted in Figures 1 and 2.

With the aforementioned data and function expressions, and using the proposed method, we can calculate the ordering quantity $q^* = 115.59$ units, the safety coefficient $k^* = 0.7293$, the length of lead time $L^* = 28.14$ days and the setup cost $A^* = 165.13$ dollars. Thus, the reorder point $r^* = 62.27$ units, the lead-time-dependent cost $R^*(L) = 15.39$ dollars, the capital investment in setup cost reduction $I^*(A) = 5970.3$ dollars, and the total expected annual cost $\text{EAC}^* = 3342.4$ dollars.

Next, we vary the value of β from 0.96 to 0.99 with equal interval 0.1 to perform sensitivity analysis. The computational results are shown in Table 1.

From the data in Table 1, several observations and managerial implications are made as follows:

(1) When the value of β is varied from 0.96 to 0.99, the ordering quantity and the safety coefficient increase while the reorder point decreases. Moreover, compared with the ordering quantity and the reorder point, the change in the safety coefficient is great. This phenomenon implies that the change in lower bound of service level has

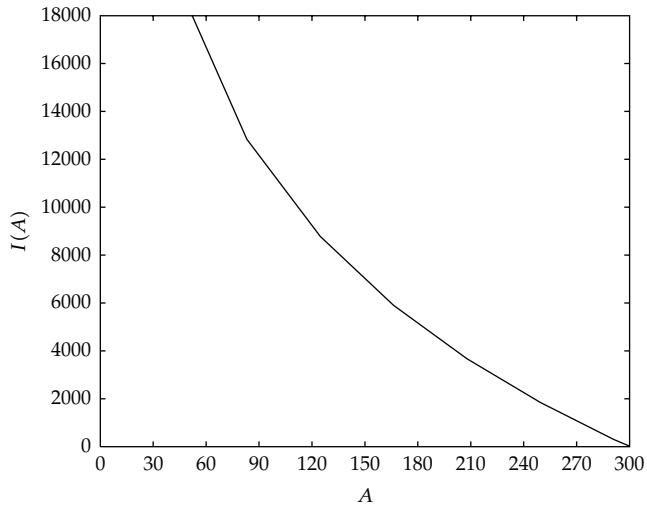

Figure 2: The capital investment function in setup cost reduction.

Table 1: Effect of change in parameter β.

β	*0.96*	*0.97*	*0.98*	*0.99*
q^*	110.74	113.32	119.00	133.86
k^*	0.3131	0.5629	0.9460	1.7613
r^*	64.48	63.04	61.51	60.78
L^*	31.65	29.46	26.62	22.38
A^*	158.19	161.89	170.00	191.23
$R^*(L)$	10.81	13.42	18.19	30.59
$I^*(A)$	6399.7	6168.6	5680.1	4502.9
EAC^*	3186.9	3280.0	3423.9	3729.9

a greater impact on the safety coefficient and the reorder point than the ordering quantity.

(2) We observe that a larger value of β yields a shorter lead time, a higher lead-time-dependent cost. This phenomenon indicates that the short lead time is favorable to the service level. Moreover, we also observe that a larger value of β leads to a higher setup cost and a smaller value of capital investment in setup cost reduction.

(3) As the value of β increases, the total expected annual cost also increases. It seems that a lower service level benefits manager in profit. However, the lower service will produce negative influences on brand and customer loyalty which are crucial to building competitive advantage in market. From this perspective, the manager should determine a proper lower bound of service level which can balance short-term income and long-term development.

6. Conclusions and Future Work

Considering the difficulty in measuring shortage cost, we proposed a distribution-free continuous review inventory model in the presence of a service level constraint. In our model,

the lead-time-dependent cost is assumed to be a power function in the length of lead time, and the capital investment in setup cost reduction is assumed to be a logarithmic function in setup cost. The proposed model guarantees that the service level constraint can be satisfied at the worst case and takes ordering quantity, safety coefficient, length of lead time and setup cost as decision variables. In the present research, we also discuss the optimal solution of the proposed model and develop an effective solution procedure. Moreover, the results contained in this research are illustrated and verified by a numerical example.

In the future research, we may take other forms of investment function into consideration. Besides, we will conduct some relevant research to extend the present model from many perspectives, such as imperfect quality, uncertain yield and so on, to develop some novel models and design the corresponding solution algorithms. Another feasible extension of the present research is to develop the inventory model and the associated solution algorithm by considering the interacted effect of capital investment in the reductions of lead time and setup cost. Additionally, in the research regarding continuous review inventory problems, the safety coefficient is usually assumed to be nonnegative. However, for some replenishment problems with short lead time and large ordering batch caused by high setup cost and low inventory holding cost, it may be economic to set a negative safety coefficient. For the negative safety coefficient, a different expression of inventory holding cost should be adopted, such as in Klouja and Antonis [36]. Therefore, it is also meaningful to relax the nonnegative assumption in safety coefficient and perform some extension on the results contained in this research.

Acknowledgments

The authors would like to express their sincere thanks to the editor and the anonymous reviewers for their valuable comments to this paper. This work was partially support by the National Natural Science Foundation of China (71071113), the Ph.D. Programs Foundation of Higher Education of China (20100072110011), the Foundation for the Author of National Excellent Doctoral Dissertation of PR China (200782), the Shanghai Pujiang Program, the Shanghai Philosophical and Social Science Program (2010BZH003), and the Fundamental Research Funds for the Central Universities.

References

[1] C. J. Liao and C. H. Shyu, "An analytical determination of lead time with normal demand," *International Journal of Operations and Production Management*, vol. 11, no. 9, pp. 72–78, 1991.

[2] M. Hariga and M. Ben-Daya, "Some stochastic inventory models with deterministic variable lead time," *European Journal of Operational Research*, vol. 113, no. 1, pp. 42–51, 1999.

[3] L. Y. Ouyang and B. R. Chuang, "Mixture inventory model involving variable lead time and controllable backorder rate," *Computers and Industrial Engineering*, vol. 40, no. 4, pp. 339–348, 2001.

[4] K. S. Wu and L. Y. Ouyang, "(Q,r,L) Inventory model with defective items," *Computers and Industrial Engineering*, vol. 39, no. 1-2, pp. 173–185, 2001.

[5] G. Yang, R. J. Ronald, and P. Chu, "Inventory models with variable lead time and present value," *European Journal of Operational Research*, vol. 164, no. 2, pp. 358–366, 2005.

[6] W.-C. Lee, "Inventory model involving controllable backorder rate and variable lead time demand with the mixtures of distribution," *Applied Mathematics and Computation*, vol. 160, no. 3, pp. 701–717, 2005.

[7] M. A. Hoque and S. K. Goyal, "An alternative simple solution algorithm of an inventory model with fixed and variable lead time crash costs under unknown demand distribution," *International Journal of Systems Science*, vol. 40, no. 8, pp. 821–827, 2009.

[8] K. Annadurai and R. Uthayakumar, "Reducing lost-sales rate in (T, R, L) inventory model with controllable lead time," *Applied Mathematical Modelling*, vol. 34, no. 11, pp. 3465–3477, 2010.
[9] M. Ben-Daya and A. Raouf, "Inventory models involving lead time as a decision variable," *Journal of the Operational Research Society*, vol. 45, no. 5, pp. 579–582, 1994.
[10] J.-W. Wu, W.-C. Lee, and H.-Y. Tsai, "Computational algorithmic procedure of optimal inventory policy involving a negative exponential crashing cost and variable lead time demand," *Applied Mathematics and Computation*, vol. 184, no. 2, pp. 798–808, 2007.
[11] M.-F. Yang, "Supply chain integrated inventory model with present value and dependent crashing cost is polynomial," *Mathematical and Computer Modelling*, vol. 51, no. 5-6, pp. 802–809, 2010.
[12] L. Y. Ouyang, C. K. Chen, and H. C. Chang, "Lead time and ordering cost reductions in continuous review inventory systems with partial backorders," *Journal of the Operational Research Society*, vol. 50, no. 12, pp. 1272–1279, 1999.
[13] L.-Y. Ouyang and H.-C. Chang, "Lot size reorder point inventory model with controllable lead time and set-up cost," *International Journal of Systems Science*, vol. 33, no. 8, pp. 635–642, 2002.
[14] L. Y. Ouyang, C. K. Chen, and H. C. Chang, "Quality improvement, setup cost and lead-time reductions in lot size reorder point models with an imperfect production process," *Computers and Operations Research*, vol. 29, no. 12, pp. 1701–1717, 2002.
[15] B. R. Chuang, L. Y. Ouyang, and K. W. Chuang, "A note on periodic review inventory model with controllable setup cost and lead time," *Computers and Operations Research*, vol. 31, no. 4, pp. 549–561, 2004.
[16] K. S. Wu and I. C. Lin, "Extend (r, Q) inventory model under lead time and ordering cost reductions when the receiving quantity is different from the ordered quantity," *Quality & Quantity*, vol. 38, no. 6, pp. 771–786, 2004.
[17] H.-C. Chang, L.-Y. Ouyang, K.-S. Wu, and C.-H. Ho, "Integrated vendor-buyer cooperative inventory models with controllable lead time and ordering cost reduction," *European Journal of Operational Research*, vol. 170, no. 2, pp. 481–495, 2006.
[18] W.-C. Lee, J.-W. Wu, and C.-L. Lei, "Computational algorithmic procedure for optimal inventory policy involving ordering cost reduction and back-order discounts when lead time demand is controllable," *Applied Mathematics and Computation*, vol. 189, no. 1, pp. 186–200, 2007.
[19] R. Uthayakumar and P. Parvathi, "A continuous review inventory model with controllable backorder rate and investments," *International Journal of Systems Science*, vol. 40, no. 3, pp. 245–254, 2009.
[20] K. Annadurai and R. Uthayakumar, "Controlling setup cost in (Q, r, L) inventory model with defective items," *Applied Mathematical Modelling*, vol. 34, no. 6, pp. 1418–1427, 2010.
[21] K. Aardal, O. Jonsson, and H. Jonsson, "Optimal inventory policies with service-level constraints," *The Journal of the Operational Research Society*, vol. 40, no. 1, pp. 65–73, 1989.
[22] L.-Y. Ouyang and K.-S. Wu, "Mixture inventory model involving variable lead time with a service level constraint," *Computers & Operations Research*, vol. 24, no. 9, pp. 875–882, 1997.
[23] W.-C. Lee, J.-W. Wu, and J.-W. Hsu, "Computational algorithm for inventory model with a service level constraint, lead time demand with the mixture of distributions and controllable negative exponential backorder rate," *Applied Mathematics and Computation*, vol. 175, no. 2, pp. 1125–1138, 2006.
[24] J. K. Jha and K. Shanker, "Two-echelon supply chain inventory model with controllable lead time and service level constraint," *Computers and Industrial Engineering*, vol. 57, no. 3, pp. 1096–1104, 2009.
[25] M. M. Tajbakhsh, "On the distribution free continuous-review inventory model with a service level constraint," *Computers and Industrial Engineering*, vol. 59, no. 4, pp. 1022–1024, 2010.
[26] S.-L. Hsu and Y.-F. Huang, "An integrated inventory model with controllable lead time and distribution-free demand," *Applied Stochastic Models in Business and Industry*, vol. 26, no. 4, pp. 416–430, 2010.
[27] K. Annadurai and R. Uthayakumar, "Ordering cost reduction in probabilistic inventory model with controllable lead time and a service level," *International Journal of Management Science and Engineering Management*, vol. 5, no. 6, pp. 403–410, 2010.
[28] C. K. Jaggi and N. Arneja, "Periodic inventory model with reduced setup cost under service level constraint," *Electronic Journal of Applied Statistical Analysis*, vol. 4, no. 2, pp. 111–123, 2011.
[29] H. J. Lin, "Effective investment to reduce setup cost in a mixture inventory model involving controllable backorder rate and variable lead time with a service level constraint," *Mathematical Problems in Engineering*, vol. 2012, Article ID 689061, 15 pages, 2012.
[30] D. Bauso, F. Blanchini, and R. Pesenti, "Robust control strategies for multi-inventory systems with average flow constraints," *Automatica*, vol. 42, no. 8, pp. 1255–1266, 2006.

[31] H. Dong, Z. Wang, D. W. C. Ho, and H. Gao, "Robust H∞ fuzzy output-feedback control with multiple probabilistic delays and multiple missing measurements," *IEEE Transactions on Fuzzy Systems*, vol. 18, no. 4, pp. 712–725, 2010.

[32] A. Jaśkiewicz and A. S. Nowak, "Stochastic games with unbounded payoffs: applications to robust control in economics," *Dynamic Games and Applications*, vol. 1, no. 2, pp. 253–279, 2011.

[33] J. Hu, Z. Wang, H. Gao, and L. K. Stergioulas, "Robust sliding mode control for discrete stochastic systems with mixed time delays, randomly occurring uncertainties, and randomly occurring nonlinearities," *IEEE Transactions on Industrial Electronics*, vol. 59, no. 7, pp. 3008–3015, 2012.

[34] G. Gallego and I. Moon, "Distribution free newsboy problem: review and extensions," *Journal of the Operational Research Society*, vol. 44, no. 8, pp. 825–834, 1993.

[35] D. P. Bertsekas, *Nonlinear Programming*, Athena Scientific, Belmont, Mass, USA, 1995.

[36] M. Khouja and A. C. Stylianou, "A (Q, R) inventory model with a drop-shipping option for e-business," *Omega*, vol. 37, no. 4, pp. 896–908, 2009.

Hindawi Publishing Corporation
Mathematical Problems in Engineering
Volume 2012, Article ID 296701, 13 pages
doi:10.1155/2012/296701

Research Article

D-Optimal Design for Parameter Estimation in Discrete-Time Nonlinear Dynamic Systems

Yu Liu,[1] Hamid Reza Karimi,[2] and Zhiwei Yu[1]

[1] *The Control Science and Engineering Department, Harbin Institute of Technology, Harbin 150001, China*
[2] *The Department of Engineering, Faculty of Engineering and Science, University of Agder, 4898 Grimstad, Norway*

Correspondence should be addressed to Yu Liu, liu_hit@126.com

Received 21 June 2012; Accepted 7 August 2012

Academic Editor: Bo Shen

An optimal input design method for parameter estimation in a discrete-time nonlinear system is presented in the paper to improve the observability and identification precision of model parameters. Determinant of the information matrix is used as the criterion function which is generally a nonconvex function about the input signals to be designed. To avoid the locally optimizing problem, a randomized design method is proposed by which a globally optimizing test plan other than input signals may be obtained. Then the randomized design can be approximated by a nonrandomized design about optimal inputs. An iterative algorithm integrated with dynamic programming is given and verified by a numerical example on experimental design for self-calibration tests of ISP system.

1. Introduction

Model parameters applied to computation or compensation in science and engineering, such as error model coefficients in INS (inertial navigation system), generally require much higher identification precision than in other applications. However, haphazard experiments not only lead to poor accuracy in parameter estimating, but also would make some parameters unobservable. A good experimental design can increase both the precision and the efficiency of a test [1] and then improve the precision of system identification or state estimation [2–5].

The field of system identification and filtering are relatively mature [6–10]; relevant experimental design methods have not made substantial advance yet. D-optimal design which allocates the experimental input variables by maximizing the determinant of information matrix of the system is recognized as the most effective method for an experimental design [11, 12]. For model parameter identification of a dynamic system, the

D-optimal design problem has a similar mathematical expression as the optimal control problem, but cannot be solved by the Pontryagin's maximum principle and dynamic programming method, due to particularity in the form of performance index [13].

On the other hand, even for a dynamic system with linear or low-order nonlinear model, the D-optimal design problems may involve global optimizing of nonconvex function and cannot achieve analytical solutions by traditional nonlinear programming methods. Although many numerical searching algorithms have been proposed to solve the nonconvex problem in global optimizing, such as genetic algorithm, simulated annealing algorithm, and so forth, most of them are either time-consuming or no guarantee of global optimization of searching results [14–16].

D-optimal design for randomized inputs is a convex optimization technique, in which the experimental variables are transformed to test plans. A test plan specifies different probability measures to each input variable in admissible set and one selects inputs for a particular trial of the experiment via randomization. The randomized design method is mainly used in regression design problems. Mehra introduces the method to optimal input design for parameter identification in a discrete-time MIMO linear system with process noise [11].

Morelli and Klein consider input design problem for LTI systems in aircraft flight tests, and the specific goals with test time optimization are achieved using principles of dynamic programming [17]. Neto et al. generalize the results to nonlinear dynamic systems and consider additive colored noises in measurement [18]. The cost function selected by Neto et al. is the trace of a dispersion matrix in which the autocorrelation matrix of the colored measurement noises is introduced. They solve the optimization problem by genetic algorithm.

Lintereur studies optimal trajectories for a 2-axis gimbaled test table by which errors in inertial systems caused by angular motion are calibrated [19]. The trace of covariance matrix computed by Kalman filtering is minimized using a conjugate gradient algorithm, but local minimum may be obtained.

In this paper, we propose a randomized design method for parameter estimation in discrete-time nonlinear dynamic systems with constraints on inputs. By this design method, the original nonconvex optimization problem can be solved by the convex optimization technique, and the global optimal maximum is guaranteed. An iterative algorithm is given and verified by a numerical example on experimental design for continuous tumbling self-calibration tests of ISP system.

2. Problem Statement

In this section we give a mathematical formulation of the D-optimal design problem, in which a time-varying MIMO nonlinear system with unknown model parameters is considered. For simplification in notation and deduction, the process noise is assumed to be zero here.

Consider the following nonlinear dynamic system:

$$\begin{aligned} x_{k+1} &= f(x_k, u_k, k, \theta), \quad x_0 = \overline{x}_0, \\ y_k &= h(x_k, t_k, \theta) + v_k, \quad k = 0, 1, \ldots, N, \end{aligned} \tag{2.1}$$

where $x_k = x(t_k)$ is a $n \times 1$ state vector, $\overline{x}_0$ is a constant vector, $u_k = u(t_k)$ is a $q \times 1$ input vector, $y_k = y(t_k)$ is a $p \times 1$ sampling output vector at moment k, and $v_k = v(t_k)$ is a $p \times 1$ measurement noise vector. v_k is the Gaussian white noise sequences with $E(v_k) = 0$ and $E(v_k v_\tau^T) = R_k \delta_{k,\tau}$, N is the number of output samples observed and is fixed. $\theta = [\theta_1\ \theta_2 \cdots \theta_m]^T$ denotes the $m \times 1$ vector of constant identifiable parameters, we estimate θ from the knowledge of $\{y_k, u_{k-1}, k = 1, \ldots, N\}$ and give an unbiased efficient estimator $\widehat{\theta}$ with covariance M^{-1}, where M is the Fisher information matrix. Therefore, the design problem is to select a series of inputs $u_k \in \Omega_u$ such that a suitable criterion function corresponding to the objectives of the identification experiment is optimized.

The Fisher information matrix is defined as follows:

$$M = \underset{\theta,Y}{E}\left[\left(\frac{\partial \log p(Y,\theta)}{\partial \theta}\right)\left(\frac{\partial \log p(Y,\theta)}{\partial \theta}\right)^T\right], \tag{2.2}$$

where Y denotes the set of observations $\{y_k,\ k = 1, \ldots, N\}$ and the expectation in (2.2) is taken over the sample space Ω_Y of observations and the parameter space Ω_θ of θ.

Using conditional expectations, M may be evaluated in two steps, first by computing $M'(\theta) = E_{Y|\theta}\{\bullet\}$ and then $M = E_\theta M'(\theta)$. The second step is generally more tedious and an *a priori* distribution $p(\theta)$ should be known exactly. Here a Taylor-series approximation is used to simplify the computation:

$$\begin{aligned} M'_{i,j}(\theta) = M'_{i,j}(\theta_0) &+ \left.\frac{\partial M'_{i,j}}{\partial \theta}\right|_{\theta_0}(\theta - \theta_0) \\ &+ \frac{1}{2}(\theta - \theta_0)^T \left.\frac{\partial^2 M'_{i,j}}{\partial \theta^2}\right|_{\theta_0}(\theta - \theta_0) + \cdots, \end{aligned} \tag{2.3}$$

where θ_0 is the *a priori* mean of $\theta, i, j = 1, \ldots, m$.

Retaining terms up to second order,

$$M_{i,j} = M'_{i,j}(\theta_0) + \frac{1}{2}\operatorname{tr}\left[\left.\frac{\partial^2 M'_{i,j}}{\partial \theta^2}\right|_{\theta_0} P_0\right], \tag{2.4}$$

where P_0 is the *a priori* covariance of θ.

The second term is typically small compared to the first term either because P_0 is small or $M'(\theta)$ is insensitive to θ.

The conditional likelihood function $L(\theta) = \log p(Y \mid \theta)$ for system (2.1) is given as follows:

$$L(\theta) = -\frac{Np}{2}\log(2\pi) - \frac{1}{2}\sum_{k=1}^{N}\left\{(v_k)^T R_k^{-1} v_k + \log|R_k|\right\}. \tag{2.5}$$

The matrix $M'(\theta)$ has elements

$$\begin{aligned} M'_{i,j}(\theta) &= E_Y\left(\frac{\partial L(\theta)}{\partial \theta_i}\frac{\partial L(\theta)}{\partial \theta_j}\right) \\ &= \sum_{K=1}^{N}\left\{\left(\frac{\partial h(x_k,t_k,\theta)}{\partial \theta_i}\right)^T R_k^{-1}\frac{\partial h(x_k,t_k,\theta)}{\partial \theta_j}\right\}. \end{aligned} \tag{2.6}$$

The sensitivity function is

$$\frac{\partial h(x_k,t_k,\theta)}{\partial \theta_i} = \frac{\partial h}{\partial x_k^T}x_{\theta_i,k} + \frac{\partial h}{\partial \theta_i}, \tag{2.7}$$

where $x_{\theta_i,k}$ is the partial derivative of $x(t)$ about θ_i at moment k, that is, $x_{\theta_i,k} = x_{\theta_i}(t_k)$ which meets the following equation:

$$x_{\theta_i,k+1} = \frac{\partial f}{\partial x_k^T}x_{\theta_i,k} + \frac{\partial f}{\partial \theta_i}, \quad x_{\theta_i,0} = 0,\ i = 1,\ldots,m. \tag{2.8}$$

Since $x_{\theta_i,k}$ and x_k all depend on the elements of U, where $U^{\mathrm{T}} = [u_0^T \cdots u_{N-1}^T] \in \Omega_U$ is the Nq-dimensional vector to be designed, we denote $M'(\theta)$ as $M'(\theta,U)$.

From (2.6), it is easy to get

$$M'(\theta,U) = \sum_{k=1}^{N}\left\{\left(\frac{\partial h(x_k,t_k,\theta)}{\partial \theta}\right)^T R_k^{-1}\frac{\partial h(x_k,t_k,\theta)}{\partial \theta}\right\}. \tag{2.9}$$

Also from (2.4), the Fisher information matrix is generally

$$M(U) = E_\theta M'(\theta,U) \approx M'(\theta_0,U). \tag{2.10}$$

There are many formulations of criterion function that measures the degree of observability about parameter θ, such as $\mathrm{tr}(M^{-1}(U))$ or $|M^{-1}(U)|$. A design which minimizes the scalar measure $|M^{-1}(U)|$ or maximizes $|M(U)|$ is called D-optimal, and it is equivalent to minimizing the volume of the uncertainty ellipsoid about parameter estimators. An important advantage of D-optimality is that it is invariant under scale changes in the parameters and linear transformations of the output.

Now, we choose $|M^{-1}(U)|$ as the criterion function and formulate the D-optimal design problem as follows:

$$\begin{aligned} &\min_{U\in\Omega_U}\left|M^{-1}(U)\right| \\ &\text{s.t.}\quad x_{k+1} = f(x_k,u_k,k,\theta), \quad x_0 = \overline{x}_0 \\ &\qquad x_{\theta_i,k+1} = \frac{\partial f}{\partial x_k^T}x_{\theta_i,k} + \frac{\partial f}{\partial \theta_i}, \quad x_{\theta_i,0} = 0,\ i = 1,\ldots,m. \end{aligned} \tag{2.11}$$

It should be pointed out that the problem in (2.11) cannot be solved by typical methods such as the Pontryagin's maximum principle and dynamic programming method since $|M^{-1}(U)|$ or $\mathrm{tr}(M^{-1}(U))$ cannot be transformed to the index form in multistage decision process. In fact, there also exists great difficulty in getting a numerical solution with global optimization since $|M^{-1}(U)|$ is not a convex function of U.

In the next section, we will present a randomized design method based on test plan theories.

3. D-Optimal Design Method

For a randomized input $U \in \Omega_U$ with probability measure $\xi(dU)$defined for all Borel sets and points of Ω_U, the definition of the information matrix is

$$M(\xi) = \int_{\Omega_U} M(U) \cdot \xi(dU), \tag{3.1}$$

where $\int_{\Omega_U} \xi(dU) = 1$.

If the probability measure is purely discrete, the information matrix is defined as follows:

$$M(\xi) = \sum_{i=1}^{l} \xi_i M(U_i), \tag{3.2}$$

where l is the number of spectrums, $\sum_{i=1}^{l} \xi_i = 1$, $0 \le \xi_i \le 1$.

$M(\xi)$ is linear in ξ, so the criteria $|M^{-1}(\xi)|$ or $\mathrm{tr}(M^{-1}(\xi))$ are convex functions of ξ, and optimization with respect to ξ gives globally optimizing design. However, we cannot find directly the optimal design ξ^* which minimizes $|M^{-1}(\xi)|$. Here, an iterative algorithm is proposed for searching ξ^* based on the following theorem [11].

Theorem 3.1. *Let ξ^* be the optimal design then the following are equivalent:*

(i) ξ^* *maximizes* $|M(\xi)|$,

(ii) ξ^* *minimizes* $\max_{U\in\Omega_U} \mathrm{tr}(M^{-1}(\xi)M(U))$,

(iii) $\max_{U\in\Omega_U} \mathrm{tr}(M^{-1}(\xi^*)M(U)) = \mathrm{tr}(M^{-1}(\xi^*)M(\xi^*)) = m$.

The D-optimal design ξ^* may be computed with the following algorithm.

Algorithm 3.2. Step 1. Start with any design ξ_0 such that $M(\xi_0)$ is nonsingular and let k=0.

Step 2. Compute $M(\xi_k)$ and $\mathrm{tr}(M^{-1}(\xi_k)M(U))$ using (2.1), (2.6)–(2.10).

Step 3. Maximize $\mathrm{tr}(M^{-1}(\xi_k)M(U))$ over $U \in \Omega_U$ and get U_k.

Step 4. If $\mathrm{tr}(M^{-1}(\xi_k)M(U_k)) = m$, stop. Otherwise, let $\xi_{k+1} = (1-\alpha_k)\xi_k + \alpha_k\xi(U_k)$, $0 < \alpha_k \le 1$ where $\xi(U_k)$ is the design at the single point U_k.

Choose α_k such that $\sum_{k=0}^{\infty} \alpha_k = \infty$, $\lim_{k\to\infty}\alpha_k = 0$, $|M(\xi_{k+1})| \ge |M(\xi_k)|$.

Step 5. Set $k = k+1$ and go to step 2.

The convergence of the above algorithm to the global maximum is proved in the appendix.

Remarks. (1) The optimal design can be depicted by the following set:

$$\{\xi_1, U_1; \xi_2, U_2; \ldots; \xi_l, U_l\}, \quad l \leq m\frac{(m+1)}{2}. \tag{3.3}$$

This can be used in a manner of randomized strategies when the experiment can be repeated. If the experiment is to be conducted only once, a nonrandomized design involving only one input U should be preferable, that is, it assigns probability one to a particular U. Since the randomized design (3.3) has been derived, we can seek nonrandomized design U^* so that $|M(U^*)|$ approximates $|\sum_{i=1}^{l} \xi_i M(U_i)|$.

(2) Step 3 is most time-consuming computationally, and the criterion function $\operatorname{tr}(M^{-1}(\xi)M(U))$ is generally not a convex function of U. Only if model (2.1) can be reduced to a linear discrete-time system, it would be a quadratic functional of U. Using (2.9) and (2.10), we get

$$\begin{aligned}\operatorname{tr}\left(M^{-1}(\xi)M(U)\right) &\approx \operatorname{tr}\left(M^{-1}(\xi)M'(\theta_0, U)\right)\\ &= \sum_{k=1}^{N} \operatorname{tr}\left\{M^{-1}(\xi)\left(\frac{\partial h(x_k, t_k, \theta)}{\partial \theta}\bigg|_{\theta_0}\right)^T R_k^{-1} \frac{\partial h(x_k, t_k, \theta)}{\partial \theta}\bigg|_{\theta_0}\right\}.\end{aligned} \tag{3.4}$$

Unlike the computing of determinant, the operations with trace and sum of matrix can exchange order. By (3.4), the optimization problem can be solved by using maximum principle or dynamic programming methods since the above equation possesses the form of criterion function in multistage decision process.

Therefore, by using randomization and Theorem 3.1 the solution to a highly nonlinear and nonconvex optimization problem, that is, minimization of $|M^{-1}(U)|$ is reduced to solving a relatively simpler optimization problem. This is mainly due to the fact that randomization produces convexity.

4. Simulation

In this section, we present a numerical example to verify the effectiveness of the proposed design method. The experiment to be designed is the continuous tumbling self-calibration test of an ISP system. Choose the determinant of information matrix as observability index and select the currents of gyro torquers or the command angular speed to the ISP as the experimental input variables, then the idea of D-optimal design can be applied to program the rotational trajectories of platform which represent the attitude and angular speed of platform at each moment.

First, we give the model equations of accelerometers and gyroscopes in the ISP system. The output equations of accelerometers that are also the observation equations are:

$$\mathbf{y} = \begin{bmatrix} 0 & A_z & -A_y \\ -A_z & 0 & A_x \\ A_y & -A_x & 0 \end{bmatrix} \begin{bmatrix} \varphi_x \\ \varphi_y \\ \varphi_z \end{bmatrix} + \begin{bmatrix} k_{0x} + k_{1x}A_x \\ k_{0y} + k_{1y}A_y - \alpha_z A_x \\ k_{0z} + k_{1z}A_z + \alpha_y A_x - \alpha_x A_y \end{bmatrix} + \varepsilon, \tag{4.1}$$

where $\alpha_x, \alpha_y, \alpha_z$ represent the misalignment angles of accelerometers' input axes with respect to platform frame.

k_{0x}, k_{0y}, k_{0z} and k_{1x}, k_{1y}, k_{1z} represent the bias and scale factors of accelerometers.

y represents outputs of accelerometers; ε denotes the observation noises in outputs with zero mean and covariance matrix $\delta_y^2 I_{3\times 3}$ at each moment.

A_x, A_y, A_z are projections of gravitational acceleration on the ideal platform frame which is defined based on x accelerometer's input axis and initially aligned to north, west, vertical direction, unit g_0, where g_0 is the local gravitational acceleration value:

$$\begin{bmatrix} A_x \\ A_y \\ A_z \end{bmatrix} = \begin{bmatrix} \sin(a)\sin(c) - \cos(a)\sin(b)\cos(c) \\ \sin(a)\cos(c) + \cos(a)\sin(b)\sin(c) \\ \cos(a)\cos(b) \end{bmatrix}, \tag{4.2}$$

where a, b, c represent three ideal angular positions of platform gimbals from outer to inner, respectively, and meet the following differential equations:

$$\begin{aligned} \begin{bmatrix} \dot{a} \\ \dot{b} \\ \dot{c} \end{bmatrix} &= \begin{bmatrix} -\cos(a)\tan(b) & \cos(b) & \sin(a)\tan(b) \\ \sin(a) & 0 & \cos(a) \\ \cos(a)\sec(b) & 0 & -\sin(a)\sec(b) \end{bmatrix} \begin{bmatrix} \omega_{ec} \\ 0 \\ \omega_{es} \end{bmatrix} \\ &\quad - \begin{bmatrix} \cos(c)\sec(b) & -\sin(c)\sec(\mathrm{b}) & 0 \\ \sin(c) & \cos(c) & 0 \\ -\cos(c)\tan(b) & \sin(c)\tan(b) & -1 \end{bmatrix} \begin{bmatrix} tg_x \\ tg_y \\ tg_z \end{bmatrix}, \end{aligned} \tag{4.3}$$

where ω_{ec}, ω_{es} represent north and vertical components of rotational speed of the earth ω_e, respectively.

ψ_x, ψ_y, ψ_z in (4.1) represent the attitude errors between the practical platform frame and ideal one:

$$\begin{bmatrix} \dot{\psi}_x \\ \dot{\psi}_y \\ \dot{\psi}_z \end{bmatrix} = \begin{bmatrix} 0 & tg_z & -tg_y \\ -tg_z & 0 & tg_x \\ tg_y & -tg_x & 0 \end{bmatrix} \begin{bmatrix} \psi_x \\ \psi_y \\ \psi_z \end{bmatrix} + \begin{bmatrix} d_{0x} + d_{1x}tg_x - \gamma_{xz}tg_y + \gamma_{xy}tg_z \\ d_{0y} + d_{1y}tg_y + \gamma_{yz}tg_x - \gamma_{yx}tg_z \\ d_{0z} + d_{1z}tg_z - \gamma_{zy}tg_x + \gamma_{zx}tg_y \end{bmatrix}, \tag{4.4}$$

where $\gamma_{xy}, \gamma_{zy}, \gamma_{zx}, \gamma_{yx}, \gamma_{yz}, \gamma_{xz}$ represent the misalignment angles of gyroscopes' input axes with respect to platform frame.

d_{0x}, d_{0y}, d_{0z} and d_{1x}, d_{1y}, d_{1z} represent the fixed drifts and scale factor errors of gyro torquers.

$u(t) = [\,tg_x\ tg_y\ tg_z\,]^T$ represent equivalent command angular speed to the ISP in an ideal platform frame and are the input variables to be designed.

Choose ψ_x, ψ_y, ψ_z and a, b, c as the state vector $x(t)$; note that only the state of (4.4) is related to partial elements of unknown parameter vector θ, where

$$\begin{gathered} \theta^T = \left[\theta_a^T\ \theta_g^T\right], \qquad \theta_a = \left[\alpha_x, \alpha_y, \alpha_z, k_{0x}, k_{0y}, k_{0z}, k_{1x}, k_{1y}, k_{1z}\right]^T, \\ \theta_g = \left[\gamma_{xy}, \gamma_{zy}, \gamma_{zx}, \gamma_{yx}, \gamma_{yz}, \gamma_{xz}, d_{0x}, d_{0y}, d_{0z}, d_{1x}, d_{1y}, d_{1z}\right]^T. \end{gathered} \tag{4.5}$$

Therefore, the equations for $x_{\theta_i}(t)$ can be derived by making partial derivative of (4.4) about θ_g.

Rewrite (4.1), (4.3), and (4.4) for abbreviation as follows:

$$\begin{aligned}
&\dot{x}_1(t) = A_1(u)x_1(t) + B_1(u)\theta_g, \qquad x_1(t_0) = x_{10}, \\
&\dot{x}_2(t) = f(x_2, u), \qquad x_2(t_0) = 0, \\
&y_k = H_1(x_{2,k})x_{1,k} + H_2(x_{2,k})\theta_a + \varepsilon_k, \quad k = 0, 1, \ldots, N,
\end{aligned} \tag{4.6}$$

where $x_1(t) = [\psi_x, \psi_y, \psi_z]^T$, $x_2(t) = [a, b, c]^T$.

Then the equations for $x_{\theta_i}(t)$ are as follows:

$$\dot{x}_{\theta_i}(t) = A_1(u)x_{\theta_i}(t) + B_{1,i}(u), \quad x_{\theta_i}(t_0) = 0, \ i = 1, \ldots, s, \tag{4.7}$$

where $B_{1,i}(u)$ denotes the ith column of matrix $B_1(u)$, and s is the dimension of θ_g.

$$M'(\theta, U) = \delta_y^{-2} \sum_{k=1}^{N} \begin{bmatrix} H_2^T(x_{2,k})H_2(x_{2,k}) & H_2^T(x_{2,k})H_1(x_{2,k})X_\theta \\ X_\theta^T H_1^T(x_{2,k})H_2(x_{2,k}) & X_\theta^T H_1^T(x_{2,k})H_1(x_{2,k})X_\theta \end{bmatrix} \tag{4.8}$$

Where $X_\theta = [x_{\theta_1,k}, \ldots, x_{\theta_s,k}]$.

It shows that $M'(\theta, U)$ is insensitive to θ since in (4.6) and (4.7), $x_{2,k}$ as well as $x_{\theta_i,k}$ is independent of the unknown parameter θ.

Thus, in this problem

$$M(U) = M'(\theta, U), \qquad M(\xi) = \sum_{i=1}^{l} \xi_i M(U_i) \tag{4.9}$$

for any θ and state equation for $x_1(t)$ can be deleted from the constraint conditions in (2.11).

Now we reformulate the design problem for self-calibration tests of ISP system as follows:

$$\begin{aligned}
&\max_{U \in \Omega_U} |M(\xi)| \\
&\text{s.t.} \quad \dot{x}_2(t) = f(x_2, u), \qquad x_2(t_0) = 0, \\
&\qquad \dot{x}_{\theta_i}(t) = A_1(u)x_{\theta_i}(t) + B_{1,i}(u), \quad x_{\theta_i}(t_0) = 0, \ i = 1, \ldots, s,
\end{aligned} \tag{4.10}$$

where $\Omega_U = \{U : u^- \le u_k \le u^+, \ k = 0, \ldots, N-1\}$ is the amplitude constraint on the precise command angular speed.

Since three state equations should be added to the constraint equations in (4.10) if one parameter in θ_g is to be estimated, the dynamic programming algorithm in Step 3 will be very time-consuming. Therefore, only 9 parameters in θ_a are considered in this example.

The initial design ξ_0 is chosen from a single-point design which maximizes $|M(U)|$ via a rough search by confining each element of the input signals $u(t)$ to a four-segment

Table 1: Design results by the propose algorithm.

i	1	2	3	4
$\log\lvert M(U_i)\rvert$	4.7	4.5	4.7	5.2
ξ_i	0.1	0.2	0.2	0.5

Table 2: Standard errors of parameter estimators ($\delta_y = 1$).

	α_x	α_y	α_z	k_{0x}	k_{0y}	k_{0z}	k_{1x}	k_{1y}	k_{1z}
U_1	0.67	0.77	0.76	0.4	0.43	0.43	0.7	0.67	0.63
U_4	0.65	0.57	0.53	0.36	0.36	0.38	0.53	0.56	0.66

square wave varying between $-10\,\omega_e$, 0, and $10\,\omega_e$. Figure 1 shows the convergence of $\mathrm{tr}(M^{-1}(\xi_k)M(U_k))$ after eleven times of iterations, and $\lvert M(\xi_{k+1})\rvert/\lvert M(\xi_k)\rvert$ tends to one which means $\lvert M(\xi_k)\rvert$ converges to a local maximum $\lvert M(\xi^*)\rvert$. Since $\lvert M(\xi)\rvert$ is a concave function about ξ, ξ^* is global optimizing as well.

The values of $\log\lvert M(U_i)\rvert$ at each supporting point U_i and measure ξ_i are listed in Table 1 with $\delta_y^2 = 1$. In addition, $\log\lvert M(\xi^*)\rvert = \log\lvert\sum_i M(U_i)\xi_i\rvert = 5.5$ and $\log\lvert M(\xi(U'))\rvert = \log\lvert M(\sum_i U_i\xi_i)\rvert = 1.7$. It shows that the randomized design ξ^* has better performance than any single-point design $\xi(U_i)$, whereas the linear combination $U' = \sum_i U_i\xi_i$, although it is also an admissible control input in Ω_U, shows poor performance and cannot be used as a nonrandomized approximation to the optimal test plan ξ^* here.

In Table 1 the 4th supporting point U_4 has the maximum $\log\lvert M(U_i)\rvert$ which approximates mostly to $\log\lvert M(\xi^*)\rvert$. So single-point design $\xi(U_4)$ is chosen as the nonrandomized approximation to ξ^*. Comparison of estimation errors between tests with U_4 and U_1 (the initial rough design) is in Table 2, which shows some improvement in budgets of estimation precision. The control input curves of U_4 are plotted in Figure 2 with unit ω_e. The whole test time is three hours, and the sampling time is 22.5 minutes. None of tg_x, tg_y, and tg_z in U_4 is the bang-bang type mainly because a constraint on angle $b(-\pi/6 \le b \le \pi/6)$ is also assumed. The projection of gravitational acceleration in the ideal platform frame is plotted in Figure 3.

The profiles of A_x, A_y, and A_z show that input axis of each accelerometer completes nearly a whole tumble in gravitational field which can provide sufficient stimulations to the error terms of accelerometers in practical testing.

5. Conclusion

A D-optimal design method for parameter estimation in nonlinear dynamic systems is presented based on test plan design theories. The corresponding iterative algorithm is proposed with a dynamic programming algorithm imbedded. The proof for the convergence of the algorithm is given as well. Simulation results on an optimal trajectory design problem in self-calibration test of ISP system demonstrate the effectiveness of the proposed algorithm.

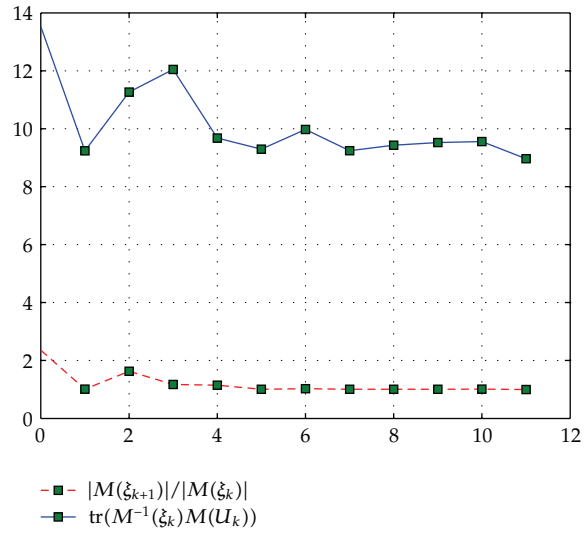

Figure 1: Convergence of the proposed algorithm.

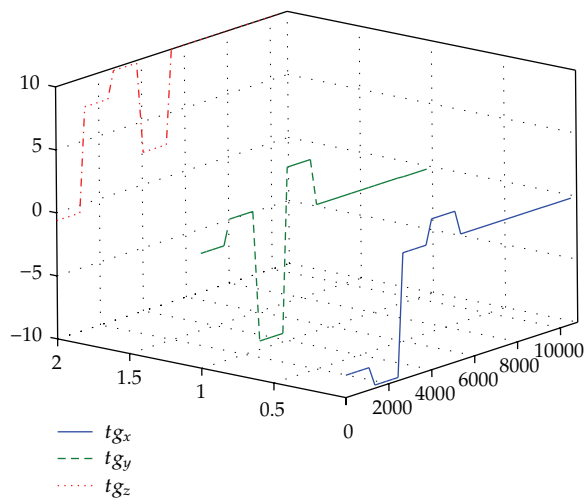

Figure 2: Curves of the supporting point U_4.

Appendix

Proof of the Convergence of Algorithm 3.2

Proof. In the algorithm, α_k is chosen such that

$$|M(\xi_0)| \leq |M(\xi_1)| \leq \cdots \leq |M(\xi^*)|. \tag{A.1}$$

Since any bounded monotone nondecreasing sequence converges, the sequence $|M(\xi_0)|, |M(\xi_1)|, \ldots, |M(\xi_k)|$ converges to some limit $|M(\widehat{\xi})|$.

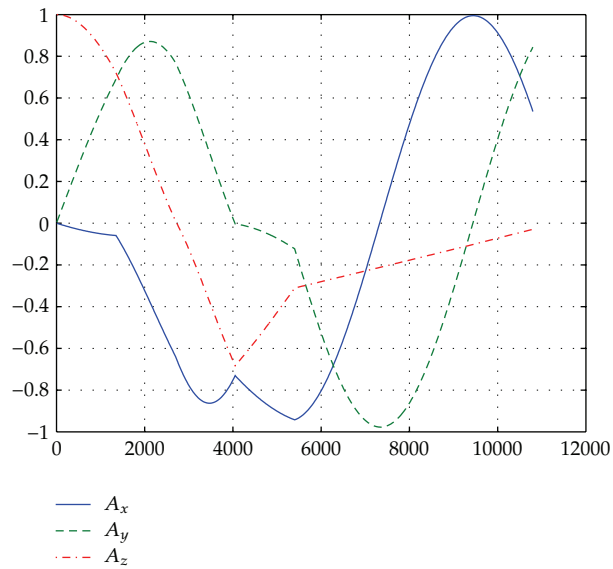

Figure 3: Acceleration projection in the ideal platform frame.

To prove $|M(\widehat{\xi})| = |M(\xi^*)|$, we assume the contrary $|M(\widehat{\xi})| < |M(\xi^*)|$. Then, by Theorem 3.1, for any k there is a constant η such that

$$\operatorname{tr}\left(M^{-1}(\xi_k)M(U_k)\right) - m > \eta > 0. \tag{A.2}$$

It follows that

$$\frac{\partial}{\partial \alpha_k} \log|M(\xi_{k+1})|\Big|_{\alpha_k=0} = \operatorname{tr}\left[M^{-1}(\xi_k)(-M(\xi_k) + M(U_k))\right] > \eta. \tag{A.3}$$

For the smoothness of the function $\log|M(\xi_{k+1})|$ about α_k and by the assumption $\lim_{k\to\infty}\alpha_k = 0$, there is a positive integer s such that for any $k \geq s$, $(\partial/\partial\alpha_k)\log|M(\xi_{k+1})| \geq \eta$.

Now integrating both sides of the above inequality over α_k from 0 to α_k, one obtains

$$\frac{|M(\xi_{k+1})|}{|M(\xi_k)|} \geq \exp(\eta\alpha_k). \tag{A.4}$$

On the other hand, in view of the convergence of the sequence $|M(\xi_0)|, \ldots$, for any small positive number γ, there is a positive integer n such that for any integer $p \geq q \geq n$, the following inequality holds:

$$|M(\xi_p)| - |M(\xi_q)| \leq \gamma. \tag{A.5}$$

Let $t = \max(n, s)$, then for any integer $p \geq q \geq t$,

$$\gamma \geq |M(\xi_p)| - |M(\xi_q)| \geq \left[\exp\left(\eta \sum_{k=q}^{p-1} \alpha_k\right) - 1\right] \cdot |M(\xi_q)|. \tag{A.6}$$

This means

$$\sum_{k=q}^{p-1} \alpha_k \leq \frac{1}{\eta}\left[\log(\gamma + |M(\xi_q)|) - \log|M(\xi_q)|\right], \tag{A.7}$$

which contradicts the assumption $\sum_{k=0}^{\infty} \alpha_k = \infty$.

Therefore, $|M(\widehat{\xi})| = |M(\xi^*)|$, the global maximum is obtained by the algorithm. □

Acknowledgment

This work was supported by the Fundamental Research Funds for the Central Universities (Grant no. HIT. NSRIF. 2013037).

References

[1] G. C. Goodwin and R. L. Payne, *Dynamic system identification*, vol. 136, Academic Press, New York, NY, USA, 1977.
[2] B. Shen, Z. Wang, H. Shu, and G. Wei, "H_∞ filtering for nonlinear discrete-time stochastic systems with randomly varying sensor delays," *Automatica*, vol. 45, no. 4, pp. 1032–1037, 2009.
[3] B. Shen, Z. Wang, and Y. S. Hung, "Distributed H_∞-consensus filtering in sensor networks with multiple missing measurements: the finite-horizon case," *Automatica*, vol. 46, no. 10, pp. 1682–1688, 2010.
[4] D. Hongli, W. Zidong, and G. Huijun, "Distributed filtering for a class of time-varying systems over sensor networks with quantization errors and successive packet dropouts," *IEEE Transactions on Signal Processing*, vol. 60, no. 6, pp. 3164–3173, 2012.
[5] H. Dong, Z. Wang, and H. Gao, "Robust H_∞ filtering for a class of nonlinear networked systems with multiple stochastic communication delays and packet dropouts," *IEEE Transactions on Signal Processing*, vol. 58, no. 4, pp. 1957–1966, 2010.
[6] H. Jun, W. Zidong, G. Huijun et al., "Probability-guaranteed H-infinity finite-horizon filtering for a class of nonlinear time-varying systems with sensor saturation," *System & Control Letters*, vol. 61, no. 4, pp. 477–484, 2012.
[7] H. Jun, W. Zidong, G. Huijun et al., "Robust sliding mode control for discrete stochastic systems with mixed time-delays, randomly occurring uncertainties and randomly occurring nonlinearities," *IEEE Transactions on Industrial Electronics*, vol. 59, no. 7, pp. 3008–3015, 2012.
[8] W. Ligang, S. Xiaojie, S. Peng et al., "Model approximation for discrete-time state-delay systems in the T-S fuzzy framework," *IEEE Transactions on Fuzzy Systems*, vol. 19, no. 2, pp. 366–378, 2011.
[9] Q. Jianbin, F. Gang, and Y. Jie, "A novel approach to filter design for T-S fuzzy discrete-time systems with time-varying delay," *IEEE Transactions on Fuzzy Systems*, vol. 17, no. 5, pp. 1044–1058, 2009.
[10] Y. Rongni, G. Huijun, and S. Peng, "Novel robust stability criteria for stochastic Hopfield neural networks with time delays," *IEEE Trans on Systems, Man and Cybernetics B*, vol. 39, no. 11, pp. 467–474, 2009.
[11] R. K. Mehra, "Optimal input signals for parameter estimation in dynamic systems—survey and new results," *IEEE Transactions on Automatic Control*, vol. 19, no. 6, pp. 753–768, 1974.
[12] V. V. Fedorov, *Theory of Optimal Experiments*, Academic Press, New York, NY, USA, 1972.
[13] A. Lew and H. Mauch, *Dynamic Programming, A Computational Tool*, Springer, 2007.

[14] D. E. Goldberg, *Genetic Algorithms in Search, Optimization and Machine Learning*, Addison-Wesley, Boston, Mass, USA, 1989.
[15] S. Kirkpatrick, C. D. Gelatt Jr., and M. P. Vecchi, "Optimization by simulated annealing," *Science*, vol. 220, no. 4598, pp. 671–680, 1983.
[16] A. A. Zhigljavsky, *Theory of Global Random Search*, vol. 65, Kluwer Academic Publishers, Dordrecht, The Netherlands, 1991.
[17] E. A. Morelli and V. Klein, "Optimal input design for aircraft parameter estimation using dynamic programming principles," in *Proceedings of the AIAA Atmospheric Flight Mechanics Conference*, pp. 249–259, 1990.
[18] N. Neto, E. Hemerly, and L. C. S. Goes, "Aircraft parameter estimation experiment design considering measurement colored residuals," in *Proceedings of the AIAA Atmospheric Flight Mechanics Conference*, pp. 1–12, 1990.
[19] L. J. Lintereur, *Optimal test trajectories for calibrating inertial systems [M.S. thesis]*, Massachusetts Institute of Technology, 1996.

Hindawi Publishing Corporation
Mathematical Problems in Engineering
Volume 2012, Article ID 623426, 20 pages
doi:10.1155/2012/623426

Research Article

Fault-Reconstruction-Based Cascaded Sliding Mode Observers for Descriptor Linear Systems

Jinyong Yu,[1] Guanghui Sun,[1] and Hamid Reza Karimi[2]

[1] *Research Institute of Intelligent Control and Systems, Harbin Institute of Technology, Harbin 150001, China*
[2] *Faculty of Engineering and Science, University of Agder, 4898 Grimstad, Norway*

Correspondence should be addressed to Jinyong Yu, yujinyong.hit@gmail.com

Received 25 May 2012; Accepted 8 July 2012

Academic Editor: Zidong Wang

This paper develops a cascaded sliding mode observer method to reconstruct actuator faults for a class of descriptor linear systems. Based on a new canonical form, a novel design method is presented to discuss the existence conditions of the sliding mode observer. Furthermore, the proposed method is extended to general descriptor linear systems with actuator faults. Finally, the effectiveness of the proposed technique is illustrated by a simulation example.

1. Introduction

With the development and applications of modern control techniques, the safety and reliability of control systems are becoming increasingly important. Therefore, the fault diagnosis has become one of the most important techniques to ensure the safety and reliability of control systems [1, 2]. During the last two decades, many significant results have been obtained for the analysis and observer design of fault diagnosis of the regular systems, such as unknown input observers [3, 4], eigenstructure assignment method [5], H_∞ filtering [6–9], parity space approach [10], and parameter identification approach [11].

Just like regular systems, the fault diagnosis for descriptor systems has recently attracted increasing attention due to their importance in real-world systems. In [12], a parametric approach is proposed to design unknown input observers to realize fault detection of descriptor linear multivariable systems with unknown disturbances. By directly identifying parity space, a model-free approach for fault detection is developed, which can be applied if the model of descriptor systems is unknown [13]. In [14], the factorization

approach for robust residual generation is extended to descriptor systems, and then a post-filter is added to ensure the robustness of fault diagnosis. In [15], H_∞ filter is utilized for providing disturbance rejection and robustness properties of the fault detection and isolation schemes of linear time-invariant descriptor systems. In [16], several sufficient conditions of existence of unknown input observers are obtained for Takagi-Sugeno descriptor systems, which are affected by unknown inputs. Unfortunately, although these methods can successfully generate residuals, they fail to reconstruct fault signals.

Recently, fault reconstruction is a promising alternative for fault detection. Instead of generating residuals, a number of methods, such as sliding mode observers (SMOs) [17–23], descriptor observer method [24–26], and PI observer [27–29], can be used to reconstruct fault signals. The sliding mode control is employed in the situations including state estimation and fault detection, since it is insensitive to matched uncertainties, nonlinearity, or disturbances [30]. Edwards et al. [17] firstly used the concept of the equivalent output error injection signals to reconstruct faults. Tan and Edwards [19] extended this work for robust reconstruction of sensor and actuator faults by minimizing the effect of uncertainty on the reconstruction in an L_2 sense. Some well-studied works, aiming at reducing the system constraints associated with the results in [17, 19], have recently appeared in the literature [18, 20–23]. In order to relax the matching conditions, the cascaded sliding mode observer method was proposed to deal with a class of systems with relative degree higher than one [20, 21]. In [22], the auxiliary outputs are defined such that the conventional sliding mode observer in [17] can be used for systems without the observer matching condition. In order to obtain those auxiliary outputs, high-order sliding-mode observers are constructed to act as exact differentiators using a super-twisting algorithm. Inspired by Floquet et al. [22], high-gain approximate differentiators and high-order sliding-mode robust differentiators were proposed to generate auxiliary outputs for the design of sliding mode observers [18, 23].

Although there are many achievements in regular systems, few results have been reported to the descriptor case despite its importance in real-world systems. In [31, 32], the sliding mode observer method was employed to detect and isolate faults and to reconstruct the faults for descriptor systems. However, the uncertainty was not considered in these results. In [33], the sliding mode observer was proposed to minimize the effect of uncertainly on the reconstruction of faults for descriptor systems. Unfortunately, the fault detection filter based sliding mode observer has to satisfy the strict condition in [31–33], which severely limits the applicability of these approaches for a wide range of practical systems.

Motivated by the above discussion, in this paper, we develop a cascaded sliding mode observer method to reconstruct actuator faults for a class of descriptor linear systems. The main contribution of this paper can be summarized as follows: (1) we present a novel cascaded sliding mode observer method to reconstruct actuator faults for a class of descriptor linear systems; (2) in the design process, we remove this restrictive assumption and extend the cascaded sliding mode observer approach of Tan et al. [20, 21] to descriptor systems; (3) a novel cascaded sliding mode observer is designed for reconstructing actuator faults for a class of descriptor linear systems.

The paper is organized as follows. In Section 2, the problem is formulated, and appropriate coordinate transformations are introduced to exploit the system structure. In Section 3 the design algorithm of cascaded sliding mode observer for linear descriptor systems is given. In Section 4, a design method of cascaded sliding mode observer and fault reconstruction for general descriptor systems are presented. In Section 5, an example is given to support the effectiveness of the proposed approach. Finally, the conclusions are drawn.

2. Problem Statement and System Analysis

Consider a descriptor linear system described by

$$\begin{aligned} E\dot{x} &= Ax + Bu + Df \\ y &= Cx, \end{aligned} \tag{2.1}$$

where $x \in R^n$ is the state variable, $u \in R^k$ is the input vector, $y \in R^p$ is the output variable, and $f \in R^q$ is unknown but bounded so that

$$\|f\| \leq \beta, \tag{2.2}$$

where the positive scalar β is known. The signal f models the actuator fault within the system. $A \in R^{m\times n}$, $B \in R^{m\times k}$, $C \in R^{p\times n}$, and $D \in R^{m\times q}$ are known constant real matrices. Without loss of generality, it is assumed that $\operatorname{rank}(D) = q$, $\operatorname{rank}(C) = p$, and E is full row rank.

In [32], a sliding mode observer is given in the following form:

$$\begin{aligned} \dot{z} &= Fz + T_1Bu + K_1y + K_2y + G_n\upsilon \\ \hat{x} &= z + T_2y \\ \hat{y} &= C\hat{x}, \end{aligned} \tag{2.3}$$

where $z \in R^{\tilde{n}}$ is the state vector of the SMO, $\hat{x}$ is the estimation of the state vector x, and υ is the discontinuous output error injection vector defined by

$$\upsilon = \begin{cases} -\eta \dfrac{P_0e_y}{\|P_0e_y\|} & e_y \neq 0 \\ 0 & \text{other}, \end{cases} \tag{2.4}$$

where $e_y = \hat{y} - y$, $\eta > 0$, F, T_1, T_2, K_1, K_2, G_n, and P_0 are parameters to be designed.

For the descriptor system (2.1), the sufficient conditions for the existence of the sliding mode observer (2.3) are as follows:

$$\operatorname{rank}\begin{bmatrix} E & D \\ C & 0 \end{bmatrix} = n + q \tag{2.5}$$

$$\operatorname{rank}\begin{bmatrix} sE - A & D \\ C & 0 \end{bmatrix} = n + q, \quad \operatorname{Re}(s) \geq 0. \tag{2.6}$$

It is well known that condition (2.5) is quite restrictive and may not apply to a wide range of systems. In the following, we give two more relaxed conditions:

$$\operatorname{rank}\begin{bmatrix} E \\ C \end{bmatrix} = n, \tag{2.7}$$

$$\operatorname{rank}\begin{bmatrix} E & D \\ C & 0 \end{bmatrix} = n + l, \tag{2.8}$$

where $l \leq q$.

Before presenting the main results, some lemmas are given as follows.

Lemma 2.1. *If the conditions* (2.7) *and* (2.8) *hold, there exists a nonsingular matrix* U *such that*

$$\operatorname{rank}\begin{bmatrix} E & D_1 \\ C & 0 \end{bmatrix} = n + l, \tag{2.9}$$

$$\operatorname{rank}\begin{bmatrix} E & D_2 \\ C & 0 \end{bmatrix} = n, \tag{2.10}$$

where $[D_1 \;\; D_2] = DU$, *and* $D_1 \in R^{m\times l}$, $D_2 \in R^{m\times(q-l)}$.

Proof. if l is equal to q, the conclusion is obviously true. So the following is to prove the case that l is less than q.

Obviously, there exists a nonsingular matrix U_1 so that $DU_1 = [D_1 \;\; \overline{D}_2]$ and (2.9) hold. Then,

$$\operatorname{rank}\begin{bmatrix} E & D \\ C & 0 \end{bmatrix} = \operatorname{rank}\begin{bmatrix} E & D_1 & \overline{D}_2 \\ C & 0 & 0 \end{bmatrix} = n + l. \tag{2.11}$$

So there exists a matrix $Y = \begin{bmatrix} Y_1 \\ Y_2 \end{bmatrix}$ so that

$$\begin{bmatrix} \overline{D}_2 \\ 0 \end{bmatrix} = \begin{bmatrix} E & D_1 \\ C & 0 \end{bmatrix}\begin{bmatrix} Y_1 \\ Y_2 \end{bmatrix}. \tag{2.12}$$

Thus, we have $\overline{D}_2 = EY_1 + D_1Y_2$ and $CY_1 = 0$.

Setting

$$U_2 = \begin{bmatrix} I & -Y_2 \\ 0 & I \end{bmatrix} \tag{2.13}$$

and $U = U_1U_2$, we have

$$\operatorname{rank}\begin{bmatrix} E & D_2 \\ C & 0 \end{bmatrix} = \operatorname{rank}\begin{bmatrix} E & EY_1 \\ C & CY_1 \end{bmatrix} = \operatorname{rank}\begin{bmatrix} E \\ C \end{bmatrix} = n. \tag{2.14}$$

□

Lemma 2.2. *If the following conditions*

$$\operatorname{rank}\begin{bmatrix} E & D_1 \\ C & 0 \end{bmatrix} = n + l,$$
$$\operatorname{rank}\begin{bmatrix} sE - A & D_1 \\ C & 0 \end{bmatrix} = n + l, \quad \operatorname{Re}(s) \geq 0 \tag{2.15}$$

hold, there exist two nonsingular matrices P and Q such that

$$PEQ = \begin{bmatrix} 0 & E_{12} \\ I_{\tilde{n}-\tilde{p}} & E_{22} \end{bmatrix}, \qquad PAQ = \begin{bmatrix} A_{11} & A_{12} \\ A_{21} & A_{22} \end{bmatrix}$$
$$PD_1 = \begin{bmatrix} D_I \\ 0 \end{bmatrix}, \qquad CQ = \begin{bmatrix} 0 & I_p \end{bmatrix}, \tag{2.16}$$

where $E_{12} \in R^{(m-n+p)\times p}$, $E_{22} \in R^{(n-p)\times p}$, $A_{11} \in R^{(m-n+p)\times(n-p)}$, $A_{12} \in R^{(m-n+p)\times p}$, $A_{21} \in R^{(n-p)\times(n-p)}$, $A_{22} \in R^{(n-p)\times p}$, $D_I = [0 \;\; I_l]^T \in R^{(m-n+p)\times l}$, and the subblock A_{11} has the structure

$$A_{11} = \begin{bmatrix} A_{111} \\ A_{112} \end{bmatrix}, \tag{2.17}$$

in which $A_{111} \in R^{(m-n+p-l)\times(n-p)}$, $A_{112} \in R^{l\times(n-p)}$, and the pair (A_{21}, A_{111}) is detectable.

It can be established easily by Lemma 2 in [33], and hence the proof is omitted.

Lemma 2.3. *If the conditions* (2.6), (2.7), *and* (2.8) *hold, there exist nonsingular matrices P, Q, and U such that*

$$PEQ = \begin{bmatrix} 0 & E_{12} \\ I_{n-p} & E_{22} \end{bmatrix}, \qquad PAQ = \begin{bmatrix} A_{11} & A_{12} \\ A_{21} & A_{22} \end{bmatrix} \tag{2.18}$$

$$PB = \begin{bmatrix} B_1 \\ B_2 \end{bmatrix}, \qquad CQ = \begin{bmatrix} 0 & I_p \end{bmatrix} \tag{2.19}$$

$$PDU = \begin{bmatrix} D_{11} & 0 \\ 0 & D_{22} \end{bmatrix}, \tag{2.20}$$

where $E_{12} \in R^{(m-n+p)\times p}$, $E_{22} \in R^{(n-p)\times p}$, $A_{11} \in R^{(m-n+p)\times(n-p)}$, $A_{12} \in R^{(m-n+p)\times p}$, $A_{21} \in R^{(n-p)\times(n-p)}$, $A_{22} \in R^{(n-p)\times p}$, $B_1 \in R^{(m-n+p)\times k}$, $B_2 \in R^{(n-p)\times k}$, $D_{11} = [0 \;\; I_l]^T \in R^{(m-n+p)\times l}$, $D_{22} \in R^{(n-p)\times(q-l)}$, and the subblock A_{11} has the structure

$$A_{11} = \begin{bmatrix} A_{111} \\ A_{112} \end{bmatrix}, \tag{2.21}$$

where $A_{111} \in R^{(m-n+p-l)\times(n-p)}$, $A_{112} \in R^{l\times(n-p)}$, and (A_{21}, A_{111}) is detectable.

Proof. By Lemma 2.1, there exists a nonsingular matrix U such that (2.9) and (2.10) hold, where $DU = [D_1 \;\; D_2]$.

Obviously,

$$\operatorname{rank}\begin{bmatrix} sE - A & D_1 \\ C & 0 \end{bmatrix} = n + l, \quad \operatorname{Re}(s) \geq 0. \tag{2.22}$$

By Lemma 2.2, there exist two nonsingular matrices P and Q such that (2.18) and (2.19) hold and

$$PD_1 = \begin{bmatrix} D_{11} \\ 0 \end{bmatrix}. \tag{2.23}$$

Setting $PD_2 = \left[\begin{smallmatrix} D_{21} \\ D_{22} \end{smallmatrix}\right]$, we have

$$\begin{aligned} \operatorname{rank}\begin{bmatrix} E & D_2 \\ C & 0 \end{bmatrix} &= \operatorname{rank}\begin{bmatrix} P & 0 \\ 0 & I \end{bmatrix}\begin{bmatrix} E & D_2 \\ C & 0 \end{bmatrix}\begin{bmatrix} Q & 0 \\ 0 & I \end{bmatrix} \\ &= \operatorname{rank}\begin{bmatrix} 0 & E_{12} & D_{21} \\ I_{n-p} & E_{22} & D_{22} \\ 0 & I_p & 0 \end{bmatrix} \\ &= \operatorname{rank}(D_{21}) + n. \end{aligned} \tag{2.24}$$

Combining (2.10) and (2.24), we have $\operatorname{rank}(D_{21}) = 0$. Obviously, $D_{21} = 0$. □

By Lemma 2.3, it can be assumed without loss of generality that system (2.1) has the following form:

$$\begin{aligned} \begin{bmatrix} 0 & E_{12} \\ I_{n-p} & E_{22} \end{bmatrix}\begin{bmatrix} \dot{x}_1 \\ \dot{x}_2 \end{bmatrix} &= \begin{bmatrix} A_{11} & A_{12} \\ A_{21} & A_{22} \end{bmatrix}\begin{bmatrix} x_1 \\ x_2 \end{bmatrix} + \begin{bmatrix} B_1 \\ B_2 \end{bmatrix} u \\ &\quad + \begin{bmatrix} D_{11} \\ 0 \end{bmatrix} f_1 + \begin{bmatrix} 0 \\ D_{22} \end{bmatrix} f_2 \\ y &= x_2, \end{aligned} \tag{2.25}$$

where $x = [x_1^T \;\; x_2^T]^T$, $x_1 \in R^{n-p}$, $x_2 \in R^p$ and

$$f \longrightarrow Uf = [f_1^T \;\; f_2^T]^T. \tag{2.26}$$

The descriptor system (2.25) may be considered as the system with the fault f_1 and the disturbance f_2. Using the fault reconstruction method in [33], the fault f_1 can be reconstructed and the L_2 gain from the f_2 to reconstruction error of fault f_1 can be minimized. But the fault f_2 and the state x_1 cannot be estimated. Inspired by Tan et al. [20, 21], the cascaded sliding mode observer is applied to estimate both the state x and fault f in the following.

3. Design of Cascaded Sliding Mode Observer

The primary sliding mode observer for system (2.25) is

$$\begin{aligned} \dot{z} &= (T_1 A - K_1 C)z + T_1 B u + K_1 y + F T_2 y + G_n \upsilon \\ \hat{x} &= z + T_2 y \\ \hat{y} &= \hat{x}_2, \end{aligned} \tag{3.1}$$

where $z \in R^n$ is the state vector of the SMO, $\hat{x} = [\hat{x}_1^T \;\; \hat{x}_2^T]^T$ with $\hat{x}_1 \in R^{n-p}$ and $\hat{x}_2 \in R^p$ is the estimation of the state vector x, $G_n = [0 \;\; I]^T$, T_1 and T_2 are defined by

$$T_1 = \begin{bmatrix} Z_1 & I_{n-p} \\ Z_2 & 0 \end{bmatrix} \tag{3.2}$$

$$T_2 = \begin{bmatrix} 0 \\ I_p \end{bmatrix} - T_1 \begin{bmatrix} E_{12} \\ E_{22} \end{bmatrix} \tag{3.3}$$

$$Z_1 = \begin{bmatrix} Z_{11} & 0 \end{bmatrix}, \tag{3.4}$$

$Z_1 \in R^{(n-p)\times(m-n+p)}$, $Z_{11} \in R^{(n-p)\times(m-n+p-q)}$, $Z_2 \in R^{p\times(m-n+p)}$ is full rank, υ is the discontinuous output error injection vector defined by:

$$\upsilon = \begin{cases} -\eta \dfrac{P_2 e_2}{\|P_2 e_2\|} & e_2 \neq 0 \\ 0 & \text{other}, \end{cases} \tag{3.5}$$

$e_2 = \hat{x}_2 - x_2$, $\eta > 0$, Z_{11}, Z_2, K_1, F, and P_2 are parameters to be designed.

In [33], it is shown that for an appropriate choice of observer parameters an ideal sliding motion takes place on $S = \{(e_1, e_2) \mid e_2 = 0\}$ in finite time.

Define $e = \hat{x} - x$ as the state estimation error, the following estimation error dynamic is obtained:

$$\begin{aligned} \dot{e}_1 &= (A_{21} + Z_1 A_{11})e_1 + (Z_1 A_{12} + A_{22} - K_{11})e_2 + D_{22} f_2 \\ \dot{e}_2 &= Z_2 A_{11} e_1 + (Z_2 A_{12} - K_{12})e_2 - Z_2 D_{11} f_1 + \upsilon, \end{aligned} \tag{3.6}$$

where $e = [e_1^T \;\; e_2^T]^T$, $e_1 \in R^{n-p}$, $K_1 = [K_{11}^T \;\; K_{12}^T]^T$, $K_{11} \in R^{(n-p)\times p}$, and $K_{12} \in R^{p\times p}$.

Assuming the primary sliding mode observer has been designed, and that a sliding motion has been achieved, then $e_2 = \dot{e}_2 = 0$, and the error equation becomes

$$\begin{aligned} \dot{e}_1 &= (A_{21} + Z_1 A_{11})e_1 + D_{22} f_2 \\ Z_2^{+} \upsilon_{\text{eq}} &= -A_{11} e_1 + D_{11} f_1, \end{aligned} \tag{3.7}$$

where Z_2^+ is the generalized inverse matrix of Z_2, υ_{eq} is the equivalent output error injection term that can be approximated to any degree of accuracy by replacing (3.8) with

$$\upsilon_{\text{eq}} = -\eta \frac{P_2 e_2}{\|P_2 e_2\| + \delta}, \tag{3.8}$$

where δ is a small positive constant.

The remaining system freedom can be used to estimate the state x_1 and reconstruct the fault f_2. Equation (3.7) can be rewritten as

$$\dot{e}_1 = (A_{21} + Z_1 A_{11}) e_1 + D_{22} f_2 \tag{3.9}$$

$$D_{11}^{\perp} Z_2^+ \upsilon_{\text{eq}} = -A_{111} e_1, \tag{3.10}$$

where $D_{11}^{\perp} = [\, I_{m+p-n-l} \quad 0 \,]$.

For any A_{111}, there exists a nonsingular matrix W so that $W A_{111} = [\, \widehat{A}_{111}^T \quad 0 \,]^T$, where $\widehat{A}_{111} \in R^{\widehat{p} \times (n-p)}$ is full row rank. We have

$$\left[I_{\widehat{p}} \;\; 0 \right] W D_{11}^{\perp} Z_2^+ \upsilon_{\text{eq}} = -\widehat{A}_{111} e_1. \tag{3.11}$$

The system (3.9) and (3.11) may be considered as the linear system with the $q-l$ faults, the $n-p$ states f_1 and the $\widehat{p}$ outputs. Using the sliding mode observer design method for the linear system in [17], we can design a secondary sliding mode observer to estimate e_1 and f_2 if the following conditions hold:

$$\begin{gathered} \operatorname{rank}\left(\widehat{A}_{111} D_{22} \right) = \operatorname{rank}(D_{22}) \\ \operatorname{rank}\begin{bmatrix} sI - (A_{21} + Z_1 A_{11}) & D_{22} \\ \widehat{A}_{111} & 0 \end{bmatrix} = n - p + q - l, \quad \operatorname{Re}(s) \geq 0. \end{gathered} \tag{3.12}$$

Obviously, (3.12) are equivalent to

$$\operatorname{rank}(A_{111} D_{22}) = \operatorname{rank}(D_{22}) \tag{3.13}$$

$$\operatorname{rank}\begin{bmatrix} sI - (A_{21} + Z_1 A_{11}) & D_{22} \\ A_{111} & 0 \end{bmatrix} = n - p + q - l, \quad \operatorname{Re}(s) \geq 0. \tag{3.14}$$

Combined with (3.4), (3.14) is equivalent to

$$\operatorname{rank}\begin{bmatrix} sI - A_{21} & D_{22} \\ A_{111} & 0 \end{bmatrix} = n - p + q - l, \quad \operatorname{Re}(s) \geq 0. \tag{3.15}$$

From the above analysis, if the conditions (3.13) and (3.15) satisfy, there exists a cascaded sliding mode observer for the descriptor system (2.1).

Next, the fault reconstruction method based cascaded sliding mode observer is given.

Assuming that the secondary sliding mode observer has been designed and the $\widehat{e}_1$ and $\widehat{f}_2$ are the estimations of e_1 and f_2, respectively. Then, the reconstruction signal of the fault f_1 is described by

$$\widehat{f}_1 = A_{112}\widehat{e}_1 + \begin{bmatrix} 0 & I_l \end{bmatrix} Z_2^{+} \upsilon_{\mathrm{eq}}, \tag{3.16}$$

and the estimation of the state x_1 is described by

$$\widehat{x}_1 - \widehat{e}_1 \longrightarrow x_1. \tag{3.17}$$

The reconstruction of fault is described by

$$\widehat{f} = U^{-1}\begin{bmatrix} \widehat{f}_1^T & \widehat{f}_2^T \end{bmatrix}^T \tag{3.18}$$

Equations (3.13) and (3.15) are the sufficient conditions for the existence of the cascaded sliding mode observer, but these cannot be checked using the parameters of the original system (2.1). Now, for system (2.1), sufficient conditions for the existence of the cascaded sliding mode observer can be given by Theorem 3.1.

Theorem 3.1. *There exists a cascaded sliding mode observer for system* (2.1) *if the following conditions hold:*

$$\operatorname{rank}\begin{bmatrix} E \\ C \end{bmatrix} = n \tag{3.19}$$

$$\operatorname{rank}\begin{bmatrix} E & A & D & 0 \\ 0 & E & 0 & D \\ C & 0 & 0 & 0 \\ 0 & C & 0 & 0 \end{bmatrix} = n + q + \operatorname{rank}\begin{bmatrix} E & D \\ C & 0 \end{bmatrix}, \tag{3.20}$$

$$\operatorname{rank}\begin{bmatrix} sE - A & D \\ C & 0 \end{bmatrix} = n + q, \quad \operatorname{Re}(s) \geq 0. \tag{3.21}$$

Proof. If l is equal to q, the conclusion is obviously true. So, the following is to prove the case that l is less than q.

Substituting (2.8) and (2.25) into (3.20), we have

$$\begin{aligned}
&\operatorname{rank}\begin{bmatrix} E & A & D & 0 \\ 0 & E & 0 & D \\ C & 0 & 0 & 0 \\ 0 & C & 0 & 0 \end{bmatrix} \\
&= \operatorname{rank}\begin{bmatrix} 0 & E_{12} & A_{11} & A_{12} & D_{11} & 0 & 0 & 0 \\ I_{n-p} & E_{22} & A_{21} & A_{22} & 0 & D_{22} & 0 & 0 \\ 0 & 0 & 0 & E_{12} & 0 & 0 & D_{11} & 0 \\ 0 & 0 & I_{n-p} & E_{12} & 0 & 0 & 0 & D_{22} \\ 0 & I_p & 0 & 0 & 0 & 0 & 0 & 0 \\ 0 & 0 & 0 & I_p & 0 & 0 & 0 & 0 \end{bmatrix} \\
&= n + p + l + \operatorname{rank}\begin{bmatrix} A_{11} & D_{11} & 0 \\ I_{n-p} & 0 & D_{22} \end{bmatrix} \\
&= n + p + l + \operatorname{rank}\begin{bmatrix} A_{111} & 0 & 0 \\ A_{112} & I_l & 0 \\ I_{n-p} & 0 & D_{22} \end{bmatrix} \\
&= n + p + 2l + \operatorname{rank}\begin{bmatrix} I_{n-p} & D_{22} \\ A_{111} & 0 \end{bmatrix} \\
&= 2n + q + l.
\end{aligned} \tag{3.22}$$

So we have

$$\operatorname{rank}\begin{bmatrix} I_{n-p} & D_{22} \\ A_{111} & 0 \end{bmatrix} = n - p + q - l. \tag{3.23}$$

By Lemma 1 in [32], (3.13) holds.
Substituting (2.18), (2.19), and (2.20) into (3.21), we can obtain (3.15). □

4. Cascaded Sliding Mode Observer Design and Fault Reconstruction for General Descriptor Systems

In Section 2, it is assumed that E is full row rank. In the following, it is discussed that E is rank deficient. Let $r := \operatorname{rank}(E) \leq \min\{m, n\}$.

Now, since $\operatorname{rank}(E) = r$, there exists a regular matrix P^* such that (2.1) is restricted system equivalent to

$$\begin{aligned}
E^*\dot{x} &= A^*x + B^*u + D^*f \\
y_1 = -\overline{B}_1 u &= \overline{A}_1 x + \overline{D}_1 f \\
y &= Cx,
\end{aligned} \tag{4.1}$$

where $P^*E = \left[\begin{smallmatrix} E^* \\ 0 \end{smallmatrix}\right]$, $P^*A = \left[\begin{smallmatrix} A^* \\ \overline{A}_1 \end{smallmatrix}\right]$, $P^*B = \left[\begin{smallmatrix} B^* \\ \overline{B}_1 \end{smallmatrix}\right]$, $P^*D = \left[\begin{smallmatrix} D^* \\ \overline{D}_1 \end{smallmatrix}\right]$, $E^* \in R^{r\times n}$, $A^* \in R^{r\times n}$, $B^* \in R^{r\times k}$, $D^* \in R^{r\times p}$, $\overline{A}_1 \in R^{(m-r)\times n}$, $\overline{B}_1 \in R^{(m-r)\times k}$, and $\overline{D}_1 \in R^{(m-r)\times q}$.

First passing the output y_1 through a nonsingular matrix P_* so that

$$P_* y_1 = \begin{cases} y_{11}(t) = A_{11}x \\ y_{12}(t) = A_{12}x + D_1 f, \end{cases} \tag{4.2}$$

where $D_1 \in R^{\overline{p}\times q}$ is row full rank.

Consider a new state $x_f \in R^{\overline{p}}$ which is a filtered version of y_{12} satisfying

$$\dot{x}_f = -A_f x_f + A_f y_{12}, \tag{4.3}$$

where $-A_f \in R^{\overline{p}\times\overline{p}}$ is a stable (filter) matrix.

Equations (4.1), (4.2), and (4.3) can be combined to form an augmented state-space system with order $\tilde{n}$ as follows:

$$\begin{aligned} E_a\dot{\tilde{x}} &= A_a\tilde{x} + B_a u + D_a f \\ y_a &= C_a\tilde{x}, \end{aligned} \tag{4.4}$$

where $E_a = \left[\begin{smallmatrix} E^* & 0 \\ 0 & I \end{smallmatrix}\right]$, $A_a = \left[\begin{smallmatrix} A^* & 0 \\ A_f A_{12} & -A_f \end{smallmatrix}\right]$, $B_a = \left[\begin{smallmatrix} B^* \\ 0 \end{smallmatrix}\right]$, $D_a = \left[\begin{smallmatrix} D^* \\ A_f D_1 \end{smallmatrix}\right]$, $C_a = \left[\begin{smallmatrix} A_{11} & 0 \\ C & 0 \\ 0 & I \end{smallmatrix}\right]$, $\tilde{x} = [x^T \quad x_f^T]^T$, $y_a = [y_{11}^T \quad y^T \quad x_f^T]^T$, $\tilde{n} = n + \overline{p}$, and $\tilde{p} = p + m - r$.

Obviously, the matrix E_a is full row rank so that the cascaded sliding mode observer can be designed using the method in Section 3.

In the following, the existence conditions of the cascaded sliding mode observer for general descriptor systems are given by Theorem 4.1.

Theorem 4.1. *There exists a cascaded sliding mode observer for system* (2.1) *with rank-deficient E if the following conditions hold:*

$$\operatorname{rank}\begin{bmatrix} E & A & D \\ 0 & C & 0 \end{bmatrix} = m + p \tag{4.5}$$

$$\operatorname{rank}\begin{bmatrix} E & A & D \\ 0 & E & 0 \\ 0 & C & 0 \end{bmatrix} = n + \operatorname{rank}\begin{bmatrix} E & D \end{bmatrix} \tag{4.6}$$

$$\operatorname{rank}\begin{bmatrix} E & A & 0 & D & 0 & 0 \\ 0 & E & A & 0 & D & 0 \\ 0 & 0 & E & 0 & 0 & D \\ 0 & C & 0 & 0 & 0 & 0 \\ 0 & 0 & C & 0 & 0 & 0 \end{bmatrix} = n + q + \operatorname{rank}\begin{bmatrix} E & A & D & 0 \\ 0 & E & 0 & D \\ 0 & C & 0 & 0 \end{bmatrix}, \tag{4.7}$$

$$\operatorname{rank}\begin{bmatrix} sE - A & D \\ C & 0 \end{bmatrix} = n + q, \quad \operatorname{Re}(s) \geq 0. \tag{4.8}$$

Proof. Define a nonsingular matrix as follows:

$$P_1 = \operatorname{diag}\left(\begin{bmatrix} I & 0 \\ 0 & P_* \end{bmatrix} P^*, \begin{bmatrix} I & 0 \\ 0 & P_* \end{bmatrix} P^*, I\right). \tag{4.9}$$

We have

$$\operatorname{rank} P^* \begin{bmatrix} E & D \end{bmatrix} = \operatorname{rank} \begin{bmatrix} E^* & D^* \\ 0 & \overline{D}_1 \end{bmatrix} = r + \overline{p} \tag{4.10}$$

$$\begin{aligned} \operatorname{rank} \begin{bmatrix} E & A & D \\ 0 & E & 0 \\ 0 & C & 0 \end{bmatrix} &= \operatorname{rank} P_1 \begin{bmatrix} E & A & D \\ 0 & E & 0 \\ 0 & C & 0 \end{bmatrix} \\ &= \operatorname{rank} \begin{bmatrix} A_{11} & 0 \\ 0 & I_{\overline{p}} \\ E^* & 0 \\ C & 0 \end{bmatrix} + r, \end{aligned} \tag{4.11}$$

$$\operatorname{rank} \begin{bmatrix} E_a \\ C_a \end{bmatrix} = \operatorname{rank} \begin{bmatrix} E^* & 0 \\ 0 & I_{\overline{p}} \\ A_{11} & 0 \\ C & 0 \\ 0 & I_{\overline{p}} \end{bmatrix} = \operatorname{rank} \begin{bmatrix} A_{11} & 0 \\ 0 & I_{\overline{p}} \\ E^* & 0 \\ C & 0 \end{bmatrix}. \tag{4.12}$$

Combining (4.6), (4.10), (4.11), and (4.12), we have

$$\operatorname{rank} \begin{bmatrix} E_a \\ C_a \end{bmatrix} = \tilde{n}. \tag{4.13}$$

Define a nonsingular matrix as follows:

$$P_2 = \operatorname{diag}\left(\begin{bmatrix} I & 0 \\ 0 & P_* \end{bmatrix} P^*, \begin{bmatrix} I & 0 \\ 0 & P_* \end{bmatrix} P^*, \begin{bmatrix} I & 0 \\ 0 & P_* \end{bmatrix} P^*, I, I\right). \tag{4.14}$$

We have

$$\operatorname{rank} P_2 \begin{bmatrix} E & A & 0 & D & 0 & 0 \\ 0 & E & A & 0 & D & 0 \\ 0 & 0 & E & 0 & 0 & D \\ 0 & C & 0 & 0 & 0 & 0 \\ 0 & 0 & C & 0 & 0 & 0 \end{bmatrix} = r + \overline{p} + \operatorname{rank} \begin{bmatrix} E^* & A^* & D^* & 0 \\ 0 & A_{12} & D_1 & 0 \\ 0 & E^* & 0 & D^* \\ 0 & 0 & 0 & D_1 \\ C & 0 & 0 & 0 \\ A_{11} & 0 & 0 & 0 \\ 0 & C & 0 & 0 \\ 0 & A_{11} & 0 & 0 \end{bmatrix} \tag{4.15}$$

$$\operatorname{rank} \begin{bmatrix} E_a & A_a & D_a & 0 \\ 0 & E_a & 0 & D_a \\ C_a & 0 & 0 & 0 \\ 0 & C_a & 0 & 0 \end{bmatrix} = 2\overline{p} + \operatorname{rank} \begin{bmatrix} E^* & A^* & D^* & 0 \\ 0 & A_{12} & D_1 & 0 \\ 0 & E^* & 0 & D^* \\ 0 & 0 & 0 & D_1 \\ A_{11} & 0 & 0 & 0 \\ C & 0 & 0 & 0 \\ 0 & A_{11} & 0 & 0 \\ 0 & C & 0 & 0 \end{bmatrix}, \tag{4.16}$$

$$\begin{aligned} \operatorname{rank} P_1 \begin{bmatrix} E & A & D & 0 \\ 0 & E & 0 & D \\ 0 & C & 0 & 0 \end{bmatrix} &= \operatorname{rank} \begin{bmatrix} E & A & D & 0 \\ 0 & A_{11} & 0 & 0 \\ 0 & A_{12} & D_1 & 0 \\ 0 & E & 0 & D \\ 0 & 0 & 0 & D_1 \\ 0 & C^* & 0 & 0 \end{bmatrix} \\ &= \operatorname{rank} \begin{bmatrix} A_{12} & D_1 & 0 \\ E & 0 & D \\ 0 & 0 & D_1 \\ A_{11} & 0 & 0 \\ C^* & 0 & 0 \end{bmatrix} + r \\ &= \operatorname{rank} \begin{bmatrix} E_a & D_a \\ C_a & 0 \end{bmatrix} + r. \end{aligned} \tag{4.17}$$

Combining (4.7), (4.15), (4.16), and (4.17), we have

$$\operatorname{rank} \begin{bmatrix} E_a & A_a & D_a & 0 \\ 0 & E_a & 0 & D_a \\ C_a & 0 & 0 & 0 \\ 0 & C_a & 0 & 0 \end{bmatrix} = \tilde{n} + q + \operatorname{rank} \begin{bmatrix} E_a & D_a \\ C_a & 0 \end{bmatrix}. \tag{4.18}$$

Define a nonsingular matrix as follows:

$$P_3 = \operatorname{diag}\left(\begin{bmatrix} I & 0 \\ 0 & P_* \end{bmatrix} P^*, I \right). \tag{4.19}$$

We have

$$\begin{aligned}\operatorname{rank}\begin{bmatrix} sE^* - A^* & D^* \\ C^* & 0 \end{bmatrix} &= \operatorname{rank} P_3 \begin{bmatrix} sE^* - A^* & D^* \\ C & 0 \end{bmatrix} \\ &= \operatorname{rank}\begin{bmatrix} sE - A & D \\ -A_{11} & 0 \\ -A_{12} & D_1 \\ C^* & 0 \end{bmatrix} = n + q;\end{aligned} \tag{4.20}$$

thus,

$$\operatorname{rank}\begin{bmatrix} sE^* - A^* & 0 & D^* \\ -A_{11} & 0 & 0 \\ -A_{12} & 0 & D_1 \\ C^* & 0 & 0 \\ 0 & I_{\overline{p}} & 0 \end{bmatrix} = n + q + \overline{p}. \tag{4.21}$$

Define

$$P_4 = \begin{bmatrix} I & 0 & 0 & 0 & 0 \\ 0 & 0 & A_f & 0 & s + A_f \\ 0 & I & 0 & 0 & 0 \\ 0 & 0 & 0 & I & 0 \\ 0 & 0 & 0 & 0 & I \end{bmatrix}, \tag{4.22}$$

Then,

$$\begin{aligned}\operatorname{rank}\begin{bmatrix} sE^* - A^* & 0 & D^* \\ -A_{11} & 0 & 0 \\ -A_{12} & 0 & D_1 \\ C^* & 0 & 0 \\ 0 & I_{\overline{p}} & 0 \end{bmatrix} &= \operatorname{rank} P_4 \begin{bmatrix} sE^* - A^* & 0 & D^* \\ -A_{11} & 0 & 0 \\ -A_f A_{12} & 0 & A_f D_1 \\ C^* & 0 & 0 \\ 0 & I_{\overline{p}} & 0 \end{bmatrix} \\ &= \operatorname{rank}\begin{bmatrix} sE^* - A^* & 0 & D^* \\ -A_f A_{12} & s + A_f & A_f D_1 \\ -A_{11} & 0 & 0 \\ C^* & 0 & 0 \\ 0 & I_{\overline{p}} & 0 \end{bmatrix} \\ &= \operatorname{rank}\begin{bmatrix} sE_a - A_a & D_a \\ C_a & 0 \end{bmatrix}.\end{aligned} \tag{4.23}$$

Hence,

$$\operatorname{rank}\begin{bmatrix} sE_a - A_a & D_a \\ C_a & 0 \end{bmatrix} = \tilde{n} + q, \quad \operatorname{Re}(s) \geq 0. \tag{4.24}$$

Combining (4.12), (4.16), and (4.24), we get the conclusion by Theorem 3.1. □

Corollary 4.2. *There exists a cascaded sliding mode observer for linear system if the following conditions hold:*

$$\operatorname{rank}\begin{bmatrix} CAD & CD \\ CD & 0 \end{bmatrix} = \operatorname{rank}(CD) + \operatorname{rank}(D), \tag{4.25}$$

$$\operatorname{rank}\begin{bmatrix} sI - A & D \\ C & 0 \end{bmatrix} = n + q, \qquad \operatorname{Re}(s) \geq 0. \tag{4.26}$$

Proof. Obviously, since $E = I$ for linear systems, (4.5), (4.6), and (4.8) hold. Hence, the following is to prove that (4.7) holds.

In [21], the canonical form of the linear system is given as follows:

$$\begin{gathered} A = \begin{bmatrix} A_1 & A_2 \\ A_3 & A_4 \end{bmatrix}, \qquad C = \begin{bmatrix} 0 & T \end{bmatrix}, \qquad D = \begin{bmatrix} D_1 & 0 \\ 0 & D_2 \end{bmatrix}, \qquad A_3 = \begin{bmatrix} A_{3a} & A_{3b} \\ A_{3c} & A_{3d} \end{bmatrix} \\ D_1 = \begin{bmatrix} D_{11} \\ 0 \end{bmatrix}, \qquad D_2 = \begin{bmatrix} 0 \\ D_{22} \end{bmatrix}, \end{gathered} \tag{4.27}$$

where $A_1 \in R^{(n-p)\times(n-p)}$, $A_{3a} \in R^{(p-l)\times(q-l)}$, $T \in R^{p\times p}$ is orthogonal, $D_1 \in R^{(n-p)\times l}$, $D_{11} \in R^{(q-l)\times(q-l)}$, and $D_{22} \in R^{l\times l}$ are invertible.

Substituting (4.27) into (4.25), we obtain

$$\operatorname{rank}\begin{bmatrix} T & 0 \\ 0 & T \end{bmatrix}\begin{bmatrix} CAD & CD \\ CD & 0 \end{bmatrix} = \operatorname{rank}(A_{3a}D_{11}) + 2l. \tag{4.28}$$

Combining (4.25) and (4.28), we obtain

$$\operatorname{rank}(A_{3a}) = q - l. \tag{4.29}$$

Substituting (4.27) into (4.7), we obtain

$$\begin{aligned} \operatorname{rank}\begin{bmatrix} E & A & 0 & D & 0 & 0 \\ 0 & E & A & 0 & D & 0 \\ 0 & 0 & E & 0 & 0 & D \\ 0 & C & 0 & 0 & 0 & 0 \\ 0 & 0 & C & 0 & 0 & 0 \end{bmatrix} &= n + \operatorname{rank}\begin{bmatrix} I_{n-p} & 0 & A_1 & A_2 & D_1 & 0 & 0 & 0 \\ 0 & I_p & A_3 & A_4 & 0 & D_2 & 0 & 0 \\ 0 & 0 & I_{n-p} & 0 & 0 & 0 & D_1 & 0 \\ 0 & 0 & 0 & I_p & 0 & 0 & 0 & D_2 \\ 0 & I_p & 0 & 0 & 0 & 0 & 0 & 0 \\ 0 & 0 & 0 & I_p & 0 & 0 & 0 & 0 \end{bmatrix} \\ &= 2n + p + \operatorname{rank}\begin{bmatrix} A_3 & D_2 & 0 & 0 \\ I_{n-p} & 0 & D_1 & 0 \\ 0 & 0 & 0 & D_2 \end{bmatrix} \end{aligned}$$

$$
\begin{aligned}
&= 3n - q + l + 2\,\mathrm{rank}(D_{22}) + \mathrm{rank}(A_{3a}) + \mathrm{rank}(D_{11}) \\
&= 3n + l + q, \\
\mathrm{rank}\begin{bmatrix} E & A & D & 0 \\ 0 & E & 0 & D \\ 0 & C & 0 & 0 \end{bmatrix} &= \mathrm{rank}\begin{bmatrix} I_{n-p} & 0 & D_1 & 0 \\ 0 & I_p & 0 & D_2 \\ 0 & I_p & 0 & 0 \end{bmatrix} + n \\
&= 2n + l.
\end{aligned}
\tag{4.30}
$$

Obviously, (4.7) holds. □

Remark 4.3. For the linear system, the rank conditions (4.25) and (4.26) are identical to the ones in [21], it is obvious that the conclusion of the paper is more general compared with [21].

5. Simulation

A machine infinite bus system linear model is described as follows [29]:

$$
\begin{aligned}
&\dot{x}_1 = x_4 \qquad \dot{x}_2 = x_5 \qquad \dot{x}_3 = x_6 \\
\dot{x}_4 &= \frac{1}{M_1}(u_1 - Y_{12}V_1V_2(x_1 - x_2) - Y_{15}V_1V_5(x_1 - x_7) - D_2x_4) \\
\dot{x}_5 &= \frac{1}{M_2}(u_2 - Y_{21}V_1V_2(x_2 - x_1) - Y_{25}V_2V_5(x_2 - x_7) - D_2x_5) \\
\dot{x}_6 &= \frac{1}{M_3}(u_3 - Y_{34}V_3V_4x_3 - Y_{35}V_3V_5(x_3 - x_7) - D_3x_6) \\
0 &= P_{ch} - Y_{51}V_5V_1(x_7 - x_1) - Y_{52}V_5V_2(x_7 - x_2) \\
&\quad - Y_{53}V_5V_3(x_7 - x_3) - Y_{54}V_5V_4x_7,
\end{aligned}
\tag{5.1}
$$

where x_1, x_2, x_3, and x_7 are the generator angles, x_4, x_5, and x_6 are the generator speeds. u_1, u_2, and u_3 are the mechanical power, P_{ch} is unknown load, the nominal values of inertia M_1, M_2 and M_3, of damping D_1, D_2, and D_3, of admittance Y_{15}, Y_{25}, Y_{35}, Y_{51}, Y_{52}, Y_{53}, and Y_{54} and of potential V_1, V_2, V_3, V_4, and V_5 are shown in

$$
\begin{array}{c|c|c|c|c}
M_1 = 0.014 & M_2 = 0.026 & M_3 = 0.02 & D_1 = 0.057 & D_2 = 0.15 \\
D_3 = 0.11 & Y_{15} = 0.5 & Y_{25} = 1.2 & Y_{34} = 0.7 & Y_{45} = 1 \\
Y_{34} = 0.7 & Y_{12} = 1 & V_i = 1 \quad (i = 1\text{–}5). & &
\end{array}
\tag{5.2}
$$

It is assumed that the available measurements are the generator angles x_1, x_2, x_3, and x_7. In order to illustrate the effectiveness of the design method, it is assumed that there exist faults on the actuator $u_1 - u_3$. It is easy to verify that the existence conditions of sliding mode

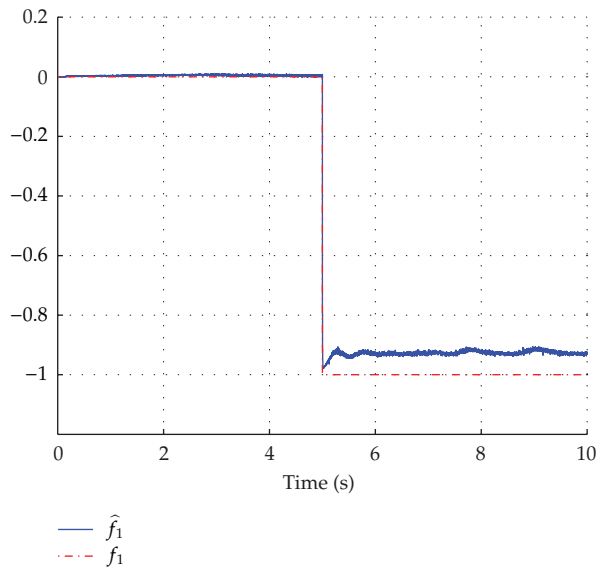

Figure 1: Fault signal f_1 and its reconstruction signal $\hat{f}_1$.

observer in [32] do not hold, but the existence conditions of cascaded sliding mode observer hold.

In the following simulation, the cascaded sliding mode observer in Section 3 is designed to reconstruct the actuator faults.

Considering system (5.1) affected by the inputs $u_1 = 1$, $u_2 = 1$, and $u_3 = 2 + \sin(5t)$, the unknown load $P_{ch} = \sin(t)$ and an uncertain admittance

$$Y_{ij} = Y_{ij} + \Delta Y_{ij}, \tag{5.3}$$

where $\Delta Y_{ij} = \delta_{ij} \sin(\omega_{ij} t)$, $|\delta_{ij}| < 0.1$, $|\omega_{ij}| < 1rd/s$, $i = 1, \ldots, 5$, $j = 1, \ldots, 5$.

Figures 1, 2, and 3 show faults and reconstruction signals. Although there exists unknown input and parameter uncertainty in the system, the cascaded sliding mode observer faithfully reconstructs the faults.

6. Conclusions and Future Works

This paper proposes a fault reconstruction method for a class of descriptor systems using cascaded sliding mode observer. The method can effectively relax the restrictions on the existence of a sliding mode observer, which allows the applicability of our proposed method to a wider range of systems. In our future work, the proposed actuator fault reconstruction schemes can be extended to some sensor fault reconstruction problems by using a suitable output filtering technique. Another interesting future research topic is to extend the current results to fault estimation of nonlinear systems based on T-S fuzzy models [34–36].

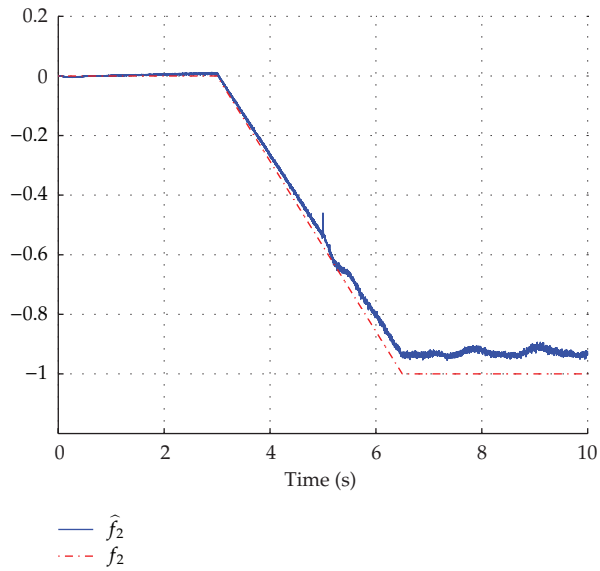

Figure 2: Fault signal f_2 and its reconstruction signal $\hat{f}_2$.

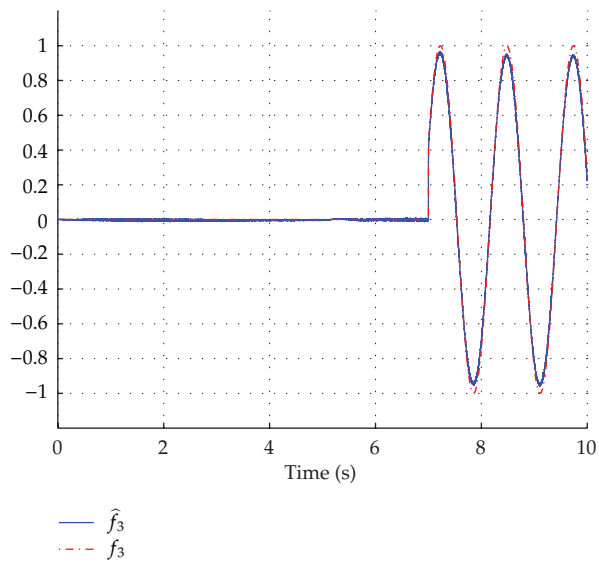

Figure 3: Fault signal f_3 and its reconstruction signal $\hat{f}_3$.

Acknowledgment

This work was supported by the Fundamental Research Funds for the Central Universities under Grant no. HIT.NSRIF.2012031.

References

[1] J. Chen and R. J. Patton, *Robust Model-Based Fault Diagnosis for Dynamic Systems*, Kluwer Academic Publishers, 1999.

[2] H. Dong, Z. D. Wang, and H. J. Gao, "Fault detection for Markovian jump systems with sensor saturations and randomly varying nonlinearities," *IEEE Transactions on Circuits and Systems*, vol. PP, no. 99, pp. 1–8, 2012.

[3] R. Martínez-Guerra and S. Diop, "Diagnosis of nonlinear systems using an unknown-input observer: an algebraic and differential approach," *IEE Proceedings: Control Theory and Applications*, vol. 151, no. 1, pp. 130–135, 2004.

[4] S. Mondal, G. Chakraborty, and K. Bhattacharyya, "Unknown input nonlinear observer for component fault detection and isolation of dynamic systems," *International Journal of Automation and Control*, vol. 3, no. 2-3, pp. 154–170, 2009.

[5] B. Chen and S. Nagarajaiah, "Linear-matrix-inequality-based robust fault detection and isolation using the eigenstructure assignment method," *Journal of Guidance, Control, and Dynamics*, vol. 30, no. 6, pp. 1831–1835, 2007.

[6] J. Hu, Z. D. Wang, Y. Niu, and S. K. Lampros, "H_∞ sliding mode observer design for a class of nonlinear discrete time-delay systems: a delay-fractioning approach," *International Journal of Robust and Nonlinear Control*. In press.

[7] B. Shen, Z. Wang, H. Shu, and G. Wei, "On nonlinear H_∞ filtering for discrete-time stochastic systems with missing measurements," *IEEE Transactions on Automatic Control*, vol. 53, no. 9, pp. 2170–2180, 2008.

[8] X. He, Z. Wang, and D. H. Zhou, "Robust fault detection for networked systems with communication delay and data missing," *Automatica*, vol. 45, no. 11, pp. 2634–2639, 2009.

[9] X. He, Z. Wang, Y. D. Ji, and D. H. Zhou, "Robust fault detection for networked systems with distributed sensors," *IEEE Transactions on Aerospace and Electronic Systems*, vol. 47, no. 1, pp. 166–177, 2011.

[10] H. Ye, G. Wang, and S. X. Ding, "A new parity space approach for fault detection based on stationary wavelet transform," *IEEE Transactions on Automatic Control*, vol. 49, no. 2, pp. 281–287, 2004.

[11] T. Jiang, K. Khorasani, and S. Tafazoli, "Parameter estimation-based fault detection, isolation and recovery for nonlinear satellite models," *IEEE Transactions on Control Systems Technology*, vol. 16, no. 4, pp. 799–808, 2008.

[12] G. R. Duan, D. Howe, and R. J. Patton, "Robust fault detection in descriptor linear systems via generalized unknown input observers," *International Journal of Systems Science*, vol. 33, no. 5, pp. 369–377, 2002.

[13] P. Zhang and S. X. Ding, "Fault detection of descriptor systems," in *Proceedings of the 6th IFAC Symposium on Fault Detection, Supervision and Safety of Technical Processes (SAFEPROCESS '06)*, pp. 378–383, September 2006.

[14] B. Marx, D. Koenig, and D. Georges, "Robust fault diagnosis for descriptor systems—a coprime factorization approach," in *Proceedings of the 6th IFAC Symposium on Fault Detection, Supervision and Safety of Technical Processeses (SAFEPROCESS '03)*, pp. 507–512, 2003.

[15] D. Koenig, S. Mammar, and B. Marx, "H_∞ fault detection and isolation for descriptor systems: a matrix inequalities approach," in *Proceedings of the American Control Conference*, pp. 1080–1081, May 2002.

[16] B. Marx, D. Koenig, and J. Ragot, "Design of observers for Takagi-Sugeno descriptor systems with unknown inputs and application to fault diagnosis," *IET Control Theory and Applications*, vol. 1, no. 5, pp. 1487–1495, 2007.

[17] C. Edwards, S. K. Spurgeon, and R. J. Patton, "Sliding mode observers for fault detection and isolation," *Automatica*, vol. 36, no. 4, pp. 541–553, 2000.

[18] W. Chen and M. Saif, "Actuator fault diagnosis for uncertain linear systems using a high-order sliding-mode robust differentiator (HOSMRD)," *International Journal of Robust and Nonlinear Control*, vol. 18, no. 4-5, pp. 413–426, 2008.

[19] C. P. Tan and C. Edwards, "Sliding mode observers for robust detection and reconstruction of actuator and sensor faults," *International Journal of Robust and Nonlinear Control*, vol. 13, no. 5, pp. 443–463, 2003.

[20] C. P. Tan, F. Crusca, and M. Aldeen, "Extended results on robust state estimation and fault detection," *Automatica*, vol. 44, no. 8, pp. 2027–2033, 2008.

[21] K. Y. Ng, C. P. Tan, C. Edwards, and Y. C. Kuang, "New results in robust actuator fault reconstruction for linear uncertain systems using sliding mode observers," *International Journal of Robust and Nonlinear Control*, vol. 17, no. 14, pp. 1294–1319, 2007.

[22] T. Floquet, C. Edwards, and S. K. Spurgeon, "On sliding mode observers for systems with unknown inputs," *International Journal of Adaptive Control and Signal Processing*, vol. 21, no. 8-9, pp. 638–656, 2007.

[23] K. Kalsi, J. Lian, S. Hui, and S. H. Żak, "Sliding-mode observers for systems with unknown inputs: a high-gain approach," *Automatica*, vol. 46, no. 2, pp. 347–353, 2010.

[24] Z. Gao and H. Wang, "Descriptor observer approaches for multivariable systems with measurement noises and application in fault detection and diagnosis," *Systems and Control Letters*, vol. 55, no. 4, pp. 304–313, 2006.

[25] Q. P. Ha and H. Trinh, "State and input simultaneous estimation for a class of nonlinear systems," *Automatica*, vol. 40, no. 10, pp. 1779–1785, 2004.

[26] Z. Gao and S. X. Ding, "Sensor fault reconstruction and sensor compensation for a class of nonlinear state-space systems via a descriptor system approach," *IET Control Theory and Applications*, vol. 1, no. 3, pp. 578–585, 2007.

[27] B. Shafai, C. T. Pi, and S. Nork, "Simultaneous disturbance attenuation and fault detection using proportional integral observers," in *Proceedings of the American Control Conference*, pp. 1647–1649, May 2002.

[28] Z. Gao and S. X. Ding, "Fault estimation and fault-tolerant control for descriptor systems via proportional, multiple-integral and derivative observer design," *IET Control Theory and Applications*, vol. 1, no. 5, pp. 1208–1218, 2007.

[29] D. Koenig, "Unknown input proportional multiple-integral observer design for linear descriptor systems: application to state and fault estimation," *IEEE Transactions on Automatic Control*, vol. 50, no. 2, pp. 212–217, 2005.

[30] J. Hu, Z. Wang, H. Gao, and L. K. Stergioulas, "Robust sliding mode control for discrete stochastic systems with mixed time delays, randomly occurring uncertainties, and randomly occurring nonlinearities," *IEEE Transactions on Industrial Electronics*, vol. 59, no. 7, Article ID 6022791, pp. 3008–3015, 2012.

[31] T. K. Yeu, H. S. Kim, and S. Kawaji, "Fault detection, isolation and reconstruction for descriptor systems," *Asian Journal of Control*, vol. 7, no. 4, pp. 356–367, 2005.

[32] J. Yu and Z. Liu, "Fault reconstruction based on sliding mode observer for linear descriptor systems," in *Proceedings of the 7th Asian Control Conference (ASCC '09)*, pp. 1132–1137, August 2009.

[33] J. Y. Yu and Z. Y. Liu, "Sliding mode observer-based fault reconstruction for uncertain descriptor linear systems," *Journal of Central South University*, vol. 40, no. 1, pp. 273–276, 2009.

[34] J. Qiu, G. Feng, and J. Yang, "A new design of delay-dependent robust H_∞ filtering for discrete-time T—S fuzzy systems with time-varying delay," *IEEE Transactions on Fuzzy Systems*, vol. 17, no. 5, pp. 1044–1058, 2009.

[35] J. Qiu, G. Feng, and H. Gao, "Nonsynchronized-State estimation of multichannel networked nonlinear systems with multiple packet dropouts Via TS Fuzzy-Affine dynamic models," *IEEE Transactions on Fuzzy Systems*, vol. 19, no. 1, pp. 75–90, 2011.

[36] H. Dong, Z. Wang, J. Lam, and H. Gao, "Fuzzy-model-based robust fault detection with stochastic mixed time delays and successive packet dropouts," *IEEE Transactions on Systems, Man, and Cybernetics B*, vol. 42, no. 2, Article ID 6020813, pp. 365–376, 2012.

Hindawi Publishing Corporation
Mathematical Problems in Engineering
Volume 2012, Article ID 467402, 17 pages
doi:10.1155/2012/467402

Research Article

Neuroendocrine-Based Cooperative Intelligent Control System for Multiobjective Integrated Control of a Parallel Manipulator

Chongbin Guo,[1,2] Kuangrong Hao,[1,2] and Yongsheng Ding[1,2]

[1] *College of Information Science and Technology, Donghua University, Shanghai 201620, China*
[2] *Engineering Research Center of Digitized Textile and Fashion Technology, Ministry of Education, Donghua University, Shanghai 201620, China*

Correspondence should be addressed to Kuangrong Hao, krhao@dhu.edu.cn and Yongsheng Ding, ysding@dhu.edu.cn

Received 7 June 2012; Accepted 1 August 2012

Academic Editor: Bo Shen

This paper presents a novel multiloop and Multi-objective cooperative intelligent control system (MMCICS) used to improve the performance of position, velocity and acceleration integrated control on a complex multichannel plant. Based on regulation mechanism of the neuroendocrine system (NES), a bioinspired motion control approach has been used in the MMCICS which includes four cooperative units. The planning unit outputs the desired signals. The selection unit chooses the real-time dominant control mode. The coordination unit uses the velocity Jacobian matrix to regulate the cooperative control signals. The execution unit achieves the ultimate task based on sub-channel controllers with the proposed hormone regulation self-adaptive Modules (HRSMs). Parameter tuning is given to facilitate the MMCICS implementation. The MMCICS is applied to an actual 2-DOF redundant parallel manipulator where the feasibility of the new control system is demonstrated. The MMCICS keeps its subchannels interacting harmoniously and systematically. Therefore, the plant has fast response, smooth velocity, accurate position, strong self-adaptability, and high stability. The HRSM improves the control performance of the local controllers and the global system as well, especially for manipulators running at high velocities and accelerations.

1. Introduction

With the development of the high-standard manufacturing requirement, plants become more complex while controlled by several of subchannels [1, 2]. Usually, the different sub-channels have different characteristics and control requirements. Therefore, the sub-channels have to interact harmoniously and systematically to achieve multiobjective integrated control [3, 4].

In that manner, the plants can have a quick start and stop, a fine uniform movement, an accurate destination, and a strong self-adaptability with stability [5]. In general, position based control cannot keep uniform velocity, while velocity-based control cannot satisfy accurate position requirement [6, 7]. It's also challenging to achieve acceleration control directly [8]. Some bio-intelligent control algorithms can overcome mathematical model problem of complex plants and have better control performances with physiological regulation to achieve multiobjective control [1, 9].

Neuroendocrine system (NES) is a major homeostatic system in human body and has some outstanding multiobjective cooperative modulation mechanisms. Being a multiloop feedback mechanism, NES can still regulate the functions of several organs and glands with high self-adaptability and stability, by means of regulating their hormone secretions synchronously [10]. Some researchers have presented several models for modulation mechanism [11], feedback control [12], and hormone release [13] of NES. Based on such mechanisms, some novel artificial neuroendocrine systems (ANES) have been developed and applied to the complex control field. Neal and Timmis [14] proposed the first artificial endocrine system (AES) which includes secretion, regulation and control of hormones. The theory is applied to design a useful emotional mechanism for robot control. Vargas et al. [15] has extended the previous work of literature [14], studied the interactions between the nervous and endocrine systems and provided a comprehensive methodology to design a novel AES for autonomous robot navigation. Córdova and Cañete [16] discussed in conceptual terms the feasibility of designing an ANES in robots and to reflect upon the bionic issues highly associated with complex automatons.

To achieve multi-objective cooperative control, some recent work concentrates on how to use multi-loop and multi-objective regulation mechanism of the NES to design some novel control structures and systems. Stear [11] summarized all hormone regulation processes and described a series of control structures. Liu et al. [17] designed a NES-based two-level structure controller, which can not only achieve accurate control but adjust control parameters in real time as well. Ding and Liu et al. [18] developed a bio-inspired decoupling controller from the bi regulation principle of growth hormone in NES. Tang et al. [19] presents an NES-inspired approach for adaptive manufacturing control system. Based on NES, Guo et al. [20] proposes a position-velocity cooperative intelligent controller for motor motion. Compared to conventional control system, these novel control systems always have better simplicity, practicality, stability, and adaptability. These approaches provide some new ideas to multi-objective integrated control field and have good results in simulation. Nevertheless, no experiment has been done on actual plants, especially for multi-objective cooperative control of the position, velocity and acceleration of different parts of the controlled plant.

In this paper, a novel multi-loop and multi-objective cooperative intelligent control system (MMCICS) based on regulation mechanism of NES is proposed. Inherited from NES, the MMCICS consists of four subunits: Planning unit regulates position, velocity and acceleration signals based on ultralong loop feedback. Selection unit is a soft switcher to smoothly select dominant motion control signal based on long loop feedback. As short loop feedback, coordination unit is responsible for processing and transmitting coordination signals to several sub-channels in execution unit. The execution unit is an integrity whose sub-channels interact harmoniously and systematically based on ultra-short loop feedback. Each channel has a proposed hormone regulation self-adaptive module (HRSM) which identifies control error and regulates control parameters in real time. The control performance of the proposed MMCICS is verified by an actual 2-DOF redundant parallel manipulator. The experimental results demonstrate that, through regulation mechanism of the MMCICS, the multiobjective

integrated control task can be achieved easily while the stability, accuracy, adaptability, and response rate of the plant is improved by proposed HRSM.

The main contribution of this paper lies in that it generalizes the characteristics of the NES for regulation, and then reveals the similarity between the NES and a motion control system where the coordination of position, velocity, and acceleration are implemented by the cooperation of different subchannels of the plant. Furthermore, based on the regulation characteristics of the NES, a bioinspired motion control approach is provided, it has been used in MMCICS design. According to our knowledge, this is the first time that the MMCICS based on biological NES is proposed and especially applied to an actual manipulator. The proposed approach is practical and easy to implement, which provides a new efficient method for the intelligent control of complex systems.

The remainder of this paper is arranged as follows. In Section 2, the regulation mechanism of the NES is described while a corresponding bio-inspired motion control approach is presented. In Section 3, the detailed design of the MMCICS is elaborated including system structure, control algorithms, and parameters tuning methods. The experimental results are given to verify the effectiveness of the proposed control system in Section 4. Finally, the work is summarized in Section 5.

2. Regulation Mechanism and Bioinspired Motion Control Approach

2.1. Regulation Mechanism of Neuroendocrine System

The NES mainly includes nervous system and endocrine system [15]. The nervous system is primarily responsible for receiving stimuli of environmental change and processing corresponding nerve impulse. The endocrine system can be viewed as a system of glands that works with the nervous system in regulating the activity of internal glands and coordinating the long-range response to external stimuli [21]. One of the most important interactions between them is regulated by means of their hormone secretions.

A typical regulation mechanism of the neuroendocrine hormone can be generalized as follows [12, 13, 20, 22]: central nervous system detects the changes in the internal and external environments and transmits the nerve impulse as appropriate response to hypothalamus. Hypothalamus receives the nerve impulses and secretes relevant releasing hormone (RH), which stimulates pituitary to secrete tropic hormone (TH). Under the influence of pituitary's TH, other glands (such as thyroid, adrenal, gonads, etc.) secrete corresponding hormones which regulate the situation of human physiological balance. There are massive of feedback loops in neuroendocrine system. Four types of typical feedbacks include ultra-short, short, long and ultra-long loop feedbacks [22, 23]. The ultrashort loop feedback means that the hormone released by a certain gland is directly fed back to its source and changes its status. In the short, long and ultralong loop feedbacks, the concentration of corresponding hormone is fed back to the pituitary, hypothalamus and central nervous system, respectively. Through the multiloop feedback mechanism, multihormone control is stable and easy to practice, as shown in Figure 1.

2.2. Regulation Characteristics and Bioinspired Motion Control Approach

The regulation characteristics of NES can be summarized as below: (1) the NES has several feedback loops and glands. Each feedback mechanism has its own function and different

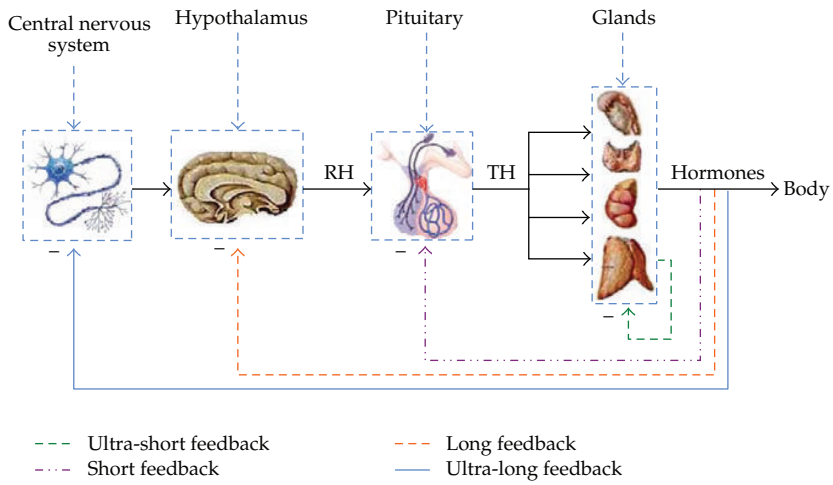

Figure 1: Hormone regulation of the NES.

messages can be transferred among them so that the whole system has a multiobjective regulation mechanism of integrity. (2) Central nervous system is the foremost command center. (3) Hypothalamus is the medium between the nervous system and the endocrine system. (4) Pituitary has the ability to achieve multi-hormone coordinative control. (5) The different glands always have different hormone secretion scopes and different hormone secretion standards. But they have the similar regulation mechanism that can enhance identification and secretion precision within a certain range of stimulus [13].

Therefore, corresponding to the motion control system, the central nervous system, the hypothalamus, the pituitary, and glands of NES can be regarded as the planning unit, the selection unit, the coordination unit, and the execution unit, respectively. In this scenario, the planning unit receives input signal and transmits the suitable motion planning signal to the selection unit. The selection unit processes the motion planning signal and chooses the dominant motion control signal. And then, the coordination unit converts dominant motion control signal to various coordination signals according to its performance characteristic. Various sub-channels in the execution unit receive their own coordination signal from the coordination unit and accomplish homologous task. Ultimately, the whole system could be controlled through the combined action of these sub-channels.

3. MMCICS Design Inspired from NES

3.1. MMCICS Structure Design

According to the bioinspired motion control approach, a novel multi-loop and multi-objective cooperative intelligent control system (MMCICS) is proposed to achieve intelligent coordination of position, velocity, and aceleration implemented by cooperation of several subchannels of plants, as shown in Figure 2.

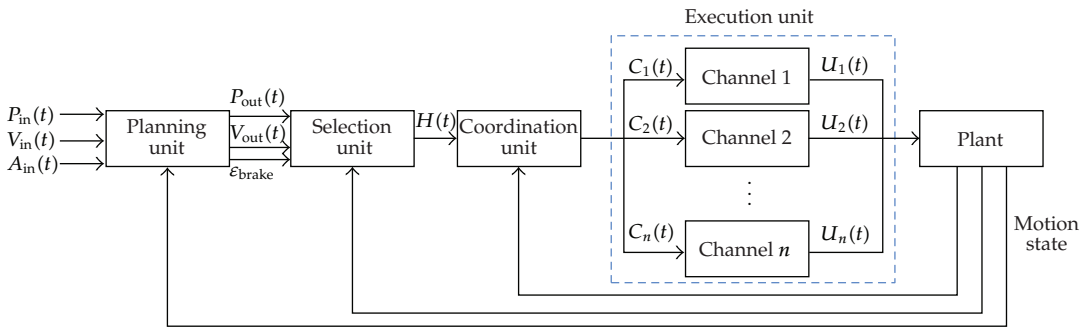

Figure 2: The structure of MMCICS.

3.2. Units Design of MMCICS

3.2.1. Planning Unit

The planning unit is primarily responsible for receiving and processing input signals of the position $P_{in}(t)$, the velocity $V_{in}(t)$, and the acceleration $A_{in}(t)$, and transmitting the desired position $P_{out}(t)$, the desired velocity $V_{out}(t)$, and the breaking factor ε_{brake} signals to the selection unit. The planning algorithm includes the automatic braking process and the cooperative planning process.

(1) Automatic braking process. The position error is defined as

$$e_{P1}(t) = P_{in}(t) - P(t). \tag{3.1}$$

When it satisfies

$$|e_{P1}(t)| \leq \varepsilon_{brake}, \tag{3.2}$$

the input velocity signal is changed automatically to

$$V_{in}(t) = 0, \tag{3.3}$$

where

$$\varepsilon_{brake} = \left| \frac{V^2(t_{brake})}{2A_{in}(t_{brake})} \right| \tag{3.4}$$

is the braking factor, t_{brake} is the initial time of the automatic braking process. The actual position signal $P(t)$ and the actual velocity signal $V(t)$ are obtained via ultra-long feedback.

(2) Cooperative planning process. Since acceleration is hardly to be controlled directly, the $V_{in}(t)$ and the $A_{in}(t)$ are regulated by the cooperative planning process while the $P_{in}(t)$ is sent to the selection unit directly. Some typical planning methods have good

results and have been used in practice for a long time. In order to test the control performance of the MMCICS more clearly, trapezoid curve method has been chosen in this paper. The algorithm can be described as

$$P_{\text{out}}(t) = P_{\text{in}}(t),$$
$$V_{\text{out}}(t) = \begin{cases} A_{\text{in}}(t) \cdot (t - t_{\text{up}}) + V(t_{\text{up}}), & t \in T_{\text{up}} \\ V_{\text{in}}(t), & t \in (T_{\text{up}} \cup T_{\text{down}})^c \\ V(t_{\text{down}}) - A_{\text{in}}(t) \cdot (t - t_{\text{down}}), & t \in T_{\text{down}}, \end{cases} \tag{3.5}$$

where

$$T_{\text{up}} = \{t \mid A_{\text{in}}(t) \cdot (t - t_{\text{up}}) + V_{\text{out}}(t_{\text{up}}) \leq V_{\text{in}}(t_{\text{up}})\},$$
$$T_{\text{down}} = \{t \mid V_{\text{out}}(t_{\text{down}}) - A_{\text{in}}(t) \cdot (t - t_{\text{down}}) \geq V_{\text{in}}(t_{\text{down}})\}, \tag{3.6}$$

where, t_{up} and t_{down} is the initial time when $V_{\text{in}}(t_{\text{up}}) > V_{\text{out}}(t_{\text{up}})$ and $V_{\text{in}}(t_{\text{down}}) < V_{\text{out}}(t_{\text{down}})$, respectively.

3.2.2. Selection Unit

The selection unit is designed as a switcher for the real-time dominant control mode. This unit receives the actual position feedback signal via long-loop feedback mechanism while the dominant motion control signal is transmitted to the coordination unit. Velocity-velocity control mode is on when the actual position is far from desired position while velocity control signal is sent to keep smooth movement. Position-velocity control mode takes over when the actual position is close to the desired position while position control signal is send to achieve accurate position. This rule for automatic switching is described as follows [6, 20]:

$$\text{strategy} = \begin{cases} \text{velocity-velocity}, & \mathbf{r} > \mathbf{r_c}, \\ \text{position-velocity}, & \mathbf{r} \leq \mathbf{r_c}, \end{cases} \tag{3.7}$$

where $\mathbf{r}$ is the distance between actual position and desired position, and $\mathbf{r_c}$ is a switcher distance which is decided by current state of plant and switching strategy. To guarantee smooth switch, a simple conversion factor K_c is also designed in the selection unit. The control algorithm can be designed as follows:

$$H(t) = \begin{cases} V_{\text{out}}(t), & |e_{P2}(t)| > \varepsilon_{\text{brake}} \cdot \eta_{\text{switch}} \\ e_{P2}(t) \cdot K_c, & |e_{P2}(t)| \leq \varepsilon_{\text{brake}} \cdot \eta_{\text{switch}}, \end{cases} \tag{3.8}$$

where

$$e_{P2}(t) = P_{\text{out}}(t) - P(t),$$
$$K_c = \frac{|V_{\text{out}}(t_{\text{switch}})|}{\varepsilon_{\text{brake}} \cdot \eta_{\text{switch}}}, \tag{3.9}$$

where $H(t)$ is the output of the selection unit, $e_{P2}(t)$ is the error signal between desired and actual position, $0\% < \eta_{\text{switch}} \leq 100\%$ is a switching coefficient which decides switching position, K_c is the conversion factor, and t_{switch} is the initial time of the switching process.

3.2.3. Coordination Unit

The coordination unit is a coordinator which sends cooperative control signals to each sub-channel of the plant. Many methods and mathematic models are suitable for this unit, the velocity Jacobian matrix is chosen in this paper due to the velocity control is our foremost object. In this scenario, all the input signals and output signals are regarded as the velocity signals whether the velocity-velocity control mode or the position-velocity control mode is selected. That output signals can be calculated by

$$[C_1(t), C_2(t), \ldots, C_n(t)]^T = J \cdot H(t), \tag{3.10}$$

where $C_i(t)$ is the ouput signal of the coordination unit to channel i, $(i = 1, 2, \ldots, n)$ of the execution unit, J is the velocity Jacobian matrix of the plant.

3.2.4. Execution Unit

The execution unit, which includes a number of sub-channels, is the core and key unit of the MMCICS. To keep sub-channels interact harmoniously and systematically, the same control method and control structure have been applied to each channel. As shown in Figure 3, each channel has its own independent control subsystem which includes a primary controller, a hormone regulation self-adaptive module (HRSM), and a controlled subpart of plant. There are two ultra-short loop feedbacks. One is that the actual velocity signal is fed back to the primary controller; the other is that the adjusted control parameters are fed back to the HRSM, which can improve the local and global control effectiveness.

Some advanced controllers widely used in industry can be applied as primary controller. The controller can obey PID control algorithm, fuzzy control algorithm [24, 25], H-infinity control algorithm [26, 27], and so forth. Due to their simpledescription, high-dependability, and satisfactory performances, in the MMCICS, the control law of primary controller obeys the conventional PID control algorithm

$$O_i(t) = Kp_i^0 \cdot e_i(t) + Ki_i^0 \cdot \int e_i(t)dt + Kd_i^0 \cdot \frac{de_i(t)}{dt}, \tag{3.11}$$

where

$$e_i(t) = C_i(t) - v_i(t) \tag{3.12}$$

is the error signal between the input signal $C_i(t)$ and the actual velocity $v_i(t)$ of the part i, $O_i(t)$ is the output of the primary controller, Kp_i^0, Ki_i^0, and Kd_i^0 are the initial PID parameters.

The HRSM is designed to improve primary controller self-adaptive performance. The regulation algorithm of HRSM is inspired from hormone regulation mechanism which includes identification and regulation processes.

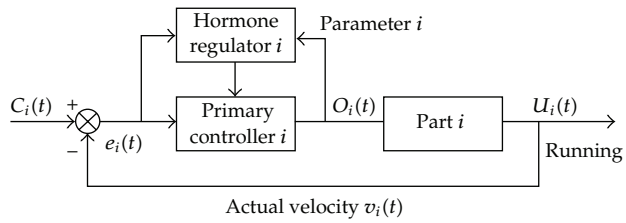

Figure 3: The structure of sub-channel.

(1) Identification. In NES, the gland can enhance identification and secretion precision within the working scope. However, when the stimulate signal beyond the control scope, hormone secretion rate is at its high limit. Similarly, the control error $e_i(t)$ in HRSM can be regarded as the stimulate signal, and its identification approach follows the principle of the hormone secretion. Therefore, the absolute value of control error $e_i(t)$ is calculated at first and then mapped to the correspond ding regulation scope. Hormone identification error $0 \leq E_i(t) \leq 1$ is defined as

$$E_i(t) = \begin{cases} \dfrac{|e_i(t)|}{e_{i\max} - e_{i\min}}, & |e_{\text{in}}(t)| < e_{i\max} - e_{i\min}, \\ 1, & |e_{\text{in}}(t)| \geq e_{i\max} - e_{i\min}, \end{cases} \tag{3.13}$$

where $e_{i\max}$ and $e_{i\min}$ are the high and low limited error of the optimal working scope, respectively.

(2) Regulation. The hormone secretion rate in NES is always nonnegative and monotone, and its secretion regulation mechanism usually follows the Hill functions, the growth curve, and so forth [13, 21]. Based on the Sigmoid function, a hormone regulation factor is designed to regulate primary controller parameter as

$$\alpha_i^j(t) = \frac{k_i^j}{1 + \left(k_i^j - 1\right) e^{-\beta_i^j((E_i(t)/\eta_i^j)-1)}}, \tag{3.14}$$

where $j = p, i, d$, $0\% < \eta_i^j \leq 100\%$ is the critical regulation coefficient, $k_i^j \geq 1$ is the high limited regulation coefficient, $0 < \beta_i^j \leq 10$ is the sensitivity regulation coefficient. These three coefficients joint control the function curve's slope. Where η_i^j decides the critical point between the up- and down-regulation, as

$$\begin{aligned} \alpha_i^j(t) &< 1, \quad E_i(t) < \eta_i^j, \\ \alpha_i^j(t) &= 1, \quad E_i(t) = \eta_i^j, \\ \alpha_i^j(t) &> 1, \quad E_i(t) > \eta_i^j. \end{aligned} \tag{3.15}$$

The k_i^j decides the high limited value. Because if $(E_i(t)/\eta_i^j) \gg 1$, then $e^{-\beta_i^j((E_i(t)/\eta_i^j)-1)} \to 0$ that $\alpha_i^j(t) \to k_i^j$. Meanwhile, it also should be noted that if $k_i^j = 1$, then $\alpha_i^j(t) = 1$. The β_i^j decides the response rate and has a major impact on the low limited value of $\alpha_i^j(t)$. When β_i^j is bigger, the $\alpha_i^j(t)$ curve changes acutely and the low limit of $\alpha_i^j(t)$ is lower; in contrast, the gentle changes results to higher low limit.

Then primary controller parameter can be regulated by its control characteristic. In the PID control algorithm, when the control error is too big, the proportion gain Kp_i^0 should decrease to weaken the control action, thus reduces the overshoot. In contrast, the proportion gain should increase to enhance control precision and eliminate control error quickly [20]. The correcting regulation of the integral coefficient Ki_i^0 and the differential coefficient Kd_i^0 are similar to that of the proportion gain. Therefore, the parameter regulation algorithm of the PID controller is

$$\begin{aligned} Kp_i(t) &= Kp_i^0/\alpha_i^p(t)Ki_i(t) \\ &= Ki_i^0 \cdot \alpha_i^i(t)Kd_i(t) \\ &= \frac{Kd_i^0}{\alpha_i^d(t)}. \end{aligned} \tag{3.16}$$

where, when $\alpha_i^p(t) > 1$, Kp_i^0 will be reduced; when $\alpha_i^p(t) < 1$, Kp_i^0 will be increased; when $\alpha_i^p(t) = 1$, Kp_i^0 will not be changed. Meanwhile, Ki_i^0 and Kd_i^0 have similar regulation characteristics. The regulation principle of the HRSM satisfies the optimization task and then (3.11) will be changed to optimized control law

$$O_i(t) = Kp_i(t) \cdot e_i(t) + Ki_i(t) \cdot \int e_i(t)dt + Kd_i(t) \cdot \frac{de_i(t)}{dt}, \tag{3.17}$$

where $Kp_i(t)$, $Ki_i(t)$, and $Kd_i(t)$ are optimized control parameters.

3.3. Parameters Tuning of MMCICS

(1) Tune the primary controller parameter. First, only take the primary controller into action, and then tune the initial control parameters Kp_i^0, Ki_i^0, and Kd_i^0 approximately.

(2) Determine the high and low limited hormone identification error. According to the response characteristics of the experimental results in step (1), determine the high limited error $e_{i\max}$ and low limited error $e_{i\min}$ of the optimal working scope.

(3) Tune the regulation coefficients of the hormone regulator. Take the execution unit into action, according to the response characteristic and overshoot of the experimental results, tune the critical regulation coefficient η_i^j to decide critical working point of the hormone regulator. And then when control error $e_i(t)$ is too big, tune the high limited regulation coefficient k_i^j to ensure a stable and faster movement of the plant with little or without overshoot. In contrast, tune the sensitivity regulation coefficient β_i^j to ensure accuracy and stability.

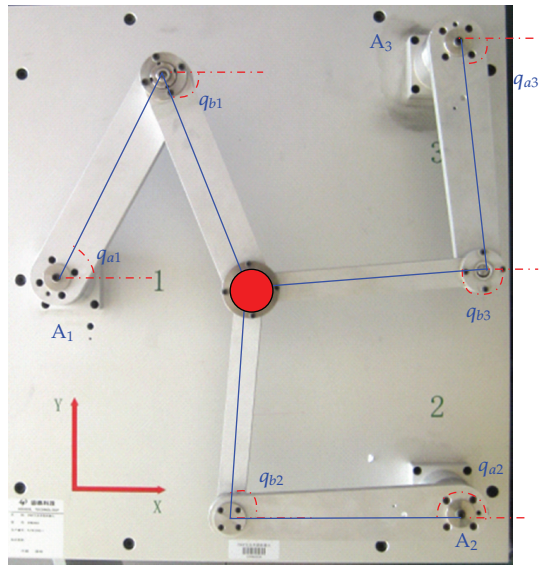

Figure 4: The 2-DOF redundant parallel manipulator.

(4) Determine the switching coefficient. Take the MMCICS into action and then determine the switching coefficient η_{switch} to ensure the control strategy switching smoothly.

4. Experimental Results and Analysis

Some typical experimental results are provided in this section to explore two main experiments of proposed MMCICS. Firstly, the control results with and without HRSM are compared to find out whether HRSM yields better in subchannel experiment. Next more comprehensive experiments are performed to verify multiobject cooperative control performance of the MMCICS, and whether HRSM has better global control effect.

As shown in Figure 4, a 2-DOF redundant parallel manipulator (Googol Tech Ltd.'s GPM2002) [28, 29] is selected as the experiment platform due to its complex redundancy structure and multi-channel inputs. Three bases of the manipulator are equipped with three AC servo motors with harmonic gear drives. The coordinates of three bases are $A_1(0, 250)$, $A_2(433, 0)$, and $A_3(433, 500)$, and all the links have the same length $l = 244$. The unit of coordinates and length is millimeter. Active joint angles are q_{a1}, q_{a2} and q_{a3}, and passive joint angles are q_{b1}, q_{b2} and q_{b3}. Position signals of the motors are measured with the absolute optical electrical encoders, and input voltage signals are controlled by a motion control board. All algorithms are implemented with Matlab/Simulink environment on an industrial controlling computer with a 2.8 GHz processor and 1024 MB memory. The real-time implementation is executed with the Real Time Workshop (RTW) of Matlab, and sampling period is 5 ms.

Firstly, to verify the effectiveness of the proposed HRSM in the execution unit, we only take active joint 1 (base A_1) without loads and links into action. The control performance of

the conventional PID controller and the PID controller with HRSM (HRSM-PID) are compared under the six different velocities of the servo motor 1, namely the motor of base A_1. To make the contrast effect more clearly, the conventional PID parameters are designed as the same as the initial PID parameters in HRSM-PID controller, as shown in Table 1.

Motor in sub-channel has different dynamic characteristics at different velocities but has similar results in the same parameter sets. Multiple experiments have the similar results, and a typical result is as shown in Figure 5(a), when motor is running at low velocities, the steady-state errors are obvious due to load influence. The HRSM-PID controller achieves better stabilities, higher accuracies, slightly faster dynamic responses, and lower or no overshoots, compared with the conventional PID controller. Figure 5(b) shows that when running at high velocities, the motor has better motion performance and spends more times to achieve higher velocity. HRSM-PID controller achieves significantly faster dynamic responses compared with the PID controller. Figure 5(c) shows a typical output control signal $O_1(t)$ when input velocity step is 5. As the expected, when the error is too big, the HRSM decreases the output control signals to reduce the overshoot. In contrast, the output control signals are increased to enhance control precision and eliminate control error quickly. With such strong self- adaptability, the HRSM improves the dynamic performances. The detailed lower quartile, median, upper quartile, average, and variance of the 10 time's results are shown in Table 2. Where, V_d is the desired velocity, t_s is the settling time, σ is the overshoot, and |ess| is the absolutely value of steady-state error. The sub-channel experimental results show that based on hormone regulation mechanism, the HRSM owns strong self-adaptability that improves the response, accuracy, and stability of the subchannel.

To verify the multiobject cooperative control performance of the MMCICS, the end-effector of the redundant parallel manipulator is viewed as a controlled plant, and three active joints are viewed as three subchannels. The velocity Jacobian matrix between the end-effector and three active joints is

$$J = \frac{1}{l}\begin{pmatrix} \dfrac{\cos q_{b1}}{\sin(q_{b1}-q_{a1})} & \dfrac{\sin q_{b1}}{\sin(q_{b1}-q_{a1})} \\ \dfrac{\cos q_{b2}}{\sin(q_{b2}-q_{a2})} & \dfrac{\sin q_{b2}}{\sin(q_{b2}-q_{a2})} \\ \dfrac{\cos q_{b3}}{\sin(q_{b3}-q_{a3})} & \dfrac{\sin q_{b3}}{\sin(q_{b3}-q_{a3})} \end{pmatrix}. \tag{4.1}$$

Due to the complex mechanism structure of the parallel manipulator with actuation redundancy, it is a typical nonlinear system and difficult to get the accurate dynamic and friction model [28, 29]. Although the manipulator has different dynamic characteristics in different positions, velocities, and accelerations, the proposed MMCICS can overcome accurate mathematical model problem. To verify the control performance of the MMCICS more thoroughly and whether the HRSM also achieves better control effectiveness in the proposed MMCICS, many different experiments were tested and have similar results. A representative contrast experimental result is shown in Figure 6, where the MMCICS without HRSM is chosen as contrast control system (CCS). The experiments are implemented with the same input signals and control parameters. The starting position, input goal position, and input

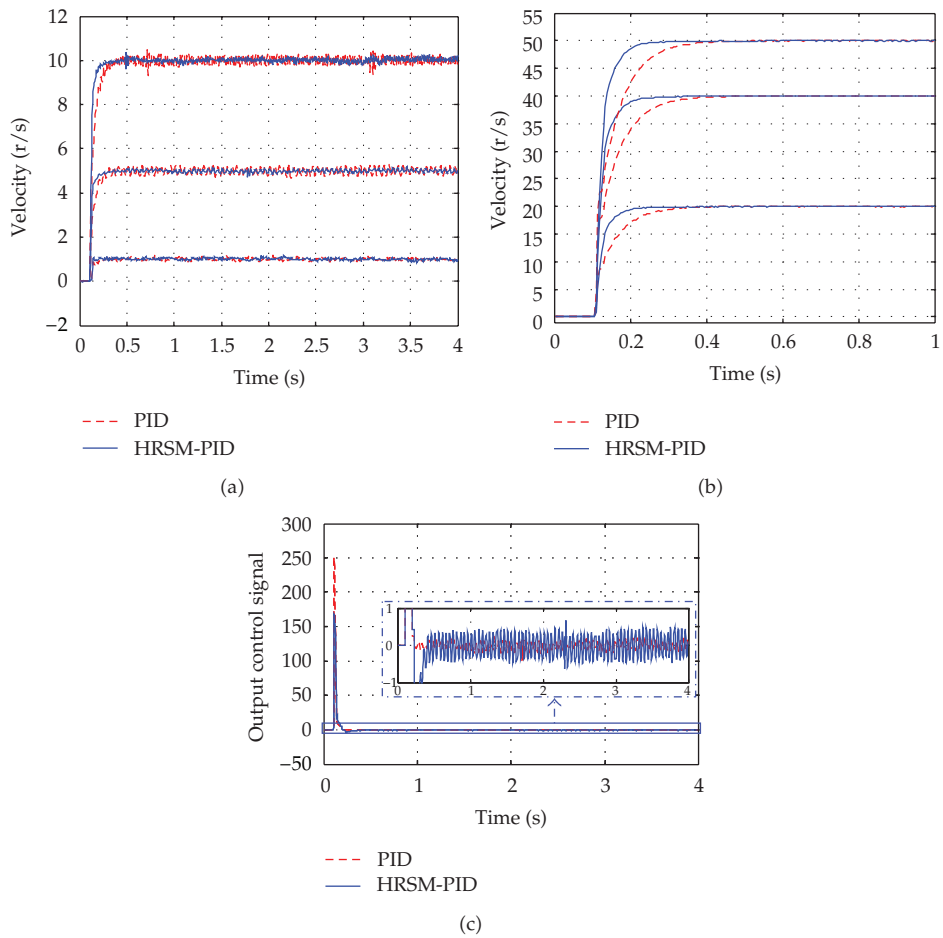

Figure 5: Contrast effect of the velocity control. (a) Low velocity control, (b) high velocity control. (c) Output control signal.

acceleration are $[216.5, 250]^T$, $[316.5, 350]^T$, and $[1500, 1500]^T$, respectively. The input velocity signal is

$$\begin{aligned} V_{\text{in}}(t) &= [0, 0]^T, \quad t \geq 0s \\ V_{\text{in}}(t) &= [100, 100]^T, \quad t \geq 0.1s \\ V_{\text{in}}(t) &= [300, 300]^T, \quad t \geq 3.5s. \end{aligned} \tag{4.2}$$

The switching coefficient is $\eta_{\text{switch}} = [20\%, 20\%]^T$ in selection unit, and control parameters in channel 1, 2, and 3 are the same as in Table 1. Similarly, the parameters of CCS are the same as MMCICS.

As shown in Figures 6(a) and 6(b), MMCICS achieves a faster response, better stability, and higher accuracy of velocity control compared with CCS. Especially, when the manipulator is running at high velocities, it is hard to achieve object velocity using CCS, due to

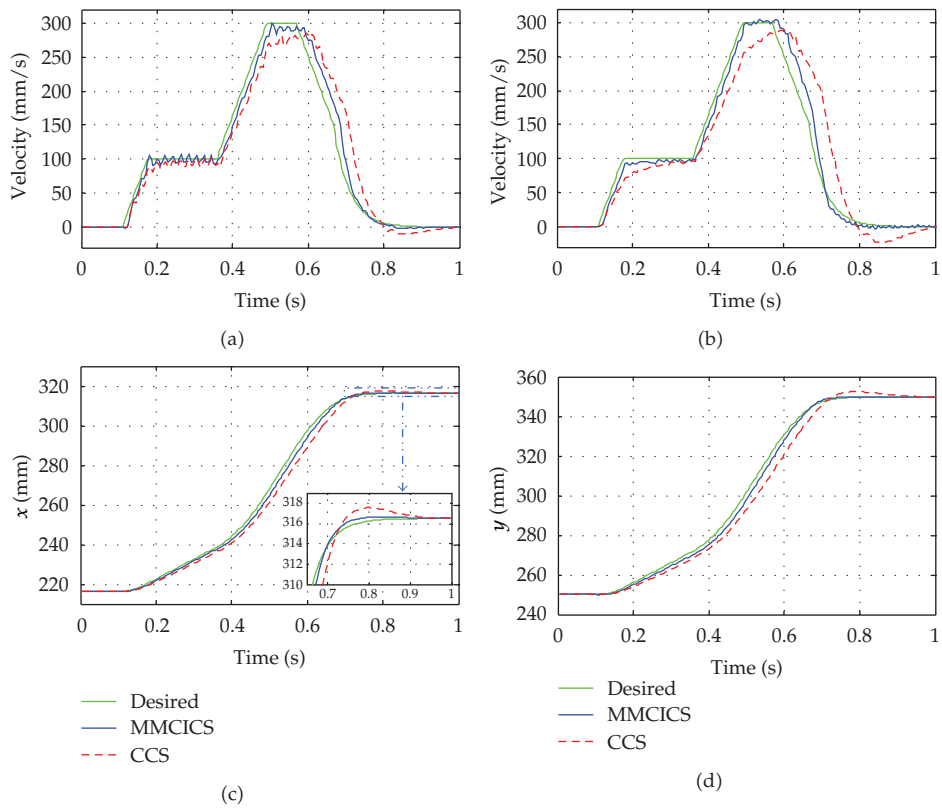

Figure 6: Multichannel control experimental results. (a) X-direction velocity. (b) Y-direction velocity. (c) X-direction position. (d) Y-direction position.

Table 1: Parameter set.

Initial PID	Error factors	Hormone regulation factors
$Kp_i^0 = 0.03$	$e_{i\max} = 1\,\mathrm{r/s}$	$k_i^p = 5$, $\beta_i^p = 1.2$, $\eta_i^p = 20\%$
$Ki_i^0 = 0.004$	$e_{i\min} = -1\,\mathrm{r/s}$	$k_i^i = 5$, $\beta_i^i = 1.2$, $\eta_i^i = 15\%$
$Kd_i^0 = 0.005$		$k_i^d = 3$, $\beta_i^d = 1$, $\eta_i^d = 10\%$

complex plan structure and big load. However, MMCICS still maintains high performance as low velocity process. From the velocity response during the ascent, it's easy to find that the MMCICS has more stable acceleration response than CCS does. That means, based on the HRSM, the cooperative planning algorithm in the planning unit can be implemented easier for acceleration control. Moreover, during control strategy switching, CCS always has a significant negative overshoot of the velocity in braking process. In contrast, MMCICS can stop quickly with little or no negative overshoot due to its strong adaptability. Compared with Figures 6(a) and 6(b), we can find that, due to uneven distribution of loads, the CCS performance in Y-direction is worse than X-direction. However, MMCICS can overcome this problem, since its local self-adaptability improves the global self-adaptability.

Figures 6(c) and 6(d) shows that due to faster, more stable, and accurate velocity response, the MMCICS can achieve better position accuracy compared with the CCS. In the braking process, because of its better adaptability when control strategy is switched from

Table 2: Performance evaluation for subchannel experiment.

V_d (r/s)		1		5		10		20		40		50	
		HRSM PID	PID	HRSM PID	PID	HRSM PID	PID	HRSM PID	PID	HRSM PID	PID	HRSM PID	PID
t_s(s)	Lower quartile	0.0475	0.1575	0.18	0.2275	0.25	0.32	0.3	0.3575	0.32	0.4275	0.3575	0.48
	Median	0.06	0.175	0.2	0.245	0.265	0.33	0.32	0.375	0.33	0.43	0.38	0.5
	Upper quartile	0.0725	0.185	0.22	0.2525	0.285	0.3525	0.34	0.385	0.3525	0.4525	0.4	0.54
	Average	0.061	0.175	0.201	0.246	0.272	0.335	0.324	0.37	0.336	0.439	0.379	0.506
	Variance	0.000309	0.000445	0.000369	0.000484	0.000496	0.000445	0.000384	0.00052	0.000524	0.000589	0.000609	0.000964
σ(r/s)	Lower quartile	0.06	0.095	0.0375	0.1675	0.04	0.16	0.02	0.0575	0.0175	0.04	0.01	0.03
	Median	0.08	0.12	0.04	0.185	0.055	0.19	0.04	0.075	0.02	0.045	0.02	0.04
	Upper quartile	0.1	0.14	0.06	0.225	0.0775	0.22	0.05	0.1	0.04	0.06	0.025	0.0525
	Average	0.079	0.12	0.049	0.195	0.11	0.192	0.038	0.077	0.024	0.049	0.021	0.045
	Variance	0.000449	0.00064	0.000449	0.001165	0.027	0.000736	0.000176	0.000501	0.000124	0.000249	0.000109	0.000225
|ess| (r/s)	Lower quartile	0.05	0.08	0.08	0.215	0.06	0.195	0.04	0.08	0.03	0.06	0.02	0.0475
	Median	0.06	0.105	0.1	0.245	0.08	0.22	0.05	0.1	0.04	0.065	0.035	0.06
	Upper quartile	0.085	0.12	0.1275	0.2525	0.085	0.2575	0.0625	0.12	0.045	0.08	0.04	0.08
	Average	0.068	0.102	0.103	0.237	0.078	0.225	0.052	0.099	0.04	0.066	0.033	0.063
	Variance	0.000576	0.000656	0.000921	0.001021	0.000376	0.001705	0.000256	0.000609	0.00014	0.000144	0.000181	0.000321

Table 3: Performance evaluation for comprehensive experiment.

	Positon		Veloctiy		
	Final error	Settling time	Error		Braking overshoot
			$V_{\text{in}}(t) = [100, 100]^T$	$V_{\text{in}}(t) = [300, 300]^T$	
MMCICS	$[0.02, 0.05]^T$	0.82 s	$[6.62, 7.50]^T$	$[7.22, 5.64]^T$	$[2.41, 3.13]^T$
CCS	$[0.05, 0.22]^T$	1.07 s	$[13.82, 18.20]^T$	$[32.2, 52.06]^T$	$[10.25, 25.20]^T$

the velocity-velocity control to the position-velocity control, the MMCICS has a faster position response, which makes position stable with lower overshoot or no overshoot.

Some compare results of the 10 time's average absolute values are shown in Table 3. The experimental results show that, with the planning algorithm in the planning unit, the soft switching algorithm in the selection unit, and the velocity cooperative control in the coordination unit, both MMCICS and CCS take advantages of position control and velocity control, and achieve cooperative control for position, velocity and acceleration. Particularly, with strong self-adaptability, faster response, and better stability of HRSM, control potentials of the MMCICS are exploited more thoroughly. The MMCICS achieves multi-objective cooperative intelligent control with higher performance even at high velocities and accelerations, for a nonlinear multi-input complex plant without accurate dynamics model.

5. Conclusions

This work presents a bioinspired cooperative intelligent control system for position, velocity, and acceleration multi-objective integrated control of a parallel plant. The similarity between the NES and motion control system revealed, and a bio-inspired motion control approach is proposed. Under the context of such approach, the MMCICS with system structure, algorithm, and steps in parameter tuning is proposed to achieve multiobjective control. The experiments are carried out with a 2-DOF redundant parallel manipulator where the feasibility of the new control system is demonstrated. The contrast effect shows that the stability, accuracy, adaptability, response rate of the proposed MMCICS is superior to those of the conventional controllers. According to our knowledge, this is the first time that NES-based MMCICS and HRSM are proposed and used for an actual parallel manipulator. The proposed MMCICS can be implemented easily and provides a new and efficient method for multiobjective integrated control of complex multichannel systems. In future works, force and torque control will be considered to establish a more complete multi-objective control system. More rigorous and advanced algorithm and proof are required instead of the PID controller. Besides, parameter optimization, dynamics, and stability analysis can be conducted on MMCICS.

Acknowledgments

This work was supported in part by the Key Project of the National Natural Science Foundation of China (No. 61134009), the National Natural Science Foundation of China (no. 60975059), Support Research Project of National ITER Program (no. 2010GB108004), Specialized Research Fund for the Doctoral Program of Higher Education from Ministry of Education of China (no. 20090075110002), Project of the Shanghai Committee of Science and Technology (Nos. 11XD1400100, 11JC1400200, 10JC1400200, and 10DZ0506500).

References

[1] D. Zhang and Z. Gao, "Optimal kinematic calibration of parallel manipulators with pseudoerror theory and cooperative coevolutionary network," *IEEE Transactions on Industrial Electronics*, vol. 59, no. 8, pp. 3221–3231, 2012.

[2] H. Dong, Z. Wang, and H. Gao, "Distributed filtering for a class of time-varying systems over sensor networks with quantization errors and successive packet dropouts," *IEEE Transactions on Signal Processing*, vol. 60, no. 6, pp. 3164–3173, 2012.

[3] Z. Wang, H. Zeng, D. W. C. Ho, and H. Unbehauen, "Multiobjective control of a four-link flexible manipulator: a robust H_∞ approach," *IEEE Transactions on Control Systems Technology*, vol. 10, no. 6, pp. 866–875, 2002.

[4] B. Shen, Z. Wang, and X. Liu, "A stochastic sampled-data approach to distributed H_∞ filtering in sensor networks," *IEEE Transactions on Circuits and Systems. I*, vol. 58, no. 9, pp. 2237–2246, 2011.

[5] A. Khoukhi, "Data-driven multi-stage motion planning of parallel kinematic machines," *IEEE Transactions on Control Systems Technology*, vol. 18, no. 6, pp. 1381–1389, 2010.

[6] Z. Sun, R. Xing, C. Zhao, and W. Huang, "Fuzzy auto-tuning PID control of multiple joint robot driven by ultrasonic motors," *Ultrasonics*, vol. 46, no. 4, pp. 303–312, 2007.

[7] K. Pathak, J. Franch, and S. K. Agrawal, "Velocity and position control of a wheeled inverted pendulum by partial feedback linearization," *IEEE Transactions on Robotics*, vol. 21, no. 3, pp. 505–513, 2005.

[8] M. S. Tsai, H. W. Nien, and H. T. Yau, "Development of integrated acceleration/deceleration look-ahead interpolation technique for multi-blocks NURBS curves," *International Journal of Advanced Manufacturing Technology*, vol. 56, no. 5–8, pp. 601–618, 2011.

[9] S. Mitra and Y. Hayashi, "Bioinformatics with soft computing," *IEEE Transactions on Systems, Man, and Cybernetics Part A*, vol. 36, no. 5, pp. 616–635, 2006.

[10] W. Savino and M. Dardenne, "Neuroendocrine control of thymus physiology," *Endocrine Reviews*, vol. 21, no. 4, pp. 412–443, 2000.

[11] E. B. Stear, "Application of control theory to endocrine regulation and control," *Annals of Biomedical Engineering*, vol. 3, no. 4, pp. 439–455, 1975.

[12] D. M. Keenan, J. Licinio, and J. D. Veldhuis, "A feedback-controlled ensemble model of the stress-responsive hypothalamo-pituitary-adrenal axis," *Proceedings of the National Academy of Sciences of the United States of America*, vol. 98, no. 7, pp. 4028–4033, 2001.

[13] L. S. Farhy, "Modeling of oscillations in endocrine networks with feedback," *Methods in Enzymology*, vol. 384, pp. 54–81, 2004.

[14] M. Neal and J. Timmis, "Timidity: a useful emotional mechanism for robot control?" *Informatica*, vol. 27, no. 2, pp. 197–204, 2003.

[15] P. Vargas, R. Moioli, L. N. d. Castro, J. Timmis, M. Neal, and F. J. V. Zuben, "Artificial homeostatic system: a novel approach," in *Advances in Artificial Life*, vol. 3630 of *Lecture Notes in Computer Science*, pp. 754–764, 2005.

[16] F. M. Córdova and L. R. Cañete, "The challenge of designing nervous and endocrine systems in robots," *International Journal of Computers, Communications & Control*, vol. 1, no. 2, pp. 33–40, 2006.

[17] B. Liu, L. Ren, and Y. Ding, "A novel intelligent controller based on modulation of neuroendocrine system," in *Proceedings of the 2nd International Symposium on Neural Networks: Advances in Neural Networks (ISNN'05)*, pp. 119–124, June 2005.

[18] Y. S. Ding and B. Liu, "An intelligent bi-cooperative decoupling control approach based on modulation mechanism of internal environment in body," *IEEE Transactions on Control Systems Technology*, vol. 19, no. 3, pp. 692–698, 2011.

[19] D. Tang, W. Gu, L. Wang, and K. Zheng, "A neuroendocrine-inspired approach for adaptive manufacturing system control," *International Journal of Production Research*, vol. 49, no. 5, pp. 1255–1268, 2011.

[20] C. Guo, K. Hao, Y. Ding, X. Liang, and Y. Dou, "A position-velocity cooperative intelligent controller based on the biological neuroendocrine system," in *Advances in Neural Networks—ISNN 2011*, vol. 6677 of *Lecture Notes in Computer Science*, pp. 112–121, 2011.

[21] C. E. Cortés, D. Sáez, F. Milla, A. Núñez, and M. Riquelme, "Hybrid predictive control for real-time optimization of public transport systems' operations based on evolutionary multi-objective optimization," *Transportation Research Part C*, vol. 18, no. 5, pp. 757–769, 2010.

[22] M. F. Prummel, L. J. S. Brokken, and W. M. Wiersinga, "Ultra short-loop feedback control of thyrotropin secretion," *Thyroid*, vol. 14, no. 10, pp. 825–829, 2004.

[23] X. Liang, Y. S. Ding, L. H. Ren, K. R. Hao, H. P. Wang, and J. J. Chen, "A bioinspired multilayered intelligent cooperative controller for stretching process of fiber production," *IEEE Transactions on Systems, Man and Cybernetics Part C*, vol. 42, no. 3, pp. 367–377, 2012.

[24] R. E. Precupa and H. Hellendoornb, "A survey on industrial applications of fuzzy control," *Computers in Industry*, vol. 62, no. 3, pp. 213–226, 2011.

[25] H. Dong, Z. Wang, D. W. C. Ho, and H. Gao, "Robust H_∞ fuzzy output-feedback control with multiple probabilistic delays and multiple missing measurements," *IEEE Transactions on Fuzzy Systems*, vol. 18, no. 4, pp. 712–725, 2010.

[26] Z. Wang, B. Shen, H. Shu, and G. Wei, "Quantized H_∞ control for nonlinear stochastic time-delay systems with missing measurements," *IEEE Transactions on Automatic Control*, vol. 7, no. 6, pp. 1431–1444, 2012.

[27] Z. Wang, B. Shen, and X. Liu, "H_∞ filtering with randomly occurring sensor saturations and missing measurements," *Automatica*, vol. 48, no. 3, pp. 556–562, 2012.

[28] W. Shang and S. Cong, "Nonlinear computed torque control for a high-speed planar parallel manipulator," *Mechatronics*, vol. 19, no. 6, pp. 987–992, 2009.

[29] W. Shang, S. Cong, and F. Kong, "Identification of dynamic and friction parameters of a parallel manipulator with actuation redundancy," *Mechatronics*, vol. 20, no. 2, pp. 192–200, 2010.

Hindawi Publishing Corporation
Mathematical Problems in Engineering
Volume 2012, Article ID 696742, 15 pages
doi:10.1155/2012/696742

Research Article

Probability-Dependent Static Output Feedback Control for Discrete-Time Nonlinear Stochastic Systems with Missing Measurements

Wangyan Li, Guoliang Wei, and Licheng Wang

Department of Control Science and Engineering, University of Shanghai for Science and Technology, Shanghai 200093, China

Correspondence should be addressed to Guoliang Wei, guoliang.wei1973@gmail.com

Received 21 June 2012; Accepted 2 August 2012

Academic Editor: Zidong Wang

This paper is devoted to the problems of gain-scheduled control for a class of discrete-time stochastic systems with infinite-distributed delays and missing measurements by utilizing probability-dependent Lyapunov functional. The missing-measurement phenomenon is assumed to occur in a random way, and the missing probability is time varying with securable upper and lower bounds that can be measured in real time. The purpose is to design a static output feedback controller with scheduled gains such that, for the admissible random missing measurements, time delays, and noises, the closed-loop system is exponentially mean-square stable. At last, a simulation example is exploited to illustrate the effectiveness of the proposed design procedures.

1. Introduction

Gain-scheduling is one of the most popular methods of controller design and has been extensively applied in engineering, such as rotation speed control of engine, aircraft control and process control. Over the past decades, the gain-scheduled control problem has been extensively studied both from theoretical and practical viewpoint, see, for example, [1–6]. For the controller design problems for parameter-varying systems, the gain-scheduling approach has been found to be one of the most effective ones, whose main idea is to design controller gains as functions of the scheduling parameters, which are supposed to be available in real time and, therefore, have much less conservatism than the conventional ones.

On the other hand, instead of using the information of system states, static output feedback (SOF) control directly makes use of system outputs to design controllers, which has also attracted attentions of many researchers over the past two decades, see, for

example, [7–12]. It is obvious that the structure of SOF controllers is simple and easy to implement. However, to the best of the authors' knowledge, there has been little research attention on the control problem for discrete-time nonlinear stochastic systems with a missing phenomenon based on the time-varying occurring probability by a gain-scheduling method.

The missing-measurement phenomenon, due to various reasons such as probabilistic network congestion and intermittent mechanical failures, usually occurs in many real-world systems, which has attracted considerable attention during the past few years, see, for example, [13–15]. The Bernoulli distribution has been successfully applied to model this phenomenon, in which 0 is used to stand for an entire signal missing and 1 denotes the intactness (i.e., there is no signal missing at all), and all sensors have the same missing probability, which is simple and effective and has become very popular during the past years, see, for example, [5, 13, 14, 16]. However, in the practical systems, the occurring probability of the missing-measurement phenomenon might be time varying; consequently, a time-varying Bernoulli distribution model is more suitable for such parameter-varying systems.

In another aspect, considering the signal propagation often distributed during a certain time period, then, a new kind of delays, namely, distributed time-delays, has drawn many researchers' attention, see, for example, [17–22], but most of the existing works on distributed delays have focused on continuous-time systems which are described either in the form of finite or infinite integral. As we all know, when it comes to implementing the control laws in a digital way, the discrete-time system is much better than continuous-time one. Naturally, it turns out to be meaningful to investigate the issue of how distributed delays influence the dynamical behavior of a discrete-time system. However, as far as authors know, based on gain-scheduled control methods, the SOF control problem for nonlinear stochastic systems with infinite-distributed delays and missing measurements with time-varying occurring probability has not been addressed yet and is still a very interesting and challenging problem.

The main contributions of this paper are summarized as follows: (1) a new SOF control problem is addressed for a class of discrete-time nonlinear stochastic systems with missing measurements and infinite-distributed delays via a gain-scheduling approach; (2) a sequence of stochastic variables satisfying Bernoulli distributions is introduced to describe the time-varying features of the missing measurements in the sensor; (3) a time-varying Lyapunov functional dependent on the missing probability is proposed and then applied to improve the performance of the gain-scheduled controller; and (4) a gain-scheduled controller is designed, in which the controller parameters can be adjusted online according to the missing probabilities estimated through statistical tests.

Notation 1. In this paper, $\mathbb{R}^n$, $\mathbb{R}^{n\times m}$, and $\mathbb{I}^+$ denote, respectively, the n-dimensional Euclidean space, and the set of all $n \times m$ real matrices, the set of all positive integers. $|\cdot|$ refers to the Euclidean norm in $\mathbb{R}^n$. I denotes the identity matrix of compatible dimension. The notation $X \geq Y$ (resp., $X > Y$), where X and Y are symmetric matrices, means that $X - Y$ is positive semidefinite (resp., positive definite). For a matrix M, M^T and M^{-1} represent its transpose and inverse, respectively. The shorthand $\mathrm{diag}\{M_1, M_2, \ldots, M_n\}$ denotes a block diagonal matrix with diagonal blocks being the matrices $M_1, M_2, \ldots, M_n$. In symmetric block matrices, the symbol $*$ is used as an ellipsis for terms induced by symmetry. Matrices, if they are not explicitly stated, are assumed to have compatible dimensions. In addition, $\mathbb{E}\{x\}$ and $\mathrm{Prob}\{y\}$ will, respectively, mean expectation of x and probability of y.

2. Problem Formulation

Consider the following discrete-time nonlinear stochastic systems with infinite-distributed delays:

$$x(k+1) = Ax(k) + Bu(k) + D\sum_{d=1}^{+\infty}\mu_d x(k-d) + Nf(z(k)) + Ex(k)w(k), \tag{2.1}$$

$$x(k) = \rho(k), \quad k = -d, -d+1, \ldots, 0, \tag{2.2}$$

where $x(k) \in \mathbb{R}^n$ is the state, $z(k) := Gx(k) + G_d \sum_{d=1}^{+\infty} \mu_d x(k-d)$. $\omega(k)$ is a one-dimensional Gaussian white noise sequence satisfying $\mathbb{E}\{\omega(k)\} = 0$ and $\mathbb{E}\{\omega^2(k)\} = \sigma^2$, $\rho(k)$ is the initial state of the system. A, B, D, N, E, G, and G_d are constant real matrices of appropriate dimensions and B is of full-column rank.

The nonlinear function $f(\cdot)$ with $(f(0) = 0)$ is assumed as nonlinear disturbances and satisfies the following sector-bounded condition:

$$\left[f(z(k)) - F_1 z(k)\right]^T \left[f(z(k)) - F_2 z(k)\right] \leq 0, \tag{2.3}$$

where $f(\cdot)$ is called to belong to the sector $[F_1, F_2]$ and F_1 and F_2 are given constant real matrices.

For the technique convenience, the nonlinear function $f(z(k))$ can be decomposed into a linear and a nonlinear part as

$$f(z(k)) = f_s(z(k)) + F_1 z(k), \tag{2.4}$$

then, from (2.3), we have

$$f_s^T(z(k))\left(f_s(z(k)) - Fz(k)\right) \leq 0, \tag{2.5}$$

where $F = F_2 - F_1 > 0$.

On the other hand, $\mu_d \geq 0$ is the convergence constant that satisfies the following condition:

$$\sum_{d=1}^{+\infty}\mu_d \leq \sum_{d=1}^{+\infty} d\mu_d < +\infty. \tag{2.6}$$

Remark 2.1. The distributed delay is one important type of time delays and has been widely recognized and intensively studied, see, for example, [17–22]. The delay term $\sum_{d=1}^{+\infty} \mu_d x(k-d)$ in the resulted stochastic system (2.1) called infinitely distributed delay. However, almost all existing references concerning distributed delays are concerned with the continuous-time systems, where the distributed delays are described in the form of a finite or infinite integral. In this paper, the constants μ_d $(d = 1, 2, \ldots)$ are assumed to satisfy the convergence conditions (2.6), which can guarantee the convergence of the terms of infinite delays as well as the Lyapunov-Krasovskii functional defined later.

The measurement output with missing sensor data is described as

$$y(k) = \xi(k)Cx(k), \tag{2.7}$$

where C is a constant real matrix of appropriate dimensions and $\xi(k) \in \mathbb{R}$ is a random white sequence characterizing the probabilistic sensor-data missing, which obeys the following time-varying Bernoulli distribution:

$$\begin{aligned} \operatorname{Prob}\{\xi(k) = 1\} &= \mathbb{E}\{\xi(k)\} = p(k), \\ \operatorname{Prob}\{\xi(k) = 0\} &= 1 - \mathbb{E}\{\xi(k)\} = 1 - p(k), \end{aligned} \tag{2.8}$$

where $p(k)$ is a time-varying positive scalar sequence and belongs to $[p_1\ p_2] \subseteq [0\ 1]$ with p_1 and p_2 being the lower and upper bounds of $p(k)$, respectively. In this paper, for simplicity, we assume that $\xi(k)$, $\omega(k)$ and $\rho(k)$ are uncorrelated.

Remark 2.2. In (2.7), a random white sequence satisfying the time-varying Bernoulli distribution is introduced to reflect the missing-measurement phenomenon that has attracted considerable attention in the past few years, see, for example, [13–15]. However, the missing probability in most relevant literatures has always been assumed to be a constant. Such an assumption, unfortunately, tends to be conservative in handling time-varying missing measurements. In this paper, the missing probability is allowed to be time-varying with known lower and upper bounds, which will then be used to schedule controller gains, thereby reducing the possible conservatism.

In this paper, we are interested in designing the following gain-scheduled controller:

$$u(k) = K(p)y(k), \tag{2.9}$$

where $K(p)$ is the controller gain sequence to be designed and assumed as the following structure:

$$K(p) = K_0 + p(k)K_u, \tag{2.10}$$

for every time step k, $p(k)$ is the time-varying parameter of the controller gain, which takes value in $[p_1, p_2]$ and K_0, K_u are the constant parameters of the controller gain to be designed.

The closed-loop system of the static output feedback gain-scheduled controller is as follows:

$$x(k+1) = Ax(k) + \xi(k)BK(p)Cx(k) + D\sum_{d=1}^{+\infty}\mu_d x(k-d) + Nf(z(k)) + Ex(k)w(k). \tag{2.11}$$

Before formulating the problem to be investigated, we first introduce the following stability concepts.

Definition 2.3. The closed-loop system (2.11) is said to be exponentially mean-square stable if, with $w(k) = 0$, there exist constants $\alpha > 0$ and $\tau \in (0,1)$ such that

$$\mathbb{E}\left\{\|\eta(k)\|^2\right\} \leq \alpha\tau^k \sup_{-d\leq i\leq 0} \mathbb{E}\left\{\|\eta(i)\|^2\right\}, \quad k \in \mathbb{I}^+. \tag{2.12}$$

In this paper, our purpose is to design a probability-dependent gain-scheduled controller of the form (2.9) for the system (2.1) by exploiting a probability-dependent Lyapunov functional and LMI method such that, for all admissible infinite-distributed delays, missing measurements with time-varying probability, and exogenous stochastic noises, the closed-loop system (2.11) is exponentially mean-square stable.

3. Main Results

The following lemmas will be used in the proofs of our main results in this paper.

Lemma 3.1 ([Schur complement] see[23]). *Given constant matrices $\Sigma_1, \Sigma_2, \Sigma_3$ where $\Sigma_1 = \Sigma_1^T$ and $0 < \Sigma_2 = \Sigma_2^T$, then $\Sigma_1 + \Sigma_3^T\Sigma_2^{-1}\Sigma_3 \geq 0$ if and only if*

$$\begin{bmatrix} \Sigma_1 & \Sigma_3^T \\ \Sigma_3 & -\Sigma_2 \end{bmatrix} \geq 0 \quad or \quad \begin{bmatrix} -\Sigma_2 & \Sigma_3 \\ \Sigma_3^T & \Sigma_1 \end{bmatrix} \geq 0. \tag{3.1}$$

Lemma 3.2 (see [24]). *Let $M \in \mathbb{R}^{n\times n}$ be a positive semidefinite matrix, $x_i \in \mathbb{R}^n$ and constant $a_i > 0$ $(i = 1, 2, \ldots)$. If the series concerned is convergent, then one has*

$$\left(\sum_{i=1}^{\infty} a_i x_i\right)^T M \left(\sum_{i=1}^{\infty} a_i x_i\right) \leq \left(\sum_{i=1}^{\infty} a_i\right) \sum_{i=1}^{\infty} a_i x_i^T M x_i. \tag{3.2}$$

Lemma 3.3 (see [25]). *Let the matrix $B \in R^{n\times m}$ be of full-column rank. There always exist two orthogonal matrices $U \in R^{n\times n}$ and $V \in R^{n\times n}$ such that*

$$\begin{gathered} B = U \begin{bmatrix} \Sigma \\ 0 \end{bmatrix} V^T, \\ \Sigma = \operatorname{diag}\{\sigma_1, \sigma_2, \ldots, \sigma_m\}. \end{gathered} \tag{3.3}$$

If matrix S has the following structure:

$$S = U \begin{bmatrix} S_{11} & S_{12} \\ 0 & S_{22} \end{bmatrix} U^T, \tag{3.4}$$

where $S_{11} \in R^{n\times m}$, $S_{12} \in R^{n\times(n-m)}$, $S_{22} \in R^{(n-m)\times(n-m)}$, then there exists a nonsingular matrix $R \in R^{m\times m}$ such that $SB = BR$.

In the following theorem, a probability-dependent gain-scheduled static output feedback control problem is dealt with for a class of discrete-time nonlinear stochastic systems

(2.1) by exploiting Lyapunov theory and LMI method. A sufficient condition is derived to guarantee the solvability of the desired gain-scheduled control problem and, simultaneously, the parameters of the gain-scheduled controller can be obtained by solving the LMIs and the measured time-varying probability.

Theorem 3.4. *Consider the discrete-time nonlinear stochastic systems* (2.11). *If there exist positive-definite matrices $Q(p(k))$ and Q_τ, slack matrix S and nonsingular matrices $Y(p)$ and R, such that the following LMIs hold:*

$$\begin{bmatrix} \overline{\mu}Q_\tau - Q(p(k)) & * & * & * & * & * \\ 0 & -\frac{1}{\overline{\mu}}Q_\tau & * & * & * & * \\ FG & FG_d & -2I & * & * & * \\ S^T\overline{A} + p(k)BY(p)C & S^T\overline{D} & S^TN & -\overline{\Lambda} & * & * \\ \sigma^2 S^T E & 0 & 0 & 0 & -\sigma^2\overline{\Lambda} & * \\ \Delta_p(k)BY(p)C & 0 & 0 & 0 & 0 & -\Delta_p(k)\overline{\Lambda} \end{bmatrix} < 0, \tag{3.5}$$

where

$$\begin{gathered} \overline{\Lambda} = -Q(p(k+1)) + S + S^T, \qquad \overline{\mu} = \sum_{d=1}^{+\infty}\mu_d, \qquad \Delta_P(k) = P(k)(1-P(k)), \\ \overline{A} = A + NF_1G, \qquad \overline{D} = D + NF_1G_d, \\ S^TB = BR, \qquad RK(p) = Y(p), \qquad K(p) = R^{-1}Y(p), \end{gathered} \tag{3.6}$$

in this case, the constant gains of the desired controller can be obtained as follows:

$$K_0 = R^{-1}Y_0, \qquad K_u = R^{-1}Y_u, \tag{3.7}$$

and the closed-system (2.11) *is then exponentially mean-square stable for all $p(k) \in [p_1\ p_2]$.*

Proof. Define the Lyapunov functional:

$$V(k) := x^T(k)Q(p(k))x(k) + \sum_{d=1}^{+\infty}\mu_d \sum_{s=k-d}^{k-1} x^T(s)Q_\tau x(s). \tag{3.8}$$

Then, noting $\mathbb{E}\{\xi(k)-p(k)\}=0$, $\mathbb{E}\{\omega(k)\}=0$ and $\mathbb{E}\{[\xi(k)-p(k)]^2\}=p(k)(1-p(k))$, we can get that

$$\begin{aligned}
\mathbb{E}\{\Delta V(k)\} &= \mathbb{E}\Bigg\{x^T(k+1)Q\big(p(k+1)\big)x(k+1)-x^T(k)Q\big(p(k)\big)x(k)+\overline{\mu}x^T(k)Q_\tau x(k) \\
&\qquad -\sum_{d=1}^{+\infty}\mu_d x^T(k-d)Q_\tau x(k-d)\Bigg\} \\
&\le \mathrm{E}\Bigg\{\Bigg[\Big(\overline{A}+p(k)BK(p)C\Big)x(k)+\overline{D}\sum_{m=1}^{+\infty}\mu_d x(k-d)+Nf_s(z(k))\Bigg]^T Q\big(p(k+1)\big) \\
&\qquad \times\Bigg[\Big(\overline{A}+p(k)BK(p)C\Big)x(k)+\overline{D}\sum_{m=1}^{+\infty}\mu_d x(k-d)+Nf_s(z(k))\Bigg] \\
&\qquad +\big[p(k)\big(1-(p(k))BK(p)C\big)x(k)\big]^T Q\big(p(k+1)\big)BK(p)Cx(k)+\sigma^2x^T(k)E^T \\
&\qquad \times Q\big(p(k+1)\big)Ex(k)-x^T(k)Q\big(p(k)\big)x(k)-\sum_{d=1}^{+\infty}\mu_d x^T(k-d)Q_\tau x(k-d) \\
&\qquad +\overline{\mu}x^T(k)Q_\tau x(k)+2f_s^T(z(k))FGx(k)+2f_s^T(z(k))FG_d\sum_{m=1}^{+\infty}\mu_d x(k-d) \\
&\qquad -2f_s^T(z(\mathrm{k}))f_s(z(k))\Bigg\}.
\end{aligned} \tag{3.9}$$

From Lemma 3.2, it is obvious that

$$-\sum_{d=1}^{+\infty}\mu_d\Big(x^T(k-d)Q_\tau x(k-d)\Big)\le-\frac{1}{\overline{\mu}}\left(\sum_{d=1}^{+\infty}\mu_d x^T(k-d)\right)Q_\tau\left(\sum_{d=1}^{+\infty}\mu_d x(k-d)\right). \tag{3.10}$$

Denote the following matrix variables

$$\eta(k)=\begin{bmatrix}x^T(k) & \displaystyle\sum_{d=1}^{+\infty}\mu_d x^T(k-d) & f_s^T(z(k))\end{bmatrix}^T. \tag{3.11}$$

Combining (3.9), (3.10), and (3.11), we can get

$$\mathbb{E}\{\Delta V(k)\} \le \mathbb{E}\left\{\eta^T(k)\Omega\eta(k)\right\},$$

$$\Omega = \begin{bmatrix} \Omega_1 & * & * \\ \Omega_2 & \Omega_3 & * \\ \Omega_4 & \Omega_5 & \Omega_6 \end{bmatrix},$$

$$\begin{aligned}
\Omega_1 &= \left(\overline{A} + p(k)BK(p)C\right)^T Q(p(k+1))\left(\overline{A} + p(k)BK(p)C\right) + \sigma^2 E^T Q(p(k+1))E \\
&\quad + p(k)(1-p(k))(BK(p)C)^T Q(p(k+1))BK(p)C + \overline{\mu}Q_\tau - Q(p(k)), \\
\Omega_2 &= \overline{D}^T Q(p(k+1))\left(\overline{A} + p(k)BK(p)C\right), \\
\Omega_3 &= \overline{D}^T Q(p(k+1))\overline{D} - \frac{1}{\overline{\mu}}Q_\tau, \\
\Omega_4 &= N^T Q(p(k+1))\left(\overline{A} + p(k)BK(p)C\right) + FG, \\
\Omega_5 &= N^T Q(p(k+1))\overline{D} + FG_d, \\
\Omega_6 &= N^T Q(p(k+1))N - 2I.
\end{aligned} \tag{3.12}$$

If $\Omega \le 0$, we can conclude the following matrix inequalities by Schur complement:

$$\begin{bmatrix}
\overline{\mu}Q_\tau - Q(p(k)) & * & * & * & * & * \\
0 & -\frac{1}{\overline{\mu}}Q_\tau & * & * & * & * \\
FG & FG_d & -2I & * & * & * \\
\overline{A} + p(k)BK(p)C & \overline{D} & N & -\Lambda & * & * \\
E & 0 & 0 & 0 & -\sigma^{-2}\Lambda & * \\
BK(p)C & 0 & 0 & 0 & 0 & -\Delta_p^{-1}(k)\Lambda
\end{bmatrix} < 0, \tag{3.13}$$

with $\Lambda = Q^{-1}(p(k+1))$.

At this time, preforming the congruence transformation $\operatorname{diag}\{I, I, I, S, \sigma^2 S, \Delta_p(k)S\}$ to (3.13), we can have

$$\begin{bmatrix}
\overline{\mu}Q_\tau - Q(p(k)) & * & * & * & * & * \\
0 & -\frac{1}{\overline{\mu}}Q_\tau & * & * & * & * \\
FG & FG_d & -2I & * & * & * \\
S^T\overline{A} + p(k)S^T BK(p)C & S^T\overline{D} & S^T N & -\widehat{\Lambda} & * & * \\
\sigma^2 S^T E & 0 & 0 & 0 & -\sigma^2\widehat{\Lambda} & * \\
\Delta_p(k)S^T BK(p)C & 0 & 0 & 0 & 0 & -\Delta_p(k)\widehat{\Lambda}
\end{bmatrix} < 0, \tag{3.14}$$

$$\widehat{\Lambda} = S^T Q^{-1}(p(k+1))S,$$

then from inequality

$$S^T Q^{-1}(p(k+1))S \geq S^T + S - Q(p(k+1)) = \overline{\Lambda}, \tag{3.15}$$

we can get

$$\begin{bmatrix} \overline{\mu}Q_\tau - Q(p(k)) & * & * & * & * & * \\ 0 & -\frac{1}{\overline{\mu}}Q_\tau & * & * & * & * \\ FG & FG_d & -2I & * & * & * \\ S^T\overline{A} + p(k)S^T BK(p)C & S^T\overline{D} & S^T N & -\overline{\Lambda} & * & * \\ \sigma^2 S^T E & 0 & 0 & 0 & -\sigma^2\overline{\Lambda} & * \\ \Delta_p(k)S^T BK(p)C & 0 & 0 & 0 & 0 & -\Delta_p(k)\overline{\Lambda} \end{bmatrix} < 0, \tag{3.16}$$

and from lemma 3, we have $S^T B = BR$ denoting $RK(p) = Y(p)$, and $K(P) = R^{-1}Y(p)$. Then (3.16) can be written as

$$\begin{bmatrix} \overline{\mu}Q_\tau - Q(p(k)) & * & * & * & * & * \\ 0 & -\frac{1}{\overline{\mu}}Q_\tau & * & * & * & * \\ FG & FG_d & -2I & * & * & * \\ S^T\overline{A} + p(k)BY(p)C & S^T\overline{D} & S^T N & -\overline{\Lambda} & * & * \\ \sigma^2 S^T E & 0 & 0 & 0 & -\sigma^2\overline{\Lambda} & * \\ \Delta_p(k)BY(p)C & 0 & 0 & 0 & 0 & -\Delta_p(k)\overline{\Lambda} \end{bmatrix} < 0, \tag{3.17}$$

Furthermore, by Lemma 3.1, we can know from that $\Omega < 0$ and, subsequently,

$$\mathbb{E}\{\Delta V(k)\} < -\lambda_{\min}(-\Omega)\mathbb{E}|\eta(k)|^2, \tag{3.18}$$

where $\lambda_{\min}(-\Omega)$ is the minimum eigenvalue of $(-\Omega)$. Finally, we can confirm from Lemma 1 of [13] that the closed-loop system is exponentially mean-square stable, then the proof of this theorem is complete. □

Remark 3.5. In the above theorem, a static output feedback controller has been designed based on a set of LMIs. However, the LMIs are actually infinite owing to the time-varying parameter $p(k) \in [p_1\ p_2]$. In this case, the desired controller cannot be obtained directly from Theorem 3.4 due to the infinite number of LMIs. To handle such a problem, in the next theorem, we have to convert this problem to a computationally accessible one by assigning a specific form to $p(k)$. Let us set $Q(p(k)) = Q_0 + p(k)Q_u$.

Theorem 3.6. *Consider the discrete-time nonlinear stochastic system with infinite-distributed delays and missing measurements* (2.11). *If there exist positive-difinite matrices Q_0, Q_u and Q_τ, slack matrix S and nonsingular matrices $Y(p)$ and R, such that the following LMIs hold:*

$$M^{ijlm} = \begin{bmatrix} \overline{\mu}Q_\tau - Q^i(p(k)) & * & * & * & * & * \\ 0 & -\frac{1}{\overline{\mu}}Q_\tau & * & * & * & * \\ FG & FG_d & -2I & * & * & * \\ S^T\overline{A} + p_iBY^mC & S^T\overline{D} & S^TN & -\overline{\Lambda}^l & * & * \\ \sigma^2S^TE & 0 & 0 & 0 & -\sigma^2\overline{\Lambda}^l & * \\ \Delta^{ij}BY^mC & 0 & 0 & 0 & 0 & -\Delta^{ij}\overline{\Lambda}^l \end{bmatrix} < 0, \tag{3.19}$$

where

$$\begin{gathered} \overline{\Lambda}^l = -Q_0 - p_lQ_u + S + S^T, \qquad \Delta^{ij} = p_i(1-p_j), \\ Q^i(p(k)) = Q_0 + p_iQ_u, \qquad Y^m = Y_0 + p_mY_u, \\ S^TB = BR, \qquad RK(p) = Y(p), \qquad K(p) = R^{-1}Y(p), \end{gathered} \tag{3.20}$$

the constant gains of the desired controller can be obtained as follows:

$$K_0 = R^{-1}Y_0, \qquad K_u = R^{-1}Y_u, \tag{3.21}$$

and the closed-system (2.11) *is then exponentially mean-square stable for all $p(k) \in [p_1\ p_2]$.*

Proof. Firstly, set

$$\alpha_1(k) = \frac{p_2 - p(k)}{p_2 - \mathrm{p}_1}, \qquad \alpha_2(k) = \frac{p(k) - p_1}{p_2 - p_1}, \tag{3.22}$$

then, we have

$$p(k) = \alpha_1(k)p_1 + \alpha_2(k)p_2, \tag{3.23}$$

with $\alpha_i(k) \geq 0$ $(i = 1, 2)$ and $\alpha_1(k) + \alpha_2(k) = 1$. Similarly, let

$$\beta_1(k) = \frac{p_2 - p(k+1)}{p_2 - p_1}, \qquad \beta_2(k) = \frac{p(k+1) - p_1}{p_2 - p_1}, \tag{3.24}$$

then we have

$$p(k+1) = \beta_1(k)p_1 + \beta_2(k)p_2, \tag{3.25}$$

with $\beta_i(k) \geq 0$ $(i = 1, 2)$, $\beta_1(k) + \beta_2(k) = 1$. From the above transformation, we can easily get

$$Q(p(k)) = \sum_{i=1}^{2} \alpha_i(k) Q^i, \qquad \overline{\Lambda} = \sum_{l=1}^{2} \beta_l(k) \overline{\Lambda}^l,$$
$$Y(p(k)) = \sum_{m=1}^{2} \alpha_m(k) Y^m(p). \tag{3.26}$$

On the other hand, it is easy to find that

$$\sum_{i,j,l,m=1}^{2} \alpha_i(k)\alpha_j(k)\alpha_m(k)\beta_l(k)\mathbb{M}^{ijlm} < 0. \tag{3.27}$$

From (3.22)–(3.27), we can have that (3.5) in Theorem 3.4 is true, then the proof is now complete. □

Remark 3.7. The above conclusions can be extended to multiple sensor case of measurement output. In this paper, to make the main idea and the proof more clear and concise, we choose the single sensor.

4. An Illustrative Example

In this section, the gain-scheduled static output feedback controller is designed for the discrete-time nonlinear stochastic systems with infinite-distributed delays and missing measurements.

The system parameters are given as follows:

$$A = \begin{bmatrix} 0.97 & 0 \\ 0 & 0.21 \end{bmatrix}, \qquad N = \begin{bmatrix} 0.13 & 0.21 \\ 0.28 & 0.33 \end{bmatrix}, \qquad B = \begin{bmatrix} 0.06 & 0 \\ 0 & 0.16 \end{bmatrix},$$
$$C = \begin{bmatrix} 0.1 & 0.2 \\ 0.15 & 0.23 \end{bmatrix}, \qquad D = \begin{bmatrix} 0.23 & 0 \\ 0.15 & 0.18 \end{bmatrix}, \qquad F_1 = \begin{bmatrix} 0.06 & 0 \\ 0 & 0.07 \end{bmatrix},$$
$$F_2 = \begin{bmatrix} 0.61 & 0 \\ 0 & 0.25 \end{bmatrix}, \qquad G = \begin{bmatrix} 0.11 & 0.12 \\ 0.18 & 0.12 \end{bmatrix}, \qquad G_d = \begin{bmatrix} 0.11 & 0.29 \\ 0.18 & 0.09 \end{bmatrix}, \qquad E = \begin{bmatrix} 0.03 & 0.19 \\ 0.21 & 0.33 \end{bmatrix},$$
$$p_1 = 0.19, \qquad p_2 = 0.51, \qquad \sigma^2 = 1, \qquad \overline{\mu} = 2^{-3}. \tag{4.1}$$

Set the time-varying Bernoulli distribution sequences as $p(k) = p_1 + (p_2 - p_1)|\sin(k)|$ and the sector nonlinear function $f(u)$ is taken as

$$f(u) = \frac{F_1 + F_2}{2} u + \frac{F_2 - F_1}{2} \sin(u), \tag{4.2}$$

which satisfies (2.3). Also, select the initial state as follows: $\rho = [2 - 2]^T$.

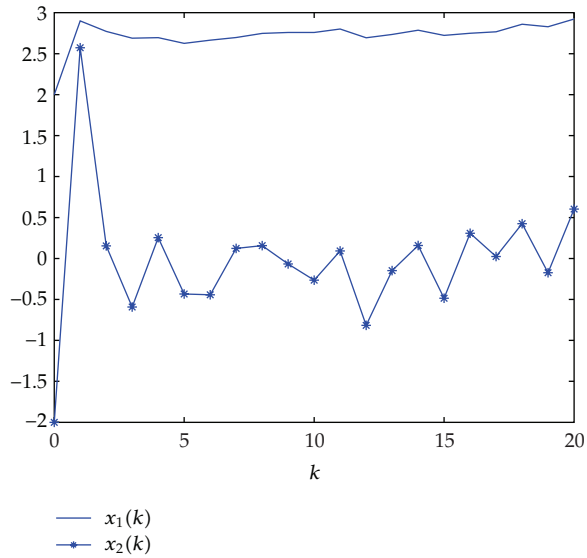

Figure 1: State evolution $x(k)$ of uncontrolled systems.

Table 1: Computing results.

k	$p(k)$	$Q(p(k))$	$K(p)$
0	0.4593	$\begin{bmatrix} 3.4334 & -0.2204 \\ -0.2204 & 2.1583 \end{bmatrix}$	$\begin{bmatrix} 606.0619 & -529.7133 \\ 10.7547 & -16.6786 \end{bmatrix}$
1	0.4810	$\begin{bmatrix} 3.4368 & -0.2282 \\ -0.2282 & 2.1833 \end{bmatrix}$	$\begin{bmatrix} 607.6342 & -531.0712 \\ 10.7201 & -16.6872 \end{bmatrix}$
2	0.2352	$\begin{bmatrix} 3.3986 & -0.1400 \\ -0.1400 & 1.9006 \end{bmatrix}$	$\begin{bmatrix} 589.8268 & -515.6926 \\ 11.1130 & -16.5901 \end{bmatrix}$
3	0.4322	$\begin{bmatrix} 3.4292 & -0.2107 \\ -0.2107 & 2.1272 \end{bmatrix}$	$\begin{bmatrix} 604.0991 & -528.0183 \\ 10.7981 & -16.6679 \end{bmatrix}$
$\vdots$	$\vdots$	$\vdots$	$\vdots$

According to Theorem 3.6, the constant controller parameters K_0, K_u can be obtained as follows:

$$K_0 = \begin{bmatrix} 572.7914 & -500.9808 \\ 11.4889 & -16.4972 \end{bmatrix}, \qquad K_u = \begin{bmatrix} 72.4419 & -62.5612 \\ -1.5985 & -0.3949 \end{bmatrix}. \tag{4.3}$$

Then, according to the measured time-varying probability parameters $p(k)$, the gain-scheduled controller gain $K(p)$ and parameter-dependent Lyapunov matrix can be calculated at every time step k as in Table 1.

Figure 1 gives the response curves of state $x(k)$ of uncontrolled systems. Figure 2 depicts the simulation results of state $x(k)$ of the controlled systems. The simulation results have illustrated our theoretical analysis.

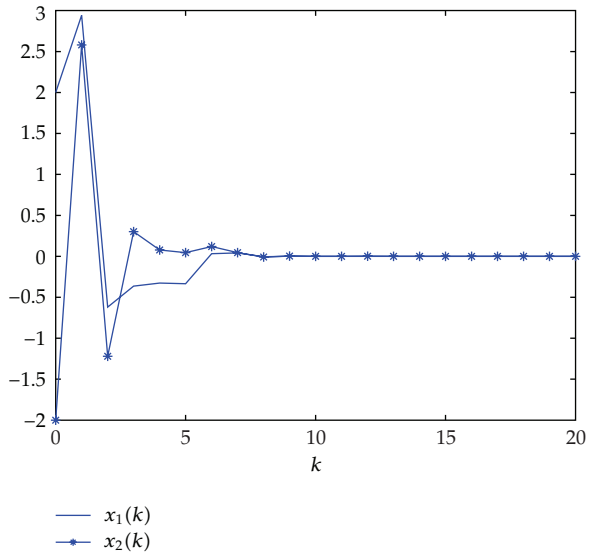

Figure 2: State evolution $x(k)$ of controlled systems.

5. Conclusions

In this paper, the problem of gain-scheduled control for a class of discrete stochastic systems with infinite-distributed delays and missing measurements has been studied, the missing-measurement phenomenon is assumed to occur in a random way, the missing probability is governed by an individual random variable satisfying a certain probabilistic distribution in the interval [0 1], and distributed delays are described in a discrete way. By employing probability-dependent Lyapunov functional, we have designed a gain-scheduled controller with the gain including both constant parameters and time-varying parameters such that, for the admissible missing measurements with time-varying probability, infinite-distributed delays, and noise disturbances, the closed-loop system is exponentially mean-square stable. Moreover, we can extend the main results to more complex and realistic systems, for instance, system with norm-bounded or polytopic uncertainties. Meanwhile, we can also consider dynamic output feedback control problem for discrete stochastic systems with missing measurements by gain-scheduling approach as well as the relevant applications in networked control system or robotic manipulator.

Acknowledgments

This work was supported in part by the National Natural Science Foundation of China under Grant 61074016, the Program for Professor of Special Appointment (Eastern Scholar) at Shanghai Institutions of Higher Learning, the Program for New Century Excellent Talents in University under Grant NCET-11-1051, the Shanghai Natural Science Foundation of China under Grant 10ZR1421200, the Leverhulme Trust of the UK, the Alexander von Humboldt Foundation of Germany, and the Innovation Fund Project for Graduate Student of Shanghai under Grant JWCXSL1202.

References

[1] P. Apkarian and R. J. Adams, "Advanced gain-scheduling techniques for uncertain systems," *IEEE Transactions On Control Systems Technology*, vol. 6, no. 1, pp. 21–32, 1998.

[2] Y. Y. Cao, Z. Lin, and Y. Shamash, "Set invariance analysis and gain-scheduling control for LPV systems subject to actuator saturation," *Systems & Control Letters*, vol. 46, no. 2, pp. 137–151, 2002.

[3] W. H. Chen, Z. H. Guan, and X. Lu, "Delay-dependent exponential stability of uncertain stochastic systems with multiple delays: an LMI approach," *Systems & Control Letters*, vol. 54, no. 6, pp. 547–555, 2005.

[4] W. J. Rugh and J. S. Shamma, "Research on gain scheduling," *Automatica*, vol. 36, no. 10, pp. 1401–1425, 2000.

[5] G. Wei, Z. Wang, and B. Shen, "Probability-dependent gain-scheduled filtering for stochastic systems with missing measure- ments," *IEEE Transactions on Circuits and Systems II: Express Briefs*, vol. 58, no. 11, pp. 753–757, 2011.

[6] G. Wei, Z. Wang, and B. Shen, "Probability-dependentgain-scheduled control for discrete stochastic delayed systems with randomly occurring nonlinearities," *International Journal of Robust and Nonlinear Control*, 2012.

[7] Y. Y. Cao, J. Lam, and Y. X. Sun, "Static output feedback stabiliztion: an LMI approach," *Automatica*, vol. 34, no. 12, pp. 1641–1645, 1998.

[8] J. C. Geromel, C. C. de Souza, and R. E. Skelton, "Static output feedback controllers: stability and convexity," *IEEE Transactions on Automatic Control*, vol. 43, no. 1, pp. 120–125, 1998.

[9] I. N. Kar, "Design of static output feedback controller for uncertain systems," *Automatica*, vol. 35, no. 1, pp. 169–175, 1999.

[10] R. E. Benton, Jr. and D. Smith, "Static output feedback stabilization with prescribed degree of stability," *IEEE Transactions on Automatic Control*, vol. 43, no. 10, pp. 1493–1496, 1998.

[11] E. Prempain and I. Postlethwaite, "Static output feedback stabilisation with H_∞ performance for a class of plants," *Systems & Control Letters*, vol. 43, no. 3, pp. 159–166, 2001.

[12] V. L. Syrmos, C. T. Abdallah, P. Dorato, and K. Grigoriadis, "Static output feedback—a survey," *Automatica*, vol. 33, no. 2, pp. 125–137, 1997.

[13] Z. Wang F, Yang, D. W. C. Ho, and X. Liu, "Robust H_∞ filtering for stochastic time-delay systems with missing measurements," *IEEE Transactions on Signal Processing*, vol. 54, no. 7, pp. 2579–2587, 2006.

[14] H. Gao and T. Chen, "H_∞ estimation for uncertain systems with limited communication capacity," *Institute of Electrical and Electronics Engineers. Transactions on Automatic Control*, vol. 52, no. 11, pp. 2070–2084, 2007.

[15] G. Wei, Z. Wang, X. He, and H. Shu, "Filtering for networked stochastic time-delay systems with sector nonlinearity," vol. 56, no. 1, pp. 71–75, 2009.

[16] G. Wei, Z. Wang, and H. Shu, "Robust filtering with stochastic nonlinearities and multiple missing measurements," *Automatica*, vol. 45, no. 3, pp. 836–841, 2009.

[17] Y. Kuang, H. L. Smith, and R. H. Martin, "Global stability for infinite-delay, dispersive Lotka-Volterra systems: weakly interacting populations in nearly identical patches," *Journal of Dynamics and Differential Equations*, vol. 3, no. 3, pp. 339–360, 1991.

[18] Y. Liu, Z. Wang, and X. Liu, "Robust H_∞ control for a class of nonlinear stochastic systems with mixed time delay," *International Journal of Robust and Nonlinear Control*, vol. 17, no. 16, pp. 1525–1551, 2007.

[19] L. Xie, E. Fridman, and U. Shaked, "Robust H_∞ control of distributed delay systems with application to combustion control," *Institute of Electrical and Electronics Engineers. Transactions on Automatic Control*, vol. 46, no. 12, pp. 1930–1935, 2001.

[20] Z. Wang, G. Wei, and G. Feng, "Reliable H_∞ control for discrete-time piecewise linear systems with infinite distributed delays," *Automatica*, vol. 45, no. 12, pp. 2991–2994, 2009.

[21] Z. Wang, Y. Liu, G. Wei, and X. Liu, "A note on control of a class of discrete-time stochastic systems with distributed delays and nonlinear disturbances," *Automatica*, vol. 46, no. 3, pp. 543–548, 2010.

[22] G. Wei, G. Feng, and Z. Wang, "Robust H_∞ control for discrete-time fuzzy systems with infinite-distributed delays," *IEEE Transactions on Fuzzy Systems*, vol. 17, no. 1, pp. 224–232, 2009.

[23] S. Boyd, L. El Ghaoui, E. Feron, and V. Balakrishnan, *Linear Matrix Inequalities in System and Control Theory*, vol. 15, Society for Industrial and Applied Mathematics (SIAM), Philadelphia, Pa, USA, 1994.

[24] Y. Liu, Z. Wang, J. Liang, and X. Liu, "Synchronization and state estimation for discrete-time complex networks with distributed delays," *Transactions on Systems, Man and Cybernetics B*, vol. 38, no. 5, pp. 1314–1325, 2008.

[25] F. Yang, Z. Wang, Y. S. Hung, and M. Gani, "H_∞ control for networked systems with random communication delays," *IEEE Transactions on Automatic Control*, vol. 51, no. 3, pp. 511–518, 2006.

Hindawi Publishing Corporation
Mathematical Problems in Engineering
Volume 2012, Article ID 748091, 13 pages
doi:10.1155/2012/748091

Research Article

Controllability of Second-Order Semilinear Impulsive Stochastic Neutral Functional Evolution Equations

Lei Zhang,[1,2] Yongsheng Ding,[1,2] Tong Wang,[1,2] Liangjian Hu,[3] and Kuangrong Hao[1,2]

[1] *College of Information Sciences and Technology, Donghua University, Shanghai 201620, China*
[2] *Engineering Research Center of Digitized Textile & Fashion Technology, Ministry of Education, Donghua University, Shanghai 201620, China*
[3] *Department of Mathematics, Donghua University, Shanghai 201620, China*

Correspondence should be addressed to Yongsheng Ding, ysding@dhu.edu.cn

Received 17 June 2012; Accepted 7 August 2012

Academic Editor: Bo Shen

We consider a class of impulsive neutral second-order stochastic functional evolution equations. The Sadovskii fixed point theorem and the theory of strongly continuous cosine families of operators are used to investigate the sufficient conditions for the controllability of the system considered. An example is provided to illustrate our results.

1. Introduction

Controllability, as a fundamental concept of control theory, plays an important role both in stochastic and deterministic control problems. The study of controllability of linear and nonlinear systems represented by infinite-dimensional systems in Banach spaces has been raised by many authors recently, see Chang [1], Sakthivel [2], Ren and Sakthivel [3], Ntouyas and Regan [4], Kang et al. [5], Sakthivel and Mahmudov [6], and Shubov et al. [7]. With the help of fixed point theorem, Luo [8, 9] and Burton [10–13] have investigated the problem of controllability of the systems in Banach spaces.

Recently, stochastic partial differential equations (SPDEs) arise in the mathematical modeling of various fields in physics and engineering science cited by Sobczyk [14]. Among them, several properties of SPDEs such as existence, controllability, and stability are studied for the first-order equations. But in many situations, it is useful to investigate the second-order abstract differential equations directly rather than to convert them to first-order systems introduced by Fitzgibbon [15]. The second-order stochastic differential equations are the right

model in continuous time to account for integrated processes that can be made stationary. For instance, it is useful for engineers to model mechanical vibrations or charge on a capacitor or condenser subjected to white noise excitation by second-order stochastic differential equations. A useful tool for the study of abstract second-order equations is the fixed point theory and the theory of strongly continuous cosine families.

In the past decades, the theory of impulsive differential equations or inclusions is emerging as an active area of investigation due to the application in area such as mechanics, electrical engineering, medicine biology, and ecology, see Benchohra and Henderson [16], Liu and Willms [17], Hernández et al. [18], Prato and Zabczyk [19], and Fattorini [20]. As an adequate model, impulsive differential equations are used to study the evolution of processes that are subject to sudden changes in their states.

The focus of this paper is the controllability of mild solutions for a class of impulsive neutral second-order stochastic evolution equations of the form:

$$\begin{gathered} d\left[x'(t) - D(x_t)\right] = \left[Ax(t) + Bu(t) + f(t, x_t)\right]dt + g(t, x_t)dw(t), \quad t \in [0, T], \quad t \neq t_k \\ \Delta x(t_k) = I_k(x(t_k)), \quad \Delta x'(t_k) = \widetilde{I}_k(x(t_k)), \quad k = 1, \ldots, n, \ x(0) = \phi, \ x'(0) = y_0. \end{gathered} \tag{1.1}$$

Here, $x(\cdot)$ is a stochastic process taking values in a real separable Hilbert space H with inner product $(\cdot,\cdot)$ and norm $\|\cdot\|$. $A : D(A) \subset H \to H$ is the infinitesimal generator of a strongly continuous cosine family on H. W is a given K-valued Wiener process with a finite trace nuclear covariance operator $Q \geq 0$ defined on a filtered complete probability space $(\Omega, F, \{F_t\}_{t\geq 0}, P)$ and K is another separable Hilbert space with inner product $(\cdot,\cdot)_K$ and norm $\|\cdot\|_K$. The fixed time $t_k, k = 1, \ldots, n$, satisfies $0 < t_1 < \cdots < t_n < T$, $x(t_k^+)$ and $x(t_k^-)$ denote the right and left limits of $x(t)$ at $t = t_k$, and $\Delta x(t_k) = x(t_k^+) - x(t_k^-)$ represents the jump in the state x at time t_k, where $I_k \in C(H, H)$ $(k = 1, 1, 2, \ldots, m)$ are bounded which determine the size of the jump. Similarly $x'(t_k^+)$ and $x'(t_k^-)$ denote, respectively, the right and left limits of x' at t_k. f, B, g are appropriate mappings specified later; x_0 and y_0 are F_0-measurable random variables with finite second moment. The main contributions are as follows. The Sadovskii fixed point theorem and the theory of strongly continuous cosine families of operators are used to investigate the sufficient conditions for the controllability of the system considered. The differences of using the fixed point theorem between our proposed method and others are that Sadovskii fixed point theorem is much easier in application, and the condition is easier to be satisfied than other fixed point theorem. To our best knowledge, there are few works about the controllability for mild solutions to second-order semilinear impulsive stochastic neutral functional evolution equations, motivated by the previous problems, our current consideration is on second-order semilinear impulsive stochastic neutral functional evolution equations. We will apply the Sadovskii fixed point theorem to investigate the controllability of mild solution of this class of equations.

The rest of this paper is arranged as follows. In Section 2, we briefly present some basic notations and preliminaries. Section 3 is devoted to the controllability of mild solutions for the system (1.1) and an example is given to illustrate our results in Section 4. Conclusion is given in Section 5.

2. Preliminaries

In this section, we briefly recall some basic definitions and results for stochastic equations in infinite dimensions and cosine families of operators. We refer to Prato and Zabczyk [19]

and Fattorini [20] for more details. Throughout this paper, let *L(K,H)* be the set of all linear bounded operators from K into H, equipped with the usual operator norm $\|\cdot\|$. Let (Ω, F, P) be a complete probability space furnished with a normal filtration$\{F_t\}_{t\geq 0}$. Suppose $\{\beta_k\}_{k\geq 1}$ is a sequence of real independent one-dimensional standard Brownian motions over (Ω, F, P). Set

$$W(t) = \sum_{k=1}^{\infty} \sqrt{\lambda_k}\beta_k(t)e_k, \quad t \geq 0, \tag{2.1}$$

where $\{e_k\}_{k\geq 1}$ is the complete orthonormal system in K and $\lambda_k,\ k \geq 1$, a bounded sequence of nonnegative real numbers. Let $Q \in L(K, K)$ be an operator defined by $Qe_k = \lambda_k e_k,\ k = 1, 2, \ldots$, with $\operatorname{tr} Q = \sum_{k=1}^{\infty} \lambda_k < \infty$. The K-valued stochastic process $W = (W_t)_{t\geq 0}$ is called a Q-Wiener process. Let $L_2^0 = L_2(Q^{1/2}K, H)$ be the space of all Hilbert-Schmidt operators from $Q^{1/2}K$ to H with the inner product $\langle \varphi, \phi\rangle_{L_2^0} = \operatorname{tr}[\varphi Q \phi^*]$.

The collection of all strongly measurable, square-integrable H-valued random variables, denoted by $L^2(\Omega, H)$, is a Banach space equipped with norm $\|x\|_{L^2} = (E\|x\|^2)^{1/2}$. An important subspace of $L^2(\Omega, H)$ is given by

$$L_0^2(\Omega, H) = \left\{L^2(\Omega, H) \ni x \text{ is } F_0 - \text{measurable}\right\}. \tag{2.2}$$

Let

$$\begin{aligned}
\wp &:= D([0,T], H) \\
&= \left\{x : [0,T] \longrightarrow H,\ x|_{(t_k,t_{k+1}]} \in C((t_k, t_{k+1}], H),\ \text{and there exists } x(t_k^+) \text{ for } k = 1, 2, \ldots, n\right\}, \\
\overline{\wp} &:= \overline{D}([0,T], H) \\
&= \left\{x \in \wp,\ x|_{(t_k,t_{k+1}]} \in C^1((t_k, t_{k+1}], H),\ \text{and there exists } x'(t_k^+) \text{ for } k = 1, 2, \ldots, n\right\}.
\end{aligned} \tag{2.3}$$

It is obvious that $D([0,T], H)$ and $\overline{D}([0,T], H)$ are Banach spaces endowed with the norm

$$\|x\|_{\wp} = \left(\sup_{t\in[0,T]} E\|x(t)\|^2\right)^{1/2} \tag{2.4}$$

and $\|x\|_{\overline{\wp}} = \|x\|_{\wp} + \|x'\|_{\wp}$, respectively.

To simplify the notations, we put $t_0 = 0$, $t_{m+1} = T$, and for $u = H_2$, we denote by $\tilde{u}_k \in C([t_k, t_{k+1}], L^2(\Omega, H))$, $k = 0, 1, \ldots, m$, the function given by

$$\tilde{u}_k(t) = \begin{cases} u(t), & t \in (t_k, t_{k+1}], \\ u(t_k^+), & t = t_k. \end{cases} \tag{2.5}$$

Moreover, for $B \subset H_2$ we denote $\tilde{B}_k = \{\tilde{u}_k : u \in B\}, k = 1, \ldots, m$. To prove our results, we need the following lemma introduced in Hernández et al. [18].

Lemma 2.1. *A set $B \subset \wp$ is relatively compact in $\wp$ if and only if the set $\widetilde{B}_k$ is relatively compact in $C([t_k, t_{k+1}], H)$, for every $k = 0, 1, \ldots, m$.*

Now, we recall some facts about cosine families of operators, see Fattorini [20] and Travis and Webb [21].

Definition 2.2. (1) The one-parameter family $\{C(t) : t \in \mathbb{R}\} \subset L(H, H)$ is said to be a strongly continuous cosine family if the following hold:

(1) $C(0) = I$;

(2) $C(t)x$ is continuous in t on $\mathbb{R}$ for any $x \in H$;

(3) $C(t+s) + C(t-s) = 2C(t)C(s)$ for all $t, s \in \mathbb{R}$.

(2) The corresponding strongly continuous sine family $\{S(t) : t \in \mathbb{R}\} \subset L(H, H)$ is defined by

$$S(t)x = \int_0^t C(s)x\,ds, \qquad t \in \mathbb{R}, x \in H. \tag{2.6}$$

(3) The (infinitesimal) generator $A : H \to H$ of $\{C(t) : t \in R\}$ is given by

$$Ax = \frac{d^2}{dt^2} C(t)x \bigg|_{t=0}, \tag{2.7}$$

for all $x \in D(A) = \{x \in H : C(\cdot)x \in C^2(\mathbb{R}, H)\}$.

It is known that the infinitesimal generator A is a closed, densely defined operator on H, and the following properties hold, see Travis and Webb [21].

Proposition 2.3. *Suppose that A is the infinitesimal generator of a cosine family of operators $\{C(t) : t \in \mathbb{R}\}$. Then, the following hold*

(i) *There exist a pair of constants $M_A \geq 1$ and $\alpha \geq 0$ such that $\|C(t)\| \leq M_A e^{\alpha|t|}$ and hence, $\|S(t)\| \leq M_A e^{\alpha|t|}$.*

(ii) $A \int_s^r S(u)x\,du = [C(r) - C(s)]x$, *for all* $0 \leq s \leq r < \infty$.

(iii) *There exist $N \geq 1$ such that $\|S(s) - S(r)\| \leq N \left| \int_s^r e^{\alpha|s|} ds \right|$, for all $0 \leq s \leq r < \infty$.*

The uniform boundedness principle: as a direct consequence we see that both $\{C(t) : t \in [0, T]\}$ and $\{S(t) : t \in [0, T]\}$ are uniformly bounded by $M^* = M_A e^{\alpha|T|}$.

At the end of this section we recall the fixed point theorem of Sadovskii [22] which is used to estimate the controllability of the mild solution to the system (1.1).

Lemma 2.4. *Let Φ be a condensing operator on a Banach space H. If $\Phi(N) \subset N$ for a convex, closed, and bounded set N of H, then Φ has a fixed point in H.*

3. Main Results

In this section we consider the system (1.1). We first present the definition of mild solutions for the system.

Definition 3.1. An F_t-adapted stochastic process $x(t) : [0,T] \to H$ is said to be a mild solution of the system (1.1) if

(1) $x_0, y_0 \in L_0^2(\Omega, H)$;

(2) $\Delta x(t_k) = x(t_k^+) - x(t_k^-) = I_k(x(t_k))$, $\Delta x'(t_k) = x'(t_k^+) - x'(t_k^-) = \widetilde{I}_k(x(t_k))$, $k = 1, \ldots, n$;

(3) $x(t)$ satisfies the following integral equation:

$$\begin{aligned} x(t) = {} & C(t)\phi(0) + S(t)\left[y_0 - D(0,\phi)\right] + \int_0^t C(t-s)D(s,x_s)ds \\ & + \int_0^t S(t-s)Bu(s)ds + \int_0^t S(t-s)f(s,x_s)ds \\ & + \int_0^t S(t-s)g(s,x_s)dW(s) + \sum_{0<t_k<t} C(t-t_k)I_k(x(t_k)) \\ & + \sum_{0<t_k<t} S(t-t_k)\widetilde{I}_k(x(t_k)). \end{aligned} \tag{3.1}$$

In this paper, we will work under the following assumptions.

(A1) The cosine family of operators $\{C(t) : t \in [0,T]\}$ on H and the corresponding sine family $\{S(t) : t \in [0,T]\}$ are compact for $t > 0$, and there exists a positive constant M such that

$$\|C(t)\| \le M, \qquad \|S(t)\| \le M. \tag{3.2}$$

(A2) D, f, g are continuous functions, and there exist some positive constants M_D, M_f, M_g, such that D, f, g satisfy the following Lipschitz condition:

$$\begin{aligned} \|D(t,\varphi) - D(t,\phi)\| &\le M_D\|\varphi - \phi\|, \\ \|f(t,\varphi) - f(t,\phi)\| &\le M_f\|\varphi - \phi\|, \\ \|g(t,\varphi) - g(t,\phi)\| &\le M_g\|\varphi - \phi\|, \end{aligned} \tag{3.3}$$

for all $\varphi, \phi \in H$, $k = 1, \ldots, n$ and $t \in [0, T]$, and there exist positive constants $\overline{M}_D$, $\overline{M}_f$, $\overline{M}_g$ that satisfy the following linear growth condition:

$$\begin{aligned} \|D(t,\varphi)\|^2 &\le \overline{M}_D\left(\|\varphi\|^2 + 1\right), \\ \|f(t,\varphi)\|^2 &\le \overline{M}_f\left(\|\varphi\|^2 + 1\right), \\ \|g(t,\varphi)\|^2 &\le \overline{M}_g\left(\|\varphi\|^2 + 1\right) \end{aligned} \tag{3.4}$$

for all $\varphi, \phi \in H$, $k = 1, \ldots, n$ and $t \in [0, T]$.

(A3) $I_k, \widetilde{I}_k : H \to H$ are continuous and there exist positive constants M_k, N_k such that

$$\|I_k(x) - I_k(y)\| \le M_k\|x - y\|^2, \qquad \left\|\widetilde{I}_k(x) - \widetilde{I}_k(y)\right\| \le N_k\|x - y\|^2 \tag{3.5}$$

for each $x, y \in H$, $k = 1, \ldots, n$.

(A4) B is a continuous operator from Ω to H and the linear operator $W : L_0^2(\Omega, H) \to X$ defined by

$$Wu = \int_0^T S(T - s)Bu(s)ds \tag{3.6}$$

has a bounded invertible operator W^{-1} which takes values in $L_0^2(\Omega, H)/\ker W$ such that $\|B\| \le M_1$, $\|W^{-1}\| \le M_2$, for some positive constants M_1, M_2.

We formulate and prove conditions for the approximate controllability of semilinear control differential systems

Theorem 3.2. *Assume that (A1)–(A4) are satisfied and $x_0, y_0 \in L_0^2(\Omega, H)$, then the system* (1.1) *is controllable on* $[0, T]$ *provided that*

$$\begin{aligned} 8M^2\Bigg[&T\overline{M}_D^2 + T\overline{M}_f^2 + \operatorname{tr}(Q)\overline{M}_g^2 + 2M^2\sum_{k=1}^{n} M_k + 2M^2\sum_{k=1}^{n} N_k \\ &+ 8M_2\left(T\overline{M}_D^2 + T\overline{M}_f^2 + \operatorname{tr}(Q)\overline{M}_g^2 + 2M^2\sum_{k=1}^{n} M_k + 2M^2\sum_{k=1}^{n} N_k\right)\Bigg] < 1. \end{aligned} \tag{3.7}$$

Proof. Define the control process with final value $\xi = x(T)$

$$\begin{aligned} u_x^T(t) = W^{-1}\Bigg\{ & \xi - S(T)\left[y_0 - D(0,\phi)\right] - C(T)\phi(0) - \int_0^T C(T-s)D(s,x_s)ds \\ & - \int_0^T S(T-s)f(s,x_s)ds - \int_0^T S(T-s)g(s,x_s)dW(s) \\ & - \sum_{0<t_k<t} C(T-t_k)I_k(x(t_k)) - \sum_{0<t_k<t} S(T-t_k)\widetilde{I}_k(x(t_k))\Bigg\}(t). \end{aligned} \tag{3.8}$$

Let $B_N = \{x \in H_2 : \|x\|_{\mathscr{P}}^2 \le N\}$, for every positive integer N. It is clear that B_N is a bounded closed convex set in H_2 for each N. Define an operator $\pi : H_2 \to H_2$ by

$$\begin{aligned} (\pi x)(t) = {} & C(t)\phi(0) + S(t)\left[y_0 - D(0,\phi)\right] + \int_0^t C(t-s)D(s,x_s)ds + \int_0^t S(t-s)Bu(s)ds \\ & + \int_0^t S(t-s)f(s,x_s)ds + \int_0^t S(t-s)g(s,x_s)dW(s) \\ & + \sum_{0<t_k<t} C(t-t_k)I_k(x(t_k)) + \sum_{0<t_k<t} S(t-t_k)\widetilde{I}_k(x(t_k)). \end{aligned} \tag{3.9}$$

Now let us show that π has a fixed point in H_2 which is a solution of (1.1) by Lemma 2.4. This will be done in the next lemmas. □

Lemma 3.3. *There exists a positive integer N such that $\pi(B_N) \subset B_N$.*

Proof. This proof can be done by contradiction. In fact, if it is not true, then for each positive number N and $t^N \in [0,T]$, there exists a function $x^N \in B_N$, but $\pi(x^N)(t^N) \notin B_N$. That is, $E\|\pi(x^N)(t^N)\|^2 > N$. By applying assumptions (A1)–(A4) one can obtain the following estimates:

$$\begin{aligned} E\left\|\sum_{0<t_k<t^N} S\left(t^N - t_k\right)\widetilde{I}_k\left(x^N(t_k)\right)\right\|^2 & \le NM^2 \sum_{0<t_k<T} E\left\|\widetilde{I}_k\left(x^N(t_k)\right) - \widetilde{I}_k(0) + \widetilde{I}_k(0)\right\| \\ & \le 2NM^2\left(\sum_{k=1}^N N_k E\left\|x^N(t_k)\right\|^2 + \sum_{k=1}^N \left\|\widetilde{I}_k(0)\right\|^2\right), \end{aligned} \tag{3.10}$$

$$\begin{aligned} E\left\|\sum_{0<t_k<t^N} C\left(t^N - t_k\right)I_k\left(x^N(t_k)\right)\right\|^2 & \le NM^2 \sum_{0<t_k<T} E\left\|I_k\left(x^N(t_k)\right) - I_k(0) + I_k(0)\right\| \\ & \le 2NM^2\left(\sum_{k=1}^N M_k E\left\|x^N(t_k)\right\|^2 + \sum_{k=1}^N \|I_k(0)\|^2\right), \end{aligned} \tag{3.11}$$

$$E\left\|\int_0^{t^N} S\left(t^N-s\right)g(s,x_s)dW(s)\right\|^2 \le \operatorname{tr}(Q)M^2\int_0^{t^N} E\left\|g(s,x_s)\right\|^2 ds$$
$$\le \operatorname{tr}(Q)M^2\overline{M}_g^2\int_0^{t^N} E\left(\|\varphi\|^2+1\right)ds, \tag{3.12}$$

$$E\left\|\int_0^{t^N} C\left(t^N-s\right)D(x_s)ds\right\|^2 \le TM^2\overline{M}_D^2\int_0^{t^N} E\left(\|\varphi\|^2+1\right)ds, \tag{3.13}$$

$$E\left\|\int_0^{t^N} S\left(t^N-s\right)f(s,x_s)ds\right\|^2 \le TM^2\overline{M}_f^2\int_0^{t^N} E\left(\|\varphi\|^2+1\right)ds, \tag{3.14}$$

$$\begin{aligned}
&E\left\|\int_0^{t^N} S\left(t^N-s\right)Bu(s)ds\right\|^2 \\
&\quad\le 8M_2M^2\Bigg(\|\xi\|^2+\|\varphi(0)\|^2+y_0^2 \\
&\qquad+(T+1)\overline{M}_D^2\int_0^{t^N} E\left(\|\varphi\|^2+1\right)ds \\
&\qquad+T\overline{M}_f^2\int_0^{t^N} E\left(\|\varphi\|^2+1\right)ds \\
&\qquad+\overline{M}_g^2\int_0^{t^N} E\left(\|\varphi\|^2+1\right)ds \\
&\qquad+2N\sum_{k=1}^{N}N_kE\left\|x^N(t_k)\right\|^2 \\
&\qquad+2N\sum_{k=1}^{N}M_kE\left\|x^N(t_k)\right\|^2\Bigg) := M^2U
\end{aligned} \tag{3.15}$$

which gives

$$\begin{aligned}
N \le{}& E\left\|\left(\pi x^N\right)\left(t^N\right)\right\|^2 \le 8E\left\|C\left(t^N\right)[\varphi(0)]\right\|^2+8E\left\|S\left(t^N\right)[y_0-D(0,\varphi)]\right\|^2 \\
&+8E\left\|\int_0^{t^N} C\left(t^N-s\right)D(s,\varphi)ds\right\|^2+8E\left\|\int_0^{t^N} S\left(t^N-s\right)f(s,\varphi)ds\right\|^2 \\
&+8E\left\|\int_0^{t^N} S\left(t^N-s\right)g(s,\varphi)dW(s)\right\|^2+8E\left\|\sum_{0<t_k<t^N} C\left(t^N-t_k\right)I_k\left(x^N(t_k)\right)\right\|^2 \\
&+8E\left\|\sum_{0<t_k<t^N} S\left(t^N-t_k\right)\tilde{I}_k\left(x^N(t_k)\right)\right\|^2+8E\left\|\int_0^{t^N} S\left(t^N-s\right)Bu(s)ds\right\|^2
\end{aligned}$$

$$\leq L + 8M^2\left[T\overline{M}_D^2 N + T\overline{M}_f^2 N + \operatorname{tr}(Q)\overline{M}_g^2 N + 2NM^2\sum_{k=1}^{n} M_k + 2NM^2\sum_{k=1}^{n} N_k \right.$$
$$\left. + 8M_2\left(T\overline{M}_D^2 N + T\overline{M}_f^2 N + \operatorname{tr}(Q)\overline{M}_g^2 N + 2NM^2\sum_{k=1}^{n} M_k + 2NM^2\sum_{k=1}^{n} N_k\right)\right], \tag{3.16}$$

where

$$L = 8M^2\left[E\|x_0\|^2 + E\|y_0\|^2 + T\overline{M}_D^2 + T\overline{M}_f^2 + \operatorname{tr}(Q)\overline{M}_g^2 + 2M^2\sum_{k=1}^{n} M_k + 2M^2\sum_{k=1}^{n} N_k \right.$$
$$\left. + 8M_2\left(T\overline{M}_D^2 + T\overline{M}_f^2 + \operatorname{tr}(Q)\overline{M}_g^2 + 2M^2\sum_{k=1}^{n} M_k + 2M^2\sum_{k=1}^{n} N_k\right)\right] \tag{3.17}$$

Dividing both sides of (3.16) by N and taking limit as $N \to \infty$, we obtain that

$$8M^2\left[T\overline{M}_D^2 + T\overline{M}_f^2 + \operatorname{tr}(Q)\overline{M}_g^2 + 2M^2\sum_{k=1}^{n} M_k + 2M^2\sum_{k=1}^{n} N_k \right.$$
$$\left. + 8M_2\left(T\overline{M}_D^2 + T\overline{M}_f^2 + \operatorname{tr}(Q)\overline{M}_g^2 + 2M^2\sum_{k=1}^{n} M_k + 2M^2\sum_{k=1}^{n} N_k\right)\right] \geq 1 \tag{3.18}$$

which is a contradiction by (3.7). Thus, $\pi(B_N) \subset B_N$, for some positive number N.

In what follows, we aim to show that the operator π has a fixed point on B_N, which implies that (1.1) is controllable. To this end, we decompose π as follows:

$$\pi = \pi_1 + \pi_2, \tag{3.19}$$

where π_1, π_2 are defined on B_N, respectively, by

$$(\pi_1 x)(t) = S(t)\left[y_0 - D(0,\varphi)\right] + \int_0^t C(t-s)D(0,\varphi)ds + \int_0^t S(t-s)f(s,x_s)ds$$
$$+ \sum_{0<t_k<t} C(t-t_k)I_k(x(t_k)) + \sum_{0<t_k<t} S(t-t_k)\widetilde{I}_k(x(t_k)), \tag{3.20}$$

$$(\pi_2 x)(t) = C(t)\phi(0) + \int_0^t S(t-s)g(s,x_s)dW(s) + \int_0^t S(t-s)Bu(s)ds. \tag{3.21}$$

□

Lemma 3.4. *The operator π_1 as above is contractive.*

Proof. Let $x, y \in B_N$. It follows from assumptions (A1)–(A4) and Hölder's inequality that

$$\begin{aligned}
&E\|(\pi_1 x)(t) - (\pi_1 y)(t)\|^2 \\
&\quad \le 5E\|S(t)[D(0,\varphi) - D(0,\phi)]\|^2 \\
&\qquad + 5E\left\|\int_0^t C(t-s)[D(0,\varphi) - D(0,\phi)]ds\right\|^2 + 5E\left\|\int_0^t S(t-s)[f(s,\varphi) - f(s,\phi)]ds\right\|^2 \\
&\qquad + 5E\left\|\sum_{0<t_k<t} C(t-t_k)[I_k(x(t_k)) - I_k(y(t_k))]\right\|^2 \\
&\qquad + 5E\left\|\sum_{0<t_k<t} S(t-t_k)\left[\widetilde{I}_k(x(t_k)) - \widetilde{I}_k(y(t_k))\right]\right\|^2 \\
&\quad \le 5M^2M_D^2 \sup_{s\in[0,T]} E\|x(s) - y(s)\|^2 + 5TM^2M_D^2 \sup_{s\in[0,T]} E\|x(s) - y(s)\|^2 \\
&\qquad + 5TM^2M_f^2 \sup_{s\in[0,T]} E\|x(s) - y(s)\|^2 + 5nM^2 \sum_{0<t_k<t} M_k E\|x(t_k) - y(t_k)\|^2 \\
&\qquad + 5nM^2 \sum_{0<t_k<t} N_k E\|x(t_k) - y(t_k)\|^2
\end{aligned} \tag{3.22}$$

which deduces

$$\begin{aligned}
&\sup_{s\in[0,T]} E\|(\pi_1 x)(s) - (\pi_1 y)(s)\|^2 \\
&\quad \le 5M^2\left[M_D^2 + TM_D^2 + TM_f^2 + n\sum_{i=0}^{n} M_k + n\sum_{i=0}^{n} N_k\right] \sup_{s\in[0,T]} E\|x(s) - y(s)\|^2
\end{aligned} \tag{3.23}$$

and the lemma follows. □

Lemma 3.5. *The operator π_2 is compact.*

Proof. Let $N > 0$ be such that $\pi_2(B_N) \subset B_N$.

We first need to prove that the set of functions $\pi_2(B_N)$ is equicontinuous on $[0, T]$. Let $0 < \varepsilon < t < T$ and $\delta > 0$ such that $\|S(s)x - S(s')x\|^2 < \varepsilon$ and $\|C(s)x - C(s')x\|^2 < \varepsilon$, for every $s, s' \in [0,T]$ with $|s - s'| \le \delta$. For $x \in B_N$ and $0 < |h| < \delta$ with $t + h \in [0,T]$ we have

$$\begin{aligned}
&E\|(\pi_2 x)(t+h) - (\pi_2 x)(t)\|^2 \\
&\quad \le 3E\|[C(t+h) - C(t)]\phi(0)\|^2 \\
&\qquad + 3E\left\|\int_0^t [S(t+h-s) - S(t-s)]g(s,x_s)dW(s) - \int_t^{t+h} S(t+h-s)g(s,x_s)dW(s)\right\|^2 \\
&\qquad + 3E\left\|\int_0^t [S(t+h-s) - S(t-s)]Bu(s)ds - \int_t^{t+h} S(t+h-s)Bu(s)ds\right\|^2
\end{aligned}$$

$$
\begin{aligned}
&\leq 3\varepsilon E\|\phi(0)\|^2 + 6\,\mathrm{tr}(Q)M^2\int_t^{t+h} E\|g(s,x'(s),x_s)\|^2 ds + 6M^2\int_t^{t+h} E\|Bu(s)\|^2 ds \\
&\quad + 6M^2\int_0^t E\|Bu(s)\|^2 ds + 6\,\mathrm{tr}(Q)\int_0^t E\|[S(t+h-s)-S(t-s)]g(s,x_s)\|^2 ds \\
&\leq 4\varepsilon E\|x_0\|^2 + 4\varepsilon E\|g(x)\|^2 + 4\varepsilon\,\mathrm{tr}(Q)\int_0^t E\|g(s,x_s)\|^2 ds \\
&\quad + 4\,\mathrm{tr}(Q)M^2\int_t^{t+h} E\|g(s,s^x(s))\|^2 ds.
\end{aligned}
\tag{3.24}
$$

Noting that $E\|g(s,s^x(s))\|^2 \leq h_N(s) \in L^1([0,T])$, we see that $\pi_2(B_N)$ is equicontinuous on $[0,T]$.

We next need to prove that π_2 maps B_N into a precompact set in B_N. That is, for every fixed $t \in [0,T]$, the set $V(t) = \{(\pi_2 x)(t) : x \in B_N\}$ is precompact in B_N. It is obvious that $V(0) = \{(\pi_2 x)(0)\}$ is precompact. Let $0 < t \leq T$ be fixed and $0 < \varepsilon < t$. For $x \in B_N$, define

$$
\begin{aligned}
(\pi_2^\varepsilon x)(t) &= C(t)\phi(0) + \int_0^{t-\varepsilon} S(t-s)g(s,x_s)dW(s) + \int_0^{t-\varepsilon} S(t-s)Bu(s)ds \\
&= C(t)\phi(0) + S(\varepsilon)\int_0^{t-\varepsilon} S(t-\varepsilon-s)g(s,x_s)dW(s) + S(\varepsilon)\int_0^{t-\varepsilon} S(t-\varepsilon-s)Bu(s)ds.
\end{aligned}
\tag{3.25}
$$

Since $C(t), S(t), t > 0$, are compact, it follows that $V_\varepsilon(t) = \{(\pi_2^\varepsilon x)(t) : x \in B_N\}$ is precompact in H for every $0 < \varepsilon < t$. Moreover, for each $x \in B_N$, we have

$$
\begin{aligned}
E\|(\pi_2 x)(t) - (\pi_2^\varepsilon x)(t)\|^2 &\leq 2\,\mathrm{tr}(Q)M^2\int_{t-\varepsilon}^t E\|g(s,x_s)\|^2 ds + 2M^2\int_{t-\varepsilon}^t E\|Bu(s)\|^2 ds \\
&\leq \varepsilon 2M^2\left[\mathrm{tr}(Q)E\left(\|\varphi\|^2+1\right) + U\right] \longrightarrow 0 \quad as \quad \varepsilon \longrightarrow 0^+
\end{aligned}
\tag{3.26}
$$

which means that there are precompact sets arbitrary close to the set $V(t)$. Thus, $V(t)$ is precompact in B_N.

Finally, from the assumptions on g, it is obvious that π_2 is continuous. Thus, Arzelá-Ascoli theorem yields that π_2 is compact. Therefore, π is a condensing map on B_N. □

4. Applications

In this section, we now give an example to illustrate the theory obtained. Considering the following impulsive neutral second-order stochastic differential equation:

$$
\begin{gathered}
d\left[\frac{\partial x(t,z)}{\partial t} + a(t)x(t,z)\right] = \frac{\partial^2}{\partial z^2}x(t,z)dt + \sigma(t,x(t,z))dW(t), \quad t \in [0,1] \\
x(t,0) = x(t,\pi) = 0, \quad t \in [0,1], \quad \frac{\partial x(0,z)}{\partial t} = x_1(z), \quad z \in [0,\pi] \\
\Delta x(t_k)(z) = I_k(x(t_k))(z), \quad \Delta x'(t_k)(z) = \widetilde{I}_k(x(t_k))(z), \quad t = t_k,
\end{gathered}
\tag{4.1}
$$

to rewrite (4.1) into the abstract form of (1.1), let $H = L^2[0,\pi]$, $A : H \to H$ be an operator by $Ax = x''$ with domain

$$D(A) = \{x \in H : x,\ x' \text{ are absolutely continuous},\ x'' \in H,\ x(0) = x(\pi) = 0\}. \tag{4.2}$$

It is well known that A is the infinitesimal generator of a strongly continuous cosine family $\{C(t) : t \in R\}$ in H and is given by

$$C(t)x = \sum_{n=1}^{\infty} \cos(nt)\langle x, e_n\rangle e_n, \quad x \in H, \tag{4.3}$$

where $e_n(\xi) = \sqrt{2/\pi}\sin(n\xi)$ and $i = 1,2,\ldots$ is the orthogonal set of eigenvalues of A. The associated sine family $\{S(t) : t > 0\}$ is compact and is given by

$$S(t)x = \sum_{n=1}^{\infty} \frac{1}{n}\sin(nt)\langle x, e_n\rangle e_n, \quad x \in H. \tag{4.4}$$

Thus, we can impose some suitable conditions on the above functions to verify the condition in Theorem 3.2.

5. Conclusions

In this paper, we have studied the controllability of second-order impulsive evolution equations. Through the Sadovskii fixed point theorem and the theory of strongly continuous cosine families of operators, we have investigated the sufficient conditions for the controllability of the system considered. At last, an example is provided to show the usefulness and effectiveness of proposed controllability results.

Acknowledgments

This work was supported in part by the Key Project of the National Nature Science Foundation of China (no. 61134009), the National Nature Science Foundation of China (no. 60975059), Specialized Research Fund for the Doctoral Program of Higher Education from Ministry of Education of China (no. 20090075110002), Specialized Research Fund for Shanghai Leading Talents, and Project of the Shanghai Committee of Science and Technology (nos. 11XD1400100, 11JC1400200, 10JC1400200).

References

[1] Y.-K. Chang, "Controllability of impulsive functional differential systems with infinite delay in Banach spaces," *Chaos, Solitons and Fractals*, vol. 33, no. 5, pp. 1601–1609, 2007.

[2] R. Sakthivel, "Approximate controllability of impulsive stochastic evolution equations," *Funkcialaj Ekvacioj*, vol. 52, no. 3, pp. 381–393, 2009.

[3] Y. Ren, L. Hu, and R. Sakthivel, "Controllability of impulsive neutral stochastic functional differential inclusions with infinite delay," *Journal of Computational and Applied Mathematics*, vol. 235, no. 8, pp. 2603–2614, 2011.

[4] S. K. Ntouyas and D. O'Regan, "Some remarks on controllability of evolution equations in Banach spaces," *Electronic Journal of Differential Equations*, vol. 2009, pp. 1–6, 2009.
[5] J. Y. Park, S. H. Park, and Y. H. Kang, "Controllability of second-order impulsive neutral functional differential inclusions in Banach spaces," *Mathematical Methods in the Applied Sciences*, vol. 33, no. 3, pp. 249–262, 2010.
[6] R. Sakthivel, N. I. Mahmudov, and J. H. Kim, "On controllability of second order nonlinear impulsive differential systems," *Nonlinear Analysis*, vol. 71, no. 1-2, pp. 45–52, 2009.
[7] M. A. Shubov, C. F. Martin, J. P. Dauer, and B. P. Belinskiy, "Exact controllability of the damped wave equation," *SIAM Journal on Control and Optimization*, vol. 35, no. 5, pp. 1773–1789, 1997.
[8] J. Luo, "Fixed points and exponential stability of mild solutions of stochastic partial differential equations with delays," *Journal of Mathematical Analysis and Applications*, vol. 342, no. 2, pp. 753–760, 2008.
[9] J. Luo and T. Taniguchi, "Fixed points and stability of stochastic neutral partial differential equations with infinite delays," *Stochastic Analysis and Applications*, vol. 27, no. 6, pp. 1163–1173, 2009.
[10] T. A. Burton, "Stability by fixed point theory or Liapunov theory: a comparison," *Fixed Point Theory*, vol. 4, no. 1, pp. 15–32, 2003.
[11] T. A. Burton, "Fixed points, stability, and exact linearization," *Nonlinear Analysis*, vol. 61, no. 5, pp. 857–870, 2005.
[12] T. A. Burton and T. Furumochi, "Asymptotic behavior of solutions of functional differential equations by fixed point theorems," *Dynamic Systems and Applications*, vol. 11, no. 4, pp. 499–519, 2002.
[13] T. A. Burton and B. Zhang, "Fixed points and stability of an integral equation: nonuniqueness," *Applied Mathematics Letters*, vol. 17, no. 7, pp. 839–846, 2004.
[14] K. Sobczyk, *Stochastic Differential Equations*, vol. 40 of *Mathematics and Its Applications (East European Series)*, Kluwer Academic, Dordrecht, The Netherlands, 1991.
[15] W. E. Fitzgibbon, "Global existence and boundedness of solutions to the extensible beam equation," *SIAM Journal on Mathematical Analysis*, vol. 13, no. 5, pp. 739–745, 1982.
[16] M. Benchohra, J. Henderson, and S. K. Ntouyas, "Existence results for impulsive semilinear neutral functional differential equations in Banach spaces," *Memoirs on Differential Equations and Mathematical Physics*, vol. 25, pp. 105–120, 2002.
[17] X. Liu and A. R. Willms, "Impulsive controllability of linear dynamical systems with applications to maneuvers of spacecraft," *Mathematical Problems in Engineering*, vol. 2, no. 4, pp. 277–299, 1996.
[18] E. Hernández, M. Pierri, and G. Goncalves, "Existence results for an impulsive abstract partial differential equation with state-dependent delay," *Computers & Mathematics with Applications*, vol. 52, no. 3-4, pp. 411–420, 2006.
[19] G. Da Prato and J. Zabczyk, *Stochastic Equations in Infinite Dimensions*, vol. 44 of *Encyclopedia of Mathematics and Its Applications*, Cambridge University Press, Cambridge, Mass, USA, 1992.
[20] H. O. Fattorini, *Second Order Linear Differential Equations in Banach Spaces*, vol. 108 of *North-Holland Mathematics Studies*, North-Holland, Amsterdam, The Netherlands, 1985.
[21] C. C. Travis and G. F. Webb, "Cosine families and abstract nonlinear second order differential equations," *Acta Mathematica Academiae Scientiarum Hungaricae*, vol. 32, no. 1-2, pp. 75–96, 1978.
[22] B. N. Sadovskiĭ, "On a fixed point principle," *Functional Analysis and Its Applications*, vol. 1, no. 2, pp. 74–76, 1967.

Hindawi Publishing Corporation
Mathematical Problems in Engineering
Volume 2012, Article ID 183729, 21 pages
doi:10.1155/2012/183729

Research Article

Almost Sure Stability and Stabilization for Hybrid Stochastic Systems with Time-Varying Delays

Hua Yang,[1,2] Huisheng Shu,[3] Xiu Kan,[1] and Yan Che[1]

[1] *School of Information Science and Technology, Donghua University, Shanghai 200051, China*
[2] *College of Information Science and Engineering, Shanxi Agricultural University, Taigu 030801, China*
[3] *Department of Applied Mathematics, Donghua University, Shanghai 200051, China*

Correspondence should be addressed to Huisheng Shu, hsshu@dhu.edu.cn

Received 21 June 2012; Accepted 1 August 2012

Academic Editor: Bo Shen

The problems of almost sure (a.s.) stability and a.s. stabilization are investigated for hybrid stochastic systems (HSSs) with time-varying delays. The different time-varying delays in the drift part and in the diffusion part are considered. Based on nonnegative semimartingale convergence theorem, Hölder's inequality, Doob's martingale inequality, and Chebyshev's inequality, some sufficient conditions are proposed to guarantee that the underlying nonlinear hybrid stochastic delay systems (HSDSs) are almost surely (a.s.) stable. With these conditions, a.s. stabilization problem for a class of nonlinear HSDSs is addressed through designing linear state feedback controllers, which are obtained in terms of the solutions to a set of linear matrix inequalities (LMIs). Two numerical simulation examples are given to show the usefulness of the results derived.

1. Introduction

In the past decades, the problems of stability analysis and stabilization synthesis of stochastic systems have received significant attentions, and many results have been reported; see, for example [1–7] and the references therein. Commonly, the above problems can be solved not only in moment sense [8–10] but also in a.s. sense [11, 12]. However, in recent years, much interest has been focused on a.s. stability problems for stochastic systems; see, for example [8, 13] and the references therein.

It is well known that a lot of dynamical systems have variable structures subject to abrupt changes in their parameters, which are usually caused by abrupt phenomena such as component failures or repairs, changing subsystem interconnections, and abrupt environmental disturbances. The HSSs, which are regarded as the stochastic systems with

Markovian switching in this paper, have been used to model the previous phenomena; see, for example [14–18] and the references therein. The HSSs combine a part of the state $x(t)$ that takes values in $\mathbb{R}^n$ continuously and another part of the state $r(t)$ that is a Markov chain taking discrete values in a finite space $S = \{1, 2, \ldots, N\}$. One of the important issues in the study of HSSs is the analysis of stability. In particular, it is not necessary for the stable HSSs to require every subsystem to be stable; in other words, even all the subsystems are unstable; as the result of Markovian switching, the HSSs may be stable. These reveal that the Markovian jumps play an important role in the stability analysis of HSSs. Therefore, in the past few decades, a great deal of literature has appeared on the topic of stability analysis and stabilization synthesis of HSSs; see, for example [2, 13, 14, 19, 20].

On the other hand, time delays are frequently encountered in a variety of dynamic systems, such as nuclear reactors, chemical engineering systems, biological systems, and population dynamics models. They are often a source of instability and poor performance of systems. So the problems of stability analysis and stabilization synthesis of HSDSs have been of great importance and interest. The classical efforts can be classified into two categories, namely, moment sense criteria, see, for example [21–23], and a.s. sense criteria, see, for example [24, 25]. Among the existing results, in [25], based on the techniques proposed in [26] which were developed via the results of [11], a.s. stability and stabilization of HSDSs were studied. In [24], the a.s. stability analysis problem for a general class of HSDSs was derived from extending the results in [25] to HSSs with mode-dependent interval delays. However, to the author's best knowledge, when the different time-varying delays in the drift part and in the diffusion part are considered, the a.s. stability analysis and stabilization synthesis problems for nonlinear HSDSs have not been adequately addressed and remain an interesting and challenging research topic. This situation motivates the present study.

In this paper, we are concerned with a.s. stability analysis and stabilization synthesis problems for HSDSs. The purpose of stability is to develop conditions such that the underlying systems are a.s. stable. Following the same idea as in dealing with the stability problem, linear state feedback controllers are designed such that the special nonlinear or linear closed-loop systems are a.s. stable. The explicit expressions for the desired state feedback controllers are given by means of the solutions to a set of LMIs. Two numerical simulation examples are exploited to verify the effectiveness of the theoretical results. The main contribution of this paper is mainly twofold: (1) *the different time-varying delays in the drift part and in the diffusion part are considered for nonlinear HSDSs;* (2) *for a class of nonlinear HSDSs, the stabilization synthesis problem is investigated in the a.s. sense.*

This paper is organized as follows. In Section 2, we formulate some preliminaries. In Section 3, we investigate the a.s. stability for the hybrid stochastic systems with time-varying delays. In Section 4, the results of Section 3 are then applied to establish a sufficient criterion for the stabilization. In Section 5, two examples are discussed for illustration. Finally, conclusions are drawn in Section 6.

Notation 1. The notation used here is fairly standard unless otherwise specified. $\mathbb{R}^n$ and $\mathbb{R}^{n\times m}$ denote, respectively, the n dimensional Euclidean space and the set of all $n \times m$ real matrices, and let $\mathbb{R}_+ = [0, +\infty)$. $(\Omega, \mathcal{F}, \{\mathcal{F}_t\}_{t\geq 0}, \mathbb{P})$ be a complete probability space with a natural filtration $\{\mathcal{F}_t\}_{t\geq 0}$ satisfying the usual conditions (i.e., it is right continuous, and $\mathcal{F}_0$ contains all $\mathbb{P}$-null sets). If x, y are real numbers, then $x \vee y$ stands for the maximum of x and y, and $x \wedge y$ the minimum of x and y. M^T represents the transpose of the matrix M. $\lambda_{\max}(M)$ and $\lambda_{\min}(M)$ denote the largest and smallest eigenvalue of M, respectively. $|\cdot|$ denotes the Euclidean norm in $\mathbb{R}^n$. $\mathbb{E}\{\cdot\}$ stands for the mathematical expectation. $\mathbb{P}\{\cdot\}$ means the probability. $C([-\tau, 0]; \mathbb{R}^n)$

denotes the family of all continuous $\mathbb{R}^n$-valued function φ on $[-\tau, 0]$ with the norm $|\varphi| = \sup\{|\varphi(\theta)| : -\tau \le \theta \le 0\}$. $C^b_{\mathcal{F}_0}([-\tau, 0); \mathbb{R}^n)$ being the family of all $\mathcal{F}_0$-measurable bounded $C([-\tau, 0); \mathbb{R}^n)$-value random variables $\xi = \{\xi(\theta) : -\tau \le \theta \le 0\}$. $L^1(\mathbb{R}_+; \mathbb{R}_+)$ denotes the family of functions $\lambda : \mathbb{R}_+ \to \mathbb{R}_+$ such that $\int_0^\infty \lambda(t)dt < \infty$.

2. Problem Formulation

In this paper, let $r(t), t \ge 0$ be a right-continuous Markov chain on the probability space taking values in a finite state space $S = \{1, 2, \ldots, N\}$ with generator $\Gamma = (\gamma_{ij})_{N\times N}$ given by

$$\mathbb{P}\{r(t+\Delta) = j \mid r(t) = i\} = \begin{cases} \gamma_{ij}\Delta + o(\Delta) & \text{if } i \ne j, \\ 1 + \gamma_{ii}\Delta + o(\Delta) & \text{if } i = j, \end{cases} \tag{2.1}$$

where $\Delta > 0$ and $\gamma_{ij} \ge 0$ is the transition rate from mode i to mode j if $i \ne j$ while $\gamma_{ii} = -\sum_{j\ne i}\gamma_{ij}$. Assume that the Markov chain $r(\cdot)$ is independent of the Brownian motion $B(\cdot)$. It is known that almost all sample paths of $r(\cdot)$ are right-continuous step functions with a finite number of simple jumps in any finite subinterval of $R_+ := [0, \infty)$.

Let us consider a class of stochastic systems with time-varying delays:

$$dx(t) = f(x(t), x(t-\tau_1(t)), t, r(t))dt + g(x(t), x(t-\tau_2(t)), t, r(t))dB(t) \tag{2.2}$$

with initial data $x_0 = \{x(\theta) : -\tau \le \theta \le 0\} = \xi \in C^b_{\mathcal{F}_0}([-\tau, 0); \mathbb{R}^n)$ and $r(0) = r_0 \in S$, where $\tau \triangleq \max\{\tau_1, \tau_2\}$, τ_1 and τ_2 are positive constant and $\tau_1(t)$ and $\tau_2(t)$ are nonnegative differential functions which denote the time-varying delays and satisfy

$$\begin{aligned} &0 \le \tau_1(t) \le \tau_1, \qquad \dot{\tau}_1(t) \le d_{\tau_1} < 1, \\ &0 \le \tau_2(t) \le \tau_2, \qquad \dot{\tau}_2(t) \le d_{\tau_2} < 1. \end{aligned} \tag{2.3}$$

The nonlinear functions $f : \mathbb{R}^n \times \mathbb{R}^n \times \mathbb{R}_+ \times S \to \mathbb{R}^n$ and $g : \mathbb{R}^n \times \mathbb{R}^n \times \mathbb{R}_+ \times S \to \mathbb{R}^{n\times m}$ satisfy the local Lipschitz condition in (x, y, z); that is, for any $K > 0$, there is $L_K > 0$ such that

$$\begin{aligned} &\left|f(x,y,t,i) - f(\overline{x},\overline{y},t,i)\right| \vee \left|g(x,z,t,i) - g(\overline{x},\overline{z},t,i)\right| \\ &\quad \le L_K\left(|x-\overline{x}| + \left|y-\overline{y}\right| + |z-\overline{z}|\right), \end{aligned} \tag{2.4}$$

for all $|x| \vee |y| \vee |z| \vee |\overline{x}| \vee |\overline{y}| \vee |\overline{z}| \le K$, $t \ge 0$ and $i \in S$, and moreover, $\sup_{t\ge 0, i\in S}\{|f(0,0,t,i)| \vee |g(0,0,t,i)| : t \ge 0, i \in S\} \le K_0$ with some nonnegative number K_0.

Remark 2.1. It should be pointed out that the systems (2.2) can be seen as the specialization of multiple time-varying delays systems which are of the form

$$\begin{aligned} dx(t) = {} & f(x(t), x(t-\tau_1(t)), x(t-\tau_2(t)), t, r(t))dt \\ & + g(x(t), x(t-\tau_1(t)), x(t-\tau_2(t)), t, r(t))dB(t). \end{aligned} \tag{2.5}$$

But it is easy to see that the results in this paper can be applied to the systems (2.5) by the similar assumption in (2.4).

Let $C^{2,1}(\mathbb{R}^n \times \mathbb{R}_+ \times S; \mathbb{R}_+)$ denote the family of all nonnegative functions $V(x,t,i)$ on $\mathbb{R}^n \times \mathbb{R}_+ \times S$ that are twice continuously differentiable in x and once in t. If $V \in C^{2,1}(\mathbb{R}^n \times \mathbb{R}_+ \times S; \mathbb{R}_+)$, define an operator $\mathcal{L}$ associated with (2.2) from $\mathbb{R}^n \times \mathbb{R}^n \times \mathbb{R}^n \times \mathbb{R}_+ \times S$ to $\mathbb{R}$ by

$$\begin{aligned}\mathcal{L}V(x,y,z,t,i) &= V_t(x,t,i) + V_x(x,t,i)f(x,y,t,i) \\ &\quad + \frac{1}{2}\operatorname{trace}\left[g^T(x,z,t,)V_{xx}(x,t,i)g(x,z,t,i)\right] + \sum_{j=1}^{N}\gamma_{ij}V(x,t,j).\end{aligned} \tag{2.6}$$

Remark 2.2. $\mathcal{L}V$ is thought as a single notation and is defined on $\mathbb{R}^n \times \mathbb{R}^n \times \mathbb{R}^n \times \mathbb{R}_+ \times S$ while V is defined on $\mathbb{R}^n \times [-\tau, \infty) \times S$.

Definition 2.3. The system (2.2) is said to be a.s. stable if for all $\xi \in C^b_{\mathcal{F}_0}([-\tau, 0); \mathbb{R}^n)$ and $r_0 \in S$

$$\mathbb{P}\left(\lim_{t\to\infty} x(t;\xi,r_0) = 0\right) = 1. \tag{2.7}$$

3. Main Results

Theorem 3.1. *Assume that there exist nonnegative functions* $V \in C^{2,1}(\mathbb{R}^n \times \mathbb{R}_+ \times S; \mathbb{R}_+)$, $\lambda \in L^1(\mathbb{R}_+; \mathbb{R}_+)$, $\omega_1, \omega_2, \omega_3 \in C(\mathbb{R}^n; \mathbb{R}_+)$ *such that*

$$\begin{aligned}\mathcal{L}V(x,y,z,t,i) &\le \lambda(t) - k_1\omega_1(x) + k_2\omega_2(y) + k_3\omega_3(z), \\ &\qquad \forall(x,y,z,t,i) \in \mathbb{R}^n \times \mathbb{R}^n \times \mathbb{R}^n \times \mathbb{R}_+ \times S,\end{aligned} \tag{3.1}$$

$$\omega_1(x) > \omega_2(x) + \omega_3(x), \quad \forall x \neq 0, \tag{3.2}$$

$$\lim_{|x|\to\infty} \inf_{t\ge 0, i\in S} V(x,t,i) = \infty, \tag{3.3}$$

where k_1, k_2 *and* k_3 *are positive numbers satisfying* $k_1 \ge \max\{k_2/(1-d_{\tau_1}), k_3/(1-d_{\tau_2})\}$. *Then system* (2.2) *is almost surely stable.*

To prove this theorem, let us present the following lemmas.

Lemma 3.2 (see [24, 25]). *If* $V \in C^{2,1}(\mathbb{R}^n \times \mathbb{R}_+ \times S; \mathbb{R}_+)$, *then for any* $t \ge 0$, *the generalized Itô's formula is given as*

$$\begin{aligned}dV(x(t),t,r(t)) &= \mathcal{L}V(x(t),x(t-\tau_1(t)),x(t-\tau_2(t)),t,r(t))dt \\ &\quad + V_x(x(t),t,r(t))g(x(t),x(t-\tau_2(t)),t,r(t))dB(t) \\ &\quad + \int_{\mathbb{R}} [V(x(t),t,r(t)+l(r(t),\alpha)) - V(x(t),t,r(t))] \times \mu(dt,d\alpha),\end{aligned} \tag{3.4}$$

where function $l(\cdot,\cdot)$ *and martingale measure* $\mu(\cdot,\cdot)$ *are defined as, for example,* (2.6) *and* (2.7) *in [25].*

Lemma 3.3 (see [27]). *Let $A_1(t)$ and $A_2(t)$ be two continuous adapted increasing processes on $t \geq 0$ with $A_1(0) = A_2(0) = 0$ a.s., let $M(t)$ be a real-valued continuous local martingale with $M(0) =$ a.s., and let ζ be a nonnegative $\mathcal{F}_0$-measurable random variable such that $\mathbb{E}\zeta < \infty$. Denote $X(t) = \zeta + A_1(t) - A_2(t) + M(t)$ for all $t \geq 0$. If $X(t)$ is nonnegative, then*

$$\left\{\lim_{t\to\infty} A_1(t) < \infty\right\} \subset \left\{\lim_{t\to\infty} X(t) < \infty\right\} \cap \left\{\lim_{t\to\infty} A_2(t) < \infty\right\} \quad a.s., \tag{3.5}$$

where $C \subset D$ a.s. means $\mathbb{P}(C \cap D^c = 0) = 0$. In particular, if $\lim_{t\to\infty} A_1(t) < \infty$ a.s., then,

$$\lim_{t\to\infty} X(t) < \infty, \qquad \lim_{t\to\infty} A_2(t) < \infty, \qquad -\infty < \lim_{t\to\infty} M(t) < \infty \quad a.s.. \tag{3.6}$$

That is, all of the three processes $X(t), A_2(t)$, and $M(t)$ converge to finite random variables with probability one.

Lemma 3.4 (see [25]). *Under the conditions of Theorem 3.1, for any initial data $\{x(\theta) : -\tau \leq \theta \leq 0\} = \xi \in C^b_{\mathcal{F}_0}([-\tau, 0); \mathbb{R}^n)$ and $r(0) = i_0 \in S$, (2.2) has a unique global solution.*

Proof. Fix any initial data ξ, r_0, and let β be the bound for ξ. For each integer $k \geq \beta$, define

$$f^{(k)}(x, y, t, i) = f\left(\frac{|x| \wedge k}{|x|}x, \frac{|y| \wedge k}{|y|}y, t, i\right), \tag{3.7}$$

where we set $(|x| \wedge k/|x|)x = 0$ when $x = 0$. Define $g^{(k)}(x, z, t, i)$ similarly. By (2.4), we can observe that $f^{(k)}$ and $g^{(k)}$ satisfy the global Lipschitz condition and the linear growth condition. By the known existence-and-uniqueness theorem, there exists a unique global solution $x_k(t)$ on $t \in [-\tau, \infty)$ to the equation

$$\begin{aligned} dx_k(t) = {} & f^{(k)}(x_k(t), x_k(t - \tau_1(t)), t, r(t))dt \\ & + g^{(k)}(x_k(t), x_k(t - \tau_2(t)), t, r(t))dB(t) \end{aligned} \tag{3.8}$$

with initial data $\{x_k(\theta) : -\tau \leq \theta \leq 0\} = \xi$ and $r(0) = r_0$.

Define the stopping time

$$\sigma_k = \inf\{t \geq 0 : |x_k(t)| \geq k\}, \tag{3.9}$$

where we set $\inf \emptyset = \infty$ as usual. It is easy to show that $x_k(t) = x_{k+1}(t)$ if $0 \leq t \leq \sigma_k$, which implies that σ_k is increasing in k. Letting $\sigma = \lim_{k\to\infty}\sigma_k$, the property above also enables us to define $x(t)$ for $t \in [-\tau, \sigma)$ as $x(t) = x_k(t)$ if $-\tau \leq t \leq \sigma_k$.

It is clear that $x(t)$ is a unique solution of (2.2) for $t \in [-\tau, \sigma)$. To complete the proof, we only need to show $\mathbb{P}\{\sigma = \infty\} = 1$. By Lemma 3.2, we have that for any $t > 0$,

$$\begin{aligned}\mathbb{E}V(x_k(t\wedge\sigma_k), t\wedge\sigma_k, r(t\wedge\sigma_k)) &= \mathbb{E}V(x_k(0), 0, r(0)) \\ &\quad + \mathbb{E}\int_0^{t\wedge\sigma_k} \mathcal{L}^{(k)}V(x_k(s), x_k(s-\tau_1(s)), x_k(s-\tau_2(s)), s, r(s))ds,\end{aligned} \tag{3.10}$$

where operator $\mathcal{L}^{(k)}V$ is defined similarly as $\mathcal{L}V$ was defined by (2.6). By the definitions of $f^{(k)}$ and $g^{(k)}$, if $0 \le s \le t\wedge\sigma_k$, we hence observe that

$$\begin{aligned}&\mathcal{L}^{(k)}V(x_k(s), x_k(s-\tau_1(s)), x_k(s-\tau_2(s)), s, r(s)) \\ &\quad = \mathcal{L}V(x_k(s), x_k(s-\tau_1(s)), x_k(s-\tau_2(s)), s, r(s)).\end{aligned} \tag{3.11}$$

By the conditions of (3.1) and (3.2), we derive that

$$\begin{aligned}&\mathbb{E}V(x_k(t\wedge\sigma_k), t\wedge\sigma_k, r(t\wedge\sigma_k)) \\ &\quad \le V(\xi(0), 0, r_0) + \mathbb{E}\int_0^t [-k_1\omega_1(x(s)) + k_2\omega_2(x(s-\tau_1(s))) + k_3\omega_3(x(s-\tau_2(s)))]ds \\ &\qquad + \int_0^t \lambda(s)ds \\ &\quad \le V(\xi(0), 0, r_0) + \mathbb{E}\int_0^t -k_1\omega_1(x(s))ds + \mathbb{E}\int_{-\tau_1}^{t-\tau_1(t)} \left(\frac{k_2}{1-d_{\tau_1}}\right)\omega_2(s)ds \\ &\qquad + \mathbb{E}\int_{-\tau_2}^{t-\tau_2(t)} \left(\frac{k_3}{1-d_{\tau_2}}\right)\omega_3(s)ds + \int_0^t \lambda(s)ds \\ &\quad \le V(\xi(0), 0, r_0) + \mathbb{E}\int_{-\tau}^0 k_1[\omega_2(\xi(\theta)) + \omega_3(\xi(\theta))]d\theta \\ &\qquad - \mathbb{E}\int_0^t k_1(\omega_1(s) - \omega_2(s) - \omega_3(s))ds + \int_0^t \lambda(s)ds \\ &\quad \le V(\xi(0), 0, r_0) + \mathbb{E}\int_{-\tau}^0 k_1[\omega_2(\xi(\theta)) + \omega_3(\xi(\theta))]d\theta + \int_0^t \lambda(s)ds.\end{aligned} \tag{3.12}$$

On the other hand,

$$\begin{aligned}\mathbb{E}V(x_k(t\wedge\sigma_k), t\wedge\sigma_k, r(t\wedge\sigma_k)) &\ge \int_{\{\sigma_k\le t\}} V(x_k(t\wedge\sigma_k), t\wedge\sigma_k, r(t\wedge\sigma_k))d\mathbb{P} \\ &\ge \mathbb{P}\{\sigma_k \le t\} \inf_{|x|\ge k, t\ge 0, i\in S} V(x, t, i).\end{aligned} \tag{3.13}$$

This yields

$$\mathbb{P}\{\sigma_k \le t\} \le \frac{V(\xi(0),0,r_0) + \mathbb{E}\int_{-\tau}^{0} k_1[\omega_2(\xi(\theta)) + \omega_3(\xi(\theta))]d\theta + \int_0^t \lambda(s)ds}{\inf_{|x|\ge k, t\ge 0, i\in S} V(x,t,i)}. \tag{3.14}$$

Letting $k \to \infty$ and using (3.3), we obtain $\mathbb{P}(\sigma \le t) = 0$. Since t is arbitrary, we must have $\mathbb{P}(\sigma = \infty) = 1$. The proof is therefore complete. □

Let us now begin to prove our main result.

Proof. Let $\omega(x) = \omega_1(x) - \omega_2(x) - \omega_3(x)$ for all $x \in \mathbb{R}^n$. Inequality (3.2) implies $\omega(x) > 0$ whenever $x \neq 0$. Fix any initial value ξ and any initial state r_0, and for simplicity write $x(t;\xi,r_0) = x(t)$.

By Lemma 3.2 and condition (3.1), we have

$$\begin{aligned}
V(x(t),t,r(t)) &= V(\xi(0),0,r_0) + \int_0^t \mathcal{L}V(x(s),x(s-\tau_1(s)),x(s-\tau_2(s)),s,r(s))ds \\
&\quad + \int_0^t V_x(x(s),s,r(s))g(x(s),x(s-\tau_2(s)),s,r(s))dB(s) \\
&\quad + \int_0^t \int_{\mathbb{R}} [V(x(s),s,r_0 + l(r(s),\alpha)) - V(x(s),s,r(s))]\mu(ds,d\alpha) \\
&\le V(\xi(0),0,r_0) + \int_0^t \lambda(s)ds - \int_0^t k_1\omega_1(x(s)) \\
&\quad + \int_0^t [k_2\omega_2(x(s-\tau_1(s))) + k_3\omega_3(x(s-\tau_2(s)))]ds \\
&\quad + \int_0^t V_x(x(s),s,r(s))g(x(s),x(s-\tau_2(s)),s,r(s))dB(s) \\
&\quad + \int_0^t \int_{\mathbb{R}} [V(x(s),s,r_0 + l(r(s),\alpha)) - V(x(s),s,r(s))]\mu(ds,d\alpha) \\
&\le V(\xi(0),0,r_0) + \int_0^t \lambda(s)ds + k_1\int_{-\tau}^{0} [\omega_2(x(s)) + \omega_3(x(s))]ds \\
&\quad - k_1\int_0^t \omega(x(s))ds + \int_0^t V_x(x(s),s,r(s))g(x(s),x(s-\tau_2(s)),s,r(s))dB(s) \\
&\quad + \int_0^t \int_{\mathbb{R}} [V(x(s),s,r_0 + l(r(s),\alpha)) - V(x(s),s,r(s))]\mu(ds,d\alpha).
\end{aligned} \tag{3.15}$$

Since $\int_0^\infty \lambda(s)ds < \infty$, applying Lemma 3.3 we obtain that

$$\lim_{t\to\infty}\int_0^t \omega(x(s))ds = \int_0^\infty \omega(x(s))ds < \infty \quad \text{a.s.,} \tag{3.16}$$

$$\lim_{t\to\infty}\sup V(x(t),t,r(t)) < \infty \quad \text{a.s..} \tag{3.17}$$

Define $\beta : R_+ \to R_+$ as $\beta(r) = \inf_{|x|\geq r, 0\leq t<\infty, i\in S} V(x,t,i)$. Then, it is obvious to see from (3.17) that

$$\sup_{0\leq t<\infty}\beta(|x(t)|) \leq \sup_{0\leq t<\infty} V(x(t),t,r(t)) < \infty \quad \text{a.s..} \tag{3.18}$$

On the other hand, by (3.3) we have $\sup_{0\leq t<\infty}|x(t)| < \infty$ a.s.. It is easy to find an integer k_0 such that $|\xi| < k_0$ a.s. because of $\xi \in C^b_{\mathcal{F}_0}([-\tau,0);\mathcal{R}^n)$. Furthermore, for any integer $k > k_0$, we can define the stopping time

$$\rho_k = \inf\{t \geq 0 : |x(t)| \geq k\}, \tag{3.19}$$

where $\inf\emptyset = \infty$ as usual. Clearly, $\rho_k \to \infty$ a.s. as $k \to \infty$. Moreover, for any given $\varepsilon > 0$, there is $k_\varepsilon \geq k_0$ such that $\mathbb{P}\{\rho_k < \infty\} \leq \varepsilon$ for any $k \geq k_\varepsilon$.

It is straightforward to see from (3.16) that $\lim_{t\to\infty}\inf\omega(x(t)) = 0$ a.s.; then we claim that

$$\lim_{t\to\infty}\omega(x(t)) = 0 \quad \text{a.s..} \tag{3.20}$$

The rest of the proof is carried out by contradiction. That is, assuming that (3.20) is false, we have

$$\mathbb{P}\left\{\lim_{t\to\infty}\sup\omega(x(t)) > 0\right\} > 0. \tag{3.21}$$

Furthermore, there exist $\varepsilon_0 > 0$ and $\varepsilon > \varepsilon_1 > 0$ such that

$$\mathbb{P}(\sigma_{2j} < \infty : j \in Z) \geq \varepsilon_0, \tag{3.22}$$

where Z is a set of natural numbers and $\{\sigma_j\}_{j\geq 1}$ are a sequence of stopping times defined by

$$\begin{aligned}
\sigma_1 &= \inf\{t \geq 0 : \omega(x(t)) \geq 2\varepsilon_1\},\\
\sigma_{2j} &= \inf\{t \geq \sigma_{2j-1} : \omega(x(t)) \leq \varepsilon_1\}, \quad j = 1,2,\ldots,\\
\sigma_{2j+1} &= \inf\{t \geq \sigma_{2j} : \omega(x(t)) \leq 2\varepsilon_1\}, \quad j = 1,2,\ldots.
\end{aligned} \tag{3.23}$$

By the local Lipschitz condition (2.4), for any given $k > 0$, there exists $L_k > 0$ such that

$$\left|f(x,y,t,i)\right| \vee \left|g(x,z,t,i)\right| \leq L_k, \tag{3.24}$$

for all $|x| \vee |y| \vee |z| \leq k, t \geq 0$ and $i \in S$.

For any $j \in Z$, let $T < \sigma_{2j} - \sigma_{2j-1}$; by Hölder's inequality and Doob's martingale inequality, we compute

$$\begin{aligned}
&\mathbb{E}\left\{\mathbb{I}_{\{\sigma_{2j}<\rho_k\}} \sup_{0\leq t\leq T}\left|x(\sigma_{2j-1}+t) - x(\sigma_{2j-1})\right|^2\right\} \\
&\quad = \mathbb{E}\left\{\mathbb{I}_{\{\sigma_{2j}<\rho_k\}} \sup_{0\leq t\leq T}\left|\int_{\sigma_{2j-1}}^{\sigma_{2j-1}+t} f(x(s), x(s-\tau_1(s)), s, r(s))ds\right.\right. \\
&\qquad\qquad \left.\left. + \int_{\sigma_{2j-1}}^{\sigma_{2j-1}+t} g(x(s), x(s-\tau_2(s)), s, r(s))dB(s)\right|^2\right\} \\
&\quad \leq 2\mathbb{E}\left\{\mathbb{I}_{\{\sigma_{2j}<\rho_k\}} \sup_{0\leq t\leq T}\left|\int_{\sigma_{2j-1}}^{\sigma_{2j-1}+t} f(x(s), x(s-\tau_1(s)), s, r(s))ds\right|^2\right\} \\
&\qquad + 8\mathbb{E}\left\{\mathbb{I}_{\{\sigma_{2j}<\rho_k\}} \sup_{0\leq t\leq T}\int_{\sigma_{2j-1}}^{\sigma_{2j-1}+t} \left|g(x(s), x(s-\tau_2(s)), s, r(s))\right|^2 ds\right\} \\
&\quad \leq 2L_k^2 T(T+4),
\end{aligned} \tag{3.25}$$

where $\mathbb{I}_A$ is the indicator of set A.

Since $\omega(x)$ is continuous in $\mathbb{R}^n$, it must be uniformly continuous in the closed ball $\overline{S}_k = \{x \in \mathbb{R}^n : |x| \leq k\}$. For any given $b > 0$, we can choose $c_b > 0$ such that $|\omega(x) - \omega(y)| < b$ whenever $x, y \in \overline{S}_k$ and $|x - y| < c_b$. Furthermore, let us choose

$$\varepsilon = \frac{\varepsilon_0}{3}, \qquad k \geq k_\varepsilon, \qquad b = \varepsilon_1. \tag{3.26}$$

By inequality (3.25) and Chebyshev's inequality, we have

$$\begin{aligned}
&\mathbb{P}(\{\rho_k \leq \sigma_{2j}\}) + \mathbb{P}\left(\{\sigma_{2j} < \rho_k\} \cap \left\{\sup_{0\leq t\leq T}\left|\omega(x(\sigma_{2j-1}+t)) - \omega(x(\sigma_{2j-1}))\right| \geq \varepsilon_1\right\}\right) \\
&\quad \leq \mathbb{P}(\{\rho_k \leq \sigma_{2j}\} \cap \{\sigma_{2j} = \infty\}) + \mathbb{P}(\{\rho_k \leq \sigma_{2j}\} \cap \{\sigma_{2j} < \infty\}) \\
&\qquad + \mathbb{P}\left(\{\sigma_{2j} < \rho_k\} \cap \left\{\sup_{0\leq t\leq T}\left|x(\sigma_{2j-1}+t) - x(\sigma_{2j-1})\right| \geq c_{\varepsilon_1}\right\}\right) \\
&\quad \leq \frac{2L_k^2 T(T+4)}{c_{\varepsilon_1}^2} + 1 - 2\varepsilon.
\end{aligned} \tag{3.27}$$

Meanwhile, we can also choose $T = T(\varepsilon, \varepsilon_1, k)$ sufficiently small for

$$\frac{2L_k^2 T(T+4)}{c_{\varepsilon_1}^2} \leq \varepsilon. \tag{3.28}$$

And then, (3.27) and (3.28) yield

$$\mathbb{P}\left(\left\{\sigma_{2j} < \rho_k\right\} \cap \Omega_j\right) \geq \varepsilon, \tag{3.29}$$

where $\Omega_j = \{\sup_{0\leq t\leq T}|\omega(x(\sigma_{2j-1}+t)) - \omega(x(\sigma_{2j-1}))| < \varepsilon_1\}$.

In the following, we can obtain from (3.16) and (3.29) that

$$\begin{aligned}
\infty &> \mathbb{E}\int_0^\infty \omega(x(t))dt \\
&\geq \sum_{j=1}^\infty \mathbb{E}\left[\mathbb{I}_{\{\sigma_{2j}<\rho_k\}}\int_{\sigma_{2j-1}}^{\sigma_{2j}} \omega(x(t))dt\right] \\
&\geq \sum_{j=1}^\infty \varepsilon_1 \mathbb{E}\left[\mathbb{I}_{\{\sigma_{2j}<\rho_k\}}\left(\sigma_{2j}-\sigma_{2j-1}\right)\right] \\
&\geq \sum_{j=1}^\infty T\varepsilon_1 \mathbb{P}\left(\left\{\sigma_{2j} < \rho_k\right\} \cap \Omega_j\right) \\
&\geq \sum_{j=1}^\infty T\varepsilon_1\varepsilon = \frac{1}{3}\sum_{j=1}^\infty T\varepsilon_0\varepsilon_1 = \infty.
\end{aligned} \tag{3.30}$$

This is a contradiction. So there is an $\overline{\Omega} \in \Omega$ with $\mathbb{P}(\overline{\Omega}) = 1$ such that

$$\lim_{t\to\infty}\omega(x(t,\omega)) = 0, \quad \sup_{0\leq t<\infty}|x(t,\omega)| < \infty, \quad \forall\omega \in \overline{\Omega}. \tag{3.31}$$

Finally, any fixed $\omega \in \overline{\Omega}$, $\{x(t,\omega)\}_{t\geq 0}$ is bounded in $\mathbb{R}^n$. By Bolzano-Weierstrass theorem, there is an increasing sequence $\{t_i\}_{i\geq 1}$ such that $\{x(t,\omega)\}_{i\geq 1}$ converges to some $z \in \mathbb{R}^n$ with $|z| < \infty$. Since $\omega(x) > 0$ whenever $x \neq 0$, we must have $\omega(x) = 0$ if and only if $x = 0$. This implies that the solution of (2.2) is a.s. stable, and the proof is therefore completed. □

Remark 3.5. The techniques proposed in Theorem 3.1 can be used to deal with the a.s. stability problem for other HSDSs, such as the ones in [25]. In a very special case when $\tau_1(t) = \tau_2(t) = \tau$ for all $t \geq 0$ and $i \in S$, it is easy to see that $\dot{\tau}_1(t) = \dot{\tau}_2(t) = 0$, and Theorem 3.1 is exactly Theorem 2.1 in [25]. Similarly, Theorem 2.2 in [25] can be generalized to system (2.2) as a LaSalle-type theorem (see [24, 26]) for HSSs with multiple time-varying delays.

4. Almost Sure Stabilization of Nonlinear HSDSs

Consider the following nonlinear HSDSs:

$$\begin{aligned} dx(t) = {} & \left[A(r(t))x(t) + A_d(r(t))x(t-\tau_1(t)) + f(x(t), x(t-\tau_1(t)), t, r(t)) + B_u(r(t))u(t)\right]dt \\ & + g(x(t), x(t-\tau_2(t)), t, r(t))dB(t), \end{aligned} \tag{4.1}$$

where $B_u(r(t))$ are known constant matrices with appropriate dimensions and $B(t)$ represents a scalar Brownian motion (Wiener process) on $(\Omega, \mathcal{F}, \{\mathcal{F}_t\}_{t\geq 0}, \mathbb{P})$ that is independent of Markov chain $r(t)$ and satisfies:

$$E\{dB(t)\} = 0, \qquad E\left\{dB(t)^2\right\} = dt, \tag{4.2}$$

f and g are both functions from $\mathbb{R}^n \times \mathbb{R}^n \times \mathbb{R}_+ \times S$ to $\mathbb{R}^n$ which satisfy local Lipschitz condition and the following assumptions:

$$\begin{aligned} & \left|f(x(t), x(t-\tau_1(t)), t, r(t))\right|^2 \\ & \quad \leq x^T(t)F_1(r(t))x(t) + x^T(t-\tau_1(t))F_2(r(t))x(t-\tau_1(t)), \\ & \left|g(x(t), x(t-\tau_2(t)), t, r(t))\right|^2 \\ & \quad \leq x^T(t)G_1(r(t))x(t) + x^T(t-\tau_2(t))G_2(r(t))x(t-\tau_2(t)), \end{aligned} \tag{4.3}$$

where, for each $r(t) = j \in S$, $A(r(t))$, $A_d(r(t))$ are known constant matrices with appropriate dimensions, and $F_i(r(t)) \in \mathbb{R}^{n\times n}$, $G_i(r(t)) \in \mathbb{R}^{n\times n}$ $(i = 1, 2)$ are positive definite matrices.

In the sequel, we denote the matrix associated with the ith mode by

$$\Gamma_i \triangleq \Gamma(r(t) = i), \tag{4.4}$$

where the matrix Γ could be A, A_d, B_u, F_1, F_2, G_1, G_2, G, or G_d.

As the given HSDSs (4.1) is nonlinear, we here consider the resulting systems can be stabilized only by linear state feedback controller which is of the form

$$u(t) = K(r(t))x(t), \tag{4.5}$$

where $K(r(t))$ are controller parameters to be designed.

Under control law (4.5), the closed-loop system can be given as follow:

$$\begin{aligned} dx(t) = {} & \left[A(r(t))x(t) + A_d(r(t))x(t-\tau_1(t)) + f(x(t), x(t-\tau_1(t)), t, r(t))\right. \\ & \left. + B_u(r(t))K(r(t))x(t)\right]dt \\ & + g(x(t), x(t-\tau_2(t)), t, r(t))dB(t). \end{aligned} \tag{4.6}$$

The stabilization problem is therefore to design matrices $K(r(t))$ for the closed-loop system (4.6) to be a.s. stable. In order to guarantee the solvability of $K(r(t))$, the following theorem is given.

Theorem 4.1. *If there exist sequences of scalars $\varepsilon_{1i} > 0$, $\varepsilon_{2i} > 0$, $\delta_i > 0$, positive definite matrices $X_i > 0$ and matrices Y_i such that the following LMIs*

$$\begin{bmatrix} M_{i1} & M_{i2} & M_{i4} \\ * & -M_{i3} & 0 \\ * & * & -M_{i5} \end{bmatrix} < 0 \quad \forall i, j \in S, \tag{4.7}$$

$$X_i \geq \delta_i I \tag{4.8}$$

hold, where

$$\begin{gathered} M_{i1} = A_i X_i + X_i A_i^T + B_{ui} Y_i + Y_i^T B_{ui}^T + \varepsilon_{1i} A_{di} A_{di}^T + \varepsilon_{2i} I + \gamma_{ii} X_i, \\ M_{i2} = [X_i, X_i, X_i, X_i, X_i], \\ M_{i3} = \operatorname{diag}\left(\varepsilon_{2i} F_{1i}^{-1}, c_1 \varepsilon_{2j} F_{2j}^{-1}, \delta_i G_{1i}^{-1}, c_2 \delta_i G_{2j}^{-1}, c_1 \varepsilon_{1j} I\right), \\ M_{i4} = \left[\sqrt{\gamma_{i1}} X_i, \ldots, \sqrt{\gamma_{i(i-1)}} X_i, \sqrt{\gamma_{i(i+1)}} X_i, \ldots, \sqrt{\gamma_{iN}} X_i\right], \\ M_{i5} = \operatorname{diag}(X_1, \ldots, X_{i-1}, X_{i+1}, \ldots, X_N), \\ c_1 = 1 - d_{\tau_1}, \qquad c_2 = 1 - d_{\tau_2}, \end{gathered} \tag{4.9}$$

then the controlled system (4.6) *is a.s. stable and the state feedback controller determined by*

$$u(t) = K_i x(t), \quad K_i = Y_i X_i^{-1}, \ i \in S. \tag{4.10}$$

Proof. Let $P_i = X_i^{-1}$ and $V(x,i) = x^T P_i x + \int_{t-\tau_1(t)}^{t} x^T(s) Q_1 x(s) ds + \int_{t-\tau_2(t)}^{t} x^T(s) Q_2 x(s) ds$.

The operator $\mathcal{L}V : \mathbb{R}^n \times \mathbb{R}^n \times \mathbb{R}^n \times S \to \mathbb{R}$ has the form

$$\begin{aligned} \mathcal{L}V(x,y,z,i) = {} & x^T Q_1 x - (1 - \dot{\tau}_1(t)) y^T Q_1 y + x^T Q_2 x - (1 - \dot{\tau}_2(t)) z^T Q_2 z \\ & + 2x^T P_i \left(A_i x + A_{di} y + f(x,y,i) + B_{ui} K_i x\right) \\ & + g^T(x,z,i) P_i g(x,z,i) + \sum_{j=1}^{N} \gamma_{ij} x^T P_j x \end{aligned}$$

$$\leq x^T \Bigg[Q_1 + Q_2 + P_i A_i + A_i^T P_i + P_i B_{ui} K_i + (B_{ui} K_i)^T P_i + \varepsilon_{1i} P_i A_{di} A_{di}^T P_i + \varepsilon_{2i} P_i^2 + \sum_{j=1}^{N} \gamma_{ij} P_j + \varepsilon_{2i}^{-1} F_{1i} + \delta_i^{-1} G_{1i} \Bigg] x + y^T \left[\varepsilon_{1i}^{-1} I + \varepsilon_{2i}^{-1} F_{2i} - (1 - d_{\tau_1}) Q_1 \right] y + z^T \left[\delta_i^{-1} G_{2i} - (1 - d_{\tau_2}) Q_2 \right] z. \tag{4.11}$$

So

$$\mathcal{L}V(x, y, z, i) \leq -\omega_{1i}(x) + (1 - d_{\tau_1})\omega_{2i}(y) + (1 - d_{\tau_2})\omega_{3i}(z), \tag{4.12}$$

where

$$\begin{aligned} \omega_{1i}(x) &= x^T \Bigg[-Q_1 - Q_2 - P_i A_i - A_i^T P_i - P_i B_{ui} K_i - (B_{ui} K_i)^T P_i - \varepsilon_{1i} P_i A_{di} A_{di}^T P_i - \varepsilon_{2i} P_i^2 - \varepsilon_{2i}^{-1} F_{1i} - \delta_i^{-1} G_{1i} - \sum_{k=1}^{N} \gamma_{ik} P_k \Bigg] x, \\ \omega_{2i}(x) &= x^T \left[c_1^{-1} \varepsilon_{1i}^{-1} I + c_1^{-1} \varepsilon_{2i}^{-1} F_{2i} - Q_1 \right] x, \\ \omega_{3i}(x) &= x^T \left[c_2^{-1} \delta_i^{-1} G_{2i} - Q_2 \right] x. \end{aligned} \tag{4.13}$$

By assumption 1, it is easy to see that we can choose Q_1 and Q_2 such that $\omega_{2i}(x) \geq 0$, $\omega_{3i}(x) \geq 0$ for all $x \in \mathbb{R}^n$, $i \in S$.

Noting that $P_i = X_i^{-1}$ and $Y_i = K_i X_i$, we can pre- and postmultiply (4.7) by $\operatorname{diag}(P_i, \ldots, P_i)$, and using Schur complements, we can obtain

$$\Phi_{ij} < 0, \tag{4.14}$$

where

$$\begin{aligned} \Phi_{ij} = {} & P_i A_i + A_i^T P_i + P_i B_{ui} K_i + (B_{ui} K_i)^T P_i + \varepsilon_{1i} P_i A_{di} A_{di}^T P_i + \varepsilon_{2i} P_i^2 + \delta_i^{-1} G_{1i} \\ & + \varepsilon_{2i}^{-1} F_{1i} + \sum_{k=1}^{N} \gamma_{ik} P_k + c_1^{-1} \varepsilon_{1j}^{-1} I + c_1^{-1} \varepsilon_{2j}^{-1} F_{2j} + c_2^{-1} \delta_j G_{2j}. \end{aligned} \tag{4.15}$$

This implies

$$\omega_{1i}(x) > \omega_{2j}(x) + \omega_{3j}(x) \geq 0, \quad \forall x \neq 0. \tag{4.16}$$

Let $\omega_1(x) = \min_{i \in S} \omega_{1i}(x)$, $\omega_2(x) = \max_{i \in S} \omega_{2i}(x)$, and $\omega_3(x) = \max_{i \in S} \omega_{3i}(x)$.

Clearly

$$\omega_1(x) > \omega_2(x) + \omega_3(x) \geq 0, \quad \forall x \neq 0. \tag{4.17}$$

Moreover, by (4.24) we further obtain

$$\mathcal{L}V(x, y, z, i) \leq -\omega_1(x) + (1 - d_{\tau_1})\omega_2(y) + (1 - d_{\tau_2})\omega_3(z). \tag{4.18}$$

The required assertion now follows from Theorem 3.1. □

If the systems (4.6) reduces to linear HSDSs of the form

$$\begin{aligned} dx(t) = {} & [A(r(t))x(t) + A_d(r(t))x(t - \tau_1(t)) \\ & + B_u(r(t))K(r(t))x(t)]dt + [G(r(t))x(t) + G_d(r(t))x(t - \tau_2(t))]dB(t), \end{aligned} \tag{4.19}$$

where $A(r(t)), A_d(r(t)), B_u(r(t)), G(r(t))$, and $G_d(r(t))$ are known constant matrices with appropriate dimensions.

Then, the following corollary follows directly from Theorem 4.1.

Corollary 4.2. *If there exist sequences of scalars $\varepsilon_{1i} > 0$, $\varepsilon_{2i} > 0$, positive definite matrices $X_i > 0$ and matrices Y_i such that the following LMIs*

$$\begin{bmatrix} M_{i1} & M_{i2} & M_{i4} \\ * & -M_{i3} & 0 \\ * & * & -M_{i5} \end{bmatrix} < 0 \quad \forall i, j \in S \tag{4.20}$$

hold, where

$$\begin{gathered} M_{i1} = A_i X_i + X_i A_i^T + B_{ui} Y_i + Y_i^T B_{ui}^T + \varepsilon_{1i} A_{di} A_{di}^T + \gamma_{ii} X_i, \\ M_{i2} = \left[\sqrt{2} X_i G_i^T, X_j, X_j, \sqrt{2} X_j^T G_{dj}\right], \\ M_{i3} = \operatorname{diag}(X_i, c_1 \varepsilon_{1j} I, \varepsilon_{2j} I, X_j), \\ M_{i4} = \left[\sqrt{\gamma_{i1}} X_i, \ldots, \sqrt{\gamma_{i(i-1)}} X_i, \sqrt{\gamma_{i(i+1)}} X_i, \ldots, \sqrt{\gamma_{iN}} X_i\right], \\ M_{i5} = \operatorname{diag}(X_1, \ldots, X_{i-1}, X_{i+1}, \ldots, X_N), \\ c_1 = 1 - d_{\tau_1}, \qquad c_2 = 1 - d_{\tau_2}, \end{gathered} \tag{4.21}$$

then the controlled system (4.19) *is a.s. stable and the state feedback controller determined by*

$$u(t) = K_i x(t), \quad K_i = Y_i X_i^{-1}, \ i \in S. \tag{4.22}$$

Proof. Let $P_i = X_i^{-1}$ and $V(x,i) = x^T P_i x + \int_{t-\tau_1(t)}^{t} x^T(s) Q_1 x(s) ds + \int_{t-\tau_2(t)}^{t} x^T(s) Q_2 x(s) ds$.

The operator $\mathcal{L}V : \mathbb{R}^n \times \mathbb{R}^n \times \mathbb{R}^n \times S \to \mathbb{R}$ has the form

$$\begin{aligned}
\mathcal{L}V(x,y,z,i) &= x^T Q_1 x - (1-\dot{\tau}_1(t)) y^T Q_1 y + x^T Q_2 x - (1-\dot{\tau}_2(t)) z^T Q_2 z \\
&\quad + 2x^T P_i \left[A_i x + A_{di} y + B_{ui} K_i x\right] + [G_i x + G_{di} z]^T P_i [G_i x + G_{di} z] \\
&\quad + \sum_{k=1}^{N} \gamma_{ik} x^T P_k x \\
&\le x^T \Bigg[Q_1 + Q_2 + P_i A_i + A_i^T P_i + P_i B_{ui} K_i + (B_{ui} K_i)^T P_i \\
&\qquad + \varepsilon_{1i} P_i A_{di} A_{di}^T P_i + \sum_{k=1}^{N} \gamma_{ik} P_k + 2G_i^T P_i G_i \Bigg] x \\
&\quad + y^T \left[\varepsilon_{1i}^{-1} I - (1-d_{\tau_1}) Q_1\right] y + z^T \left[\varepsilon_{2i}^{-1} I + 2G_{di}^T P_i G_{di} - (1-d_{\tau_2}) Q_2\right] z.
\end{aligned} \tag{4.23}$$

So

$$\mathcal{L}V(x,y,z,i) \le -\omega_{1i}(x) + (1-d_{\tau_1})\omega_{2i}(y) + (1-d_{\tau_2})\omega_{3i}(z), \tag{4.24}$$

where

$$\begin{aligned}
\omega_{1i}(x) &= x^T \Bigg[-Q_1 - Q_2 - P_i A_i - A_i^T P_i - P_i B_{ui} K_i - (B_{ui} K_i)^T P_i \\
&\qquad - \varepsilon_{1i} P_i A_{di} A_{di}^T P_i - \sum_{k=1}^{N} \gamma_{ik} P_k - 2G_i^T P_i G_i \Bigg] x, \\
\omega_{2i}(x) &= x^T \left[c_1^{-1} \varepsilon_{1i}^{-1} I - Q_1\right] x, \\
\omega_{3i}(x) &= x^T \left[\varepsilon_{2i}^{-1} I + 2c_2^{-1} G_{di}^T P_i G_{di} - Q_2\right] x.
\end{aligned} \tag{4.25}$$

It is easy to see that we can choose Q_1 and Q_2 such that $\omega_{2i}(x) \ge 0$, $\omega_{3i}(x) \ge 0$ for all $x \in \mathbb{R}^n$, $i \in S$.

Noting that $P_i = X_i^{-1}$ and $Y_i = K_i X_i$, we can pre- and postmultiply (4.7) by $\operatorname{diag}(P_i, \ldots, P_i)$, and using Schur complements, we can obtain

$$\Phi_{ij} < 0, \tag{4.26}$$

where

$$\begin{aligned}\Phi_{ij} &= P_iA_i + A_i^TP_i + P_iB_{ui}K_i + (B_{ui}K_i)^TP_i + \varepsilon_{1i}P_iA_{di}A_{di}^TP_i \\ &\quad + \sum_{k=1}^{N}\gamma_{ik}P_k + 2G_i^TP_iG_i + c_1^{-1}\varepsilon_{1j}^{-1}I + \varepsilon_{2j}^{-1}I + 2c_2^{-1}G_{dj}^TP_jG_{dj}.\end{aligned} \tag{4.27}$$

This implies

$$\omega_{1i}(x) > \omega_{2j}(x) + \omega_{3j}(x) \geq 0, \quad \forall x \neq 0. \tag{4.28}$$

Let $\omega_1(x) = \min_{i\in S}\omega_{1i}(x), \omega_2(x) = \max_{i\in S}\omega_{2i}(x)$, and $\omega_3(x) = \max_{i\in S}\omega_{3i}(x)$. Clearly

$$\omega_1(x) > \omega_2(x) + \omega_3(x) \geq 0, \quad \forall x \neq 0. \tag{4.29}$$

Moreover, by (4.24) we further obtain

$$\mathcal{L}V(x,y,z,i) \leq -\omega_1(x) + (1-d_{\tau_1})\omega_2(y) + (1-d_{\tau_2})\omega_3(z). \tag{4.30}$$

The required assertion now follows from Theorem 3.1. □

5. Examples

In this section we will provide two examples to illustrate our results. In the following examples we assume that $B(t)$ is a scalar Brownian motion, $\gamma(t)$ is a right-continuous Markov chain independent of $B(t)$ and taking values in $S = \{1,2\}$, and the step size $\Delta = 0.0001$. By using the YALMIP toolbox, simulations results are shown in Figures 1–3. Figure 1 gives a portion of state $\gamma(t)$ of Example 5.1 for clear display. Figure 2 simulates the numerical results for Example 5.1. The simulation results have illustrated our theoretical analysis. Following from Theorem 4.1, the simulation results for Example 5.2 can be founded in Figure 3, which verify our desired results.

Example 5.1. Let

$$\Gamma = (\gamma_{ij})_{2\times 2} = \begin{pmatrix} -0.8 & 0.8 \\ 0.3 & -0.3 \end{pmatrix}. \tag{5.1}$$

Consider scalar nonlinear HSDSs:

$$dx(t) = f(x(t),t,r(t))dt + g(x(t),x(t-\tau_2(t)),t,r(t))dB(t), \tag{5.2}$$

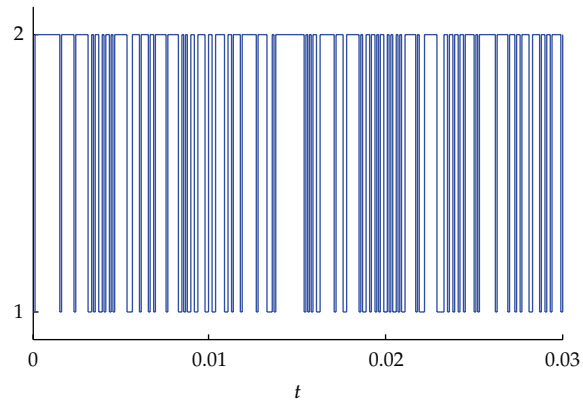

Figure 1: The state $\gamma(t)$ of Example 5.1.

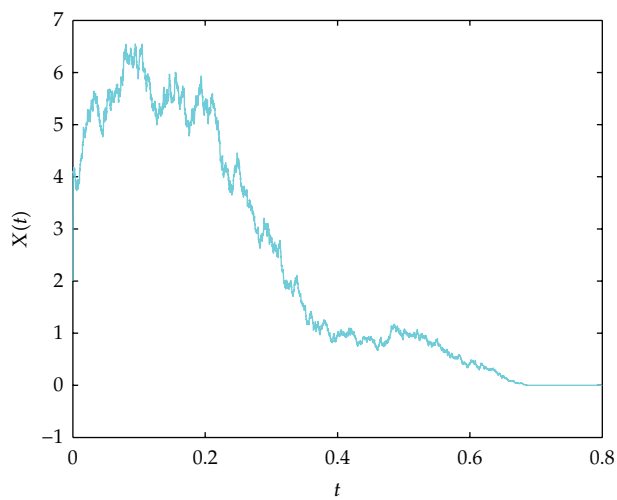

Figure 2: The state evolution of Example 5.1.

where

$$
\begin{aligned}
f(x,t,1) &= -6\sqrt[5]{x}, \\
g(x,z,t,1) &= -\sqrt[5]{x^3} + 2\sqrt[5]{z^3}, \\
f(x,t,2) &= \frac{3}{2\sqrt[3]{1+t}} - 4\sqrt[5]{x}, \\
g(x,z,t,2) &= \sqrt[5]{x^3}\cos(t) + \frac{5}{4}\sqrt[5]{z^3}\sin(t),
\end{aligned}
\tag{5.3}
$$

$\tau_2(t) = 0.3 + 0.3\sin(t)$.

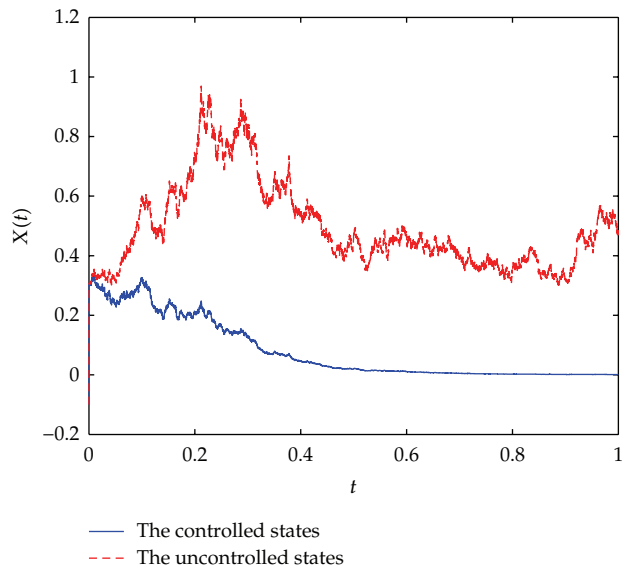

Figure 3: The state evolution of Example 5.2.

To examine the stability of system (5.2), we consider a Lyapunov function candidate $V : \mathbb{R} \times S \to \mathbb{R}_+$ as $V(x,i) = x^2$ for $i = 1,2$. Then we have

$$\begin{aligned} \mathcal{L}V(x,z,t,1) &\le -10x^{6/5} + 4z^{6/5}, \\ \mathcal{L}V(x,z,t,2) &\le \frac{3x}{\sqrt[3]{1+t}} - 6x^{6/5} + \frac{25}{8}z^{6/5}. \end{aligned} \tag{5.4}$$

By the elementary inequality $\alpha^c\beta^{1-c} \le c\alpha + (1-c)\beta$ for all $\alpha \ge 0$, $\beta \ge 0$, and $0 \le c \le 1$, we see that inequality

$$\frac{3x}{\sqrt[3]{1+t}} = \left(\frac{6}{5}\kappa x^{6/5}\right)^{6/5}\left(6\left(\frac{\kappa}{5}\right)^{-5}(1+t)^{-2}\right)^{1/6} \le \kappa x^{6/5} + \frac{\kappa_1}{(1+t)^2} \tag{5.5}$$

holds for any $\kappa > 0$, where $\kappa_1 = (\kappa/5)^{-5}$.

From inequalities (5.4)–(5.5), we have

$$\mathcal{L}V(x,z,t,i) \le \frac{\kappa_1}{(1+t)^2} - (6-\kappa)x^{6/5} + 4z^{6/5}, \tag{5.6}$$

for all $t \ge 0$ and $i \in S$. By $\tau_2(t) = 0.3 + 0.3\sin(t)$, it is easy to see that $d_{\tau_2}(t) < 1/3$; then, we choose constant κ such that $0 < \kappa < (2 - 6d_{\tau_2})/(1 - d_{\tau_2})$, and hence conditions of Theorem 3.1 are satisfied.

Example 5.2. Let

$$\Gamma = (\gamma_{ij})_{2\times 2} = \begin{pmatrix} -0.6 & 0.6 \\ 0.5 & -0.5 \end{pmatrix}. \tag{5.7}$$

Consider scalar nonlinear closed-loop HSDSs:

$$\begin{aligned} dx(t) = {} & \left[f(x(t), x(t-\tau_1(t)), t, r(t)) + B(r(t))K(r(t))x(t)\right]dt \\ & + g(x(t), x(t-\tau_2(t)), t, r(t))dB(t) \end{aligned} \tag{5.8}$$

with

$$\begin{aligned} f(x,y,t,1) &= x + \frac{1}{2}y + \frac{2x^3}{(|x|+1)^2} + y\sin(t), \\ g(x,z,t,1) &= x\cos(t) + \frac{z^3}{(|z|+1)^2}, \end{aligned} \tag{5.9}$$

$$\begin{aligned} f(x,y,t,2) &= -2x + y + \frac{x^3}{(|x|+2)^2} + \frac{y^3}{(|y|+1)^2}, \\ g(x,z,t,2) &= 2x\sin(t) + \frac{x^3}{2(|x|+1)^2} + \frac{z^3}{(|z|+2)^2}, \end{aligned} \tag{5.10}$$

$\tau_1(t) = 0.1 + 0.1\sin(t)$, $\tau_2(t) = 0.2 + 0.2\sin(2t)$, $B_1 = 2$, $B_2 = -3$, $A_1 = 1$, $A_2 = 2$, $A_{d1} = 1/2$, $A_{d2} = 1$, $F_{11} = 8$, $F_{12} = G_{11} = 2$, $G_{12} = F_{21} = F_{22} = 2$, $G_{21} = 1/2$, $G_{22} = 2$.

By Theorem 4.1 we can find the feasible solution $K_1 = -3$, $K_2 = 2$ for the a.s. stability.

6. Conclusions

In this paper, we have investigated the a.s. stability analysis and stabilization synthesis problems for nonlinear HSDSs. Some sufficient conditions are given to guarantee the resulting systems to be a.s. stable. Under these conditions, a.s. stabilization problem for a class of nonlinear HSDSs is solved in terms of the solutions to a set of LMIs. Finally, the results of this paper have been demonstrated by two numerical simulation examples.

Acknowledgment

This work is supported in part by the National Natural Science Foundation of P.R. China (no. 60974030).

References

[1] J. Hu, Z. Wang, H. Gao, and L. K. Stergioulas, "Robust sliding mode control for discrete stochastic systems with mixed time delays, randomly occurring uncertainties, and randomly occurring nonlinearities," *IEEE Transactions on Industrial Electronics*, vol. 59, no. 7, pp. 3008–3015, 2012.

[2] L. Hu and X. Mao, "Almost sure exponential stabilisation of stochastic systems by state-feedback control," *Automatica*, vol. 44, no. 2, pp. 465–471, 2008.

[3] X. Li and C. E. De Souza, "Criteria for robust stability and stabilization of uncertain linear systems with state delay," *Automatica*, vol. 33, no. 9, pp. 1657–1662, 1997.

[4] X. Li and C. E. De Souza, "Delay-dependent robust stability and stabilization of uncertain linear delay systems: a linear matrix inequality approach," *IEEE Transactions on Automatic Control*, vol. 42, no. 8, pp. 1144–1148, 1997.

[5] S. Ma, Z. Cheng, and C. Zhang, "Delay-dependent robust stability and stabilisation for uncertain discrete singular systems with time-varying delays," *Control Theory & Applications*, vol. 1, no. 4, pp. 1086–1095, 2007.

[6] B. Shen, Z. Wang, Y. S. Hung, and G. Chesi, "Distributed H_∞ filtering for polynomial nonlinear stochastic systems in sensor networks," *IEEE Transactions on Industrial Electronics*, vol. 58, no. 5, pp. 1971–1979, 2011.

[7] D. Yue and Q. L. Han, "Delay-dependent exponential stability of stochastic systems with time-varying delay, nonlinearity, and Markovian switching," *IEEE Transactions on Automatic Control*, vol. 50, no. 2, pp. 217–222, 2005.

[8] L. Liu, Y. Shen, and F. Jiang, "The almost sure asymptotic stability and th moment asymptotic stability of nonlinear stochastic differential systems with polynomial growth," *IEEE Transactions on Automatic Control*, vol. 56, no. 8, pp. 1985–1990, 2011.

[9] G. Wei, Z. Wang, H. Shu, and J. Fang, "Robust H_∞ control of stochastic time-delay jumping systems with nonlinear disturbances," *Optimal Control Applications and Methods*, vol. 27, no. 5, pp. 255–271, 2006.

[10] G. Wei, Z. Wang, and H. Shu, "Nonlinear H_∞ control of stochastic time-delay systems with Markovian switching," *Chaos, Solitons and Fractals*, vol. 35, no. 3, pp. 442–451, 2008.

[11] X. Mao, "Stochastic versions of the LaSalle theorem," *Journal of Differential Equations*, vol. 153, no. 1, pp. 175–195, 1999.

[12] X. Mao, Y. Shen, and C. Yuan, "Almost surely asymptotic stability of neutral stochastic differential delay equations with Markovian switching," *Stochastic Processes and their Applications*, vol. 118, no. 8, pp. 1385–1406, 2008.

[13] B. Bercu, F. Dufour, and G. G. Yin, "Almost sure stabilization for feedback controls of regime-switching linear systems with a hidden Markov Chain," *IEEE Transactions on Automatic Control*, vol. 54, no. 9, pp. 2114–2125, 2009.

[14] Z. Lin, Y. Lin, and W. Zhang, "H_∞ filtering for non-linear stochastic Markovian jump systems," *Control Theory & Applications*, vol. 4, no. 12, pp. 2743–2756, 2010.

[15] L. Wu, D. W. C. Ho, and C. W. Li, "Stabilisation and performance synthesis for switched stochastic systems," *Control Theory & Applications*, vol. 4, no. 10, pp. 1877–1888, 2010.

[16] L. Wu, D. W. C. Ho, and C. W. Li, "Sliding mode control of switched hybrid systems with stochastic perturbation," *Systems and Control Letters*, vol. 60, no. 8, pp. 531–539, 2011.

[17] J. Yao, F. Lin, and B. Liu, "H_∞ control for stochastic stability and disturbance attenuation in a class of networked hybrid systems," *Control Theory & Applications*, vol. 5, no. 15, pp. 1698–1708, 2011.

[18] N. Zeng, Z. Wang, Y. Li, M. Du, and X. Liu, "a Hybrid EKF and switching PSO algorithm for joint state and parameter estimation of lateral flow immunoassay models," *IEEE/ACM Transactions on Computational Biology and Bioinformatics*, vol. 9, no. 2, pp. 321–329, 2012.

[19] X. Mao, "Stability of stochastic differential equations with Markovian switching," *Stochastic Processes and their Applications*, vol. 79, no. 1, pp. 45–67, 1999.

[20] C. Yuan and J. Lygeros, "Stabilization of a class of stochastic differential equations with Markovian switching," *Systems and Control Letters*, vol. 54, no. 9, pp. 819–833, 2005.

[21] X. Mao, J. Lam, and L. Huang, "Stabilisation of hybrid stochastic differential equations by delay feedback control," *Systems and Control Letters*, vol. 57, no. 11, pp. 927–935, 2008.

[22] Z. Wang, H. Qiao, and K. J. Burnham, "On stabilization of bilinear uncertain time-delay stochastic systems with Markovian jumping parameters," *IEEE Transactions on Automatic Control*, vol. 47, no. 4, pp. 640–646, 2002.

[23] Z. Wang, Y. Liu, and X. Liu, "Exponential stabilization of a class of stochastic system with markovian jump parameters and mode-dependent mixed time-delays," *IEEE Transactions on Automatic Control*, vol. 55, no. 7, pp. 1656–1662, 2010.

[24] L. Huang and X. Mao, "On almost sure stability of hybrid stochastic systems with mode-dependent interval delays," *IEEE Transactions on Automatic Control*, vol. 55, no. 8, pp. 1946–1952, 2010.

[25] C. Yuan and X. Mao, "Robust stability and controllability of stochastic differential delay equations with Markovian switching," *Automatica*, vol. 40, no. 3, pp. 343–354, 2004.
[26] X. Mao, "A note on the LaSalle-type theorems for stochastic differential delay equations," *Journal of Mathematical Analysis and Applications*, vol. 268, no. 1, pp. 125–142, 2002.
[27] R. S. Lipster and A. N. Shiryayev, *Theory of Martingales*, Kluwer Academic, Dodrecht, The Netherlands, 1989.

Hindawi Publishing Corporation
Mathematical Problems in Engineering
Volume 2012, Article ID 421754, 20 pages
doi:10.1155/2012/421754

Research Article

Uniform Approximate Estimation for Nonlinear Nonhomogenous Stochastic System with Unknown Parameter

Xiu Kan and Huisheng Shu

School of Information Science and Technology, Donghua University, Shanghai 200051, China

Correspondence should be addressed to Huisheng Shu, hsshu@dhu.edu.cn

Received 21 June 2012; Accepted 3 August 2012

Academic Editor: Jun Hu

The error bound in probability between the approximate maximum likelihood estimator (AMLE) and the continuous maximum likelihood estimator (MLE) is investigated for nonlinear nonhomogenous stochastic system with unknown parameter. The rates of convergence of the approximations for Itô and ordinary integral are introduced under some regular assumptions. Based on these results, the in probability rate of convergence of the approximate log-likelihood function to the true continuous log-likelihood function is studied for the nonlinear nonhomogenous stochastic system involving unknown parameter. Finally, the main result which gives the error bound in probability between the ALME and the continuous MLE is established.

1. Introduction

It is now well known that the parameter estimation is one of the foundational problems in stochastic differential equations which are used to model practical systems that with random influences. Since 1962, Arato et al. who first applied parameter estimation to a geophysical problem in [1]. Various parameter estimation methods have been developed for many advanced models with an increasing number of application to physical, biological and financial systems. Over the past few decades, a lot of effective approaches have proposed in this research area, see for example, [2–5]. In particular, maximum likelihood estimation (MLE) gives a unified approach to estimation, which is well defined in the case of the normal distribution and many other statistical models. Therefore the MLE technique has been widely used for the parameter estimation problem of stochastic systems [6]. Byes estimation (BE), which is a decision rule that minimizes the posterior expected value of a loss function, has been developed in [7]. Since some inconvenience is encountered in the

real-time application that location and scale parameters are not uniquely determined, M-estimator has been studied toward the theory of robust estimation [8]. Other widely used parameter estimation methods can be generally categorized as least squares estimation (LSE), maximum probability estimation (MPE), minimum distance estimation (MDE), minimum contrast estimation (MCE), and filtering method for parameter estimation, see for example, [9–18] and the references therein.

In reality, nonhomogenous stochastic differential equations are useful for modeling term structure of interest rates in finance and other fields. A large number of results have been published in the literature on a variety of research topics including strong or weak consistency and asymptotic efficiency as well as asymptotic normality on various parameter estimators of nonhomogenous stochastic systems [19, 20]. On the other hand, recognizing that nonlinearity is commonly encountered in engineering practice, the parameter estimation problem for nonlinear nonhomogenous stochastic systems deserves more research attention from both the theoretical and practical viewpoints and, accordingly, some promising results have been reported. For example, weak consistency, asymptotic normality, and convergence of moments of MLE and BE of the drift parameter in the nonlinear nonhomogenous Itô stochastic differential equations having nonstationary solutions have been studied in [21] for the small noise asymptotic case. In [22], the martingale approach but under some stronger regularity conditions has been used to study strong consistency and asymptotic normality for nonlinear nonhomogenous stochastic system in the large sample case. It should be pointed out that, so far, many parameter estimation methods and corresponding probability properties have been widely investigated for nonlinear nonhomogenous Itô stochastic differential equation with constant diffusion. Unfortunately, the parameter problem of general nonlinear nonhomogenous system has gained much less research attention despite its potential in practical application.

The stochastic processes which can be observed continuously over a specified time period are first used to model real system for the most part [23, 24]. In practice, it is obviously impossible to observe a process continuously over any given time period, due to the limitations on the precision of the measuring instrument or to unavailability of observations at every time point, and so forth. In other words, stochastic inference based on discrete observations is of major importance in dealing with practical problems. Hence, parameter estimation problem based on discrete observations has naturally become a hot topic in recent years [25, 26]. An approximation method has been proposed based on the discretization of the continuous time likelihood function in [27] for linear stochastic differential equation. A numerical approximate likelihood method has been developed in [28] based on iterations of the Gaussian transition densities emanating from the Euler scheme. [29] has used a specific transformation of the diffusion to obtain accurate theoretical approximations based on the Hermite function expansions and studied the asymptotic behavior of the approximate MLE. Up to now, although some parameter estimation problems have been established based on discretization scheme, how close are the discrete parameter estimator to the true continuous one for general nonlinear nonhomogenous stochastic system has not been fully studied due probably to the mathematical complexity, and this situation motivates our present paper.

Summarizing the above discussions, in this paper, we are motivated to study the rate of convergence of the approximate maximum likelihood estimator (AMLE) to the true continuous MLE for a class of general nonlinear nonhomogenous stochastic system with unknown parameter. The main contributions of this paper lie in the following aspects. (1) *The Itô type approximation for the stochastic integral is introduced to obtain an approximate log-likelihood function.* (2) *The rate of convergence of the approximation is investigated for Itô type*

integral. (3) *The in probability rate of convergence of the approximate log-likelihood function is established for the nonlinear nonhomogenous stochastic system involving unknown parameter.* (4) *The error bound in probability of the ALME and the LME is studied for the nonlinear nonhomogenous stochastic system.* The rest of this paper is outlined as follows. In Section 2, the approximate log-likelihood function is proposed and the problem under consideration is formulated. In Section 3, several lemmas are given to analyze the rates of convergence of the approximations for Itô and ordinary integral; furthermore, the main results are discussed to analyze the rate of convergence of the approximate log-likelihood function and the error bound of the ALME and the LME. Finally, we conclude the paper in Section 4.

2. Problem Formulation and Preliminaries

Consider the real valued diffusion process X_t, $t \geq 0$ on $(\Omega, \mathcal{F}, \{\mathcal{F}_t\}_{t\geq 0}, \mathbf{P})$ satisfying the following stochastic differential equation:

$$dX_t = \theta f(t, X_t)dt + g(t, X_t)dW_t, \tag{2.1}$$

where W_t, $t \geq 0$ is a standard Wiener process adapted to $\mathcal{F}_t$, $t \geq 0$ such that for $0 \leq s < t$, $W_t - W_s$ is independent of $\mathcal{F}_s$, $\theta \in \Theta$ open in $\mathbb{R}$ is the unknown parameter to be estimated. Let θ_0 be the true value of the parameter θ.

Throughout this paper C is a generic constant, we use following notations:

$$f_x = \frac{\partial f}{\partial x}, \qquad f_t = \frac{\partial f}{\partial t}, \qquad f_{xx} = \frac{\partial^2 f}{\partial x^2}, \qquad f_{tt} = \frac{\partial^2 f}{\partial t^2}, \qquad f_{tx} = \frac{\partial^2 f}{\partial t \partial x}. \tag{2.2}$$

We assume the following condition:

(A1) $f(\cdot,\cdot)$ and $g(\cdot,\cdot)$ are Lipschitz continuous in $X_t \in \mathbb{R}$ uniformly in $t \in \mathbb{R}_+$, that is, there exists a constant $K \geq 0$ such that

$$\left|f(t, X_1) - f(t, X_2)\right|^2 \vee \left|g(t, X_1) - g(t, X_2)\right|^2 \leq K|X_1 - X_2|^2, \tag{2.3}$$

for any $t \in \mathbb{R}_+$ and $X_1, X_2 \in \mathbb{R}$.

(A2) $f(\cdot,\cdot)$ and $g(\cdot,\cdot)$ satisfy linear growth condition, that is, there exists a constant $K \geq 0$ such that

$$\left|f(t, x)\right|^2 \vee \left|g(t, x)\right|^2 \leq K\left(1 + |x|^2\right), \tag{2.4}$$

for any $t \in \mathbb{R}_+$ and $x \in \mathbb{R}$.

(A3)

$$\inf_{\{t, X_t\}} g^2(t, X_t) > 0. \tag{2.5}$$

(A4)

$$\forall p \geq 0, \quad \sup_{\{t,X_t\}} \mathbb{E}\left|f(t,X_t)\right|^p < \infty, \quad \sup_{\{t,X_t\}} \mathbb{E}\left|g(t,X_t)\right|^p < \infty. \tag{2.6}$$

$(\mathrm{A5})_j$ $f(\cdot,\cdot)$ and $g(\cdot,\cdot)$ are continuously differentiable with respect to X_t up to order $j \geq 1$ and

$$\begin{aligned} &\sup_{0\leq t\leq T} \mathbb{E}\left|f_x(t,X_t)\right|^8 < \infty, \qquad \sup_{0\leq t\leq T} \mathbb{E}\left|g_x(t,X_t)\right|^{16} < \infty, \\ &\sup_{0\leq t\leq T} \mathbb{E}\left|f_{xx}(t,X_t)\right|^8 < \infty, \qquad \sup_{0\leq t\leq T} \mathbb{E}\left|g_{xx}(t,X_t)\right|^{16} < \infty. \end{aligned} \tag{2.7}$$

$(\mathrm{A6})_k$ $f(\cdot,\cdot)$ and $g(\cdot,\cdot)$ are continuously differentiable with respect to t up to order $k \geq 1$ and

$$\begin{aligned} &\sup_{0\leq t\leq T} \mathbb{E}\left|f_t(t,X_t)\right|^4 < \infty, \qquad \sup_{0\leq t\leq T} \mathbb{E}\left|g_t(t,X_t)\right|^8 < \infty, \\ &\sup_{0\leq t\leq T} \mathbb{E}\left|f_{tt}(t,X_t)\right|^4 < \infty, \qquad \sup_{0\leq t\leq T} \mathbb{E}\left|g_{tt}(t,X_t)\right|^4 < \infty. \end{aligned} \tag{2.8}$$

(A7)

$$\sup_{0\leq t\leq T} \mathbb{E}\left|f_{tx}(t,X_t)\right|^8 < \infty, \qquad \sup_{0\leq t\leq T} \mathbb{E}\left|g_{tx}(t,X_t)\right|^8 < \infty. \tag{2.9}$$

(A8)

$$\mathbb{E}|X_0|^8 < \infty. \tag{2.10}$$

Remark 2.1. As (A1) and (A2) are established, it is well known that stochastic differential equation (2.1) has a unique solution. Please see the details in [30].

Denote $X_0^T = \{X_t,\ 0 \leq t \leq T\}$. Let P_θ^T be the measure generated on the space (C_T, B_T) of the continuous functions on $[0,T]$ with the associated Borel σ-algebra B_T generated under the supremum norm by the process X_0^T and P_0^T be the standard Wiener measure. Under assumptions (A3) and (A4), the measure P_θ^T and P_0^T are equivalent and the Randon-Nikodym derivative of P_θ^T with respect to P_0^T is given by

$$\frac{dP_\theta^T}{dP_0^T} = \exp\left\{\theta \int_0^T \frac{f(t,X_t)}{g^2(t,X_t)} dX_t - \frac{\theta^2}{2} \int_0^T \frac{f^2(t,X_t)}{g^2(t,X_t)} dt\right\}, \tag{2.11}$$

along the sample path X_0^T. Let

$$L_T(\theta) = \log \frac{dP_\theta^T}{dP_0^T} = \theta \int_0^T \frac{f(t, X_t)}{g^2(t, X_t)} dX_t - \frac{\theta^2}{2} \int_0^T \frac{f^2(t, X_t)}{g^2(t, X_t)} dt \tag{2.12}$$

be the log-likelihood function. The maximum likelihood estimate (MLE) of θ is defined as

$$\theta_T = \arg\max_{\theta \in \Theta} L_T(\theta) \left\{ \int_0^T \frac{f(t, X_t)}{g^2(t, X_t)} dX_t \right\} \left\{ \int_0^T \frac{f^2(t, X_t)}{g^2(t, X_t)} dt \right\}^{-1}. \tag{2.13}$$

Now, we study the approximation of the MLE θ_T when stochastic X_t is observed at the discrete-time points $0 = t_0 < t_1 < \cdots < t_n = T$ with $t_i - ih,\ i = 0, 1, 2, \ldots, n$ such that $h \to 0$ as $n \to \infty$. Itô approximation of the stochastic integral and rectangular approximation of the ordinary integral in the log-likelihood (2.12) yields the approximate log-likelihood function:

$$L_{n,T}(\theta) = \theta \left\{ \sum_{i=1}^n \frac{f(t_{i-1}, X_{t_{i-1}})}{g^2(t_{i-1}, X_{t_{i-1}})} (X_{t_i} - X_{t_{i-1}}) \right\} - \frac{\theta^2}{2} \left\{ \sum_{i=1}^n \frac{f^2(t_{i-1}, X_{t_{i-1}})}{g^2(t_{i-1}, X_{t_{i-1}})} (t_i - t_{i-1}) \right\}. \tag{2.14}$$

The corresponding approximate maximum likelihood estimator (AMLE) is established as follow:

$$\theta_{n,T} = \left\{ \sum_{i=1}^n \frac{f(t_{i-1}, X_{t_{i-1}})}{g^2(t_{i-1}, X_{t_{i-1}})} (X_{t_i} - X_{t_{i-1}}) \right\} \left\{ \sum_{i=1}^n \frac{f^2(t_{i-1}, X_{t_{i-1}})}{g^2(t_{i-1}, X_{t_{i-1}})} (t_i - t_{i-1}) \right\}^{-1}. \tag{2.15}$$

The main purpose of this paper is to study the rate of the convergence of the approximate log-likelihood functions and furthermore analyze the error bound in probability between the AMLE and the continuous MLE.

3. Main Results

Firstly, let us give the following lemmas which will be used in the proof of our main results.

Lemma 3.1. *Under the assumptions (A1)–(A4), $(A5)_2$, and $(A6)_1$, one has*

$$\mathbb{E} \left| \sum_{i=1}^n \frac{f^2(t_{i-1}, X_{i-1})}{g^2(t_{i-1}, X_{i-1})} (t_i - t_{i-1}) - \int_0^T \frac{f^2(t, X_t)}{g^2(t, X_t)} dt \right|^2 \le C \frac{T^3}{n^2}. \tag{3.1}$$

Proof. By Itô formula we can derive that for $t \in [0,T]$,

$$
\begin{aligned}
&\frac{f^2(t,X_t)}{g^2(t,X_t)} - \frac{f^2(t_{i-1},X_{i-1})}{g^2(t_{i-1},X_{i-1})} \\
&\quad = \int_{t_{i-1}}^{t} \frac{2f(u,X_u)f_u(u,X_u)g^2(u,X_u) - 2f^2(u,X_u)g(u,X_u)g_u(u,X_u)}{g^4(u,X_u)}du \\
&\qquad + \int_{t_{i-1}}^{t} \frac{2f(u,X_u)f_x(u,X_u)g^2(u,X_u) - 2f^2(u,X_u)g(u,X_u)g_x(u,X_u)}{g^4(u,X_u)}\theta f(u,X_u)du \\
&\qquad + \int_{t_{i-1}}^{t} \left[f_x^2(u,X_u)g^2(u,X_u) + 3f^2(u,X_u)g_x^2(u,X_u) - 4f(u,X_u)g(u,X_u)f_x(u,X_u)g_x(u,X_u)\right]du \\
&\qquad + \int_{t_{i-1}}^{t} \left[f(u,X_u)g^2(u,X_u)f_{xx}(u,X_u) - f^2(u,X_u)g(u,X_u)g_{xx}(u,X_u)\right]du \\
&\qquad + \int_{t_{i-1}}^{t} \frac{2f(u,X_u)f_x(u,X_u)g^2(u,X_u) - 2f^2(u,X_u)g(u,X_u)g_x(u,X_u)}{g^4(u,X_u)}dW_u \\
&\quad \triangleq \int_{t_{i-1}}^{t} F_1(u,X_u)du + \int_{t_{i-1}}^{t} F_2(u,X_u)dW_u,
\end{aligned}
\tag{3.2}
$$

where

$$
\begin{aligned}
F_1(u,X_u) &= F_{11}(u,X_u) + F_{12}(u,X_u) + F_{13}(u,X_u) + F_{14}(u,X_u), \\
F_{11}(u,X_u) &= \frac{2f(u,X_u)f_u(u,X_u)g^2(u,X_u) - 2f^2(u,X_u)g(u,X_u)g_u(u,X_u)}{g^4(u,X_u)}, \\
F_{12}(u,X_u) &= \frac{2f(u,X_u)f_x(u,X_u)g^2(u,X_u) - 2f^2(u,X_u)g(u,X_u)g_x(u,X_u)}{g^4(u,X_u)}\theta f(u,X_u), \\
F_{13}(u,X_u) &= f_x^2(u,X_u)g^2(u,X_u) + 3f^2(u,X_u)g_x^2(u,X_u) - 4f(u,X_u)g(u,X_u)f_x(u,X_u)g_x(u,X_u), \\
F_{14}(u,X_u) &= f(u,X_u)g^2(u,X_u)f_{xx}(u,X_u) - f^2(u,X_u)g(u,X_u)g_{xx}(u,X_u).
\end{aligned}
\tag{3.3}
$$

For $F_{11}(u, X_u)$ and $F_{13}(u, X_u)$, by assumption (A3), (A4), $(A5)_2$, $(A6)_1$, and Hölder's inequality, one has

$$\begin{aligned}
&\mathbb{E}\left(\int_{t_{i-1}}^{t} F_{11}(u, X_u)\right)^2 \\
&\quad = \mathbb{E}\left(\int_{t_{i-1}}^{t} \frac{2f(u, X_u) f_u(u, X_u) g^2(u, X_u) - 2f^2(u, X_u) g(u, X_u) g_u(u, X_u)}{g^4(u, X_u)} du\right)^2 \\
&\quad \le C\mathbb{E}\int_{t_{i-1}}^{t} f^2(u, X_u) du + C\mathbb{E}\int_{t_{i-1}}^{t} f_u^2(u, X_u) du + C\mathbb{E}\int_{t_{i-1}}^{t} g_u^2(u, X_u) du \\
&\quad \le C, \\
&\mathbb{E}\left(\int_{t_{i-1}}^{t} F_{13}(u, X_u)\right)^2 \\
&\quad = \mathbb{E}\left(\int_{t_{i-1}}^{t} f_x^2(u, X_u) g^2(u, X_u) + 3f^2(u, X_u) g_x^2(u, X_u)\right. \\
&\qquad\qquad \left. -4f(u, X_u) g(u, X_u) f_x(u, X_u) g_x(u, X_u) du\right)^2 \\
&\quad \le C\mathbb{E}\int_{t_{i-1}}^{t} f^4(u, X_u) du + C\mathbb{E}\int_{t_{i-1}}^{t} g^4(u, X_u) du + C\mathbb{E}\int_{t_{i-1}}^{t} f_x^4(u, X_u) du + C\mathbb{E}\int_{t_{i-1}}^{t} g_x^4(u, X_u) du \\
&\quad \le C.
\end{aligned} \tag{3.4}$$

Similarly, we have

$$\mathbb{E}\left(\int_{t_{i-1}}^{t} F_{12}(u, X_u)\right)^2 \le C, \qquad \mathbb{E}\left(\int_{t_{i-1}}^{t} F_{14}(u, X_u)\right)^2 \le C. \tag{3.5}$$

This means

$$\mathbb{E}\left(\int_{t_{i-1}}^{t} F1(u, X_u)\right)^2 \le C. \tag{3.6}$$

Hence, it follows C_r inequality that

$$\begin{aligned}
&\mathbb{E}\left|\sum_{i=1}^{n}\frac{f^2(t_{i-1},X_{i-1})}{g^2(t_{i-1},X_{i-1})}(t_i-t_{i-1})-\int_0^T\frac{f^2(t,X_t)}{g^2(t,X_t)}dt\right|^2\\
&\quad=\mathbb{E}\left|\sum_{i=1}^{n}\int_{t_{i-1}}^{t_i}\left[\frac{f^2(t_{i-1},X_{i-1})}{g^2(t_{i-1},X_{i-1})}(t_i-t_{i-1})-\int_0^T\frac{f^2(t,X_t)}{g^2(t,X_t)}\right]dt\right|^2\\
&\quad=\mathbb{E}\left|\sum_{i=1}^{n}\int_{t_{i-1}}^{t_i}\left[\int_{t_{i-1}}^{t}F_1(u,X_u)du+\int_{t_{i-1}}^{t}F_2(u,X_u)dW_u\right]dt\right|^2\\
&\quad\le 2\mathbb{E}\left|\sum_{i=1}^{n}\int_{t_{i-1}}^{t_i}\int_{t_{i-1}}^{t}F_1(u,X_u)du\,dt\right|^2+2\mathbb{E}\left|\sum_{i=1}^{n}\int_{t_{i-1}}^{t_i}\int_{t_{i-1}}^{t}F_2(u,X_u)dW_u dt\right|^2\triangleq 2G_1+2G_2.
\end{aligned}\tag{3.7}$$

By assumptions (A3), (A4), $(A5)_2$, and $(A6)_1$, we obtain

$$\begin{aligned}
G_1&=\mathbb{E}\left|\sum_{i=1}^{n}\int_{t_{i-1}}^{t_i}\int_{t_{i-1}}^{t}F_1(u,X_u)du\,dt\right|^2\\
&\le\mathbb{E}\sum_{i=1}^{n}\left(\int_{t_{i-1}}^{t_i}\int_{t_{i-1}}^{t}F_1(u,X_u)du\,dt\right)^2\\
&\quad+\mathbb{E}\sum_{1=i\neq j}^{n}\left(\int_{t_{i-1}}^{t_i}\int_{t_{i-1}}^{t}F_1(u,X_u)du\,dt\right)\left(\int_{t_{j-1}}^{t_j}\int_{t_{j-1}}^{t}F_1(u,X_u)du\,dt\right)\\
&\le\mathbb{E}\sum_{i=1}^{n}(t_i-t_{i-1})\int_{t_{i-1}}^{t_i}\left|\int_{t_{i-1}}^{t}F_1(u,X_u)du\,dt\right|^2dt\\
&\quad+\sum_{1=i\neq j}^{n}\left\{\mathbb{E}\left(\int_{t_{i-1}}^{t_i}\int_{t_{i-1}}^{t}F_1(u,X_u)du\,dt\right)^2\mathbb{E}\left(\int_{t_{j-1}}^{t_j}\int_{t_{j-1}}^{t}F_1(u,X_u)du\,dt\right)^2\right\}^{1/2}\\
&\le\sum_{i=1}^{n}(t_i-t_{i-1})\int_{t_{i-1}}^{t_i}\mathbb{E}\left|\int_{t_{i-1}}^{t}F_1(u,X_u)du\,dt\right|^2dt\\
&\quad+\sum_{1=i\neq j}^{n}\left\{(t_i-t_{i-1})\int_{t_{i-1}}^{t_i}\mathbb{E}\left(\int_{t_{i-1}}^{t}F_1(u,X_u)du\right)^2dt(t_j-t_{j-1})\int_{t_{j-1}}^{t_j}\mathbb{E}\left(\int_{t_{j-1}}^{t}F_1(u,X_u)du\right)^2dt\right\}^{1/2}\\
&\le C\sum_{i=1}^{n}(t_i-t_{i-1})^3+C\sum_{1=i\neq j}^{n}\left\{(t_i-t_{i-1})^3(t_j-t_{j-1})^3\right\}^{1/2}\le C\frac{T^3}{n^2}.
\end{aligned}\tag{3.8}$$

Due to the orthogonality, Itô isomorphism, the Cauchy-Schwarz inequality, assumption (A3), (A4), and $(A5)_1$, we get

$$\begin{aligned}
G_2 &= \mathbb{E}\left|\sum_{i=1}^{n}\int_{t_{i-1}}^{t_i}\int_{t_{i-1}}^{t} F_2(u,X_u)dW_u dt\right|^2 \\
&\le \mathbb{E}\sum_{i=1}^{n}\left(\int_{t_{i-1}}^{t_i}\int_{t_{i-1}}^{t} F_2(u,X_u)dW_u dt\right)^2 \\
&\quad + \sum_{1=i\neq j}^{n}\mathbb{E}\left(\int_{t_{i-1}}^{t_i}\int_{t_{i-1}}^{t} F_2(u,X_u)dW_u dt\right)\left(\int_{t_{j-1}}^{t_j}\int_{t_{j-1}}^{t} F_2(u,X_u)dW_u dt\right) \\
&\le \sum_{i=1}^{n}(t_i-t_{i-1})\int_{t_{i-1}}^{t_i}\mathbb{E}\left|\int_{t_{i-1}}^{t} F_2(u,X_u)dW_u dt\right|^2 dt \\
&\le \sum_{i=1}^{n}(t_i-t_{i-1})\int_{t_{i-1}}^{t_i}\int_{t_{i-1}}^{t}\mathbb{E}|F_2(u,X_u)|^2 du\, dt \\
&\le C\sum_{i=1}^{n}(t_i-t_{i-1})\int_{t_{i-1}}^{t_i}(t-t_{i-1})dt \\
&\le C\sum_{i=1}^{n}(t_i-t_{i-1})^3 \\
&\le C\frac{T^3}{n^2}.
\end{aligned} \tag{3.9}$$

Obviously, it follows from bounds for G_1 and G_2 that

$$\mathbb{E}\left|\sum_{i=1}^{n}\frac{f^2(t_{i-1},X_{i-1})}{g^2(t_{i-1},X_{i-1})}(t_i-t_{i-1})-\int_0^T\frac{f^2(t,X_t)}{g^2(t,X_t)}dt\right|^2 \le C\frac{T^3}{n^2}. \tag{3.10}$$

The proof is now complete. □

Next, we will go on to analyze the rate of convergence of the approximations for Itô integral whose result will be used in the following theorems.

Lemma 3.2. *Under the assumptions (A1)–(A4), $(A5)_2$, $(A6)_2$, (A7), and (A8), one has*

$$\mathbb{E}\left|\sum_{i=1}^{n}\frac{f(t_{i-1},X_{t_{i-1}})}{g(t_{i-1},X_{t_{i-1}})}(W_{t_i}-W_{t_{i-1}})-\int_0^T\frac{f(t,X_t)}{g(t,X_t)}dW_t\right|^2 \le C\frac{T^3}{n^2}. \tag{3.11}$$

Proof. Let π_n be the partition $\pi_n = 0 = t_0 < t_1 < \cdots < t_n = T,\ t_i = ih,\ i = 0, 1, \ldots, n$ such that $h \to 0$. Define S and S_n as

$$S = \int_0^T \frac{f^2(t, X_t)}{g^2(t, X_t)} dW_t,$$
$$S_n = \sum_{i=1}^{n} \frac{f(t_{i-1}, X_{t_{i-1}})}{g(t_{i-1}, X_{t_{i-1}})} (W_{t_i} - W_{t_{i-1}}). \tag{3.12}$$

Let π_n' be a partition which is finer than π_n, obtained by choosing the mid point $\widehat{t}_{i-1}$ from each of the interval $t_{i-1} < \widehat{t}_{i-1} < t_i$, $i = 0, 1, \cdots, n$. Let $0 = t_0' < t_1' < \cdots < t_{2n}' = T$ be the points of subdivision of the refined partition π_n'. Define the approximating sum $S_{\pi_n'}$ as before. We take two steps to prove the assertion in this lemma.

Step 1. We will first obtain the bounds on $E|S_{\pi_n} - S_{\pi_n'}|^2$.

Let $0 \le \widetilde{t}_0 < \widetilde{t}_1 < \widetilde{t}_2 \le T$ be three equally space points on $[0, T]$ and let us denote $X_{\widetilde{t}_i}$ by X_i and $W_{\widetilde{t}_i}$ by $W_i,\ i = 0, 1, \ldots, n$. Define

$$\begin{aligned} H &= \frac{f\left(\widetilde{t}_0, X_0\right)}{g\left(\widetilde{t}_0, X_0\right)} (W_2 - W_0) - \left\{ \frac{f\left(\widetilde{t}_1, X_1\right)}{g\left(\widetilde{t}_1, X_1\right)} (W_2 - W_1) + \frac{f\left(\widetilde{t}_0, X_0\right)}{g\left(\widetilde{t}_0, X_0\right)} (W_1 - W_0) \right\} \\ &= (W_2 - W_1) \left\{ \frac{f\left(\widetilde{t}_0, X_0\right)}{g\left(\widetilde{t}_0, X_0\right)} - \frac{f\left(\widetilde{t}_1, X_1\right)}{g\left(\widetilde{t}_1, X_1\right)} \right\}. \end{aligned} \tag{3.13}$$

Denote

$$I = \int_{\widetilde{t}_0}^{\widetilde{t}_1} \frac{f(t, X_t)}{g(t, X_t)} dt. \tag{3.14}$$

Applying the Taylor expansion, one has

$$\begin{aligned} &\frac{f\left(\widetilde{t}_0, X_0\right)}{g\left(\widetilde{t}_0, X_0\right)} - \frac{f\left(\widetilde{t}_1, X_1\right)}{g\left(\widetilde{t}_1, X_1\right)} \\ &\quad = (X_0 - X_1) \frac{f_x g - g_x f}{g^2} \left(\widetilde{t}_1, X_1\right) + \left(\widetilde{t}_0 - \widetilde{t}_1\right) \frac{f_t g - g_t f}{g^2} \left(\widetilde{t}_1, X_1\right) \\ &\qquad + \frac{1}{2} (X_0 - X_1)^2 \frac{\left(f_{xx} g^2 - g_{xx} f\right) g - 2\left(f_x g - g_x f\right) g g_x}{g^4} (t^*, X^*) \\ &\qquad + \frac{1}{2} \left(\widetilde{t}_0 - \widetilde{t}_1\right)^2 \frac{\left(f_{tt} g^2 - g_{tt} f\right) g - 2\left(f_t g - g_t f\right) g g_t}{g^4} (t^*, X^*) \end{aligned}$$

$$
\begin{aligned}
&+\left(\tilde{t}_0-\tilde{t}_1\right)(X_0-X_1)\frac{(f_{tx}g-fgtx-f_xg_t-f_tg_x)g^2+2fgg_tg_x}{g^4}(t^*,X^*)\\
&=-(W_1-W_0+I)\frac{f_xg-g_xf}{g^2}\left(\tilde{t}_1,X_1\right)+\left(\tilde{t}_0-\tilde{t}_1\right)\frac{f_tg-g_tf}{g^2}\left(\tilde{t}_1,X_1\right)\\
&\quad+\frac{1}{2}(X_0-X_1)^2\frac{(f_{xx}g^2-g_{xx}f)g-2(f_xg-g_xf)gg_x}{g^4}(t^*,X^*)\\
&\quad+\frac{1}{2}\left(\tilde{t}_0-\tilde{t}_1\right)^2\frac{(f_{tt}g^2-g_{tt}f)g-2(f_tg-g_tf)gg_t}{g^4}(t^*,X^*)\\
&\quad+\left(\tilde{t}_0-\tilde{t}_1\right)(X_0-X_1)\frac{(f_{tx}g-fgtx-f_xg_t-f_tg_x)g^2+2fgg_tg_x}{g^4}(t^*,X^*),
\end{aligned}
\tag{3.15}
$$

where $|X_1-X^*|<|X_0-X_1|$, $|\tilde{t}_1-t^*|<|\tilde{t}_0-\tilde{t}_1|$.

Relations (3.15) to (3.13) show that

$$
\begin{aligned}
H&=-(W_2-W_1)I\frac{f_xg-g_xf}{g^2}\left(\tilde{t}_1,X_1\right)+(W_2-W_1)\left(\tilde{t}_0-\tilde{t}_1\right)\frac{f_tg-g_tf}{g^2}\left(\tilde{t}_1,X_1\right)\\
&\quad+(W_2-W_1)\frac{1}{2}(X_0-X_1)^2\frac{(f_{xx}g^2-g_{xx}f)g-2(f_xg-g_xf)gg_x}{g^4}(t^*,X^*)\\
&\quad+(W_2-W_1)\frac{1}{2}\left(\tilde{t}_0-\tilde{t}_1\right)^2\frac{(f_{tt}g^2-g_{tt}f)g-2(f_tg-g_tf)gg_t}{g^4}(t^*,X^*)\\
&\quad+(W_2-W_1)\left(\tilde{t}_0-\tilde{t}_1\right)(X_0-X_1)\frac{(\mathrm{f}_{tx}g-fg_{tx}-f_xg_t-f_tg_x)g^2+2fgg_tg_x}{g^4}(t^*,X^*).
\end{aligned}
\tag{3.16}
$$

Notice that H's corresponding to different subintervals of $[0,T]$-generated by π_n form a martingale difference sequence. Observe that

$$
\begin{aligned}
\mathbb{E}|H|^2=\mathbb{E}(W_2-W_1)^2\mathbb{E}\Bigg\{&-I\frac{f_xg-g_xf}{g^2}\left(\tilde{t}_1,X_1\right)+\left(\tilde{t}_0-\tilde{t}_1\right)\frac{f_tg-g_tf}{g^2}\left(\tilde{t}_1,X_1\right)\\
&+\frac{1}{2}(X_0-X_1)^2\frac{(f_{xx}g^2-g_{xx}f)g-2(f_xg-g_xf)gg_x}{g^4}(t^*,X^*)\\
&+\frac{1}{2}\left(\tilde{t}_0-\tilde{t}_1\right)^2\frac{(f_{tt}g^2-g_{tt}f)g-2(f_tg-g_tf)gg_t}{g^4}(t^*,X^*)\\
&+\left(\tilde{t}_0-\tilde{t}_1\right)(X_0-X_1)\frac{(\mathcal{S})g^2+2fgg_tg_x}{g^4}(t^*,X^*)\Bigg\}^2
\end{aligned}
$$

$$
\begin{aligned}
&\leq 4\left(\tilde{t}_2-\tilde{t}_1\right)\Bigg\{\mathbb{E}\left(I\frac{f_xg-g_xf}{g^2}\left(\tilde{t}_1,X_1\right)\right)^2+\left(\tilde{t}_0-\tilde{t}_1\right)^2\mathbb{E}\left(\frac{f_tg-g_tf}{g^2}\left(\tilde{t}_1,X_1\right)\right)^2\\
&\quad+\frac{1}{4}\mathbb{E}\left[(X_0-X_1)^4\left(\frac{(f_{xx}g^2-g_{xx}f)g-2(f_xg-g_xf)gg_x}{g^4}(t^*,X^*)\right)^2\right]\\
&\quad+\frac{1}{4}\left(\tilde{t}_0-\tilde{t}_1\right)^4\mathbb{E}\left(\frac{(f_{tt}g^2-g_{tt}f)g-2(f_tg-g_tf)gg_t}{g^4}(t^*,X^*)\right)^2\\
&\quad+\left(\tilde{t}_0-\tilde{t}_1\right)^2\mathbb{E}\left[(X_0-X_1)^2\left(\frac{(\mathcal{S})g^2+2fgg_tg_x}{g^4}(t^*,X^*)\right)^2\right]\Bigg\}\\
&\leq 4\left(\tilde{t}_2-\tilde{t}_1\right)\Bigg\{\left[\mathbb{E}I^4\mathbb{E}\left(\frac{f_xg-g_xf}{g^2}\left(\tilde{t}_1,X_1\right)\right)^4\right]^{1/2}+\left(\tilde{t}_0-\tilde{t}_1\right)^2\mathbb{E}\left(\frac{f_tg-g_tf}{g^2}\left(\tilde{t}_1,X_1\right)\right)^2\\
&\quad+\frac{1}{4}\left[\mathbb{E}(X_0-X_1)^8\mathbb{E}\left(\frac{(f_{xx}g^2-g_{xx}f)g-2(f_xg-g_xf)gg_x}{g^4}(t^*,X^*)\right)^8\right]^{1/2}\\
&\quad+\frac{1}{4}\left(\tilde{t}_0-\tilde{t}_1\right)^4\mathbb{E}\left(\frac{(f_{tt}g^2-g_{tt}f)g-2(f_tg-g_tf)gg_t}{g^4}(t^*,X^*)\right)^2\\
&\quad+\left(\tilde{t}_0-\tilde{t}_1\right)^2\left[\mathbb{E}(X_0-X_1)^4\mathbb{E}\left(\frac{(\mathcal{S})g^2+2fgg_tg_x}{g^4}(t^*,X^*)\right)^4\right]^{1/2}\Bigg\}\\
&\leq 4\left(\tilde{t}_2-\tilde{t}_1\right)\Bigg\{\left(\mathbb{E}I^4\right)^{1/2}C\left[\left(\mathbb{E}f_x^8\left(\tilde{t}_1,X_1\right)\right)^{1/2}+\left(\mathbb{E}g_x^8\left(\tilde{t}_1,X_1\right)\right)^{1/2}+\left(\mathbb{E}f^8\left(\tilde{t}_1,X_1\right)\right)^{1/2}\right]^{1/2}\\
&\quad+\left(\tilde{t}_0-\tilde{t}_1\right)^2C\left[\left(\mathbb{E}f_t^4\left(\tilde{t}_1,X_1\right)\right)^{1/2}+\left(\mathbb{E}g_t^4\left(\tilde{t}_1,X_1\right)\right)^{1/2}+\left(\mathbb{E}f^4\left(\tilde{t}_1,X_1\right)\right)^{1/2}\right]\\
&\quad+\frac{1}{4}\left(\mathbb{E}(X_0-X_1)^8\right)^{1/2}C\Bigg[\left(\mathbb{E}f_{xx}^8(t^*,X^*)\right)^{1/2}+\left(\mathbb{E}g_{xx}^8(t^*,X^*)\right)^{1/2}\\
&\qquad+\left(\mathbb{E}f^8(t^*,X^*)\right)^{1/2}+\left(\mathbb{E}f_x^8(t^*,X^*)\right)^{1/2}\\
&\qquad+\left(\mathbb{E}f_x^{16}(t^*,X^*)\right)^{1/2}\Bigg]^{1/2}\\
&\quad+\frac{1}{4}\left(\tilde{t}_0-\tilde{t}_1\right)^4C\Bigg[\left(\mathbb{E}f_{tt}^4(t^*,X^*)\right)^{1/2}+\left(\mathbb{E}g_{tt}^4(t^*,X^*)\right)^{1/2}+\left(\mathbb{E}f_t^4(t^*,X^*)\right)^{1/2}\\
&\qquad+\left(\mathbb{E}g_t^4(t^*,X^*)\right)^{1/2}+\left(\mathbb{E}g_t^8(t^*,X^*)\right)^{1/2}\Bigg]
\end{aligned}
$$

$$+\left(\tilde{t}_0-\tilde{t}_1\right)^2\left[\mathbb{E}(X_0-X_1)^4\right]^{1/2}\left[\left(\mathbb{E}f_{tx}^8(t^*,X^*)\right)^{1/2}+\left(\mathbb{E}g_{tx}^8(t^*,X^*)\right)^{1/2}\right.$$
$$+\left(\mathbb{E}f_x^8\left(\tilde{t}_1,X_1\right)\right)^{1/2}+\left(\mathbb{E}g_x^8\left(\tilde{t}_1,X_1\right)\right)^{1/2}$$
$$\left.+\left(\mathbb{E}f_t^8\left(\tilde{t}_1,X_1\right)\right)^{1/2}+\left(\mathbb{E}g_t^8\left(\tilde{t}_1,X_1\right)\right)^{1/2}\right]^{1/2}\Bigg\}. \tag{3.17}$$

where $\mathcal{S}$ denotes $f_{tx}g - fg_{tx} - f_xg_t - f_tg_x$.

By Theorem 4 of [31], for any $0 \le s < t \le T$, there exists $C > 0$ such that

$$\mathbb{E}(X_t - X_s)^{2m} \le C\left(\mathbb{E}X_0^{2m} + 1\right)(t-s)^m, \quad m \ge 1. \tag{3.18}$$

Hence

$$\begin{aligned}\mathbb{E}(X_t - X_s)^8 &\le C\left(\mathbb{E}X_0^8 + 1\right)(t-s)^4,\\ \mathbb{E}(X_t - X_s)^4 &\le C\left(\mathbb{E}X_0^4 + 1\right)(t-s)^2.\end{aligned} \tag{3.19}$$

Furthermore by (A2) and (A3), we have

$$\begin{aligned}\mathbb{E}I^4 &= \mathbb{E}\left(\int_{\tilde{t}_0}^{\tilde{t}_1}\frac{f(t,X_t)}{g(t,X_t)}dt\right)^4\\ &\le C\mathbb{E}\left(\int_{\tilde{t}_0}^{\tilde{t}_1} f^4(t,X_t)dt\right)\\ &\le C\mathbb{E}\left(\int_{\tilde{t}_0}^{\tilde{t}_1}\left(1+|X_t|^2\right)^2 dt\right)\\ &\le C\left(\tilde{t}_1-\tilde{t}_0\right)^4\sup_{0\le t\le T}\mathbb{E}\left(1+|X_t|^2\right)^2\\ &\le C\left(\tilde{t}_1-\tilde{t}_0\right)^4.\end{aligned} \tag{3.20}$$

Thus

$$\mathbb{E}(H)^2 \le C\left(\tilde{t}_2-\tilde{t}_1\right)\left(\tilde{t}_1-\tilde{t}_0\right)^2. \tag{3.21}$$

Using the property that H corresponding to different subintervals forms a martingale difference sequence, it follows that

$$\mathbb{E}\left|S_{\pi_n} - S_{\pi_n'}\right|^2 \leq C\frac{T^3}{n^2}, \tag{3.22}$$

for some constant $C > 0$.

Step 2. We will show now the bounds on $E|S_{\pi_n'} - S|^2$.

Let $\pi_n^{(p)}$, $p \geq 0$ be the sequence of partitions such that $\pi_n^{(i+1)}$ is a refinement of $\pi_n^{(n)}$ by choosing the midpoint of the subintervals generated by $\pi_n^{(n)}$. Note that $\pi_n^{(0)} = \pi_n$ and $\pi_n^{(1)} = \pi_n'$. The analysis given above proves that

$$\mathbb{E}\left|S_{\pi_n}(p) - S_{\pi_n(p+1)}\right|^2 \leq C\frac{T^3}{2^p n^2}, \quad p \geq 0, \tag{3.23}$$

where $S_{\pi_n}(p)$ is the approximation corresponding to $\pi_n^{(p)}$ and $S_{\pi_n}(0) = S_{\pi_n}$.

Therefore, applying the Hölder inequality and the Minkovski inequality, one gets

$$\begin{aligned}
&\mathbb{E}\left|S_{\pi_n}(0) - S_{\pi_n(p+1)}\right|^2 \\
&\quad \leq \mathbb{E}\left[\sum_{k=0}^{p}\left(S_{\pi_n}(k) - S_{\pi_n(k+1)}\right)\right]^2 \\
&\quad \leq \left[\sum_{k=0}^{p}\left(\mathbb{E}\left|S_{\pi_n}(k) - S_{\pi_n(k+1)}\right|^2\right)^{1/2}\right]^2 \\
&\quad \leq \left[\sum_{k=0}^{p}\left(\frac{CT^3}{2^p n^2}\right)^{1/2}\right]^2 \\
&\quad \leq C\frac{T^3}{n^2},
\end{aligned} \tag{3.24}$$

for all $p \geq 0$. Let $p \to \infty$. Since the integral S exists, $S_{\pi_n}(p+1)$ converges in $\mathcal{L}_2$ to S as $p \to \infty$. Note that $\pi_n^{(p+1)}$, $P \geq 0$ is a sequence of partitions such that the mesh of the partition tends to zero as $p \to \infty$ for any fixed n.

Thus

$$\mathbb{E}|S_{\pi_n} - S|^2 \leq C\frac{T^3}{2^p n^2}, \quad p \geq 0, \tag{3.25}$$

where

$$S = \lim_{n\to\infty} S_{\pi_n} = \int_0^T \frac{f(t,X_t)}{g(t,X_t)} dW_t. \tag{3.26}$$

The proof is now complete. □

Theorem 3.3. *Under assumptions (A1)–(A4), $(A5)_2$, $(A6)_2$, (A7), and (A8), one has*

$$\begin{aligned} \mathbb{E}|L_{n,T}(\theta) - L_T(\theta)|^2 &\le C\frac{T^3}{n^2}, \\ \mathbb{E}\left|L'_{n,T}(\theta) - L'_T(\theta)\right|^2 &\le C\frac{T^3}{n^2}. \end{aligned} \tag{3.27}$$

Proof. By the analysis given above, one has

$$\begin{aligned} &|L_{n,T}(\theta) - L_T(\theta)|^2 \\ &= \left|\theta\left[\sum_{i=1}^n \frac{f(t_{i-1},X_{t_{i-1}})}{g^2(t_{i-1},X_{t_{i-1}})}(X_{t_i} - X_{t_{i-1}}) - \int_0^T \frac{f(t,X_t)}{g^2(t,X_t)} dX_t\right]\right. \\ &\quad \left. -\frac{\theta^2}{2}\left[\sum_{i=1}^n \frac{f^2(t_{i-1},X_{t_{i-1}})}{g^2(t_{i-1},X_{t_{i-1}})}(t_i - t_{i-1}) - \int_0^T \frac{f^2(t,X_t)}{g^2(t,X_t)} dt\right]\right|^2 \\ &\le \frac{\theta^4}{2}\left|\sum_{i=1}^n \frac{f^2(t_{i-1},X_{t_{i-1}})}{g^2(t_{i-1},X_{t_{i-1}})}(t_i - t_{i-1}) - \int_0^T \frac{f^2(t,X_t)}{g^2(t,X_t)} dt\right|^2 \\ &\quad + 2\theta^2\left|\sum_{i=1}^n \frac{f(t_{i-1},X_{t_{i-1}})}{g^2(t_{i-1},X_{t_{i-1}})}(W_{t_i} - W_{t_{i-1}}) - \int_0^T \frac{f(t,X_t)}{g^2(t,X_t)} dW_t\right|^2. \end{aligned} \tag{3.28}$$

Hence, it follows from Lemmas 3.1 and 3.2 that

$$\begin{aligned} &\mathbb{E}|L_{n,T}(\theta) - L_T(\theta)|^2 \\ &\le \frac{\theta^4}{2}\mathbb{E}\left|\sum_{i=1}^n \frac{f^2(t_{i-1},X_{t_{i-1}})}{g^2(t_{i-1},X_{t_{i-1}})}(t_i - t_{i-1}) - \int_0^T \frac{f^2(t,X_t)}{g^2(t,X_t)} dt\right|^2 \\ &\quad + 2\theta^2\mathbb{E}\left|\sum_{i=1}^n \frac{f(t_{i-1},X_{t_{i-1}})}{g^2(t_{i-1},X_{t_{i-1}})}(W_{t_i} - W_{t_{i-1}}) - \int_0^T \frac{f(t,X_t)}{g^2(t,X_t)} dW_t\right|^2 \\ &\le C\frac{T^3}{n^2}. \end{aligned} \tag{3.29}$$

Next, note that

$$\begin{aligned}
&\left|L'_{n,T}(\theta) - L'_T(\theta)\right|^2 \\
&\quad = \left|\theta \sum_{i=1}^{n} \frac{f(t_{i-1}, X_{t_{i-1}})}{g^2(t_{i-1}, X_{t_{i-1}})}(X_{t_i} - X_{t_{i-1}})\right. \\
&\qquad \left. -\theta \sum_{i=1}^{n} \frac{f^2(t_{i-1}, X_{t_{i-1}})}{g^2(t_{i-1}, X_{t_{i-1}})}(t_i - t_{i-1}) - \left[\int_0^T \frac{f(t, X_t)}{g^2(t, X_t)} dX_t - \int_0^T \frac{f^2(t, X_t)}{g^2(t, X_t)} dt\right]\right|^2 \\
&\quad = (1-\theta)^2 \left|\sum_{i=1}^{n} \frac{f^2(t_{i-1}, X_{t_{i-1}})}{g^2(t_{i-1}, X_{t_{i-1}})}(t_i - t_{i-1}) - \int_0^T \frac{f^2(t, X_t)}{g^2(t, X_t)} dt\right|^2 \\
&\qquad + \left|\sum_{i=1}^{n} \frac{f(t_{i-1}, X_{t_{i-1}})}{g^2(t_{i-1}, X_{t_{i-1}})}(W_{t_i} - W_{t_{i-1}}) - \int_0^T \frac{f(t, X_t)}{g^2(t, X_t)} dW_t\right|^2.
\end{aligned} \tag{3.30}$$

Similarly, by Lemmas 3.1 and 3.2, we obtain

$$\mathbb{E}\left|L'_{n,T}(\theta) - L'_T(\theta)\right|^2 \le C\frac{T^3}{n^2}. \tag{3.31}$$

The proof is now complete. □

Remark 3.4. The rate of convergence of the approximations for Itô and ordinary integral have been investigated in Lemmas 3.1 and 3.2. Based on these analysis results, the rate of convergence of the approximate log-likelihood function for nonlinear nonhomogenous stochastic system with unknown parameter has been established in Theorem 3.3. It should be pointed out that the corresponding approximate result gained in [27] is the special case for linear stochastic differential equation, furthermore, the conclusions in [9] also can be regarded as a special example under the result in Theorem 3.3 for nonlinear nonhomogenous stochastic system with constant diffusion.

Finally, we will study the error bound in probability between the AMLE and the continuous MLE for nonlinear nonhomogenous stochastic system with unknown parameter.

Theorem 3.5. *Under assumption (A1)–(A4), $(A5)_2$, $(A6)_2$, (A7), and (A8), one has*

$$\mathbb{E}|\theta_{n,T} - \theta_T|^2 \le C\frac{T^3}{n^2}. \tag{3.32}$$

Proof. We know $\theta_{n,T}$ and θ_T are the solutions of equations $L'_{n,T}(\theta) = 0$ and $L'_T(\theta) = 0$, respectively.

Hence, one gets

$$
\begin{aligned}
&|\theta_{n,T}-\theta_T|^2 \\
&\quad= \left|\frac{\sum_{i=1}^{n}\left(f(t_{i-1},X_{t_{i-1}})/g^2(t_{i-1},X_{t_{i-1}})\right)(X_{t_i}-X_{t_{i-1}})}{\sum_{i=1}^{n}\left(f^2(t_{i-1},X_{t_{i-1}})/g^2(t_{i-1},X_{t_{i-1}})\right)(t_i-t_{i-1})}-\frac{\int_0^T\left(f(t,X_t)/g^2(t,X_t)\right)dX_t}{\int_0^T\left(f^2(t,X_t)/g^2(t,X_t)\right)dt}\right|^2 \\
&\quad= \left|\frac{\sum_{i=1}^{n}\left(f(t_{i-1},X_{t_{i-1}})/g(t_{i-1},X_{t_{i-1}})\right)(W_{t_i}-W_{t_{i-1}})}{\sum_{i=1}^{n}\left(f^2(t_{i-1},X_{t_{i-1}})/g^2(t_{i-1},X_{t_{i-1}})\right)(t_i-t_{i-1})}-\frac{\int_0^T\left(f(t,X_t)/g(t,X_t)\right)dW_t}{\int_0^T\left(f^2(t,X_t)/g^2(t,X_t)\right)dt}\right|^2 \\
&\quad= \left|\frac{\sum_{i=1}^{n}\left(f(t_{i-1},X_{t_{i-1}})/g(t_{i-1},X_{t_{i-1}})\right)(W_{t_i}-W_{t_{i-1}})-\int_0^T\left(f(t,X_t)/g(t,X_t)\right)dW_t}{\sum_{i=1}^{n}\left(f^2(t_{i-1},X_{t_{i-1}})/g^2(t_{i-1},X_{t_{i-1}})\right)(t_i-t_{i-1})}\right. \\
&\qquad\left.-\frac{\int_0^T\left(f(t,X_t)/g(t,X_t)\right)dW_t\left[\sum_{i=1}^{n}\left(f^2(t_{i-1},X_{t_{i-1}})/g^2(t_{i-1},X_{t_{i-1}})\right)(t_i-t_{i-1})-\mathcal{A}\right]}{\left[\sum_{i=1}^{n}\left(f^2(t_{i-1},X_{t_{i-1}})/g^2(t_{i-1},X_{t_{i-1}})\right)(t_i-t_{i-1})\right]\int_0^T\left(f^2(t,X_t)/g^2(t,X_t)\right)dt}\right|^2 \\
&\quad\le 2\left|\frac{\sum_{i=1}^{n}\left(f(t_{i-1},X_{t_{i-1}})/g(t_{i-1},X_{t_{i-1}})\right)(W_{t_i}-W_{t_{i-1}})-\int_0^T\left(f(t,X_t)/g(t,X_t)\right)dW_t}{\sum_{i=1}^{n}\left(f^2(t_{i-1},X_{t_{i-1}})/g^2(t_{i-1},X_{t_{i-1}})\right)(t_i-t_{i-1})}\right|^2 \\
&\qquad+2\left|\frac{\int_0^T\left(f(t,X_t)/g(t,X_t)\right)dW_t\left[\sum_{i=1}^{n}\left(f^2(t_{i-1},X_{t_{i-1}})/g^2(t_{i-1},X_{t_{i-1}})\right)(t_i-t_{i-1})-\mathcal{A}\right]}{\left[\sum_{i=1}^{n}\left(f^2(t_{i-1},X_{t_{i-1}})/g^2(t_{i-1},X_{t_{i-1}})\right)(t_i-t_{i-1})\right]\int_0^T\left(f^2(t,X_t)/g^2(t,X_t)\right)dt}\right|^2.
\end{aligned}
\tag{3.33}
$$

As we know that $\sum_{i=1}^{n}(f^2(t_{i-1},X_{t_{i-1}})/g^2(t_{i-1},X_{t_{i-1}}))(t_i-t_{i-1}) > 0$, so there exists a constant $C>0$ such that

$$
\frac{1}{\sum_{i=1}^{n}\left(f^2(t_{i-1},X_{t_{i-1}})/g^2(t_{i-1},X_{t_{i-1}})\right)(t_i-t_{i-1})}\le C. \tag{3.34}
$$

Therefore, applying Itô isomorphism, the Cauchy-Schwarz inequality, Lemmas 3.1 and 3.2, we obtain

$$
\begin{aligned}
&\mathbb{E}|\theta_{n,T}-\theta_T|^2 \\
&\quad\le 2\mathbb{E}\left|\frac{\sum_{i=1}^{n}\left(f(t_{i-1},X_{t_{i-1}})/g(t_{i-1},X_{t_{i-1}})\right)(W_{t_i}-W_{t_{i-1}})-\int_0^T\left(f(t,X_t)/g(t,X_t)\right)dW_t}{\sum_{i=1}^{n}\left(f^2(t_{i-1},X_{t_{i-1}})/g^2(t_{i-1},X_{t_{i-1}})\right)(t_i-t_{i-1})}\right|^2 \\
&\qquad+2\mathbb{E}\left|\frac{\int_0^T\left(f(t,X_t)/g(t,X_t)\right)dW_t\left[\sum_{i=1}^{n}\left(f^2(t_{i-1},X_{t_{i-1}})/g^2(t_{i-1},X_{t_{i-1}})\right)(t_i-t_{i-1})-\mathcal{A}\right]}{\left[\sum_{i=1}^{n}\left(f^2(t_{i-1},X_{t_{i-1}})/g^2(t_{i-1},X_{t_{i-1}})\right)(t_i-t_{i-1})\right]\int_0^T\left(f^2(t,X_t)/g^2(t,X_t)\right)dt}\right|^2
\end{aligned}
$$

$$
\begin{aligned}
&\leq C\mathbb{E}\left|\sum_{i=1}^{n}\left(f(t_{i-1},X_{t_{i-1}})/g(t_{i-1},X_{t_{i-1}})\right)(W_{t_i}-W_{t_{i-1}})-\int_0^T\left(f(t,X_t)/g(t,X_t)\right)dW_t\right|^2\\
&\quad+C\mathbb{E}\left|\sum_{i=1}^{n}\left(f^2(t_{i-1},X_{t_{i-1}})/g^2(t_{i-1},X_{t_{i-1}})\right)(t_i-t_{i-1})-\int_0^T\left(f^2(t,X_t)/g^2(t,X_t)\right)dt\right|^2\\
&\leq C\frac{T^3}{n^2},
\end{aligned}
\tag{3.35}
$$

where $\mathcal{A}$ denotes $\int_0^T(f^2(t,X_t)/g^2(t,X_t))dt$.

The proof is now complete. □

Remark 3.6. Up to present, the rate of the convergence of the approximate log-likelihood functions and the error bound in probability between the AMLE and the continuous MLE have been obtained for the nonlinear nonhomogenous stochastic system with unknown parameter. As well, the corresponding results gained in [9, 27] are the direct conclusions after applying Chebyshev's inequality on (3.32).

4. Conclusions

In this paper, we have investigated the error bound in probability between the ALME and the continuous MLE for a class of general nonlinear nonhomogenous stochastic system with unknown parameter. The rates of convergence of the approximations for Itô and ordinary integral have been derived under some regular assumptions. On the basis of these analysis results, we have studied the in probability rate of convergence of the approximate log-likelihood function to the true continuous log-likelihood function for the nonlinear nonhomogenous stochastic system involving unknown parameter. Finally, the main result which gives the error bound in probability between the ALME and the continuous MLE has been established. It should be noted that one of the future research topics would be to investigate the asymptotic normality of the ALME for the nonlinear nonhomogenous stochastic system with unknown parameter mentioned in this paper.

Acknowledgment

This work was supported in part by the National Natural Science Foundation of China under Grant 60974030.

References

[1] M. Arato, A. N. Kolmogrorov, and Y. G. Sinai, "On parameter estimation of a complex stationary gaussian process," *Doklady of Academy of Sciences*, vol. 146, no. 4, pp. 747–750, 1962.

[2] H. Dong, Z. Wang, and H. Gao, "H_∞ fuzzy control for systems with repeated scalar nonlinearities and random packet losses," *IEEE Transactions on Fuzzy Systems*, vol. 17, no. 2, pp. 440–450, 2009.

[3] H. Dong, Z. Wang, and H. Gao, "Robust H_∞ filtering for a class of nonlinear networked systems with multiple stochastic communication delays and packet dropouts," *IEEE Transactions on Signal Processing*, vol. 58, no. 4, pp. 1957–1966, 2010.

[4] H. Dong, Z. Wang, and H. Gao, "Distributed filtering for a class of time-varying systems over sensor networks with quantizationerrors and successive packet dropouts," *IEEE Transactions on Signal Processing*, vol. 60, no. 6, pp. 3164–3173, 2012.

[5] W. B. Michael and S. C. Pedro, "Simulated likelihood estimation of diffusions with an application to exchange rate dynamics inincomplete markets," *Journal of Financial Economics*, vol. 63, no. 2, pp. 161–210, 2002.

[6] F. Konecny, "Maximum likelihood estimation of a drift parameter from a partially observed diffusion in the case of small measurement noise," *Statistics & Decisions*, vol. 8, no. 2, pp. 115–130, 1990.

[7] B. L. S. Prakasa Rao, "On Bayes estimation for diffusion fields," in *Statistics: Applications and New Directions, Proceedings of the ISI Golden Jubilee Conferences*, J. K. Ghosh and J. Roy, Eds., pp. 504–511, Indian Statistical Institute, Calcutta, India, 1981.

[8] P. J. Huber, "Robust estimation of a location parameter," *Annals of Mathematical Statistics*, vol. 35, pp. 73–101, 1964.

[9] J. P. N. Bishwal, *Prameter Estimation in Stochastic Differential Equations*, vol. 1923 of *Lecture Notes in Mathematics*, Springer, Berlin, Germany, 2008.

[10] V. Genon-Catalot, "Maximum contrast estimation for diffusion processes from discrete observations," *Statistics*, vol. 21, no. 1, pp. 99–116, 1990.

[11] J. Hu, Z. Wang, H. Gao, and L. K. Stergioulas, "Robust H_∞ sliding mode control for discrete time-delay systems with stochastic nonlinearities," *Journal of the Franklin Institute*, vol. 349, no. 4, pp. 1459–1479, 2012.

[12] J. Hu, Z. Wang, H. Gao, and L. K. Stergioulas, "Probability-guaranteed H_∞ finite-horizon filtering for a class of nonlinear timevaryingsystems with sensor saturation," *System and Control Letters*, vol. 61, no. 4, pp. 477–484, 2012.

[13] J. Hu, Z. Wang, G. Niu, and L. K. Stergioulas, "H_∞ sliding mode observer design for a class of nonlinear discrete time-delaysystems: a delay-fractioningapproach," *International Journal of Robust and Nonlinear Control*. In press.

[14] V. Lánská, "Minimum contrast estimation in diffusion processes," *Journal of Applied Probability*, vol. 16, no. 1, pp. 65–75, 1979.

[15] L. Birgé and P. Massart, "Rates of convergence for minimum contrast estimators," *Probability Theory and Related Fields*, vol. 97, no. 1-2, pp. 113–150, 1993.

[16] B. Shen, Z. Wang, H. Shu, and G. Wei, "On nonlinear H_∞ filtering for discrete-time stochastic systems with missing measurements," *IEEE Transactions on Automatic Control*, vol. 53, no. 9, pp. 2170–2180, 2008.

[17] B. Shen, Z. Wang, Y. S. Hung, and G. Chesi, "Distributed H_∞ filtering for polynomial nonlinear stochastic systems in sensor networks," *IEEE Transactions on Industrial Electronics*, vol. 58, no. 5, pp. 1971–1979, 2011.

[18] B. Shen, Z. Wang, and X. Liu, "A stochastic sampled-data approach to distributed H_∞ filtering in sensor networks," *IEEE Transactions on Circuits and Systems I*, vol. 58, no. 9, pp. 2237–2246, 2011.

[19] V. Harison, "The Bernstein-von Mises theorem for a certain class of Gaussion diffusion processes," Publications du Service deMathematiques, Umiversite d'Antananarivo, vol. 6, pp. 1–7, 1992.

[20] D. Levanony, A. Shwartz, and O. Zeitouni, "Recursive identification in continuous-time stochastic processes," *Stochastic Processes and Their Applications*, vol. 49, no. 2, pp. 245–275, 1994.

[21] Ju. A. Kutojanc, "Estimation of a parameter of a diffusion type process," *Akademiya Nauk SSSR. Teoriya Veroyatnosteĭ i ee Primeneniya*, vol. 23, no. 3, pp. 665–672, 1978.

[22] V. Borkar and A. Bagchi, "Parameter estimation in continuous-time stochastic processes," *Stochastics*, vol. 8, no. 3, pp. 193–212, 1982.

[23] J. Hu, Z. Wang, and H. Gao, "A delay fractioning approach to robust sliding mode control for discrete-time stochastic systems with randomly occurring non-linearities," *IMA Journal of Mathematical Control and Information*, vol. 28, no. 3, pp. 345–363, 2011.

[24] J. Hu, Z. Wang, H. Gao, and L. K. Stergioulas, "Robust sliding mode control for discrete stochastic systems with mixed timedelays, randomly occurring uncertainties and randomly occurring nonlinearities," *IEEE Transactions on Industrial Electronics*, vol. 59, no. 7, pp. 3008–3015, 2012.

[25] D. Dacunha-Castelle and D. Florens-Zmirou, "Estimation of the coefficients of a diffusion from discrete observations," *Stochastics*, vol. 19, no. 4, pp. 263–284, 1986.

[26] B. L. S. Prakasa Rao, *Statistical Inference for Diffusion Type Processes*, vol. 8 of *Kendall's Library of Statistics*, Edward Arnold, Oxford University Press, London, UK, 1999.

[27] A. Le Breton, "On continuous and discrete sampling for parameter estimation in diffusion type processes," *Mathematical Programming Study*, vol. 5, pp. 124–144, 1976.

[28] A. R. Pedersen, "Consistency and asymptotic normality of an approximate maximum likelihood estimator for discretely observed diffusion processes," *Bernoulli*, vol. 1, no. 3, pp. 257–279, 1995.
[29] Y. Ait-Sahalia, "Maximum likelihood estimation of discretely sampled diffusions: a closed-form approximation approach," *Econometrica*, vol. 70, no. 1, pp. 223–262, 2002.
[30] X. Mao, *Stochastic Differential Equations and Their Applications*, Horwood Publishing Series in Mathematics & Applications, Horwood Publishing, Chichester, UK, 1997.
[31] I. I. Gikham and A. V. Skorohod, *Stochastic Differential Equations*, Springer, Berlin, Germany, 1972.

Hindawi Publishing Corporation
Mathematical Problems in Engineering
Volume 2012, Article ID 768212, 22 pages
doi:10.1155/2012/768212

Research Article

Linear Matrix Inequalities in Multirate Control over Networks

Ángel Cuenca, Ricardo Pizá, Julián Salt, and Antonio Sala

Departamento de Ingeniería de Sistemas y Automática, Instituto Universitario de Automática e Informática Industrial, Universitat Politecnica de Valencia, Camino de Vera, s/n, 46022 Valencia, Spain

Correspondence should be addressed to Ángel Cuenca, acuenca@isa.upv.es

Received 4 June 2012; Revised 19 July 2012; Accepted 23 July 2012

Academic Editor: Bo Shen

This paper faces two of the main drawbacks in networked control systems: bandwidth constraints and timevarying delays. The bandwidth limitations are solved by using multirate control techniques. The resultant multirate controller must ensure closed-loop stability in the presence of time-varying delays. Some stability conditions and a state feedback controller design are formulated in terms of linear matrix inequalities. The theoretical proposal is validated in two different experimental environments: a crane-based test-bed over Ethernet, and a maglev based platform over Profibus.

1. Introduction

Networked control systems (NCSs) [1, 2] are becoming a powerful research area because of introducing considerable advantages [3] (wiring reduction, easier and cheaper maintenance, cost optimization) in several kinds of control applications (teleoperation, supervisory control, avionics, chemical plants, etc). Nevertheless, as a consequence of sharing the same communication medium among different devices (sensor, actuator, controller), some problems such as time-varying delays [4–6], bandwidth limitations [7, 8], packet dropouts [9–13], packet disorder [14], and lack of synchronization [15] can arise in this kind of systems. So, the analysis and design of NCS is a complex problem and, usually, some simplifying assumptions are made.

In this work, neither packet dropouts nor packet disorder will be considered (as later detailed). In addition, devices will be assumed to be synchronized (by means of a suitable initial synchronization procedure or by implementing time-stamping techniques). Thus, only

bandwidth limitations and time-varying delays will be faced. To solve these issues, some previous authors' developments such as those in [4, 16–19] are revised and conveniently adapted and gathered together in the present work.

Regarding bandwidth constraints, this could be the case if the network configuration imposes a limitation in the control frequency (say, because of an excessive number of devices sharing the communication link). In this context, the consideration of a dual-rate controller [20–22] might be useful in terms of achievable performance [23, 24], since the controller can work at a faster rate than the network one which provides the measurements (a multirate input control (MRIC) structure will be considered, which is able to generate N control actions for each sampled output).

As time-varying delays are assumed in an NCS, the control problem becomes a linear time-varying (LTV) one. Then, stability and design for arbitrary time-varying network delays must be carried out. Depending on what kind of information about the delay is provided, different stability analysis can be performed. So, if the probability density function of the network delay is unknown, a robust stability analysis must be proved. However, if the probability function is provided, stochastic stability can be analyzed. In this work, in order to prove any of these situations in a dual-rate NCS, linear matrix inequalities (LMIs) [25] will be considered. So, both LMIs for the robust case and for the probabilistic one (with extension to a multiobjective analysis) will be formulated. With respect to design approaches, a state feedback controller enunciated in terms of LMIs will be presented. The reader is referred, for example, to [6, 13] to find other LMI-based state feedback controller approaches. As well in terms of LMIs, in [11, 12] $\mathscr{H}_\infty$ controllers are enunciated, and in [21] a multirate controller is proposed.

As a summary, the main novelties introduced by this work can be lumped as the followoing.

(i) NCS analysis improvements: in [4, 16] control system stability is studied via LMIs. In the former work, a robust analysis is treated, whereas in the latter work, a stochastic analysis is presented. Both works use as a controller an output feedback one. In the present work, notation used in both approaches is unified and extended to the state feedback controller case. In addition, a hierarchical structure for the controller is contemplated.

(ii) NCS design improvements: firstly, in [19], a multirate controller design procedure is introduced by splitting the controller into two sides—the slow-rate side and the fast-rate side. No shared communication medium is considered between both sides. Now, in the present work, from the previous idea a distributed controller for the proposed multirate NCS can be implemented (details in Section 2). Secondly, in [18], a single-rate state feedback controller to deal with time-varying delays is proposed. Now, this controller is adapted to be included in the slow-rate side of the multirate NCS. In addition, in order to reach a null steady-state error, an integral action can be added to this controller. The obtained results show a better control system performance than that achieved in [17].

The paper is divided into five parts: in Section 2 the dual-rate NCS scenario is exposed. Closed-loop realizations from lifted plant and controller are formulated in Section 3. By means of LMIs, for this kind of LTV systems, Section 4 proposes several stability analysis, and Section 5 introduces a state feedback controller. Finally, Section 6 presents stability and design results obtained for the test-bed platforms, and Section 7 enumerates the main conclusions.

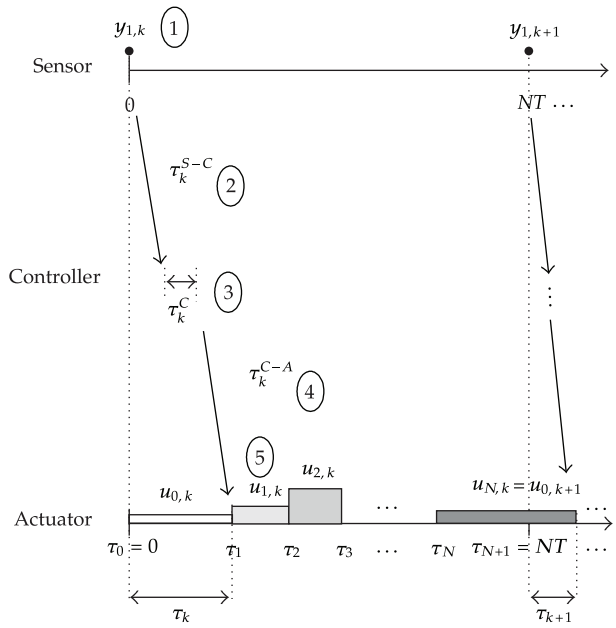

Figure 1: Chronogram of the proposed NCS.

2. Problem Scenario

Depending on the network configuration, three main options arise when integrating a dual-rate controller in an NCS.

(i) The dual-rate controller is located at a remote side (with no direct link to the plant), and its fast-rate control actions can be sent from this side to the local actuator (directly connected to the plant) following a packet-based approach [26].

(ii) The dual-rate controller is located at the local side, being directly connected to the actuator [16].

(iii) The dual-rate controller is split into two subcontrollers [19] (a slow-rate one located at the remote side, and a fast-rate one situated at the local side); then a rude slow-rate control action is sent from the remote side to the local one in order to be refined and converted to a fast-rate control signal by the local subcontroller [4].

From the last option, Figure 1 represents a typical chronogram for this kind of dual-rate NCS. Both time-driven and event-driven policies are required [27]. The meaning of the encircled numbers is now detailed.

(1) The sensor works in a time-triggered operation mode, sampling the process output $y_{1,k}$ at period NT (the measurement period). The output is sent through the network.

(2) After a certain processing and propagation time has elapsed τ_k^{S-C}, the remote controller receives the packet.

(3) Then, at the remote controller an event is triggered. As a consequence, after a computation delay τ_k^C, a slow-rate control action is generated and sent to the local controller, which is directly connected to the actuator.

(4) After a certain processing and propagation time has elapsed τ_k^{C-A}, the local controller receives the packet.

(5) Then, at the local side an event is triggered. Its main consequence is the application of N faster-rate control actions to the process. Such actions are scheduled to be applied taking into account the total delay:

$$\tau_k = \tau_k^{S-C} + \tau_k^{C} + \tau_k^{C-A}, \tag{2.1}$$

where, in this work, $\tau_k \in [0, \tau_{\max}]$, being $\tau_{\max} < NT$ in order to avoid causality and packet order issues, and no sample losses. Note that the lumped delay in (2.1) can be adopted if the controller is a static one. In addition, if the total delay τ_k can be measured and finally compensated at the local side (as assumed in this work), (2.1) can also be considered in the control strategy. In any other case, it is inappropriate or impossible to lump all delays as one. Please, see for example in [28, 29] on how to deal with delays on different communication links separately.

Regarding the N control actions, the first of them will be applied at the time of arrival of the packet (τ_k time units after the measurement was taken). The remaining control actions, as they are not influenced by the network delay, will be applied every T time units (the control period), triggered by a fast-rate clock signal. Note, if the delay fulfills

$$\tau_k \geq dT, \quad d \in \mathbf{N}^+, \tag{2.2}$$

the first d control actions will never be applied to the process.

3. Preliminaries and Notation

Consider a continuous linear time-invariant plant P, which admits a state-space realisation $\Sigma_c = (A_c, B_c, C, D)$, with suitable dimensions, fulfilling the followig:

$$\begin{aligned} \dot{x} &= A_c x + B_c u, \\ y &= Cx + Du. \end{aligned} \tag{3.1}$$

Being an arbitrary number, ξ is denoted as

$$B(\xi) = \begin{cases} \displaystyle\int_0^{\xi} e^{A_c \gamma} B_c d\gamma, & \xi > 0 \\ 0, & \xi \leq 0. \end{cases} \tag{3.2}$$

It is well known [30, 31] that, in the case the input changes every T time units, being constant in the intersample period (zero-order hold, ZOH) and the output is sampled synchronously to that input, the sampled output verifies the discrete-time equations:

$$\begin{aligned} x_{k+1} &= e^{A_c T} x_k + B(T) u_k \\ y_k &= C x_k + D u_k. \end{aligned} \tag{3.3}$$

When the input change and output sampling do not follow such a conventional sampling pattern, but they follow an arbitrary but periodic one with period NT, the discretization is a periodic linear time-varying discrete system. However, the process can be equivalently represented by a multivariable linear time-invariant discrete system with period NT and the so-called "lifted" input and output vectors, which are formed by stacking all the input and output signals; this methodology is denoted as "lifting" [32].

3.1. Lifted Plant Realization

Consider the above system (3.1) (as most physical system have $D = 0$, it will be assumed on the sequel) being subject to inputs u_i at time τ_i, $i = 0, \ldots, N$ under ZOH conditions (i.e., input at time τ_i is held constant until time reaches τ_{i+1}), and $\tau_0 = 0$, $\tau_{N+1} = NT$ (see Figure 1). It is easy to show [31, 33] that the state at an arbitrary time t is given by:

$$x(t) = e^{A_c t} x(0) + \sum_{i=0}^{N} B(\min(t, \tau_{i+1}) - \tau_i) e^{A_c (t - \min(t, \tau_{i+1}))} u_i, \tag{3.4}$$

and, from the above formula, a lifted realization can be computed when inputs are applied at times τ_i and outputs are read at times η_j, $j = 1, \ldots, m$ inside a metaperiod NT. Indeed, the discrete state equations comes from replacing $t = NT$ in (3.4), and the output equation comes from replacing $t = \eta_j$ in (3.4) and multiplying by C. In the following, as the above equations will be evaluated every NT seconds, notation $u_{i,k}$ will describe the input at time $kNT + \tau_i$, and similarly, $y_{j,k}$ will denote the sample at time $kNT + \eta_j$.

In a networked control framework, since $u_{0,k}$ is the last controller output from the previous sampling period (the controller will be assumed to apply (with delay τ_1) a set of N control actions $(u_{1,k}, \ldots, u_{N,k})$ (see Figure 1), an additional set of states φ must be added [18, 34]. So, incorporating the "memory" equation $\varphi_{k+1} = u_{N,k}$, and replacing $u_{0,k}$ by φ_k, (3.4) yields the following:

$$\begin{aligned} x(kNT + t) = {} & e^{A_c t} x_k + B(\min(t, \tau_0)) e^{A_c (t - \min(t, \tau_0))} \varphi_k \\ & + \sum_{i=1}^{N} B(\min(t, \tau_{i+1}) - \tau_i) e^{A_c (t - \min(t, \tau_{i+1}))} u_{i,k}. \end{aligned} \tag{3.5}$$

The output equations would be built by stacking for all needed η_j the following expression:

$$\begin{aligned} y_{j,k} &= Ce^{A_c\eta_j}x_k + CB\left(\min\left(\eta_j,\tau_0\right)\right)e^{A_c(\eta_j-\min(\eta_j,\tau_0))}\varphi_k \\ &\quad + \sum_{i=1}^{N} CB\left(\min\left(\eta_j,\tau_{i+1}\right)-\tau_i\right)e^{A_c(\eta_j-\min(\eta_j,\tau_{i+1}))}u_{i,k}. \end{aligned} \tag{3.6}$$

As described, an MRIC strategy is considered in this work, and hence only the first sampled output $y_{1,k}$ is needed to be sent to the controller. Then, for the sake of simplicity, let us describe the lifted plant model $\Sigma_P = (A_P, B_P, C_P, D_P)$ in this way:

$$\begin{aligned} \tilde{x}_{k+1} &= A_P\tilde{x}_k + B_P\overline{U}_k, \\ \overline{Y}_k &= C_P\tilde{x}_k + D_P\overline{U}_k, \end{aligned} \tag{3.7}$$

where $\tilde{x}_k = (x_k, \varphi_k)^T$, $\overline{U}_k = (u_{1,k}, \ldots, u_{N,k})^T$, $\overline{Y}_k \equiv y_{1,k}$, and

$$A_P = \begin{pmatrix} e^{A_cNT} & B_0^* \\ 0 & 0 \end{pmatrix}, \qquad B_P = \begin{pmatrix} B_1^* & \cdots & B_N^* \\ 0 & \cdots & 1 \end{pmatrix} \tag{3.8}$$

$$C_P = \begin{pmatrix} C & 0 \end{pmatrix}, \qquad D_P = \begin{pmatrix} 0 & \cdots & 0 \end{pmatrix}, \tag{3.9}$$

being $B_i^* = B(\tau_{i+1} - \tau_i)e^{A_c(NT-\tau_{i+1})}$. Standard complete C_P and D_P matrices can be reviewed, for instance, in [32].

3.2. Controller and Closed-Loop Realization

In this paper, two different structures for the controller will be taken into account: a one-degree-of-freedom linear regulator R, and a hierarchical controller H.

For the first case, the regulator R, two alternative cases can be treated as follows:

(i) an output feedback regulator, whose lifted discrete realization will be $\Sigma_R = (A_R, B_R, C_R, D_R)$ [32]:

$$\begin{aligned} \zeta_{k+1} &= A_R\zeta_k - B_R\overline{Y}_k, \\ \overline{U}_k &= C_R\zeta_k - D_R\overline{Y}_k, \end{aligned} \tag{3.10}$$

where set-points are considered to be zero, so $-y = e$ (being e the loop error),

(ii) a state feedback regulator, with a gain F:

$$\overline{U}_k = -F\tilde{x}_k. \tag{3.11}$$

From the previous plant representation $\Sigma_P = (A_P, B_P, C_P, D_P)$, its closed-loop connection to the output feedback regulator implies a dynamical system governed by this expression [31]:

$$\begin{pmatrix} \zeta_{k+1} \\ \tilde{x}_{k+1} \end{pmatrix} = \begin{pmatrix} A_R & -B_R C_P \\ B_P C_R & A_P - B_P D_R C_P \end{pmatrix} \begin{pmatrix} \zeta_k \\ \tilde{x}_k \end{pmatrix} = \overline{A}_{cl} \overline{x}_k. \tag{3.12}$$

For the state feedback regulator, the closed-loop realization will yield the following [31]:

$$\tilde{x}_{k+1} = (A_P - B_P F)\tilde{x}_k = \tilde{A}_{cl}\tilde{x}_k. \tag{3.13}$$

Regarding the second regulator, the hierarchical one H, it will be decomposed into two parts at different rates (remember Section 2). Different alternatives could be used to design each part. For brevity, let us consider and formulate the option developed in the second example of Section 6, where

(i) fast-rate local subcontrollers are designed by means of robust $\mathcal{H}_\infty$ control techniques [42],

(ii) a coordinating, slow-rate remote subcontroller is designed using a state feedback approach (to be detailed in Section 5).

Then, the representation of each local subcontroller will be similar to (3.10). And, the remote subcontroller will yield an expression like in (3.11) but with these variations:

$$U_{sr,k} = -F^* \overline{x}_k, \tag{3.14}$$

where $U_{sr,k}$ is the slow-rate control action, and F^* is the resultant controller gain when considering the augmented state $\overline{x}$, which includes the overall local side state (controller + plant, remember (3.12)).

Let us denote the lifted expression $\Sigma^* = (A^*, B^*, C^*, D^*)$, where, respectively, A^*, B^*, C^*, D^* are obtained like A_P, B_P, C_P, D_P in (3.8), but now considering the overall local side state $\overline{x}$ (details omitted for brevity). Then, the closed-loop realization for the hierarchical control structure will be similar to (3.13), but now

$$\overline{x}_{k+1} = (A^* - B^* F^*)\overline{x}_k = A^*_{cl}\overline{x}_k. \tag{3.15}$$

4. Stability Analysis

As commented, time-varying delays can appear in an NCS framework. Thus, a variation in the instants where the outputs are measured (η_j) or those in which the input commands are presented to the plant (τ_i) is expected. Let us denote the set of parameters that might vary from metaperiod to metaperiod as $\rho_k = \{\eta_{1,k}, \eta_{2,k}, \ldots, \tau_{1,k}, \tau_{2,k}, \ldots\}$. Since matrices in (3.7) depend on ρ_k, then $\Sigma_P = (A_P, B_P, C_P, D_P)$, or $\Sigma^* = (A^*, B^*, C^*, D^*)$, can vary from metaperiod to metaperiod. Further time variance occurs if the controller is also intentionally dependent on all or some of the parameters included in ρ_k; this is the case, for example, in

a gain-scheduling approach [16, 35]. Subsequently, the closed-loop realization $\overline{A}_{cl}$, $\widetilde{A}_{cl}$, A^*_{cl} does depend on the above parameters, and then it will be replaced by $\overline{A}_{cl}(\rho_k)$ in (3.12), by $\widetilde{A}_{cl}(\rho_k)$ in (3.13), and by $A^*_{cl}(\rho_k)$ in (3.15), representing a discrete LTV system. For the sake of simplicity, only one of the closed-loop realizations ($\overline{A}_{cl}$) will be considered on the sequel. In addition, in this work the actual time-varying parameter ρ_k used will be the network delay τ_k, that is, the delay of the first control action $\rho_k = \{\tau_{1,k}\} \equiv \{\tau_k\}$.

Three different scenarios will be studied as follows.

(i) Consideration of arbitrary delay changes with unknown probability: a robust stability analysis will be needed.

(ii) A probability density function of the network delay for each network situation is assumed known: a stochastic stability analysis can be independently carried out for each situation.

(iii) Several network states are considered, which are defined by different probability density functions and different performance objectives: a multiobjective analysis will be developed.

4.1. Robust Analysis

In order to prove robust stability of the discrete LTV system:

$$\overline{x}_{k+1} = \overline{A}_{cl}(\tau_k)\overline{x}_k, \tag{4.1}$$

with a geometric decay rate (the geometric decay rate is a performance measure for nonlinear and LTV systems which guarantees that there exists $\lambda \in \mathbb{R}$ so $\|\overline{x}_k\| \leq \lambda\|\overline{x}_0\|\alpha^k$. When particularized to a discrete linear time-invariant system, the decay rate is the modulus of the dominant pole), $0 \leq \alpha \leq 1$, a common Lyapunov function

$$V(\overline{x}) = \overline{x}^T Q\overline{x}, \quad Q > 0, \tag{4.2}$$

must be found [18, 25, 36] so that $V(\overline{x}_{k+1}) < \alpha^2 V(\overline{x}_k)$ (obviously, $\alpha < 1$ implies stability, given by the decrescence condition $V(\overline{x}_{k+1}) < V(\overline{x}_k)$). Replacing the closed-loop equations in (4.2), the Lyapunov decrescence condition can be written as the following LMI:

$$\overline{A}_{cl}(\vartheta)^T Q\overline{A}_{cl}(\vartheta) - \alpha^2 Q < 0 \quad \forall\vartheta \in \Theta, \tag{4.3}$$

where ϑ is a dummy parameter ranging in a set Θ, where the time-varying parameters τ_k are assumed to take values in, and matrix Q is composed of decision variables to be found by the semidefinite programming solver. In this work, Θ will be an interval $[0, \tau_{\max}]$ (as defined in (2.1)).

If $\overline{A}_{cl}$ is an affine function of τ_k and Θ is polytopic, then (4.3) can be checked with a finite number of LMIs. Otherwise, for bounded Θ a dense enough gridding must be set up in order to approximately check for the above conditions. This procedure is denoted as LMI gridding [18, 36].

4.2. Probabilistic Analysis

Now, a probabilistic model of the network delay τ_k will be considered, so a probability density function $p(\tau_k)$ is assumed known.

As the network delay is supposed to vary in a random way, stability of the closed-loop system will be analyzed in the mean square sense [37] (a particular case of the Martingales convergence theorem [38]), by means of the quadratic Lyapunov function (4.2), which will be shown to decrease in average. So, denoting $E[\cdot]$ as the statistical expectation, $E[V(\overline{x}_k)]$ will tend to zero, and hence the state will converge to zero with probability one. The average descent to prove will be expressed as

$$E[V(\overline{x}_{k+1})] \leq E[V(\overline{x}_k)], \tag{4.4}$$

or, considering an average decay rate $0 < \alpha < 1$, the descent expression yields

$$E[V(\overline{x}_{k+1})] \leq \alpha^2 E[V(\overline{x}_k)]. \tag{4.5}$$

Replacing the closed-loop equations in (4.2), the Lyapunov decrescence condition (4.5) can be written as the following probabilistic LMI:

$$\int p(\vartheta)\left(\overline{A}_{cl}(\vartheta)^T Q \overline{A}_{cl}(\vartheta) - \alpha^2 Q\right) d\vartheta < 0, \tag{4.6}$$

where ϑ, Θ, and Q were defined after (4.3).

For a generic probability distribution, working with the above integral may be cumbersome. For bounded Θ, a dense enough gridding in ϑ must be set up in order to approximately check for the above conditions. This procedure extends the LMI gridding in [18, 36] to a probabilistic case. Choosing a set of l equally spaced values ϑ_j, $j = 1, \ldots, l$ so that $\vartheta_1 = 0$, $\vartheta_l = \tau_{\max}$ (Θ is an interval $[0, \tau_{\max}]$), (4.6) can be approximately rewritten as

$$\sum_{j=1}^{l} p(\vartheta_j)\overline{A}_{cl}(\vartheta_j)^T Q \overline{A}_{cl}(\vartheta_j) - \alpha^2 Q < 0, \tag{4.7}$$

which is a standard LMI to be solved by widely known methods [25, 39].

Note that the above results are more relaxed than those in the robust case. Indeed, in a probabilistic case there is only one LMI constraint (average decay) instead of one for each possible sampling period. In this way, temporal random increases of the Lyapunov function are tolerated as long as the average over time is decreasing. Hence, better results in stability analysis can be obtained; however, the gridding approach leaves intermediate points out of the analysis so, in rigor, the results are not valid unless the grid is very fine.

4.3. Multiobjective Analysis

The above idea can be extended to considering several possible network states, say n_o, with different performance objectives. Each network state will be described by a probability

density of the network delay $p_i(\tau_k)$, and a performance objective α_i, $i = 1, \ldots, n_o$. For example, two objectives can be considered: the first one can be defined by the probability function for an unloaded network (with a probability distribution around a "short" delay mean), and the other objective for a saturated network case (with a larger delay mean).

Then, the Lyapunov decrescence conditions can be written as the following probabilistic LMI (expressed, for computation, in its discrete approximation):

$$\sum_{j=1}^{l} p_i(\vartheta_j)\overline{A}_{cl}(\vartheta_j)^T Q \overline{A}_{cl}(\vartheta_j) - \alpha_i^2 Q < 0. \tag{4.8}$$

It is well known that the optimal result of multiobjective analysis will be a Pareto front with the optimal performance α_i' for a particular i', being the rest fixed. If the performance bounds on the rest of constraints are made more restrictive, the resulting $\alpha_{i'}$ decreases. The reader is referred to [40] for basic ideas on multiobjective optimization.

Note that the use of the shared Lyapunov function in (4.8) proves stability of the networked control system for any probabilistic mixture of the considered network states (i.e., a network state whose probability density can be expressed as a convex combination of those in LMIs (4.8)).

5. State Feedback Controller Design

Apart from stability and decay rate, well-known LMI conditions can be set up for pole region placement, $\mathcal{H}_\infty$ and $\mathcal{H}_2$ norms, and so forth. The reader is referred to [25, 41] for details. In this section, a state feedback synthesis approach will be presented. The resultant controller can be used as a slow-rate subcontroller in a dual-rate framework.

As previously shown, from a lifted model $\Sigma^* = (A^*, B^*, C^*, D^*)$, the control synthesis problem can be cast as a state-feedback one (3.14). But, as a consequence of time-varying network-induced delays, a different F^* must be designed for each possible delay value τ_k (leading to, e.g., gain scheduling approaches [16, 35]). Another possibility is to achieve a unique stabilizing controller F^* subject to any possible time-varying delay. In this case, an LMI gridding procedure can be considered. So, from [18], if there exist matrices X and M so that

$$\begin{bmatrix} e^{-2\beta NT}X & XA^{*T} - M^T B^{*T} \\ A^*X - B^*M & X \end{bmatrix} > 0 \tag{5.1}$$

is verified for any τ_k, the feedback controller $F^* = MX^{-1}$ stabilizes $\Sigma^* = (A^*, B^*, C^*, D^*)$ with decay rate β (which is the continuous-time equivalent exponential decay rate, that is, $\alpha = e^{-\beta NT}$), and $V(\overline{x}_k) = \overline{x}_k^T X^{-1} \overline{x}_k$ is the associated Lyapunov function.

Due to the existence of time-varying delays, the lifted state $\overline{x}_k$ could not be known when updating the control gain F^*. This problem can be solved by adding any kind of state observer to the control strategy, for example, a nonstationary Kalman filter [18].

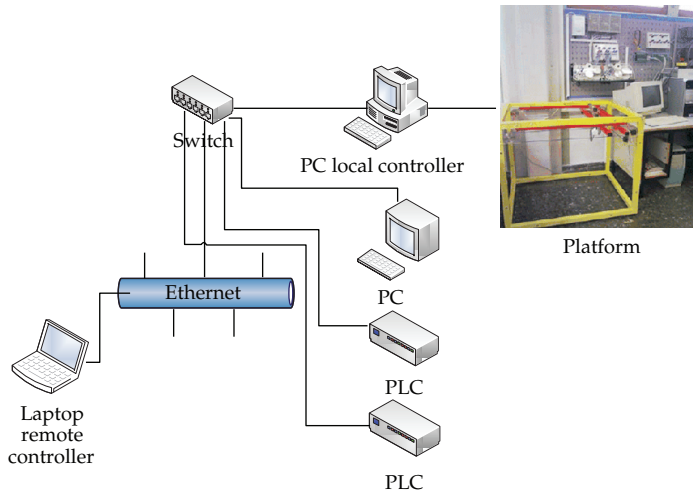

Figure 2: Test-bed Ethernet environment.

6. Experimental Results

6.1. A Crane-Based Platform over Ethernet: A Stability Analysis Example

In this section, a test-bed Ethernet environment is used to implement a dual-rate NCS, where the controller will be split into two parts. The proposed NCS includes the following devices (see Figure 2):

(i) an industrial crane platform (to be controlled) equipped with three cc motors (to actuate each axis: x, y, z) and five encoders (to sense the three axis and two different angles). The motors are controlled by an analog signal in the range ± 1 V. The encoders provide a position measurement of 1 V/m. In this application only the X-axis is actuated and sensed, whose behavior is modeled by

$$p(s) = \frac{6.3}{s(s+17.7)}. \tag{6.1}$$

Details on the crane characteristics can be obtained at http://www.inteco.com.pl (3D crane apparatus).

(ii) A local computer which is connected to the platform by means of a DAQ board, and where the local subcontroller is implemented.

(iii) Two PLCs and one computer working as interference nodes in order to introduce different load scenarios.

(iv) A switch shared by the previous devices to connect them to Ethernet.

(v) A remote laptop computer where the remote subcontroller is implemented.

In this example, the controller will be a dual-rate PID one. Its parameters will be retuned according to Ethernet network delays, leading to a gain-scheduling proposal. In this case, the scheduling follows a Taylor-series-based approach (see [16] for details).

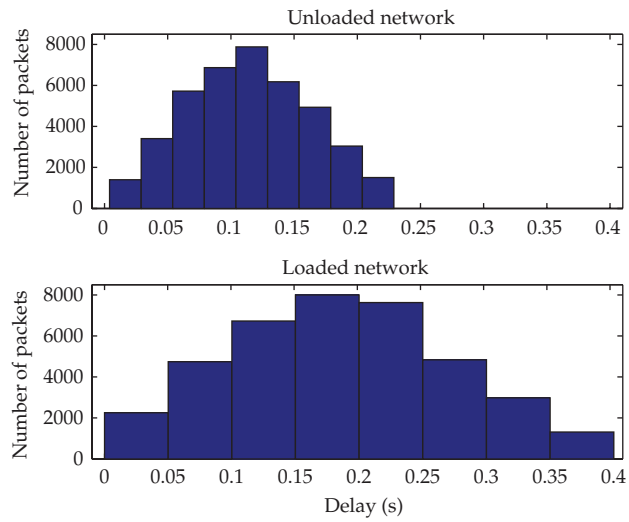

Figure 3: Experimental delay histograms.

Table 1: LMI decay rate for the dual-rate PD controller (robust stability).

Max. delay bound (in s)	Scheduled PD	Nominal PD
0.1	0.42	0.59
0.15	0.63	0.73
0.20	0.84	0.84
0.30	1	0.99

An LMI analysis will be required to observe the stability benefits of the scheduled controller compared with the nominal unscheduled one. Finally, from experimental implementation, time response for both controllers will be obtained in order to observe transient behavior.

First of all, several experiments are carried out, where the number and complexity of the tasks developed by the interference nodes is modified in order to obtain different load scenarios ranging between the two extreme histograms on Figure 3. According to this figure, the output sampling time is chosen to be $NT = 0.4\,\text{s}$, since the largest delay obtained is $0.39\,\text{s}$ (delay bound: $\tau_{\max} = 0.39\,\text{s}$), and then the requirement commented after (2.1), that is $\tau_{\max} < NT$, is fulfilled.

Since the crane model (6.1) includes an integrator, a dual-rate PD is designed in order to achieve an overshoot of 8% and a settling time of $0.65\,\text{s}$ (with no steady-state error). The resultant controller's gains are: $K_p = 6.95$, $K_i = 0$, $K_d = 2.2$, $f = 0.1$ (derivative filter).

6.1.1. Robust Stability Analysis

Let us suppose that no information about probability distribution is known. Then, the worst-case behavior of the proposed PD regulator can be assessed by means of the LMIs in (4.3). Testing different maximum delay bounds, the consequent results appear on Table 1.

As a conclusion, the proposed gain scheduled regulator improves worst-case performance for small delays (up to $0.2\,\text{s}$). In large delays, the approach used for retuning the PD

Table 2: LMI decay rate for the dual-rate PD controller (with probability information).

Network context	Scheduled PD	Nominal PD
Only unloaded	0.50	0.65
Only loaded	0.68	0.83

parameters (based on Taylor-series) loses precision and results are similar (marginally worse) than those of a nonscheduled regulator. In fact, there are delay distributions involving delays larger than 0.3 s which might render the system unstable.

6.1.2. Probabilistic Stability Analysis: Extension to the Multiobjective Case

Now, information about probability distribution provided by experimental tests is taken into account. So, stability of the setup in probabilistic time-varying delays can be assessed. The LMI gridding in (4.7) can be carried out computing the closed-loop realization for the delay bound $\tau_{\max} = 0.39$ s ($\Theta = [0, 0.39]$). According to Figure 3, the number of grid points l for the probability density approximation is taken as $l = 16$.

Two cases are analyzed as follows:

(i) firstly, considering each network situation separately (a different Lyapunov function for each load scenario), the LMI in (4.7) is applied to each situation to obtain the minimum α for which a feasible solution Q exists,

(ii) secondly, a multiobjective analysis is performed by considering a unique Lyapunov function for both network load scenarios.

The second case is more conservative but allows stability guarantees for mixtures and random switching between both scenarios. The two proposed cases are somehow extreme situations from which would happen in a practical situation. If each of the network behaviors is very likely to remain active for a dwell time significantly longer than the loop's settling time, then assumptions in case 1 will be closer to reality. If arbitrary, fast, network load changes were expected, then case 1 would be too optimistic and the analysis in case 2 would be recommended.

Regarding the first analysis, results are presented in Table 2, both for the scheduled PD and for the nominal one. In conclusion, the less the network is loaded, the better worst-case performance can be guaranteed. In addition, the scheduled approach shows better behavior than the nominal one.

Now, the second (multiobjective) study is carried out. Figure 4 shows a Pareto front that summarizes the analysis, which is developed by setting the decay-rate of one objective and optimizing the other's one. As depicted, the decay-rates obtained in the previous study for the unloaded network case (here, the first objective) can not be now achieved, despite considering the highest decay-rate for the second objective ($\alpha_2 = 0.99$), that is, the loaded network scenario. However, if $\alpha_1 = 0.99$, the previous decay-rates for the loaded network case can be achieved. Finally, the figure reveals the scheduled approach outperforms again the nominal one.

In summary, from the analysis of both Tables 1 and 2, two main conclusions arise:

(i) if the probability of large delays is low, the use of probabilistic information indicates (as intuitively expected) that the gain scheduling approach used in this example

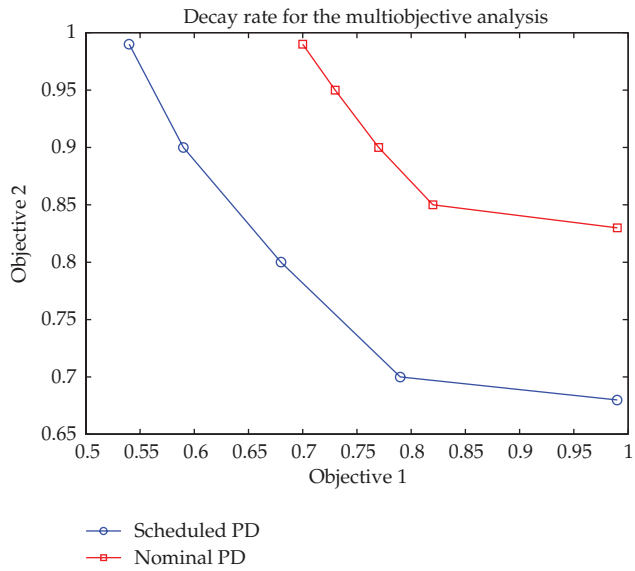

Figure 4: LMI decay-rate for the multiobjective study.

(based on Taylor-series) seems a sensible practical procedure, because of improving average performance.

(ii) if no likelihood of (transient) instability is required, then the network must be reconfigured so the maximum delay does not exceed 0.3 s, or the initial controller specifications must be changed (reducing gains to improve robustness).

6.1.3. Control System Time Response

Since the previous figures indicate only stability and decay rate, to complete the study the control system time response is obtained. So, other performance differences (such as overshoot) can be evaluated.

Figures 5 and 6 present one of the different experiments tested for each network situation. As observed in the LMI analysis, the scheduled PD controller points out a better behavior than the nominal PD controller, being a more marked trend when working in a loaded network. So, Figures 5 and 6 show that the scheduled controller reduces the overshoot at least a 10% and up to a 40%, and the settling time up to a 60%, with a 30% on the average.

6.2. A Maglev-Based Platform over Profibus: A State Feedback Design Example

In this example, the position of a triangular platform assembled by joining three maglevs is hierarchically controlled by means of a dual-rate controller over Profibus. The proposed NCS (see Figure 7) includes:

(i) a levitated platform with an equilateral triangle shape where each maglev is located at each corner. The maglevs provide position information from an infrared sensor array in ±10 V. The control signal is provided to a power amplifier, being in ±10 V.

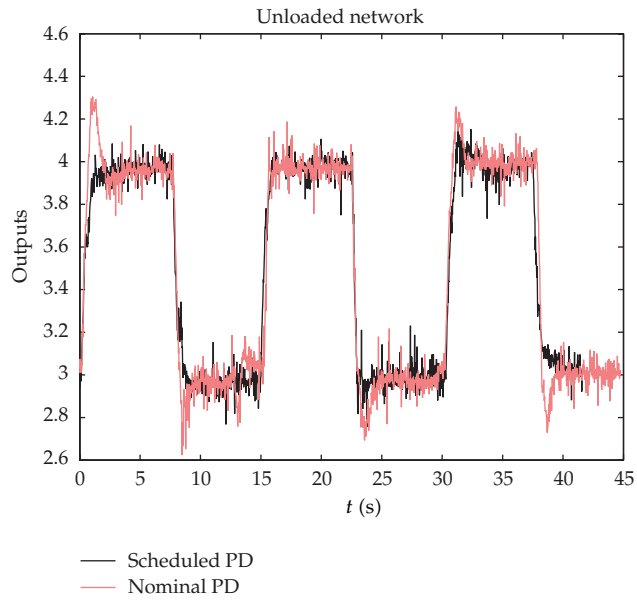

Figure 5: Experimental closed loop output (unloaded network).

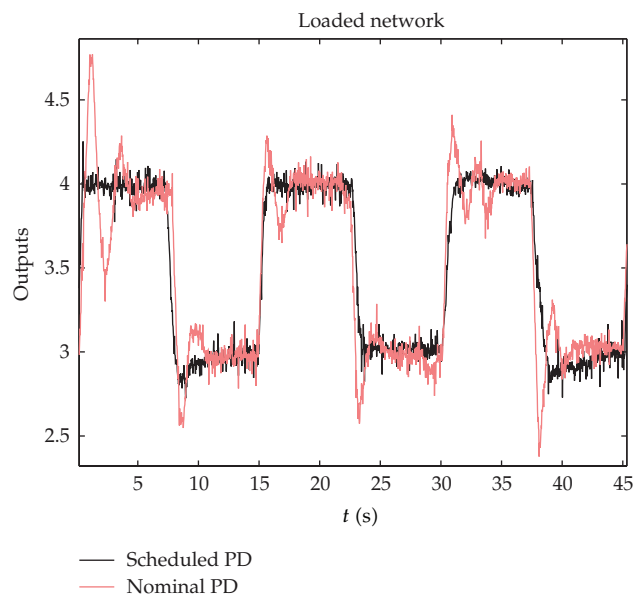

Figure 6: Experimental closed loop output (loaded network).

For more information about these levitators see http://www.xdtech.com, model ML-EA,

(ii) a National Instruments CompactRio 9074 acting as local subcontrollers,

(iii) a desktop PC acting as a remote subcontroller,

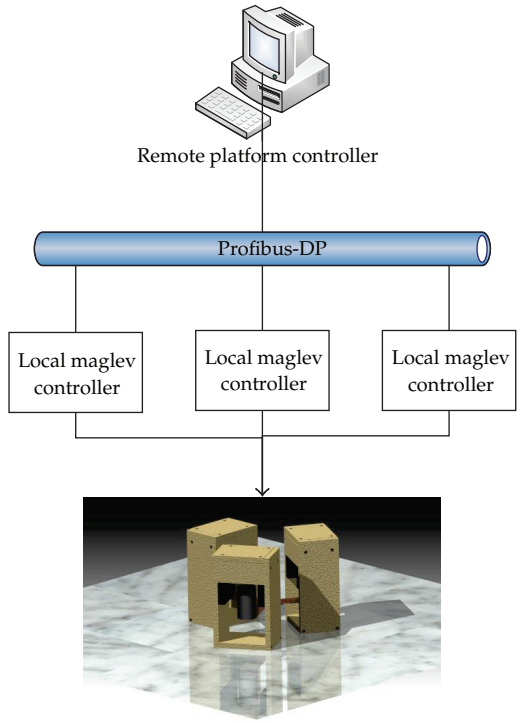

Figure 7: Hierarchical control structure.

Table 3: Experimental network round-trip time delay histogram.

Delay	5 ms	10 ms	15 ms
Occurrences	123,154	1,084,502	292,357
Percentage	8.21%	72.3%	19.49%

(iv) a Profibus-DP network configured to work with a bus rate of 187.5 kBits/s, and with asynchronous operation mode. This enables sending a remote control action every 20 ms.

In this example, a standalone, fast-rate local subcontroller is designed for each maglev by using robust $\mathcal{H}_\infty$ control techniques [42]. The coordinating, slow-rate remote subcontroller is a state feedback one, designed by using the LMI-gridding techniques presented in Section 5. So, the controller is assured to be robust in the presence of time-varying network-induced delays. Experimental time responses will validate this aspect.

After carrying out several experimental tests, network-induced time delays are measured (see histogram in Table 3). The main conclusion is that the most repeated round-trip time delay corresponds to a 10 ms period, with eventual delays at 5 ms and 15 ms. So, to design the state feedback controller, the grid of delay values to be considered will be $(5, 10, 15)$ ms, and hence (5.1) will be actually a collection of 3 LMIs. As the least delay value is 5 ms, then $T = 5$ ms. And according to the bus rate, $NT = 20$ ms, and hence $N = 4$.

Now, the linearized state space for a generic maglev i is presented as follows:

$$\begin{pmatrix} \dot{I}_i(t) \\ \dot{z}_i(t) \\ \ddot{z}_i(t) \end{pmatrix} = \begin{pmatrix} \dfrac{-R_i}{L_i} & 0 & \dfrac{-Q_i}{L_i} \\ 0 & 0 & 1 \\ \dfrac{3K_1^i}{M} & \dfrac{3K_2^i}{M} & 0 \end{pmatrix} \cdot \begin{pmatrix} I_i(t) \\ z_i(t) \\ \dot{z}_i(t) \end{pmatrix} + \begin{pmatrix} \dfrac{1}{L_i} \\ 0 \\ 0 \end{pmatrix} \cdot v_i(t),$$
$$y_i(t) = \begin{pmatrix} 0 & K_3^i & 0 \end{pmatrix} \cdot \begin{pmatrix} I_i(t) \\ z_i(t) \\ \dot{z}_i(t) \end{pmatrix}, \tag{6.2}$$

where I_i is intensity on levitator's electromagnetic circuit, z_i is the system output (i.e., a measure of airgap between levitated load and magnet taken with infrared sensors), R_i, L_i are resistance and inductance of the electromagnetic circuit for levitator i, M is mass of the levitated body, and K_1^i, K_2^i, K_3^i, Q_i are constants of the magnetic levitator i.

From this representation, and using the robust control toolbox in Matlab, a fast-rate, local $\mathscr{H}_\infty$ subcontroller for each single maglev is designed ($T = 5\,\text{ms}$). All the controllers are very similar, and hence one of them is now presented as follows:

$$G_R(z) = \frac{u(z)}{e(z)} = \frac{10.845(z+1)(z-0.878)(z-0.641)}{(z+0.93)\left((z-0.54)^2 + 0.27^2\right)}. \tag{6.3}$$

If the coupled global platform model is obtained (details omitted for brevity; more information in [17]), the slow-rate, remote state feedback subcontroller will be designed. First, denoting the state, input, and output vectors as

$$x = \begin{pmatrix} I_1 \\ I_2 \\ I_3 \\ z \\ \dot{z} \\ \alpha \\ \dot{\alpha} \\ \gamma \\ \dot{\gamma} \end{pmatrix}, \qquad u = \begin{pmatrix} v_1 \\ v_2 \\ v_3 \end{pmatrix}, \qquad y = \begin{pmatrix} K_3^1 z_1 \\ K_3^2 z_2 \\ K_3^3 z_3 \end{pmatrix}, \tag{6.4}$$

where α, γ are angles of rotation of the levitated platform around X- and Y-axes, respectively, and being $v_i = L_i \dot{I}_i + Q_i \dot{z}_i + R_i I_i$. Then, the linearized state space for the coupled platform yields

$$\begin{aligned} \dot{x} &= Ax + Bu, \\ y &= Cx, \end{aligned} \tag{6.5}$$

where

$$A = \begin{pmatrix} A_{11} & A_{12} \\ A_{21} & A_{22} \end{pmatrix},$$

$$A_{11} = \begin{pmatrix} -\frac{R_1}{L_1} & 0 & 0 & 0 \\ 0 & -\frac{R_2}{L_2} & 0 & 0 \\ 0 & 0 & -\frac{R_3}{L_3} & 0 \\ 0 & 0 & 0 & 0 \end{pmatrix},$$

$$A_{21} = \begin{pmatrix} \frac{K_1^1}{M} & \frac{K_1^2}{M} & \frac{K_1^3}{M} & 0 \\ 0 & 0 & 0 & 0 \\ \frac{LK_1^1}{J_{xx}} & -\frac{LK_1^2}{J_{xx}} & -\frac{LK_1^3}{J_{xx}} & 0 \\ 0 & 0 & 0 & 0 \\ 0 & \frac{LK_1^2 \sin(\pi/3)}{J_{yy}} & \frac{LK_1^3 \sin(\pi/6)}{J_{yy}} & 0 \end{pmatrix},$$

$$A_{12} = \begin{pmatrix} 0 & 0 & -\frac{Q_1 L}{L_1} & 0 & 0 \\ 0 & 0 & \frac{Q_2 L \sin(\pi/6)}{L_2} & 0 & -\frac{Q_2 L \sin(\pi/3)}{L_2} \\ 0 & 0 & -\frac{Q_3 L \sin(\pi/6)}{L_3} & 0 & \frac{Q_3 L \sin(\pi/3)}{L_3} \\ 1 & 0 & 0 & 0 & 0 \end{pmatrix},$$

$$A_{22} = \begin{pmatrix} 0 & \frac{L\left(K_2^1 + \sin(\pi/6)\left(K_2^3 - K_2^2\right)\right)}{M} & 0 & \frac{L \sin(\pi/3)\left(K_2^3 - K_2^2\right)}{M} & 0 \\ 0 & 0 & 1 & 0 & 0 \\ 0 & \frac{L^2\left(K_2^1 + \sin^2(\pi/6)\left(K_2^2 - K_2^3\right)\right)}{J_{xx}} & 0 & \frac{L^2 \sin(\pi/6) \sin(\pi/3)\left(K_2^3 - K_2^2\right)}{J_{xx}} & 0 \\ 0 & 0 & 0 & 0 & 1 \\ 0 & \frac{L^2 \sin(\pi/6)\left(K_2^3 \sin(\pi/6) - K_2^2 \sin(\pi/3)\right)}{J_{yy}} & 0 & \frac{L^2 \sin(\pi/3)\left(K_2^2 \sin(\pi/3) - K_2^3 \sin(\pi/6)\right)}{J_{yy}} & 0 \end{pmatrix},$$

$$B = \begin{pmatrix} \frac{1}{L_1} & 0 & 0 \\ 0 & \frac{1}{L_2} & 0 \\ 0 & 0 & \frac{1}{L_3} \\ 0 & 0 & 0 \\ 0 & 0 & 0 \\ 0 & 0 & 0 \\ 0 & 0 & 0 \\ 0 & 0 & 0 \\ 0 & 0 & 0 \end{pmatrix},$$

$$C = \begin{pmatrix} 0 & 0 & 0 & K_3^1 & 0 & K_3^1 L & 0 & 0 & 0 \\ 0 & 0 & 0 & K_3^2 & 0 & -K_3^2 L \sin(\pi/6) & 0 & K_3^2 L \sin(\pi/3) & 0 \\ 0 & 0 & 0 & K_3^3 & 0 & K_3^3 L \sin(\pi/6) & 0 & -K_3^3 L \sin(\pi/3) & 0 \end{pmatrix}, \tag{6.6}$$

being, respectively, J_{xx}, J_{yy} moments of inertia around x- and y-axes of the levitated body.

From the previous model, the resulting state feedback controller in (3.14) obtained for a decay rate $\beta = 1.45$ in (5.1) has the next gain matrix of dimensions 3×21:

$$F^* = \begin{pmatrix} -5.36 & 383.2 & -0.63 & 44.76 & -0.001 & -0.008 & 0.57 & 0.001 & 0 & 0.22 & 0.12 & \cdots & -0.013 & 0.001 & 0.044 & 0 & 0.001 & 0.012 & 0 & 0.104 & 0.0004 & 0 \\ -4.75 & 349.4 & 0.29 & -20.32 & -0.5 & 35.34 & -0.003 & 0.33 & -0.0003 & -0.003 & -0.120 & \cdots & 0 & 0.194 & -2.45 & -0.008 & -0.001 & -0.02 & 0 & -0.001 & 0.06 & -0.001 \\ 1.963 & 395.7 & -0.11 & -23.14 & -0.19 & 40.08 & 0.0004 & -00002 & 0.06 & 0.0008 & 0.037 & \cdots & -0.0001 & 0.0001 & 0.007 & 0 & 0.042 & -6.86 & -0.004 & 0.001 & 0 & -0.15 \end{pmatrix}. \tag{6.7}$$

As the design strategy contemplated in this example is the same than that used in [17], the controllers obtained in both cases show negligible differences.

6.2.1. *Control System Time Response*

Once the dual-rate controller is designed, the next experiment is carried out in the proposed network scenario (adding a nonstationary Kalman filter as a state observer) .

The experiment starts with the platform in equilibrium point, as shown in Figure 8. In this figure, the top graphic shows the position error (center of mass), the middle one shows the control signal applied to the maglev, and the bottom one shows the supervision signal generated by the remote subcontroller and sent through the network to the local subcontroller. For clarity, only one of the three control and supervision signals is plotted. At time $t = 1.75$ s, some load (a coin of 2 euros, 8.5 g) is applied. After a transient, the system reaches a new, stable equilibrium point, but with some position error (experiment 1). Possible disturbances introduced by coupling between the three maglevs are compensated by the coordinating remote subcontroller.

Next, as position error is presented, a new remote subcontroller that includes accumulated error in system state is developed. So the controller is designed considering

$$\begin{pmatrix} \overline{x}_{k+1} \\ s_{k+1} \end{pmatrix} = \begin{pmatrix} A^* & 0 \\ -C^* & I \end{pmatrix} \cdot \begin{pmatrix} \overline{x}_k \\ s_k \end{pmatrix} + \begin{pmatrix} B^* \\ -0 \end{pmatrix} \cdot U_{sr,k}, \tag{6.8}$$

where A^*, B^*, C^* were introduced before (3.15), and the position error in $C^*\overline{x}$ will be zero in steady state [31].

Following this reasoning, the system state vector is expanded by adding the accumulated error for each one of the three maglevs. According to this new plant model, the feedback state controller is recalculated via LMI gridding, obtaining a new state feedback gain

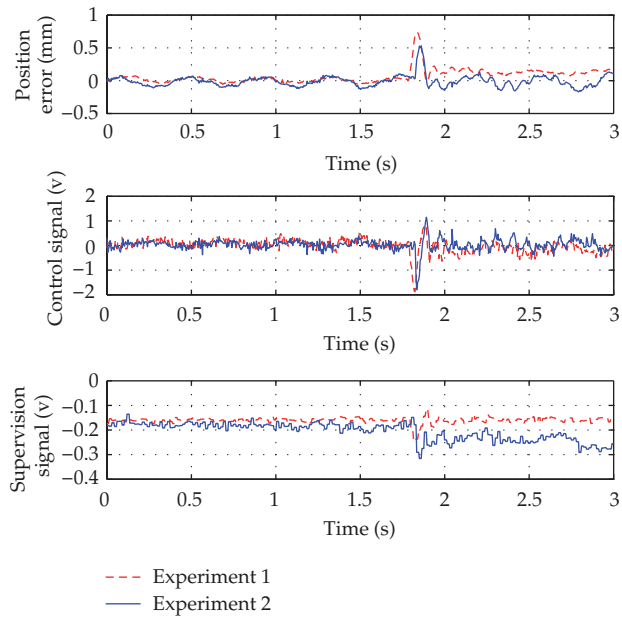

Figure 8: Figure results for experiments 1 and 2.

F^* with dimensions 3×24 (details omitted for brevity). As shown in Figure 8 (experiment 2), despite time-varying delays this new remote subcontroller (with the integral action) can keep the platform stable even with load variations (coin), improving control system performance with respect to that obtained in experiment 1 (which is related to [17]).

7. Conclusions

In this paper, in order to face arbitrary time-varying delays in a dual-rate NCS framework, different stability conditions and a state feedback design approach are presented in terms of LMIs. Multirate control techniques are proposed to avoid bandwidth limitations.

Regarding the stability conditions, three scenarios are treated: the robust case, the probabilistic case, and its extension to the multiobjective case. With respect to the state feedback controller, it is designed to assure robust stability for any possible time delay measured for the considered network.

Experimental results from two different dual-rate NCS implementations (a crane system over Ethernet, and a maglev-based platform over Profibus) validates the applicability of these LMI-based dual-rate control techniques.

Acknowledgments

The authors A. Cuenca, R. Pizá, and J. Salt are grateful to the Spanish Ministry of Education research Grants DPI2011-28507-C02-01 and DPI2009-14744-C03-03, and Generalitat Valenciana Grant GV/2010/018. A. Sala is grateful to the financial support of Spanish

Ministry of Economy research Grant DPI2011-27845-C02-01, and Generalitat Valenciana Grant PROMETEO/2008/088.

References

[1] Y. Tipsuwan and M. Y. Chow, "Control methodologies in networked control systems," *Control Engineering Practice*, vol. 11, no. 10, pp. 1099–1111, 2003.

[2] Y. Halevi and A. Ray, "Integrated communication and control systems. Part 1—analysis," *Journal of Dynamic Systems, Measurement and Control, Transactions of the ASME*, vol. 110, no. 4, pp. 367–373, 1988.

[3] T. C. Yang, "Networked control system: a brief survey," *IEE Proceedings: Control Theory and Applications*, vol. 153, no. 4, pp. 403–412, 2006.

[4] Á. Cuenca, J. Salt, A. Sala, and R. Pizá, "A delay-dependent dual-rate PID controller over an ethernet network," *IEEE Transactions on Industrial Informatics*, vol. 7, no. 1, pp. 18–29, 2011.

[5] Y. Tipsuwan and M. Y. Chow, "On the gain scheduling for networked PI controller over IP network," *IEEE/ASME Transactions on Mechatronics*, vol. 9, no. 3, pp. 491–498, 2004.

[6] J. Hu, Z. Wang, H. Gao, and L. Stergioulas, "Robust sliding mode control for discrete stochastic systems with mixed time delays, randomly occurring uncertainties, and randomly occurring nonlinearities," *IEEE Transactions on Industrial Electronics*, vol. 59, no. 7, pp. 3008–3015, 2012.

[7] W. S. Wong and R. W. Brockett, "Systems with finite communication bandwidth constraints. II. Stabilization with limited information feedback," *IEEE Transactions on Automatic Control*, vol. 44, no. 5, pp. 1049–1053, 1999.

[8] V. Casanova, J. Salt, A. Cuenca, and R. Pizá, "Networked Control Systems: control structures with bandwidth limitations," *International Journal of Systems, Control and Communications*, vol. 1, no. 3, pp. 267–296, 2009.

[9] A. Cuenca, P. García, P. Albertos, and J. Salt, "A non-uniform predictor-observer for a networked control system," *International Journal of Control, Automation and Systems*, vol. 9, no. 6, pp. 1194–1202, 2011.

[10] Y. C. Tian and D. Levy, "Compensation for control packet dropout in networked control systems," *Information Sciences*, vol. 178, no. 5, pp. 1263–1278, 2008.

[11] Z. Wang, B. Shen, H. Shu, and G. Wei, "Quantized H_∞ control for nonlinear stochastic time-delay systems with missing measurements," *IEEE Transactions on Automatic Control*, vol. 57, no. 6, pp. 1431–1444, 2012.

[12] Z. Wang, B. Shen, and X. Liu, "H_∞ filtering with randomly occurring sensor saturations and missing measurements," *Automatica*, vol. 48, no. 3, pp. 556–562, 2012.

[13] L. Ma, Z. Wang, Y. Bo, and Z. Guo, "Finite-horizon H_2/H_∞ control for a class of nonlinear Markovian jump systems with probabilistic sensor failures," *International Journal of Control*, vol. 84, no. 11, pp. 1847–1857, 2011.

[14] J.-N. Li, Q.-L. Zhang, Y.-L. Wang, and M. Cai, "H_∞ control of networked control systems with packet disordering," *IET Control Theory & Applications*, vol. 3, no. 11, pp. 1463–1475, 2009.

[15] S. Johannessen, "Time synchronization in a local area network," *IEEE Control Systems Magazine*, vol. 24, no. 2, pp. 61–69, 2004.

[16] A. Sala, Á. Cuenca, and J. Salt, "A retunable PID multi-rate controller for a networked control system," *Information Sciences*, vol. 179, no. 14, pp. 2390–2402, 2009.

[17] R. Pizá, J. Salt, A. Sala, and A. Cuenca, "Maglev platform networked control: a profibus DP application," in *Proceedings of the 8th IEEE International Conference on Industrial Informatics (INDIN '10)*, pp. 160–165, July 2010.

[18] A. Sala, "Computer control under time-varying sampling period: an LMI gridding approach," *Automatica*, vol. 41, no. 12, pp. 2077–2082, 2005.

[19] J. Salt and P. Albertos, "Model-based multirate controllers design," *IEEE Transactions on Control Systems Technology*, vol. 13, no. 6, pp. 988–997, 2005.

[20] Á. Cuenca, J. Salt, and P. Albertos, "Implementation of algebraic controllers for non-conventional sampled-data systems," *Real-Time Systems*, vol. 35, no. 1, pp. 59–89, 2007.

[21] S. Lall and G. Dullerud, "An LMI solution to the robust synthesis problem for multi-rate sampled-data systems," *Automatica*, vol. 37, no. 12, pp. 1909–1922, 2001.

[22] Y. Shi, H. Fang, and M. Yan, "Kalman filter-based adaptive control for networked systems with unknown parameters and randomly missing outputs," *International Journal of Robust and Nonlinear*

Control, vol. 19, no. 18, pp. 1976–1992, 2009.
[23] M. Araki, "Recent developments in digital control theory," in *Proceedings of the 12th World Congress of the International Federation of Automatic Control (IFAC '93)*, vol. 9, pp. 951–960, 1993.
[24] D. Li, S. L. Shah, and T. Chen, "Analysis of dual-rate inferential control systems," *Automatica*, vol. 38, no. 6, pp. 1053–1059, 2002.
[25] S. Boyd, L. El Ghaoui, E. Feron, and V. Balakrishnan, *Linear Matrix Inequalities in System and Control Theory*, vol. 15, Society for Industrial and Applied Mathematics, Philadelphia, Pa, USA, 1994.
[26] Y. B. Zhao, G. P. Liu, and D. Rees, "Modeling and stabilization of continuous-time packet-based networked control systems," *IEEE Transactions on Systems, Man, and Cybernetics, Part B*, vol. 39, no. 6, pp. 1646–1652, 2009.
[27] J. Salt, V. Casanova, A. Cuenca, and R. Pizá, "Networked-control based systems. modelling and control structures design," *Revista Iberoamericana de Automática e Informática Industrial*, vol. 5, no. 3, pp. 5–20, 2008.
[28] Y. Shi and B. Yu, "Output feedback stabilization of networked control systems with random delays modeled by Markov chains," *IEEE Transactions on Automatic Control*, vol. 54, no. 7, pp. 1668–1674, 2009.
[29] Y. Shi and B. Yu, "Robust mixed H_2/H_∞ control of networked control systems with random time delays in both forward and backward communication links," *Automatica*, vol. 47, no. 4, pp. 754–760, 2011.
[30] C. F. Van Loan, "Computing integrals involving the matrix exponential," *IEEE Transactions on Automatic Control*, vol. 23, no. 3, pp. 395–404, 1978.
[31] P. Albertos and A. Sala, *Multivariable Control Systems: An Engineering Approach*, Springer, 2004.
[32] P. P. Khargonekar, K. Poolla, and A. Tannenbaum, "Robust control of linear time-invariant plants using periodic compensation," *IEEE Transactions on Automatic Control*, vol. 30, no. 11, pp. 1088–1096, 1985.
[33] K. Ogata, *Discrete-Time Control Systems*, Prentice-Hall, Upper Saddle River, NJ, USA, 1987.
[34] P. Martí, J. Yépez, M. Velasco, R. Villà, and J. M. Fuertes, "Managing quality-of-control in network-based control systems by controller and message scheduling co-design," *IEEE Transactions on Industrial Electronics*, vol. 51, no. 6, pp. 1159–1167, 2004.
[35] Y. Tipsuwan and M. Y. Chow, "Gain scheduler middleware: a methodology to enable existing controllers for networked control and teleoperation—part I: networked control," *IEEE Transactions on Industrial Electronics*, vol. 51, no. 6, pp. 1218–1227, 2004.
[36] P. Apkarian and R. J. Adams, "Advanced gain-scheduling techniques for uncertain systems," *IEEE Transactions on Control Systems Technology*, vol. 6, no. 1, pp. 21–32, 1998.
[37] L. A. Montestruque and P. Antsaklis, "Stability of model-based networked control systems with time-varying transmission times," *IEEE Transactions on Automatic Control*, vol. 49, no. 9, pp. 1562–1572, 2004.
[38] M. M. Rao, *Foundations of Stochastic Analysis*, Academic Press, 1981.
[39] J. F. Sturm, "Using SeDuMi 1.02, a MATLAB toolbox for optimization over symmetric cones," *Optimization Methods and Software*, vol. 11/12, no. 1–4, pp. 625–653, 1999.
[40] Y. Sawaragi, H. Nakayama, and T. Tanino, *Theory of Multiobjective Optimization*, vol. 176, Academic Press, Orlando, Fla, USA, 1985.
[41] R. Sanchez-Pena and M. Sznaier, *Robust Systems Theory and Application*, John Wiley & Sons, New York, NY, USA, 1998.
[42] K. Zhou, *Essentials of Robust Control*, Prentice Hall, 1998.

Hindawi Publishing Corporation
Mathematical Problems in Engineering
Volume 2012, Article ID 342705, 15 pages
doi:10.1155/2012/342705

Research Article

Asymptotic Parameter Estimation for a Class of Linear Stochastic Systems Using Kalman-Bucy Filtering

Xiu Kan,[1] Huisheng Shu,[2] and Yan Che[1]

[1] *School of Information Science and Technology, Donghua University, Shanghai 200051, China*
[2] *School of Science, Donghua University, Shanghai 200051, China*

Correspondence should be addressed to Huisheng Shu, hsshu@dhu.edu.cn

Received 21 June 2012; Accepted 21 July 2012

Academic Editor: Jun Hu

The asymptotic parameter estimation is investigated for a class of linear stochastic systems with unknown parameter $\theta : dX_t = (\theta\alpha(t) + \beta(t)X_t)dt + \sigma(t)dW_t$. Continuous-time Kalman-Bucy linear filtering theory is first used to estimate the unknown parameter θ based on Bayesian analysis. Then, some sufficient conditions on coefficients are given to analyze the asymptotic convergence of the estimator. Finally, the strong consistent property of the estimator is discussed by comparison theorem.

1. Introduction

Stochastic differential equations (SDEs) are a natural choice to model the time evolution of dynamic systems which are subject to random influences. Such models have been used with great success in a variety of application areas, including biology, mechanics, economics, geophysics, oceanography, and finance. For instance, refer to [1–8]. In reality, it is unavoidable that a stochastic system contains unknown parameters. Since 1962, Arato et al. [10] first applied parameter estimation to geophysical problem. Parameter estimation for SDEs has attracted the close attention of many researchers, and many parameter estimation methods for various advanced models have been studied, such as maximum likelihood estimation (MLE), Bayes estimation (BE), maximum probability estimation (MPE), minimum distance estimation (MDE), minimum contrast estimation (MCE), and M-estimation (ME). See [10–15] for details.

In practice, most stochastic systems cannot be observed completely, but the development of filtering theory provides an effective method to solve this problem. Over the past few decades, a lot of effective approaches have been proposed to overcome the difficulties in parameter estimation for stochastic models by filtering methods. It turns out to be

helpful both in computability and asymptotic studies. See [9, 16–26]. In particular, the parameter estimation has been studied based on filtering observation, and the strong consistency property has also been shown in [27, 28]. In [29], a large deviation inequality has been obtained which implies the strong consistency, local asymptotic normality, and the convergence of moments. The asymptotic properties of estimators have been studied for a class of special Gaussian Itô processes with noisy observations in [30]. It should be pointed out that, so far, although the parameter estimation problem has been widely investigated for SDEs, the parameter estimation problem for stock price model has gained much less research attention due probably to the mathematical complexity.

Stock return volatility process is an important topic in options pricing theory. During the past decades, many SDEs have been modeled to solve the financial problems. For instance, refer to [2, 31–35]. Particularly, the so-called Hull-White model has been established by Hull and White [34] to analyze European call options prices under stochastic volatility at 1987. Using Taylor series expansion, an accurate formula for call options has been derived where stock returns and stock volatilities are uncorrelated. In addition, the Hull-White model readily lends itself to the estimation of underlying stochastic process parameters. Since the Hull-White formula is an effective options pricing model, it has been widely used to model the practice stock price problem. Therefore, it is reasonable to study the parameter estimation problem for Hull-White model with unknown parameter. Unfortunately, to the best of the authors' knowledge, the parameter estimation for Hull-White model with unknown parameter based on Kalman-Bucy linear filtering theory has not been fully studied despite its potential in practical application, and this situation motivates our present investigation.

Summarizing the above discussions, in this paper, we aim to investigate the parameter estimation problem for a general class of linear stochastic systems. The main contributions of this paper lie in the following aspects. (1) *Kalman-Bucy linear filtering is used to solve the parameter estimation problem.* (2) *The asymptotic convergence of the estimator is investigated by analyzing Riccati equation.* (3) *The strong consistent property is studied by comparison theorem*. The rest of this paper is organized as follows. In Section 2, we formulate the problem and state the well-known fact which would be used later. In Section 3, we study the asymptotic convergence of the estimator. In Section 4, the strong consistent of estimator is given. In Section 5, some conclusions are drawn.

Notation. The notation used here is fairly standard except where otherwise stated. $\mathbb{R} = (-\infty, +\infty)$ and $\mathbb{R}_+ = [0, +\infty)$. For a vector $x =\in \mathbb{R}$, $|x|$ is the Euclidean norm (or L^2 norm) with $|x| = \sqrt{x \cdot x}$. M^T and M^{-1} represent the transpose and inverse of the matrix M. $\det(M)$ denotes the determinant of the matrix M. I denotes the identity matrix of compatible dimension. Moreover, let $(\Omega, \mathcal{F}, \mathbf{P})$ be a complete probability space with a natural filtration $\{\mathcal{F}_t\}_{t\geq 0}$ satisfying the usual conditions (i.e., it is right continuous, and $\mathcal{F}_0$ contains all $\mathbf{P}$-null sets). $\mathbb{E}[x]$ stands for the expectation of the stochastic variable x with respect to the given probability measure $\mathbf{P}$. $C(\mathbb{R}_+)$ denotes the class of all continuous time on $t \in \mathbb{R}_+$.

2. Problem Statement

Hull-White model is a continuous-time, real stochastic process as follows:

$$X_t = X_0 + \int_0^t \left(\alpha(s) + \beta(s) X_s\right) ds + \int_0^t \sigma(s) dW_s \tag{2.1}$$

with initial value X_0 as a Gaussian random variable, where α, β, σ are deterministic continuous functions on time t, W_t is a Brownian motion independent of the initial value X_0. Obviously, Hull-White model (2.1) is a general continuous-time linear SDE for X_t, and we assume that the coefficient α contains an unknown parameter $\theta \in R$ as follows:

$$dX_t = \left(\theta\alpha(t) + \beta(t)X_t\right)dt + \sigma(t)dW_t \quad t \geq 0, \tag{2.2}$$

and we observe the process X_t by the following filtering observations:

$$dY_t = \mu(t)X_t dt + \gamma(t)dV_t \quad t \geq 0, \tag{2.3}$$

where μ, γ are deterministic bounded continuous functions on time t, and V_t is a Brownian motion independent of W_t.

Now, our aim is to estimate θ in (2.2) based on the observation of (2.3). First, we can use Bayesian analysis to deal with the unknown parameter θ. We model θ as a random variable and denoted it as θ_0. We assume θ_0 normally distributed and independent of $\sigma(W_t, V_t, t \geq 0)$. Then, we can rewrite (2.2) as a two-component system for (X_t, θ_t) as follows:

$$\begin{pmatrix} dX_t \\ d\theta_t \end{pmatrix} = \begin{pmatrix} \beta(t) & \alpha(t) \\ 0 & 0 \end{pmatrix} \begin{pmatrix} X_t \\ \theta_t \end{pmatrix} dt + \begin{pmatrix} \sigma(t) \\ 0 \end{pmatrix} dW_t \quad t \geq 0. \tag{2.4}$$

Similarly, filtering observations system (2.3) can be expressed as follows:

$$dY_t = \begin{pmatrix} \mu(t) & 0 \end{pmatrix} \begin{pmatrix} X_t \\ \theta_t \end{pmatrix} dt + \gamma(t)dV_t \quad t \geq 0. \tag{2.5}$$

Therefore, we can use the Kalman-Bucy linear filtering theory to estimate θ_0 as follows:

$$\widehat{\theta}_t = \mathbb{E}[\theta_0 \mid Y_s, 0 \leq s \leq t], \tag{2.6}$$

and moreover, we also have $\widehat{X}_t = \mathbb{E}[X_t | Y_s, 0 \leq s \leq t]$.

For given Gaussian initial conditions X_0 and θ_0, it is well known from Kalman-Bucy linear filtering theory that error covariance matrix $S(t)$ satisfies the following Riccati equation:

$$\dot{S}(t) = AS + SA^T - SC^T\left(DD^T\right)^{-1}CS + BB^T, \tag{2.7}$$

where $A = \left(\begin{smallmatrix} \beta(t) & \alpha(t) \\ 0 & 0 \end{smallmatrix}\right), B = \left(\begin{smallmatrix} \sigma(t) \\ 0 \end{smallmatrix}\right), C = (\mu(t)\ 0), D = \gamma(t)$, and as we all know the error covariance matrix $S(t)$ is defined as follows:

$$S(t) = \begin{pmatrix} S_{xx}(t) & S_{x\theta}(t) \\ S_{\theta x}(t) & S_{\theta\theta}(t) \end{pmatrix} = \begin{pmatrix} \mathbb{E}\left[\left(X_t - \widehat{X}_t\right)^2\right] & \mathbb{E}\left[\left(X_t - \widehat{X}_t\right)\left(\theta_0 - \widehat{\theta}_t\right)\right] \\ \mathbb{E}\left[\left(X_t - \widehat{X}_t\right)\left(\theta_0 - \widehat{\theta}_t\right)\right] & \mathbb{E}\left[\left(\theta_0 - \widehat{\theta}_t\right)^2\right] \end{pmatrix}. \tag{2.8}$$

Set $a = S_{xx}$, $b = S_{x\theta} = S_{\theta x}$, and $c = S_{\theta\theta}$. From Riccati equation (2.7), one can get the following system:

$$\begin{aligned} \dot{a} &= 2\beta a + 2\alpha b + \sigma^2 - \frac{\mu^2}{\gamma^2} a^2, \\ \dot{b} &= \beta b + \alpha c - \frac{\mu^2}{\gamma^2} ab, \\ \dot{c} &= -\frac{\mu^2}{\gamma^2} b^2. \end{aligned} \tag{2.9}$$

Remark 2.1. Equation (2.9) is a nontrivial nonlinear ordinary differential equation system, and it is well known from the Kalman-Bucy linear filtering theory that such Riccati equations have unique solutions for all $t \in \mathbb{R}_+$.

Remark 2.2. From the equation $\dot{c} = -(\mu^2/\gamma^2)b^2$, we can see that the error variance $\mathbb{E}[(\theta_0 - \widehat{\theta}_t)^2]$ is monotonically decreasing.

3. Asymptotic Convergence Analysis

Assume that the initial conditions X_0 and θ_0 are independent and have nonvariances, so that $b(0) = 0$ and $a(0) = \mathbb{E}[X_0^2] > 0$, $c(0) = \mathbb{E}[\theta_0^2] > 0$; thus, $S(0)$ is a regular matrix. For the property of continuity of $S(t)$, $S^{-1}(t)$ exists at least for small times. In order to obtain the rate of convergence of the estimator, $S(t)$ should satisfy the regularity conditions. The following Theorem certifies the regularity of $S(t)$.

Theorem 3.1. *(a1) Assume the initial conditions X_0 and θ_0 for system* (2.2) *are independent and have nonvanishing variances.*

(a2) Let $\alpha(t), \beta(t), \sigma(t), \mu(t), \gamma(t) \in C(\mathbb{R}_+)$.

Then, the error covariance matrix $S(t)$ satisfies $\det(S(t)) > 0$ *for all $t \geq 0$, and*

$$S_{xx}(t) > 0, \quad S_{\theta\theta}(t) > 0 \quad \forall t \geq 0. \tag{3.1}$$

Proof. By Kalman-Bucy linear filtering theory, we know that $\det(S(t)) > 0$ for all $t \geq 0$. Furthermore, it is not difficult to show that (3.1) holds for all $t \geq 0$.

Since $\det(S(t)) > 0$, it follows that $S^{-1}(t)$ exists. Set

$$R(t) = S^{-1}(t) = \begin{pmatrix} e(t) & f(t) \\ f(t) & g(t) \end{pmatrix}. \tag{3.2}$$

As we know that $R = 1/S$ implies that $\dot{R} = -(1/S^2)\dot{S}$, one can easily have that

$$\dot{R} = -R\dot{S}R. \tag{3.3}$$

It follows readily form (2.9) and (3.3) that

$$\dot{R} = -RA - A^T R + C^T \left(DD^T\right)^{-1} C - RBB^T R. \tag{3.4}$$

Using a similar computation as (2.9), we can get

$$\begin{aligned} \dot{e} &= \frac{\mu^2}{\gamma^2} - 2\beta e - \sigma^2 e^2, \\ \dot{f} &= -\alpha e - \beta f - \sigma^2 e f, \\ \dot{g} &= -2\alpha f - \sigma^2 f^2. \end{aligned} \tag{3.5}$$

The condition (a1) shows that $a(0) > 0$, $b(0) = 0$, and $c(0) > 0$, which implies that $e(0) > 0$, $f(0) = 0$, and $g(0) > 0$. Since the Riccati equations (2.9) have unique solutions on R_+, thus the nonlinear system (3.5) has a unique solution on $\mathbb{R}_+$. Furthermore, the first equation $\dot{e} = \mu^2/\gamma^2 - 2\beta e - \sigma^2 e^2$ with initial condition $e(0) > 0$ has a unique solution on a maximal time interval $[0, T)$, where $T \in \mathbb{R}_+$. Assume that there exists a smallest time $\bar{t} \in (0, T)$ such that $e(\bar{t}) = 0$. By the property of continuity of $e(t)$, we have $e(t) > 0$, for $0 \le t < \bar{t}$. Thus,

$$\dot{e}(t) = \lim_{\Delta t \to 0} \frac{e\left(\bar{t}\right) - e\left(\bar{t} - \Delta t\right)}{\Delta t} < 0, \tag{3.6}$$

this contradicts with $\dot{e}(t) = \mu^2(\bar{t})/\gamma^2(\bar{t}) - 2\beta(\bar{t})e(\bar{t}) - \sigma^2(\bar{t})e^2(\bar{t}) \le \mu^2(\bar{t})/\gamma^2(\bar{t})$ for all $t \in [0, T)$. Therefore, $e(t) > 0$, for $t \in [0, T)$.

As long as $\dot{e}(t) = \mu^2(\bar{t})/\gamma^2(\bar{t}) - 2\beta(\bar{t})e(\bar{t}) - \sigma^2(\bar{t})e^2(\bar{t}) \le \mu^2(\bar{t})/\gamma^2(\bar{t})$ for all $t \in [0, T)$ and $\mu(t), \gamma(t)$ are bounded, we have $\dot{e}(t) \le C$, where C is a constant. So that $e(t)$ is bounded from below by 0 and from above by $e(0) + t$, which implies that $e(t)$ cannot explode in finite time, thus $T = +\infty$. This shows that system (3.5) has a unique solution on $\mathbb{R}_+$ because the second equation is a linear equation for f which can be solved analytically on $\mathbb{R}_+$, and g can get by integration.

Define $h(t) := \det(R(t)) = e(t)g(t) - f^2(t)$. Since $\det(S(t)) > 0$ for all $t \ge 0$, thus $h(t) = \det(R(t)) = 1/\det(S(t)) > 0$ for all $t \ge 0$, moreover, $S_{\theta\theta} > 0$ for all $t \ge 0$. Finally, we assume that there exists t_0 such that, $S_{xx}(t_0) = 0$, then $g(t_0) = S_{xx}(t_0)h(t_0) = 0$, so that $h(t_0) = e(t_0)g(t_0) - f^2(t_0) \le 0$, and this contradicts $h(t_0) > 0$. Hence, $S_{xx} > 0$ for all $t \ge 0$.

The proof is complete. □

In order to obtain the convergence rate, the Riccati equation must be solved, and we just need the solution of (3.5). Now, we solve the equation $\dot{e} = \mu^2/\gamma^2 - 2\beta e - \sigma^2 e^2$ when $\beta, \sigma, \mu, \gamma$ are equal to constants.

In the case $e(0) \ne l_2$, we get

$$e(t) = \frac{l_1 + l_2 L \exp\left[(l_1 + l_2)\sigma^2 t\right]}{L \exp\left[(l_1 + l_2)\sigma^2 t\right] - 1}, \tag{3.7}$$

where $L = (e(0) + l_1)/(e(0) - l_2)$, $l_1 = (2\beta/\sigma^2 + \sqrt{4\beta^2/\sigma^4 + 4\mu^2/\sigma^2\gamma^2})/2$, $l_2 = (-(2\beta/\sigma^2) + \sqrt{4\beta^2/\sigma^4 + 4\mu^2/\sigma^2\gamma^2})/2$.

In the other case $e(0) = l_2$, the solution shows that $e(t) = l_2$ for all $t \geq 0$.

Thus, for each $\alpha > 0$, $\beta > 0$, $\sigma > 0$, $\mu > 0$, $\gamma > 0$, the solution $e(t)$ obviously satisfies

$$e(t) \longrightarrow l_2 \quad \text{as } t \longrightarrow +\infty. \tag{3.8}$$

The convergence rate of the estimator is given by following theorem.

Theorem 3.2. *Assume that $\alpha, \beta, \sigma, \mu, \gamma \in C(\mathbb{R}_+)$, are all bounded, and there are constants α_1, α_2, β_1, β_2, σ_1, σ_2, μ_1, μ_2, γ_1, γ_2, and t_0, such that*

(b1) *: $0 < \alpha_1 \leq |\alpha(t)| \leq \alpha_2$ for all $t \geq t_0$;*

(b2) *: $0 < \beta_1 \leq |\beta(t)| \leq \beta_2$ for all $t \geq t_0$;*

(b3) *: $0 < \sigma_1 \leq |\sigma(t)| \leq \sigma_2$ for all $t \geq t_0$;*

(b4) *: $0 < \mu_2 \leq |\mu(t)| \leq \mu_1$ for all $t \geq t_0$;*

(b5) *: $0 < \gamma_1 \leq |\gamma(t)| \leq \gamma_2$ for all $t \geq t_0$;*

(b6) *: $2\alpha_1(\beta_1 + \sigma_1^2 l_{22}) > \sigma_2^2 l_{21}$ where $l_{2i} = (-2\beta_i/\sigma_i^2 + \sqrt{(4\beta_i^2)/(\sigma_i^4) + (4\mu_i^2)/(\sigma_i^2\ \gamma_i^2)})/2$, $i = 1, 2$.*

Then, for arbitrary $\epsilon > 0$ and $T > 0$, we have

$$P\left(\left|\theta_0 - \widehat{\theta}_t\right| > \epsilon\right) \leq \frac{1}{\epsilon^2} C T^{-1}, \tag{3.9}$$

where C is a positive constant independent of ϵ and T.

Proof. Let e_i be the solution to $\dot{e}_i = \mu_i^2/\gamma_i^2 - 2\beta_i e_i - \sigma_i^2 e_i^2$, $i = 1, 2$, and $e_i(t_0) = e(t_0)$.

Since $\mu_2^2/\gamma_2^2 - 2\beta_2 e - \sigma_2^2 e^2 \leq \dot{e} = \mu^2/\gamma^2 - 2\beta e - \sigma^2 e^2 \leq \mu_1^2/\gamma_1^2 - 2\beta_1 e - \sigma_1^2 e^2$ for all $t \geq t_0$, by the comparison theorem [2, 36], we obtain that

$$e_2(t) \leq e(t) \leq e_1(t) \quad \forall t \geq t_0. \tag{3.10}$$

It follows from (3.7) that e is bounded, and for any given $\delta \in (0, 1)$, there is a $t_1 \geq t_0$ such that

$$0 < l_{22}(1 - \delta) \leq e(r) \leq l_{21}(1 + \delta) \quad \forall r \geq t_1. \tag{3.11}$$

For $t \geq t_1$, we can obtain from (3.5) and $f(0) = 0$ that

$$\begin{aligned} f(t) = & -\int_0^t \exp\left[-\int_s^t \left(\beta(r) + \sigma^2(r)e(r)\right)dr\right]\alpha(s)e(s)ds \\ = & -\exp\left[-\int_0^t \left(\beta(r) + \sigma^2(r)e(r)\right)dr\right]\int_0^{t_1} \exp\left[\int_0^s \left(\beta(r) + \sigma^2(r)e(r)\right)dr\right]\alpha(s)e(s)ds \\ & -\int_{t_1}^t \exp\left[-\int_s^t \left(\beta(r) + \sigma^2(r)e(r)\right)dr\right]\alpha(s)e(s)ds. \end{aligned} \tag{3.12}$$

As $\beta(r) + \sigma^2(r)e(r) \geq \beta_1 + \sigma_1^2 l_{22}(1-\delta)$ holds for all $t \geq t_1$, thus, the first term in (3.12) goes to 0 as $t \to \infty$. For the second term in (3.12), we have

$$\begin{aligned} & \left|\int_{t_1}^t \exp\left[-\int_s^t \left(\beta(r) + \sigma^2(r)e(r)\right)dr\right]\alpha(s)e(s)ds\right| \\ & \quad \leq \int_0^t \exp\left[-\left(\beta_1 + \sigma_1^2 l_{22}(1-\delta)\right)(t-s)\right] l_{21}(1+\delta)ds \\ & \quad = \frac{l_{21}(1+\delta)}{\beta_1 + \sigma_1^2 l_{22}(1-\delta)} \int_0^t \exp\left[-\left(\beta_1 + \sigma_1^2 l_{22}(1-\delta)\right)(t-s)\right] d\left(\beta_1 + \sigma_1^2 l_{22}(1-\delta)\right)s \\ & \quad = \frac{l_{21}(1+\delta)}{\beta_1 + \sigma_1^2 l_{22}(1-\delta)}\left(1 - \exp\left[-\left(\beta_1 + \sigma_1^2 l_{22}(1-\delta)\right)t\right]\right) \\ & \quad \leq \frac{l_{21}(1+\delta)}{\beta_1 + \sigma_1^2 l_{22}(1-\delta)}. \end{aligned} \tag{3.13}$$

By similar arguments, we obtain that

$$\left|\int_{t_1}^t \exp\left[-\int_s^t \left(\beta(r) + \sigma^2(r)e(r)\right)dr\right]\alpha(s)e(s)ds\right| \geq \frac{l_{22}(1-\delta)}{\beta_2 + \sigma_2^2 l_{21}(1+\delta)}. \tag{3.14}$$

Therefore, for any $\xi > 0$, there exists $t(\xi) > 0$ such that

$$\frac{l_{22}(1-\delta)}{\beta_2 + \sigma_2^2 l_{21}(1+\delta)} \leq |f(t)| \leq \frac{l_{21}(1+\delta)}{\beta_1 + \sigma_1^2 l_{22}(1-\delta)} \quad \forall t \geq t(\xi). \tag{3.15}$$

For all $t \geq t(\xi)$, we can get from (3.5) that

$$\begin{aligned}
\dot{g} &= \left(2|\alpha| - \sigma^2|f|\right)|f| \\
&\geq \left(2\alpha_1 - \sigma_2^2 \frac{l_{21}(1+\delta)}{\beta_1 + \sigma_1^2 l_{22}(1-\delta)}\right) \frac{l_{22}(1-\delta)}{\beta_2 + \sigma_2^2 l_{21}(1+\delta)} \\
&= \left(\frac{2\alpha_1(\beta_1 + \sigma_1^2 l_{22}) - \sigma_2^2(l_{21}(1+\delta))}{\beta_1 + \sigma_1^2 l_{22}(1-\delta)}\right) \frac{l_{22}(1-\delta)}{\beta_2 + \sigma_2^2 l_{21}(1+\delta)}.
\end{aligned} \tag{3.16}$$

By assumption (b6), we get $\dot{g} > 0$ for a sufficiently small $\xi > 0$. This implies that $g(t)$ goes to infinity at least as a linear function. Thus, there exists a constant $C > 0$, such that

$$\mathbb{E}\left(\theta_0 - \widehat{\theta}_t\right)^2 = S_{\theta\theta} = \frac{e}{h} \leq Ct^{-1}. \tag{3.17}$$

Hence, for arbitrary $\epsilon > 0$ and all $T > 0$, it follows from Chebyshev's inequality that

$$P\left(\left|\theta_0 - \widehat{\theta}_t\right| > \epsilon\right) \leq \frac{1}{\epsilon^2} CT^{-1}. \tag{3.18}$$

The proof is complete. □

Remark 3.3. From the proof of Theorem 3.2, we can see that $\theta_0 - \widehat{\theta}_t$ goes to 0 in L^2-sense under the given conditions. In other words, $\widehat{\theta}_t$ is asymptotically unbiased.

Remark 3.4. It is well known that Kalman-Bucy linear filtering theory remains valid if one replaces the Brownian motion (W_t, V_t) in systems (2.2) and (2.3) by an arbitrary centered orthogonal increment process of the same covariance structure. Thus, Theorem 3.2 remains valid under this replacement.

4. Strong Consistency

In last section, we give the conditions for the convergence rate of the estimator. Furthermore, we use the comparison theorem to proof the strong consistency in this section. As we all know, if the parameter θ is, a genuine Gaussian random variable, then we can have a clear statistical interpretation for the convergence rate. Firstly, we pick θ_0 at random; secondly, let system (2.2) run up to time t and simultaneously observe Y by system (2.3); finally, compute $\widehat{\theta}_t$ as the following form.

The Kalman-Bucy linear filtering theory shows us

$$\begin{aligned}\begin{pmatrix} dX_t \\ d\theta_t \end{pmatrix} &= \left(A(t) - \frac{C^T(t)C(t)}{D^2(t)} S(t) \right) \begin{pmatrix} X_t \\ \theta_t \end{pmatrix} dt + \frac{C(t)}{D^2(t)} S(t) dY_t \\ &= \begin{pmatrix} \beta(t) - \dfrac{\mu^2(t)}{\gamma^2(t)} S_{xx}(t) & \alpha(t) \\ -\dfrac{\mu^2(t)}{\gamma^2(t)} S_{\theta x}(t) & 0 \end{pmatrix} \begin{pmatrix} X_t \\ \theta_t \end{pmatrix} dt + \frac{\mu^2(t)}{\gamma^2(t)} \begin{pmatrix} S_{xx}(t) \\ S_{\theta x}(t) \end{pmatrix} dY_t \end{aligned} \tag{4.1}$$

with initial conditions $\widehat{X}_0 = \mathbb{E}[X_0]$ and $\widehat{\theta}_0 = \mathbb{E}[\theta_0]$. If we denote that $\Phi(t)$ is the matrix fundamental solution of the deterministic linear system

$$\begin{pmatrix} \dot{x}_t \\ \dot{y}_t \end{pmatrix} = \begin{pmatrix} \beta(t) - \dfrac{\mu^2(t)}{\gamma^2(t)} S_{xx}(t) & \alpha(t) \\ -\dfrac{\mu^2(t)}{\gamma^2(t)} S_{\theta x}(t) & 0 \end{pmatrix} \begin{pmatrix} x(t) \\ y(t) \end{pmatrix}, \tag{4.2}$$

then the solution to (4.1) is given by

$$\begin{pmatrix} \widehat{X}_t \\ \widehat{\theta}_t \end{pmatrix} = \Phi(t)\Phi^{-1}(0) \begin{pmatrix} \mathbb{E}[X_0] \\ \mathbb{E}[\theta_0] \end{pmatrix} + \int_0^t \Phi(t)\Phi^{-1}(s) \begin{pmatrix} S_{xx}(t) \\ S_{\theta x}(t) \end{pmatrix} dY_s. \tag{4.3}$$

And for every particular experiment ω, the quantity $(\theta_0(\omega) - \widehat{\theta}_t(\omega))^2$ would be the squared estimation error.

But in this paper θ is a fixed parameter, so we can only choose $\theta_0(\omega) = \theta$, and then the statistical mean over different values of $\theta_0(\omega)$ has no experimental meaning. The true estimation error is given by $\theta - \widehat{\theta}_t$, not $\theta_0 - \widehat{\theta}_t$. It is therefore desirable that estimator $\widehat{\theta}_t$ converges to θ_0 for "all fixed values $\upsilon = \theta_0$" a.s. To establish such an assertion we work with a product space $(R \times \Omega, \mathcal{B}(R) \otimes \mathcal{F}, \eta \otimes P)$, where η denotes the law of θ_0, and $(\Omega, \mathcal{F}, P)$ is the underlying probability space for Brownian motion $(W_t, V_t)_{t\geq 0}$. This space is most appropriate because one can make P a.s. statements for fixed $\upsilon \in \mathbb{R}$. Notice that in this representation we have $\theta_0(\upsilon, \omega) = \upsilon$ for all $(\upsilon, \omega) \in \mathbb{R} \times \Omega$. Assuming this underlying probability space, we use the comparison theorem to get the following consistency result.

In the proof of Theorem 3.2, we know that e, f is bonded and g is monotonically increasing, moreover, $S_{xx}(t) = a = g/h = g/(eg - f^2) = (g - f^2/e + f^2/e)/(eg - f^2) = 1/e + f^2/e(eg - f^2)$ and $S_{\theta x}(t) = b = f/h = f/(eg - f^2)$. Thus, there exist positive constants a_1, a_2, b_1, and b_2 such that $a_1 \leq a \leq a_2$ and $b_1 \leq b \leq b_2$.

Theorem 4.1. *Assume that the following two conditions are satisfied:*

(c1) *: $\widehat{\theta}_t$ converges to θ_0 in $L^2(\eta \otimes P)$;*

(c2) *: $\beta_2 - \mu_2^2/\gamma_2^2 < 0$;*

(c3) *: $(\beta_2 - (\mu_2^2/\gamma_2^2)a_2)^2 - 4\alpha_2(\mu_2^2/\gamma_2^2)b_2 < 0$.*

Then, for all fixed $\upsilon \in \mathbb{R}$, we have

$$\widehat{\theta}_t(\upsilon, \cdot) \longrightarrow \upsilon, \quad P\text{-}a.s., \quad as\, t \longrightarrow \infty. \tag{4.4}$$

Proof. We will show that (4.4) holds for all $\upsilon \in N^c$, where $\eta(N) = 0$.

By Kalman-Bucy linear filtering theory, we know

$$\begin{aligned}\begin{pmatrix} dX_t \\ d\theta_t \end{pmatrix} &= \left(A(t) - \frac{C^T(t)C(t)}{D^2(t)}S(t)\right)\begin{pmatrix} X_t \\ \theta_t \end{pmatrix}dt + \frac{C(t)}{D^2(t)}S(t)dY_t \\ &= \begin{pmatrix} \beta(t) - \dfrac{\mu^2(t)}{\gamma^2(t)}S_{xx}(t) & \alpha(t) \\ -\dfrac{\mu^2(t)}{\gamma^2(t)}S_{\theta x}(t) & 0 \end{pmatrix}\begin{pmatrix} X_t \\ \theta_t \end{pmatrix}dt + \frac{\mu^2(t)}{\gamma^2(t)}\begin{pmatrix} S_{xx}(t) \\ S_{\theta x}(t) \end{pmatrix}dY_t \end{aligned} \tag{4.5}$$

with initial conditions $\widehat{X}_0 = \mathbb{E}[X_0]$ and $\widehat{\theta}_0 = \mathbb{E}[\theta_0] = \mathbb{E}[\upsilon] = \upsilon$.

Since the following linear equations:

$$\begin{pmatrix} \dot{x}_t \\ \dot{y}_t \end{pmatrix} = \begin{pmatrix} \beta(t) - \dfrac{\mu^2(t)}{\gamma^2(t)}S_{xx}(t) & \alpha(t) \\ -\dfrac{\mu^2(t)}{\gamma^2(t)}S_{\theta x}(t) & 0 \end{pmatrix}\begin{pmatrix} x(t) \\ y(t) \end{pmatrix} \tag{4.6}$$

equal to

$$\begin{aligned} \dot{x}_t &= \left[\beta(t) - \frac{\mu^2(t)}{\gamma^2(t)}S_{xx}(t)\right]x(t) + \alpha(t)Y(t), \\ \dot{y}_t &= -\frac{\mu^2(t)}{\gamma^2(t)}S_{\theta x}(t)x(t), \end{aligned} \tag{4.7}$$

it follows from (c1)–(c3) that

$$\begin{gathered} \beta_1 - \frac{\mu_1^2}{\gamma_1^2}a_1 \le \beta(t) - \frac{\mu^2(t)}{\gamma^2(t)}S_{xx}(t) \le \beta_2 - \frac{\mu_2^2}{\gamma_2^2}a_2 < 0, \\ \alpha_1 \le \alpha(t) \le \alpha_2, \\ -\frac{\mu_1^2}{\gamma_1^2}b_1 \le -\frac{\mu^2(t)}{\gamma^2(t)}S_{\theta x}(t) \le -\frac{\mu_2^2}{\gamma_2^2}b_2. \end{gathered} \tag{4.8}$$

For linear equations:

$$\begin{pmatrix} \dot{x}_t \\ \dot{y}_t \end{pmatrix} = \begin{pmatrix} \beta_1 - \dfrac{\mu_1^2}{\gamma_1^2} a_1 & \alpha_1 \\ -\dfrac{\mu_1^2}{\gamma_1^2} b_1 & 0 \end{pmatrix} \begin{pmatrix} x(t) \\ y(t) \end{pmatrix},$$
$$\begin{pmatrix} \dot{x}_t \\ \dot{y}_t \end{pmatrix} = \begin{pmatrix} \beta_2 - \dfrac{\mu_2^2}{\gamma_2^2} a_2 & \alpha_2 \\ -\dfrac{\mu_2^2}{\gamma_2^2} b_2 & 0 \end{pmatrix} \begin{pmatrix} x(t) \\ y(t) \end{pmatrix}, \tag{4.9}$$

if we set $\Phi_1(t)$ and $\Phi_2(t)$ that are the matrix fundamental solution of (4.9), we can obtain from the comparison theorem that

$$\Phi_1(t) \le \Phi(t) \le \Phi_2(t). \tag{4.10}$$

It is not difficult to explore (4.9), and get

$$\Phi_1(t) = \begin{pmatrix} -\dfrac{\lambda_1'}{N_{21}} e^{\lambda_1' t} & -\dfrac{\lambda_2'}{N_{21}} e^{\lambda_2' t} \\ e^{\lambda_1' t} & e^{\lambda_2' t} \end{pmatrix}, \qquad \Phi_2(t) = \begin{pmatrix} -\dfrac{\lambda_1}{M_{21}} e^{\lambda_1 t} & -\dfrac{\lambda_2}{M_{21}} e^{\lambda_2 t} \\ e^{\lambda_1 t} & e^{\lambda_2 t} \end{pmatrix},$$
$$\Phi_1^{-1}(t) = \begin{pmatrix} -\dfrac{N_{21}}{\lambda_1' - \lambda_2} e^{-\lambda_1' t} & -\dfrac{\lambda_2'}{\lambda_1' - \lambda_2'} e^{-\lambda_1' t} \\ \dfrac{N_{21}}{\lambda_1' - \lambda_2'} e^{-\lambda_2' t} & \dfrac{\lambda_1'}{\lambda_1' - \lambda_2'} e^{-\lambda_2' t} \end{pmatrix}, \qquad \Phi_2^{-1}(t) \begin{pmatrix} -\dfrac{M_{21}}{\lambda_1 - \lambda_2} e^{-\lambda_1 t} & -\dfrac{\lambda_2}{\lambda_1 - \lambda_2} e^{-\lambda_1 t} \\ \dfrac{M_{21}}{\lambda_1 - \lambda_2} e^{-\lambda_2 t} & \dfrac{\lambda_1}{\lambda_1 - \lambda_2} e^{-\lambda_2 t} \end{pmatrix}, \tag{4.11}$$

where $N_{11} = \beta_1 - (\mu_1^2/\gamma_1^2)a_1$, $N_{12} = \alpha_1$, $N_{21} = (\mu_1^2/\gamma_1^2)b_1$, $\lambda_1' = (N_{11} + \sqrt{N_{11}^2 - 4N_{12}N_{21}})/2$, $\lambda_2' = (N_{11} - \sqrt{N_{11}^2 - 4N_{12}N_{21}})/2$, $M_{11} = \beta_2 - (\mu_2^2/\gamma_2^2)a_2$, $M_{12} = \alpha_2$, $M_{21} = (\mu_2^2/\gamma_2^2)b_2$, $\lambda_1 = (M_{11} + \sqrt{M_{11}^2 - 4M_{12}M_{21}})/2$, $\lambda_2 = (M_{11} - \sqrt{M_{11}^2 - 4M_{12}M_{21}})/2$.

By assumption (c2) and (c3), we know that $\lambda_1' < 0$, $\lambda_2' < 0$, $\lambda_1 < 0$, and $\lambda_2 < 0$.

By the ODE theory [37, 38] and above discussion, we know that the solution of (4.1) is given by

$$\begin{pmatrix} \widehat{X}_t \\ \widehat{\theta}_t \end{pmatrix} = \Phi(t)\Phi^{-1}(0) \begin{pmatrix} \mathbb{E}[X_0] \\ \mathbb{E}[\theta_0] \end{pmatrix} + \int_0^t \Phi(t)\Phi^{-1}(s) \begin{pmatrix} S_{xx}(t) \\ S_{\theta x}(t) \end{pmatrix} d\Upsilon_s. \tag{4.12}$$

Using the similar method, we can also obtain the solutions for the following two equations:

$$\begin{pmatrix} d\widehat{X}_t \\ d\widehat{\theta}_t \end{pmatrix} = \begin{pmatrix} \beta_1 - \dfrac{\mu_1^2}{\gamma_1^2} a_1 & \alpha_1 \\ -\dfrac{\mu_1^2}{\gamma_1^2} b_1 & 0 \end{pmatrix} \begin{pmatrix} \widehat{X}_t \\ \widehat{\theta}_t \end{pmatrix} dt + \frac{\mu_1}{\gamma_1} \begin{pmatrix} a_1 \\ b_1 \end{pmatrix} dY_t, \tag{4.13}$$

$$\begin{pmatrix} d\widehat{X}_t \\ d\widehat{\theta}_t \end{pmatrix} = \begin{pmatrix} \beta_2 - \dfrac{\mu_2^2}{\gamma_2^2} a_2 & \alpha_2 \\ -\dfrac{\mu_2^2}{\gamma_2^2} b_2 & 0 \end{pmatrix} \begin{pmatrix} \widehat{X}_t \\ \widehat{\theta}_t \end{pmatrix} dt + \frac{\mu_2}{\gamma_2} \begin{pmatrix} a_2 \\ b_2 \end{pmatrix} dY_t, \tag{4.14}$$

where $\widehat{X}_0 = \mathbb{E}[X_0]$ and $\widehat{\theta}_0 = \mathbb{E}[\theta_0] = \mathbb{E}[\upsilon] = \upsilon$.

The solutions of the two equations are explored as the following form:

$$\begin{aligned} \begin{pmatrix} \widehat{X}_t \\ \widehat{\theta}_t \end{pmatrix} &= \Phi_1(t)\Phi_1^{-1}(0) \begin{pmatrix} \mathbb{E}[X_0] \\ \mathbb{E}[\theta_0] \end{pmatrix} + \int_0^t \Phi_1(t)\Phi_1^{-1}(s) \begin{pmatrix} a_1 \\ b_1 \end{pmatrix} dY_s, \\ \begin{pmatrix} \widehat{X}_t \\ \widehat{\theta}_t \end{pmatrix} &= \Phi_2(t)\Phi_2^{-1}(0) \begin{pmatrix} \mathbb{E}[X_0] \\ \mathbb{E}[\theta_0] \end{pmatrix} + \int_0^t \Phi_2(t)\Phi_2^{-1}(s) \begin{pmatrix} a_2 \\ b_2 \end{pmatrix} dY_s. \end{aligned} \tag{4.15}$$

For (4.14), we have that

$$\begin{pmatrix} \widehat{X}_t \\ \widehat{\theta}_t \end{pmatrix} = \Phi_2(t)\Phi_2^{-1}(0) \begin{pmatrix} \mathbb{E}[X_0] \\ \mathbb{E}[\theta_0] \end{pmatrix} + \int_0^t \Phi_2(t)\Phi_2^{-1}(s) \begin{pmatrix} a_2 \\ b_2 \end{pmatrix} dY_s \tag{4.16}$$

yields that

$$\begin{aligned} \widehat{\theta}_t = {} & \int_0^t \left[a_2 \left(\frac{M_{21}}{\lambda_1 - \lambda_2} e^{-\lambda_2(t-s)} - \frac{M_{21}}{\lambda_1 - \lambda_2} e^{-\lambda_2(t-s)} \right) + b_2 \left(\frac{\lambda_1}{\lambda_1 - \lambda_2} e^{-\lambda_2(t-s)} - \frac{\lambda_2}{\lambda_1 - \lambda_2} e^{-\lambda_2(t-s)} \right) \right] dY_s \\ & + \left(\frac{M_{21}}{\lambda_1 - \lambda_2} e^{-\lambda_2 t} - \frac{M_{21}}{\lambda_1 - \lambda_2} e^{-\lambda_2 t} \right) X_0 + \left(\frac{\lambda_1}{\lambda_1 - \lambda_2} e^{-\lambda_2 t} - \frac{\lambda_2}{\lambda_1 - \lambda_2} e^{-\lambda_2 t} \right) \theta_0. \end{aligned} \tag{4.17}$$

Since $\lambda_1 < 0$ and $\lambda_2 < 0$, it is easy to get

$$\widehat{\theta}_t(\upsilon, \cdot) \longrightarrow \upsilon, P\text{-a.s.}, \quad \text{as } t \longrightarrow \infty. \tag{4.18}$$

For (4.13), we can also get

$$\widehat{\theta}_t(\upsilon, \cdot) \longrightarrow \upsilon, P\text{-a.s.}, \quad \text{as } t \longrightarrow \infty. \tag{4.19}$$

Hence, for (4.1), we can get the following result:

$$\widehat{\theta}_t(\upsilon,\cdot) \longrightarrow \upsilon, P\text{-a.s.}, \quad \text{as } t \longrightarrow \infty. \tag{4.20}$$

The proof is complete. □

Remark 4.2. Under the probability space used in this paper, we can see that Theorem 3.2 is the particular form of Theorem 4.1 if we use Chebyshev's inequality on the result of Theorem 4.1.

Remark 4.3. The strong consistency in Deck [30] requires that $\widehat{\theta}_t$ is a martingale, while, in our result, $\widehat{\theta}_t$ can be not a martingale. Furthermore, when $\widehat{\theta}_t$ is a martingale, our result is more strong than Deck's, so in that case we can relax the conditions as Deck.

5. Conclusions

In this paper, we have investigated the parameter estimation problem for a class of linear stochastic systems called Hull-White stochastic differential equations which are important models in finance. Firstly, Bayesian viewpoint is first chosen to analyze the parameter estimation problem based on Kalman-Bucy linear filtering theory. Secondly, some sufficient conditions on coefficients are given to study the asymptotic convergence problem. Finally, the strong consistent property of estimator is discussed by Kalman-Bucy linear filtering theory and comparison theorem.

Acknowledgments

This work was supported by the National Nature Science Foundation of China under Grant no. 60974030 and the Science and Technology Project of Education Department in Fujian Province JA11211.

References

[1] B. M. Bibby and M. Sørensen, "Martingale estimation functions for discretely observed diffusion processes," *Bernoulli*, vol. 1, no. 1-2, pp. 17–39, 1995.

[2] C. Corrado and T. Su, "An empirical test of the Hull-White option pricing model," *Journal of Futures Markets*, vol. 18, no. 4, pp. 363–378, 1998.

[3] H. Dong, Z. Wang, and H. Gao, "H_∞ fuzzy control for systems with repeated scalar nonlinearities and random packet losses," *IEEE Transactions on Fuzzy Systems*, vol. 17, no. 2, pp. 440–450, 2009.

[4] J. Hu, Z. Wang, and H. Gao, "A delay fractioning approach to robust sliding mode control for discrete-time stochastic systems with randomly occurring non-linearities," *IMA Journal of Mathematical Control and Information*, vol. 28, no. 3, pp. 345–363, 2011.

[5] J. Hu, Z. Wang, H. Gao, and L. K. Stergioulas, "Robust sliding mode control for discrete stochastic systems with mixed time delays, randomly occurring uncertainties, and randomly occurring non-linearities," *IEEE Transactions on Industrial Electronics*, vol. 59, no. 7, pp. 3008–3015, 2012.

[6] J. Hu, Z. Wang, and H. Gao, "Robust H_∞ sliding mode control for discrete time-delay systems with stochastic nonlinearities," *Journal of the Franklin Institute*, vol. 349, no. 4, pp. 1459–1479, 2012.

[7] E. Ince, *Ordinary Differential Equations*, Dover, New York, NY, USA, 1956.

[8] C. R. Rao, *Linear Statistical Inference and its Applications*, John Wiley & Sons, New York, NY, USA, 1973.

[9] M. H. A. Davis, *Linear Estimation and Stochastic Control*, Chapman and Hall, London, UK, 1977.

[10] M. Arato, A. Kolmogrorov, and Y. Sinai, *On Parameter Estimation of a Complex Stationary Gaussian Process*, vol. 146, Doklady Academy, USSR, 1962.

[11] H. Frydman and P. Lakner, "Maximum likelihood estimation of hidden Markov processes," *The Annals of Applied Probability*, vol. 13, no. 4, pp. 1296–1312, 2003.

[12] L. Galtchouk and V. Konev, "On sequential estimation of parameters in semimartingale regression models with continuous time parameter," *The Annals of Statistics*, vol. 29, no. 5, pp. 1508–1536, 2001.

[13] N. R. Kristensen, H. Madsen, and S. B. Jørgensen, "Parameter estimation in stochastic grey-box models," *Automatica*, vol. 40, no. 2, pp. 225–237, 2004.

[14] B. L. S. Prakasa Rao, *Statistical Inference for Diffusion Type Processes*, vol. 8, Edward Arnold, London, UK, 1999.

[15] I. Shoji and T. Ozaki, "Comparative study of estimation methods for continuous time stochastic processes," *Journal of Time Series Analysis*, vol. 18, no. 5, pp. 485–506, 1997.

[16] H. Dong, Z. Wang, and H. Gao, "Robust H_∞ filtering for a class of nonlinear networked systems with multiple stochastic communication delays and packet dropouts," *IEEE Transactions on Signal Processing*, vol. 58, no. 4, pp. 1957–1966, 2010.

[17] H. Dong, Z. Wang, and H. Gao, "Distributed filtering for a class of time-varying systems over sensor networks with quantization errors and successive packet dropouts," *IEEE Transactions on Signal Processing*, vol. 60, no. 6, pp. 3164–3173, 2012.

[18] J. Hu, Z. Wang, H. Gao, and L. K. Stergioulas, "Probability-guaranteed H finite-horizon filtering for a class of nonlinear time-varying systems with sensor saturations," *Systems and Control Letters*, vol. 61, no. 4, pp. 477–484, 2012.

[19] J. Hu, Z. Wang, Y. Niu, and L. K. Stergioulas, "H_∞ sliding mode observer design for aclass of nonlinear discrete time-delay systems: a delay-fractioning approach," *International Journal of Robust and Nonlinear Control*. In press.

[20] J. Picard, "Asymptotic study of estimation problems with small observation noise," in *Stochastic Modelling and Filtering (Rome, 1984)*, vol. 91 of *Lecture Notes in Control and Inference Science*, Springer, 1987.

[21] B. Shen, Z. Wang, and Y. S. Hung, "Distributed H_∞-consensus filtering in sensor networks with multiple missing measurements: the finite-horizon case," *Automatica*, vol. 46, no. 10, pp. 1682–1688, 2010.

[22] B. Shen, Z. Wang, and X. Liu, "Bounded H_∞ synchronization and state estimation for discrete time-varying stochastic complex networks over a finite-horizon," *IEEE Transactions on Neural Networks*, vol. 22, no. 1, pp. 145–157, 2011.

[23] B. Shen, Z. Wang, Y. Hung, and G. Chesi, "Distributed H_∞ filtering for polynomial nonlinear stochastic systems in sensor networks," *IEEE Transactions on Industrial Electronics*, vol. 58, no. 5, pp. 1971–1979, 2011.

[24] Z. Wang, J. Lam, and X. Liu, "Filtering for a class of nonlinear discrete-time stochastic systems with state delays," *Journal of Computational and Applied Mathematics*, vol. 201, no. 1, pp. 153–163, 2007.

[25] Z. Wang, X. Liu, Y. Liu, J. Liang, and V. Vinciotti, "An extended Kalman filtering approach to modelling nonlinear dynamic gene regulatory networks via short gene expression time series," *IEEE/ACM Transactions on Computational Biology and Bioinformatics*, vol. 6, no. 3, pp. 410–419, 2009.

[26] G. Wei and H. Shu, "H_∞ filtering on nonlinear stochastic systems with delay," *Chaos, Solitons and Fractals*, vol. 33, no. 2, pp. 663–670, 2007.

[27] M. R. James and F. Le Gland, "Consistent parameter estimation for partially observed diffusions with small noise," *Applied Mathematics and Optimization*, vol. 32, no. 1, pp. 47–72, 1995.

[28] R. S. Liptser and A. N. Shiryayev, *Statistics of Random Processes. I*, Springer, New York, NY, USA, 1977.

[29] Yu. A. Kutoyants, "Parameter estimation for diffusion type processes of observation," *Mathematische Operationsforschung und Statistik Series Statistics*, vol. 15, no. 4, pp. 541–551, 1984.

[30] T. Deck, "Asymptotic properties of Bayes estimators for Gaussian Itô-processes with noisy observations," *Journal of Multivariate Analysis*, vol. 97, no. 2, pp. 563–573, 2006.

[31] J. P. N. Bishwal, *Parameter Estimation in Stochastic Differential Equations*, Springer, Berlin, Germany, 2008.

[32] A. Brace, D. Gatarek, and M. Musiela, "The market model of interest rate dynamics," *Mathematical Finance*, vol. 7, no. 2, pp. 127–155, 1997.

[33] D. Heath, R. Jarrow, and A. Morton, "Bond pricing and the term structure of interest-rates: a new methodology," *Econometrica*, vol. 60, no. 1, pp. 77–105, 1992.

[34] J. Hull and A. White, "The pricing of option on assets with stochastic volatilities," *The Journal of Finance*, vol. 42, no. 2, pp. 281–300, 1987.
[35] J. Hull and A. White, "The general Hull-White model and super calibration," *Financial Analysis Journal*, vol. 57, no. 6, pp. 34–43, 2001.
[36] G. Kallianpur and R. S. Selukar, "Parameter estimation in linear filtering," *Journal of Multivariate Analysis*, vol. 39, no. 2, pp. 284–304, 1991.
[37] V. I. Arnold, *Geometrical Methods in the Theory of Ordinary Differential Equations*, Springer, New York, NY, USA, 1983.
[38] E. L. Ince, *Ordinary Differential Equations*, Dover, New York, NY, USA, 1944.

Hindawi Publishing Corporation
Mathematical Problems in Engineering
Volume 2012, Article ID 581040, 22 pages
doi:10.1155/2012/581040

Research Article

Optimality Condition-Based Sensitivity Analysis of Optimal Control for Hybrid Systems and Its Application

Chunyue Song

State Key Laboratory of Industrial Control Technology, Institute of Industrial Process Control, Zhejiang University, Hangzhou 310027, China

Correspondence should be addressed to Chunyue Song, cysong@iipc.zju.edu.cn

Received 4 April 2012; Revised 21 June 2012; Accepted 11 July 2012

Academic Editor: Jun Hu

Gradient-based algorithms are efficient to compute numerical solutions of optimal control problems for hybrid systems (OCPHS), and the key point is how to get the sensitivity analysis of the optimal control problems. In this paper, optimality condition-based sensitivity analysis of optimal control for hybrid systems with mode invariants and control constraints is addressed under a priori fixed mode transition order. The decision variables are the mode transition instant sequence and admissible continuous control functions. After equivalent transformation of the original problem, the derivatives of the objective functional with respect to control variables are established based on optimal necessary conditions. By using the obtained derivatives, a control vector parametrization method is implemented to obtain the numerical solution to the OCPHS. Examples are given to illustrate the results.

1. Introduction

In many fields of applications, such as powertrain systems of automobiles and multistage chemical processes, dynamics of the systems involve a sequence of distinct modes with fixed mode transition order, forming a hybrid system characterized by the coexistence and interaction of discrete and continuous dynamics (the mode is commonly denoted by a discrete state of the systems in hybrid systems literature). To achieve some overall optimal performance for the systems, the duration and the admissible continuous control function of each mode must be determined as a whole [1–3]; thus, it necessitates the use of theories and techniques for the analysis and synthesis of hybrid dynamical systems. With the growing importance of hybrid models, various classes of hybrid systems for analysis, design, and

optimization have been addressed by research communities in recent years. For more discussions on various literature results, the reader is referred to [4–8], and the references therein.

The existed results on OCPHS can be divided into the following two categories. One is about the optimal control theory on OCPHS. The theory inherits conventional optimal control theory and can be regarded as the extension of conventional optimal control theory [3, 9–14]. When control can take any value, Xu and Antsaklis [3] and Hwang et al. [9] addressed the variational method for hybrid systems. Sussmann [10], Shaikh and Caines [11], and Dmitruk and Kaganovich [12] established the Maximum Principle for hybrid systems with control constraints. Branicky et al. [14] and Bensoussan and Menaldi [13] provided the dynamic programming principle for general hybrid systems.

The other results focus on how to compute optimal control for OCPHS, which can be carried out by using a wide variety of methods (see [3, 6, 11, 15–20] and the references therein). Given a prespecified order of mode transitions, Xu and Antsaklis [3] obtained the optimal continuous control and optimal switching instants based on parameterization of the switching instant for switching hybrid systems with free control. Under a fixed switching sequence of modes, Attia et al. [19] considered an optimization problem for a class of impulsive hybrid systems where continuous control function is not involved. When switching hybrid systems with control constraints are considered, Shaikh and Caines [11] proposed two algorithms for obtaining the optimal control. As far as switching hybrid systems without external continuous control function are concerned, Egerstedt et al. [6] and Johnson and Murphey [18] derived the gradients and second-order derivatives of the cost functional, respectively, and used them to design an associated algorithm to get the mode transition instants. Based on the hybrid Maximum Principle, Taringoo and Caines [20] provided gradient geodesic and Newton geodesic algorithms for the optimization of autonomous hybrid systems, and convergence analysis for the algorithms was also provided. From the view of dynamic programming, Seatzu et al. [16] provided an optimal state feedback control law to switched piecewise affine autonomous systems. Generally, these algorithms pose the hierarchy [17, 21, 22], and the basic module of the hierarchical algorithms is how to get optimal continuous control and optimal mode transition instants, though the main challenge of OCPHS is how to get the optimal mode transition order. The basic module of the hierarchical algorithms is commonly gradient based due to that gradient information can provide a better searching direction and hence reduce computation burden and help the gradient-based algorithms converge quickly, which motivates us to pay attention to the sensitivity analysis of optimal control for hybrid systems.

Although the derivative of cost functional with respect to switching instants has been discussed in the aforementioned literature [3, 6, 18], the derivative of cost functional with respect to control function is not involved. When hybrid systems are considered, due to the coexistence and interaction of discrete and continuous dynamics, the derivative of cost functional w.r.t control functions is nontrivial and is not directly formulated by $\partial H/\partial u$ as conventional optimal control indicates, where H is the Hamiltonian function. The derivative will be a function of the derivatives of continuous states w.r.t control functions at the instants of subsequent modes. In this paper, the derivatives of cost functional w.r.t control functions are established analytically, which can facilitate the design of associated gradient-based algorithms.

Motivated by the work of Vassiliadis et al. [1, 2] and Jennings et al. [23], in this paper, optimal control problem of hybrid systems (OCPHS) with mode invariants which describe the conditions that continuous states have to satisfy at this mode are considered. Based on optimal necessary conditions, the derivatives of the objective functional w.r.t control

variables, that is, the mode transition instant sequence and admissible continuous control functions, are derived analytically. As a result, a control vector parametrization method is implemented to obtain the numerical solution to optimal control of the hybrid systems with the obtained derivatives. The sensitivity analysis in Vassiliadis et al. [1, 2] is similar to the work, in which the sensitivity of states w.r.t control parameters is directly obtained from the state equations and the sensitivity of objective functional with respect to control parameters is not involved. In contrast, this paper derives the derivatives of cost functional w.r.t control variables based on the optimality conditions and gives the explicitly expression of the derivatives. Therefore, the main contributions of this paper are listed as follows. (a) Optimality conditions-based sensitivity analysis of optimal control for hybrid systems with mode invariants are given explicitly, and (b) following the given derivatives, a control vector parameterization method is designed to obtain the numerical solution. Compared with the existing results on the OCPHS with fixed mode transition order, the settings in this paper cover not only the control constraints, but also the continuous states constraints, which makes the results here more general.

The paper is organized as follows. In the next section, the hybrid system with mode invariants and its optimal control problem are formulated. In Section 3, the equivalent problem and associated optimal conditions are analyzed. The derivatives of the objective functional w.r.t control variables are established in Section 4, and a control vector parametrization approach is also proposed in this section. Some numerical examples are presented in Section 5, and Section 6 contains conclusions.

Terminology and Notation

$\mathbb{N}$ denotes the set of positive integers. $\mathbb{R}$ and $\mathbb{R}_+$ denote the set of real numbers and nonnegative real numbers, respectively. A^T denotes the transpose of a vector (or a matrix) A. $C^l([a,b],\mathbb{R}^n)$ denotes the family of continuous functions f from $[a,b]$ to $\mathbb{R}^n$ with up to l order derivatives. $\|\cdot\|$ denotes the Euclidean norm.

2. Hybrid Systems and Its Optimal Control Problem

2.1. Hybrid Systems

Engineered systems, such as chemical engineering systems and powertrain systems of automobiles, always undergo multiple modes which are represented by a discrete state i taking values from set $I \doteq \{1,2,\ldots,M\}$ and pose hybrid characters. The evolution of discrete state i is determined by mode transition sequence. A mode transition sequence schedules the sequence of active modes $i_j, i_j \in I$ and is a sequence of pairs of (t_{j-1}, i_j), which can be defined by $\{(t_0,i_1),(t_1,i_2),\ldots\} \doteq (\theta,\pi)$ where $\theta \doteq \{t_0,t_1,\ldots\}$ and $\pi \doteq \{i_1,i_2,\ldots\}$ are referred to as mode transition instants and mode transition order, respectively. A pair of (t_{j-1}, i_j) indicates that at instant t_{j-1}, the hybrid system transits from mode i_{j-1} to mode i_j. During the time interval $[t_{j-1}, t_j)$, mode i_j is active and unchanged.

The mode transition order π of the considered hybrid dynamical systems is known a priori. Without loss of generality, it is supposed that the mode transition order is $\{i_1,i_2,\ldots,i_K\}$ over the finite horizon $[t_0,t_f]$, $i_j \in I$, $j = 1,2,\ldots,K$. Moreover, according to each distinct mode, the continuous states are restricted in a specified range which is referred to as mode invariants. Here, the mode invariants are formulated by a set of inequalities. Thus, for each

mode $i_j \in I$ and its active horizon $[t_{j-1}, t_j)$, the dynamics of the considered systems can be formulated by

$$\begin{gathered} \dot{x} = f_{i_j}(x,u), \\ p_{i_j}(x) < 0, \\ x(t_{j-1}) = \varphi_{i_j}\left(x\left(t_{j-1}^-\right)\right), \\ g_{i_j}\left(x\left(t_j^-\right)\right) = 0, \end{gathered} \tag{2.1}$$

where $x \in \mathbb{R}^n$, $u \in \mathbf{U}_{i_j} \subseteq \mathbb{R}^m$ is a piecewise continuous function, $f_{i_j} : \mathbb{R}^n \times \mathbf{U}_{i_j} \to \mathbb{R}^n$, t_j is the mode transition instant when a particular mode transition occurs, p_{i_j}, φ_{i_j}, and g_{i_j} are $h_{i_j} < n$, n and $r_{i_j} \leq n$ dimensional vectors for $i_j \in I$, respectively. $n, m, h_{i_j}, r_{i_j} \in \mathbb{N}$. To make the hybrid systems formulated by (2.1) well defined, the following assumption is needed.

Assumption 2.1. For any $i_j \in I$, $f_{i_j} \in C^l(\mathbb{R}^n \times \mathbf{U}_{i_j}; \mathbb{R}^n)$, $l \geq 1$, $l \in \mathbb{N}$, and such that a uniform Lipschitz condition holds, that is, there exists $K_f < \infty$ such that

$$\left\| f_{i_j}(x,u) - f_{i_j}(x',u) \right\| \leq K_f \|x - x'\|, \tag{2.2}$$

where $x, x' \in \mathbb{R}^n, u \in \mathbf{U}_{i_j}$.

Remark 2.2. $p_{i_j}(x) < 0$ indicates mode invariant for mode $i_j \in I$, which describes the conditions that the continuous states have to satisfy at this mode and can be referred to as the *path constraints* of the continuous states in Vassiliadis et al. [1, 2].

Remark 2.3. $g_{i_j}(x(t_j^-)) = 0$ can be referred to as mode transition conditions which describe the conditions on the continuous states under which a particular mode transition takes place. When mode i_j is active over $[t_{j-1}, t_j)$, then, at t_j^-, x meets an $(n - r_{i_j})$-dimensional smooth manifold $S_{i_j} = \{x \mid g_{i_j}(x) = 0\}$ and mode transition from i_j to i_{j+1} occurs. The mode transition conditions implicitly define the mode i_j's active horizon $[t_{j-1}, t_j)$. To prevent Zeno behavior from occurrence, $t_{j-1} < t_j$ is assumed. Physically, the mode transition conditions are always the boundary of closure of the mode invariant $p_{i_j} < 0$.

Remark 2.4. $x(t_{j-1}) = \varphi_{i_j}(x(t_{j-1}^-))$ is the outcome of the mode transition and describes the effect that the transition will have on the continuous states. It can be viewed as *junction conditions* in Vassiliadis et al. [1, 2]. It is assumed that $\varphi_{i_j} \in C^l(\mathbb{R}^n)$, $l \geq 1$, $l \in \mathbb{N}$.

Remark 2.5. Basically, for general hybrid systems, the evaluation of i should be formulated by a function of impulsive control or a graph, which generates mode transition sequence, as formulated in Song and Li [24] and Cassandras and Lygeros [8]. However, the order of the mode transition π is known a prior here thus, the evaluation of i is determined only by the transition instants t_j, and the evaluation function of i is omitted here.

Besides Assumption 2.1, to make the considered systems to be well defined, there are some additional assumptions on mode invariants and mode transition conditions should be

imposed. Here, it is supposed that the mode invariants and mode transition conditions meet the requirements as in Taringoo and Caines [20].

2.2. Optimal Control Problem for Hybrid Systems

Let $L_i \in C^l(\mathbb{R}^n \times \mathbf{U}_i; \mathbb{R})$ be a running cost function, $\varphi_{ij} \in C^l(\mathbb{R}^n; \mathbb{R}_+)$ be a discrete state transition cost function, and $\phi \in C^l(\mathbb{R}^n; \mathbb{R}_+)$ be a terminal cost function, $i, j \in I$, $l \geq 1$, $l \in \mathbb{N}$, respectively. The optimal control problem for the hybrid systems (2.1) is stated as follows.

Optimal Problem A

Consider a hybrid system formulated by (2.1), given a fixed time interval $[t_0, t_f]$ and a prespecified mode transition order $\pi = \{i_1, i_2, \ldots, i_K\}$, find a continuous control $u \in \mathbf{U}_{i_j}$ in each mode $i_j \in I$ and mode transition instants $\theta = \{t_1, \ldots, t_{K-1}\}$, such that the corresponding continuous state trajectory x departs from a given initial state $x(t_0) = x_0$ and meets an $(n-l_f)$-dimensional smooth manifold $S_f = \{x \mid \vartheta(x) = 0, \vartheta : \mathbb{R}^n \to \mathbb{R}^{l_f}\}$, $l_f \in \mathbb{N}$, at t_f and the cost functional

$$J(\theta, u) = \phi(x(t_f)) + \int_{t_0}^{t_f} L_{i(t)}(x(t), u(t))dt + \sum_{j=1}^{K-1} \varphi_{i_j i_{j+1}}\left(x\left(t_j^-\right)\right) \tag{2.3}$$

is minimized.

Remark 2.6. As it is well known, when t_0 and t_f are unknown points in some fixed interval $T \subset \mathbb{R}_+$, this problem can be transformed to one with fixed time essentially by introducing an additional state variable.

There are fruitful strategies about how to compute OCPHS (see [15] and the references therein), and the basic idea is briefly reviewed as follows for completeness.

Obtaining the optimal control for hybrid systems is very difficult due to the interactions between the continuous states and discrete states which produce a mode transition sequence that increases the feasibility range of the decision variables. One algorithm framework for dealing with this complexity is the decomposition method as follows:

$$\min_{((\pi,\theta),u)} J((\pi,\theta),u) = \min_{(\pi,\theta)} \min_{u} J(u \mid (\pi,\theta)) = \min_{\pi} \min_{\theta} \min_{u} J((u,\theta) \mid \pi), \tag{2.4}$$

where $J(\cdot \mid b)$ means that b is given.

According to this framework, the master problem is how to get the optimum of the inner functional, that is, minimize $J(u, \theta)$ given π. The key point of finding the optimal solution of $J(u, \theta)$ is how to get the sensitivity of the objective with respect to control variables, which provides a better direction for searching and hence reduces computational burden and help associated algorithms converge quickly and accelerate the primary problem convergence eventually.

In next section, the derivatives of cost functional with respect to control variables are established analytically based on optimality condition, which can facilitate the design of associated gradient-based algorithms.

3. Equivalent Problem and Its Optimal Conditions

When control vector parametrization methods are implemented to obtain numerical solution to the OCPHS, updating the parameters of control profiles should be at the same time point when iterative procedure is running. However, the fact is that the mode active horizon $[t_{j-1}, t_j)$ for mode $i_j \in I$ is varying during the procedure running, so a fixed horizon should be introduced, which will guarantee the updating of parameters of control profiles is at the same time point. For this purpose, let $\tau \in [0, K]$ be a time independent variable, and $t \in [t_{j-1}, t_j)$ can be formulated by

$$t = t_{j-1} + (\tau - (j-1))(t_j - t_{j-1}), \quad \tau \in [j-1, j),\ j = 1, \ldots, K. \tag{3.1}$$

In addition, to deal with mode invariants constraints $p_{i_j}(x) < 0$, slack algebraic variable $s_{i_j} = [s_{i_j 1}, \ldots, s_{i_j h_{i_j}}]^T \in \mathbb{R}_+^{h_{i_j}}$ is introduced for each mode $i_j \in I$, such that $p_{i_j}(x) + \operatorname{diag}[s_{i_j 1}, \ldots, s_{i_j h_{i_j}}] s_{i_j} = 0$. For $\tau \in [j-1, j)$, denote $\mathbf{x}_j(\tau) \doteq x(t_{j-1} + (\tau - (j-1))(t_j - t_{j-1}))$, $\mathbf{u}_j(\tau) \doteq u(t_{j-1} + (\tau - (j-1))(t_j - t_{j-1}))$, $\mathbf{s}_j(\tau) \doteq s_{i_j}(t_{j-1} + (\tau - (j-1))(t_j - t_{j-1}))$, and let $\mathbf{x} = [\mathbf{x}_1, \ldots, \mathbf{x}_K]^T$, $\mathbf{u} = [\mathbf{u}_1, \ldots, \mathbf{u}_K]^T$, and $\mathbf{s} = [\mathbf{s}_1, \ldots, \mathbf{s}_K]^T$.

According to the above definition, the Optimal Problem A can be transcribed into an equivalent Optimal Problem B as follows:

Optimal Problem B

Given a fixed interval $[0, K]$, find continuous inputs $\mathbf{u} \in \mathbf{U}_{i_1} \times \cdots \times \mathbf{U}_{i_K}$, $\mathbf{s} \in \mathbb{R}_+^{h_{i_1}} \times \cdots \times \mathbb{R}_+^{h_{i_K}}$ and θ, such that the corresponding continuous state trajectory $\mathbf{x}_1$ departs from a given initial state $\mathbf{x}_1(0) = x_0$ and $\mathbf{x}_K$ meets an $(n - l_f)$-dimensional smooth manifold $S_f = \{\mathbf{x}_K \mid \vartheta(\mathbf{x}_K) = 0, \vartheta : \mathbb{R}^n \to \mathbb{R}^{l_f}\}$ at K, and the cost functional

$$\widetilde{J}(\theta, \mathbf{u}, \mathbf{s}) = \phi(\mathbf{x}_K(K)) + \sum_{j=1}^{K} \int_{j-1}^{j} \widetilde{L}_{i_j}(\mathbf{x}_j(\tau), \mathbf{u}_j(\tau), \mathbf{s}_j(\tau)) d\tau + \sum_{j=1}^{K-1} \varphi_{i_j i_{j+1}}(\mathbf{x}_j(j^-)) \tag{3.2}$$

is minimized, subject to

$$\begin{aligned} \frac{d\mathbf{x}_j(\tau)}{d\tau} &= \widetilde{f}_{i_j}(\mathbf{x}_j(\tau), \mathbf{u}_j(\tau)) \doteq (t_j - t_{j-1}) f_{i_j}(\mathbf{x}_j(\tau), \mathbf{u}_j(\tau)), \\ \mathbf{x}_j(j-1) &= \varphi_{i_j}\left(\mathbf{x}_{j-1}\left((j-1)^-\right)\right), \\ g_{i_j}(\mathbf{x}_j(j^-)) &= 0, \end{aligned} \tag{3.3}$$

where

$$\widetilde{L}_{i_j}(\mathbf{x}_j, \mathbf{u}_j, \mathbf{s}_j) = (t_j - t_{j-1}) \overline{L}_{i_j}, \qquad \overline{L}_{i_j} = L_{i_j}(\mathbf{x}_j, \mathbf{u}_j) + M \sum_{l=1}^{h_{i_j}} \left(p_{i_j l}(\mathbf{x}_j) + s_{i_j l}^2\right)^2, \tag{3.4}$$

and M is a large positive constant.

According to Theorems 2 and 3 in Dmitruk and Kaganovich [12], when M is big enough Optimal Problem B is equivalent to Optimal Problem A.

Remark 3.1. The penalty function term, say, $M\sum_{l=1}^{h_{i_j}}(p_{i_jl}(\mathbf{x}_j)+\mathbf{s}_{i_jl}^2)^2$, cannot always guarantee the state satisfies the mode invariant conditions. However, the method works well in practice; moreover, the mode transition order is fixed in this paper which reduces the negative effect of the penalty function method for OCPHS.

For $\tau\in[j-1,j)$, $j=1,\ldots,K$, let $\lambda_j\in\mathbb{R}^n$, and define Hamiltonian function H_j by

$$H_j(\lambda_j,\mathbf{x}_j,\mathbf{u}_j,\mathbf{s}_j)=\widetilde{L}_{i_j}(\mathbf{x}_j,\mathbf{u}_j,\mathbf{s}_j)+\lambda_j^T\widetilde{f}_{i_j}(\mathbf{x}_j,\mathbf{u}_j), \tag{3.5}$$

and according to Sussmann [10], Shaikh and Caines [11], and Dmitruk and Kaganovich [12], the following Theorem 3.2 holds.

Theorem 3.2. *In order that* $\mathbf{u}$ *and* $\mathbf{s}$ *are optimal for Optimal Problem B, it is necessary that there exist vector functions* λ_j, $j=1,\ldots,K$, *such that the following conditions hold:*

(a) *for almost any* $\tau\in[j-1,j)$, *the following state equations hold:*

$$\frac{d\mathbf{x}_j(\tau)}{d\tau}=\widetilde{f}_{i_j}(\mathbf{x}_j(\tau),\mathbf{u}_j(\tau)), \tag{3.6}$$

(b) *for almost any* $\tau\in[j-1,j)$, *the following costate equations hold:*

$$\dot{\lambda}_j=-\left(\frac{\partial\widetilde{L}_{i_j}}{\partial\mathbf{x}_j}\right)^T-\left(\frac{\partial\widetilde{f}_{i_j}}{\partial\mathbf{x}_j}\right)^T\lambda_j, \tag{3.7}$$

(c) *for a.e.* $\tau\in[j-1,j)$,

$$H_j\left(\lambda_j^*,\mathbf{x}_j^*,\mathbf{u}_j^*,\mathbf{s}_j^*\right)=0, \tag{3.8}$$

(d) *minimality condition: for all* $\tau\in[j-1,j)$,

$$\min_{\left\{\mathbf{u}_j\in\mathbf{U}_{i_j},\mathbf{s}_j\in\mathbb{R}_+^{h_{i_j}}\right\}}H_j\left(\lambda_j^*,\mathbf{x}_j^*,\mathbf{u}_j,\mathbf{s}_j^*\right)=0, \tag{3.9}$$

(e) *transversality conditions for* λ_j,

$$\begin{aligned}
&\lambda_{j+1}(j) = \beta_j, \quad j = 1, \ldots, K-1, \\
&\lambda_j(j^-) = \left(\frac{\partial g_{i_j}}{\partial \mathbf{x}_j(j^-)}\right)^T \alpha_j - \left(\frac{\partial \varphi_{i_{j+1}}}{\partial \mathbf{x}_j(j^-)}\right)^T \beta_j + \left(\frac{\partial \varphi_{i_j i_{j+1}}}{\partial \mathbf{x}_j(j^-)}\right)^T, \quad j = 1, \ldots, K-1, \\
&\lambda_K(K) = \left(\frac{\partial \phi}{\partial \mathbf{x}_K(K)}\right)^T + \left(\frac{\partial \vartheta}{\partial \mathbf{x}_K(K)}\right)^T \alpha_K,
\end{aligned} \tag{3.10}$$

where $\alpha_j \in \mathbb{R}^{h_i}$, $\beta_j \in \mathbb{R}^n$ *are Lagrangian multipliers. Based on Theorem 3.2, the sensitivity analysis is established in the next section for Optimal Problem B.*

4. Sensitivity Analysis and Parametrization Method

For finding numerical solution to the OCPHS effectively, based on Theorem 3.2, the derivatives of the objective functional $\widetilde{J}(\cdot)$ with respect to the control $\mathbf{u}$, $\mathbf{s}$, and the mode transition instant t_j, $j = 1, \ldots, K-1$ are established in this section, and by using the obtained derivatives associated parametrization method is proposed.

4.1. Sensitivity Analysis

Lemma 4.1. *The derivatives of* $\mathbf{x}_j(j^-)$, $j = 1, \ldots, K$, *w.r.t* t_k *and* $\mathbf{u}_k$ *are given, respectively, as follows for* $k = 1, \ldots, K-1$,

$$\begin{aligned}
&\frac{d\mathbf{x}_j(j^-)}{dt_k} = 0, \quad j = 1, \ldots, k-1, \\
&\frac{d\mathbf{x}_k(k^-)}{dt_k} = f_{i_k}(\mathbf{x}_k(k^-), \mathbf{u}_k(k^-)), \\
&\frac{d\mathbf{x}_{k+1}((k+1)^-)}{dt_k} = \Omega_{k+1}, \\
&\frac{d\mathbf{x}_j(j^-)}{dt_k} = \left[\prod_{l=k+2}^{j} \Phi_l(l, l-1) \frac{d\varphi_{i_l}}{d\mathbf{x}_{l-1}((l-1)^-)}\right] \Omega_{k+1}, \quad j = k+2, \ldots, K,
\end{aligned} \tag{4.1}$$

$$\begin{aligned}
&\frac{\delta\mathbf{x}_j(j^-)}{\delta\mathbf{u}_k} = 0, \quad j = 1, \ldots, k-1, \\
&\frac{\delta\mathbf{x}_k(k^-)}{\delta\mathbf{u}_k} = \Gamma_k(\tau), \\
&\frac{\delta\mathbf{x}_j(j^-)}{\delta\mathbf{u}_k} = \prod_{l=k+1}^{j} \left[\Phi_l(l, l-1) \frac{d\varphi_{i_l}}{d\mathbf{x}_{l-1}((l-1)^-)}\right] \Gamma_k(\tau), \quad j = k+1, \ldots, K,
\end{aligned} \tag{4.2}$$

where

$$\Omega_{k+1} = \Phi_{k+1}(k+1,k)\frac{d\psi_{i_{k+1}}}{d\mathbf{x}_k(k^-)} f_{i_k}\left(\mathbf{x}_k\left(k^-\right), \mathbf{u}_k\left(k^-\right)\right) - f_{i_{k+1}}(\mathbf{x}_{k+1}(k), \mathbf{u}_{k+1}(k)),$$
$$\Gamma_k(\tau) = (t_k - t_{k-1})\Phi_k(k,\tau)\frac{\partial f_{i_k}}{\partial \mathbf{u}_k}, \qquad \Phi_l(\tau, v) = \exp\left(\int_v^\tau (t_l - t_{l-1})\frac{\partial f_{i_l}}{\partial \mathbf{x}_l} da\right). \tag{4.3}$$

Note that $\mathbf{x}(t_j)$ is a functional vector of $\mathbf{u}_k$, and the expression $\delta\mathbf{x}_j/\delta\mathbf{u}_k$ is used, where the notation $\delta\mathbf{x}_j/\delta\mathbf{u}_k$ is the functional derivatives which describe the response of the functional $\mathbf{x}_j$ to an infinitesimal change in the function $\mathbf{u}_k$ at each point.

Proof. The proof of (4.1) is only going to be shown for easily reading. The proof for (4.2) can be found in Appendix.

When $j = 1, \ldots, k-1$, $\mathbf{x}_j(j^-)$ and $\mathbf{x}_{j+1}(j)$ are independent of t_k, and obviously $d\mathbf{x}_j(j^-)/dt_k = 0$ holds. In the case of $j = k$, $\mathbf{x}_k(k^-)$ is a function of t_k which gives rise to $d\mathbf{x}_k(k^-)/dt_k = f_{i_k}(\mathbf{x}_k(k^-), \mathbf{u}_k(k^-))$.

Case i. ($j = k+1$). In this case, $\mathbf{x}_{k+1}$ is a function of t_k and $\mathbf{x}_{k+1}(k)$, and we have

$$\frac{d\mathbf{x}_{k+1}(\tau)}{dt_k} = \frac{\partial \mathbf{x}_{k+1}}{\partial t_k} + \frac{\partial \mathbf{x}_{k+1}}{\partial \mathbf{x}_{k+1}(k)}\frac{\partial \mathbf{x}_{k+1}(k)}{\partial t_k}. \tag{4.4}$$

Note that in (4.4), $\partial\mathbf{x}_{k+1}/\partial t_k$ is produced by the perturbation of t_k, and $(\partial\mathbf{x}_{k+1}/\partial\mathbf{x}_{k+1}(k))(\partial\mathbf{x}_{k+1}(k)/\partial t_k)$ is produced by the perturbation of $\mathbf{x}_{k+1}(k)$ with respect to t_k. Obviously, for $\tau \in [k, k+1)$,

$$\frac{\partial \mathbf{x}_{k+1}(\tau)}{\partial t_k} = -f_{i_{k+1}}(\mathbf{x}_{k+1}(k), \mathbf{u}_{k+1}(k)). \tag{4.5}$$

The solution to $\partial\mathbf{x}_{k+1}(\tau)/\partial\mathbf{x}_{k+1}(k)$ is given by

$$\frac{\partial \mathbf{x}_{k+1}(\tau)}{\partial \mathbf{x}_{k+1}(k^+)} = I + (t_{k+1} - t_k)\int_k^\tau \frac{\partial f_{i_{k+1}}}{\partial \mathbf{x}_{k+1}}\frac{\partial \mathbf{x}_{k+1}(v)}{\partial \mathbf{x}_{k+1}(k)} dv. \tag{4.6}$$

Equation (4.6) is a linear system about $\partial\mathbf{x}_{k+1}/\partial\mathbf{x}_{k+1}(k)$. Define the state transition matrix $\Phi_l(\tau, v)$ by

$$\Phi_l(\tau, v) = \exp\left(\int_v^\tau (t_l - t_{l-1})\frac{\partial f_{i_l}(a)}{\partial \mathbf{x}_l(a)} da\right), \tag{4.7}$$

according to (4.6), and we have

$$\frac{\partial \mathbf{x}_{k+1}(\tau)}{\partial \mathbf{x}_{k+1}(k)} = \Phi_{k+1}(\tau, k). \tag{4.8}$$

Thus,

$$\frac{d\mathbf{x}_{k+1}(\tau)}{dt_k} = \Phi_{k+1}(\tau,k)\frac{\partial \mathbf{x}_{k+1}(k)}{\partial t_k} - f_{i_{k+1}}(\mathbf{x}_{k+1}(k),\mathbf{u}_{k+1}(k)). \tag{4.9}$$

At transition instants t_j, since $\mathbf{x}_{j+1}(j) = \psi_{i_{j+1}}(\mathbf{x}_j(j^-))$, so

$$\frac{d\mathbf{x}_{j+1}(j)}{dt_k} = \frac{d\psi_{i_{j+1}}}{d\mathbf{x}_j(j^-)}\frac{d\mathbf{x}_j(j^-)}{dt_k}, \tag{4.10}$$

which implies

$$\frac{\partial \mathbf{x}_{k+1}(k)}{\partial t_k} = \frac{d\psi_{i_{k+1}}}{d\mathbf{x}_k(k^-)}\frac{d\mathbf{x}_k(k^-)}{dt_k} = \frac{d\psi_{i_{k+1}}}{d\mathbf{x}_k(k^-)} f_{i_k}(\mathbf{x}_k(k^-),\mathbf{u}_k(k^-)). \tag{4.11}$$

According to (4.9), and we have

$$\begin{aligned}\frac{d\mathbf{x}_{k+1}((k+1)^-)}{dt_k} &= \Phi_{k+1}(k+1,k)\frac{d\psi_{i_{k+1}}}{d\mathbf{x}_k(k^-)} f_{i_k}(\mathbf{x}_k(k^-),\mathbf{u}_k(k^-)) \\ &\quad - f_{i_{k+1}}(\mathbf{x}_{k+1}(k),\mathbf{u}_{k+1}(k)) \doteq \Omega_{k+1}.\end{aligned} \tag{4.12}$$

Case *ii*. $(j = k+2,\ldots,K)$. When $j = k+2,\ldots,K$, the following holds:

$$\frac{d\mathbf{x}_j(\tau)}{dt_k} = \frac{d\mathbf{x}_j(j-1)}{dt_k} + (t_j - t_{j-1})\int_{j-1}^{\tau}\frac{\partial f_{i_j}}{\partial \mathbf{x}_j}\frac{d\mathbf{x}_j(v)}{dt_k}dv, \quad \tau \in [j-1,j). \tag{4.13}$$

Then,

$$\frac{d\mathbf{x}_j(\tau)}{dt_k} = \Phi_j(\tau,j-1)\frac{d\mathbf{x}_j(j-1)}{dt_k}. \tag{4.14}$$

Substituting the term $d\mathbf{x}_j(j-1)/dt_k$ in (4.14) by (4.10), we obtain

$$\frac{d\mathbf{x}_j(j^-)}{dt_k} = \left[\prod_{l=k+2}^{j}\Phi_l(l,l-1)\frac{d\psi_{i_l}}{d\mathbf{x}_{l-1}((l-1)^-)}\right]\Omega_{k+1}. \tag{4.15}$$

□

Theorem 4.2. *The derivatives of the objective functional $\widetilde{J}(\cdot)$ w.r.t t_k, $\mathbf{u}_k$ and $\mathbf{s}_k$ are given, respectively, as follows:*

$$\begin{aligned}
\frac{d\widetilde{J}}{dt_k} &= \overline{L}_{i_k}\left(\mathbf{x}_k(k^-), \mathbf{u}_k(k^-), \mathbf{s}_k(k^-)\right) - \overline{L}_{i_{k+1}}(\mathbf{x}_{k+1}(k), \mathbf{u}_{k+1}(k), \mathbf{s}_{k+1}(k)) \\
&\quad + \lambda_k(k^-)^T f_{i_k}\left(\mathbf{x}_k(k^-), \mathbf{u}_k(k^-)\right) - \lambda_{k+1}(k)^T f_{i_{k+1}}(\mathbf{x}_{k+1}(k), \mathbf{u}_{k+1}(k)) \\
&\quad - \sum_{j=k}^{K-1} \alpha_j^T \frac{\partial g_{i_j}}{\partial \mathbf{x}_j(j^-)} \frac{d\mathbf{x}_j(j^-)}{dt_k} - \alpha_K^T \frac{\partial \vartheta}{\partial \mathbf{x}_K(K)} \frac{d\mathbf{x}_K(K)}{dt_k} \\
\frac{\delta \widetilde{J}}{\delta \mathbf{u}_k} &= \frac{\partial H_k}{\partial \mathbf{u}_k} - \sum_{j=k}^{K-1} \alpha_j^T \frac{\partial g_{i_j}}{\partial \mathbf{x}_j(j^-)} \frac{\delta \mathbf{x}_j(j^-)}{\delta \mathbf{u}_k} - \alpha_K^T \frac{\partial \vartheta}{\partial \mathbf{x}_K(K)} \frac{\delta \mathbf{x}_K(K)}{\delta \mathbf{u}_k} \\
\frac{\delta \widetilde{J}}{\delta \mathbf{s}_k} &= \frac{\partial H_k}{\partial \mathbf{s}_k}.
\end{aligned} \tag{4.16}$$

Before proving Theorem 4.2, Lemma 4.3 is firstly given as follows.

Lemma 4.3. *For $j = k+2, \ldots, K$,*

$$\frac{d}{dt_k} \int_{j-1}^{j} \widetilde{L}_{i_j}(\mathbf{x}_j, \mathbf{u}_j, \mathbf{s}_j) d\tau = \lambda_j(j-1)^T \frac{d\mathbf{x}_j(j-1)}{dt_k} - \lambda_j(j^-)^T \frac{d\mathbf{x}_j(j^-)}{dt_k}. \tag{4.17}$$

Proof. For any $j = k+2, \ldots, K$, we have

$$\begin{aligned}
\frac{d}{dt_k} \int_{j-1}^{j} \widetilde{L}_{i_j}(\mathbf{x}_j, \mathbf{u}_j, \mathbf{s}_j) d\tau &= \int_{j-1}^{j} \frac{d}{dt_k}\left(H_j(\lambda_j, \mathbf{x}_j, \mathbf{u}_j, \mathbf{s}_j) - \lambda_j^T \widetilde{f}_{i_j}\right) d\tau \\
&= \int_{j-1}^{j} \left(\frac{\partial H_j}{\partial \mathbf{x}_j} \frac{d\mathbf{x}_j}{dt_k} + \frac{\partial H_j}{\partial \lambda_j} \frac{d\lambda_j}{dt_k} - \left(\frac{d\lambda_j}{dt_k}\right)^T \widetilde{f}_{i_j} - \lambda_j^T \frac{d}{dt_k} \widetilde{f}_{i_j} \right) d\tau.
\end{aligned} \tag{4.18}$$

Since the following holds by Theorem 3.2,

$$\left(\frac{\partial H_j}{\partial \mathbf{x}_j}\right)^T = -\dot{\lambda}_j, \qquad \left(\frac{\partial H_j}{\partial \lambda_j}\right)^T = \widetilde{f}_{i_j}, \tag{4.19}$$

then

$$\begin{aligned}\frac{d}{dt_k}\int_{j-1}^{j}\widetilde{L}_{i_j}(\mathbf{x}_j,\mathbf{u}_j,\mathbf{s}_j)d\tau &= \int_{j-1}^{j}\left(-(\dot{\lambda}_j)^T\frac{d\mathbf{x}_j}{dt_k}+\left(\widetilde{f}_{i_j}\right)^T\frac{d\lambda_j}{dt_k}-\left(\frac{d\lambda_j}{dt_k}\right)^T\widetilde{f}_{i_j}-\lambda_j^T\frac{d}{dt_k}\widetilde{f}_{i_j}\right)d\tau\\ &= \int_{j-1}^{j}\left(-(\dot{\lambda}_j)^T\frac{d\mathbf{x}_j}{dt_k}-\lambda_j^T\frac{d}{dt_k}\widetilde{f}_{i_j}\right)d\tau=-\int_{j-1}^{j}\frac{d}{d\tau}\left(\lambda_j^T\frac{d\mathbf{x}_j}{dt_k}\right)d\tau\\ &= \lambda_j(j-1)^T\frac{d\mathbf{x}_j(j-1)}{dt_k}-\lambda_j(j^-)^T\frac{d\mathbf{x}_j(j^-)}{dt_k}.\end{aligned} \tag{4.20}$$

□

Obviously, when $j=k,k+1$, we have

$$\frac{d}{dt_k}\int_{k-1}^{k}\widetilde{L}_{i_k}(\mathbf{x}_k,\mathbf{u}_k,\mathbf{s}_k)d\tau=\frac{d}{dt_k}\int_{t_{k-1}}^{t_k}\overline{L}_{i_k}(x,u,s_{i_k})dt=\overline{L}_{i_k}(\mathbf{x}_k(k^-),\mathbf{u}_k(k^-),\mathbf{s}_k(k^-)), \tag{4.21}$$

$$\begin{aligned}\frac{d}{dt_k}\int_{k}^{k+1}\widetilde{L}_{i_{k+1}}(\mathbf{x}_{k+1},\mathbf{u}_{k+1},\mathbf{s}_{k+1})d\tau &= \lambda_{k+1}(k)^T\frac{d\mathbf{x}_{k+1}(k)}{dt_k}-\lambda_{k+1}((k+1)^-)^T\frac{d\mathbf{x}_{k+1}((k+1)^-)}{dt_k}\\ &\quad-\overline{L}_{i_{k+1}}(\mathbf{x}_{k+1}(k),\mathbf{u}_{k+1}(k),\mathbf{s}_{k+1}(k)).\end{aligned} \tag{4.22}$$

Now we prove Theorem 4.2. We are only going to show $d\widetilde{J}/dt_k$ for easily reading. The proofs for $\delta\widetilde{J}/\delta\mathbf{u}_k$ and $\delta\widetilde{J}/\delta\mathbf{s}_k$ can be found in Appendix.

Proof. $\widetilde{J}(\theta,\mathbf{u},\mathbf{s})$ can be formulated as

$$\begin{aligned}\widetilde{J}(\theta,\mathbf{u},\mathbf{s}) &= \phi(\mathbf{x}_K(K))+\sum_{j=1}^{k-1}\int_{j-1}^{j}\widetilde{L}_{i_j}(\mathbf{x}_j,\mathbf{u}_j,\mathbf{s}_j)d\tau\\ &\quad+\sum_{j=k}^{K}\int_{j-1}^{j}\widetilde{L}_{i_j}(\mathbf{x}_j,\mathbf{u}_j,\mathbf{s}_j)d\tau+\sum_{j=1}^{K-1}\varphi_{i_ji_{j+1}}(\mathbf{x}_j(j^-)).\end{aligned} \tag{4.23}$$

Since $\widetilde{L}_{i_j}(\cdot)$ is independent of t_k for $j=1,\ldots,k-1$, then $d\widetilde{J}/dt_k$ can be obtained by

$$\begin{aligned}\frac{d\widetilde{J}}{dt_k}(\theta,\mathbf{u},\mathbf{s}) &= \frac{\partial\phi(\mathbf{x}_K(K))}{\partial\mathbf{x}_K(K)}\frac{d\mathbf{x}_K(K)}{dt_k}\\ &\quad+\frac{d}{dt_k}\sum_{j=k}^{K}\int_{j-1}^{j}\widetilde{L}_{i_j}(\mathbf{x}_j,\mathbf{u}_j,\mathbf{s}_j)d\tau+\sum_{j=1}^{K-1}\frac{\partial\varphi_{i_ji_{j+1}}}{\partial\mathbf{x}_j(j^-)}\frac{d\mathbf{x}_j(j^-)}{dt_k}.\end{aligned} \tag{4.24}$$

Substituting (4.17), (4.21), and (4.22) into (4.24), we have

$$\begin{aligned}\frac{d\tilde{J}}{dt_k}(\theta,\mathbf{u},\mathbf{s}) = {} & \frac{\partial\phi(\mathbf{x}_K(K))}{\partial\mathbf{x}_K(K)}\frac{d\mathbf{x}_K(K)}{dt_k} + \overline{L}_{i_k}(\mathbf{x}_k(k^-),\mathbf{u}_k(k^-),\mathbf{s}_k(k^-)) \\ & - \overline{L}_{i_{k+1}}(\mathbf{x}_{k+1}(k),\mathbf{u}_{k+1}(k),\mathbf{s}_{k+1}(k)) + \lambda_{k+1}(k)^T\frac{d\mathbf{x}_{k+1}(k)}{dt_k} + \frac{\partial\varphi_{i_k i_{k+1}}}{\partial\mathbf{x}_k(k^-)}\frac{d\mathbf{x}_k(k^-)}{dt_k} \\ & - \sum_{j=k+1}^{K-1}\left(\lambda_j(j^-)^T\frac{d\mathbf{x}_j(j^-)}{dt_k} - \lambda_{j+1}(j)^T\frac{d\mathbf{x}_{j+1}(j)}{dt_k} - \frac{\partial\varphi_{i_j i_{j+1}}}{\partial\mathbf{x}_j(j^-)}\frac{d\mathbf{x}_j(j^-)}{dt_k}\right) \\ & - \lambda_K(K)^T\frac{d\mathbf{x}_K(K)}{dt_k}.\end{aligned} \tag{4.25}$$

Due to Theorem 3.2 and (4.10), $d\tilde{J}/dt_k$ can be formulated by

$$\begin{aligned}\frac{d\tilde{J}}{dt_k}(\theta,\mathbf{u},\mathbf{s}) = {} & \left(\frac{\partial\phi(\mathbf{x}_K(K))}{\partial\mathbf{x}_K(K)} - \lambda_K(K)^T\right)\frac{d\mathbf{x}_K(K)}{dt_k} + \overline{L}_{i_k}(\mathbf{x}_k(k^-),\mathbf{u}_k(k^-),\mathbf{s}_k(k^-)) \\ & - \overline{L}_{i_{k+1}}(\mathbf{x}_{k+1}(k),\mathbf{u}_{k+1}(k),\mathbf{s}_{k+1}(k)) + \lambda_k(k^-)^T\frac{d\mathbf{x}_k(k^-)}{dt_k} \\ & - \lambda_{k+1}(k)^T f_{i_{k+1}}(\mathbf{x}_{k+1}(k),\mathbf{u}_{k+1}(k)) \\ & - \alpha_k^T\frac{\partial p_{i_k}}{\partial\mathbf{x}_k(k^-)}\frac{d\mathbf{x}_k(k^-)}{dt_k} - \sum_{j=k}^{K-1}\alpha_j^T\frac{\partial g_{i_j}}{\partial\mathbf{x}_j(j^-)}\frac{d\mathbf{x}_j(j^-)}{dt_k} \\ = {} & \overline{L}_{i_k}(\mathbf{x}_k(k^-),\mathbf{u}_k(k^-),\mathbf{s}_k(k^-)) - \overline{L}_{i_{k+1}}(\mathbf{x}_{k+1}(k),\mathbf{u}_{k+1}(k),\mathbf{s}_{k+1}(k)) \\ & + \lambda_k(k^-)^T f_{i_k}(\mathbf{x}_k(k^-),\mathbf{u}_k(k^-)) - \lambda_{k+1}(k)^T f_{i_{k+1}}(\mathbf{x}_{k+1}(k),\mathbf{u}_{k+1}(k)) \\ & - \sum_{j=k}^{K-1}\alpha_j^T\frac{\partial g_{i_j}}{\partial\mathbf{x}_j(j^-)}\frac{d\mathbf{x}_j(j^-)}{dt_k} - \alpha_K^T\frac{\partial\vartheta}{\partial\mathbf{x}_K(K)}\frac{d\mathbf{x}_K(K)}{dt_k}.\end{aligned} \tag{4.26}$$

□

Note that when second-order derivatives are needed, there is no difficulty to obtain the second-order derivatives following the above procedure.

4.2. Parametrization Method

To obtain the numerical solution to optimal control for hybrid systems, continuous control profiles are parameterized on each mode active horizon in this section. Then the numerical solution to optimal controls can be computed based on the obtained sensitivity analysis results. The basic idea behind the proposed method using finite parameterizations of the controls is to transcribe the original infinite dimensional problem, that is, C-problem, into a finite dimensional nonlinear programming problem, that is, P-problem [25]. Here, the parametrization method that the control profiles are approximated by a family of Lagrange form polynomials is implemented.

Partition each horizon $[j-1, j)$ into N_j elements as $j-1 = \tau_{j0} < \tau_{j1} < \cdots < \tau_{jN_j} = j$ where τ_{jl} are referred to as collocation points, $l = 0, \ldots, N_j$. Let $\mathbf{u}_{jl}$ denote the value of $\mathbf{u}_j$ at τ_{jl}, $l = 0, \ldots, N_j$. Thus, the control variable $\mathbf{u}_j$ is represented approximately by a Lagrange interpolation profile for $j = 1, \ldots, K$,

$$\mathbf{u}_j(\tau) = \sum_{l=0}^{N_j} \widehat{l}_l(\tau) u_{jl}, \quad \tau \in [j-1, j), \tag{4.27}$$

where $\widehat{l}_l(\tau) = \prod_{m=0, m\neq l}^{N_j} ((\tau - \tau_{jm})/(\tau_{jl} - \tau_{jm}))$. $\mathbf{s}_j$ is also parameterized by

$$\mathbf{s}_j(\tau) = \sum_{l=0}^{N_j} \widehat{l}_l(\tau) \mathbf{s}_{jl}, \quad \tau \in [j-1, j), \tag{4.28}$$

where $\mathbf{s}_{jl}$ is the value of $\mathbf{s}_j$ at the collocation points τ_{jl}, $l = 0, \ldots, N_j$.

As a result, based on the obtained derivatives, the numerical solution of u and θ to optimal control for the hybrid systems can be solved simultaneously and efficiently by adopting gradient-based algorithms as described in Xu and Antsaklis [3] and Egerstedt et al. [6]. Note that the derivatives are functions of costate λ_j as formulated in Theorem 4.2. When control polynomial profiles are implemented, a multipoint boundary value problem about state and costate expressed by (3.6), (3.7), and (3.10) will be solved, which produces the derivatives.

Although the Lagrange interpolation profiles may cause the state or/and control trajectories violate their constraints, this parameterizations method has been proved useful in practice. Moreover, there are some techniques to decrease the defect [1, 2].

Remark 4.4. Control variable $\mathbf{u}_j$ can be approximated by several piecewise Lagrange interpolation profiles by further partitioning the element $[j-1, j)$. More detail of the parameterizations methods can be found in Vassiliadis et al. [1, 2], Kameswaran and Biegler [26], and the references therein. Only one Lagrange interpolation profile is used here to show the process of the proposed method.

5. Some Examples

To illustrate the effectiveness of the developed method, two examples with different situations are presented in the following. Numerical examples are conducted on an ThinkPad X61 2.10-GHz PC with 2G of RAM. The program is implemented using MatLab 7. The order of Lagrange polynomials in the examples is 3.

Example 5.1. The prototype of this example comes from Vassiliadis et al. [1]. The hybrid system consists of two batch reactors as shown in Figure 1. The first reactor denoted by mode 1 is fitted with a heating coil which can be used to manipulate the reactor temperature u over time and is initially loaded with $0.1\,\mathrm{m}^3$ of an aqueous solution of component x_1 of concentration $2000\,\mathrm{mol/m}^3$. This reacts to form components x_2 according to the consecutive reaction scheme $2x_1 \rightarrow x_2$. After completion of the first reaction, an amount of dilute aqueous solution of component x_2 of concentration $600\,\mathrm{mol/m}^3$ is added instantaneously to the products of

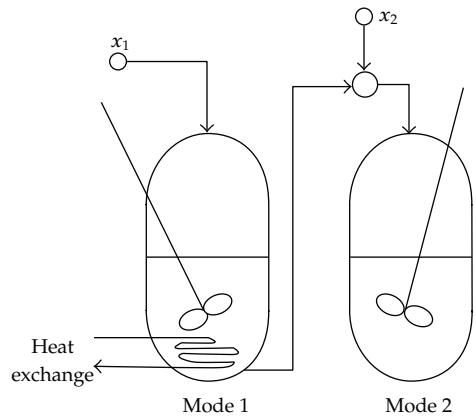

Figure 1: Two batch reactors system.

the first reactor, and the mixture is loaded into the second reactor denoted by mode 2 where the reaction $x_2 \rightarrow x_3$ takes place under isothermal conditions at a fixed temperature. The decision variables are the temperature u of the mode 1, and the durations of the two mode over the horizon $[0, 180]$. The dynamics of the hybrid systems can be described by

Mode 1:

$$\begin{aligned} \dot{x}_1 &= -0.0888e^{(-2500/u)}x_1^2, \\ \dot{x}_2 &= 0.0444e^{(-2500/u)}x_1^2 - 6889.0e^{(-5000/u)}x_2, \\ \dot{x}_3 &= 0. \end{aligned} \tag{5.1}$$

Mode 2:

$$\begin{aligned} \dot{x}_1 &= 0, \\ \dot{x}_2 &= -0.07x_2 - 8.0 \times 10^{-5}x_2^2, \\ \dot{x}_3 &= 0.02x_2, \end{aligned} \tag{5.2}$$

with $x(0) = [2000 \quad 0 \quad 0]^T$. The system transits once at $t = t_1 (t_0 < t_1 < t_f)$ from mode 1 to 2 with $x_1(t_1) = x_1(t_1^-)/1.7$, $x_2(t_1) = (x_2(t_1^-) + 420)/1.7$. The OCPHS is to find an optimal mode transition instant t_1 and an optimal input $298 \leq u(t) \leq 398$, $t \in [t_0, t_1]$, to maximize the cost functional

$$\max_{t_1, u} x_3(t_f), \tag{5.3}$$

with $x_3(t_f) \geq 150$ must be satisfied.

By using the proposed method, the optimal mode transition instant is $t_1 = 105$ and the corresponding optimal cost is $J^* = 150.0285$. The corresponding continuous control and state trajectories are shown in Figure 2. In Vassiliadis et al. [1], the transition instants and

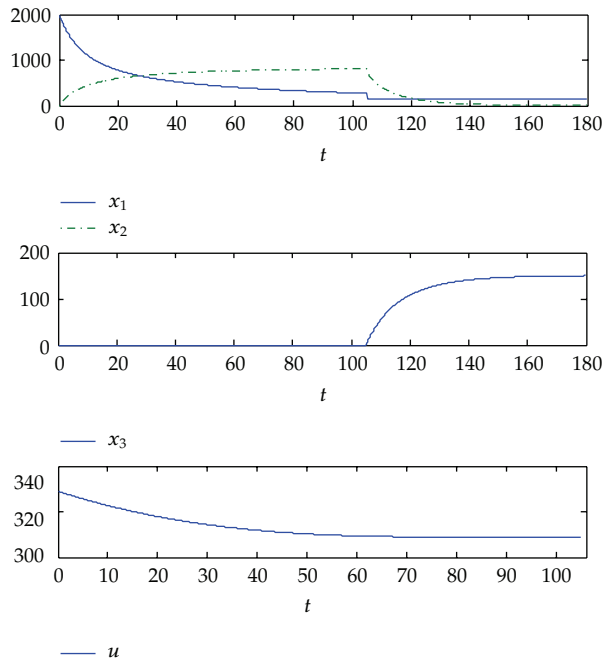

Figure 2: State trajectories and control input of Example 5.1.

the optimal cost are $t_1 = 106$, $J^* = 150.294$, respectively, which are solved by software package DAEOPT.

Example 5.2. Example 5.2 comes from Xu and Antsaklis [3] and is also reconsidered by Hwang et al. [9]. Different from the example in the two references, the control constraint is imposed. The example can be referred to as autonomous switching hybrid systems with mode invariants. Consider the hybrid system consisting of

Mode 1:

$$\dot{x} = \begin{pmatrix} 1.5 & 0 \\ 0 & 1 \end{pmatrix} x + \begin{pmatrix} 1 \\ 1 \end{pmatrix} u, \tag{5.4}$$

Mode 2:

$$\dot{x} = \begin{pmatrix} 0.5 & 0.866 \\ 0.866 & -0.5 \end{pmatrix} x + \begin{pmatrix} 1 \\ 1 \end{pmatrix} u, \tag{5.5}$$

with $x_0 = [1 \quad 1]^T$. Assume that $t_0 = 0$, $t_f = 2$ and the system transits once at $t = t_1$ ($t_0 < t_1 < t_f$) from Mode 1 to 2 when the state trajectories intersect the linear manifold defined by $m(x) = x_1 + x_2 - 7 = 0$. Mode 1 is active with its mode invariant $x_1 + x_2 - 7 < 0$ and Mode

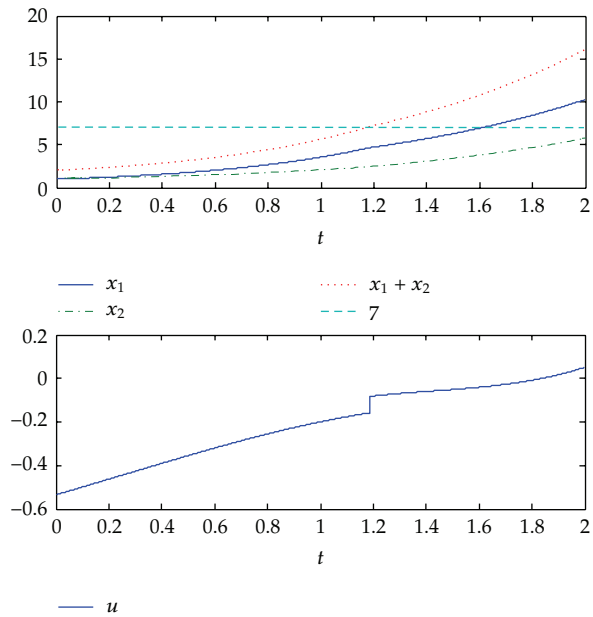

Figure 3: State trajectories and control input of Example 5.2.

2 is active with its mode invariant $x_1 + x_2 - 7 > 0$. The OCPHS is to find an optimal mode transition instant t_1 and an optimal input $u(t) \in [-1, 1]$ such that the cost functional

$$J(t_1, u) = \frac{1}{2}\left[\left(x_1(t_f) - 10\right)^2 + \left(x_2(t_f) - 6\right)^2 + \int_{t_0}^{t_f} u^2(t)dt\right] \tag{5.6}$$

is minimized.

By using the method developed here, the optimal mode transition instant is $t_1 = 1.1857$ and the corresponding optimal cost is $J^* = 0.1246$. The corresponding continuous control and state trajectories are shown in Figure 3. In Xu and Antsaklis [3], the transition instants and the optimal cost are $t_1 = 1.1624$, $J^* = 0.1130$, respectively. The bad performance results from that the optimal control is approximated by polynomial.

6. Conclusions

The optimal control problem for hybrid systems (OCPHS) with mode invariants and control constraints is addressed under a priori fixed mode transition order. By introducing new independent variables and auxiliary algebraic variables, the original OCPHS is transformed into an equivalent optimal control problem, and the optimality conditions for the OCPHS is stated. Based on the optimality conditions, the derivatives of the objective functional w.r.t control variables, that is, mode transition instant sequence and admissible continuous control functions, are established analytically. As a result, a control vector parametrization method is implemented to obtain the numerical solution by using gradient-based algorithms with the obtained derivatives. Compared with the existing results on the OCPHS with fixed mode

transition order, the settings cover not only the control constraints but also the continuous states constraints, which makes the obtained results more general. Note that when no information about the mode transition sequence is known a priori, the discrete model methods formulated in Bemporad and Morari [27], Barton et al. [15], and Song et al. [28] seem appropriate. In addition, when uncertainties are considered in the systems, the reader is referred to Hu et al. [29] and the references therein.

Appendix

For any $\tau \in [k-1, k)$, $k = 1, \ldots, K$, let $\mathbf{u}_k(\tau) \in \mathbf{U}_{i_k}$ be given and let $\delta\mathbf{u}_k(\tau) \in \mathbf{U}_{i_k}$ be arbitrary but fixed. Define a perturbation of $\mathbf{u}_k$ as

$$\mathbf{u}_k(\tau;\varepsilon) = \mathbf{u}_k(\tau) + \varepsilon\delta\mathbf{u}_k(\tau), \tag{A.1}$$

where $\varepsilon \in \mathbb{R}$ is arbitrarily small such that $\mathbf{u}_k(\tau;\varepsilon) \in \mathbf{U}_{i_k}$. For the time being, assume that the other controls, $\mathbf{u}_j$, $j = 1, \ldots, K$, $j \neq k$, be given and fixed. For brevity, let $\mathbf{x}_j$ and $\mathbf{x}_j(\cdot;\varepsilon)$ denote the state trajectories corresponding to $\mathbf{u}_k$ and $\mathbf{u}_k(\tau;\varepsilon)$, respectively. Similarly, let λ_j and $\lambda_j(\cdot;\varepsilon)$ denote the costate trajectories corresponding to $\mathbf{u}_k$ and $\mathbf{u}_k(\varepsilon)$, respectively, which are the solutions of the costate equations

$$\begin{aligned} \mathbf{x}_j(\cdot;\varepsilon) &= \mathbf{x}_j(\cdot) + \varepsilon\delta\mathbf{x}_j(\cdot), \\ \lambda_j(\cdot;\varepsilon) &= \lambda_j(\cdot) + \varepsilon\delta\lambda_j(\cdot). \end{aligned} \tag{A.2}$$

Proof of (4.2) *in Lemma 4.1.* When $j = 1, \ldots, k-1$, obviously in these cases $\mathbf{x}_j$ is independent of $\mathbf{u}_k$, that is, $\delta\mathbf{x}_j(j^-;\varepsilon) = 0$, which leads to

$$\frac{\delta\mathbf{x}_j(j^-)}{\delta\mathbf{u}_k} = 0, \quad j = 1, \ldots, k-1. \tag{A.3}$$

Case i ($j = k$). Since

$$\delta\dot{\mathbf{x}}_k = (t_k - t_{k-1})\left(\frac{\partial f_{i_k}}{\partial\mathbf{x}_k}\delta\mathbf{x}_k + \frac{\partial f_{i_k}}{\partial\mathbf{u}_k}\delta\mathbf{u}_k\right), \tag{A.4}$$

with $\delta\mathbf{x}_k(k-1) = 0$, thus we have

$$\delta\mathbf{x}_k(k^-) = \int_{k-1}^{k} \Phi_k(k,\tau)(t_k - t_{k-1})\frac{\partial f_{i_k}}{\partial\mathbf{u}_k}\delta\mathbf{u}_k d\tau, \tag{A.5}$$

where Φ_k is the state transition matrix defined in Section 3. Based on the definition of functional derivative, there exists

$$\frac{\delta\mathbf{x}_k(k^-)}{\delta\mathbf{u}_k} = (t_k - t_{k-1})\Phi_k(k,\tau)\frac{\partial f_{i_k}}{\partial\mathbf{u}_k} \doteq \Gamma_k(\tau). \tag{A.6}$$

Case (*ii*) ($j = k+1, \ldots, K$). In this case,

$$\delta\dot{\mathbf{x}}_j(\tau;\varepsilon) = (t_j - t_{j-1})\frac{\partial f_{i_j}}{\partial \mathbf{x}_j}\delta\mathbf{x}_j, \quad \tau \in [j-1, j), \tag{A.7}$$

which gives rise to

$$\delta\mathbf{x}_j(j^-;\varepsilon) = \Phi_j(j, j-1)\delta\mathbf{x}_j(j-1). \tag{A.8}$$

At mode transition instant t_j, $j = 1, \ldots, K-1$, $\mathbf{x}_{j+1}(j) = \varphi_{i_{j+1}}(\mathbf{x}_j(j^-))$ holds, which results in

$$\delta\mathbf{x}_{j+1}(j) = \frac{d\varphi_{i_{j+1}}}{d\mathbf{x}_j(j^-)}\delta\mathbf{x}_j(j^-). \tag{A.9}$$

Substituting (A.9) into (A.8), we obtain

$$\delta\mathbf{x}_j(j^-) = \prod_{l=k+1}^{j}\left[\Phi_l(l, l-1)\frac{d\varphi_{i_l}}{d\mathbf{x}_{l-1}((l-1)^-)}\right]\delta\mathbf{x}_k(k^-). \tag{A.10}$$

According to the definition of functional derivative, we have

$$\frac{\delta\mathbf{x}_j(j^-)}{\delta\mathbf{u}_k} = \prod_{l=k+1}^{j}\left[\Phi_l(l, l-1)\frac{d\varphi_{i_l}}{d\mathbf{x}_{l-1}((l-1)^-)}\right]\Gamma_k(\tau). \tag{A.11}$$

This completes the proof. □

Before proving the $\delta\tilde{J}/\delta\mathbf{u}_k$ in Theorem 4.2, Lemma A.1 is firstly given as follows.

Lemma A.1. *For any* $j = k+1, \ldots, K$,

$$\delta\int_{j-1}^{j}\tilde{L}_{i_j}(\mathbf{x}_j, \mathbf{u}_j, \mathbf{s}_i)d\tau = \lambda_j(j-1)^T\delta\mathbf{x}_j(j-1) - \lambda_j(j^-)^T\delta\mathbf{x}_j(j^-). \tag{A.12}$$

Proof. Note that

$$\begin{aligned}\delta\int_{j-1}^{j}\tilde{L}_{i_j}(\mathbf{x}_j, \mathbf{u}_j, \mathbf{s}_j)d\tau &= \delta\int_{j-1}^{j}\left(H_j(\lambda_j, \mathbf{x}_j, \mathbf{u}_j, \mathbf{s}_j) - \lambda_j^T\tilde{f}_{i_j}\right)d\tau \\ &= \int_{j-1}^{j}\left(\frac{\partial H_j}{\partial \mathbf{x}_j}\delta\mathbf{x}_j + \frac{\partial H_j}{\partial \lambda_j}\delta\lambda_j - (\delta\lambda_j)^T\tilde{f}_{i_j} - \lambda_j^T\delta\tilde{f}_{i_j}\right)d\tau.\end{aligned} \tag{A.13}$$

Since the following holds by Theorem 3.2:

$$\left(\frac{\partial H_j}{\partial \mathbf{x}_j}\right)^T = -\dot{\lambda}_j, \qquad \left(\frac{\partial H_j}{\partial \lambda_j}\right)^T = \tilde{f}_{i_j}, \tag{A.14}$$

therefore,

$$\begin{aligned}\delta \int_{j-1}^{j} \tilde{L}_{i_j}(\mathbf{x}_j, \mathbf{u}_j, \mathbf{s}_j)d\tau &= -\int_{j-1}^{j}\left((\dot{\lambda}_j)^T \delta \mathbf{x}_j + \lambda_j^T \delta \tilde{f}_{i_j}\right)d\tau = -\int_{j-1}^{j}\left((\dot{\lambda}_j)^T \delta \mathbf{x}_j + \lambda_j^T \delta \dot{\mathbf{x}}_{i_j}\right)d\tau \\ &= -\int_{j-1}^{j} \frac{d}{d\tau}\left(\lambda_j^T \delta \mathbf{x}_j\right)d\tau = \lambda_j(j-1)^T \delta \mathbf{x}_j(j-1) - \lambda_j(j^-)^T \delta \mathbf{x}_j(j^-).\end{aligned} \tag{A.15}$$

□

Obviously, when $j = k$, we have

$$\delta \int_{k-1}^{k} \tilde{L}_{i_k}(\mathbf{x}_k, \mathbf{u}_k, \mathbf{s}_k)d\tau = \lambda_k(k-1)^T \delta \mathbf{x}_k(k-1) - \lambda_k(k^-)^T \delta \mathbf{x}_k(k^-) + \int_{k-1}^{k} \frac{\partial H_k}{\partial \mathbf{u}_k}\delta \mathbf{u}_k d\tau. \tag{A.16}$$

Proof of $\delta\tilde{J}/\delta\mathbf{u}_k$ in Theorem 4.2. $\tilde{J}(\theta, \mathbf{u}(\varepsilon), \mathbf{s})$ can be rewritten by

$$\begin{aligned}\tilde{J}(\theta, \mathbf{u}(\varepsilon), \mathbf{s}) = \phi(\mathbf{x}_K(K)) &+ \sum_{j=1}^{k-1}\int_{j-1}^{j} \tilde{L}_{i_j}(\mathbf{x}_j, \mathbf{u}_j, \mathbf{s}_j)d\tau + \int_{k-1}^{k} \tilde{L}_{i_k}(\mathbf{x}_k(\varepsilon), \mathbf{u}_k(\varepsilon), \mathbf{s}_k)d\tau \\ &+ \sum_{j=k+1}^{K}\int_{j-1}^{j} \tilde{L}_{i_j}(\mathbf{x}_j(\varepsilon), \mathbf{u}_j, \mathbf{s}_j)d\tau + \sum_{j=1}^{K-1}\varphi_{i_j i_{j+1}}(\mathbf{x}_j(j^-)).\end{aligned} \tag{A.17}$$

Applying a δ-operation to (A.17) leads to

$$\begin{aligned}\delta\tilde{J} = \left.\frac{d\tilde{J}(\rho, \mathbf{u}(\varepsilon), \mathbf{s})}{d\varepsilon}\right|_{\varepsilon=0} &= \frac{\partial \phi(\mathbf{x}_K(K))}{\partial \mathbf{x}_K(K)}\delta \mathbf{x}_K(K) + \int_{k-1}^{k} \frac{\partial H_k}{\partial \mathbf{u}_k}\delta \mathbf{u}_k d\tau \\ &+ \sum_{j=k}^{K}\left(\lambda_j(j-1)^T \delta \mathbf{x}_j(j-1) - \lambda_j(j^-)^T \delta \mathbf{x}_j(j^-)\right) + \sum_{j=1}^{K-1}\frac{\partial \varphi_{i_j i_{j+1}}}{\partial \mathbf{x}_j(j^-)}\delta \mathbf{x}_j(j^-) \\ &= \frac{\partial \phi(\mathbf{x}_K(K))}{\partial \mathbf{x}_K(K)}\delta \mathbf{x}_K(K) + \int_{k-1}^{k} \frac{\partial H_k}{\partial \mathbf{u}_k}\delta \mathbf{u}_k d\tau + \lambda_k(k-1)^T \delta \mathbf{x}_k(k-1) \\ &- \sum_{j=k}^{K-1}\left(\lambda_j(j^-)^T \delta \mathbf{x}_j(j^-) - \lambda_{j+1}(j)^T \delta \mathbf{x}_{j+1}(j) - \frac{\partial \varphi_{i_j i_{j+1}}}{\partial \mathbf{x}_j(j^-)}\delta \mathbf{x}_j(j^-)\right) \\ &- \lambda_K(K)^T \delta \mathbf{x}_K(K).\end{aligned} \tag{A.18}$$

Due to Theorem 3.2 and (A.9), $\delta\tilde{J}$ can be reformulated by

$$\begin{aligned}\delta\tilde{J} &= \left(\frac{\partial\phi(\mathbf{x}_K(K))}{\partial\mathbf{x}_K(K)} - \lambda_K(K)^T\right)\delta\mathbf{x}_K(K) + \int_{k-1}^{k}\frac{\partial H_k}{\partial\mathbf{u}_k}\delta\mathbf{u}_k d\tau \\ &\quad - \sum_{j=k}^{K-1}\alpha_j^T\frac{\partial g_{i_j}}{\partial\mathbf{x}_j(j^-)}\delta\mathbf{x}_j(j^-) \\ &= \int_{k-1}^{k}\frac{\partial H_k}{\partial\mathbf{u}_k}\delta\mathbf{u}_k d\tau - \sum_{j=k}^{K-1}\alpha_j^T\frac{\partial g_{i_j}}{\partial\mathbf{x}_j(j^-)}\delta\mathbf{x}_j(j^-) - \alpha_K^T\frac{\partial\vartheta}{\partial\mathbf{x}_K(K)}\delta\mathbf{x}_K(K).\end{aligned} \tag{A.19}$$

Then according to the definition of functional derivative, we have

$$\frac{\delta\tilde{J}}{\delta\mathbf{u}_k} = \frac{\partial H_k}{\partial\mathbf{u}_k} - \sum_{j=k}^{K-1}\alpha_j^T\frac{\partial g_{i_j}}{\partial\mathbf{x}_j(j^-)}\frac{\delta\mathbf{x}_j(j^-)}{\delta\mathbf{u}_k} - \alpha_K^T\frac{\partial\vartheta}{\partial\mathbf{x}_K(K)}\frac{\delta\mathbf{x}_K(K)}{\delta\mathbf{u}_k}. \tag{A.20}$$

Obviously, the functional derivative of $\tilde{J}$ with respect to $\mathbf{s}_k$ can be directly given by

$$\frac{\delta\tilde{J}}{\delta\mathbf{s}_k} = \frac{\partial H_k}{\partial\mathbf{s}_k}. \tag{A.21}$$

This completes the proof. □

Acknowledgments

The authors would like to express their sincere thanks to Professor Michael Fu at the University of Maryland (College Park) for suggestions on this work. This work was supported by the NSF under grant 60974023 of China, the State Key Development Program for Basic Research of China (2012CB720503), and the Fundamental Research Funds for the Central Universities.

References

[1] V. S. Vassiliadis, R. W. H. Sargent, and C. C. Pantelides, "Solution of a class of multistage dynamic optimization problems. 1. Problems without path constraints," *Industrial and Engineering Chemistry Research*, vol. 33, no. 9, pp. 2111–2122, 1994.

[2] V. S. Vassiliadis, R. W. H. Sargent, and C. C. Pantelides, "Solution of a class of multistage dynamic optimization problems. 2. Problems with path constraints," *Industrial and Engineering Chemistry Research*, vol. 33, no. 9, pp. 2123–2133, 1994.

[3] X. Xu and P. J. Antsaklis, "Optimal control of switched systems based on parameterization of the switching instants," *IEEE Transactions on Automatic Control*, vol. 49, no. 1, pp. 2–16, 2004.

[4] P. J. Antsaklis and A. Nerode, "Special issue on hybrid control systems," *IEEE Transactions on Automatic Control*, vol. 43, no. 4, 1998.

[5] P. E. Caines and Y.-J. Wei, "Hierarchical hybrid control systems: a lattice-theoretic formulation," *IEEE Transactions on Automatic Control*, vol. 43, no. 4, pp. 501–508, 1998.

[6] M. Egerstedt, Y. Wardi, and H. Axelsson, "Transition-time optimization for switched-mode dynamical systems," *IEEE Transactions on Automatic Control*, vol. 51, no. 1, pp. 110–115, 2006.

[7] D. Flieller, P. Riedinger, and J. P. Louis, "Computation and stability of limit cycles in hybrid systems," *Nonlinear Analysis*, vol. 64, no. 2, pp. 352–367, 2006.
[8] C. G. Cassandras and J. Lygeros, *Stochastic Hybrid Systems*, chapter 1, 2, 6, 7, Taylor & Francis, Boca Raton, Fla, USA, 2007.
[9] I. Hwang, J. Li, and D. Du, "A numerical algorithm for optimal control of a class of hybrid systems: differential transformation based approach," *International Journal of Control*, vol. 81, no. 2, pp. 277–293, 2008.
[10] H. J. Sussmann, "A maximum principle for hybrid optimal control problems," in *Proceedings of the 38th IEEE Conference on Decision and Control (CDC '99)*, pp. 425–430, Phoenix, Ariz, USA, December 1999.
[11] M. S. Shaikh and P. E. Caines, "On the hybrid optimal control problem: theory and algorithms," *IEEE Transactions on Automatic Control*, vol. 52, no. 9, pp. 1587–1603, 2007.
[12] A. V. Dmitruk and A. M. Kaganovich, "The hybrid maximum principle is a consequence of Pontryagin maximum principle," *Systems & Control Letters*, vol. 57, no. 11, pp. 964–970, 2008.
[13] A. Bensoussan and J. L. Menaldi, "Stochastic hybrid control," *Journal of Mathematical Analysis and Applications*, vol. 249, no. 1, pp. 261–288, 2000.
[14] M. S. Branicky, V. S. Borkar, and S. K. Mitter, "A unified framework for hybrid control: model and optimal control theory," *IEEE Transactions on Automatic Control*, vol. 43, no. 1, pp. 31–45, 1998.
[15] P. I. Barton, C. K. Lee, and M. Yunt, "Optimization of hybrid systems," *Computers and Chemical Engineering*, vol. 30, no. 10–12, pp. 1576–1589, 2006.
[16] C. Seatzu, D. Corona, A. Giua, and A. Bemporad, "Optimal control of continuous-time switched affine systems," *IEEE Transactions on Automatic Control*, vol. 51, no. 5, pp. 726–741, 2006.
[17] H. Axelsson, Y. Wardi, M. Egerstedt, and E. I. Verriest, "Gradient descent approach to optimal mode scheduling in hybrid dynamical systems," *Journal of Optimization Theory and Applications*, vol. 136, no. 2, pp. 167–186, 2008.
[18] E. R. Johnson and T. D. Murphey, "Second order switching time optimization for time-varying nonlinear systems," in *Proceedings of the 48th IEEE Conference on Decision and Control (CDC '09)*, pp. 5281–5286, Shanghai, China, 2009.
[19] S. A. Attia, V. Azhmyakov, and J. Raisch, "On an optimization problem for a class of impulsive hybrid systems," *Discrete Event Dynamic Systems*, vol. 20, no. 2, pp. 215–231, 2010.
[20] F. Taringoo and P. E. Caines, "Gradient geodesic and Newton geodesic HMP algorithms for the optimization of hybrid systems," *Annual Reviews in Control*, vol. 35, pp. 187–198, 2011.
[21] X. Xu and P. J. Antsaklis, "A dynamic programming approach for optimal control of switched systems," in *Proceedings of the 39th IEEE Confernce on Decision and Control (CDC '00)*, pp. 1822–1827, Sydney, Australia, December 2000.
[22] K. Gokbayrak and C. G. Cassandras, "Hybrid controllers for hierarchically decomposed systems," in *Proceedings of the Hybrid System Control Confernce*, pp. 117–129, March 2000.
[23] L. S. Jennings, K. L. Teo, V. Rehbock, and W. X. Zheng, "Optimal control of singular systems with a cost on changing control," *Dynamics and Control*, vol. 6, no. 1, pp. 63–89, 1996.
[24] C. Song and P. Li, "Near optimal control for a class of stochastic hybrid systems," *Automatica*, vol. 46, no. 9, pp. 1553–1557, 2010.
[25] R. Findeisen, L. Imsland, F. Allgöwer, and B. A. Foss, "State and output feedback nonlinear model predictive control: an overview," *European Journal of Control*, vol. 9, no. 2-3, pp. 190–206, 2003.
[26] S. Kameswaran and L. T. Biegler, "Simultaneous dynamic optimization strategies: recent advances and challenges," *Computers and Chemical Engineering*, vol. 30, no. 10–12, pp. 1560–1575, 2006.
[27] A. Bemporad and M. Morari, "Control of systems integrating logic, dynamics, and constraints," *Automatica*, vol. 35, no. 3, pp. 407–427, 1999.
[28] C. Song, B. Wu, and P. Li, "A hybrid model-based optimal control method for nonlinear systems using simultaneous dynamic optimization strategies," *Journal of Process Control*, vol. 22, no. 5, pp. 852–860, 2012.
[29] J. Hu, Z. Wang, H. Gao, and L. K. Stergioulas, "Probability-guaranteed H_∞ finite-horizon filtering for a class of nonlinear time-varying systems with sensor saturation," *System and Control Letters*, vol. 61, no. 4, pp. 477–484, 2012.

Hindawi Publishing Corporation
Mathematical Problems in Engineering
Volume 2012, Article ID 781542, 17 pages
doi:10.1155/2012/781542

Research Article

Observer-Based Stabilization of Stochastic Systems with Limited Communication

Junli Wu,[1] Hamid Reza Karimi,[2] and Peng Shi[3,4]

[1] *Mechanical Engineering Institute, Huaqiao University, Xiamen 360000, China*
[2] *Department of Engineering, Faculty of Engineering and Science, University of Agder, 4898 Grimstad, Norway*
[3] *Faculty of Advanced Technology, University of Glamorgan, Pontypridd CF37 1DL, UK*
[4] *School of Engineering and Science, Victoria University, Melbourne, VIC 8001, Australia*

Correspondence should be addressed to Junli Wu, wfdwjl@gmail.com

Received 6 May 2012; Accepted 7 June 2012

Academic Editor: Zidong Wang

This paper studies the problem of observer-based stabilization of stochastic nonlinear systems with limited communication. A communication channel exists between the output of the plant and the input of the dynamic controller, which is considered network-induced delays, data packet dropouts, and measurement quantization. A new stability criterion is derived for the stochastic nonlinear system by using the Lyapunov functional approach. Based on this, the design procedure of observer-based controller is presented, which ensures asymptotic stability in the meansquare of the closed-loop system. Finally, an illustrative example is given to illustrate the effectiveness of the proposed design techniques.

1. Introduction

Stochastic variables frequently exist in practical systems such as aircraft systems, biology systems, and electronic circuits. Without taking them into account in the system design, the stochastic variables can bring negative effects on the performance of control systems and even make the systems unstable. According to the way stochastic variable occurs, stochastic system mode can be classified as Itô stochastic differential equation [1, 2], Markov switched systems [3–5], and other systems with stochastic variables [6–9]. Since the introduction of the concept of stochastic differential equation by Itô [10] in 1951, Itô stochastic system model has been used successfully in numerous applications, such as the analysis of stock systems and prediction for ecosystem. In automatic control of stochastic systems, a great number of important results have been reported in the literature [11, 12].

In the past two decades, network-based control technology has been developed to combine a communication network with conventional control systems to form the Network

Control Systems (NCSs), which have wide applications due to their advantages, such as reduced weight, power requirements, low installation cost, and easy maintenance [13]. Since the capacity of the communication channel is limited [14–16], signal transmission delay and data packet dropout are two fundamental problems in NCSs. To deal with these issues, considerable research results on this topic have been reported, see for example [17–20] and the references therein. In [21], the robust H_∞ control problem was considered for a class of networked systems with random communication packet losses.

Among the reported results, most NCSs are mainly based on deterministic physical plant. However, stochastic systems models also have wide applications in the dynamical systems. This has motivated the researches on networked control for stochastic systems and many results have been reported in the literature. In [22], the problem of network-based control for stochastic plants was studied, and a new model of stochastic time-delay systems was presented including both network-induced delays and packet dropouts. In [23], the problem of sampled-data control for networked control systems was considered. In recent years, much attention is paid to the problem of the observer-based controller design for NCSs [24–27]. In [28], the problem of the NCS design for continuous-time systems with random measurement was investigated, where the measurement channel is assumed to be subjected to random sensor delay. To the authors' knowledge, the problem of observer-based controller design for stochastic nonlinear systems with limited communication has not been fully investigated and still remains challenging, which motivates us for the present study.

In this paper, we investigate the problem of observer-based stabilization of stochastic nonlinear systems with limited communication. A new model is proposed to describe the stochastic nonlinear systems with a communication channel, which exists between the output of the stochastic plant and the input of the observer-based controller. Based on this, the design procedure of observer-based controller is proposed, which ensures the asymptotic stability of the resulting closed-loop system. Finally, a mechanical system example consisted of two cars, a spring and a damper, is given to illustrate the effectiveness of the proposed controller design method.

Notation. The notation used throughout the paper is fairly standard. $\mathbb{R}^n$ denotes the n-dimensional Euclidean space and the notation $P > 0$ (≥ 0) means that P is real symmetric and positive definite (semidefinite). In symmetric block matrices or complex matrix expressions, we use an asterisk $(*)$ to represent a term that is induced by symmetry and $\operatorname{diag}\{\cdots\}$ standing for a block-diagonal matrix. $\operatorname{sym}(A)$ is defined as $A + A^T$. Matrices, if their dimensions are not explicitly stated, are assumed to be compatible for algebraic operations. $\mathbb{E}\{x\}$ means the expectation of x. The space of square-integrable vector functions over $[0,\infty)$ is denoted by $L_2[0,\infty)$, and for $w = \{w(t)\} \in L_2[0,\infty)$, its norm is given by: $\|w\|_2 = \sqrt{\int_{t=0}^{\infty} |w(t)|^2 dt}$.

2. Problem Formulation

Consider the following stochastic nonlinear system:

$$\begin{aligned} dx(t) &= \left[Ax(t) + Bu(t) + g(x(t))\right]dt + Ex(t)d\omega(t), \\ y(t) &= Cx(t), \\ x(t) &= \phi(t), \quad t \in [-2\kappa, 0], \end{aligned} \tag{2.1}$$

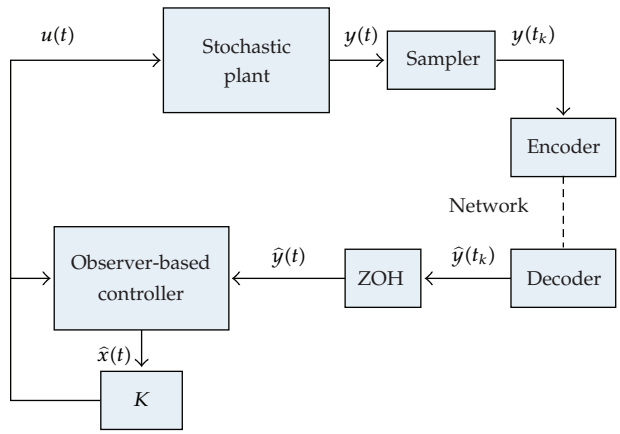

Figure 1: The stochastic systems with limited communication.

where $x(t) \in \mathbb{R}^n$ is the state vector; $u(t) \in \mathbb{R}^m$ is the control input; $y(t) \in \mathbb{R}^p$ is the control output; $g(\cdot) : \mathbb{R}^n \to \mathbb{R}^{n_f}$ is unknown nonlinear function; C and E are constant matrices with an appropriate dimension; κ is the maximum delay; $\omega(t)$ is a zero-mean real scalar Wiener process, which satisfies $\mathbb{E}\{d\omega(t)\} = 0$ and $\mathbb{E}\{d\omega(t)^2\} = dt$.

For system (2.1), it is assumed that the states are not fully measured. Thus, we consider the following observer-based controller:

$$\begin{gathered} d\hat{x}(t) = \left[A\hat{x}(t) + Bu(t) + g(\hat{x}(t)) + L\left(\hat{y}(t) - C\hat{x}(t)\right)\right]dt, \\ u(t) = K\hat{x}(t), \end{gathered} \tag{2.2}$$

where $\hat{x}(t) \in \mathbb{R}^n$ is the estimation of the state vector $x(t)$; $\hat{y}(t) \in \mathbb{R}^p$ denotes the output of the zero-order hold (ZOH); K and L are the controller and observer gains.

Under control law (2.2), the closed-loop system in (2.1) is given by

$$dx(t) = \left[Ax(t) + BK\hat{x}(t) + g(x(t))\right]dt + Ex(t)d\omega(t). \tag{2.3}$$

The structure of the stochastic systems with limited communication is shown in Figure 1. In this system, for convenience of analysis, it is assumed that communication delay occurs only in the sampler-to-controller side. The stochastic plant continuously sends the output signal $y(t)$ to the controller by a network. $y(t)$ is firstly sampled by the sampler, which is assumed to be clock-driven. Then, $y(t_k)$, where t_k denotes the sampling instant for $k = 0, 1, 2, \ldots$, is encoded and decoded by the quantizer and sent to ZOH, which are assumed to be event-driven. $\hat{y}(t)$ and $u(t)$ are the input of the observer-based controller and $\hat{x}(t)$ is the output of the observer-based controller.

In this paper, the quantizer is chosen as the logarithmic quantizer. The set of quantized levels is described by:

$$\mathcal{U}_i = \left\{\pm u_i^{(j)},\ u_i^{(j)} = \rho_j^i u_0^{(j)},\ i = \pm 1, \pm 2, \ldots\right\} \cup \left\{\pm u_0^{(j)}\right\} \cup \{0\}, \quad 0 < \rho_j < 1,\ u_0^{(j)} > 0. \tag{2.4}$$

Each of the quantization level $u_i^{(j)}$ corresponds to a segment such that the quantizer maps the whole segment to this quantization level. In addition, these segments form a partition of $\mathbb{R}$, that is, they are disjoint and their union for i equals to $\mathbb{R}$. For the logarithmic quantizer, the associated quantizer $f_i(\cdot)$ is defined as

$$f_i(v) = \begin{cases} u_i^{(j)} & \text{if } \dfrac{1}{1+\sigma_j} u_i^{(j)} < v \leq \dfrac{1}{1-\sigma_j} u_i^{(j)},\ v > 0, \\ 0 & \text{if } v = 0, \\ -f_j(-v) & \text{if } v < 0, \end{cases} \tag{2.5}$$

where $\sigma_j = (1-\rho_j)/(1+\rho_j)$.

When taking into account signal transmission delays η_k from sampler to ZOH, the quantized output signal takes the following form:

$$\hat{y}(t_k) = f(y(t_k - \eta_k)) = \left[f_1(y_1(t_k - \eta_k)) \ \ f_2(y_2(t_k - \eta_k)) \ \ \cdots \ \ f_n(y_n(t_k - \eta_k))\right]^T. \tag{2.6}$$

Considering the behavior of the ZOH, we have

$$\hat{y}(t) = f(y(t_k - \eta_k)), \quad t_k \leq t < t_{k+1}, \tag{2.7}$$

with t_{k+1} being the next updating instant of the ZOH after t_k.

A natural assumption on the network induced delays η_k can be made as

$$0 \leq \eta_k \leq \overline{\eta}, \tag{2.8}$$

where $\overline{\eta}$ denotes the maximum delay. In addition, at the updating instant t_{k+1} the number of accumulated data packet dropouts since the last updating instant t_k is denoted as δ_{k+1}. We assume that the maximum number of data packet dropouts is $\overline{\delta}$, that is,

$$\delta_{k+1} \leq \overline{\delta}. \tag{2.9}$$

Then, it can be seen from (2.8) and (2.9) that

$$t_{k+1} - t_k = (\delta_{k+1} + 1)h + \eta_{k+1} - \eta_k, \tag{2.10}$$

where h denotes the sampling period.

As the time sequence t_k depends on both the network-induced delays and data packet dropouts, the period $t_{k+1} - t_k$ for the sampled-data system in (2.3) is variable and uncertain. Now let us represent $t_k - \eta_k$ in (2.7) as

$$t_k - \eta_k = t - \eta(t), \tag{2.11}$$

where

$$\eta(t) = t - t_k + \eta_k. \tag{2.12}$$

Then, from (2.10) we have

$$0 \leq \eta(t) \leq \kappa, \tag{2.13}$$

where

$$\kappa = \overline{\eta} + \left(\overline{\delta} + 1\right)h. \tag{2.14}$$

Considering the quantization shown in (2.5) and by substituting (2.11) into (2.7), (2.2) can be expressed as

$$\begin{gathered} d\hat{x}(t) = \left[A\hat{x}(t) + Bu(t) + g(\hat{x}(t)) + L\left((I + \Lambda(t))y\left(t - \eta(t)\right) - C\hat{x}(t)\right)\right]dt, \\ u(t) = K\hat{x}(t), \end{gathered} \tag{2.15}$$

where

$$\Lambda(t) = \operatorname{diag}\{\Lambda_1(t), \Lambda_2(t), \ldots, \Lambda_n(t)\}, \tag{2.16}$$

with

$$\Lambda_j(t) \in \left[-\sigma_j, \sigma_j\right], \quad j = 1, \ldots, n. \tag{2.17}$$

Defining the estimation error $e(t) = x(t) - \hat{x}(t)$, we obtain

$$\begin{aligned} dx(t) &= \left[(A + BK)x(t) - BKe(t) + g(x(t))\right]dt + Ex(t)d\omega(t), \\ de(t) &= \left[LCx(t) + (A - LC)e(t) + g(x(t)) - g(x(t) - e(t))\right. \\ &\quad \left. -L(I + \Lambda(t))Cx\left(t - \eta(t)\right)\right]dt + Ex(t)d\omega(t). \end{aligned} \tag{2.18}$$

Before proceeding further, we introduce the following assumption and lemma, which will be used in subsequent developments.

Assumption 2.1. For a stochastic system mode, there exists known real constant matrices $G \in \mathbb{R}^{n\times n}$, such that the unknown nonlinear vector function $g(\cdot)$ satisfies the following boundedness condition:

$$\left|g(x(t))\right| \leq |Gx(t)|, \quad \forall x(t) \in \mathbb{R}^n. \tag{2.19}$$

Lemma 2.2 (see [29]). *Given appropriately dimensioned matrices Σ_1, Σ_2 and Σ_3, with $\Sigma_1^T = \Sigma_1$, then,*

$$\Sigma_1 + \Sigma_3 H(t)\Sigma_2 + \Sigma_2^T H^T(t)\Sigma_3^T < 0 \tag{2.20}$$

holds for all $H(t)$ satisfying $H^T(t)H(t) \leq I$ if and only if for some $\varepsilon > 0$,

$$\Sigma_1 + \varepsilon^{-1}\Sigma_3\Sigma_3^T + \varepsilon\Sigma_2^T\Sigma_2 < 0. \tag{2.21}$$

3. Main Results

In this section, the problem of asymptotical stabilization of stochastic system with limited communication is studied. We are first concerned with the asymptotical stability analysis problem. The following theorem develops a sufficient condition for system (2.18) to be asymptotically stable in the meansquare.

Theorem 3.1. *The nominal stochastic system* (2.18) *is asymptotically stable in the mean square if there exist scalars $\varepsilon_i > 0$, $(i = 1, 2, 3)$ and matrices $P_j > 0$, $R_j > 0$, S_j, U_j, $(j = 1, 2)$ satisfying*

$$\begin{bmatrix} \Pi_1 + \varepsilon_3\Pi_4^T\Pi_4 & \sqrt{\kappa+1}V & \Pi_2^T & \Pi_3^T & \Pi_5^T \\ * & \Pi_6 & 0 & 0 & 0 \\ * & * & -R_1^{-1} & 0 & 0 \\ * & * & * & -R_2^{-1} & -L \\ * & * & * & * & -\varepsilon_3 I \end{bmatrix} < 0, \tag{3.1}$$

where

$$\begin{aligned}
\Pi_1 = {} & \operatorname{sym}\left(W_x^T P_1 W_{r_1} + W_e^T P_2 W_{r_2} + V W_v - W_x^T\left(\varepsilon_2 G^T G\right)W_e\right) + W_g^T \Psi_1 W_g \\
& + W_x^T E^T (P_1 + \kappa R_1 + P_2 + \kappa R_2) W_x, \\
& W_x = \left[I_n \;\; 0_{n,5n}\right], \qquad W_e = \left[0_{n,2n} \;\; I_n \;\; 0_{n,3n}\right], \qquad V = \left[\tilde{S} \;\; \tilde{U}\right], \\
& \Psi_1 = \operatorname{diag}\left\{(\varepsilon_1 + \varepsilon_2)G^T G, \varepsilon_2 G^T G, -\varepsilon_1 I, -\varepsilon_2 I\right\}, \\
& \tilde{S} = \left[S_1^T \;\; S_2^T \;\; 0_n \;\; 0_n \;\; 0_n \;\; 0_n\right]^T, \qquad \tilde{U} = \left[0_n \;\; 0_n \;\; U_1^T \;\; U_2^T \;\; 0_n \;\; 0_n\right]^T, \\
& W_v = \left[\begin{array}{cccc} I_n & -I_n & 0_{n,4n} & \\ \hline 0_{n,2n} & I_n & -I_n & 0_{n,2n} \end{array}\right], \qquad W_g = \left[\begin{array}{ccc} I_n & 0_{n,5n} & \\ \hline 0_{n,2n} & I_n & 0_{n,3n} \\ \hline 0_{n,4n} & I_n & 0_n \\ \hline 0_{n,5n} & I_n & \end{array}\right], \\
& \Pi_2 = \sqrt{\kappa} W_{r_1}, \qquad W_{r_1} = \left[A + BK \;\; 0_n \;\; -BK \;\; 0_n \;\; I_n \;\; 0_n\right], \\
& \Pi_3 = \sqrt{\kappa} W_{r_2}, \qquad W_{r_2} = \left[LC \;\; -LC \;\; A - LC \;\; 0_n \;\; I_n \;\; -I_n\right], \\
& \Pi_4 = \left[0_n \;\; \Lambda C \;\; 0_n \;\; 0_n \;\; 0_n \;\; 0_n\right], \qquad \Lambda = \operatorname{diag}\{\Lambda_1, \Lambda_2, \ldots, \Lambda_n\}, \\
& \Pi_5 = \left[0_{n,p} \;\; 0_{n,p} \;\; -L^T P_2 \;\; 0_{n,p} \;\; 0_{n,p} \;\; 0_{n,p}\right], \qquad \Pi_6 = \operatorname{diag}\{-R_1, -R_2\}.
\end{aligned} \tag{3.2}$$

Proof. For technical convenience, we rewrite (2.18) as

$$\begin{aligned} dx(t) &= r_1(t)dt + Ex(t)d\omega(t), \\ de(t) &= r_2(t)dt + Ex(t)d\omega(t), \end{aligned} \tag{3.3}$$

where

$$\begin{aligned} r_1(t) &= (A+BK)x(t) - BKe(t) + g(x(t)), \\ r_2(t) &= LCx(t) + (A-LC)e(t) + g(x(t)) \\ &\quad - g(x(t)-e(t)) - L(I+\Lambda(t))Cx\big(t-\eta(t)\big). \end{aligned} \tag{3.4}$$

Now, choose the following Lyapunov-Krasovskii functional:

$$\begin{aligned} V(t) &= x^T(t)P_1x(t) + \int_{t-\kappa}^{t}\int_{s}^{t} r_1^T(\theta)R_1r_1(\theta)d\theta ds + \int_{t-\kappa}^{t}\int_{s}^{t} x^T(\theta)E^TR_1Ex(\theta)d\theta ds \\ &\quad + e^T(t)P_2e(t) + \int_{t-\kappa}^{t}\int_{s}^{t} r_2^T(\theta)R_2r_2(\theta)d\theta ds + \int_{t-\kappa}^{t}\int_{s}^{t} x^T(\theta)E^TR_2Ex(\theta)d\theta ds, \end{aligned} \tag{3.5}$$

where $P_j > 0$, $R_j > 0$, $(j = 1, 2)$ are matrices to be determined. Then, by Itô's formula and from (3.5), we obtain the stochastic differential as

$$dV(t) = \mathcal{L}V(t)dt + 2\Big(x^T(t)P_1Ex(t) + e^T(t)P_2Ex(t)\Big)d\omega(t) \tag{3.6}$$

and

$$\begin{aligned} \mathcal{L}V(t) &= 2x^T(t)P_1r_1(t) + r_1^T(t)\kappa R_1r_1(t) \\ &\quad - \int_{t-\kappa}^{t} r_1^T(s)R_1r_1(s)ds + x^T(t)E^T(P_1+\kappa R_1)Ex(t) \\ &\quad - \int_{t-\kappa}^{t} x^T(s)E^TR_1Ex(s)ds + 2e^T(t)P_2r_2(t) + r_2^T(t)\kappa R_2r_2(t) - \int_{t-\kappa}^{t} r_2^T(s)R_2r_2(s)ds \\ &\quad + x(t)^TE^T(P_2+\kappa R_2)Ex(t) - \int_{t-\kappa}^{t} x^T(s)E^TR_2Ex(s)ds \\ &\le 2x^T(t)P_1r_1(t) + r_1^T(t)\kappa R_1r_1(t) + x(t)^TE^T(P_1+\kappa R_1+P_2+\kappa R_2)Ex(t) \\ &\quad - \int_{t-\eta(t)}^{t} r_1^T(s)R_1r_1(s)ds - \int_{t-\eta(t)}^{t} x^T(s)E^TR_1Ex(s)ds \\ &\quad + 2e^T(t)P_2r_2(t) + r_2^T(t)\kappa R_2r_2(t) \\ &\quad - \int_{t-\eta(t)}^{t} r_2^T(s)R_2r_2(s)ds - \int_{t-\eta(t)}^{t} x^T(s)E^TR_2Ex(s)ds + 2X_1(t) + 2X_2(t), \end{aligned} \tag{3.7}$$

where

$$\begin{aligned}
X_1(t) &= \xi_1^T(t)S\left(x(t) - x(t-\eta(t)) - \int_{t-\eta(t)}^{t} r_1(s)ds - \int_{t-\eta(t)}^{t} Ex(s)d\omega(s)\right) = 0,\\
X_2(t) &= \xi_2^T(t)U\left(e(t) - e(t-\eta(t)) - \int_{t-\eta(t)}^{t} r_2(s)ds - \int_{t-\eta(t)}^{t} Ex(s)d\omega(s)\right) = 0,\\
\xi_1^T(t) &= \left[x^T(t) \quad x^T(t-\eta(t))\right], \qquad S = \left[S_1^T \quad S_2^T\right]^T,\\
\xi_2^T(t) &= \left[e^T(t) \quad e^T(t-\eta(t))\right], \qquad U = \left[U_1^T \quad U_2^T\right]^T.
\end{aligned} \tag{3.8}$$

From (2.19), we obtain

$$\begin{aligned}
Y_1(t) &= \varepsilon_1 x^T(t)G^T Gx(t) - \varepsilon_1 g^T(x(t))g(x(t)) \geq 0,\\
Y_2(t) &= \varepsilon_2(x(t) - e(t))^T G^T G(x(t) - e(t))\\
&\quad - \varepsilon_2 g^T(x(t) - e(t))g(x(t) - e(t)) \geq 0,
\end{aligned} \tag{3.9}$$

where ε_1 and ε_2 are positive constants. Then, taking expectation on both sides of (3.7), we have

$$\mathbb{E}\{\mathcal{L}V(t)\} + Y_1(t) + Y_2(t) \leq \mathbb{E}\left\{\xi^T(t)\left[\overline{\Pi}_6 + \Sigma_4 + \Sigma_5\right]\xi(t)\right\} + \Sigma_6 + \Sigma_7, \tag{3.10}$$

where

$$\begin{aligned}
\overline{\Pi}_1 &= \operatorname{sym}\left(W_x^T P_1 W_{r_1} + W_e^T P_2 W_{\tilde{r}_2} + VW_v\right) + W_x^T E^T(P_1 + \kappa R_1 + P_2 + \kappa R_2)W_x + W_g^T \Psi_1 W_g,\\
\Sigma_4 &= \kappa W_{r_1}^T R_1 W_{r_1} + \kappa W_{\tilde{r}_2}^T R_2 W_{\tilde{r}_2}, \qquad \Sigma_5 = (\kappa+1)\tilde{S}R_1^{-1}\tilde{S}^T + (\kappa+1)\tilde{U}R_2^{-1}\tilde{U}^T,\\
W_{\tilde{r}_2} &= \left[LC \quad -L(I+\Lambda(t))C \quad A - LC \quad 0 \quad I \quad -I\right],\\
\Sigma_6 &= -\int_{t-\eta(t)}^{t}\left[\xi_1^T(t)S + r_1(s)R_1\right]R_1^{-1}\left[S^T\xi_1(t) + R_1 r_1(s)\right]ds,\\
\Sigma_7 &= -\int_{t-\eta(t)}^{t}\left[\xi_2^T(t)U + r_2(s)R_2\right]R_2^{-1}\left[U^T\xi_2(t) + R_2 r_2(s)\right]ds,\\
\xi^T(t) &= \left[\xi_1^T(t) \quad \xi_2^T(t) \quad g^T(x(t)) \quad g^T(x(t) - e(t))\right].
\end{aligned} \tag{3.11}$$

Note that $R_1 > 0$ and $R_2 > 0$, thus Σ_6 and Σ_7 are nonpositive. Therefore, from (3.10) we know that $\mathbb{E}\{\mathcal{L}V(t)\} + Y_1(t) + Y_2(t) < 0$ if

$$\overline{\Pi}_1 + \Sigma_4 + \Sigma_5 < 0, \tag{3.12}$$

which by Schur complements, is equivalent to

$$\begin{bmatrix} \overline{\Pi}_1 & \sqrt{\kappa+1}V & \Pi_2^T & \overline{\Pi}_7^T \\ * & \Pi_6 & 0 & 0 \\ * & * & -R_1^{-1} & 0 \\ * & * & * & -R_2^{-1} \end{bmatrix} < 0, \tag{3.13}$$

where $\overline{\Pi}_7 = \sqrt{\kappa} W_{\tilde{r}_2}$. Now, rewrite (3.13) in the form (2.20) with

$$\Sigma_1 = \begin{bmatrix} \Pi_1 & \sqrt{\kappa+1}V & \Pi_2^T & \Pi_3^T \\ * & \Pi_6 & 0 & 0 \\ * & * & -R_1^{-1} & 0 \\ * & * & * & -R_2^{-1} \end{bmatrix},$$
$$\Sigma_2 = \begin{bmatrix} \Pi_4 & 0 & 0 & 0 \end{bmatrix}, \qquad \Sigma_3 = \begin{bmatrix} \Pi_5 & 0 & 0 & -L^T \end{bmatrix}^T, \qquad H(t) = \Lambda(t)\Lambda^{-1}. \tag{3.14}$$

By Lemma 2.2 together with a Schur complement operation, (3.13) holds if for some $\varepsilon > 0$, (3.1) holds. Thus, we have

$$\mathbb{E}\{\mathcal{L}V(t)\} < 0, \tag{3.15}$$

which ensures that the closed-loop system in (2.18) is asymptotically stable by [30]. Theorem 3.1 is proved. □

Since our main objective is to design K and L to stabilize the system (2.18), (3.1) is actually a nonlinear matrix inequality. We will transform them into tractable conditions to solve the control synthesis problem.

Theorem 3.2. *There exists an observer-based controller such that the closed-loop system in* (2.18) *is asymptotically stable in the mean square if there exist scalars $\varepsilon_i > 0$ ($i = 1, 2, 3$) and matrices $\overline{P}_1 > 0$, $P_2 \geq 0$, $R_1 > 0$, $R_2 > 0$, $Z_i > 0$, $Q_i > 0$ and S, U, $\overline{K}$, $\overline{L}$, satisfying*

$$\begin{bmatrix} \Xi_1 & \Xi_2 \\ * & \Xi_3 \end{bmatrix} < 0, \tag{3.16}$$

$$\begin{bmatrix} \Phi_1 & \Phi_2 \\ * & \Phi_3 \end{bmatrix} < 0, \tag{3.17}$$

$$\begin{bmatrix} Z_1 & I \\ * & Q_1 \end{bmatrix} > 0, \qquad \begin{bmatrix} Z_3 & I \\ * & Q_2 \end{bmatrix} > 0, \qquad \begin{bmatrix} R_1 & I \\ * & Q_3 \end{bmatrix} > 0, \tag{3.18}$$

where

$$\Xi_1 = \operatorname{sym}\left(W_{\bar{e}}^T P_2 W_{\bar{r}_2} + \overline{V} W_{\bar{v}} - W_{\hat{x}}^T \left(\varepsilon_2 G^T G\right) W_{\bar{e}}\right) + W_{\bar{g}}^T \Psi_1 W_{\bar{g}} + W_z^T Z W_z,$$

$$\Xi_2 = \left[\sqrt{\kappa}\Upsilon_1^T \quad \sqrt{\kappa+1}\,\overline{V} \quad \Upsilon_2^T \quad \Upsilon_3^T\right], \qquad Z = \operatorname{diag}\{-Z_1, Z_2, Z_3\},$$

$$\Xi_3 = \operatorname{diag}\{R_2 - 2P_2, -R_1, -R_2, -P_2, -R_2, -\varepsilon_3 I\},$$

$$\Phi_1 = \operatorname{sym}\left(W_{\bar{x}}^T W_{\bar{r}_1}\right) - W_y^T \overline{Z} W_y, \qquad \overline{Z} = \operatorname{diag}\left\{Z_2, 2\overline{P}_1 - Q_2\right\},$$

$$\Phi_2 = \begin{bmatrix} \sqrt{\kappa}\left(\overline{P}_1 A^T + \overline{K}^T B^T\right) & \overline{P}_1 E^T & \sqrt{\kappa}\,\overline{P}_1 E^T & \overline{P}_1 \\ \sqrt{\kappa} I & 0 & 0 & 0 \\ -\sqrt{\kappa}\,\overline{K}^T B^T & 0 & 0 & 0 \end{bmatrix},$$

$$\Phi_3 = \operatorname{diag}\left\{-Q_3, -\overline{P}_1, -Q_3, -Q_1\right\}, \qquad \overline{V} = \left[\overline{S} \quad \overline{U}\right], \qquad W_{\hat{x}} = \left[0_{n,3n} \quad I_n \quad 0_{n,2n}\right],$$

$$\overline{S} = \left[0_n \quad S_2^T \quad 0_n \quad S_1^T \quad 0_n \quad 0_n\right]^T, \qquad \overline{U} = \left[U_2^T \quad 0_{n,4n} \quad U_1^T\right]^T,$$

$$W_{\bar{x}} = \left[I_n \quad 0_{n,2n}\right], \qquad W_{\bar{r}_1} = \left[A\overline{P} + B\overline{K} \quad I_n \quad -B\overline{K}\right],$$

$$W_{\bar{e}} = \left[0_{n,5n} \quad I_n\right], \qquad W_{\bar{r}_2} = \left[0_n \quad -\overline{L}C \quad -I_n \quad \overline{L}C \quad I_n \quad A - \overline{L}C\right],$$

$$\Upsilon_1 = \left[0_n \quad -\overline{L}C \quad -P_2 \quad \overline{L}C \quad P_2 \quad P_2 A - \overline{L}C\right],$$

$$\Upsilon_2 = \begin{bmatrix} 0 & 0 & 0 & P_2 E & 0 & 0 \\ 0 & 0 & 0 & \sqrt{\kappa} R_2 E & 0 & 0 \end{bmatrix},$$

$$\Upsilon_3 = \left[0 \quad 0 \quad 0 \quad 0 \quad 0 \quad -\overline{L}^T\right],$$

$$W_{\bar{v}} = \left[\begin{array}{cccccc} 0_n & -I_n & 0_n & I_n & 0_{n,2n} \\ \hline -I_n & -0_{n,4n} & & I_n & \end{array}\right], \qquad W_y = \left[\begin{array}{ccc} 0_n & I_n & 0_n \\ \hline 0_{n,2n} & I_n & \end{array}\right],$$

$$W_{\bar{g}} = \left[\begin{array}{ccc} 0_{n,3n} & I_n & 0_{n,2n} \\ \hline 0_{n,5n} & I_n & \\ \hline 0_{n,4n} & I_n & 0_n \\ \hline 0_{n,2n} & I_n & 0_{n,3n} \end{array}\right], \qquad W_z = \left[\begin{array}{ccc} 0_{n,3n} & I_n & 0_{n,2n} \\ \hline 0_{n,4n} & I_n & 0_n \\ \hline 0_{n,5n} & I_n & \end{array}\right]. \tag{3.19}$$

Moreover, if the above conditions are satisfied, a desired controller gain and observer gain are given as follows:

$$K = \overline{K}\,\overline{P}_1^{-1}, \qquad L = \overline{P}_2^{-1}\overline{L}. \tag{3.20}$$

Proof. Define the following matrix:

$$W = \begin{bmatrix} 0_{n,3n} & I_n & 0_{n,2n} \\ 0_n & I_n & 0_{n,4n} \\ 0_{n,5n} & I_n & \\ I_n & 0_{n,5n} & \\ 0_{n,4n} & I_n & 0_n \\ 0_{n,2n} & I_n & 0_{n,3n} \end{bmatrix}. \tag{3.21}$$

Perform a congruence transformation to (3.1) by $W_1 = \operatorname{diag}\{W, I, I, I, I, I\}$, which are to exchange the first row and the forth row with the third row and the sixth row, then exchange the first column and the forth column with the third column and the sixth column.

Then, by using Lemma 1 in [25] and Theorem 3.2, we have

$$\begin{bmatrix} \overline{\Xi}_1 & \overline{\Xi}_2 \\ * & \overline{\Xi}_3 \end{bmatrix} < 0, \tag{3.22}$$

$$\begin{bmatrix} \overline{\Phi}_1 & \overline{\Phi}_2 \\ * & \overline{\Phi}_3 \end{bmatrix} < 0, \tag{3.23}$$

where

$$\begin{gathered}
\overline{\Xi}_1 = \operatorname{sym}\left(W_{\overline{e}}^T P_2 W_{\overline{r}_2} + \overline{V} W_{\overline{v}} - W_{\hat{x}}^T \left(\varepsilon_2 G^T G\right) W_{\overline{e}}\right) + W_{\overline{g}}^T \Psi_1 W_{\overline{g}} + W_z^T Z W_z, \\
\overline{\Xi}_2 = \left[\overline{\Upsilon}_1^T \quad \sqrt{\kappa + 1}\,\overline{V} \quad \overline{\Upsilon}_2^T \quad \overline{\Upsilon}_3^T\right], \\
\overline{\Xi}_3 = \operatorname{diag}\left\{-R_2^{-1}, -R_1, -R_2, -P_2^{-1}, -R_2^{-1}, -\varepsilon_3 I\right\}, \\
\overline{\Upsilon}_1 = \sqrt{\kappa} W_{\overline{r}_2}, \qquad W_{\overline{r}_2} = \left[0_n \quad -LC \quad -I_n \quad LC \quad I_n \quad A - LC\right], \\
\overline{\Upsilon}_2 = \begin{bmatrix} 0 & 0 & 0 & E & 0 & 0 \\ 0 & 0 & 0 & \sqrt{\kappa} E & 0 & 0 \end{bmatrix}, \qquad \overline{\Upsilon}_3 = \left[0 \quad 0 \quad 0 \quad 0 \quad 0 \quad -L^T P_2\right], \\
\overline{\Phi}_1 = \operatorname{sym}\left(W_{\overline{x}}^T P_1 W_{\overline{r}_1}\right) - W_{\overline{y}}^T Z W_{\overline{y}}, \qquad W_{\overline{r}_1} = \left[A + BK \quad I_n \quad -BK\right], \\
\overline{\Phi}_2 = \begin{bmatrix} \sqrt{\kappa}\left(A^T + K^T B^T\right) & E^T & \sqrt{\kappa} E^T \\ \sqrt{\kappa} I & 0 & 0 \\ -\sqrt{\kappa} K^T B^T & 0 & 0 \end{bmatrix}, \qquad W_{\overline{y}} = \begin{bmatrix} I_n & 0_{n,2n} & \\ 0_n & I_n & 0_n \\ 0_{n,2n} & I_n & \end{bmatrix}, \\
\overline{\Phi}_3 = \operatorname{diag}\left\{-R_1^{-1}, -P_1^{-1}, -R_1^{-1}\right\}.
\end{gathered} \tag{3.24}$$

Perform a congruence transformation to (3.22) by $J_2 = \operatorname{diag}\{I_{6n}, J_1\}$ with $J_1 = \operatorname{diag}\{P_2, I_{2n}, P_2, R_2, I_n\}$. Defining $\overline{L} = P_2 L$, we have (3.16). Performing a congruence transformation to (3.23) by $J_4 = \operatorname{diag}\{J_3, I_{3n}\}$ with $J_3 = \operatorname{diag}\{P_1^{-1}, I, P_1^{-1}\}$ and defining $\overline{P}_1 = P_1^{-1}$, $\overline{K} = K P_1^{-1}$, $Q_1 = Z_1^{-1}$, $Q_2 = Z_3^{-1}$, $Q_3 = R_1^{-1}$, $-P_1^{-1} Z_3 P_1^{-1} \leq Z_3^{-1} - 2P_1^{-1}$ and $-P_2 R_2^{-1} P_2 \leq R_2 - 2P_2$ we have (3.17). We can solve the inequalities (3.18) by using of the cone complementarity linearization (CCL) algorithm in [31]. The proof is completed. □

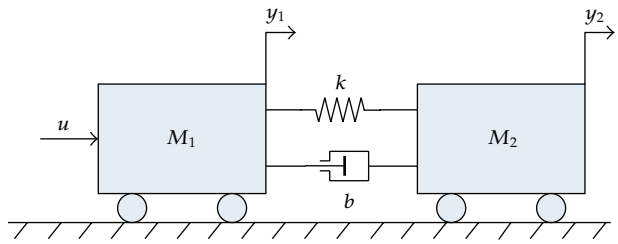

Figure 2: Mechanical system.

4. Illustrative Example

In this section, we use a mechanical example to illustrate the applicability of the theoretical results developed in this paper.

The controlled plant is a mechanical system consisted of two cars, a spring, and a damper, as shown in Figure 2. The objective is to design controllers such that the system will maintain the zero position ($y_1 = 0$ and $y_2 = 0$) when the disturbance disappears. M_1 and M_2 denote the two car mass, respectively; k is the elastic coefficient of the spring; b is the viscous damping coefficient of the damper; u denotes control input; y_1 and y_2 are the displacements of the two cars, respectively. The right is the positive direction of the force and the displacement. When $u = 0$, the balance positions are the zero place of the two cars y_1 and y_2.

Choose the following set of state variables:

$$x = \begin{bmatrix} x_1 & x_2 & x_3 & x_4 \end{bmatrix} = \begin{bmatrix} y_1 & y_2 & \dot{y}_1 & \dot{y}_2 \end{bmatrix}. \tag{4.1}$$

The equations of the mechanical system are in the following:

$$\begin{aligned} dx_1 &= x_3 dt, \\ dx_2 &= x_4 dt, \\ dx_3 &= \left(-\frac{k}{m_1}(x_1 - x_2) - \frac{b}{m_1}(x_3 - x_4) + u(t) + 0.001\sin(0.5t)\right)dt \\ &\quad + 0.01 x_1 d\omega(t), \\ dx_4 &= \left(\frac{k}{m_2}(x_1 - x_2) + \frac{b}{m_2}(x_3 - x_4) + 0.001\sin(0.2t)\right)dt. \end{aligned} \tag{4.2}$$

The parameters of the mechanical system are $m_1 = 1\,\text{kg}$, $m_2 = 2\,\text{kg}$, $k = 36\,\text{N/m}$, and $b = 0.06\,\text{Ns/m}$. Then the state-space matrices are given by

$$\begin{aligned} A &= \begin{bmatrix} 0 & 0 & 1 & 0 \\ 0 & 0 & 0 & 1 \\ -36 & 36 & -0.6 & 0.6 \\ 18 & -18 & 0.3 & -0.3 \end{bmatrix}, \qquad B = \begin{bmatrix} 0 \\ 0 \\ 1 \\ 0 \end{bmatrix}, \qquad C = \begin{bmatrix} 1 & 0 & 0 & 0 \\ 0 & 1 & 0 & 0 \end{bmatrix}, \\ E &= \begin{bmatrix} 0 & 0 & 0 & 0 \\ 0 & 0 & 0 & 0 \\ 0.01 & 0 & 0 & 0 \\ 0 & 0 & 0 & 0 \end{bmatrix}, \qquad G = \begin{bmatrix} 0.05 & 0 & 0 & 0 \\ 0 & 0.05 & 0 & 0 \\ 0 & 0 & 0.05 & 0 \\ 0 & 0 & 0 & 0.05 \end{bmatrix}. \end{aligned} \tag{4.3}$$

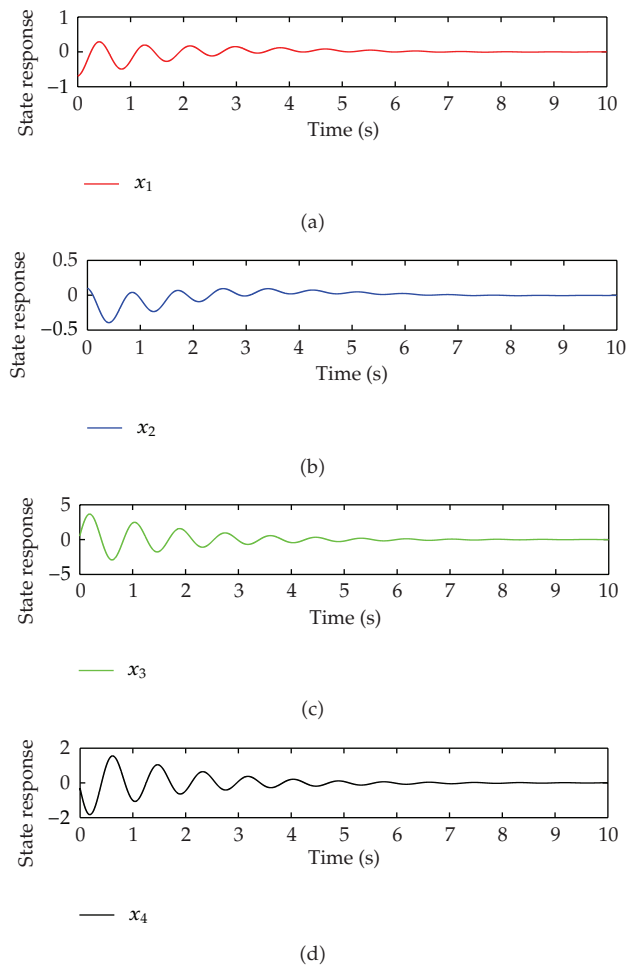

Figure 3: State responses of closed-loop system.

The eigenvalues of A are $-0.4500 \pm 7.3347i, 0, 0$, and thus this system is unstable. Our objective is to design an observer-based controller in the form of (2.2) such that the closed-loop system (2.1) is asymptotically stable in mean square. The network-related parameters are assumed: the sampling period $h = 2\,\text{ms}$, the maximum delay $\overline{\eta} = 4\,\text{ms}$, the maximum number of data packet dropouts $\overline{\delta} = 1$, the quantizer parameters $\rho = 0.9$, and $u_0 = 2$. By Theorem 3.2, we obtain the following matrices (other associated matrices are omitted here):

$$\overline{P}_1 = \begin{bmatrix} 0.5130 & 0.4367 & -0.1801 & -0.1547 \\ 0.4367 & 0.4903 & -0.1504 & -0.1654 \\ -0.1801 & -0.1504 & 3.4095 & -1.2803 \\ -0.1547 & -0.1654 & -1.2803 & 1.0595 \end{bmatrix}, \qquad \overline{K}^T = \begin{bmatrix} -0.4605 \\ -0.4650 \\ -1.6411 \\ 0.0173 \end{bmatrix},$$
$$P_2 = \begin{bmatrix} 2.7987 & -0.4600 & -0.7901 & -1.4199 \\ -0.4600 & 5.3953 & -1.2876 & -2.5287 \\ -0.7901 & -1.2876 & 0.7402 & 1.3478 \\ -1.4199 & -2.5287 & 1.3478 & 2.7867 \end{bmatrix}, \qquad \overline{L} = \begin{bmatrix} 9.2859 & -4.2200 \\ -6.3928 & 7.7879 \\ 0.5443 & 0.8766 \\ 1.2269 & 1.3828 \end{bmatrix}. \tag{4.4}$$

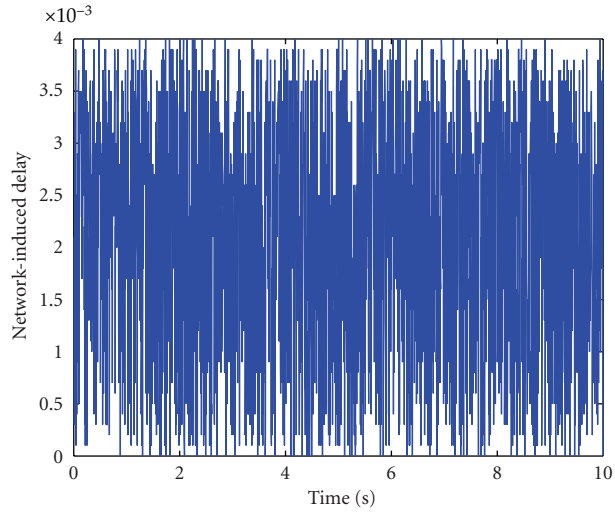

Figure 4: Network-induced delays.

According to (3.20), the gain matrices for the observer-based controller is given by:

$$K^T = \begin{bmatrix} -0.9531 \\ -1.1033 \\ -1.2654 \\ -1.8243 \end{bmatrix}, \qquad L = \begin{bmatrix} 7.7216 & 2.5661 \\ 2.8715 & 4.5438 \\ 10.5690 & 8.6714 \\ 1.8687 & 1.7328 \end{bmatrix}. \tag{4.5}$$

In the following, we provide simulation results. The initial condition is assumed to be $[-0.3, 0.7, 0.1, -0.5]$. The state responses are depicted in Figure 3, from which we can see that all the four state components of the closed-loop system converge to zero. In the simulation, the network-induced delays and the data packet dropouts are generated randomly (uniformly distributed within their ranges) according to the above assumptions, and shown in Figures 4 and 5. The output signals $y(t)$ and the successfully transmitted signal arriving at the ZOH $\hat{y}(t)$ (denotes as y_{ZOH} in figure) are shown in Figure 6, where we can see the discontinuous behavior of the transmitted measurements.

5. Conclusion

In this paper, the problem of observer-based stabilization of the stochastic nonlinear systems with limited communication has been studied. A new model has been proposed to describe the stochastic nonlinear systems with a communication channel, which exists between the output of the physical plant and the input of the dynamic controller. Based on this, the design procedure of observer-based controller has been proposed, which guarantees the asymptotic stability of the closed-loop systems. Finally, a mechanical system example is given to show the effectiveness of the proposed controller design method.

Acknowledgments

This work was partly supported by the Postdoctoral Science Foundation of China (2011M501076), the Research Foundation of Education Bureau of Heilongjiang province (11551492), the National Key Basic Research Program of China (2012CB215202), the 111 Project (B12018), and the National Natural Science Foundation of China (61174058).

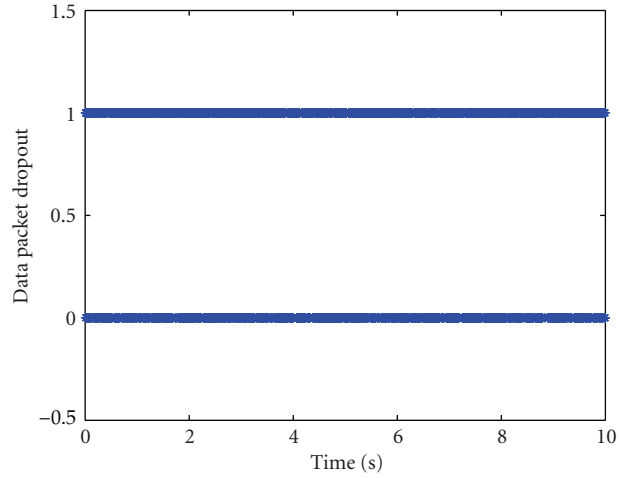

Figure 5: Data packet dropouts.

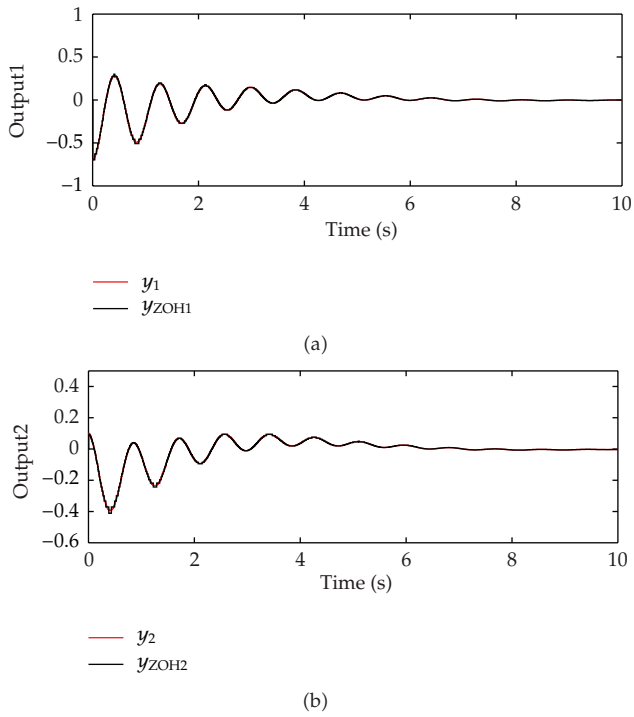

Figure 6: Measurements and transmitted signals.

References

[1] X. X. Liao and X. Mao, "Exponential stability of stochastic delay interval systems," *Systems & Control Letters*, vol. 40, no. 3, pp. 171–181, 2000.

[2] Z. Mao, B. Jiang, and P. Shi, "Fault-tolerant control for a class of nonlinear sampled-data systems via a Euler approximate observer," *Automatica*, vol. 46, no. 11, pp. 1852–1859, 2010.

[3] Z. Wang, Y. Liu, and X. Liu, "Exponential stabilization of a class of stochastic system with Markovian jump parameters and mode-dependent mixed time-delays," *IEEE Transactions on Automatic Control*, vol. 55, no. 7, pp. 1656–1662, 2010.

[4] H. R. Karimi, "Robust delay-dependent H_∞ control of uncertain time-delay systems with mixed neutral, discrete, and distributed time-delays and Markovian switching parameters," *IEEE Transactions on Circuits and Systems. I. Regular Papers*, vol. 58, no. 8, pp. 1910–1923, 2011.

[5] A. P. C. Gonçalves, A. R. Fioravanti, and J. C. Geromel, "H_∞ filtering of discrete-time Markov jump linear systems through linear matrix inequalities," *IEEE Transactions on Automatic Control*, vol. 54, no. 6, pp. 1347–1351, 2009.

[6] H. Gao, J. Wu, and P. Shi, "Robust sampled-data H_∞ control with stochastic sampling," *Automatica*, vol. 45, no. 7, pp. 1729–1736, 2009.

[7] Z. Wang, D. W. C. Ho, Y. Liu, and X. Liu, "Robust H_∞ control for a class of nonlinear discrete time-delay stochastic systems with missing measurements," *Automatica*, vol. 45, no. 3, pp. 684–691, 2009.

[8] R. Yang, P. Shi, G. Liu, and H. Gao, "Network-based feedback control for systems with mixed delays based on quantization and dropout compensation," *Automatica*, vol. 47, no. 12, pp. 2805–2809, 2011.

[9] X. Luan, P. Shi, and F. Liu, "Stabilization of networked control systems with random delays," *IEEE Transactions on Industrial Electronics*, vol. 45, no. 3, pp. 4323–4330, 2011.

[10] K. Itô, "On stochastic differential equations," *Memoirs of the American Mathematical Society*, no. 4, pp. 1–51, 1951.

[11] X. Mao, "Robustness of exponential stability of stochastic differential delay equations," *IEEE Transactions on Automatic Control*, vol. 41, no. 3, pp. 442–447, 1996.

[12] S. Xu and T. Chen, "H_∞ output feedback control for uncertain stochastic systems with time-varying delays," *Automatica*, vol. 40, no. 12, pp. 2091–2098, 2004.

[13] P. Antsaklis and J. Baillieul, "Guest editorial. Special issue on networked control systems," *IEEE Transactions on Automatic Control*, vol. 49, no. 9, pp. 1421–1423, 2004.

[14] N. Elia and S. K. Mitter, "Stabilization of linear systems with limited information," *IEEE Transactions on Automatic Control*, vol. 46, no. 9, pp. 1384–1400, 2001.

[15] G. N. Nair and R. J. Evans, "Exponential stabilisability of finite-dimensional linear systems with limited data rates," *Automatica*, vol. 39, no. 4, pp. 585–593, 2003.

[16] S. Tatikonda and S. Mitter, "Control under communication constraints," *IEEE Transactions on Automatic Control*, vol. 49, no. 7, pp. 1056–1068, 2004.

[17] H. Gao and T. Chen, "H_∞ estimation for uncertain systems with limited communication capacity," *IEEE Transactions on Automatic Control*, vol. 52, no. 11, pp. 2070–2084, 2007.

[18] D. Xie, D. Zhang, and Z. Wang, "Robust H_∞ faulttolerant control for uncertain networked control system with two additive random delays," *International Journal of Innovative Computing, Information and Control*, vol. 7, no. 1, pp. 315–326, 2011.

[19] H. Yang, Y. Xia, and P. Shi, "Stabilization of networked control systems with nonuniform random sampling periods," *International Journal of Robust and Nonlinear Control*, vol. 21, no. 5, pp. 501–526, 2011.

[20] Y. Zhao, J. Lam, and H. Gao, "Fault detection for fuzzy systems with intermittent measurements," *IEEE Transactions on Fuzzy Systems*, vol. 17, no. 2, pp. 398–410, 2009.

[21] Z. Wang, F. Yang, D. W. C. Ho, and X. Liu, "Robust H∞ control for networked systems with random packet losses," *IEEE Transactions on Systems, Man, and Cybernetics, Part B*, vol. 37, no. 4, pp. 916–924, 2007.

[22] X. Meng, J. Lam, and H. Gao, "Network-based H_∞ control for stochastic systems," *International Journal of Robust and Nonlinear Control*, vol. 19, no. 3, pp. 295–312, 2009.

[23] L.-S. Hu, T. Bai, P. Shi, and Z. Wu, "Sampled-data control of networked linear control systems," *Automatica*, vol. 43, no. 5, pp. 903–911, 2007.

[24] H. R. Karimi, "Observer-based mixed H_2/H∞ control design of linear systems with time-varying delays: an LMI approach," *International Journal of Control, Automation and Systems*, vol. 6, no. 1, pp. 1–14, 2008.

[25] E. Tian, D. Yue, and C. Peng, "Quantized output feedback control for networked control systems," *Information Sciences*, vol. 178, no. 12, pp. 2734–2749, 2008.

[26] Y. Cheng, B. Jiang, Y. Fu, and Z. Gao, "Robust observer based reliable control for satellite attitude control systems with sensor faults," *International Journal of Innovative Computing, Information and Control*, vol. 7, no. 7 B, pp. 4149–4160, 2011.

[27] I. Saboori, M. B. Menhaj, and B. Karimi, "A nonlinear adaptive observer based on neural networks for nonlinear systems including secure communication problems," *International Journal of Innovative Computing, Information and Control*, vol. 6, no. 11, pp. 4771–4782, 2010.

[28] C. Lin, Z. Wang, and F. Yang, "Observer-based networked control for continuous-time systems with random sensor delays," *Automatica*, vol. 45, no. 2, pp. 578–584, 2009.

[29] L. Xie, M. Fu, and C. E. de Souza, "H_∞-control and quadratic stabilization of systems with parameter uncertainty via output feedback," *IEEE Transactions on Automatic Control*, vol. 37, no. 8, pp. 1253–1256, 1992.

[30] V. B. Kolmanovskii and A. D. Myshkis, *Applied Theory of Functional Differential Equations*, Kluwer Academic Publishers, Dordrecht, The Netherlands, 1992.

[31] L. El Ghaoui, F. Oustry, and M. AitRami, "A cone complementarity linearization algorithm for static output-feedback and related problems," *IEEE Transactions on Automatic Control*, vol. 42, no. 8, pp. 1171–1176, 1997.

Hindawi Publishing Corporation
Mathematical Problems in Engineering
Volume 2012, Article ID 705828, 12 pages
doi:10.1155/2012/705828

Research Article

Finite-Time Boundedness and Stabilization of Networked Control Systems with Time Delay

Yeguo Sun and Jin Xu

Department of Mathematics and Computational Science, Huainan Normal University, 238 Dongshan West Road, Huainan 232038, China

Correspondence should be addressed to Yeguo Sun, yeguosun@126.com

Received 30 March 2012; Revised 6 June 2012; Accepted 26 June 2012

Academic Editor: Bo Shen

The finite-time control problem of a class of networked control systems (NCSs) with time delay is investigated. The main results provided in the paper are sufficient conditions for finite-time stability via state feedback. An augmentation approach is proposed to model NCSs with time delay as linear systems. Based on finite time stability theory, the sufficient conditions for finite-time boundedness and stabilization of the underlying systems are derived via linear matrix inequalities (LMIs) formulation. Finally, an illustrative example is given to demonstrate the effectiveness of the proposed results.

1. Introduction

Networked control systems (NCSs) are feedback control systems with control loops closed via digital communication channels. Compared with the traditional point-to-point wiring, the use of the communication channels can reduce the costs of cables and power, simplify the installation and maintenance of the whole system, and increase the reliability. NCSs have many industrial applications in automobiles, manufacturing plants, aircrafts, and HVAC systems [1]. However, the insertion of communication networks in feedback control loops makes the NCSs analysis and synthesis complex; see [2–8] and the references therein.

One issue inherent to NCSs, however, is the network-induced delay that occurs while exchanging date among devices connected to the shared medium. This delay, either constant or time varying, can degrade the performance of control systems designed without considering it and even destabilize the system. Thus the issues of stability analysis for NCSs have received considerable attention for decades [9–15]. In [9, 10], NCSs with random delays are modelled as jump linear systems with two modes; the necessary and sufficient conditions on the existence of stabilizing controllers are given. By introducing indicator functions, mean-square asymptotic stability is derived for the closed-loop networked control system in [11].

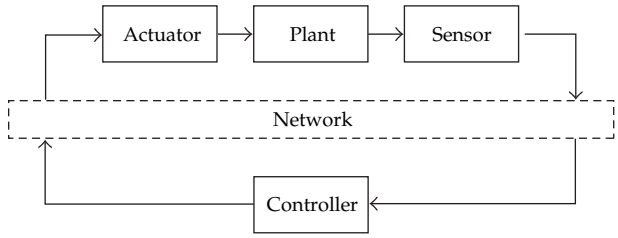

Figure 1: Illustration of NCSs over communication network.

Based on a discrete system model with time-varying input delays, stability analysis and control design are carried out in [12, 13]. In [14], an observer-based stabilizing controller has been designed for networked systems involving both random measurement and actuation delays. In [15], a novel state feedback H_∞ control with the compensator for the effects of network delays in both forward and feedback channels is proposed by introducing an augmented state variable.

On the other hand, finite-time boundedness and stability can be used in all those applications where large values of the state should not be attained, for instance, in the presence of saturations. However, most of the results in the literature are focused on Lyapunov stability. Some early results on finite-time stability (FTS) can be found in [16], more recently the concept of FTS has been revisited in the light of recent results coming from linear matrix inequalities (LMIs) theory, which has made it possible to find less conservative conditions for guaranteeing FTS and finite time stabilization of discrete-time and continuous-time systems [17–26]. In [27, 28], sufficient conditions for finite-time stability of networked control systems with packet dropout are provided; however, controller design methods are not given.

To the best of our knowledge, the finite-time stabilization problems for NCSs with delay have not been fully investigated to date. Especially for the case where the plant subjects to external interference, very few results related to NCSs are available in the existing literature, which motivates the study of this paper. The main contributions of this paper are definitions of finite-time boundedness and stabilization are extended to NCSs. Furthermore, sufficient conditions for finite-time boundedness and stabilization linear matrix inequalities formulation are given.

In this paper, the finite-time stabilization and boundedness problems of a class of NCSs with time delay are studied. The sufficient conditions for finite-time stabilization and boundedness of the underlying systems are derived via LMIs formulation. Lastly, an illustrative example is given to demonstrate the effectiveness of the proposed methods.

This paper is organized as follows. An augmentation approach is proposed to model NCSs with time delay as linear system in Section 2. The finite-time stabilization and boundedness conditions for NCSs with time delay are derived via LMIs in Section 3. Section 4 provides a numerical example to illustrate the effectiveness of our results. Finally, Section 5 gives some concluding remarks.

2. Problem Formulation and Preliminaries

Consider NCS depicted in Figure 1 consists of three components: a plant to be controlled, a network such as the Internet, and a controller.

In this paper, it is assumed that the plant is described by

$$\dot{x}(t) = Ax(t) + Bu(t) + Gw(t) \tag{2.1}$$

and time-invariant controller

$$u(kh) = -Kx(Kh), \quad k = 0, 1, 2, \ldots, \tag{2.2}$$

where $x(t) \in \mathbb{R}^n$ is the state, $u(t) \in \mathbb{R}^m$ is the control input, and $w(t) \in \mathbb{R}^q$ is the exogenous input. A, B, and G are known real constant matrices with appropriate dimensions. The sampling period h is fixed and known. There are two sources of delays from the network: the sensor-to-controller delay τ_{sc} and the controller-to-actuator delay τ_{ca}. For the fixed control law, the sensor-to-controller delay and the controller-to-actuator delay can be lumped together as $\tau = \tau_{sc} + \tau_{ca}$ for analysis purpose. We make the following assumptions about NCSs.

Assumption 2.1. The sensors are clock-driven sensors, and controllers and actuators are event-driven.

Assumption 2.2. The network-induced delay is constant and less than one sampling period.

Assumption 2.3. During the finite time T, there exists a positive constant d, such that the exogenous input $w(t)$ satisfies

$$\int_0^T w^T(t)w(t)dt \leq d^2. \tag{2.3}$$

Then the system equation can be written as

$$\begin{gathered} \dot{x}(t) = Ax(t) + Bu(t) + Gw(t), \quad t \in [kh + \tau, (k+1)h + \tau), \\ y(t) = Cx(t), \\ u(t^+) = -Kx(t - \tau), \quad t \in \{kh + \tau, k = 1, 2, \ldots\}. \end{gathered} \tag{2.4}$$

Sampling the system with period h, we obtain

$$\begin{gathered} x(k+1) = \Phi x(k) + \Gamma_0(\tau)u(k) + \Gamma_1(\tau)u(k-1) + \Psi w(k), \\ y(t) = Cx(t), \end{gathered} \tag{2.5}$$

where

$$\Phi = e^{Ah}, \qquad \Psi = \int_0^h e^{As} G\, ds. \tag{2.6}$$

$\Gamma_0(\tau)$ and $\Gamma_1(\tau)$ are defined as follows:

$$\Gamma_0(\tau) = \int_0^{h-\tau} e^{As} B\, ds, \qquad \Gamma_1(\tau) = \int_{h-\tau}^{h} e^{As} B\, ds. \tag{2.7}$$

Define the augmented state vector $\tilde{x}(k)$ as follows:

$$\tilde{x}(k) = [x(k), u(k-1)]^T \tag{2.8}$$

and the augmented exogenous input vector $\tilde{w}(k)$ as

$$\tilde{w}(k) = [w(k), 0]^T. \tag{2.9}$$

Then we have the augmented closed-loop system

$$\tilde{x}(k+1) = \left(\tilde{A} + \tilde{B}\tilde{K}\right)\tilde{x}(k) + \tilde{G}\tilde{w}(k), \tag{2.10}$$

where

$$\tilde{A} = \begin{bmatrix} \Phi & \Gamma_1(\tau) \\ 0 & 0 \end{bmatrix}, \qquad \tilde{B} = \begin{bmatrix} -\Gamma_0(\tau) \\ -I \end{bmatrix}, \qquad \tilde{G} = \begin{bmatrix} \Psi & 0 \\ 0 & 0 \end{bmatrix} \tag{2.11}$$

and $\tilde{K}$ is defined as follows

$$\tilde{K} = \begin{bmatrix} K & 0 \end{bmatrix}. \tag{2.12}$$

Remark 2.4. According to Assumption 2.3, we can derive that there exists a positive constant d, such that the condition

$$\sum_{k=1}^{N} \tilde{w}^T(k)\tilde{w}(k) \le d^2 \tag{2.13}$$

is satisfied, for finite positive integer N.

Remark 2.5. When the delay is longer than one sampling period, that is to say, $h < \tau < lh$, where $l > 1$, the augmented state vector $\tilde{x}(k)$ is defined as

$$\tilde{x}(k) = [x(k), u(k-l), \ldots, u(k-1)]^T \tag{2.14}$$

and the corresponding augmented closed-loop system can be derived.

The main aim of this paper is to find some sufficient conditions which guarantee that the system given by (2.10) is bounded over a finite-time interval. The general idea of finite-time stability concerns the boundedness of the state of a system over a finite time interval for given initial conditions; this concept can be formalized through the following definitions.

Definition 2.6. System (2.10) with (2.13) is said to be finite-time bounded with respect to (α, d, β, R, N), where R is a positive-definite matrix, $0 < \alpha < \beta$, if

$$x^T(0)Rx(0) \le \alpha^2 \Longrightarrow x^T(k)Rx(k) \le \beta^2, \quad k \in \{1, \ldots, N\}. \tag{2.15}$$

Definition 2.7. System (2.10) with $w(k) = 0$ is said to be finite-time stable with respect to (α, β, R, N), where R is a positive-definite matrix, $0 < \alpha < \beta$, if

$$x^T(0)Rx(0) \le \alpha^2 \Longrightarrow x^T(k)Rx(k) \le \beta^2, \quad k \in \{1, \ldots, N\}. \tag{2.16}$$

To this end, the following lemma will be essential for the proofs in the next section and its proof can be found in the cited references.

Lemma 2.8 (Schur complement lemma, see [29]). *For a given symmetric matrix* $W = \begin{bmatrix} W_{11} & W_{12} \\ W_{12}^T & W_{22} \end{bmatrix}$, *where* $W_{11} \in \mathbb{R}^{p\times p}, W_{22} \in \mathbb{R}^{q\times q}$, *and* $W_{12} \in \mathbb{R}^{p\times q}$, *the following three conditions are mutually equivalent:*

(1) $W < 0$,

(2) $W_{11} < 0$, $W_{22} - W_{12}^T W_{11}^{-1} W_{12} < 0$,

(3) $W_{22} < 0$, $W_{11} - W_{12} W_{22}^{-1} W_{12}^T < 0$.

3. Main Results

In this section, we will find a state feedback control matrix K, such that system (2.10) is finite-time bounded with respect to (α, d, β, R, N). In order to solve the problem, the following theorem will be essential.

Theorem 3.1. *For given state feedback control matrix K, system* (2.10) *is finite-time bounded with respect to* (α, d, β, R, N), *if there exist symmetric positive definite matrices P_1 and P_2 and a scalar $\gamma \ge 1$, such that the following conditions hold:*

$$\begin{bmatrix} \left(\tilde{A} + \tilde{B}\tilde{K}\right)^T P_1 \left(\tilde{A} + \tilde{B}\tilde{K}\right) - \gamma P_1 & \left(\tilde{A} + \tilde{B}\tilde{K}\right)^T P_1 \tilde{G} \\ \tilde{G}^T P_1 \left(\tilde{A} + \tilde{B}\tilde{K}\right) & \tilde{G}^T P_1 \tilde{G} - \gamma P_2 \end{bmatrix} < 0, \tag{3.1}$$

$$\frac{\lambda_2}{\lambda_1}\gamma^N \alpha^2 + \frac{\lambda_3}{\lambda_1}\gamma^N d^2 < \beta^2, \tag{3.2}$$

where

$$\begin{aligned} \lambda_1 &= \lambda_{\min}\left(\tilde{P}_1\right), \\ \lambda_2 &= \lambda_{\max}\left(\tilde{P}_1\right), \\ \lambda_3 &= \lambda_{\max}(P_2), \\ \tilde{P}_1 &= R^{-1/2} P_1 R^{1/2}. \end{aligned} \tag{3.3}$$

Proof. Choose the Lyapunov function as

$$V(\tilde{x}(k)) = \tilde{x}^T(k)P_1\tilde{x}(k). \tag{3.4}$$

Then we have

$$\begin{aligned} V(\tilde{x}(k+1)) &= \tilde{x}^T(k+1)P_1\tilde{x}(k+1) \\ &= \left(\left(\tilde{A}+\tilde{B}\tilde{K}\right)\tilde{x}(k)+\tilde{G}w(k)\right)^T P_1\left(\left(\tilde{A}+\tilde{B}\tilde{K}\right)\tilde{x}(k)+\tilde{G}w(k)\right) \\ &= \begin{bmatrix}\tilde{x}(k)\\ w(k)\end{bmatrix}^T \begin{bmatrix}\left(\tilde{A}+\tilde{B}\tilde{K}\right)^T P_1\left(\tilde{A}+\tilde{B}\tilde{K}\right) & \left(\tilde{A}+\tilde{B}\tilde{K}\right)^T P_1\tilde{G} \\ \tilde{G}^T P_1\left(\tilde{A}+\tilde{B}\tilde{K}\right) & \tilde{G}^T P_1\tilde{G}\end{bmatrix}\begin{bmatrix}\tilde{x}(k)\\ w(k)\end{bmatrix}. \end{aligned} \tag{3.5}$$

It follows from (3.1) that

$$V(\tilde{x}(k+1)) \le \gamma V(\tilde{x}(k)) + \gamma w^T(k)P_2w(k). \tag{3.6}$$

Applying iteratively (3.6), we obtain

$$\begin{aligned} V(\tilde{x}(k)) &\le \gamma^k V(\tilde{x}(0)) + \sum_{j=1}^{k}\gamma^j w^T(k-j)P_2w(k-j) \\ &= \gamma^k\left(V(\tilde{x}(0)) + \sum_{j=1}^{k}\gamma^{j-k}w^T(k-j)P_2w(k-j)\right) \\ &\le \gamma^k\left(V(\tilde{x}(0)) + \lambda_3\sum_{j=1}^{k}\gamma^{j-k}w^T(k-j)w(k-j)\right). \end{aligned} \tag{3.7}$$

Using the fact that $\gamma \ge 1$, we have

$$\begin{aligned} V(\tilde{x}(k)) &\le \gamma^k\left(V(\tilde{x}(0)) + \lambda_3\sum_{j=1}^{k}w^T(k-j)w(k-j)\right) \\ &\le \gamma^N\left(\lambda_2\alpha^2+\lambda_3d^2\right). \end{aligned} \tag{3.8}$$

On the other hand,

$$V(\tilde{x}(k)) = \tilde{x}^T(k)P_1\tilde{x}(k) \ge \lambda_1\tilde{x}^T(k)R\tilde{x}(k). \tag{3.9}$$

From (3.8) and (3.19), it can be seen that

$$\tilde{x}^T(k)R\tilde{x}(k) \le \frac{\lambda_2}{\lambda_1}\gamma^N\alpha^2 + \frac{\lambda_3}{\lambda_1}\gamma^N d^2 < \beta^2 \tag{3.10}$$

which means that

$$\tilde{x}^T(k)R\tilde{x}(k) \leq \beta^2, \quad k = 1, \ldots, N. \tag{3.11}$$

This completes the proof. □

Corollary 3.2. *For given state feedback control matrix K, system* (2.10) *with the disturbance $\tilde{w}(k) = 0$ is finite-time stable with respect to (α, β, R, N), if there exist symmetric positive definite matrix P and a scalar $\gamma \geq 1$, such that the following conditions hold:*

$$\begin{gathered} \left(\tilde{A} + \tilde{B}\tilde{K}\right)^T P\left(\tilde{A} + \tilde{B}\tilde{K}\right) - \gamma P < 0, \\ \operatorname{cond}\left(\tilde{P}\right) < \frac{1}{\gamma^N}\frac{\beta^2}{\alpha^2}, \end{gathered} \tag{3.12}$$

where

$$\tilde{P} = R^{-1/2}PR^{1/2}, \quad \operatorname{cond}\left(\tilde{P}\right) = \frac{\lambda_{\max}\left(\tilde{P}\right)}{\lambda_{\min}\left(\tilde{P}\right)}. \tag{3.13}$$

Now we turn back to our original problem, that is, to find sufficient conditions which guarantee that the system (2.4) with the controller (2.2) is finite-time bounded with respect to (α, d, β, R, N). The solution of this problem is given by the following theorem.

Theorem 3.3. *System* (2.10) *is finite-time bounded with respect to (α, d, β, R, N) if there exist symmetric positive definite matrices Q_{11}, Q_{12}, and Q_2, a matrix L, and a scalar $\gamma \geq 1$, such that the following conditions hold:*

$$\begin{bmatrix} -\gamma Q_1 & 0 & \left(\tilde{A}Q_1 + \tilde{B}LS\right)^T \\ 0 & -\gamma Q_2 & \tilde{G}^T \\ \tilde{A}Q_1 + \tilde{B}LS & \tilde{G} & -Q_1 \end{bmatrix} < 0, \tag{3.14}$$

$$\frac{\lambda_5}{\lambda_4}\gamma^N\alpha^2 + \lambda_5\lambda_6\gamma^N d^2 < \beta^2, \tag{3.15}$$

where

$$\begin{gathered} \lambda_4 = \lambda_{\min}\left(\tilde{Q}_1\right), \\ \lambda_5 = \lambda_{\max}\left(\tilde{Q}_1\right), \\ \lambda_6 = \lambda_{\max}(Q_2), \\ \tilde{Q}_1 = R^{-1/2}Q_1R^{1/2} \end{gathered} \tag{3.16}$$

S and Q_1 are defined as follows

$$S = \begin{bmatrix} I & 0 \\ 0 & 0 \end{bmatrix}, \qquad Q_1 = \begin{bmatrix} Q_{11} & 0 \\ 0 & Q_{12} \end{bmatrix}. \tag{3.17}$$

Then the controller K is given by the first p columns of $\widetilde{K} = LSQ_1^{-1}$, which is in the form (2.12).

Proof. Let us consider Theorem 3.1 with $Q_1 = P_1^{-1}$ and $Q_2 = P_2$. Condition (3.2) can be rewritten as in (3.15) recalling that for a positive definite matrix Q

$$\lambda_{\max}(Q) = \frac{1}{\lambda_{\min}(Q^{-1})}. \tag{3.18}$$

Denote $\widehat{A} = \widetilde{A} + \widetilde{B}\widetilde{K}$. Then condition (3.1) can be rewritten as

$$\begin{bmatrix} \widehat{A}^T Q_1^{-1} \widehat{A} - \gamma Q_1^{-1} & \widehat{A}^T Q_1^{-1} \widetilde{G} \\ \widetilde{G}^T Q_1^{-1} \widehat{A} & \widetilde{G}^T Q_1^{-1} \widetilde{G} - \gamma Q_2 \end{bmatrix} < 0. \tag{3.19}$$

Pre- and postmultiplying (3.19) by the symmetric matrix

$$\begin{bmatrix} Q_1 & 0 \\ 0 & I \end{bmatrix}, \tag{3.20}$$

the following equivalent condition is obtained

$$\begin{bmatrix} Q_1 \widehat{A}^T Q_1^{-1} \widehat{A} Q_1 - \gamma Q_1 & Q_1 \widehat{A}^T Q_1^{-1} \widetilde{G} \\ \widetilde{G}^T Q_1^{-1} \widehat{A} Q_1 & \widetilde{G}^T Q_1^{-1} \widetilde{G} - \gamma Q_2 \end{bmatrix} < 0. \tag{3.21}$$

By using Lemma 2.8, (3.21) is equivalent to the following:

$$\begin{bmatrix} Q_1 \widehat{A}^T Q_1^{-1} \widehat{A} Q_1 - \gamma Q_1 & Q_1 \widehat{A}^T Q_1^{-1} \widetilde{G} & 0 \\ \widetilde{G}^T Q_1^{-1} \widehat{A} Q_1 & -\gamma Q_2 & \widetilde{G}^T \\ 0 & \widetilde{G} & -Q_1 \end{bmatrix} < 0. \tag{3.22}$$

Premultiply (3.22) by

$$\begin{bmatrix} I & 0 & -Q_1 \widehat{A}^T Q_1^{-1} \\ 0 & I & 0 \\ 0 & 0 & I \end{bmatrix} \tag{3.23}$$

and postmultiply it by the transpose of (3.23). In this way, we obtain the following equivalent condition:

$$\begin{bmatrix} -\gamma Q_1 & 0 & Q_1\widehat{A}^T \\ 0 & -\gamma Q_2 & \widetilde{G}^T \\ \widehat{A}Q_1 & \widetilde{G} & -Q_1 \end{bmatrix} < 0. \tag{3.24}$$

Recalling that $\widehat{A} = \widetilde{A} + \widetilde{B}\widetilde{K}$ and letting $\widetilde{K}Q_1 = LS$, we obtain that condition (3.1) is equivalent to (3.14). This completes the proof. □

Remark 3.4. The chosen structures for matrices S and Q_1 guarantee that $\widetilde{K}$ is in the form (2.12). In fact

$$\widetilde{K} = LSQ_1^{-1} = L\begin{bmatrix} I & 0 \\ 0 & 0 \end{bmatrix}\begin{bmatrix} Q_{11} & 0 \\ 0 & Q_{12} \end{bmatrix} = L\begin{bmatrix} Q_{11}^{-1} & 0 \\ 0 & 0 \end{bmatrix} = \begin{bmatrix} K & 0 \end{bmatrix}. \tag{3.25}$$

Remark 3.5. Once we have fixed γ, the feasibility of the conditions stated in (3.14) can be turned into LMI feasibility problems. On the other hand, for $\theta_1 > 0, \theta_2 > 0$, it is easy to check that condition (3.15) can be guaranteed by

$$\begin{gathered} \theta_1 R^{-1} < Q_1 < R^{-1}, \\ 0 < Q_2 < \theta_2 I, \\ \begin{bmatrix} \beta^2 - \theta_2 d^2 \gamma^N & \alpha\sqrt{\gamma^N} \\ \alpha\sqrt{\gamma^N} & \theta_1 \end{bmatrix} > 0. \end{gathered} \tag{3.26}$$

Corollary 3.6. *System* (2.10) *with the disturbance* $\widetilde{w}(k) = 0$ *is finite-time stable with respect to* (α, β, R, N)*, if there exist symmetric positive definite matrices* Q_1*,* Q_2*, a matrix* L*, and a scalar* $\gamma \geq 1$*, such that the following conditions hold:*

$$\begin{gathered} \begin{bmatrix} -\gamma Q & \left(\widetilde{A}Q + \widetilde{B}LS\right)^T \\ \widetilde{A}Q + \widetilde{B}LS & -Q \end{bmatrix} < 0, \\ R^{-1} < Q < \frac{1}{\gamma^N}\frac{\beta^2}{\alpha^2}R^{-1}, \end{gathered} \tag{3.27}$$

where

$$S = \begin{bmatrix} I & 0 \\ 0 & 0 \end{bmatrix}, \qquad Q = \begin{bmatrix} Q_1 & 0 \\ 0 & Q_2 \end{bmatrix}. \tag{3.28}$$

Then the controller K *is given by the first* p *columns of* $\widetilde{K} = LSQ^{-1}$.

4. Numerical Example

Consider the following system:

$$\dot{x}(t) = \begin{bmatrix} 0 & 1 \\ 0 & -0.1 \end{bmatrix} x(t) + \begin{bmatrix} 0 \\ 0.1 \end{bmatrix} u(t) + \begin{bmatrix} 1 & 0 \\ 0 & 1 \end{bmatrix} w(t),$$
$$y(t) = \begin{bmatrix} 0.1 & 0.5 \end{bmatrix} x(t). \tag{4.1}$$

Choose the sampling $h = 0.3s$. Suppose $\tau = 0.1s$. The corresponding matrices are given by

$$\Phi = \begin{bmatrix} 1.0000 & 0.2955 \\ 0 & 0.9704 \end{bmatrix}, \qquad \Psi = \begin{bmatrix} 0.3000 & 0.0446 \\ 0 & 0.2955 \end{bmatrix}, \tag{4.2}$$

$$\Gamma_0(\tau) = \begin{bmatrix} 0.0020 \\ 0.0198 \end{bmatrix}, \qquad \Gamma_1(\tau) = \begin{bmatrix} 0.0025 \\ 0.0098 \end{bmatrix} \tag{4.3}$$

which yields

$$\tilde{A} = \begin{bmatrix} 1.0000 & 0.2955 & 0.0025 \\ 0 & 0.9704 & 0.0098 \\ 0 & 0 & 0 \end{bmatrix}, \qquad \tilde{B} = \begin{bmatrix} -0.0020 \\ -0.0198 \\ -1 \end{bmatrix}, \qquad \tilde{G} = \begin{bmatrix} 0.3000 & 0.0446 & 0 \\ 0 & 0.2955 & 0 \\ 0 & 0 & 0 \end{bmatrix}. \tag{4.4}$$

It is assumed that $\alpha = 1$, $d = 3$, $\beta = 20$, $R = I$, $N = 10$. Applying Theorem 3.3 with $\gamma = 1.5$, it is found that

$$Q_1 = \begin{bmatrix} 0.9472 & 0.0318 & 0 \\ 0.0318 & 0.7947 & 0 \\ 0 & 0 & 0.8616 \end{bmatrix},$$
$$L = \begin{bmatrix} 0.0030 & 0.0187 & 0 \end{bmatrix}. \tag{4.5}$$

Therefore, the desired controller gain is given by

$$\tilde{K} = LSQ_1^{-1} = \begin{bmatrix} K & 0 \end{bmatrix} = \begin{bmatrix} 0.0024 & 0.0235 & 0 \end{bmatrix}. \tag{4.6}$$

5. Conclusions

In this paper, we have considered the finite-time boundedness problems of a class of networked control systems (NCSs) subject to disturbances. Based on the augmentation approach, the NCSs with time delay as linear systems. The sufficient conditions for finite-time boundedness of the underlying systems are derived via linear matrix inequalities (LMIs) formulation. Lastly, an illustrative example is given to demonstrate the effectiveness of the proposed results.

Acknowledgment

This work was partly supported by the program of science and technology of Huainan no. 2011A08005.

References

[1] J. P. Hespanha, P. Naghshtabrizi, and Y. Xu, "A survey of recent results in networked control systems," *Proceedings of the IEEE*, vol. 95, no. 1, pp. 138–172, 2007.

[2] J. Wu and T. Chen, "Design of networked control systems with packet dropouts," *IEEE Transactions on Automatic Control*, vol. 52, no. 7, pp. 1314–1319, 2007.

[3] D. Yue, E. Tian, Z. Wang, and J. Lam, "Stabilization of systems with probabilistic interval input delays and its applications to networked control systems," *IEEE Transactions on Systems, Man, and Cybernetics Part A*, vol. 39, no. 4, pp. 939–945, 2009.

[4] E. Tian, D. Yue, and C. Peng, "Reliable control for networked control systems with probabilistic sensors and actuators faults," *IET Control Theory and Applications*, vol. 4, no. 8, pp. 1478–1488, 2010.

[5] Z. Wang, B. Shen, H. Shu, and G. Wei, "Quantized H_∞ control for nonlinear stochastic time-delay systems with missing measurements," *IEEE Transactions on Automatic Control*, vol. 57, no. 6, pp. 1431–1444, 2012.

[6] B. Shen, Z. Wang, H. Shu, and G. Wei, "H_∞ filtering for uncertain time-varying systems with multiple randomly occurred nonlinearities and successive packet dropouts," *International Journal of Robust and Nonlinear Control*, vol. 21, no. 14, pp. 1693–1709, 2011.

[7] B. Shen, Z. Wang, H. Shu, and G. Wei, "Robust H_∞ finite-horizon filtering with randomly occurred nonlinearities and quantization effects," *Automatica*, vol. 46, no. 11, pp. 1743–1751, 2010.

[8] Z. Wang, B. Shen, and X. Liu, "H_∞ filtering with randomly occurring sensor saturations and missing measurements," *Automatica*, vol. 48, no. 3, pp. 556–562, 2012.

[9] L. Zhang, Y. Shi, T. Chen, and B. Huang, "A new method for stabilization of networked control systems with random delays," *IEEE Transactions on Automatic Control*, vol. 50, no. 8, pp. 1177–1181, 2005.

[10] Y. Shi and B. Yu, "Output feedback stabilization of networked control systems with random delays modeled by Markov chains," *IEEE Transactions on Automatic Control*, vol. 54, no. 7, pp. 1668–1674, 2009.

[11] H. J. Gao, X. Y. Meng, and T. W. Chen, "Stabilization of networked control systems with a new delay characterization," *IEEE Transactions on Automatic Control*, vol. 53, no. 9, pp. 2142–2148, 2008.

[12] M. B. G. Cloosterman, N. van de Wouw, W. P. M. H. Heemels, and H. Nijmeijer, "Stability of networked control systems with uncertain time-varying delays," *IEEE Transactions on Automatic Control*, vol. 54, no. 7, pp. 1575–1580, 2009.

[13] M. B. G. Cloosterman, L. Hetel, N. van de Wouw, W. P. M. H. Heemels, J. Daafouz, and H. Nijmeijer, "Controller synthesis for networked control systems," *Automatica*, vol. 46, no. 10, pp. 1584–1594, 2010.

[14] X. L. Luan and P. Shi, "Stabilization of networked control systems with random delays," *IEEE Transactions on Industrial Electronics*, vol. 58, no. 9, pp. 4323–4330, 2011.

[15] E. G. Tian and D. Yue, "A new state feedback H_∞ control of networked control systems with time-varying network conditions," *Journal of the Franklin Institute*, vol. 349, pp. 891–914, 2012.

[16] L. Weiss and E. F. Infante, "Finite time stability under perturbing forces and on product spaces," *IEEE Transactions on Automatic Control*, vol. 12, pp. 54–59, 1967.

[17] F. Amato, M. Ariola, and P. Dorato, "Finite-time control of linear systems subject to parametric uncertainties and disturbances," *Automatica*, vol. 37, no. 9, pp. 1459–1463, 2001.

[18] F. Amato and M. Ariola, "Finite-time control of discrete-time linear systems," *IEEE Transactions on Automatic Control*, vol. 50, no. 5, pp. 724–729, 2005.

[19] F. Amato, M. Ariola, and C. Cosentino, "Finite-time stabilization via dynamic output feedback," *Automatica*, vol. 42, no. 2, pp. 337–342, 2006.

[20] F. Amato, R. Ambrosino, M. Ariola, and C. Cosentino, "Finite-time stability of linear time-varying systems with jumps," *Automatica*, vol. 45, no. 5, pp. 1354–1358, 2009.

[21] F. Amato, C. Cosentino, and A. Merola, "Sufficient conditions for finite-time stability and stabilization of nonlinear quadratic systems," *IEEE Transactions on Automatic Control*, vol. 55, no. 2, pp. 430–434, 2010.

[22] F. Amato, M. Ariola, and C. Cosentino, "Finite-time stability of linear time-varying systems: analysis and controller design," *IEEE Transactions on Automatic Control*, vol. 55, no. 4, pp. 1003–1008, 2010.
[23] F. Amato, M. Ariola, and C. Cosentino, "Finite-time control of discrete-time linear systems: analysis and design conditions," *Automatica*, vol. 46, no. 5, pp. 919–924, 2010.
[24] G. Garcia, S. Tarbouriech, and J. Bernussou, "Finite-time stabilization of linear time-varying continuous systems," *IEEE Transactions on Automatic Control*, vol. 54, no. 2, pp. 364–369, 2009.
[25] L. Liu and J. Sun, "Finite-time stabilization of linear systems via impulsive control," *International Journal of Control*, vol. 81, no. 6, pp. 905–909, 2008.
[26] S. Zhao, J. Sun, and L. Liu, "Finite-time stability of linear time-varying singular systems with impulsive effects," *International Journal of Control*, vol. 81, no. 11, pp. 1824–1829, 2008.
[27] S. Mastellone, C. T. Abdallah, and P. Dorato, "Stability and finite-time stability analysis of discrete-time nonlinear networked control systems," in *Proceedings of the American Control Conference (ACC '05)*, pp. 1239–1244, June 2005.
[28] S. Mastellone, C. T. Abdallah, and P. Dorato, "Model-based networked control for finite-time stability of nonlinear systems: the deterministic case," in *Proceedings of the Mediterranean Conference on Control and Automation*, pp. 1091–1096, June 2005.
[29] Y. Sun and S. Qin, "Stability analysis and controller design for networked control systems with random time delay," *International Journal of Systems Science*, vol. 42, no. 3, pp. 359–367, 2011.

Hindawi Publishing Corporation
Mathematical Problems in Engineering
Volume 2012, Article ID 261274, 14 pages
doi:10.1155/2012/261274

Research Article

Exponential Synchronization Analysis and Control for Discrete-Time Uncertain Delay Complex Networks with Stochastic Effects

Tianbo Wang,[1,2] Wuneng Zhou,[2] Dejun Zhao,[1] and Shouwei Zhao[1]

[1] *College of Fundamental Studies, Shanghai University of Engineering Science, Shanghai 201620, China*
[2] *College of Information Sciences and Technology, Donghua University, Shanghai 201620, China*

Correspondence should be addressed to Tianbo Wang, tb_wang@163.com

Received 18 April 2012; Accepted 3 June 2012

Academic Editor: Bo Shen

The exponential synchronization for a class of discrete-time uncertain complex networks with stochastic effects and time delay is investigated by using the Lyapunov stability theory and discrete Halanay inequality. The uncertainty arises from the difference of the nodes' reliability in the complex network. Through constructing an appropriate Lyapunov function and applying inequality technique, some synchronization criteria and two control methods are obtained to ensure the considered complex network being exponential synchronization. Finally, a numerical example is provided to show the effectiveness of our proposed methods.

1. Introduction

Since the discovery of small-world effect [1] and scale-free feature [2] of complex networks, many researchers in the fields of science and engineering have paid more attention to the topic and provided some valuable results which can be found in [3–9] and the references therein. Particularly, the broad application in the fields of ecosystems, the Internet, biological neural networks, and large-scale robotic system (see [10–12]), and so forth, promotes the complex network becoming a more significant topic.

Synchronization, as one of the important dynamical characters of the complex networks, has been studied in many papers. For example, the authors studied the pinning synchronization problem of stochastic impulsive network by using Lyapunov stability theory and provided some sufficient criteria to ensure that the dynamical network is asymptotical synchronization and exponential synchronization in mean square in [13]. Based

on the parameter-dependent Lyapunov function, the authors considered the synchronization problem for a network family with different network structure and proposed some synchronization criteria in [14]. Similar with the continuous complex networks, there also exist many control methods to study the synchronization stability for discrete complex networks recently, which can be found in [15–20] and the references therein. For instance, the authors investigated the synchronization problem for the discrete-time complex networks with distributed time delays by using the Lyapunov stability theory, Kronecker product, and the linear matrix inequalities method in [17]. In [18], the authors revisited the synchronization stability problem for discrete complex dynamical networks with a time varying delay and constructed a new Lyapunov-Krasovskii functional by dividing the time-varying delay into a constant part and a variant part. In [20], the authors investigated the synchronization and state estimation problems for discrete-time complex network by utilizing a time varying real-valued function and the Kronecker product and provided a novel concept of bounded H_∞ synchronization.

However, in the real world, some nodes in a complex network usually do not normally work for some reasons. Particularly, this phenomenon easily appears in a complex network composed of many electronic components since that the reliability of every electric component exists the difference in general. The reason resulted in this phenomenon can be found in [21–23]. Therefore, it is necessary to study the synchronization problem for this kind of complex network with uncertain nodes. Motivated by the above discussion, we intend to study the exponential synchronization problem for a discrete-time uncertain complex network with stochastic effects in this paper. Different from some previous papers, the contributions of our paper are as follows. (1) We consider the uncertainty arising from the nodes' reliability in the complex network. (2) We consider the case that all the nodes in the complex network are effected by the working circumstance. (3) Our approach used in the paper is different from the methods in the papers listed.

The rest of this paper is organized as follows. In Section 2, the investigated discrete complex network and some necessary lemmas, assumptions are given. In Section 3, the exponential synchronization criteria and control methods for the complex network are derived. In Section 4, a numerical example is provided to illustrate the effectiveness of our method. Finally, this paper is ended with a conclusion in Section 5.

Notation 1. In this paper, R^n and $R^{n\times m}$, respectively, denote the n-dimensional Euclidean space and the set of all $n \times m$ real matrices. For a vector $x(t) = (x_1(t), x_2(t), \ldots, x_n(t))^T \in R^n$, $\|x(t)\| = \sqrt{\sum_{i=1}^n x_i^2(t)}$ denotes its norm. A^T denotes the transpose of matrix A. $(\Omega, \mathcal{F}, \{\mathcal{F}_t\}_{t\geq 0}, \mathcal{P})$ denotes the complete probability space with a filtration $\{\mathcal{F}_t\}_{t\geq 0}$ satisfying right continuous and $\mathcal{F}_0$ containing all $\mathcal{P}$-null sets. I_n is the $n \times n$ identical matrix. $\mathbf{1}_n = (1, 1, \ldots, 1)^T$ and $\mathbf{1}_{n\times n} \in R^{n\times n}$ are an n-dimensional vector and an $n \times n$ matrix with all the elements being 1, respectively. $\otimes$ is the Kronecker product. $\lambda_{\max}(H)$ stands for the biggest eigenvalues of matrix H. $E\{\cdot\}$ denotes the mathematical expectation.

2. Preliminaries

In this paper, we consider the following discrete-time complex network consisting of N identical nodes with diffusive couplings. Each node is an n-dimensional dynamical system

and the state equation is

$$x_i(k+1) = Ax_i(k) + f(x_i(k), x_i(k-\tau(k))) + c\sum_{j=1, j\neq i}^{N} \xi_i g_{ij}\Gamma\left[x_j(k-\tau(k)) - x_i(k-\tau(k))\right] + u_i(k)$$
$$+ \varphi(x_i(k))w(k), \quad i = 1, 2, \ldots, N, \tag{2.1}$$

where N is the number of coupled nodes. $x_i(k) = (x_{i1}(k), x_{i2}(k), \ldots, x_{in}(k))^T \in R^n$ is the state vector of node i at sampling time kT with sampling period $T > 0$, $A \in R^{n\times n}$ is a constant matrix, $f(\cdot) : R^n \times R^n \rightarrow R^n$ is a nonlinear vector function, and scalar $c > 0$ denotes the coupling strength. The working situation of every node in the complex network is described by two random events:

$$\begin{aligned} &\text{Event 1 : the node is available,} \\ &\text{Event 2 : the node is unavailable.} \end{aligned} \tag{2.2}$$

Random variables ξ_i $(i = 1, 2, \ldots, N)$ are defined as

$$\xi_i = \begin{cases} 1, & \text{if Event 1 occurs,} \\ 0, & \text{if Event 2 occurs,} \end{cases} \tag{2.3}$$

where $\xi_i (i = 1, 2, \ldots, N)$ are N independent random variables with mathematical expectation $E\{\xi_i\} = p_i$ and the variance $\mathrm{Var}\{\xi_i\} = q_i$. In practice, since the availability of each node in the considered complex network is usually not identical, so it is very reasonable to describe the working situation using different random variables for different nodes. Outer-coupling matrix

$$G = \begin{bmatrix} g_{11} & g_{12} & \cdots & g_{1N} \\ g_{21} & g_{22} & \cdots & g_{2N} \\ \cdots & \cdots & \cdots & \cdots \\ g_{N1} & g_{N2} & \cdots & g_{NN} \end{bmatrix} = \begin{bmatrix} g_{11} & G_{12} \\ G_{21} & G_{22} \end{bmatrix}, \tag{2.4}$$

where $g_{ii} = -\sum_{j=1, j\neq i}^{N} g_{ij}$, $G_{12} = [\, g_{12}\ g_{13}\ \cdots\ g_{1N} \,]$, and $G_{21} = [\, g_{21}\ g_{31}\ \cdots\ g_{N1} \,]^T$. g_{ij} $(i, j = 1, 2, \ldots, N)$ are defined as follows: if there exists a connection between node i with node j, then $g_{ij} = 1$, or else $g_{ij} = 0$. Inner-coupling matrix $\Gamma \in R^{n\times n}$ is a positive definite diagonal matrix. $\tau(k)$ denotes the transmission time delay and satisfies $0 \leq \tau(k) \leq \tau$ for a positive scalar $\tau > 0$. $w(k)$ is a scalar Wiener process defined on a probability space $(\Omega, \mathcal{F}, \{\mathcal{F}_t\}_{t\geq 0}, \mathcal{P})$ with

$$E\{w(k)\} = 0, \qquad E\left\{w^2(k)\right\} = 1, \qquad E\{w(i)w(j)\} = 0, \quad i \neq j. \tag{2.5}$$

The noise strength $\varphi(\cdot) : R^n \to R^n$ is a vector function. $u_i(k) \in R^n$ $(i = 1, 2, \ldots, N)$ are the control input to be designed. The complex network (2.1) can be written as

$$\begin{aligned} x_i(k+1) = {} & Ax_i(k) + f(x_i(k), x_i(k-\tau(k))) + c\sum_{j=1}^{N}\xi_i g_{ij}\Gamma x_j(k-\tau(k)) + u_i(k) \\ & + \varphi(x_i(k))w(k), \quad i = 1, 2, \ldots, N. \end{aligned} \tag{2.6}$$

Letting $e_i(k) = x_i(k) - x_1(k)$, we get

$$\begin{aligned} e_i(k+1) = {} & Ae_i(k) + f(x_i(k), x_i(k-\tau(k))) - f(x_1(k), x_1(k-\tau(k))) + c\sum_{j=1}^{N}\xi_i g_{ij}\Gamma x_j(k-\tau(k)) \\ & - c\sum_{j=1}^{N}\xi_1 g_{1j}\Gamma x_j(k-\tau(k)) + u_i(k) - u_1(k) + \left[\varphi(x_i(k)) - \varphi(x_1(k))\right]w(k), \\ & i = 2, \ldots, N. \end{aligned} \tag{2.7}$$

Define

$$\begin{gathered} e(k) = \left(e_2^T(k), e_3^T(k), \ldots, e_N^T(k)\right)^T, \qquad \widehat{\xi} = \operatorname{diag}(\xi_2, \xi_3, \ldots, \xi_N), \qquad \overline{\xi} = \xi_1 \cdot I_{N-1}, \\ \widehat{P} = \operatorname{diag}(p_2, p_3, \ldots, p_N), \qquad \overline{P} = p_1 \cdot I_{N-1}, \qquad \widehat{Q} = \operatorname{diag}(q_2, q_3, \ldots, q_N), \qquad \overline{Q} = q_1 \cdot I_{N-1}, \\ F_i(e_i(k)) = f(x_i(k), x_i(k-\tau(k))) - f(x_1(k), x_1(k-\tau(k))), \\ F(e(k)) = \left(F_2^T(e_2(k)), F_3^T(e_3(k)), \ldots, F_N^T(e_N(k))\right)^T, \\ u(k) = \left(u_2^T(k), u_3^T(k), \ldots, u_N^T(k)\right)^T, \\ \Psi_i(e_i(k)) = \varphi(x_i(k)) - \varphi(x_1(k)), \qquad \Psi(e(k)) = \left(\Psi_2^T(e_2(k)), \Psi_3^T(e_3(k)), \ldots, \Psi_N^T(e_N(k))\right)^T, \\ G_1 = \begin{bmatrix} g_{12} & g_{13} & \cdots & g_{1N} \\ g_{12} & g_{13} & \cdots & g_{1N} \\ \cdots & \cdots & \cdots & \cdots \\ g_{12} & g_{13} & \cdots & g_{1N} \end{bmatrix} \in R^{(N-1)\times(N-1)}, \end{gathered} \tag{2.8}$$

then the error system (2.7) can be written as the following form

$$\begin{aligned} e(k+1) = {} & (I_{N-1}\otimes A)e(k) + F(e(k)) + c\left(\widehat{\xi}G_{22}\right)\otimes\Gamma e(k-\tau(k)) - c\left(\overline{\xi}G_1\right)\otimes\Gamma e(k-\tau(k)) \\ & + u(k) - \mathbf{1}_{N-1}\otimes u_1(k) + \Psi(e(k))w(k). \end{aligned} \tag{2.9}$$

Note that (2.9) is equivalent to

$$\begin{aligned} e(k+1) = {} & (I_{N-1} \otimes A)e(k) + F(e(k)) + c\left(\widehat{P}G_{22}\right) \otimes \Gamma e(k-\tau(k)) - c\left(\overline{P}G_1\right) \otimes \Gamma e(k-\tau(k)) \\ & + c\left[\left(\widehat{\xi} - \widehat{P}\right)G_{22}\right] \otimes \Gamma e(k-\tau(k)) - c\left[\left(\overline{\xi} - \overline{P}\right)G_1\right] \otimes \Gamma e(k-\tau(k)) \\ & + u(k) - \mathbf{1}_{N-1} \otimes u_1(k) + \Psi(e(k))w(k). \end{aligned} \tag{2.10}$$

Letting $\Theta_1 = c\widehat{P}G_{22} - c\overline{P}G_1$, $\Theta_2 = c(\widehat{\xi} - \widehat{P})G_{22} - c(\overline{\xi} - \overline{P})G_1$, then we have

$$\begin{aligned} e(k+1) = {} & (I_{N-1} \otimes A)e(k) + F(e(k)) + \Theta_1 \otimes \Gamma e(k-\tau(k)) + \Theta_2 \otimes \Gamma e(k-\tau(k)) + u(k) \\ & - \mathbf{1}_{N-1} \otimes u_1(k) + \Psi(e(k))w(k). \end{aligned} \tag{2.11}$$

Throughout this paper, the following assumptions are needed.

(A1) The nonlinear vector function $f(\cdot)$ in the system (2.1) satisfies

$$\begin{aligned} & \left\| f(x(k), x(k-\tau(k))) - f\left(y(k), y(k-\tau(k))\right) \right\|^2 \\ & \quad \le L_1 \left\| x(k) - y(k) \right\|^2 + L_2 \left\| x(k-\tau(k)) - y(k-\tau(k)) \right\|^2 \end{aligned} \tag{2.12}$$

for any $x(k) \in R^n$ and $y(k) \in R^n$, where $L_1 \ge 0$ and $L_2 \ge 0$ are positive constants.

From (2.12), it can be verified that

$$\|F_i(e_i(k))\|^2 \le L_1 \|e_i(k)\|^2 + L_2 \|e_i(k-\tau(k))\|^2 \tag{2.13}$$

for $i = 2, 3, \ldots, N$.

(A2) There exists a positive constant $M > 0$ such that the nonlinear vector function $\varphi(\cdot)$ in the system (2.1) satisfies

$$\left\| \varphi(x(k)) - \varphi\left(y(k)\right) \right\| \le M \left\| x(k) - y(k) \right\| \tag{2.14}$$

for any $x(k) \in R^n$ and $y(k) \in R^n$.

From (2.14), one can conclude that

$$\begin{aligned}\Psi^T(e(k))\Psi(e(k)) &= \sum_{i=2}^{N}\Psi_i^T(e_i(k))\Psi_i(e_i(k))\\ &\le \sum_{i=2}^{N}M^2e_i^T(k)e_i(k)\\ &= M^2e^T(k)e(k).\end{aligned} \tag{2.15}$$

Definition 2.1. The complex network (2.1) is said to be exponential synchronization in mean square if there exist positive constants $h > 0$ and $\gamma \in (0,1)$ such that

$$E\left\{\left\|x_i(k) - x_j(k)\right\|^2\right\} \le h\gamma^k, \quad i,j = 1,2,\ldots,N,\ k = 1,2,\ldots \tag{2.16}$$

for any initial values $x(s), s = -\tau,\ldots,0$, where γ is called the exponential convergence rate.

Remark 2.2. From Definition 2.1, it is easy to see that the complex network (2.1) is exponential synchronization in mean square only if there exist positive constants $h > 0$ and $\gamma \in (0,1)$ such that

$$E\left\{\|x_i(k) - x_1(k)\|^2\right\} \le h\gamma^k, \quad i = 2,\ldots,N,\ k = 1,2,\ldots \tag{2.17}$$

for any initial values $x(s), s = -\tau,\ldots,0$.

Remark 2.3. The complex network model (2.1) not only includes time delay and stochastic disturbances, but also considers the uncertainty of nodes' working situation. To date, there have existed many literatures [13, 15, 19] to study the synchronization control problem for discrete-time complex networks. However, for this case, there exist less results. Moreover, different from [13, 17], we are not necessary to use the information of target node given beforehand in the paper.

Lemma 2.4 (see [24]). *Let $d > 0$ be a natural number and $\{U(k)\}_{k\ge -d}$ a sequence of real numbers satisfying the inequality*

$$\Delta U(k) \le -aU(k) + b\cdot\max\{U(k), U(k-1),\ldots,U(k-d)\}, \quad k \ge 0, \tag{2.18}$$

where $\Delta U(k) = U(k+1) - U(k)$. If $0 < b < a \le 1$, then there exists a constant $\eta_0 \in (0,1)$ such that

$$U(k) \le \max\{0, U(0), U(-1),\ldots,U(-d)\}\eta_0^k, \quad k \ge 0. \tag{2.19}$$

Moreover, η_0 can be chosen as the root of the equation

$$\eta^{d+1} + (a-1)\eta^d - b = 0 \tag{2.20}$$

in the interval $(0,1)$.

Lemma 2.5 (see [25]). *The Kronecker product $\otimes$ has the following properties:*

(1) $(A+B)\otimes C = A\otimes C + B\otimes C, C\otimes(A+B) = C\otimes A + C\otimes B,$

(2) $(A\otimes B)^T = A^T\otimes B^T,$

(3) $(A\otimes B)^{-1} = A^{-1}\otimes B^{-1},$

(4) $(A\otimes C)(B\otimes D) = AB\otimes CD.$

where, $A, B, C,$ and D are real matrices with appropriate dimensions.

3. Synchronization Analysis and Control

In this section, we will derive some synchronization criteria for the complex network (2.1) without input and two different synchronization control methods, respectively.

Theorem 3.1. *Under assumptions (A1)~(A2), if there exist positive constants $\delta_1 > 0, \delta_2 > 0, \alpha > 0,$ and $\beta > 0$ such that*

$$\begin{gathered}\beta < \alpha \le 1,\\ \Pi_1 = \begin{bmatrix} I_{N-1}\otimes\left[\left(M^2+\alpha\right)\cdot I_n + (1+\delta_1+\delta_2)L_1\cdot I_n + A^TA - I_n\right] & I_{N-1}\otimes A^T \\ I_{N-1}\otimes A & -\delta_1\cdot I_{n(N-1)}\end{bmatrix} < 0,\\ \Pi_2 = \begin{bmatrix} (1+\delta_1+\delta_2)L_2\cdot I_{n(N-1)} - \beta I_{n(N-1)} + \left(\Theta_1^T\Theta_1+\Theta_3\right)\otimes\Gamma^T\Gamma & \Theta_1^T\otimes\Gamma^T \\ \Theta_1\otimes\Gamma & -\delta_2\cdot I_{n(N-1)}\end{bmatrix} < 0,\end{gathered} \tag{3.1}$$

where $\Theta_3 = c^2G_{22}^T\widehat{Q}G_{22} + c^2G_1^T\overline{Q}G_1$, then the complex network (2.1) *without input is exponential synchronization in mean square.*

Proof. Choosing the following Lyapunov function:

$$V(e(k)) = e^T(k)e(k), \tag{3.2}$$

and calculating the difference of $V(e(k))$ along the trajectories of the system (2.11) without the input, we get

$$\begin{aligned}
E\{\Delta V(e(k))\} &= E\{V(e(k+1)) - V(e(k))\} \\
&= E\Big\{[(I_{N-1}\otimes A)e(k) + F(e(k)) + \Theta_1\otimes\Gamma e(k-\tau(k)) + \Theta_2\otimes\Gamma e(k-\tau(k))]^T \\
&\quad \times [(I_{N-1}\otimes A)e(k) + F(e(k)) + \Theta_1\otimes\Gamma e(k-\tau(k)) + \Theta_2\otimes\Gamma e(k-\tau(k))] \\
&\quad - e^T(k)e(k) + \Psi^T(e(k))\Psi(e(k))\Big\} \\
&= E\Big\{e^T(k)\Big[I_{N-1}\otimes\Big(A^TA\Big)\Big]e(k) + 2e^T(k)\Big(I_{N-1}\otimes A^T\Big)F(e(k)) \\
&\quad + 2e^T(k)\Big(\Theta_1\otimes A^T\Gamma\Big)e(k-\tau(k)) + 2e^T(k)\Big(\Theta_2\otimes A^T\Gamma\Big)e(k-\tau(k)) \\
&\quad + F^T(e(k))F(e(k)) + 2F^T(e(k))(\Theta_1\otimes\Gamma)e(k-\tau(k)) \\
&\quad + 2F^T(e(k))(\Theta_2\otimes\Gamma)e(k-\tau(k)) \\
&\quad + e^T(k-\tau(k))\Big[\Big(\Theta_1^T\Theta_1 + 2\Theta_1^T\Theta_2 + \Theta_2^T\Theta_2\Big)\otimes\Gamma^T\Gamma\Big]e(k-\tau(k)) \\
&\quad - e^T(k)e(k) + \Psi^T(e(k))\Psi(e(k))\Big\} \\
&= E\Big\{e^T(k)\Big[I_{N-1}\otimes\Big(A^TA - I_n\Big)\Big]e(k) + 2e^T(k)\Big(I_{N-1}\otimes A^T\Big)F(e(k)) \\
&\quad + 2e^T(k)\Big(\Theta_1\otimes A^T\Gamma\Big)e(k-\tau(k)) + F^T(e(k))F(e(k)) \\
&\quad + 2F^T(e(k))(\Theta_1\otimes\Gamma)e(k-\tau(k)) + \Psi^T(e(k))\Psi(e(k)) \\
&\quad + e^T(k-\tau(k))\Big[\Big(\Theta_1^T\Theta_1 + \Theta_3\Big)\otimes\Gamma^T\Gamma\Big]e(k-\tau(k))\Big\}.
\end{aligned} \tag{3.3}$$

It is noted that

$$\begin{aligned}
&E\Big\{2e^T(k)\Big(I_{N-1}\otimes A^T\Big)F(e(k))\Big\} \\
&\quad \le E\Big\{\delta_1^{-1}e^T(k)\Big(I_{N-1}\otimes A^T\Big)(I_{N-1}\otimes A)e(k) + \delta_1F^T(e(k))F(e(k))\Big\} \\
&\quad \le E\Big\{\delta_1^{-1}e^T(k)\Big(I_{N-1}\otimes A^T\Big)(I_{N-1}\otimes A)e(k) \\
&\qquad + L_1\delta_1e^T(k)e(k) + L_2\delta_1e^T(k-\tau(k))e(k-\tau(k))\Big\},
\end{aligned}$$

$$
\begin{aligned}
&E\left\{2F^T(e(k))(\Theta_1\otimes\Gamma)e(k-\tau(k))\right\}\\
&\quad\le E\left\{\delta_2F^T(e(k))F(e(k))+\delta_2^{-1}e^T(k-\tau(k))\left(\Theta_1^T\otimes\Gamma^T\right)(\Theta_1\otimes\Gamma)e(k-\tau(k))\right\}\\
&\quad\le E\left\{\delta_2L_1e^T(k)e(k)+\delta_2L_2e^T(k-\tau(k))e(k-\tau(k))\right.\\
&\qquad\left.+\ \delta_2^{-1}e^T(k-\tau(k))\left(\Theta_1^T\otimes\Gamma^T\right)(\Theta_1\otimes\Gamma)e(k-\tau(k))\right\},\\
&E\left\{F^T(e(k))F(e(k))\right\}\le E\left\{L_1e^T(k)e(k)+L_2e^T(k-\tau(k))e(k-\tau(k))\right\},\\
&\Psi^T(e(k))\Psi(e(k))\le M^2e^T(k)e(k).
\end{aligned}
\tag{3.4}
$$

From (3.4), one can get

$$
\begin{aligned}
E\{\Delta V(e(k))\}\le E\Big\{&e^T(k)\Big[I_{N-1}\otimes\left(A^TA-I_n\right)+\delta_1^{-1}\left(I_{N-1}\otimes A^T\right)(I_{N-1}\otimes A)\\
&+\ (1+\delta_1+\delta_2)L_1\cdot I_{n(N-1)}+M^2\cdot I_{n(N-1)}\Big]e(k)\\
&+e^T(k-\tau(k))\Big[\left(\Theta_1^T\Theta_1+\Theta_3\right)\otimes\Gamma^T\Gamma+(1+\delta_1+\delta_2)L_2\cdot I_{n(N-1)}\\
&+\ \delta_2^{-1}\left(\Theta_1^T\otimes\Gamma^T\right)(\Theta_1\otimes\Gamma)\Big]e(k-\tau(k))\Big\}\\
\le E\Big\{&e^T(k)\Omega_1e(k)+e^T(k-\tau(k))\Omega_2e(k-\tau(k))\Big\},
\end{aligned}
\tag{3.5}
$$

where

$$
\begin{aligned}
\Omega_1&=M^2\cdot I_{n(N-1)}+(1+\delta_1+\delta_2)L_1\cdot I_{n(N-1)}+I_{N-1}\otimes\left(A^TA-I_n\right)+\delta_1^{-1}\left(I_{N-1}\otimes A^T\right)(I_{N-1}\otimes A),\\
\Omega_2&=(1+\delta_1+\delta_2)L_2\cdot I_{n(N-1)}+\left(\Theta_1^T\Theta_1+\Theta_3\right)\otimes\Gamma^T\Gamma+\delta_2^{-1}\left(\Theta_1^T\otimes\Gamma^T\right)(\Theta_1\otimes\Gamma).
\end{aligned}
\tag{3.6}
$$

By the Schur complement lemma, we know that (3.1) is equivalent to $\Omega_1<-\alpha I_{n(N-1)}$ and $\Omega_2<\beta I_{n(N-1)}$. So, we have

$$
E\{\Delta V(e(k))\}\le E\{-\alpha V(e(k))+\beta\cdot\max\{V(e(k)),V(e(k-1)),\ldots,V(e(k-\tau))\}\}.
\tag{3.7}
$$

By Lemma 2.4, there exists a constant $\eta_0\in(0,1)$ such that

$$
E\{V(e(k))\}\le\max\{V(e(0)),V(e(-1)),\ldots,V(e(-\tau))\}\eta_0^k,\quad k\ge0.
\tag{3.8}
$$

In particular, η_0 is the root of the equation

$$\eta^{d+1} + (\alpha - 1)\eta^d - \beta = 0 \tag{3.9}$$

in the interval $(0, 1)$. Therefore, the complex network (2.1) is exponential synchronization in mean square. This completes the proof of Theorem 3.1. □

While using the following state feedback controller:

$$u_i(k) = -kx_i(k), \quad i = 1, 2, \ldots, N, \tag{3.10}$$

to control every node in the complex network (2.1), we can obtain the error system

$$\begin{aligned} e(k+1) = {} & [I_{N-1} \otimes (A - kI_n)]e(k) + F(e(k)) + \Theta_1 \otimes \Gamma e(k - \tau(k)) \\ & + \Theta_2 \otimes \Gamma e(k - \tau(k)) + \Psi(e(k))w(k), \end{aligned} \tag{3.11}$$

where $k > 0$ is the control gain to be determined. So, by Theorem 3.1, we can obtain the following result.

Theorem 3.2. *Under assumptions (A1)~(A2), if there exist positive constants $k > 0$, $\delta_1 > 0, \delta_2 > 0, \alpha > 0$, and $\beta > 0$ such that*

$$\begin{gathered} \beta < \alpha \leq 1, \\ \widehat{\Pi}_1 = \begin{bmatrix} \widehat{\Pi}_{1,11} & I_{N-1} \otimes (A - kI_n)^T & I_{N-1} \otimes (A - kI_n)^T \\ I_{N-1} \otimes (A - kI_n) & -\delta_1 \cdot I_{n(N-1)} & 0 \\ I_{N-1} \otimes (A - kI_n) & 0 & -I_{n(N-1)} \end{bmatrix} < 0, \\ \Pi_2 = \begin{bmatrix} (1 + \delta_1 + \delta_2)L_2 \cdot I_{n(N-1)} - \beta I_{n(N-1)} + \left(\Theta_1^T \Theta_1 + \Theta_3\right) \otimes \Gamma^T \Gamma & \Theta_1^T \otimes \Gamma^T \\ \Theta_1 \otimes \Gamma & -\delta_2 \cdot I_{n(N-1)} \end{bmatrix} < 0, \end{gathered} \tag{3.12}$$

where

$$\widehat{\Pi}_{1,11} = I_{N-1} \otimes \left\{ \left[M^2 + \alpha + (1 + \delta_1 + \delta_2)L_1 - 1 \right] \cdot I_n \right\}, \tag{3.13}$$

then the complex network (2.1) *is exponential synchronization in mean square under the action of the controller* (3.10).

While using the pinning controller to control arbitrary l nodes in the complex network (2.1), we suppose that the number of the controlled nodes are $2, 3, \ldots, l + 1$, respectively. Substituting the following control law:

$$u_i(k) = -k_i x_i(k), \quad i = 2, 3, \ldots, l + 1, \tag{3.14}$$

into the error system (2.11), we get

$$\begin{aligned} e(k+1) = {} & [I_{N-1} \otimes A - K \otimes I_n]e(k) + F(e(k)) + \Theta_1 \otimes \Gamma e(k-\tau(k)) \\ & + \Theta_2 \otimes \Gamma e(k-\tau(k)) + \Psi(e(k))w(k), \end{aligned} \tag{3.15}$$

where $k_i > 0$ $(i = 2, 3, .., l+1)$ are the control gains to be determined, $K = \operatorname{diag}(k_2, k_3, \ldots, k_{l+1}, \underbrace{0, \ldots, 0}_{N-1-l})$. By Theorem 3.1, we can obtain the following result.

Theorem 3.3. *Under assumptions (A1)~(A2), if there exist positive constants $k_i > 0$ (i=2,3,...,l+1), $\delta_1 > 0, \delta_2 > 0, \alpha > 0$, and $\beta > 0$ such that*

$$\begin{gathered} \beta < \alpha \leq 1, \\ \widetilde{\Pi}_1 = \begin{bmatrix} \widetilde{\Pi}_{1,11} & I_{N-1} \otimes A^T - K \otimes I_n & I_{N-1} \otimes A^T - K \otimes I_n \\ I_{N-1} \otimes A - K \otimes I_n & -\delta_1 \cdot I_{n(N-1)} & 0 \\ I_{N-1} \otimes A - K \otimes I_n & 0 & -I_{n(N-1)} \end{bmatrix} < 0, \\ \Pi_2 = \begin{bmatrix} (1+\delta_1+\delta_2)L_2 \cdot I_{n(N-1)} - \beta I_{n(N-1)} + \left(\Theta_1^T\Theta_1 + \Theta_3\right) \otimes \Gamma^T\Gamma & \Theta_1^T \otimes \Gamma^T \\ \Theta_1 \otimes \Gamma & -\delta_2 \cdot I_{n(N-1)} \end{bmatrix} < 0, \end{gathered} \tag{3.16}$$

where

$$\widetilde{\Pi}_{1,11} = I_{N-1} \otimes \left\{ \left[M^2 + \alpha + (1+\delta_1+\delta_2)L_1 - 1 \right] \cdot I_n \right\}, \tag{3.17}$$

then the complex network (2.1) *is exponential synchronization in mean square under the action of the pinning controller* (3.14).

Remark 3.4. If the time delay $\tau(k) = 0$ in the complex network (2.1), applying the same method in the paper, we can also obtain the synchronization criteria and synchronization controllers for the following complex network:

$$\begin{aligned} x_i(k+1) = {} & Ax_i(k) + f(x_i(k)) + c\sum_{j=1, j\neq i}^{N} \xi_i g_{ij} \Gamma \left[x_j(k) - x_i(k) \right] \\ & + u_i(k) + \varphi(x_i(k))w(k) \end{aligned} \tag{3.18}$$

for $i = 1, 2, \ldots, N$.

Remark 3.5. Similar with [21–23], we will investigate the H_∞ synchronization for the uncertain complex network (2.1) in our future work.

4. A Numerical Example

Example 4.1. Consider the complex network (2.1) with ten nodes, and let each node be a three-dimensional dynamical subsystem whose parameters are as follows: $A = \operatorname{diag}\{0.3, 0.5, 0.4\}$,

$$f(x_i(k), x_i(k-\tau(k))) = \begin{bmatrix} \tanh(0.2x_{i1}(k)) + \tanh[-0.4x_{i1}(k-\tau(k))] \\ \tanh(0.3x_{i2}(k)) + \tanh[-0.2x_{i2}(k-\tau(k))] \\ \tanh(0.4x_{i3}(k)) + \tanh[0.1x_{i3}(k-\tau(k))] \end{bmatrix},$$

$$c = 0.1, \qquad \Gamma = \operatorname{diag}\{0.1, 0.2, 0.3\}, \qquad \tau(k) = 2 + \frac{1}{k}, \qquad \varphi(x_i(k)) = 0.4x_i(k),$$

$$G = \begin{bmatrix} -6 & 1 & 0 & 1 & 1 & 1 & 0 & 1 & 0 & 1 \\ 1 & -5 & 1 & 0 & 1 & 0 & 0 & 1 & 0 & 1 \\ 0 & 1 & -6 & 0 & 1 & 1 & 1 & 0 & 1 & 1 \\ 1 & 0 & 0 & -5 & 1 & 1 & 0 & 1 & 0 & 1 \\ 1 & 1 & 1 & 1 & -7 & 0 & 1 & 1 & 0 & 1 \\ 1 & 0 & 1 & 1 & 0 & -6 & 1 & 1 & 1 & 0 \\ 0 & 0 & 1 & 0 & 1 & 1 & -5 & 0 & 1 & 1 \\ 1 & 1 & 0 & 1 & 1 & 1 & 0 & -7 & 1 & 1 \\ 1 & 0 & 1 & 0 & 0 & 1 & 1 & 1 & -5 & 0 \\ 1 & 1 & 1 & 1 & 1 & 0 & 1 & 1 & 0 & -7 \end{bmatrix}, \tag{4.1}$$

$$E\{\xi_1\} = 0.6, \qquad E\{\xi_2\} = 0.7, \qquad E\{\xi_3\} = 1, \qquad E\{\xi_4\} = 0.9, \qquad E\{\xi_5\} = 0.7,$$
$$E\{\xi_6\} = 1, \qquad E\{\xi_7\} = 0.5, \qquad E\{\xi_8\} = 0.8, \qquad E\{\xi_9\} = 0.6, \qquad E\{\xi_{10}\} = 0.9.$$

It is easy to verify that assumptions (A1)~(A2) hold while $L_1 = L_2 = M = 0.2$. By the LMI toolbox in the Matlab, we can obtain a feasible solution of inequalities (3.12) as follows:

$$\delta_1 = 0.2748, \qquad \delta_2 = 0.3624, \qquad \alpha = 0.5126, \qquad \beta = 0.5047, \qquad k = 0.4003. \tag{4.2}$$

Therefore, according to Theorem 3.2, we know that all the nodes in the complex network can exponentially synchronize each other. The state error curves are shown in Figure 1, and these figures show that all the nodes synchronize well. However, for this example, inequalities (3.16) are infeasible. So, from Theorem 3.3, we know that all the nodes in the complex network cannot achieve exponential synchronization by using the pinning controller (3.14).

5. Conclusions

This paper has investigated the exponential synchronization problem for a class of discrete-time uncertain delay complex network with stochastic effects based on the Lyapunov stability theory and discrete Halanay inequality and provided some synchronization criteria and two different control schemes. Different from some existing results, this paper has considered the uncertainty arising from the nodes' working situation. Moreover, we do not need the state information of the target node given beforehand. The numerical illustration has shown that our proposed methods are effective.

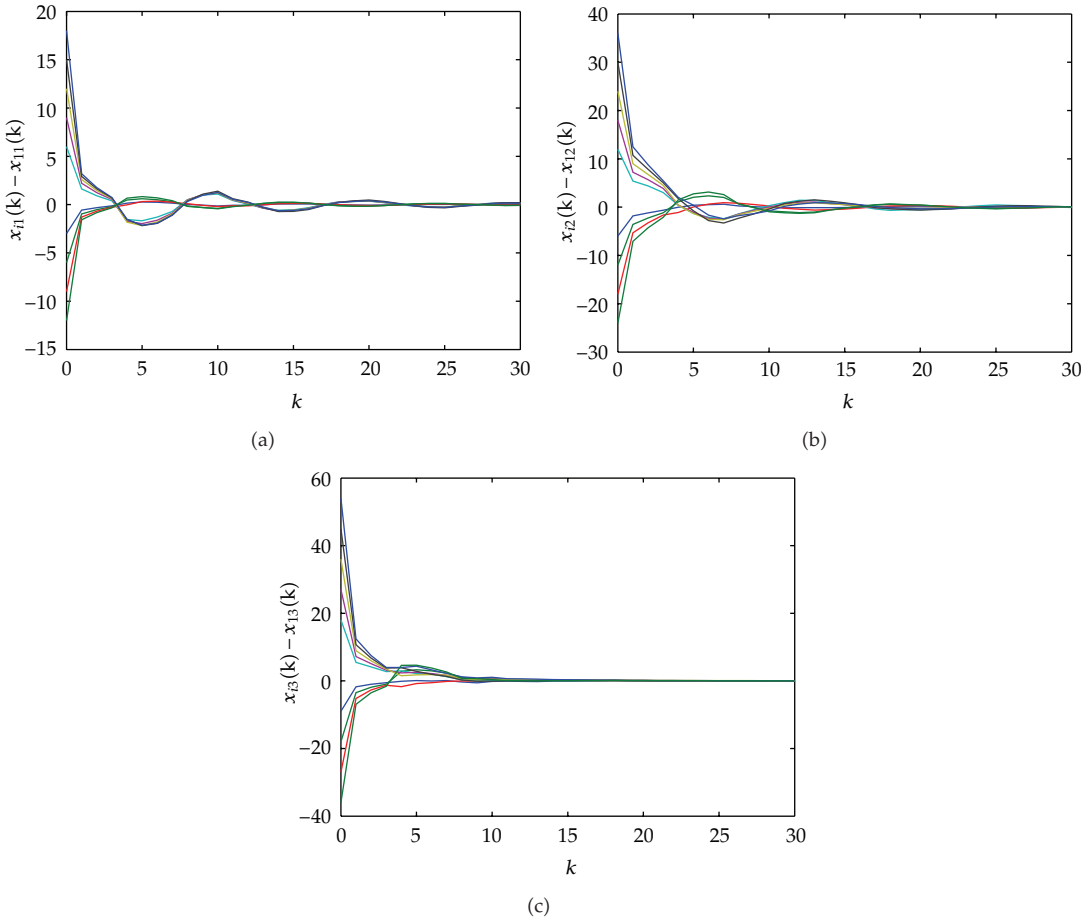

Figure 1: The state error curves of the complex network (2.1) with the given parameters in Example 4.1 ($i = 2, \ldots, 10$).

Acknowledgments

This work was supported by the National Natural Science Foundation of China (61075060), the National 863 Key Program of China (2008AA042902), the Innovation Program of Shanghai Municipal Education Commission (12zz064,11xk11), the Doctoral Start-Up Research Foundation of Shanghai University of Engineering Science (A-0501-10-0200), and the Outstanding Young Teachers Foundation of Shanghai Municipal Education Commission (gjd10009).

References

[1] D. J. Watts and S. H. Strogatz, "Collective dynamics of 'small-world9 networks," *Nature*, vol. 393, no. 6684, pp. 440–442, 1998.

[2] A.-L. Barabási and R. Albert, "Emergence of scaling in random networks," *American Association for the Advancement of Science*, vol. 286, no. 5439, pp. 509–512, 1999.

[3] H. J. Gao, J. Lam, and G. R. Chen, "New criteria for synchronization stability of general complex dynamical networks with coupling delays," *Physics Letters, Section A*, vol. 360, no. 2, pp. 263–273, 2006.
[4] H. J. Li, "New criteria for synchronization stability of continuous complex dynamical networks with non-delayed and delayed coupling," *Communications in Nonlinear Science and Numerical Simulation*, vol. 16, no. 2, pp. 1027–1043, 2011.
[5] T. P. Chen, X. W. Liu, and W. L. Lu, "Pinning complex networks by a single controller," *IEEE Transactions on Circuits and Systems. I*, vol. 54, no. 6, pp. 1317–1326, 2007.
[6] W. W. Yu, G. R. Chen, and J. H. Lü, "On pinning synchronization of complex dynamical networks," *Automatica*, vol. 45, no. 2, pp. 429–435, 2009.
[7] H. J. Li, W. K. Wong, and Y. Tang, "Global synchronization stability for stochastic complex dynamical networks with probabilistic interval time-varying delays," *Journal of Optimization Theory and Applications*, vol. 152, no. 2, pp. 496–516, 2012.
[8] B. X. Wang and Z.-H. Guan, "Chaos synchronization in general complex dynamical networks with coupling delays," *Nonlinear Analysis. Real World Applications*, vol. 11, no. 3, pp. 1925–1932, 2010.
[9] J. M. Yang, C. Z. Yao, W. C. Ma, and G. R. Chen, "A study of the spreading scheme for viral marketing based on a complex network model," *Physica A*, vol. 389, no. 4, pp. 859–870, 2010.
[10] X. F. Wang and G. R. Chen, "Synchronization in scale-free dynamical networks: robustness and fragility," *IEEE Transactions on Circuits and Systems I*, vol. 49, no. 1, pp. 54–62, 2002.
[11] M. E. J. Newman, "The structure and function of complex networks," *SIAM Review*, vol. 45, no. 2, pp. 167–256, 2003.
[12] H. L. Zhu, H. Luo, H. P. Peng, L. X. Li, and Q. Luo, "Complex networks-based energy-efficient evolution model for wireless sensor networks," *Chaos, Solitons and Fractals*, vol. 41, no. 4, pp. 1828–1835, 2009.
[13] Y. Tang, S. Y. S. Leung, W. K. Wong, and J. A. Fang, "Impulsive pinning synchronization of stochastic discrete-time networks," *Neurocomputing*, vol. 73, no. 10–12, pp. 2132–2139, 2010.
[14] C. Huang, D. W. C. Ho, and J. Q. Lu, "Synchronization analysis of a complex network family," *Nonlinear Analysis. Real World Applications*, vol. 11, no. 3, pp. 1933–1945, 2010.
[15] Z. D. Wang, Y. Wang, and Y. R. Liu, "Global synchronization for discrete-time stochastic complex networks with randomly occurred nonlinearities and mixed time delays," *IEEE Transactions on Neural Networks*, vol. 21, no. 1, pp. 11–25, 2010.
[16] H. J. Li, "Synchronization stability for discrete-time stochastic complex networks with probabilistic interval time-varying delays," *International Journal of Innovative Computing, Information and Control*, vol. 7, no. 2, pp. 697–708, 2011.
[17] Y. R. Liu, Z. D. Wang, J. L. Liang, and X. H. Liu, "Synchronization and state estimation for discrete-time complex networks with distributed delays," *IEEE Transactions on Systems, Man, and Cybernetics, Part B*, vol. 38, no. 5, pp. 1314–1325, 2008.
[18] Z. Y. Fei, D. Z. Wang, H. J. Gao, and Y. W. Zhang, "Discrete-time complex networks: a new synchronisation stability criterion," *International Journal of Systems Science*, vol. 40, no. 9, pp. 931–936, 2009.
[19] Q. J. Zhang, J.-A. Lu, and J. C. Zhao, "Impulsive synchronization of general continuous and discrete-time complex dynamical networks," *Communications in Nonlinear Science and Numerical Simulation*, vol. 15, no. 4, pp. 1063–1070, 2010.
[20] B. Shen, Z. D. Wang, and X. H. Liu, "Bounded H_∞ synchronization and state estimation for discrete time-varying stochastic complex networks over a finite horizon," *IEEE Transactions on Neural Networks*, vol. 22, no. 1, pp. 145–157, 2011.
[21] D. R. Ding, Z. D. Wang, B. Shen, and H. S. Shu, "H_∞ state estimation for discrete-time complexnetworks with randomly occurring sensor saturations and randomly varying sensor delays," *IEEE Transactions on Neural Networks and Learning Systems*, vol. 23, pp. 725–736, 2012.
[22] Z. D. Wang, B. Shen, and X. H. Liu, "H_∞ filtering with randomly occurring sensor saturations and missing measurements," *Automatica*, vol. 48, no. 3, pp. 556–562, 2012.
[23] B. Shen, Z. D. Wang, and X. H. Liu, "Sampled-data synchronization control of complex dynamical networks with stochastic sampling," *IEEE Transactions on Automatic Control*. In press.
[24] E. Liz and J. B. Ferreiro, "A note on the global stability of generalized difference equations," *Applied Mathematics Letters*, vol. 15, no. 6, pp. 655–659, 2002.
[25] R. A. Horn and C. R. Johnson, *Matrix Analysis*, Cambridge University Press, Cambridge, UK, 1985.

Hindawi Publishing Corporation
Mathematical Problems in Engineering
Volume 2012, Article ID 132597, 16 pages
doi:10.1155/2012/132597

Research Article

Stabilization of Time-Varying System by Controllers with Internal Loop

Yufeng Lu and Chengkai Shi

School of Mathematical Sciences, Dalian University of Technology, Dalian 116024, China

Correspondence should be addressed to Chengkai Shi, shichengkai2001@163.com

Received 18 April 2012; Accepted 10 May 2012

Academic Editor: Zidong Wang

We study the concept of stabilization with internal loop for infinite-dimensional discrete time-varying systems in the framework of nest algebra. We originally give a parametrization of all stabilizing controllers with internal loop, and it covers the parametrization of canonical or dual canonical controllers with internal loop obtained before. We show that, in practical application, the controller with internal loop overcomes the awkwardness brought by the extra invertibility condition in the parametrization of the conventional controllers. We also prove that the strong stabilization problem can be completely solved in the closed-loop system with internal loop. Thus the advantage of the controller with internal loop is addressed in the framework of nest algebra.

1. Introduction

The closed-loop system whose stability is achieved by the controller with internal loop has attracted the attention of many authors in recent years (see [1–5]). This system was originally introduced by Weiss and Curtain in 1997 in [1]. When they extended the theory of dynamic stabilization to regular linear systems (a subclass of the well-posed linear systems), it was shown in Example 6.5 of [1] that even the standard observer-based controller is not a well-posed linear system as needed, correspondingly, its transfer function is not well-posed. To overcome this difficulty, a new type of controller, the so-called stabilizing controller with internal loop, was introduced. This controller is more general and useful than the standard feedback controller. Until now, only a special class of stabilizing controllers with internal loop called canonical controllers is widely investigated. In [1], a procedure was developed to design the canonical controllers for stabilizable and detectable plants. In [6], the parametrization for all canonical controllers is given which is clean and avoids the extra invertibility condition in the parametrization for the controller in the standard feedback

system. In [7], the author extended the theory to non-well posed systems, and the robust stabilization problem is considered by using the canonical controller.

In recent years, the study of time-varying systems using modern mathematical methods has come into its own. This was a scientific necessity. After all, many common physical systems are time varying. In [8], A. Feintuch specifically introduced a framework of nest algebra and the control theory for linear time-varying systems was studied in this framework. Meanwhile, many stabilization problems for various nonlinear time-varying systems were widely considered as well (see [9–16]). Based on these cases, we are motivated to consider the new model of closed-loop feedback system with internal loop for time-varying systems.

In this paper, we study the concept of stabilization with internal loop for the linear time-varying system under the framework of nest algebra. We extend our study of controllers with internal loop to more general cases and originally give a parametrization of all stabilizing controllers with internal loop. It is found that the parametrization of the canonical controller obtained in [6] can be viewed as a special case of the parametrization obtained here. As we know, the parametrization of the conventional controller is not clean, and there is always an extra invertibility condition on the parameter. This in turn makes it awkward to use this parametrization to solve the practical problems. While the controller with internal loop overcomes this awkwardness. We take the sensitivity minimization problem as an example to show this advantage of the controller with internal loop. The strong stabilization problem is known as the design of a stable controller which stabilizes the given plant. In the framework of nest algebra, it is still an open problem and only a necessary condition is addressed in [17] for this problem. We prove that any stabilizable plant can be strongly stabilized by the controller with internal loop. This means that the strong stabilization problem can be completely solved in the system with internal loop. We also give a simple example to show how to design the strongly stabilizing controller with internal loop.

This paper is organized as follows. In Section 2, we recall some basic concepts of the linear systems in the framework of nest algebra. In Section 3, we introduce the closed-loop system whose stability is achieved by the controller with internal loop and firstly give a parametrization for all stabilizing controllers with internal loop. In Section 4, we focus on the canonical controller and show the benefit of the controller with internal loop in the practical application. In Section 5, we define the strongly stabilizing controller with internal loop and address an advantage of the controller with internal loop in the framework of nest algebra.

2. Preliminaries

Let $\mathscr{H}$ be the complex infinite dimensional Hilbert sequence space:

$$\ell^2 = \left\{ (x_0, x_1, x_2, \ldots) : x_i \in \mathbb{C}, \sum_{i=0}^{\infty} |x_i|^2 < \infty \right\}, \tag{2.1}$$

where $|\cdot|$ denotes the standard Euclidean norm on $\mathbb{C}$ with inner product $(x, y) = \sum_{i=0}^{\infty} x_i \overline{y}_i$. $\mathscr{H}_e$ will denote the extended space:

$$\mathscr{H}_e = \{ (x_0, x_1, x_2, \ldots) : x_i \in \mathbb{C} \}. \tag{2.2}$$

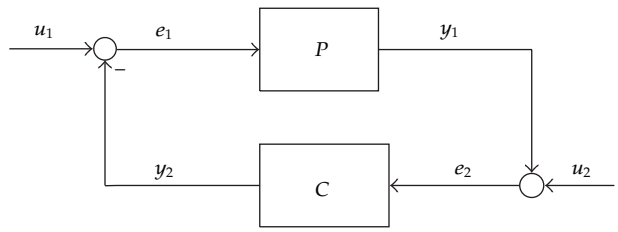

Figure 1: Standard feedback configuration.

For each $n \geq 0$, let P_n denote the standard truncation projection defined on $\mathscr{H}$ and $\mathscr{H}_e$ by

$$P_n(x_0, x_1, \ldots, x_n, x_{n+1}, \ldots) = (x_0, x_1, \ldots, x_n, 0, 0, \ldots). \tag{2.3}$$

A continuous linear transformation T on $\mathscr{H}_e$ with the standard seminorm topology ([8, Chapter 5]) is a causal linear system (or a linear system) if for each $n \geq 0$, $P_nT = P_nTP_n$. Let $\mathscr{L}$ be the set of all linear systems on $\mathscr{H}_e$. Then any element of $\mathscr{L}$ is a lower triangular matrix (with respect to the standard basis, see [8, Chapter 5]).

A linear system T is stable if its restriction to $\mathscr{H}$ is a bounded operator ([8, Chapter 5]). We denote the set of stable systems by $\mathscr{S}$, then $\mathscr{S}$ is a weakly closed algebra containing the identity, referred to in the operator algebra literature as a nest algebra ([8, Chapter 5]).

For $P, C \in \mathscr{L}$, we consider the standard feedback configuration with plant P and controller C shown in Figure 1.

u_1, u_2 denote the externally applied inputs; e_1, e_2 denote the inputs to the plant and compensator, respectively, and y_1, y_2 denote the outputs of the plant and compensator, respectively. The closed loop system equations are

$$\begin{bmatrix} u_1 \\ u_2 \end{bmatrix} = \begin{bmatrix} I & C \\ -P & I \end{bmatrix} \begin{bmatrix} e_1 \\ e_2 \end{bmatrix}. \tag{2.4}$$

The system is well posed if the internal input $e = \left[\begin{smallmatrix} e_1 \\ e_2 \end{smallmatrix}\right]$ can be expressed as a causal function of the external input $u = \left[\begin{smallmatrix} u_1 \\ u_2 \end{smallmatrix}\right]$. This is equivalent to requiring that $\left[\begin{smallmatrix} I & C \\ -P & I \end{smallmatrix}\right]$ be invertible. This inverse can be easily computed and is given by the transfer matrix

$$H(P, C) = \begin{bmatrix} (I + CP)^{-1} & -C(I + PC)^{-1} \\ P(I + CP)^{-1} & (I + PC)^{-1} \end{bmatrix}. \tag{2.5}$$

Definition 2.1 (see [8]). The closed loop system $\{P, C\}$ is stable if all the entries of $H(P, C)$ are stable systems on $\mathscr{H}$. The plant P is stabilizable if there exists a causal linear system C such that $\{P, C\}$ is stable.

Recall that the graph of a linear transformation P with domain $\mathfrak{D}(P) = \{x \in \mathscr{H} : Px \in \mathscr{H}\}$ is $\mathcal{G}(P) = \{\left[\begin{smallmatrix} x \\ Px \end{smallmatrix}\right] : x \in \mathfrak{D}(P)\}$. Then we can give the definitions of strong right representation and strong left representation.

Definition 2.2 (see [8]). A plant P has a strong right representation $\left[\begin{smallmatrix} M \\ N \end{smallmatrix}\right]$ with M and N stable if

(1) $\mathcal{G}(P) = \mathrm{Ran}\left[\begin{smallmatrix} M \\ N \end{smallmatrix}\right]$,

(2) there exist $X, Y \in \mathcal{S}$ such that $[YX]\left[\begin{smallmatrix} M \\ N \end{smallmatrix}\right] = I$.

A plant P has a strong left representation $[-\widehat{N}\widehat{M}]$ with $\widehat{M}$ and $\widehat{N}$ stable if

(1) $\mathcal{G}(P) = \mathrm{Ker}[-\widehat{N}\widehat{M}]$,

(2) there exist $\widehat{X}, \widehat{Y} \in \mathcal{S}$ such that $[-\widehat{N}\widehat{M}]\left[\begin{smallmatrix} -\widehat{X} \\ \widehat{Y} \end{smallmatrix}\right] = I$.

The following result on strong right representation is proved in [8].

Theorem 2.3 (see [8]). *Suppose $M, N \in \mathcal{S}$. Then $\left[\begin{smallmatrix} M \\ N \end{smallmatrix}\right]$ is a strong right representation of $P \in \mathcal{L}$ if and only if*

(1) *there exist $X, Y \in \mathcal{S}$ such that $[YX]\left[\begin{smallmatrix} M \\ N \end{smallmatrix}\right] = I$,*

(2) *M is invertible in $\mathcal{L}$.*

We say that a plant P has a right coprime factorization if there exist $M, N, X, Y \in \mathcal{S}$ such that $P = NM^{-1}$ and $YM + XN = I$. The proof of Theorem 2.1 in [8] implies that $\left[\begin{smallmatrix} M \\ N \end{smallmatrix}\right]$ is a strong right representation of P if and only if NM^{-1} is a right coprime factorization of P. Similarly, $[-\widehat{N}\widehat{M}]$ is a strong left representation of P if and only if $\widehat{M}^{-1}\widehat{N}$ is a left coprime factorization of P.

The following theorem is the classical Youla Parametrization Theorem.

Theorem 2.4 (see [8]). *A causal linear system $P \in \mathcal{L}$ is stabilizable if and only if P has a strong right and a strong left representation. If this is the case, the representations can be chosen so that one has the double Bezout identity*

$$\begin{bmatrix} Y & X \\ -\widehat{N} & \widehat{M} \end{bmatrix}\begin{bmatrix} M & -\widehat{X} \\ N & \widehat{Y} \end{bmatrix} = \begin{bmatrix} M & -\widehat{X} \\ N & \widehat{Y} \end{bmatrix}\begin{bmatrix} Y & X \\ -\widehat{N} & \widehat{M} \end{bmatrix} = \begin{bmatrix} I & 0 \\ 0 & I \end{bmatrix}. \tag{2.6}$$

A causal linear system C stabilizes P if and only if it has a strong right representation $\left[\begin{smallmatrix} \widehat{Y}-NQ \\ \widehat{X}+MQ \end{smallmatrix}\right]$ and a strong left representation $[-(X + Q\widehat{M})Y - Q\widehat{N}]$ for some $Q \in \mathcal{S}$.

3. Controllers with Internal Loop

In this section, we investigate the stabilization of the time-varying system by controllers with internal loop in the framework of nest algebra. This system is illustrated in Figure 2.

The intuitively interpretation of Figure 2: $P \in \mathcal{L}$ is the plant and K_I is a transfer map from $\left[\begin{smallmatrix} e_2 \\ e_3 \end{smallmatrix}\right]$ to $\left[\begin{smallmatrix} y_2 \\ y_3 \end{smallmatrix}\right]$ when all the connections are open. Then the connection from y_3 to e_3 is called internal loop. The closed loop system determined by the plant P and the controller K_I with internal loop is denoted by $\{P, K_I\}$.

Partitioning K_I into

$$\begin{bmatrix} C_{11} & C_{12} \\ C_{21} & C_{22} \end{bmatrix}, \tag{3.1}$$

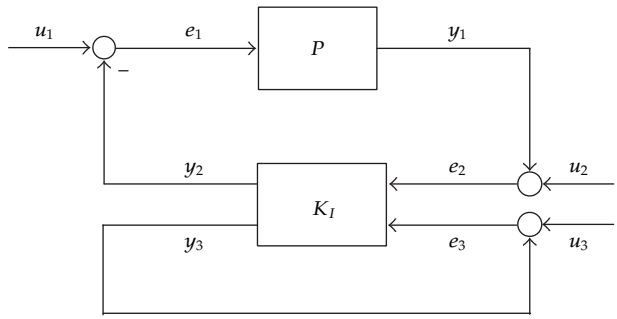

Figure 2: The plant P connected to a controller K_I with internal loop.

where $C_{ij} \in \mathcal{L}$, $i, j = 1, 2$, the closed loop system equations are

$$\begin{bmatrix} u_1 \\ u_2 \\ u_3 \end{bmatrix} = \begin{bmatrix} I & C_{11} & C_{12} \\ -P & I & 0 \\ 0 & -C_{21} & I - C_{22} \end{bmatrix} \begin{bmatrix} e_1 \\ e_2 \\ e_3 \end{bmatrix}. \tag{3.2}$$

We say that the system is well posed if $\begin{bmatrix} I & C_{11} & C_{12} \\ -P & I & 0 \\ 0 & -C_{21} & I-C_{22} \end{bmatrix}$ is invertible and We denote this inverse by $H(P, K_I)$.

Definition 3.1. The closed loop system $\{P, K_I\}$ determined by the plant $P \in \mathcal{L}$ and the controller with internal loop K_I is stable if all the entries of $H(P, K_I)$ are stable. The plant P is stabilizable by a controller with internal loop if there exists a K_I such that $H(P, K_I)$ is stable. In this case, K_I is called a stabilizing controller with internal loop for P.

In the previous papers, the study of stabilizing controller with internal loop is mainly focused on the case that P and K_I are both well-posed transfer functions (bounded and analytic on some right half plane). And in all applications, the controller K_I is assumed to be stable and satisfy two conditions proposed in [1] (refer to Proposition 4.8 in [1]). While, in the framework of nest algebra, we extend the study to the more general case that $C_{ij} \in \mathcal{L}$, $i, j = 1, 2$ and K_I need not to satisfy the two conditions proposed in [1].

Suppose $I - C_{22}$ is invertible in $\mathcal{L}$, then we have that

$$H(P, K_I) = \begin{bmatrix} (I + CP)^{-1} & -C(I + PC)^{-1} & T_{13} \\ P(I + CP)^{-1} & (I + PC)^{-1} & T_{23} \\ T_{31} & T_{32} & T_{33} \end{bmatrix}, \tag{3.3}$$

where

$$\begin{aligned} C &= C_{11} + C_{12}(I - C_{22})^{-1}C_{21}, \\ T_{13} &= -(I + CP)^{-1}C_{12}(I - C_{22})^{-1}, \\ T_{23} &= -P(I + CP)^{-1}C_{12}(I - C_{22})^{-1}, \end{aligned}$$

$$
\begin{aligned}
T_{31} &= (I - C_{22})^{-1} C_{21} P (I + CP)^{-1}, \\
T_{32} &= (I - C_{22})^{-1} C_{21} (I + PC)^{-1}, \\
T_{33} &= \left(I - (I - C_{22})^{-1} C_{21} P (I + CP)^{-1} C_{12}\right)(I - C_{22})^{-1}.
\end{aligned}
\tag{3.4}
$$

Remark 3.2. Notice that the upper left 2×2 corner of the above transfer matrix $H(P, K_I)$ is just the transfer matrix $H(P, C)$ of the standard feedback system with the plant P and the controller $C = C_{11} + C_{12}(I - C_{22})^{-1} C_{21}$. This implies that the closed-loop system stabilized by controllers with internal loop is more general than the standard feedback system and its transfer matrix provides more information.

Now we can give a parametrization of all stabilizing controllers with internal loop with $I - C_{22}$ invertible in $\mathcal{L}$.

Theorem 3.3. *Suppose $P \in \mathcal{L}$ and there exist $M, N, X, Y, \widehat{M}, \widehat{N}, \widehat{X}, \widehat{Y} \in \mathcal{S}$ such that $\left[\begin{smallmatrix} M \\ N \end{smallmatrix}\right]$ and $[-\widehat{N}\,\widehat{M}]$ are, respectively, strong right and left representation for P that satisfy the double Bezout identity*

$$
\begin{bmatrix} Y & X \\ -\widehat{N} & \widehat{M} \end{bmatrix} \begin{bmatrix} M & -\widehat{X} \\ N & \widehat{Y} \end{bmatrix} = \begin{bmatrix} M & -\widehat{X} \\ N & \widehat{Y} \end{bmatrix} \begin{bmatrix} Y & X \\ -\widehat{N} & \widehat{M} \end{bmatrix} = \begin{bmatrix} I & 0 \\ 0 & I \end{bmatrix}. \tag{3.5}
$$

Then all stabilizing controllers with internal loop $K_I = \left[\begin{smallmatrix} C_{11} & C_{12} \\ C_{21} & C_{22} \end{smallmatrix}\right]$ are parameterized by

$$
\begin{aligned}
C_{11} &= \left(\widehat{X} + MQ\right)\left(\widehat{Y} - NQ\right)^{-1} \\
&\quad - \left(Y - Q\widehat{N}\right)^{-1} R_1 \left(R_3 + R_2\left(\widehat{Y} - NQ\right)^{-1} N R_1\right)^{-1} R_2 \left(\widehat{Y} - NQ\right)^{-1}, \\
C_{12} &= \left(Y - Q\widehat{N}\right)^{-1} R_1 \left(R_3 + R_2\left(\widehat{Y} - NQ\right)^{-1} N R_1\right)^{-1}, \\
C_{21} &= \left(R_3 + R_2\left(\widehat{Y} - NQ\right)^{-1} N R_1\right)^{-1} R_2 \left(\widehat{Y} - NQ\right)^{-1}, \\
C_{22} &= I - \left(R_3 + R_2\left(\widehat{Y} - NQ\right)^{-1} N R_1\right)^{-1},
\end{aligned}
\tag{3.6}
$$

for some $Q, R_1, R_2, R_3 \in \mathcal{S}$.

In order to prove this theorem clearly, we need the following result which is an improvement of Theorem 2.4. It is interesting that while the two representations for the controller in Theorem 2.4 are independent, the same Q will in fact work for both.

Theorem 3.4. *Suppose P satisfies the assumption in Theorem 2.4. Then the stabilizing controller C for P has the form $C = (Y - Q\widehat{N})^{-1}(X + Q\widehat{M}) = (\widehat{X} + MQ)(\widehat{Y} - NQ)^{-1}$ for some $Q \in \mathcal{S}$.*

Proof. Suppose C stabilizes P. By Theorem 2.4, we have that C has a right coprime factorization $C = (\widehat{X} + MQ)(\widehat{Y} - NQ)^{-1}$ for some $Q \in \mathcal{S}$. It is easy to check that

$$\begin{aligned}\begin{bmatrix} -\left(X + Q\widehat{M}\right) & Y - Q\widehat{N} \\ \widehat{M} & \widehat{N} \end{bmatrix}\begin{bmatrix} -N & \widehat{Y} - NQ \\ M & \widehat{X} + MQ \end{bmatrix} &= \begin{bmatrix} -N & \widehat{Y} - NQ \\ M & \widehat{X} + MQ \end{bmatrix}\begin{bmatrix} -\left(X + Q\widehat{M}\right) & Y - Q\widehat{N} \\ \widehat{M} & \widehat{N} \end{bmatrix} \\ &= \begin{bmatrix} I & 0 \\ 0 & I \end{bmatrix}.\end{aligned} \tag{3.7}$$

Thus,

$$\left[-\left(X + Q\widehat{M}\right) \quad Y - Q\widehat{N}\right]\begin{bmatrix} \widehat{Y} - NQ \\ \widehat{X} + MQ \end{bmatrix} = 0. \tag{3.8}$$

This implies that

$$\mathcal{G}(C) = \operatorname{Ran}\begin{bmatrix} \widehat{Y} - NQ \\ \widehat{X} + MQ \end{bmatrix} \subseteq \operatorname{Ker}\left[-\left(X + Q\widehat{M}\right) \quad Y - Q\widehat{N}\right]. \tag{3.9}$$

On the other hand, for any $\left[\begin{smallmatrix} x \\ y \end{smallmatrix}\right] \in \operatorname{Ker}[-(X + Q\widehat{M}) \quad Y - Q\widehat{N}]$, we have

$$\begin{aligned}\begin{bmatrix} x \\ y \end{bmatrix} &= \begin{bmatrix} -N & \widehat{Y} - NQ \\ M & \widehat{X} + MQ \end{bmatrix}\begin{bmatrix} -\left(X + Q\widehat{M}\right) & Y - Q\widehat{N} \\ \widehat{M} & \widehat{N} \end{bmatrix}\begin{bmatrix} x \\ y \end{bmatrix} \\ &= \left(\begin{bmatrix} -N \\ M \end{bmatrix}\left[-\left(X + Q\widehat{M}\right) \quad Y - Q\widehat{N}\right] + \begin{bmatrix} \widehat{Y} - NQ \\ \widehat{X} + MQ \end{bmatrix}\left[\widehat{M} \quad \widehat{N}\right]\right)\begin{bmatrix} x \\ y \end{bmatrix} \\ &= \begin{bmatrix} \widehat{Y} - NQ \\ \widehat{X} + MQ \end{bmatrix}\left[\widehat{M} \quad \widehat{N}\right]\begin{bmatrix} x \\ y \end{bmatrix} \in \mathcal{G}(C),\end{aligned} \tag{3.10}$$

that is,

$$\operatorname{Ker}\left[-\left(X + Q\widehat{M}\right) \quad Y - Q\widehat{N}\right] \subseteq \mathcal{G}(C). \tag{3.11}$$

Thus,

$$\mathcal{G}(C) = \operatorname{Ker}\left[-\left(X + Q\widehat{M}\right) \quad Y - Q\widehat{N}\right]. \tag{3.12}$$

Since

$$\left[-\left(X + Q\widehat{M}\right) \quad Y - Q\widehat{N}\right]\begin{bmatrix} -N \\ M \end{bmatrix} = I, \tag{3.13}$$

we obtain that $[-(X + Q\widehat{M})\ \ Y - Q\widehat{N}]$ is a strong left representation of C and $C = (Y - Q\widehat{N})^{-1}(X + Q\widehat{M})$. This completes the proof. □

Now we can give the proof of Theorem 3.3.

Proof of Theorem 3.3. Suppose $\{P, K_I\}$ is stable, then every entry of the matrix

$$\begin{bmatrix} (I + CP)^{-1} & -C(I + PC)^{-1} \\ P(I + CP)^{-1} & (I + PC)^{-1} \end{bmatrix} \tag{3.14}$$

is in $\mathcal{S}$ and $T_{13}, T_{23}, T_{31}, T_{32}, T_{33} \in \mathcal{S}$. Note that (3.14) is just the transfer matrix $H(P, C)$ for the standard feedback system. By Theorem 3.4, we see that C has the following representation:

$$C = \left(Y - Q\widehat{N}\right)^{-1}\left(X + Q\widehat{M}\right) = \left(\widehat{X} + MQ\right)\left(\widehat{Y} - NQ\right)^{-1}, \tag{3.15}$$

for some $Q \in \mathcal{S}$. In this case,

$$\begin{aligned} T_{13} &= -(I + CP)^{-1}C_{12}(I - C_{22})^{-1} \\ &= -M\left(Y - Q\widehat{N}\right)C_{12}(I - C_{22})^{-1} \in \mathcal{S}, \\ T_{23} &= -P(I + CP)^{-1}C_{12}(I - C_{22})^{-1} \\ &= -N\left(Y - Q\widehat{N}\right)C_{12}(I - C_{22})^{-1} \in \mathcal{S}, \end{aligned} \tag{3.16}$$

if and only if

$$\left(Y - Q\widehat{N}\right)C_{12}(I - C_{22})^{-1} \in \mathcal{S}. \tag{3.17}$$

It follows that

$$C_{12}(I - C_{22})^{-1} = \left(Y - Q\widehat{N}\right)^{-1}R_1 \tag{3.18}$$

for some $R_1 \in \mathcal{S}$.

In the same way, we obtain that

$$(I - C_{22})^{-1}C_{21} = R_2\left(\widehat{Y} - NQ\right)^{-1}, \tag{3.19}$$

for some $R_2 \in \mathcal{S}$. So we get

$$\begin{aligned} C_{12} &= \left(Y - Q\widehat{N}\right)^{-1}R_1(I - C_{22}), \\ C_{21} &= (I - C_{22})R_2\left(\widehat{Y} - NQ\right)^{-1}. \end{aligned} \tag{3.20}$$

Since

$$\begin{aligned} T_{33} &= \left(I - (I - C_{22})^{-1} C_{21} P (I + CP)^{-1} C_{12}\right)(I - C_{22})^{-1} \\ &= (I - C_{22})^{-1} - R_2\left(\widehat{Y} - NQ\right)^{-1} N\left(Y - Q\widehat{N}\right)\left(Y - Q\widehat{N}\right)^{-1} R_1 \\ &= (I - C_{22})^{-1} - R_2\left(\widehat{Y} - NQ\right)^{-1} N R_1 \in \mathcal{S}, \end{aligned} \tag{3.21}$$

we have

$$(I - C_{22})^{-1} = R_3 + R_2\left(\widehat{Y} - NQ\right)^{-1} N R_1, \tag{3.22}$$

for some $R_3 \in \mathcal{S}$. Thus,

$$C_{22} = I - \left(R_3 + R_2\left(\widehat{Y} - NQ\right)^{-1} N R_1\right)^{-1}. \tag{3.23}$$

Then we can obtain the following representations for C_{12} and C_{21}:

$$\begin{aligned} C_{12} &= \left(Y - Q\widehat{N}\right)^{-1} R_1 \left(R_3 + R_2\left(\widehat{Y} - NQ\right)^{-1} N R_1\right)^{-1}, \\ C_{21} &= \left(R_3 + R_2\left(\widehat{Y} - NQ\right)^{-1} N R_1\right)^{-1} R_2\left(\widehat{Y} - NQ\right)^{-1}. \end{aligned} \tag{3.24}$$

Substituting the representations of C, C_{12}, C_{21}, and C_{22} into $C_{11} = C - C_{12}(I - C_{22})^{-1} C_{21}$, we obtain

$$\begin{aligned} C_{11} = {} & \left(\widehat{X} + MQ\right)\left(\widehat{Y} - NQ\right)^{-1} - \left(Y - Q\widehat{N}\right)^{-1} \\ & \times R_1 \left(R_3 + R_2\left(\widehat{Y} - NQ\right)^{-1} N R_1\right)^{-1} R_2\left(\widehat{Y} - NQ\right)^{-1}. \end{aligned} \tag{3.25}$$

This completes the proof. □

It was said in [1] that the controller with internal loop was particularly well suited for tracking, and a physical interpretation was given for the system with internal loop. In [6], the author described a seemingly impossible problem, the "intriguing control problem", which can be easily solved by the system with internal loop. In the next two sections, we will show the other great advantages of the controller with internal loop.

4. Canonical Controllers and Dual Canonical Controllers

In this section, we focus on two special classes of controllers with internal loop called canonical controllers and dual canonical controllers, respectively. Here below it is given their definitions in the framework of nest algebra.

Definition 4.1. A controller with internal loop is called the canonical controller for the plant P if it is of the form $K_I = \left[\begin{smallmatrix} 0 & I \\ C_{21} & C_{22} \end{smallmatrix}\right]$ with $C_{21}, C_{22} \in \mathcal{S}$. Analogously, a controller with internal loop is called a dual canonical controller for the plant P if it is of the form $\left[\begin{smallmatrix} 0 & C_{12} \\ I & C_{22} \end{smallmatrix}\right]$ with C_{12}, $C_{22} \in \mathcal{S}$.

For canonical controllers, we have the following results.

Theorem 4.2. *The canonical controller $K_I = \left[\begin{smallmatrix} 0 & I \\ C_{21} & C_{22} \end{smallmatrix}\right]$ stabilizes $P \in \mathcal{L}$ with internal loop if and only if $\Delta = I - C_{22} + C_{21}P$ is invertible in $\mathcal{L}$ and Δ^{-1}, $P\Delta^{-1} \in \mathcal{S}$.*

If P has a strong right representation $\left[\begin{smallmatrix} M \\ N \end{smallmatrix}\right]$, then the canonical controller K_I stabilizes P if and only if $D = M - C_{22}M + C_{21}N$ is invertible in $\mathcal{S}$.

Proof. According to the system equations in (3.2), we have that, for the canonical controllers $K_I = \left[\begin{smallmatrix} 0 & I \\ C_{21} & C_{22} \end{smallmatrix}\right]$, the transfer matrix $H(P, K_I)$ can be given by

$$H(P, K_I) = \begin{bmatrix} I - \Delta^{-1}C_{21}P & -\Delta^{-1}C_{21} & -\Delta^{-1} \\ P(I - \Delta^{-1}C_{21}P) & I - P\Delta^{-1}C_{21} & -P\Delta^{-1} \\ \Delta^{-1}C_{21}P & \Delta^{-1}C_{21} & \Delta^{-1} \end{bmatrix}. \tag{4.1}$$

Thus, $H(P, K_I) \in M_3(\mathcal{S})$ if and only if Δ^{-1}, $P\Delta^{-1}$, $\Delta^{-1}C_{21}P$, and $P(I - \Delta^{-1}C_{21}P)$ are all in $\mathcal{S}$. Since $\Delta^{-1}C_{21}P = \Delta^{-1}(\Delta + C_{21}P) - I = \Delta^{-1}(I - C_{22}) - I$ and $P(I - \Delta^{-1}C_{21}P) = P\Delta^{-1}(I - C_{22})$. We have that all the entries of $H(P, K_I)$ are in $\mathcal{S}$ if and only if Δ^{-1} and $P\Delta^{-1}$ are in $\mathcal{S}$. Thus the first statement is proved.

Let us prove the second assertion in the theorem. If $P = NM^{-1}$ and $D^{-1} \in \mathcal{S}$, we have that $\Delta^{-1} = M(M - C_{22}M + C_{21}N)^{-1} = MD^{-1} \in \mathcal{S}$ and $P\Delta^{-1} = ND^{-1} \in \mathcal{S}$. By using the first result, we have that $K_I = \left[\begin{smallmatrix} 0 & I \\ C_{21} & C_{22} \end{smallmatrix}\right]$ stabilizes P. Conversely, if $K_I = \left[\begin{smallmatrix} 0 & I \\ C_{21} & C_{22} \end{smallmatrix}\right]$ stabilizes P. By the first result, we have that Δ^{-1}, $P\Delta^{-1}$ are both in $\mathcal{S}$. Suppose that M, N, X, and Y are as in Definition 2.2, then

$$Y\Delta^{-1} + XP\Delta^{-1} = (YM + XN)(M - C_{22}M + C_{21}N) = D^{-1}. \tag{4.2}$$

Since X and Y are in $\mathcal{S}$, we see that $D^{-1} \in \mathcal{S}$. This completes the proof. □

There is a similar result for the dual canonical controller.

Theorem 4.3. *The dual canonical controller $K_I = \left[\begin{smallmatrix} 0 & C_{12} \\ I & C_{22} \end{smallmatrix}\right]$ stabilizes $P \in \mathcal{L}$ with internal loop if and only if $\widehat{\Delta} = I - C_{22} + PC_{12}$ is invertible in $\mathcal{L}$ and $\widehat{\Delta}^{-1}$, $\widehat{\Delta}^{-1}P \in \mathcal{S}$.*

If P has a strong left representation $[-\widehat{N} \quad \widehat{M}]$, then the dual canonical controller K_I stabilizes P if and only if $\widehat{D} = \widehat{M} - \widehat{M}C_{22} + \widehat{N}C_{12}$ is invertible in $\mathcal{S}$.

In [6], the parametrization of all canonical controllers and dual canonical controllers is given and it can be easily extended to our framework.

Theorem 4.4. *Suppose $P \in \mathcal{L}$ satisfies the assumption of Theorem 3.3. Then all canonical controllers that stabilize P are parameterized by*

$$\begin{bmatrix} 0 & I \\ E\left(X + Q\widehat{M}\right) & I - E\left(Y - Q\widehat{N}\right) \end{bmatrix}, \tag{4.3}$$

where $Q \in \mathcal{S}$ and E is invertible in $\mathcal{S}$.

Analogously, all dual canonical controllers that stabilize P are parameterized by

$$\begin{bmatrix} 0 & \left(\widehat{X} + MQ\right)R \\ I & I - \left(\widehat{Y} - NQ\right)R \end{bmatrix}, \tag{4.4}$$

where $Q \in \mathcal{S}$ and R is invertible in $\mathcal{S}$.

Remark 4.5. Indeed, if we choose the parameters in Theorem 3.3 such that $R_1 = E^{-1}$, $R_2 = \widehat{X} + MQ$, and $R_3 = ME^{-1}$, we can obtain the same result of the above theorem. This implies that the result derived in [6] can be regarded as a special case of Theorem 3.3.

The following theorem gives a strong relation between the stabilization with canonical controller and the usual concept of stabilization.

Theorem 4.6. *Suppose $I - C_{22}$ is invertible in $\mathcal{L}$, then P can be stabilized by a canonical controller with internal loop if and only if P is stabilizable in the framework of standard feedback system.*

Proof. Suppose P is stabilized by a canonical controller $K_I = \left[\begin{smallmatrix} 0 & C_{12} \\ I & C_{22} \end{smallmatrix}\right]$ with $I - C_{22}$ invertible in $\mathcal{L}$. Then all entries of $H(P, K_I)$ in (4.1) are in $\mathcal{S}$. By computation, we can easily obtain that the upper left 2×2 corner of the transfer matrix $H(P, K_I)$ is just the transfer matrix $H(P, C)$ in the standard feedback system with the plant P and the controller $C = (I - C_{22})^{-1}C_{21}$. It follows that P is stabilizable in the standard feedback system.

On the other hand, suppose P is stabilizable in the standard feedback system. Then, from Theorem 2.4, all the stabilizing controllers can be given by $C = (Y - Q\widehat{N})^{-1}(X + Q\widehat{M})$ with some $Q \in \mathcal{S}$. Let $C_{21} = X + Q\widehat{M}$, $C_{22} = Y - Q\widehat{N}$, then we obtain a canonical controller $K_I = \left[\begin{smallmatrix} 0 & I \\ X+Q\widehat{M} & Y-Q\widehat{N} \end{smallmatrix}\right]$ and it is easy to verify that K_I stabilizes P. □

Naturally, there exists a dual result for the dual canonical controller.

Now we can explain the advantage of the controller with internal loop in the practical application.

Recall the parametrization of the conventional controllers in Theorem 2.4, it is not clean and an extra invertibility condition is imposed on the Youla parameter. This in turn makes it awkward to use this parametrization to solve the practical problems. For example, in [8, Section 7], the sensitivity minimization problem for the system described in Figure 3 is studied. The weighted sensitivity operator for this system is defined by $S_W = (I + PC)^{-1}W$ and the weighted sensitivity minimization problem is to find

$$\inf\{\|S_W\| : C \text{ stabilizes } P\}. \tag{4.5}$$

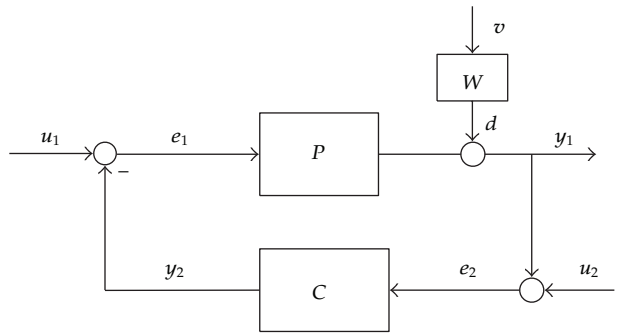

Figure 3: Standard feedback system with outside disturbance d and W invertible.

Suppose $P \in \mathcal{L}$ satisfy the condition in Theorem 2.4, then all stabilizing controllers can be given by $C = (\widehat{X} + MQ)(\widehat{Y} - NQ)^{-1}$ with $Q \in \mathcal{S}$ and $\widehat{Y} - NQ$ is invertible in $\mathcal{L}$. By simple computation, we can obtain that the weighted sensitivity minimization problem is to find

$$\inf\left\{\left\|\widehat{Y}\widehat{M}W - NQ\widehat{M}W\right\| : Q \in \mathcal{S}, \widehat{Y} - NQ \text{ is invertible in } \mathcal{L}\right\}. \tag{4.6}$$

Obviously, the extra condition that $\widehat{Y} - NQ$ is invertible in $\mathcal{L}$ makes the practical control engineers difficult to continue their computations. So they have to choose to ignore the fact that the Youla parameter can not be taken for all the elements in $\mathcal{S}$.

Fortunately, the controller with internal loop overcomes this awkwardness. Let us consider the sensitivity minimization problem for the system with internal loop as described in Figure 4. We consider this problem for the dual canonical controller $K_I = \left[\begin{smallmatrix} 0 & C_{12} \\ I & C_{22} \end{smallmatrix}\right]$ with C_{12}, $C_{22} \in \mathcal{S}$. When $u_1 = u_2 = u_3 = 0$, it is easy to check that the weighted sensitivity operator for this system is

$$S_W = \left[I - PC_{12}(I - C_{22} + PC_{12})^{-1}\right]W, \tag{4.7}$$

and the weighted sensitivity minimization problem is to find

$$\inf\left\{\|S_W\| : K_I = \begin{bmatrix} 0 & C_{12} \\ I & C_{22} \end{bmatrix} \text{ stabilizes } P\right\}. \tag{4.8}$$

By using the parametrization of the dual canonical controller given in Theorem 4.4, the weighted sensitivity minimization problem is to find

$$\inf\left\{\left\|\widehat{Y}\widehat{M}W - NQ\widehat{M}W\right\| : Q \in \mathcal{S}\right\}. \tag{4.9}$$

Obviously, it avoids the extra invertibility condition for the parameter Q as it appears in the standard feedback system. This overcomes the difficulty arisen in the standard feedback system.

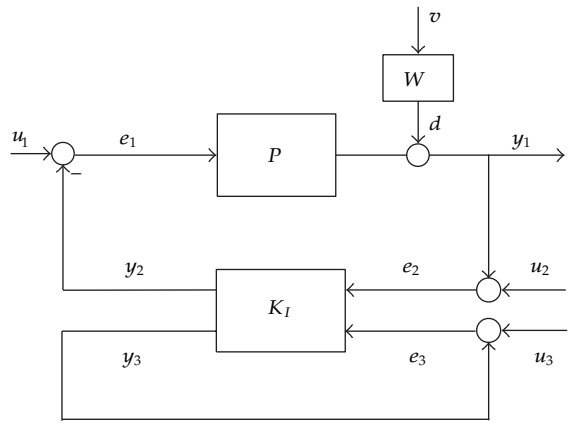

Figure 4: System with internal loop with outside disturbance d and W invertible.

5. Strong Stabilization with Internal Loop

Practicing control engineers is reluctant to use unstable compensators for the purpose of stabilization. This motivated considering the strong stabilization problem whether among the stabilizing controllers for a given stabilizable plant P, there exist stable ones. If there exists such a controller, P is said to be strongly stabilizable and the stable controller is called the strongly stabilizing controller. In this section, we consider the strong stabilization problem for the system with internal loop and address another advantage of the controller with internal loop.

Definition 5.1. $P \in \mathcal{L}$ is said to be strongly stabilizable with internal loop if it can be stabilized by the controller $K_I = \begin{bmatrix} C_{11} & C_{12} \\ C_{21} & C_{22} \end{bmatrix}$ with $C_{ij} \in \mathcal{S}$, $i, j = 1, 2$. This controller K_I is called the strongly stabilizing controller with internal loop.

Obviously, the canonical controller and dual canonical controller are both the strongly stabilizing controller with internal loop. From the parametrization of controllers with internal loop given in Theorem 3.3, we see that the strongly stabilizing controller with internal loop can be characterize by choosing the parameters Q, R_1, R_2, and R_3 in Theorem 3.3 such that $\widehat{Y} - NQ$ and $R_3 + R_2(\widehat{Y} - NQ)^{-1}NR_1$ are invertible in $\mathcal{S}$. The following theorem shows the existence of the strongly stabilizing controller with internal loop.

Theorem 5.2. *Suppose $P \in \mathcal{L}$ is stabilizable, then P can be strongly stabilized by the controller with internal loop.*

Proof. Suppose P is stabilizable. From Theorem 2.4, the controller stabilizes P has the parametrization that $C = (Y - Q\widehat{N})^{-1}(X + Q\widehat{M})$ for some stable Q. Set $C_{11} = 0$, $C_{12} = I$, $C_{21} = (X + Q\widehat{M})$ and $C_{22} = I - (Y - Q\widehat{N})$, then $K_I = \begin{bmatrix} 0 & I \\ X+Q\widehat{M} & I-(Y-Q\widehat{N}) \end{bmatrix}$ is a stable controller with internal loop and it strongly stabilizes the plant P. □

Remark 5.3. In [17], it is proved that a given plant P with left coprime factorization $P = \widehat{M}^{-1}\widehat{N}$ can be strongly stabilized in the standard feedback system if $\widehat{N}$ is compact. While in the case where $\widehat{N}$ is not compact, it is still an open problem whether or not there exists a stable

controller that stabilizes the plant. Theorem 5.2 shows that any stabilizable plant can be stabilized by a stable controller with internal loop. It implies that the strong stabilization problem can be completely solved by the controller with internal loop. And this addresses an advantage of the controller with internal loop in the framework of nest algebra.

From the proof of Theorem 5.2, we see that it also provides a method to design the strongly stabilizing controller with internal loop. We end our paper with a simple example to show this design method.

Example 5.4. Suppose $P = I$, it is obviously stabilizable. Take

$$N = \widehat{N} = M = \widehat{M} = I,$$

$$Y = \widehat{Y} = \begin{bmatrix} 1 & & & & \\ 0 & \frac{1}{2} & & & \\ 0 & 0 & \frac{1}{3} & & \\ 0 & 0 & 0 & \frac{1}{4} & \\ \vdots & \vdots & \vdots & \vdots & \ddots \end{bmatrix}, \qquad X = \widehat{X} = \begin{bmatrix} 0 & & & & \\ 0 & \frac{1}{2} & & & \\ 0 & 0 & \frac{2}{3} & & \\ 0 & 0 & 0 & \frac{3}{4} & \\ \vdots & \vdots & \vdots & \vdots & \ddots \end{bmatrix}. \tag{5.1}$$

From Theorem 2.4, we obtain the parametrization of the stabilizing controller $C = (Y - Q\widehat{N})^{-1}(X + Q\widehat{M})$ for some stable Q. Take $Q = 0$, then

$$C = Y^{-1}X \text{ stabilizes } P \text{ and } C = \begin{bmatrix} 0 & & & & \\ 0 & 1 & & & \\ 0 & 0 & 2 & & \\ 0 & 0 & 0 & 3 & \\ \vdots & \vdots & \vdots & \vdots & \ddots \end{bmatrix} \tag{5.2}$$

is unstable. In order to satisfy the practicing control engineers' requirement, we set $C_{11} = 0$, $C_{12} = I$, $C_{21} = X$ and $C_{22} = I - Y$. Then we obtain a stable controller $K_I = \left[\begin{smallmatrix} 0 & I \\ X & I-Y \end{smallmatrix}\right]$ with internal loop which stabilizes the plant P.

6. Conclusion

In this paper, the closed-loop system whose stability is achieved by the controller with internal loop is studied in the framework of nest algebra. The controllers with internal loop considered here are more general than those in the previous paper and they are not necessarily stable and need not to satisfy the two conditions proposed in [1]. We give a parametrization for all stabilizing controllers with internal loop which has never been studied before. Then we show that this parametrization covers the parametrization for canonical or dual canonical controllers obtained in [6]. By taking the sensitivity minimization problem as an example, we show that, in the practical application, the controller with internal loop solves the difficulty brought by the invertibility condition in the parametrization of the conventional controller. In the framework of nest algebra, the strong stabilization problem is still an open problem, and no sufficient and necessary condition was found to characterize the plant

which can be strongly stabilized. While, with the help of the concept of stabilization with internal loop, we show that any stabilizable plant can be strongly stabilized by the controller with internal loop. This addresses an advantage of the controller with internal loop in the framework of nest algebra. By using the parametrization of the controller with internal loop, we are considering other questions in the control theory for the this model of closed-loop systems with internal loop.

Acknowledgments

The authors would like to thank Doctor Liu Liu for pointing out Lemma 3.1 and Doctor Gong Ting for her invaluable suggestions. This research is supported by NSFC, item number: 10971020.

References

[1] G. Weiss and R. F. Curtain, "Dynamic stabilization of regular linear systems," *Institute of Electrical and Electronics Engineers*, vol. 42, no. 1, pp. 4–21, 1997.

[2] R. Curtain, G. Weiss, and M. Weiss, "Coprime factorization for regular linear systems," *Automatica*, vol. 32, no. 11, pp. 1519–1531, 1996.

[3] S. Townley, G. Weiss, and Y. Yamamoto, "Discretizing continuous time controllers for infinite-dimensional linear systems," in *Proceedings of the MTNS Symposium*, pp. 547–550, Padova, Italy, July 1998.

[4] G. Weiss and R. Rebarber, "Optimizability and estimatability for infinite-dimensional linear systems," *SIAM Journal on Control and Optimization*, vol. 39, no. 4, pp. 1204–1232, 2000.

[5] K. M. Mikkola, "Coprime factorization and dynamic stabilization of transfer functions," *SIAM Journal on Control and Optimization*, vol. 45, no. 6, pp. 1988–2010, 2007.

[6] R. F. Curtain, G. Weiss, and M. Weiss, "Stabilization of irrational transfer functions by controllers with internal loop, Systems, approximation, singular integral operators, and related topics," in *Proceedings of the International Workshop on Operator Theory and Applications (IWOTA)*, A. A. Borichev and N. K. Nikolski, Eds., vol. 129 of *Advances in Operator Theory and Applications*, pp. 179–207, Birkhäauser, Basel, 2000.

[7] R. F. Curtain, "Robustly stabilizing controllers with internal loop," in *Control of uncertain systems: modelling, approximation, and design*, vol. 329 of *Lecture Notes in Control and Inform. Sci.*, pp. 79–98, Springer, Berlin, Germany, 2006.

[8] A. Feintuch, *Robust Control Theory in Hilbert Space*, vol. 130, Springer, New York, NY, USA, 1998.

[9] L. Ma, Z. Wang, Y. Bo, and Z. Guo, "A game theory approach to mixed $\mathscr{H}_2/\mathscr{H}_\infty$ control for a class of stochastic time-varying systems with randomly occurring nonlinearities," *Systems and Control Letters*, vol. 60, no. 12, pp. 1009–1015, 2011.

[10] J. Hu, Z. Wang, H. Gao, and L. K. Stergioulas, "Probability-guaranteed H_∞ finite-horizon filtering for a class of nonlinear time-varying systems with sensor saturations," *Systems and Control Letters*, vol. 61, no. 4, pp. 477–484, 2012.

[11] G. Wei, Z. Wang, and B. Shen, "Error-constrained finite-horizon tracking control with incomplete measurements and bounded noises," *International Journal of Robust and Nonlinear Control*, vol. 22, no. 2, pp. 223–238, 2012.

[12] B. Shen, Z. Wang, H. Shu, and G. Wei, "H_∞ filtering for uncertain time-varying systems with multiple randomly occurred nonlinearities and successive packet dropouts," *International Journal of Robust and Nonlinear Control*, vol. 21, no. 14, pp. 1693–1709, 2011.

[13] B. Shen, Z. Wang, and X. Liu, "Bounded H_∞ synchronization and state estimation for discrete time-varying stochastic complex networks over a finite horizon," *IEEE Transactions on Neural Networks*, vol. 22, no. 1, Article ID 5640676, pp. 145–157, 2011.

[14] G. Wei, Z. Wang, and B. Shen, "Error-constrained filtering for a class of nonlinear time-varying delay systems with non-Gaussian noises," *IEEE Transactions on Automatic Control*, vol. 55, no. 12, pp. 2876–2882, 2010.

[15] Z. Wang, D. W. C. Ho, H. Dong, and H. Gao, "Robust $\mathcal{H}_\infty$ finite-horizon control for a class of stochastic nonlinear time-varying systems subject to sensor and actuator saturations," *IEEE Transactions on Automatic Control*, vol. 55, no. 7, pp. 1716–1722, 2010.

[16] H. Dong, Z. Wang, D. W. C. Ho, and H. Gao, "Variance-constrained $\mathcal{H}_\infty$ filtering for a class of nonlinear time-varying systems with multiple missing measurements: the finite-horizon case," *IEEE Transactions on Signal Processing*, vol. 58, no. 5, pp. 2534–2543, 2010.

[17] A. Feintuch, "On strong stabilization for linear time-varying systems," *Systems & Control Letters*, vol. 54, no. 11, pp. 1091–1095, 2005.